



ELECTRIC POWER
RESEARCH INSTITUTE

MRP Materials Reliability Program

MRP 2016-039

(via email)

DATE: November 8, 2016

TRD 50669

TO: Document Control Desk
U.S. Nuclear Regulatory Commission
Washington, DC 20555-001

FROM: David Czufin, TVA, PMMP Chairman
Brian Burgos, EPRI, MRP Program Manager

SUBJECT: Transmittal of *Materials Reliability Program: Topical Report for Primary Water Stress Corrosion Cracking Mitigation by Surface Stress Improvement (MRP-335 Revision 3-A)*, EPRI, Palo Alto, CA: 2016. 3002009241.

References:

1. *Materials Reliability Program: Topical Report for Primary Water Stress Corrosion Cracking Mitigation by Surface Stress Improvement (MRP-335 Revision 3)*, EPRI, Palo Alto, CA: 2016. 3002007392.
2. U.S. NRC, Final Safety Evaluation of the Electric Power Research Institute MRP-335, Revision 3, "Materials Reliability Program: Topical Report for Primary Water Stress Corrosion Cracking Mitigation by Surface Stress Improvement [Peening]" (TAC No. MF2429), August 24, 2016. [NRC ADAMS Accession No.: ML16208A485]
3. U.S. NRC, Request for Additional Information related Electric Power Research Institute MRP-335, Revision 1, "Topical Report for Primary Water Stress Corrosion Cracking Mitigation by Surface Stress Improvement [Peening]" (TAC No. MF2429), September 8, 2014. [NRC ADAMS Accession No.: ML14181A025]
4. U.S. NRC, Second Request for Additional Information for MRP-335, Revision 1, "Topical Report for Primary Water Stress Corrosion Cracking Mitigation by Surface Stress Improvement [Peening]" (TAC No. MF2429), April 2, 2015. [NRC ADAMS Accession No.: ML15057A028]
5. Letter from B. C. Rudell and A. Demma to U.S. NRC, "Response to the NRC Request for Additional Information (RAI) related to Electric Power Research Institute (EPRI) MRP-335, Revision 1, 'Topical Report for Primary Water Stress Corrosion Cracking Mitigation by Surface Stress Improvement [Peening]' (TAC No. MF2429)," MRP 2014-027, October 10, 2014. [NRC ADAMS Accession No.: ML14288A370]
6. Letter from B. C. Rudell and A. Demma to U.S. NRC, "Response to the NRC Second Request for Additional Information related to MRP-335, Revision 1, 'Topical Report for Primary Water Stress Corrosion Cracking Mitigation by Surface Stress

Together . . . Shaping the Future of Electricity

PALO ALTO OFFICE

3420 Hillview Avenue, Palo Alto, CA 94304-1338 USA • 650.855.2000 • Customer Service 800.313.3774 • www.epri.com

DO 35
T010

Improvement [Peening]' (TAC No. MF2429)," MRP 2015-020, June 12, 2015. [NRC ADAMS Accession No.: ML15167A106]

7. *Materials Reliability Program: Topical Report for Primary Water Stress Corrosion Cracking Mitigation by Surface Stress Improvement (MRP-335, Revision 1)*, EPRI, Palo Alto, CA: 2013. 3002000073.

This letter transmits the subject EPRI Topical Report, MRP-335 Revision 3-A. This non-proprietary report is a revision to MRP-335 Revision 3 [1] that incorporates the four Conditions specified in the corresponding U.S. Nuclear Regulatory Commission Safety Evaluation [2]. All changes to the report from Revision 3 to Revision 3-A, except corrections to any typographic errors, are marked with margin bars and summarized in the Record of Revisions table of the report. In accordance with a NRC request, the SE cover letter and final SE are reproduced at the beginning of the report and the report number includes an "-A" indicating the version of the report accepted by the NRC staff.

In addition to incorporation of the NRC Conditions, Revision 3-A includes the following changes to Revision 3:

- Section 3.6 was updated and revised to ensure that its intention is clear. Section 3.6 of MRP-335R3 discussed a project completed in February 2016 to determine if peening has an effect on the results for ultrasonic testing applied to reactor pressure vessel head penetration nozzles (RPVHPNs). This project involved an RPVHPN mockup peened using a single peening process of one peening vendor and examined per the qualified examination procedures of one NDE vendor. Section 3.6 of MRP-335R3-A was updated and revised to make clear that this project was cited as an example of one process and exam procedure validity test and refers utilities to continuing support and the need and plans to validate other peening methods and ultrasonic procedures.
- Sections 5.1 and 5.2.3.2 were updated to clarify the modeled stress conditions in the deterministic analyses and deterministic matrix for RPVHPNs subsequent to peening.
- Editorial wording changes were made to the Abstract and Section 1.2. These changes do not affect the meaning of the text.

Note that there were no Requests for Additional Information (RAIs) from NRC in conjunction with NRC's review of MRP-335 Revision 3. Thus, no RAIs or RAI responses are included in the attached version of the topical report. There were two sets of RAIs ([3], [4]) and RAI responses ([5], [6]) in the previous review process for MRP-335 Revision 1 [7]. EPRI MRP's previous request for review of MRP-335 Revision 1 was withdrawn without NRC publishing a Safety Evaluation on that version of the topical report.

If you should have any questions concerning this letter, please contact Paul Crooker, EPRI MRP Project Manager, at (pcrooker@epri.com) or 650-855-2028.

Together . . . Shaping the Future of Electricity

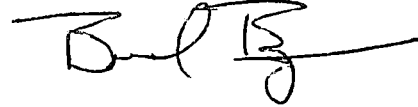
PALO ALTO OFFICE

3420 Hillview Avenue, Palo Alto, CA 94304-1338 USA • 650.855.2000 • Customer Service 800.313.3774 • www.epri.com

Sincerely,



David Czufin
Chairman, PMMP
Tennessee Valley Authority



Brian Burgos
EPRI MRP Program Manager
Electric Power Research Institute

cc: Joe Holonich, NRC
Paul Crooker, EPRI
William Sims, Entergy

Attachments:

1. Materials Reliability Program: Topical Report for Primary Water Stress Corrosion Cracking Mitigation by Surface Stress Improvement (MRP-335 Revision 3-A)

Together . . . Shaping the Future of Electricity

PALO ALTO OFFICE

3420 Hillview Avenue, Palo Alto, CA 94304-1338 USA • 650.855.2000 • Customer Service 800.313.3774 • www.epri.com

Materials Reliability Program:
Topical Report for Primary Water Stress Corrosion
Cracking Mitigation by Surface Stress Improvement
(MRP-335, Revision 3-A)

2016 TECHNICAL REPORT



Materials Reliability Program: Topical Report for Primary Water Stress Corrosion Cracking Mitigation by Surface Stress Improvement (MRP-335, Revision 3-A)

3002009241

Final Report, November 2016

EPRI Project Manager
P. Crooker

All or a portion of the requirements of the EPRI Nuclear
Quality Assurance Program apply to this product.

YES



DISCLAIMER OF WARRANTIES AND LIMITATION OF LIABILITIES

THIS DOCUMENT WAS PREPARED BY THE ORGANIZATION(S) NAMED BELOW AS AN ACCOUNT OF WORK SPONSORED OR COSPONSORED BY THE ELECTRIC POWER RESEARCH INSTITUTE, INC. (EPRI). NEITHER EPRI, ANY MEMBER OF EPRI, ANY COSPONSOR, THE ORGANIZATION(S) BELOW, NOR ANY PERSON ACTING ON BEHALF OF ANY OF THEM:

(A) MAKES ANY WARRANTY OR REPRESENTATION WHATSOEVER, EXPRESS OR IMPLIED, (I) WITH RESPECT TO THE USE OF ANY INFORMATION, APPARATUS, METHOD, PROCESS, OR SIMILAR ITEM DISCLOSED IN THIS DOCUMENT, INCLUDING MERCHANTABILITY AND FITNESS FOR A PARTICULAR PURPOSE, OR (II) THAT SUCH USE DOES NOT INFRINGE ON OR INTERFERE WITH PRIVATELY OWNED RIGHTS, INCLUDING ANY PARTY'S INTELLECTUAL PROPERTY, OR (III) THAT THIS DOCUMENT IS SUITABLE TO ANY PARTICULAR USER'S CIRCUMSTANCE; OR

(B) ASSUMES RESPONSIBILITY FOR ANY DAMAGES OR OTHER LIABILITY WHATSOEVER (INCLUDING ANY CONSEQUENTIAL DAMAGES, EVEN IF EPRI OR ANY EPRI REPRESENTATIVE HAS BEEN ADVISED OF THE POSSIBILITY OF SUCH DAMAGES) RESULTING FROM YOUR SELECTION OR USE OF THIS DOCUMENT OR ANY INFORMATION, APPARATUS, METHOD, PROCESS, OR SIMILAR ITEM DISCLOSED IN THIS DOCUMENT.

REFERENCE HEREIN TO ANY SPECIFIC COMMERCIAL PRODUCT, PROCESS, OR SERVICE BY ITS TRADE NAME, TRADEMARK, MANUFACTURER, OR OTHERWISE, DOES NOT NECESSARILY CONSTITUTE OR IMPLY ITS ENDORSEMENT, RECOMMENDATION, OR FAVORING BY EPRI.

THE FOLLOWING ORGANIZATION, UNDER CONTRACT TO EPRI, PREPARED THIS REPORT:

Dominion Engineering, Inc.

THE TECHNICAL CONTENTS OF THIS PRODUCT WERE **NOT** PREPARED IN ACCORDANCE WITH THE EPRI QUALITY PROGRAM MANUAL THAT FULFILLS THE REQUIREMENTS OF 10 CFR 50, APPENDIX B. THIS PRODUCT IS **NOT** SUBJECT TO THE REQUIREMENTS OF 10 CFR PART 21.

NOTE

For further information about EPRI, call the EPRI Customer Assistance Center at 800.313.3774 or e-mail askepri@epri.com.

Electric Power Research Institute, EPRI, and TOGETHER...SHAPING THE FUTURE OF ELECTRICITY are registered service marks of the Electric Power Research Institute, Inc.

Copyright © 2016 Electric Power Research Institute, Inc. All rights reserved.

ACKNOWLEDGMENTS

The following organization, under contract to the Electric Power Research Institute (EPRI), prepared this report:

Dominion Engineering, Inc.
12100 Sunrise Valley Dr., Suite 220
Reston, VA 20191

Principal Investigators

G. White
J. Gorman
K. Schmitt
K. Fuhr
M. Burkardt

This report describes research sponsored by EPRI.

The contributions of the MRP utility participants, EPRI consultants, and participating surface stress improvement vendors are gratefully acknowledged. The MRP utility participants and EPRI consultants included Gary Alkire (Exelon), Edward Blackard (Entergy), Guy DeBoo (Exelon), Richard Gimple (Wolf Creek Nuclear Operating Corporation), Jamie GoBell (Entergy), Beth Haluska (Dominion Generation), Scott Koernschild (Exelon), Bernie Rudell (Constellation Energy Group), William Sims (Entergy), Dennis Weakland (Ironwood Consulting), and Tim Wells (Southern Nuclear). The participating surface stress improvement vendors were AREVA, Hitachi-GE, Metal Improvement Company, Mitsubishi Heavy Industries / Mitsubishi Nuclear Energy Systems, and Toshiba / Westinghouse.

This publication is a corporate document that should be cited in the literature in the following manner:

Materials Reliability Program: Topical Report for Primary Water Stress Corrosion Cracking Mitigation by Surface Stress Improvement (MRP-335, Revision 3-A), EPRI, Palo Alto, CA: 2016. 3002009241.

ABSTRACT

Given the demonstrated effectiveness of surface stress improvement (SSI) techniques such as laser peening and water jet peening (aka cavitation peening), relaxation of inspection requirements for certain components is appropriate after SSI treatment. The objective of this report is to define appropriate inspection requirements and intervals for Alloy 600 reactor pressure vessel head penetration nozzles and Alloy 82/182 dissimilar metal welds in primary system piping treated by SSI methods to mitigate primary water stress corrosion cracking (PWSCC). These requirements apply in case relaxation of the applicable inspection requirements for unmitigated components is sought. It is important to note that the requirements of this report are generally not applicable where peening is performed for asset management without request for inspection relief.

Specific inspection requirements are supported by detailed deterministic and probabilistic modeling that assumes the peening process meets applicable minimum performance criteria. This report defines performance criteria and discusses the technical bases, which include an increased nuclear safety margin and a large reduction in the probability of leakage occurring. While plant experience has shown that the probability of leakage under current inspection requirements is low, the analyses documented here demonstrate that the probability further decreases by performing peening and inspecting per the relaxed inspection requirements. Peening mitigation implemented in accordance with the requirements of this report provides a substantial risk benefit for a risk that is already low.

Inspection requirements for these components are prescribed by U.S. Nuclear Regulatory Commission (NRC) regulations (based on American Society of Mechanical Engineers Boiler and Pressure Vessel Code Cases). NRC approval is thus required for relaxation of these inspection requirements following peening mitigation. Licensees may reference this topical report in support of site-specific relief requests.

Keywords

Alloy 600
Cavitation peening
Laser peening
Primary water stress corrosion cracking (PWSCC)
Surface stress improvement (SSI)
Water jet peening

Deliverable Number: 3002009241

Product Type: Technical Report

Product Title: Materials Reliability Program: Topical Report for Primary Water Stress Corrosion Cracking Mitigation by Surface Stress Improvement (MRP-335, Revision 3-A)

PRIMARY AUDIENCE: Organizations considering peening surface stress improvement (SSI) to mitigate primary water stress corrosion cracking (PWSCC), peening vendors

SECONDARY AUDIENCE: Nuclear regulatory agencies

KEY RESEARCH QUESTION

Given the demonstrated effectiveness of surface stress improvement (SSI) techniques such as laser peening and water jet peening (aka cavitation peening), relaxation of inspection requirements for certain components is appropriate after SSI treatment. The objective of this report is to define appropriate inspection requirements and intervals for Alloy 600 reactor pressure vessel head penetration nozzles (RPVHPNs) and Alloy 82/182 dissimilar metal welds (DMWs) in primary system piping treated by SSI methods to mitigate primary water stress corrosion cracking (PWSCC). These requirements apply in case utilities seek to relax the applicable inspection requirements for unmitigated components. It is important to note that the requirements of this report are generally not applicable where peening is performed for asset management without request for inspection relief.

RESEARCH OVERVIEW

Specific inspection requirements are supported by detailed deterministic and probabilistic modeling that assumes the peening process meets applicable minimum performance criteria. This topical report defines performance criteria and discusses the technical bases, which include an increased nuclear safety margin and a large reduction in the probability of leakage occurring. While plant experience has shown that the probability of leakage under current inspection requirements is low, the analyses documented here demonstrate that the probability further decreases by performing peening and inspecting per the relaxed inspection requirements. Peening mitigation implemented in accordance with the requirements of this report provides a substantial risk benefit for a risk that is already low.

KEY FINDINGS

- Extensive industrial experience shows that peening of many types is effective at inhibiting the initiation of both fatigue and stress corrosion cracks.
- The deterministic and probabilistic calculations discussed in Section 5 and appendices A and B of this report show that peening provides significant benefits in terms of preventing initiation of new PWSCC. Furthermore, any cracks that could be present after pre-peening inspections and repairs are effectively addressed by inspection subsequent to peening.
- A set of deterministic crack growth rate calculations using a range of deterministic inputs demonstrate that a large fraction of cases with peening show no leakage subsequent to the extension of inspection intervals. Although some cases do show leakage, the frequency of such cases is greatly reduced versus that for unpeened components inspected per the current inspection requirements. Most of the cases that do show leakage represent very unlikely combinations of conditions resulting in crack growth rates near the upper bound of credible behavior.
- Extensive testing—including examination of many peened samples and test blocks—has been performed of peening processes as described in MRP-267, Revision 1 (EPRI 1025839). No adverse effects have been identified in this testing.

- Peening has been extensively used in Japanese pressurized water reactors (PWRs) and boiling water reactors (BWRs) for 14 years with no reported adverse effects to the peened components.

WHY THIS MATTERS

PWSCC can lead to increased costs for operation, maintenance, assessment, repair, and replacement of PWR components. Alloy 600 and Alloy 82/182 materials, which are widely used in PWR systems, are susceptible to PWSCC. This report demonstrates the acceptability of relaxing inspection intervals for RPVHPN and DMW components mitigated using a SSI process that meets applicable performance criteria. Such relaxation of intervals maintains an acceptably low effect on nuclear safety in terms of PWSCC, while also maintaining defense in depth.

HOW TO APPLY RESULTS

The inspection requirements for RPVHPN and DMW components are prescribed by U.S. NRC regulations (based on ASME Boiler and Pressure Vessel Code Cases). To date, the U.S. NRC has not generically approved inspection relief for peening within 10 CFR 50.55a (such as approval of ASME Code Cases N-7295, N-729-6, or N-770-4). Until such time, application-specific relief must be approved by the NRC before implementing inspection relief for peening. Before implementing the inspection relief defined in this report, therefore, a relief request must be submitted for NRC review and approval. This report identifies technical information that must be included in the relief request and lists additional technical information that must be included in the peening qualification report. Relaxed inspection intervals and performance criteria are developed to credit peening performance within the framework of the respective Code Cases upon which existing inspection requirements are based. This report may also serve as the technical basis for revision of the respective Code Cases to credit peening.

LEARNING AND ENGAGEMENT OPPORTUNITIES

- MRP-267, Revision 1 (EPRI 1025839) establishes the technical basis for applying peening SSI treatments for mitigating PWSCC as a viable method to protect key PWR plant assets. The report presents extensive data showing the effectiveness of laser peening and water jet peening methods to mitigate PWSCC.
- MRP-336, Revision 1 (EPRI 3002008084) provides guidance to utilities regarding technical specification of the requirements the peening vendor must meet to ensure that the peening mitigation process is effective and reliable.

EPRI CONTACTS: Paul Crooker, EPRI Project Manager, pcrooker@epri.com

PROGRAM: 2016 Program 41.01.04 Pressurized Water Reactor Materials Reliability Program (MRP)

IMPLEMENTATION CATEGORY: Category 2

Together...Shaping the Future of Electricity®

Electric Power Research Institute

3420 Hillview Avenue, Palo Alto, California 94304-1338 • PO Box 10412, Palo Alto, California 94303-0813 USA
800.313.3774 • 650.855.2121 • askepri@epri.com • www.epri.com

© 2016 Electric Power Research Institute (EPRI), Inc. All rights reserved. Electric Power Research Institute, EPRI, and TOGETHER...SHAPING THE FUTURE OF ELECTRICITY are registered service marks of the Electric Power Research Institute, Inc.

NRC SAFETY EVALUATION

In accordance with an NRC request, the NRC Safety Evaluation immediately follows this page.

Note: the changes proposed by the NRC in the Safety Evaluation have been incorporated into the current version of the report (MRP-335R3-A)

August 24, 2016

Matthew Sunseri, Chair
PWR Materials Management Program
Electric Power Research Institute
3420 Hillview Avenue
Palo Alto, CA 94304

SUBJECT: FINAL SAFETY EVALUATION OF THE ELECTRIC POWER RESEARCH
INSTITUTE MRP-335, REVISION 3, "MATERIALS RELIABILITY PROGRAM:
TOPICAL REPORT FOR PRIMARY WATER STRESS CORROSION CRACKING
MITIGATION BY SURFACE STRESS IMPROVEMENT [PEENING]"
(TAC NO. MF2429)

Dear Mr. Sunseri:

By letter dated May 1, 2013 (Agencywide Documents Access and Management System Package Accession No. ML131260010), the Electric Power Research Institute (EPRI) on behalf of nuclear power industry's Materials Reliability Program (MRP), submitted to U.S. Nuclear Regulatory Commission (NRC) staff for review "Materials Reliability Program: Topical Report for Primary Water Stress Corrosion Cracking Mitigation by Surface Stress Improvement (MRP 335, Revision 3)."

By letter dated July 14, 2016 (ADAMS Package Accession No. ML16083A010), an NRC draft safety evaluation (SE) was provided for your review and comment. By letter dated July 27, 2016 (ADAMS Accession No. ML16214A253), the Electric Power Research Institute (EPRI) provided comments on the NRC draft SE. The comments provided by EPRI were related to clarifications and accuracy. No proprietary information was identified in the draft SE. The NRC staff dispositioned the EPRI comments as shown in Table 5 of the enclosed final SE.

The NRC staff has found that MRP-335, Revision 3 is acceptable for referencing in licensing applications for nuclear power plants to the extent specified and under the limitations delineated in the TR and in the enclosed final SE. The final SE defines the basis for our acceptance of the TR.

Our acceptance applies only to material provided in the subject TR. We do not intend to repeat our review of the acceptable material described in the TR. When the TR appears as a reference in licensing action requests, our review will ensure that the material presented applies to the specific plant involved. Request for licensing actions that deviate from this TR will be subject to a plant-specific review in accordance with applicable review standards.

Mr. Sunseri

- 2 -

In accordance with the guidance provided on the NRC website, we request that EPRI publish an approved version of MRP-335, Revision 3 within three months of receipt of this letter. The approved version shall incorporate this letter and the enclosed final SE after the title page. Also, it must contain historical review information, including NRC requests for additional information (RAIs) and your responses. The approved version shall include an "-A" (designating approved) following the TR identification symbol.

As an alternative to including the RAIs and RAI responses behind the title page, if changes to the TR were provided to the NRC staff to support the resolution of RAI responses, and if the NRC staff reviewed and approved those changes as described in the RAI responses, there are two ways that the accepted version can capture the RAIs:

1. The RAIs and RAI responses can be included as an Appendix to the accepted version.
2. The RAIs and RAI responses can be captured in the form of a table (inserted after the final SE) which summarizes the changes as shown in the approved version of the TR. The table should reference the specific RAIs and RAI responses which resulted in any changes, as shown in the accepted version of the TR.

If future changes to the NRC's regulatory requirements affect the acceptability of this TR, EPRI will be expected to revise the TR appropriately or justify its continued applicability for subsequent referencing. Licensees referencing this TR would be expected to justify its continued applicability or evaluate their plant using the revised TR.

Sincerely,

/RA/

Kevin Hsueh, Chief
Licensing Processes Branch
Division of Policy and Rulemaking
Office of Nuclear Reactor Regulation

Project No. 669

Enclosure:
Final SE

Together...Shaping the Future of Electricity®

Electric Power Research Institute

3420 Hillview Avenue, Palo Alto, California 94304-1338 • PO Box 10412, Palo Alto, California 94303-0813 USA
800.313.3774 • 650.855.2121 • askepri@epri.com • www.epri.com

© 2016 Electric Power Research Institute (EPRI), Inc. All rights reserved. Electric Power Research Institute, EPRI, and TOGETHER...SHAPING THE FUTURE OF ELECTRICITY are registered service marks of the Electric Power Research Institute, Inc.

In accordance with the guidance provided on the NRC website, we request that EPRI publish an approved version of MRP-335, Revision 3 within three months of receipt of this letter. The approved version shall incorporate this letter and the enclosed final SE after the title page. Also, it must contain historical review information, including NRC requests for additional information (RAIs) and your responses. The approved version shall include an "-A" (designating approved) following the TR identification symbol.

As an alternative to including the RAIs and RAI responses behind the title page, if changes to the TR were provided to the NRC staff to support the resolution of RAI responses, and if the NRC staff reviewed and approved those changes as described in the RAI responses, there are two ways that the accepted version can capture the RAIs:

1. The RAIs and RAI responses can be included as an Appendix to the accepted version.
2. The RAIs and RAI responses can be captured in the form of a table (inserted after the final SE) which summarizes the changes as shown in the approved version of the TR. The table should reference the specific RAIs and RAI responses which resulted in any changes, as shown in the accepted version of the TR.

If future changes to the NRC's regulatory requirements affect the acceptability of this TR, EPRI will be expected to revise the TR appropriately or justify its continued applicability for subsequent referencing. Licensees referencing this TR would be expected to justify its continued applicability or evaluate their plant using the revised TR.

Sincerely,

/RA/

Kevin Hsueh, Chief
Licensing Processes Branch
Division of Policy and Rulemaking
Office of Nuclear Reactor Regulation

Project No. 669

Enclosure:
Final SE

DISTRIBUTION:

PUBLIC	RidsNrrDeEvib	RidsNrrDpr	DAlley	JCollins
RidsNrrDir	RidsNrrDirRarb	RidsNrrLADHarrison	RidsNroOd	RidsNrrDeEmcb
RidsACRS_MailCTR	RidsResOd	RidsOgcMailCenter	RidsNrrDprPlpb	RidsNrrDe
KHsueh	SCumblidge	JTsao		

EXTERNAL DISTRIBUTION:

Crooker, Paul> pcrooker@epri.com

ADAMS Accession No.: ML16208A485; *concurred via e-mail

NRR-106

OFFICE	NRR/DPR/PLPB	NRR/DPR/PLPB*	DE/EPNB/BC	NRR/DPR/PLPB
NAME	JHolonich	DHarrison	DAlley	KHsueh
DATE	07/27/2016	08/04/2016	08/11/2016	08/24/2016

OFFICIAL RECORD COPY

FINAL SAFETY EVALUATION ON THE TOPICAL REPORT
"MATERIALS RELIABILITY PROGRAM: PRIMARY WATER STRESS CORROSION
CRACKING MITIGATION BY SURFACE STRESS IMPROVEMENT (MRP-335 REVISION 3)"
TAC NO. MF2429

1.0 INTRODUCTION

1.1 PURPOSE

By letter dated May 1, 2013 (Agencywide Documents Access and Management System (ADAMS) Accession No. ML13126A009), the Electric Power Research Institute (EPRI) on behalf of nuclear power industry's Materials Reliability Program (MRP), submitted to the U.S. Nuclear Regulatory Commission (NRC) staff for review and approval the topical report (TR), "Materials Reliability Program: Topical Report for Primary Water Stress Corrosion Cracking Mitigation by Surface Stress Improvement (MRP-335, Revision 1)," EPRI, 3002000073, January 2013.

By letters dated October 10, 2014, and June 12, 2015 (ADAMS Accession Nos. ML14288A370 and ML15167A112, respectively), the MRP responded to the NRC staff's requests for additional information.

By letter dated August 14, 2015 (ADAMS Accession No. ML15230A173), the MRP submitted MRP-335, Revision 2, 3002006654, EPRI, August 2015 (ADAMS Package Accession No. ML15230A201).

By letter dated February 19, 2016 (ADAMS Accession No. ML16055A216), the MRP submitted MRP-335, Revision 3 (MRP-335R3), 3002007392, EPRI January 2016 (ADAMS Package Accession No. ML166055A215).

The MRP proposed to apply peening as a mitigation method to prevent primary water stress corrosion cracking (PWSCC) from occurring at dissimilar metal butt welds (DMWs) in primary loop piping, reactor pressure vessel head penetration nozzles (RPVHPNs), and associated J-groove welds that are fabricated from nickel-based Alloy 600/82/182 material. As part of peening, the MRP proposed to relax the current inspection requirements for the peened DMWs and RPVHPNs. MRP-335R3 contains the technical basis for peening application, including affected components, peening processes, performance criteria, analyses, and alternative inspection requirements.

1.2 BACKGROUND

Pressurized water reactor (PWR) plants have experienced PWSCC in Alloy 82/182 DMWs, Alloy 600 RPVHPNs, and associated Alloy 82/182 J-groove welds. Circumferential and axial cracks have been found in these components in several U.S. and international nuclear power plants, challenging the leak-tightness and structural integrity of the subject components. As a result of PWSCC, the NRC requires augmented inspections for these DMWs, RPVHPNs, and associated J-groove welds as summarized in Table 2 at the end of this safety evaluation (SE) and as specified in the following NRC regulations:

Title 10 of the *Code of Federal Regulations* (10 CFR) Section 50.55a(g)(6)(ii)(D), "Reactor Vessel Head Inspections," requires PWR plants to augment their inservice inspection (ISI) of the RPVHPNs and associated J-groove welds using American Society of Mechanical Engineers *Boiler and Pressure Vessel Code* (ASME Code) Case N-729-1, "Alternative Examination Requirements for PWR Reactor Vessel Upper Heads With Nozzles Having Pressure-Retaining Partial-Penetration Welds, Section XI, Division 1," with conditions.

The regulation at 10 CFR 50.55a(g)(6)(ii)(E), "Reactor Coolant Pressure Boundary Visual Inspections," requires PWR plants to augment their ISI of Class 1 components that are fabricated from Alloy 600/82/182 materials based on ASME Code Case N-722-1, "Additional Examinations for PWR Pressure Retaining Welds in Class 1 Components Fabricated With Alloy 600/82/182 Materials Section XI, Division 1," with conditions.

The regulation at 10 CFR 50.55a(g)(6)(ii)(F) requires augmented inservice volumetric inspection of DMWs in PWR plants in accordance with ASME Code Case N-770-1, "Alternative Examination Requirements and Acceptance Standards for Class 1 PWR Piping and Vessel Nozzle Butt Welds Fabricated With UNS N06082 or UNS W86182 Weld Filler Material with or without Application of Listed Mitigation Activities Section XI, Division 1," with conditions.

In addition to the NRC regulations, TR MRP-267, Revision 1, "Materials Reliability Program: Technical Basis for Primary Water Stress Corrosion Cracking Mitigation by Surface Stress Improvement," MRP, Palo Alto, CA, 2012. 1025839, provides the mockup testing to demonstrate the effectiveness of peening.

2.0 Scope of NRC Staff Review

The NRC staff limited its review of MRP-335R3 to determining whether the MRP proposed inspection intervals provide reasonable assurance of structural and leak tight integrity of the DMWs and RPVHPNs given the peening performance criteria (e.g., area of coverage, magnitude of residual stresses on the peened surfaces), stress/depth profile, and associated analyses.

In making the above determination, the NRC staff concentrated on three issues. First, whether the proposed post-peening operating stresses at the surface of the subject components are sufficient to prevent PWSCC initiation. Second, whether the proposed inspections requirements are sufficient to monitor the presence and growth of postulated PWSCC cracks which predate the peening process and were not discovered in the pre-peening inspection. Third, how the

peening process considers fabrication flaws or other defects that may penetrate past the peening layer and grow later.

Of equal importance to what is included in this safety evaluation (SE) is what is not included. Three concepts central to peening are not included. The first issue is the regulatory authority by which peening may be conducted. As will be discussed below, this issue has been resolved and requires no further consideration here. The second issue not addressed in the SE is the qualification of a specific peening process and whether the application of the peening process meets the requirements contained in MRP-335R3. Additional information concerning this issue is also provided below. The third issue not included in this SE is regulatory authority to take any action regarding peening application. As described below, this authority will lie in a plant-specific licensing action.

Relative to the first and third issues, the NRC staff has determined that the application of peening, as described in MRP-335R3, is not in conflict with any aspect of the ASME Code, Sections III and XI, or NRC regulations. The NRC staff notes that relief from the ASME Code and NRC regulations is not required to perform peening on DMWs or RPVHPNs. The NRC staff further notes that the peening application as described in MRP-335R3 is distinctly different than peening for the purpose of distortion control as described in the ASME Code, Section III.

Each nuclear power plant may apply peening to components and evaluate its acceptability in accordance with the requirements of 10 CFR 50.59, "Changes, Tests, and Experiments." However, the ability of a licensee to self-evaluate the acceptability of peening plant components does not extend to the modification (i.e., relaxation) of current inspection requirements of peened components. The current inspection requirements for DMWs and RPVHPNs are promulgated in 10 CFR 50.55a which incorporates by reference the inspection requirements of ASME Code, Section XI, and relevant ASME code cases. Should a licensee desire to modify inspections of peened components, a licensing action (i.e., a proposed alternative under 10 CFR 50.55a(z)) is required to be submitted for NRC review and authorization prior to implementing inspection relaxation.

Relative to the second issue, this SE does not address the qualification of a specific peening process or whether a specific peening application has achieved the required performance criteria such as, stresses on the peened surface of a component. Specifically, the SE does not address the uncertainty associated with the measurement of weld residual stresses on the surface and effective depth of peened components. The stress on the surface and effective depth is a significant parameter in crack growth calculations and affects the inspection frequency (intervals) after peening application. These issues should be addressed via demonstration testing, including the effects of measurement uncertainties, in a plant-specific relief request with respect to the inspection requirements of the ASME Code and NRC regulations under 10 CFR 50.55a(z).

Relative to the third issue, this SE, in and of itself, has no impact on any regulatory requirement. This SE may, however, be cited in a plant-specific relief request to document the NRC's evaluation of proposed inspection requirements based on successful application of peening. Additionally, the plant-specific relief request should describe the peening process used,

including issues associated with quality control, and demonstrate that the essential variables and performance criteria assessed in this SE are satisfied.

The NRC staff notes that the MRP made changes to Revisions 1 and 2 of MRP-335. This SE is applicable to MRP-335, Revision 3, only.

3.0 Summary of MRP-335, Revision 3

3.1 Affected Components of Peening Application

The MRP proposed to apply peening to the following components and locations:

- The inner diameter surfaces of DMWs in PWR reactor coolant system piping.
- The inside diameter and outside diameter surfaces of RPVHPNs in the area with high weld residual stresses caused by the presence of J-groove attachment welds.
- The surfaces of the J-groove attachment welds at RPVHPNs, including the surfaces of the Alloy 82/182 filler and butter metal that are normally wetted during operation.

3.2 Proposed Peening Processes

The MRP-335R3 discussed two major peening processes (methods): laser peening and water jet peening, also known as cavitation peening. The key aspects of peening processes are performance criteria (e.g., stress improvement depth, geometric limitations, surface conditions, and peening coverage), process variables, inspectability, and quality control and quality assurance.

The MRP stated that the effectiveness of peening in preventing crack initiation is independent of the peening process and is dependent only on the final compressive stresses and depth into the part that compressive stresses exist. As such, the MRP noted that the proposed inspection requirements are acceptable irrespective of the peening process used provided that the performance criteria as specified in MRP-335R3, such as depth of compression, magnitude of compression, and area peened, are satisfied.

The MRP further stated that each peening vendor is required to demonstrate that the essential variables and corresponding values of its peening process documented in the application-specific procedures will satisfy the requirements and applicable performance criteria in MRP-335R3 such as coverage and compressive stress magnitude and depth parameters. The MRP noted that the vendor will demonstrate satisfaction of these requirements through representative mockup testing. The MRP requires that this testing and the proof of peening effectiveness be documented in a plant-specific report.

3.3 Proposed Alternative

Table 1 at the end of this SE summarizes the MRP proposed performance criteria for peening parameters (e.g., the area of the component that will be peened, the effective depth of peening, and the stresses that will be achieved after peening).

Table 3 at the end of this SE summarizes the MRP proposed inspection requirements, which include a pre-peening examination, follow-up examinations, ISI examinations, and bare metal visual examinations. The following paragraphs describe significant aspects of proposed inspection requirements.

DMWs

Pre-Peening Examination

For DMWs, the MRP stated that prior to peening an ultrasonic examination and an eddy current examination of the DMW inner surface will be performed during the same refueling outage when peening is applied.

Follow-up Examination

For DMWs in hot leg piping, the MRP stated that a volumetric and surface examination will be performed within 5 years following the peening application. In addition, a second volumetric and surface examination will be performed within 10 years following the peening application.

For DMWs in cold leg piping, the MRP stated that a volumetric and surface examination will be performed once within 10 years, but no sooner than the third refueling outage following the peening application.

ISI Examination

The MRP stated that all peened DMWs will receive a surface and a volumetric examination once each inspection interval (nominally 10 years). The MRP specified that the surface examination shall be performed from the DMW inside surface and the volumetric examination shall be performed from either the inside or outside surface of the DMW.

RPVHPNs

Pre-Peening Examination

The MRP stated that before peening application but during the same refueling outage, a volumetric examination of each RPVHPN tube will be performed as the baseline inspection. As an alternative, a surface examination will be performed on the nozzle inner surface and the wetted surface of the nozzle outside diameter and J-groove weld. This examination will be considered as the baseline inspection. Additionally, a demonstrated volumetric or surface leak path assessment through all J-groove welds will be performed.

Follow-up Examination

The MRP stated that a volumetric examination of 100 percent of the required volume or equivalent surfaces of the RPVHPN tube and a leak path examination will be performed as part of the follow-up examination. The frequency of the follow-up inspections is as follows:

For plants whose RPVHPNs have experienced greater than or equal to 8 effective degradation years (EDY) at the time of peening, a follow-up inspection is performed in the first and second refueling outages after peening application. For plants with fewer than 8 EDY, a follow-up inspection is performed in the second refueling outage after peening application.

ISI Examination

The MRP stated that after peening, a bare metal visual examination (VE) will be performed for RPVHPNs each refueling outage. This interval may be extended in the following cases for RPVHPNs with less than 8 EDYs at the time of peening:

For RPVHPNs where the VE interval immediately before peening is permitted to be at least two refueling outages, the interval for performance of VE after peening is every second refueling outage. In this case, a VE must be performed either during the refueling outage of the peening or during the subsequent refueling outage.

If no unacceptable flaws are detected in the two refueling outages following peening, the interval for VE of RPVHPNs may be extended to every third refueling outage or 5 calendar years, whichever is less.

The MRP states that VT-2 visual examinations of peened RPVHPNs under the insulation through multiple access points are required to be performed during refueling outages in which the VE is not performed.

In addition to the VE and VT-2, the MRP stated that volumetric or surface examinations of peened RPVHPNs are performed once at an interval not to exceed one inspection interval (nominally 10 years). In addition, a demonstrated volumetric or surface leak path assessment through all J-groove welds is performed each time the periodic volumetric or surface examination is performed.

3.4 Basis for Use

The MRP performed deterministic and probabilistic flaw analyses with the intent of demonstrating that the safety of the plant is either maintained or improved when the peened DMWs and RPVHPNs in conjunction with the proposed inspection requirement is compared to the unmitigated condition with the current inspection requirements. The MRP's flaw analyses will demonstrate that the length of time for a postulated flaw to grow to the unacceptable size in the peened components will be longer than the proposed inspection intervals. Following the proposed inspection requirements, a licensee would detect the flaw early in the peened components and take corrective actions. Thereby, the structural integrity and leak-tightness of the peened components are adequately monitored and maintained.

3.4.1 Deterministic Analyses—General Information

The MRP's deterministic analyses investigate the impact of peening on PWSCC crack growth versus time at various assumed crack locations from various initial crack sizes. The MRP considered stress profiles which it proposed to be representative of those present in components before peening and after peening. The MRP stated that in areas where the superposition of peening residual stress and operating stress results in a layer of compressive stresses near the peened surface, shallow cracks located within this compressive layer do not grow through the layer because of the lack of tensile forces acting on the crack flanks and the lack of a positive stress intensity factor at the crack tip. However, the deterministic crack growth analyses demonstrate that flaws significantly deeper than the compressive layer tend to grow in depth at a rate similar to that for the unmitigated case. The MRP calculated crack growth based on stress profiles which it proposed to be representative of those present in components before and after peening.

The MRP characterized the post-peening stress profile by a thin compressive layer near the peened surface followed by a rapid transition to the pre-peening stresses. The key attributes of this stress profile are the compressive stress magnitude at the surface and the penetration depth—the depth to which peening imparts compressive stresses (i.e., depth of effect).

The MRP also performed sensitivity studies on crack growth based on combinations of key input variables to investigate the effect of input variability. The key variables considered were PWSCC crack growth rates, weld residual stresses, operating temperatures, initial crack aspect ratios, initial crack depths, and bending loads. The end result of the sensitivity studies is the time for the initial postulated crack to reach the detectable limit and the time for the crack to grow from the detectable limit to leakage. From the sensitivity studies, the MRP determined acceptability of the proposed inspection requirements in detecting potential flaw growth in the peened component before the flaw challenges the structural integrity and leak tightness of the peened components.

3.4.2 Probabilistic Analyses—General Information

The MRP's probabilistic analyses use the deterministic crack growth methodology to assess the effectiveness of follow-up and ISI examinations in addressing the effects of any pre-existing flaws not detected during the pre-peening examination. The MRP's probabilistic analyses predict the effect of peening on PWSCC, considering component loading, crack initiation, crack growth, and crack detection. The probabilistic model, which integrates the various models into a probabilistic simulation framework, allows the prediction of PWSCC throughout the operating lifetime of the plant. The end condition (component failure) of the probabilistic analysis for the DWM is leakage and for the RPVHPN is nozzle ejection.

The integrated probabilistic model includes a loading and stress model, a crack initiation model, a crack growth model, a nondestructive examinations model, and a leakage criterion. The MRP also performed sensitivity studies with respect to various probabilistic model parameters to characterize the impact of probabilistic modeling assumptions and input uncertainty on leakage and nozzle ejection predictions.

The probabilistic modeling framework for DMWs accepts both deterministic and distributed inputs. The values of the deterministic inputs are constant for every Monte Carlo realization. The values of the distributed inputs are determined by sampling probability distributions (e.g., normal distribution, log-normal distribution, triangular distribution, etc.) during each Monte Carlo realization. The probabilistic model accepts an array of inputs that is used to define the distribution of each distributed input. For example, for DMW, the inputs are component geometry, operating time, temperature, and component loading.

The MRP also performed sensitivity studies for the probabilistic models. The MRP investigated variations in modeling and inspection scheduling such as magnitude and depth of the peening stresses, and inspection frequencies.

3.4.3 Deterministic Analyses—DMW

Definition of Component Failure

The MRP predicted crack growth versus time, at various assumed crack locations, from various initial crack sizes to 100 percent through wall. The failure of a peened DMW in the deterministic analysis is defined as a leaking DMW.

DMW Configuration

The MRP postulated a circumferential flaw located at the point of maximum tensile bending and an axial crack (of arbitrary location) in the DMWs at the reactor vessel inlet (cold leg) and outlet (hot leg) nozzles. The MRP used a DMW with a wall thickness of 2.75 inches, an outside diameter of 35.5 inches, and a weld width of 1.752 inches based on a typical Westinghouse reactor design. The normal operating pressure used in the calculations is 2,250 psi. The MRP calculation assumes that the hot leg temperature is 625 degrees Fahrenheit (F) and the cold leg temperature is 563 degrees F.

Stress Profile

For the bounding case, the MRP modeled the post-peening residual stress profile in a DMW by a thin compressive region near the peened surface followed by a rapid transition to the pre-peening residual stresses. The key attributes of this stress profile are the compressive residual stress magnitude at the surface and the penetration depth – the depth to which peening imparts compressive residual stresses. The MRP assumed that for DMWs, the residual plus normal operating stress remains compressive for all wetted surfaces along the susceptible material. Thus, the bounding peening compressive stress at the peened surface is set to result in a total (operating plus residual) stress of 0 ksi (ksi = 1000 pound per square inch) at the circumferential location and for the principal stress direction with the maximum operating stress.

For the sensitivity study cases, the MRP assumed a compressive residual stress of 100 ksi at the peened inside surface of the DMW. The MRP stated that data and other information from peening vendors suggest that a compressive surface stress magnitude between 58 to 145 ksi can be achieved by peening. While thermal and load cycling may reduce the compressive

stress over the operating lifetime of the plant (with a large majority of relaxation occurring during the first operational cycle after peening), the stress for these cases is chosen to demonstrate the crack growth behavior in components where peening induces a highly compressive residual stress.

The MRP stated that the uncertainty in measurement of the surface residual stress shall be considered in the analysis to determine the surface stress including operating and residual stress. The MRP further stated that the basis for that consideration shall be documented in the relief request.

Depth of Peening Effect

The MRP assumed compressive residual stresses exist from the peened surface to a depth of 0.04 inches. The MRP stated that the nominal depth refers to the depth of the compressive residual stress that is reliably obtained in demonstration testing, i.e., for at least 90% of the locations measured.

The MRP clarified that some advanced peening processes result in a very thin surface layer (i.e., within 0.001 to 0.002 inch from the surface) where the residual stress is tensile. The tensile residual stresses in this very thin surface layer may be excluded in the flaw analysis when the above requirement (i.e., compressive stresses achieved at a depth of 0.04 inches) is met. The testing shall demonstrate that the nominal depth of the compressive surface residual stress field, excluding the very thin layer of tensile stress at the surface, is at least 0.04 inches. The depth measurement shall be from the surface to the point where the compressive residual stress becomes neutral.

Peening Coverage

The MRP stated that the required peening coverage (the area that will be peened) is the full area of the susceptible material along the entire wetted surface under steady-state operation. Susceptible material includes the weld, butter, and base material, as applicable. In addition, the peening coverage shall be extended at least 0.25 inches beyond the area of susceptible material.

Examination Coverage

The MRP stated that the required examination volume is defined by volume C-D-E-F of Figure 1 in ASME Code Case N-770-1. The required examination surface shall be surface E-F in the same figure. In accordance with 10 CFR 50.55a(g)(6)(ii)(F)(4), essentially 100% coverage is required for the examination for axial flaws instead of the requirements in -2500(c) of ASME Code Case N-770-1.

Crack Growth Calculation

The MRP used the following three crack growth models:

A model based on the classical weight function method to predict the stress intensity factors at the crack surface and deepest point locations.

- 1) A model that disregards the effect of peening on the growth of the crack surface point locations. This convention is used to approximate the realistic "balloon"-type growth of the crack front below the peening compressive layer. Numerical studies have demonstrated that the depth growth of a realistic crack is generally bounded by the classical weight function approach and balloon growth approximation.
- 2) A model that accounts for the effects of partial crack closure. When partial crack closure occurs, membrane stresses are produced over the area of closure and are assumed to act equal and opposite to the compressive stresses over the same area. This results in a balancing of some of the compressive load. So, if partial crack closure is not accounted for, a larger benefit to peening may be predicted.

The MRP used the crack growth rates based on the 75th percentile of material variability, consistent with MRP-115, "Materials Reliability Program Crack Growth Rates for Evaluating Primary Water Stress Corrosion Cracking (PWSCC) of Alloy 82, 182, and 132 Welds (MRP-115)," EPRI, Palo Alto, CA: 2004, 1006696.

Results of DMW Deterministic Analysis

The MRP reported that peening is most effective on the arrest of micro-crack growth in a peened DMW. For example, the growth of an axial flaw with an initial depth of 0.7 percent (0.02 inches) through wall will be arrested completely.

The MRP stated that peening will slow the growth of small cracks. For example, the MRP reported that for a 1.3-percent deep circumferential flaw (0.036 inches), it took approximately 4.3 effective full power years (EFPY) and 2.6 EFPY to grow 100-percent through wall for the peened and unpeened DMW, respectively. For a 1.3-percent deep axial flaw, it took approximately 3.6 EFPY and 1.8 EFPY to grow 100-percent through wall for the peened and unpeened DMW, respectively.

The MRP noted that peening has a limited effect on the growth of a relatively large flaw size such as an initial through-wall of 10 percent depth (0.3 inches) or more. The 10-percent deep circumferential flaw in the peened DMW would reach 100-percent through-wall in 2.4 EFPY whereas as the same flaw in an unpeened DMW would reach 100-percent through-wall in 1.85 EFPY, delaying crack growth by approximately 7 months. For a 10-percent depth axial flaw, the crack growth to leakage is delayed by less than 1 month between the peened and unpeened DMW.

The MRP noted that a longer crack in length, with the same initial depth, is predicted to grow through 0 to 40 percent of wall thickness faster than the shorter crack. The lower operating temperature of a reactor vessel inlet nozzle (cold leg) results in a much greater period of growth before a crack penetrates through wall (i.e., the lower the operating temperature the slower the crack growth).

The MRP's sensitivity study shows that only three of 72 cases for peened DMWs result in leakage after the extension of the inspection interval whereas 24 of 72 cases for unpeened DMWs result in leakage per the current inspection requirements. The MRP noted that the leakage cases in the peened DMWs resulted from using conservative inputs which may not occur in the field (high tensile weld residual stresses, high operating temperature and 95th percentile crack growth rate). The MRP stated that the sensitivity study demonstrates that peened DMWs with proposed inspection relaxation will result in less leakage than unpeened DMW with the current inspection requirements.

3.4.4 Probabilistic Analyses—DMW

Definition of Component Failure

The failure of a DMW in the probabilistic analyses is defined as when the initial crack becomes 100 percent through wall (i.e., leakage) at which point Monte Carlo simulation ends and summary statistics are compiled.

Crack Initiation Model

The MRP used a statistical Weibull approach to predict crack initiation. It allows for adjustments for operating temperature and surface stress which are significant parameters for crack initiation prediction. The model allows for independent initiation of multiple flaws with axial or circumferential orientations. The crack size, location, capacity for growth, material properties, and environmental conditions were also considered.

Load and Stress Model

Load models are used to calculate the stress in the DMW component during each Monte Carlo realization. Separate load models are used for hoop stresses (propagating axial cracks) and axial stresses (propagating circumferential cracks). The load models account for pre-peening and post-peening welding residual stresses, internal pressure, and piping loads (dead weight, thermal expansion, and thermal stratification, if applicable). In addition, a peening residual stress model is introduced for modeling crack growth during cycles after a peening application. The load models differentiate between residual stress and operational stress (which can all be combined to obtain total stress) as well as membrane stress and bending stress.

The MRP assumed that after the peening application, no new cracks will initiate. As with weld residual stress, the peening stress profile is assumed to be axisymmetric and varying through wall. The through-wall post-peening residual stress, in both the hoop and axial directions, is modeled using a piecewise stress equation that captures the minimum depth of the compressive residual stress layer and the limiting magnitude of the residual plus normal operating stress. The MRP modeled the post-peening stress profile into the following four general regions:

- the compressive region (nearest to the peened surface)
- the first transition region

- the second transition region
- the "minimally affected" region (farthest from the peened surface)

Crack Growth Model

The MRP used a model to allow the prediction of PWSCC growth rate as a function of crack geometry, component loading, and other conditions. Assuming that cracks maintain a semi-elliptical shape as they grow through wall, the model predicts growth rates of the surface tips (in the length direction) and the deepest point (in the depth direction) of the crack. The model incorporates the major factors affecting flaw growth rate: temperature and stress intensity factor.

The MRP also performed a sensitivity study to show the effect of the balloon crack growth phenomenon by allowing crack length growth independent of peening (i.e., using the pre-peening stresses).

Examination Model

The probabilistic analyses include examination models to simulate ultrasonic examinations of DMWs. The MRP used probability of detection curves to estimate the likelihood of a crack being detected, given its size. The examination models are used to predict leakage probabilities because cracks that lead to leaks are often those that are undetected during one or more scheduled examinations. The models include methods of examination schedules before and after peening, the probability of detection, the crack geometry, and detection and repair modeling.

Uncertainty

The probabilistic modeling framework for DMWs accepts both deterministic and distributed inputs. The values of the deterministic inputs are constant for every Monte Carlo realization. The values of the distributed inputs (i.e., probabilistic modeling) are determined by sampling probability distributions (e.g., normal distribution, log-normal distribution, triangular distribution, etc.) during each Monte Carlo realization. The probabilistic model accepts an array of inputs that is used to define the distribution of each distributed input.

The MRP managed uncertainty propagation by sampling input and parameter values from selected probability distributions (with appropriately selected bounds). The MRP stated that, for simplicity, the model does not treat epistemic (i.e., caused by incomplete knowledge) and aleatory (i.e., caused by random variation) uncertainties differently. The parameters that the MRP sampled were the component temperature, weld residual stress profiles, and model parameters for the crack initiation model, crack growth model, flaw inspection and detection model, and effect of peening on residual stresses.

Results of Probabilistic Analysis of DMW

The MRP predicted that for the reactor vessel outlet nozzle (hot leg), the cumulative probability of leakage after peening (1.0×10^{-3} to 2.5×10^{-3}) would be reduced by a factor of between

60 and 150, as compared to cumulative leakage probabilities on the same span of time for an unmitigated reactor vessel outlet nozzle (1.5×10^{-1}), depending on the post-peening follow-up examination and ISI scheduling. The MRP noted that, in general, the degree of improvement is not significantly influenced by the follow-up inspection time or the ISI frequency. The MRP explained that the reason for the former is that most of the cracks that were undetected at the pre-peening inspection are small and, accordingly, grow slowly after peening. The reason for the latter is because nearly all cracks are detected during the pre-peening or follow-up inspection and no new cracks are expected to initiate after peening.

For the reactor vessel inlet nozzle (cold leg), the MRP predicted that the cumulative probability of leakage after peening (8.8×10^{-5} to 2.3×10^{-4}) is reduced by a factor of between 8 and 24, as compared to cumulative leakage probabilities on the same span of time for an unmitigated reactor vessel inlet nozzle (2.1×10^{-3}) depending on the post-peening follow-up examination and ISI scheduling. This degree of improvement is smaller than that predicted for the reactor vessel outlet nozzle because the inspection schedule for an unmitigated inlet nozzle conservatively takes little credit for its reduced temperature in comparison to that for hot-leg locations. The MRP stated that for both the reactor vessel outlet nozzle and inlet nozzle peening base cases, the probability of leaking after the follow-up inspection is very low.

The MRP stated that the results of the probabilistic analysis of PWSCC on a peened reactor vessel outlet nozzle support the relaxed ultrasonic test (UT) inspection schedules. Specifically, the cumulative leakage probability after peening is predicted to be reduced by a factor of 97 and 142, depending on when the follow-up inspection is performed.

The MRP stated that the results of the probabilistic analysis of PWSCC on a peened reactor vessel inlet nozzle support the relaxed UT inspection schedules. Specifically, the cumulative leakage probability after peening is predicted to be reduced by a factor of 9 to 12, depending on when the follow-up inspection is performed.

The MRP concluded that the large reduction in leakage probability with peening (approximately between a factor of 10 and 100) supports the conclusion that rupture frequency (and boric acid wastage potential) is also reduced through peening application with inspection relaxation.

The MRP stated that the sensitivity cases show that conclusions drawn from the base peening case results are not highly sensitive to the precise input values used. Specifically, sensitivity cases showed that only minimal risk benefit for peened DMVs with increased depth of the peening stress effect or with more compressive stresses at the peened surface. The MRP stated that no case negates the prediction that a peened reactor vessel outlet nozzle or inlet nozzle can maintain a lower probability of leakage with a relaxed inspection schedule (as compared to the unmitigated component). This is because the large margin of improvement predicted for the base peening cases. The sensitivity studies also showed the importance of a pre-peening UT inspection.

3.4.5 Deterministic Analyses—RPVHPN

Definition of Component Failure

The MRP stated that for the RPVHPN, the failure mode is nozzle ejection. The MRP assumed that when leakage occurs because of a flaw at any location, this flaw immediately transitions to a through-wall circumferential crack that grows along the top of the J-groove weld contour until it is repaired or it becomes large enough to fulfill the ejection criterion.

Flaw Configuration

For its calculations, the MRP used a wall thickness of 0.622 inches for the RPVHPN, nozzle outer diameter of 4 inches, a reactor vessel head thickness of 5.984 inches, a hot head temperature of 605 degrees F, and cold head temperature of 561 degrees F. The normal operating pressure used is 2,250 psi.

MRP-335R3 postulated the following four types of crack on the RPVHPN: (1) an axial crack on the nozzle inside diameter initiating above the J-groove weld, (2) an axial crack on the nozzle outside diameter initiating below the J-groove weld, (3) a crack initiating on the J-groove weld, and (4) a circumferential through-wall crack growing along the J-groove weld contour.

Stress Profile

Section 4.3.1 of MRP-335R3 requires that for the performance criteria of the RPVHPN, the residual stress in combination with the operating stress on the peened surface does not exceed +10 ksi tensile stress.

The MRP stated that peening will prevent PWSCC initiation because the stresses imparted on the peened surface are below the threshold stress necessary for PWSCC initiation over plant life. The MRP stated that while it is considered that there is no firm "threshold" below which PWSCC will never occur, a tensile stress of +20 ksi is a conservative lower bound of the stress level below which PWSCC initiation will not occur during plant life. The MRP stated that the 20 ksi threshold stress corresponds to about 80 percent of the lower bound yield strength for Alloy 600 materials at operating temperatures. The MRP noted that this limit applies to steady-state stresses during normal operation as stress corrosion cracking initiation is a long-term process, and does not apply to transient stresses that occur only for short periods of time.

The MRP noted that consistent with the yield strength range known to be applicable to RPVHPNs fabricated from Alloy 600 wrought material, laboratory testing for Alloy 600 materials with yield strengths could be up to 65 ksi. The MRP concluded from its literature review that the room-temperature yield stresses for PWR plant Alloy 600 materials are in the range 35-60 ksi. Applying a factor of 0.8 to obtain the at-temperature (at operating condition) yield stress and an 80 percent conservative margin factor, the stresses required for PWSCC initiation are 22-38 ksi. The MRP explained that +20 ksi is a conservatively low limit for the stress level required for PWSCC initiation over plant service periods. The MRP stated that its proposed limit of +10 ksi provides substantial additional margin for post-peening stresses to prevent PWSCC initiation.

Depth of Peening Effect

The MRP assumed a 0.01 inches deep layer of compressive residual stress exists on the inside diameter of a RPVHPN. For the outside diameter and J-groove weld wetted surfaces of a RPVHPN, the MRP assumed the compressive residual stress exists on the surface to a depth of 0.04 inches of the peened RPVHPN.

For the sensitivity study case, the MRP assumed a 0.02 inches deep layer of compressive residual stress on the inside diameter of a RPVHPN. For the outside diameter and J-groove weld wetted surfaces of a RPVHPN, the MRP assumed a 0.12 inches deep layer of compressive residual stress.

Peening Coverage

The MRP stated that the required peening coverage is the full wetted surfaces of the attachment weld, butter, and nozzle base material in the region defined in Figure 4-1 through Figure 4-4 of MRP-335R3. The MRP specified the peening coverage to ensure that areas susceptible to PWSCC initiation are mitigated. Section 4.3.8.1 of MRP-335R3 requires that the boundaries of the area required to be effectively peened in Figure 4-1 through Figure 4-4 be extended a suitable distance for the specific peening method to provide high assurance that the areas susceptible to PWSCC receive the required peening effect.

Due to geometry, some peening techniques of interest cannot be used to peen the threaded areas that are present in some cases near the bottom of the nozzle tube. MRP-335R3 stated that because any such threaded areas are located below the weld toward the end of the nozzle and are not part of the pressure boundary, it is not necessary that peening be performed of the threaded regions when present.

Examination Coverage

The MRP stated that the required examination volume and surface are defined in Figure 2 of ASME Code Case N-729-1. Note (5) of Table 4-3 of MRP-335R3 states that if the examination area or volume requirements of Figure 2 of Code Case N-729-1 cannot be met, the alternative requirements of Appendix I of Code Case N-729-1 shall be used and the evaluation shall be submitted to the regulatory authority having jurisdiction at the plant site. The MRP stated that in accordance with 10 CFR 50.55a(g)(6)(ii)(D)(6), implementation of Note (5) of Table 4-3 requires prior NRC approval.

Crack Growth Calculation

Growth predictions for each crack type can be made for the uphill and downhill locations on the penetration by using stress profiles that are representative of each location. Consistent with the DMW calculations, the MRP used the 75th percentile value of crack growth rates in topical reports, MRP-55, "Materials Reliability Program (MRP) Crack Growth Rates for Evaluating Primary Water Stress Corrosion Cracking (PWSCC) of Thick-Wall Alloy 600 Materials (MRP-55), Revision 1," EPRI, Palo Alto, CA: 2002, 1006695, and MRP-115 to calculate crack growth in RPVHPNs.

For the first three crack types, the MRP predicted growth from a part-depth flaw until the time of leakage. For the fourth crack type, growth is predicted from an initially through-wall flaw until the time of ejection. For the nozzle ejection calculation (i.e., the fourth crack type), the MRP assumed an initial circumferential flaw that is 100 percent through wall and a length of 30 degrees in circumferential extent of the RPVHPN. When the initial circumferential flaw grows to the 300 degree circumferential extent, the nozzle is assumed to eject.

The critical crack length for ejection, or net section collapse, is based on calculations presented in MRP-110, "Materials Reliability Program: Reactor Vessel Closure Head Penetration Safety Assessment for U.S. PWR Plants (MRP-110 NP): Evaluations Supporting the MRP Inspection Plant," EPRI, Palo Alto, CA: 2004, 1009807(ADAMS Accession No. ML041680506).

Results of Deterministic Analysis of RPVHPN

The MRP stated that for an axial crack on the inside diameter of a RPVHPN with an initial through-wall flaw depth of 1 percent (0.006 inches), the effect of peening is predicted to delay 100 percent through-wall growth by approximately 5 EFPY.

The MRP stated that growth of axial cracks on the RPVHPN outside diameter through the wall does not cause leakage. Instead, leakage occurs once an outside diameter axial crack grows in length to reach the outside diameter nozzle annulus beyond the J-groove weld. The MRP reported that the effect of peening on growth of axial outside diameter shallow flaws is large, delaying leakage by 1- 4 EFPY for flaws up to about 30 percent (0.20 inches) through-wall at the time of peening.

The MRP reported that peening is predicted to arrest growth for cracks less than 80 percent of the compressive layer depth. Peening is predicted to be beneficial for slowing the growth of cracks significantly deeper than the compressive residual stress layer depth. The MRP explained that the potency of this effect depends on the nature of the operating stresses and residual stresses beyond the peening compressive layer (i.e. the pre-peening stresses). The MRP further explained that the effect of peening on the crack growth time rapidly fades for weld cracks deeper than the compressive layer depth.

At the RPVHPN outside diameter and J-groove weld locations, where the peening penetration depth is assumed to be 0.118 inches, cracks less than approximately 15 percent - 35 percent through-wall may be arrested upon the application of peening. For the first three crack configurations, the downhill locations tend to grow to leak faster because of characteristically more tensile weld residual stresses.

The MRP noted that for some initial crack depths, leakage occurs in the peened RPVHPN slightly faster than in the unmitigated RPVHPN. The MRP stated that this occurs for relatively deep cracks and is because of the modeling assumption that the effective forces on the cross-section of the peened component balance (i.e., tensile stresses) are displaced from the peened surface and are redistributed to deeper locations.

The MRP showed that if the RPVHPN is operated near the cold leg temperature, as opposed to the hot leg temperature, it would result in a longer period of growth before a crack grows through wall.

The MRP noted that the effect of peening on the growth of cracks that are deeper than the compressive residual stress layer depth is predicted to be small when balloon crack growth is approximated. The effect of the balloon growth approximation is not observed at J-groove weld locations, where crack surface length growth is constrained by the width of the J-groove weld.

The MRP stated that downhill circumferential cracks in RPVHPN are predicted to cause ejection approximately 18 EFPY after crack initiation, and uphill circumferential cracks are predicted to cause ejection approximately 23 EFPY after crack initiation. In the rare case in which two circumferential through-wall cracks initiate—one from the uphill location and one from the downhill location—RPVHPN ejection is predicted approximately 9.5 EFPY after crack initiation.

3.4.6 Probabilistic Analyses—RPVHPN

Crack Initiation Model

Each RPVHPN is divided into an uphill and downhill side. Each cracking mode may initiate on either the uphill or downhill sides, both of which have their own unique loading conditions.

Inside diameter axial cracks (Mode 1)—partial through-wall cracks located on the RPVHPN inside diameter surface. These cracks are assumed to initiate in the region above the J-groove weld such that they immediately result in leakage if they penetrate through wall into the outside diameter nozzle annulus. These cracks are opened by hoop stresses in the RPVHPN.

Outside diameter axial cracks (Mode 2)—partial through-wall cracks located on the RPVHPN outside diameter surface below the J-groove weld. These cracks cause leakage if they grow in length to reach the nozzle outside diameter annulus. They may transition to through-wall axial cracks if they grow through wall before reaching the annulus. These cracks are opened by hoop stresses in the RPVHPN.

Radially oriented weld cracks (Mode 3)—cracks located on the J-groove weld that grow toward the weld toe. These cracks are opened by hoop stresses in the J-groove weld.

Through-wall axial cracks (Mode 4)—through-wall cracks located below the J-groove weld. These cracks may only form if an outside diameter axial crack reaches through-wall before reaching the nozzle outside diameter annulus. These cracks cause leakage if they grow long enough to reach the nozzle outside diameter annulus. These cracks are opened by hoop stresses in the RPVHPN.

Circumferential through-wall cracks (Mode 5)—through-wall cracks located on the weld contour above the J-groove weld. These cracks are assumed to occur immediately following leakage caused by any of the preceding crack modes, either by branching of the flaw causing the leakage or by initiation of a new flaw on the outside diameter surface of the nozzle. These cracks are opened by a complex stress field acting orthogonally to the weld contour.

The MRP used a statistical Weibull approach for predicting crack initiation that is similar to the approach used in the DMW probabilistic analyses. The key difference in the initiation models is that the RPVHPN initiation model does not include a surface stress adjustment.

Load and Stress Model

The MRP stated that total stresses and operational stresses (i.e., those stresses caused by loads present during operation) are derived from finite element analysis results, and welding residual stresses are attained from the difference between the total and operational stresses. After peening is applied, the post-peening residual stress profile is superimposed with the operational stresses to attain the total stress profiles used to predict crack growth.

The MRP further stated that for RPVHPNs, the compressive residual stress depths are sampled from separate distributions for the inside diameter locations, as compared to the outside diameter and J-groove weld locations.

For J-groove weld locations, the through-element dimension is the weld path length instead of the RPVHPN thickness. Inside diameter peening stresses above the weld are assumed to have no effect on the growth of circumferential through-wall cracks. The growth of circumferential through-wall cracks is based on stress intensity factors that were calculated with finite element software.

The MRP assumed that outside diameter peening stresses below the J-groove weld have no effect on the growth of partial through-wall axial outside diameter cracks that have grown under the weld far enough that the upper crack surface tip is outside of the peening compressive layer.

Inside diameter peening stresses do not affect nearly through-wall axial outside diameter cracks (i.e., the thin compressive region near the inside diameter is not given credit for abating the growth of most (90 to 100 percent) through-wall cracks).

Crack Growth Model

The crack growth model used for RPVHPN is similar to the crack growth model in the probabilistic analyses of DMW.

Examination Model

The examination model includes simulation of ultrasonic and visual examinations of RPVHPNs. The model includes the examination schedules before and after peening, probability of detection, and detection and repair modeling rules.

Uncertainty

The uncertainty treatment in the probability analysis of RPVHPN is similar to that of DMW probabilistic analysis. Uncertainty propagation is handled by sampling input and parameter values from selected probability distributions (with selected bounds), including correlations during each Monte Carlo realization. The sampled inputs include component geometry,

RPVHPN operating temperature, and welding residual stresses, as well as model parameters for the crack initiation model, crack growth model, flaw inspection and detection model, effect of peening on residual stresses, and flaw stability model.

Sensitivity Study

The MRP conducted sensitivity studies with the RPVHPN probabilistic model in order to demonstrate the relative change in the predicted results given one or more changes to modeling or input assumptions. The MRP classified each sensitivity case as either a Model Sensitivity Case (in which an approximated input or model characteristic is varied) or an Inspection Scheduling Sensitivity Case (in which a controllable inspection option is varied).

Results of Probabilistic Analysis for RPVHPN

The results of the probabilistic analysis of PWSCC on a peened hot head: (a) the MRP predicted that the cumulative leakage probability after peening will be reduced by a factor of approximately 5.5 relative to the unmitigated case and (b) the MRP predicted that the average RPVHPN ejection frequency after peening will be reduced to 81 percent of the average ejection frequency of the unmitigated case.

The results of the probabilistic analysis of PWSCC on a peened cold head: (a) the MRP predicted that the cumulative leakage probability after peening will be reduced by a factor of approximately 4.6 relative to the unmitigated case and (b) the MRP predicted that the average RPVHPN ejection frequency after peening will be reduced to 64 percent of the average ejection frequency of the unmitigated case.

The MRP showed that peening mitigation with proposed inspections results in an average nozzle ejection frequency of approximately 1.7×10^{-5} per reactor year or less. The MRP stated that an ejection frequency of 1.7×10^{-5} will result in a core damage frequency that does not exceed the acceptance criterion contained in NRC Regulatory Guide (RG) 1.174, "An Approach for Using Probabilistic Risk Assessment in Risk-Informed Decisions on Plant-Specific Changes to the Licensing Basis," for permanent changes in plant equipment (i.e., 1×10^{-6} events per reactor year).

In addition, the ratio of the maximum incremental RPVHPN ejection frequency to the time average nozzle ejection frequency is of an acceptable magnitude (only a factor of 3 - 4). Thus, the MRP contended that the peening mitigation in combination with the proposed inspection requirements will result in an acceptably small effect of PWSCC. Furthermore, the probabilistic results show a reduced average nozzle ejection frequency with peening and the proposed inspection requirements compared to the case of no mitigation with current inspection regiment.

Lastly, cumulative probability of nozzle leakage after peening is reduced by about a factor of 5 to 8 for the case of peening mitigation compared to the no mitigation case. This demonstrates that the concern for boric acid corrosion of the RPVHPN is addressed by, and defense-in-depth is supported by, the peening and proposed inspections, which maintains the same basic intervals for periodic direct visual examinations for evidence of leakage as prior to peening.

The MRP stated that its sensitivity cases show that conclusions drawn from the base case results are not highly sensitive to the precise input values used. Specifically, sensitivity cases showed minimal risk benefit for peened RPVHPNs with increased depth of the peening stress effect or with more compressive stresses at the peened surface. Sensitivity cases that model a range of bare metal visual (VE) examination frequencies indicate that performing VE examinations at an interval nominally equivalent to the examination frequency for unmitigated heads is effective in reducing the risk of nozzle ejection. The MRP stated that performing VE more frequently for peened RPVHPN than for unpeened RPVHPN only provide a limited additional risk benefit for nozzle ejection. According to the MRP, its sensitivity results show that there would be minimal benefit to requiring a more compressive stress effect than that specified by the performance criteria. All sensitivity cases for peened components result in a cumulative probability of leakage substantially below that of the equivalent sensitivity case for an unmitigated component. The MRP noted that the probabilistic analyses presented in MRP-335R3 include the license renewal period (60 years) and subsequent license renewal period (80 years).

4.0 NRC STAFF EVALUATION

4.1 General Considerations

Based on independent research conducted by the NRC staff, which is not limited to the information contained in MRP-335R3, the NRC staff has determined the following:

1. Peening methods are currently available which, when executed in accordance with controlled procedures, are capable of imparting compressive stresses into the surface of a part without damaging the part through such mechanisms as cracking or spalling.
2. The NRC staff views the ability of the peened surface of a component to resist cracking to be a function of the compressive stresses achieved rather than the peening process employed. As a result, the NRC considered only the proposed set of input parameters in determining whether the analyses in MRP-335R3 supports the proposed inspection relaxation. The manner in which those stresses are achieved, e.g., the peening process, was not considered in this SE.
3. The NRC staff notes that the process of measuring residual stresses on the near surface of a peened component, particularly in welds, is not precise. At present there are significant differences in stress values obtained by various measurement methods and uncertainties in stress values obtained by a single method. The measurement uncertainty issue is not considered in this SE. Measurement uncertainties will need to be addressed by licensees in plant-specific relief requests for alternatives to the ASME Code inspection requirements.
4. Peening has been used on new parts in industries other than nuclear power plants as a way to reduce fatigue cracking.
5. The use of peening in the U.S. nuclear industry on safety-related components, to date, has been applied to steam generator tubes, repaired reactor vessel closure head

penetration nozzles (e.g., abrasive water jet peening), and pressurizer heater sheaths. The NRC has not approved any inspection relaxation as a result of peening on these components.

6. Peening of nuclear reactor vessel internals and piping has been conducted outside the United States. However, the NRC staff is not aware of any relaxation in inspection requirements that has been authorized by international regulators in response to peening of DMWs and RPVHPNs.
7. The NRC staff finds probabilistic analyses to be useful tools in assessing changes in procedures or configurations of nuclear power plants. The NRC routinely uses probabilistic fracture mechanics analyses in assessing structural integrity of reactor vessels and environmental fatigue degradation of piping. In each of these cases, the approach used in the probabilistic evaluation of these issues has been fully evaluated by the NRC staff and is the subject of an NRC SE or NUREG reports. Probabilistic fracture mechanics analyses are very complex processes that require thorough verification, validation, and assessment of data input quality through sensitivity studies. The NRC staff did not evaluate the probabilistic model used in MRP-335R3 accordingly, did not base its regulatory decisions on the probabilistic analyses in MRP-335R3.
8. The NRC considered the MRP evaluation of a threshold stress for PWSCC initiation. The rationale for this threshold is described in section 2.3.4 of MRP-335R3. The MRP document states: "While it is considered that there is no firm "threshold" below which PWSCC will never occur, from a practical experience perspective a tensile stress of +20 ksi (+140 MPa) is a conservative lower bound of the stress level below which PWSCC initiation will not occur during plant lifetimes...." The NRC notes that initiation of PWSCC is a function of time, temperature, applied stress, material properties and environmental factors. While extensive testing and evaluation of service experience supports a conclusion that PWSCC initiation is unlikely when applied stresses are less than 80 percent of material yield strength, this conclusion is based on practical considerations rather than theoretical derivations. There may be combinations of materials, stress, temperature, time and environment variables, particularly at long test or operational durations, where PWSCC initiation may occur even though it is not expected. The NRC staff use of the term "threshold" in this SE is consistent with the discussion in MRP-335R3. The "threshold" stress for PWSCC initiation is an applied surface stress below which initiation of PWSCC is unlikely for exposure durations that exceed plant operational periods.
9. Although beyond the scope of this SE, the NRC staff finds that the adequacy of the process should be demonstrated by peening mockups and by measuring residual stresses. Licensees should confirm that its peening process is performed with an acceptable set of essential variables and corresponding values to ensure that the required stress and coverage parameters are met or exceeded in accordance with MRP-335R3 to demonstrate that the peening mitigation is effective. This information should be reported in plant-specific relief requests.

4.2 NRC Staff Evaluation Approach

The objective of this SE is to determine, given the peening input variables and performance criteria (e.g., area peened, effective peening depth, and compressive stresses on the peened surface), whether the analyses presented in MRP-335R3 support the requested inspection requirements. In performing this evaluation the NRC staff separately considered two questions: first, given the proposed peening parameters, will the initiation of new flaws be prevented; and second, with respect to cracks which predate peening, are the inspection intervals proposed in MRP-335R3 sufficient to maintain the level of plant safety currently achieved for non-peened components which are inspected in accordance with current regulations. In addressing both questions, the NRC staff adhered to the concepts that the peening process was done correctly, that full coverage was achieved, and that residual stresses and distributions proposed in MRP-335R3 are achieved (uncertainty in measurements is not considered). These issues, while important, are subject to future plant-specific review. The NRC staff ensures that the acceptance criteria applied to assessing the peened DMWs and RPVHPNs with proposed inspection relaxation were reasonable, not absolute, assurance of the adequate protection of public health and safety.

Safety Implications

As a background information, PWSCC in reactor coolant system pressure boundary components can lead to the following safety issues:

1. Axial cracks in DMWs are stable even if they crack completely through wall because the maximum length of the crack is constrained to the susceptible material and the axial length of susceptible material in a DMW is much less than the length at which an axial crack could exhibit unstable crack growth. However, leakage from an axial crack can lead to boric acid corrosion of carbon and alloy steel surfaces of piping. Corrosion of low alloy steel piping surfaces adjacent to a leaking DMW can lead to a loss-of-coolant accident (LOCA).
2. Circumferential cracks in DMWs can grow to a size where unstable crack growth occurs, (e.g., 360 degrees in circumferential extent and 100% through wall) which would cause a LOCA.
3. Leaks from circumferential cracks in DMWs can lead to boric acid corrosion of adjacent steel surfaces of piping, which can lead to a LOCA.
4. Cracks anywhere on RPVHPNs can lead to leakage. Leakage can lead to initiation of circumferential cracks on the outside diameter surface, which can eventually lead to nozzle ejection, which would cause a LOCA.
5. Cracks anywhere on RPVHPNs can lead to leakage. Leakage can cause boric acid corrosion of nearby steel surfaces, such as the RPV head, which could cause a LOCA.

Of these five potentially safety significant effects of PWSCC, four of them, boric acid corrosion from leaking axial cracks in DMWs, boric acid corrosion from circumferential cracks in DMWs, boric acid corrosion from cracks in RPVHPNs, and outside diameter initiated circumferential cracking of RPVHPNs, involve a period of leakage during which it is possible to observe the boric acid and repair the leak prior to occurrence of boric acid corrosion severe enough to compromise the structural integrity of the reactor coolant pressure boundary. Periodic bare metal visual examinations are a means to detect leaks before the safety significant effects of severe boric acid corrosion occur. Ultrasonic examination is used to detect cracks. Cracks

could grow to leaks or to unstable dimensions without exhibiting prior leakage. The combination of periodic bare metal visual examination and ultrasonic examination is used to minimize the potential for through wall leakage and rupture.

Current regulations require a combination of bare metal visual examinations and ultrasonic examinations be performed on susceptible materials to ensure PWSCC is detected and repaired or mitigated before plant safety is challenged.

Crack Initiation

The fundamental technical basis of peening is to prevent crack initiation in DMWs and RPVHPNs. As such the NRC staff has considered the following assessment.

DMWs

The MRP proposes that, once peened, DMWs will not develop new cracks because:

1. All susceptible surfaces plus a margin on each side of the DMW will be peened.
2. At room temperature without operational loading, the peening will result in compressive stresses from the DMW wetted surface to a depth of 0.04 inches.
3. Under operating conditions, the stress at the wetted surface of the DMW will not be in tension (not more tensile than 0 ksi).

The NRC staff evaluated the basis for why crack initiation is not expected in DMWs following peening as proposed in MRP-335R3. As part of the review, the NRC staff notes the following design parameters:

1. The entire wetted surface of susceptible material plus a margin will be peened,
2. Crack initiation is a surface phenomenon,
3. The wetted surface of the DMW will be inspected to identify any surface breaking flaws or significant fabrication defects in the DMW, and
4. At operating pressure, the surface stress will be more compressive (0 ksi) than MRP-335R3 proposed lower bound stress for PWSCC initiation (20 ksi in tension).

The NRC staff notes that the peening surface condition under operating conditions of 0 ksi is consistent with the NRC previously approved surface stress condition of Paragraph I-1 of Appendix I to ASME Code Case N-770-1, which is mandated by 10 CFR 50.55a(g)(6)(ii)(F) for the surface stress condition required for the Mechanical Stress Improvement Process (MSIP)TM. The NRC staff notes that the MSIPTM process typically maintains a compressive stress field under operating conditions for approximately 50 percent of the weld depth.

The NRC also reviewed the MRP's deterministic analysis and performed independent calculations to determine if any missed PWSCC or fabrication flaws in the DMW from which PWSCC cracks could initiate, could threaten the structural integrity or leak tightness of the DMW. In considering such situations the NRC staff determined that the use of eddy current examinations in combination with volumetric examinations at the time of peening and in subsequent inspections provide reasonable assurance that a flaw would be detected at the time

of peening or, if not, it would be detected prior to affecting plant safety, i.e., the loss of structural integrity. Therefore, given the design parameters above, the NRC staff finds that once a DMW is peened, there is reasonable assurance that cracking should not initiate. However, if initiation does occur, the inspections, identified in this SE, will provide reasonable assurance of structural integrity and leak tightness for peened DMW.

RPVHPNs

The MRP proposes that, once peened, RPVHPN components will not develop new PWSCC cracks because:

1. All susceptible surfaces of the RPVHPN and J-groove weld will be peened.
2. At room temperature, the peening will result in compressive stresses from the outside diameter surface to a depth of 0.04 inches of the RPVHPN and J-groove weld, and from the inside diameter surface to a depth of 0.01 inch of the RPVHPN.
3. Under operating conditions the stress at the wetted surface of the RPVHPN will not exceed 10 ksi (tension) which is less than the MRP-335R3 proposed limit for PWSCC crack initiation of 20 ksi. Section 5.2.1 of MRP-335R3 states that "the peening compressive stress at the surface is set to result in a net tensile stress of +70 MPa (10 ksi) in the direction of maximum operating stress for flaws on the nozzle ID surface, and a residual stress value that results in a net stress of 0 MPa (0 ksi) is assumed for the peened surface of the nozzle OD and weld since the operating stress in those regions is small."

The NRC staff evaluated the basis for why crack initiation is not expected in RPVHPNs following peening. As part of the review, the NRC staff notes the following design parameters:

1. The inside and outside diameter surfaces of RPVHPN and J-groove weld that are susceptible to PWSCC will be peened,
2. Crack initiation is a surface phenomenon and,
3. At steady state operating conditions, the surface stress will be more compressive (10 ksi tension) than the MRP-335R3 proposed threshold for PWSCC crack initiation, 20 ksi tension. As stated previously, the threshold is the level of applied surface stress below which initiation of PWSCC is unlikely during RPVHPN lifetime.

The NRC notes three significant differences between the peening parameters for the DMW versus RPVHPN. First, a surface examination is not required on the RPVHPN and J-groove weld while a surface examination is required on the DMW. Second, a 10 ksi tensile steady state operating stress condition is permitted on the RPVHPN while 0 ksi is the maximum stress permitted on the DMW. Finally, for the RPVHPN, peening is to be performed on highly stressed alloy 600, 82 and 182 surfaces, with lower stressed surfaces remaining unpeened, while the entire surface of the DMW plus 0.25 inches on either side of the DMW will be peened.

As the peening coverage does not cover the entire RPVHPN inside diameter and outside diameter region associated with PWSCC and as there are no surface examinations of the surfaces prior to peening, it is not possible to obtain absolute assurance that new cracks will not initiate. The only new initiations that are postulated to occur would be located at areas where

subsurface original fabrication features such as hot tears and lack of fusion are located near the surface. The only ones of these hypothetical defects that can initiate are those that have not already initiated and grown into PWSCC during prior periods of unpeened service time. Their initiation requires a subcritical crack growth mechanism other than PWSCC (fatigue is a possibility) to cause them to propagate to the component surface where, once in contact with the reactor coolant, cracks would be initiated based on the PWSCC degradation mechanism.

The NRC reviewed the proposed stress threshold for PWSCC crack initiation provided in MRP-335R3. The topical report cited technical references describing multiple independent test programs to investigate the applied stress necessary to permit initiation of PWSCC. In all but one cited test program showed that PWSCC did not initiate below the yield strength of the material. In that one set of tests, initiation occurred in two exposures at 360°C (680°F) between 28,000 and 53,500 hours at a stress ratio as low as 0.78 between the applied stress and the test temperature yield stress. If these data are adjusted to account for lower temperature operation in service, the test exposures equate to greater than 222,900 hours of operation at hot leg temperatures.

The MRP report evaluated typical minimum yield strength values for Alloys 600, 82 and 182 and determined 30 ksi was a conservative minimum value. The ASME Code minimum specified yield strength is 35 ksi. The at-temperature (at operating condition) yield strength is lower than the room temperature yield strength. The report discussed the ASME and other methods for estimating higher temperature yield strength using room temperature test data and concluded that the yield strength at 325°C (617°F) would be approximately 80% of the room temperature yield strength of the material.

The NRC staff used the information in the MRP report to calculate a conservative estimate of the minimum applied stress to support initiation (i.e., the threshold stress, the surface stress below which PWSCC is unexpected to occur during the RPVHPN lifetime). Using the ASME Code minimum specified of 35 ksi for minimum yield strength, a factor of 80% to convert room temperature yield strength to yield strength at 325°C and the 0.78 ratio between yield strength and applied stress in the test samples that exhibited PWSCC with the lowest ratio of applied stress to yield strength, the NRC estimates that PWSCC will not initiate in specimens exposed with less than approximately 22 ksi tensile stress at the surface. This is consistent with past NRC determinations. For example, in NRC letter to Palo Verde Nuclear Generating Station Unit 1, dated May 5, 2004 (ADAMS Accession No. ML041260228) and NRC letter to Palo Verde Nuclear Generating Station Unit 2, dated February 23, 2005 (ADAMS Accession No. ML050540726) regarding reactor vessel head inspections, the NRC states: "The stress level of 20 ksi is a conservative value below which PWSCC initiation is unlikely." Additionally, NRC First Revised Order EA-03-009, specified the need to perform inspections on "...all RPV head penetration nozzle surfaces below the J-groove weld that have an operating stress level (including all residual and normal operation stresses) of 20 ksi tension and greater...." Since the proposed performance criterion of +10 ksi is lower than the threshold for PWSCC initiation, the NRC finds that the performance criterion of 10 ksi should prevent initiation of new cracks. The NRC staff is performing confirmatory research to validate that PWSCC initiation does not occur on peened specimens with surface stress of +10 ksi.

One method of assessing the safety implications of reducing crack initiation rates would be to perform probabilistic fracture mechanics evaluations to calculate the effect of reduced initiation on future cracking, degradation, and operation loading. The MRP did perform a probabilistic fracture mechanics analysis but as stated previously, the NRC did not perform a detailed review of that analysis. However, it is possible to perform a qualitative assessment of the impact of applying peening on future initiation rates. Comparing crack initiation on unpeened surfaces, where crack initiation is equally likely anywhere, with crack initiation on peened surfaces, where crack initiation is only possible at these special hypothetical spots, ratioing the susceptible surface areas would be an appropriate method of assessing the potential number of expected initiations following peening. Given the very large differences in susceptible surface areas, the NRC concludes that peening will substantially reduce crack initiation. As will be discussed below, this reduction in the rate of crack initiation can be qualitatively assessed to reduce plant risk (i.e., improve plant safety). Alternatively, the reduction in the rate of crack initiation can be combined with an extension in inspection intervals in a manner which can be qualitatively assessed so as to show that the safety of the plant is improved from the current situation (i.e., unpeened components with current inspection intervals).

Despite the low probability of a crack initiating post-peening, the NRC staff considered the implications of the initiation of such a crack from the surface of a J-groove weld or RPVHPN. The NRC staff noted that, at the present, the J-groove weld cannot be volumetrically inspected.

In considering the implications of a crack which grows within the J-groove weld, the NRC staff notes that the crack will eventually reach the annulus between the nozzle and the reactor head. Such a crack will not be detected by volumetric examinations and will result in a leak. The NRC staff further notes that numerous means are available to detect significant leakage from these locations, such as, reactor coolant inventory balances, boric acid program walkdowns, radiation monitoring, and containment air cooler performance. The primary means for identifying leakage from this location, due primarily to the low volume of leakage, is bare metal visual examinations. MRP-335R3 does require bare metal visual examinations of peened RPVHPN. However, the NRC believes that, due at least in part to the above scenario, additional bare metal visual examinations are appropriate and has imposed Condition 5.1 to increase the proposed frequency of bare metal visual examinations above both the levels proposed in MRP-335R3 and above the current regulatory requirements.

In considering the implications of a crack growing into the RPVHPN, the NRC staff notes that it will become detectable by way of volumetric examinations when the crack enters the wall thickness of the RPVHPN to a sufficient depth. The NRC staff also notes that such a crack will typically be oriented axially with respect to the nozzle. Such a crack could eventually grow through wall and elongate to the point where it intersects the annulus between the nozzle and the reactor vessel closure head. As proposed in MRP-335R3, during this growth period the nozzle would be subject to volumetric inspection at 10-year intervals. These inspections would be capable of identifying the crack if it is of sufficient size in the nozzle material. Should such a crack not be identified prior to reaching the annulus, a leak would result. As mentioned for the case in which the crack remains in the J-groove weld, a leak in the annulus is subject to detection by a wide variety of means and is specifically the subject of bare metal visual examinations as imposed by Condition 5.1.

The NRC staff further notes that the allowance of a 10 ksi tensile stress on the surface with increasing tensile stress into the thickness of the J-groove weld or RPVHPN provides no benefit to stop crack growth through these materials. The allowance of any tensile stress would allow growth of any potential missed existing cracks or cracks initiating from surface flaws. However, the allowed residual stress profile under steady state operating conditions of MRP-335R3 could allow a wider range of tensile stresses, even within the peened area identified in MRP-335R3. The NRC considered these aspects when evaluating the follow-up and inservice inspections for the RPVHPN.

Current regulatory requirements in 10 CFR 50.55a for unpeened RPVHPNs establish inspection periodicities and modalities (techniques) that ensure the probability of PWSCC crack growth to a through wall flaw size is sufficiently low to provide adequate assurance of structural integrity. The NRC considered the qualification and testing information on peening performance provided in the deterministic evaluations in MRP-335R3 and concluded that peened RPVHPNs will have lower probability of crack initiation as compared to unpeened RPVHPNs. The probability of PWSCC initiation on peened RPVHPNs will be lower because the potential sites for crack initiation will have surface stresses reduced by peening to a level below the threshold for crack initiation. The threshold represents the surface stress below which PWSCC is unexpected to occur during the RPVHPN lifetime. The reduction in crack initiation will reduce the probability of through wall cracking because when fewer cracks initiate, fewer cracks can grow through wall. MRP-335R3 states that two RPVHPNs, one with peened penetrations and one with no peening, subjected to the same inspections schedules, will result in different levels of safety. The peened RPVHPN would be more safe (has less frequent through wall cracks) than the unpeened case. The NRC staff finds that the peened RPVHPN will have a lower probability of failure than unpeened RPVHPN because the likelihood of crack initiation is lower in the peened RPVHPN than the unpeened RPVHPN.

The MRP seeks to establish alternative inspection schedules with longer inspection periods for peened RPVHPNs such that a peened RPVHPN subjected to the alternative schedule would have a lower probability of cracking than the probability of cracking that would be expected for an unpeened RPVHPN subjected to current inspection requirements for inspection periodicity. MRP-335R3 uses a series of deterministic and probabilistic calculations to quantify the relationship among peening, inspection frequency and modality, and through wall cracking probability. The NRC reviewed the deterministic calculations in Section 5 of MRP-335R3. The NRC considered insights provided in the probabilistic analyses described in Appendix B of MRP-335R3. The NRC qualitatively considered the deterministic and probabilistic information and, combined with an understanding of the relationship between peening and a reduction in through wall cracking probability due to a reduction in surface stress, concluded that a peened RPVHPN with proposed inspection intervals could have the same or improved level of assurance of structural integrity as an unpeened head subjected to current regulatory requirements.

Given the design parameters above for RPVHPN and associated J-groove welds, the NRC finds that there is reasonable assurance that crack initiation will be significantly reduced. However, the NRC does not find that crack initiation or growth could be entirely mitigated through peening such that there would be absolute assurance of no new cracking. Therefore, the NRC staff established conditions as shown in Section 5 of this SE, which when implemented along with

the proposed requirements of MRP-335R3 provide reasonable assurance of the structural integrity of the RPVHPN.

Inspections for Postulated Preexisting Cracks

The NRC staff evaluated the analyses presented in MRP-335R3 in support of the adequacy of the proposed inspection intervals. For each analysis type (DMW deterministic, DMW probabilistic, RPVHPNs deterministic, and RPVHPNs probabilistic) the NRC staff evaluated each significant topic of the analysis to determine its adherence to accepted standards and the quality of the data used. When applicable, the NRC staff also considered the sufficiency of MRP's sensitivity studies. Following the evaluation of each analysis topic, the NRC staff considered the effect of any shortcomings identified in each analysis topic on the overall analysis results.

In addition to the input variables and analyses provided, the NRC noted that MRP-335R3 contains additional examination requirements which the NRC considers in its evaluation. To determine the acceptability of each of these requirements, the NRC considered each requirement and its implications to the analyses conducted, the overall level of quality and safety of the peened components, and current regulatory requirements as contained in 10 CFR 50.55a, as appropriate.

The NRC staff established conditions as the final aspect of its evaluation. In previous phases of the NRC staff's evaluation, input variables had been considered fixed. In this portion of the evaluation, if the NRC staff discovered a deficiency in MRP's analysis to support the proposed inspection requirements, the NRC staff conditioned the MRP requirement, or the proposed inspection intervals, as appropriate, to achieve reasonable assurance of structural integrity of the peened components from one inspection to the next.

4.3 Probabilistic Analysis—DMW and RPVHPN

While the NRC staff regularly uses probabilistic fracture mechanics calculations to make regulatory decisions, this is only done after significant verification and validation on the probabilistic fracture mechanics computer codes and inputs. As an example, the NRC staff used the FAVOR code to develop the alternate pressurized thermal shock rules found in 10 CFR 50.61a. The FAVOR code has been extensively verified and validated by the NRC staff, and several NUREG reports describe the FAVOR code and its use. Additionally, since 2013, the NRC staff has collaborated with industry to develop the xLPR (Extremely Low Probability of Rupture) code which is a probabilistic fracture mechanics tool to estimate the frequency of failure for reactor coolant system piping. This program has some similarity to the probabilistic analyses performed for MRP-335R3 but remains under development. The NRC staff has not performed verification and validation of the probabilistic fracture mechanics calculations in MRP-335R3. Such work would take significant time and resources to perform and document.

Nevertheless, the NRC staff has reviewed MRP's probabilistic fracture mechanics analysis as part of supporting the proposed inspection requirements. The NRC staff has identified several concerns regarding general uncertainties and basis for input parameters in the probabilistic

analyses in MRP-335R3. The NRC staff's concerns limited, but did not preclude, its ability to rely upon the probabilistic analysis to review MRP's proposed inspection requirements. Therefore, the NRC staff used MRP's probabilistic analyses to provide information for MRP's deterministic analysis in the review of MRP proposed inspection requirements.

The NRC staff has identified inputs to MRP's probabilistic fracture mechanics analyses that contain significant uncertainties that can affect the final outcome of the analysis. The NRC staff has raised questions on some of these inputs, such as on the flaw initiation model and the weld residual stress profiles in the NRC's requests for additional information for previous version of MRP-335. The NRC staff determines that several variables, such as " α " in the crack growth equation, with very large uncertainties, can significantly alter the conclusions if the data used are nearer to one end of the distribution rather than another. The NRC staff determined that further uncertainty analyses would need to be conducted to identify models and input distributions that would most benefit from additional data collection or testing.

The NRC staff was able to use the results of both the MRP and the NRC deterministic analyses to evaluate the peening application. The NRC staff, did not review in detail the probabilistic fracture mechanics calculations in MRP-335R3. However, the NRC staff used the probabilistic results in combination with the deterministic analyses to confirm reasonable assurance of the MRP's proposed inspection requirements, as no instances of significant failure were identified through the MRP's analysis.

The MRP requested the NRC to complete the review of MRP-335R3 in a timely manner because some licensees plan to apply peening at their plants in year 2016. The MRP proposed review schedule precludes the NRC from a detailed review of MRP's probabilistic fracture mechanics analysis because it would take NRC significant time and resources to adequately review the MRP's probabilistic fracture mechanics analysis. The NRC focused its review of MRP-335R3 on the deterministic analysis. The NRC staff may review the probabilistic fracture mechanics analysis in MRP-335R3 at some future date.

4.4 Deterministic Analysis—DMW

DMW and Crack Configuration

The NRC staff finds that the physical parameters (dimensions) and operating conditions (pressure and temperature) used in the model of the DMW are representative of pressurized water reactor plants, but are not bounding for either hot or cold leg DMWs.

Peening Depth

The NRC staff finds that the peening depth used in the MRP's deterministic analysis of DWM is consistent with the performance criteria specified in Section 4 of MRP-335R3 and, therefore, is acceptable.

Peening Coverage

The NRC staff notes that the required peening coverage for a DMW is the full area of the susceptible material along the entire wetted surface under steady-state operation, including the weld, butter, and base material. The MRP requires that the peening coverage be extended at least 0.25 inches beyond the area of susceptible material. The NRC staff finds that the peening coverage for the DMW is acceptable because it covers the susceptible material, including 0.25 inches of non-susceptible base material.

Deterministic Time-to-Failure Analyses for DMW

Table 5-5 to Table 5-11 of MRP-335R3 provide comparisons of the time to failure for DMW. This analysis is based on a variety of postulated crack growth rates, initial flaw sizes and residual stresses.

The deterministic calculations performed in MRP-335R3 used a 100 percent probability of detection (POD) for 0.04 inches deep flaws, based on the use of eddy current testing in accordance with the ASME Code, Section XI, Appendix IV. The NRC staff does not consider a 100 percent POD for PWSCC under field conditions (rough inside diameter surfaces, irregular geometries, etc.) in MRP's calculations conservative. The NRC staff noted that the weld residual stresses used in the deterministic calculations in MRP-335R3 varied in magnitude but not in overall stress profile, thereby, reducing their usefulness in the flaw analysis. Additionally, the assumed flaws in MRP-335R3 are smaller than or equal to the penetration depth of the peening method.

The NRC staff performed an independent analysis using various weld residual stress profiles, including calculated axial and hoop stresses for components with and without safe ends, and with a variety of inner-diameter repair depths. Based on its independent calculations, the NRC staff finds that the proposed inspection requirements for the DMW for cold leg welds are acceptable. The NRC staff finds that the proposed inspection requirements for the hot leg DMWs are unacceptable. For the hot leg DMWs, the NRC calculations support the timing of the first follow-up examination to follow the schedule described in ASME Code Case N-770-1, i.e. on the second refueling outage for hot leg temperatures above 625° F and by the fifth year for hot leg temperatures less than or equal to 625° F. This is reflected in Condition 5.3. In both cases the second follow-up examination would occur within ten years after peening.

4.5 Deterministic Analysis—RPVHPN

RPVHPN Crack Configuration

The NRC staff finds that the RPVHPN modeled in the deterministic analysis is consistent with the relevant design and fabrication of the RPVHPN at pressurized water reactor plants. The NRC staff also finds that MRP-335R3 has considered crack configurations and locations that are consistent with the currently accepted practice of analyzing the initiation and growth of cracks associated with the RPVHPN and J-groove weld. Therefore, the NRC staff finds the configuration of the RPVHPNs and cracks modeled in the deterministic analysis acceptable.

Peening Depth and Required Stresses

MRP-335R3 proposes that, following peening, the depth to which compression will exist in the inside diameter surface of the RPVHPNs is 0.01 inches. MRP-335R3 also proposes that, following peening, compression will exist in the J-groove weld and the outer diameter surface of the RPVHPN to a depth of 0.04 inches. Section 4.3 of MRP-335R3 stated that the operating stress plus the residual stress for the peened RPVHPN (inside and outside diameter surfaces) and J-groove weld shall not exceed 10 ksi (tension). However, the NRC staff finds that the MRP's flaw analysis of RPVHPN in Section 5 of MRP-335R3 used a value for stress at operating conditions on RPVHPNs of 0 ksi on the outside diameter and J-groove weld surfaces, yet the performance criteria specified in Section 4.3 of MRP-335R3 indicate the stress at operating conditions may be up to +10 ksi for the inside and outside diameter surfaces of the RPVHPN and J-groove weld. In addition, the period for small flaws to grow to 10% through-wall or leakage, as shown in the RPVHPN and the J-groove weld summary tables in Section 5 of MRP-335R3, do not seem to be consistent with operating stress profiles that range from 10 ksi tension on the inside diameter to a tensile stress of 30 to 60 ksi at depths of 0.01 to 0.04-inches. The NRC staff finds that the MRP's flaw analysis for the RPVHPN is inconsistent with the performance criteria in Section 4 of MRP-335R3. Therefore, the NRC establishes Conditions 5.1 and 5.4 to address this issue.

Peening Coverage

The NRC staff finds that the peening coverage is adequate because Figure 4-1 through Figure 4-4 of MRP-335R3 show the susceptible surface areas of the RPVHPN and J-groove weld that will be peened.

Section 2.3.3 of MRP-335R3 states that the proposed peening coverage zone for the RPVHPN covers surfaces that are susceptible to PWSCC initiation. The MRP recognized that the proposed peening coverage is in contrast to the inspection coverage zone per ASME Code Case N-729-1. The MRP explained that the difference between the proposed peening coverage and the inspection areas per ASME Code Case N-729-1 is the nozzle areas below the J-groove weld that are not susceptible to PWSCC initiation and that are not part of the pressure boundary. The MRP noted that the proposed peening coverage required for RPVHPNs was established using the stress results in MRP-95, Revision 1, "Generic Evaluation of Examination Coverage Requirements for Reactor Pressure Vessel Head Penetration Nozzles," and the stress limit of +20 ksi (tensile). The NRC staff finds acceptable that the limited RPVHPN areas below the J-groove weld are not peened because those areas are not susceptible to crack initiation and are not part of the RCS pressure boundary. The NRC staff noted that even if a flaw is developed in the unpeened RPVHPN areas and grow into the peened areas, the flaw growth may be limited because the peened areas will have a 10 ksi stress to resist such growth. The 10 ksi stress state may delay the flaw growth. Therefore, the NRC finds that the proposed peening coverage for RPVHPN and J-groove weld is acceptable.

Deterministic Time-to-Failure Analyses for RPVHPN

Table 5-13 to Table 5-19 of MRP-335R3 provide comparisons of the time to failure for the peened RPVHPN. The MRP's deterministic analyses were based on a variety of postulated

crack growth rates, initial flaw sizes and residual stress distributions. The NRC staff found the postulated flaw sizes and crack growth rates used to be both reasonably understood and consistent with the objectives of the analysis. The MRP used the deterministic analyses to demonstrate that there were very limited cases in which a hypothetical crack, missed during the pre-peening inspection or below NDE detectability limits, would grow to leakage under the proposed MRP-335R3 performance criteria.

The NRC staff also evaluated the pre-peening stress profiles for the RPVHPN and, to the extent possible, the post-peening stress profiles. As described below, the NRC staff found these stress profiles to be questionable for several reasons and the variability between high and low stress conditions was not sufficiently large to bound available data.

Of particular note was the NRC staff's comparison of the residual stress profiles in Figure 5-35 through Figure 5-38 of MRP-335R3 with the residual stress profiles of MRP-95, Revision 1. Appendix A of MRP-95R1 provides the residual stress profiles for four limiting plants. The stress profiles in Figure 5-35 through Figure 5-38 present the mean and plus one standard deviation and minus one standard deviation stress profiles calculated using a finite element analysis. The variability of the stress profiles from inside to outside diameter of the RPVHPN are significantly more varied in MRP-95R1 than those used in Figure 5-35 through Figure 5-38 in part because MRP-95R1 reported bounding profiles while Figure 5-35 through Figure 5-38 used a single standard deviation level for the limiting analyses. As such, the NRC staff finds the weld residual stress profiles for the deterministic calculations in MRP-335R3 were neither high enough nor low enough to bound the stress profiles of the peened RPVHPN.

The NRC staff performed a series of independent calculations of a hypothetical flaw of 0.01 inch based on the following considerations: 10 ksi tension on the inside diameter surface of RPVHPNs under operating conditions, the residual stress value will increase sharply with depth, the depth affected by peening is 0.01 inches, and the residual stress not affected by peening is approximately 20 to 70 ksi in tension. The NRC staff found that peening, in accordance with the performance criteria of MRP-335R3, may not prevent flaw growth and flaws may grow through-wall. As a defense-in-depth measure, NRC staff finds that, in addition to the proposed inspections in MRP-335R3 (follow-up inspection at the second refueling outage), for peened RPVHPN and associated J-groove welds that, at the time of peening, having experienced < 8 effective degradation years (EDYs), and that contained flaws prior to peening, should also be examined in the first refueling outage following the peening application as specified in Condition 5.4.

4.6 NRC Review of Proposed Inspection Requirements

4.6.1 Pre-Peening Examinations

DMW

MRP-335R3 proposed to perform ultrasonic examination and eddy current testing on the inside diameter surface of DMW. The NRC staff evaluated these examinations and finds them to be acceptable because the proposed pre-peening examination requirement is consistent with ASME Code Case N-770-1 and 10 CFR 50.55a(g)(6)(ii)(F).

RPVHPN

MRP-335R3 proposed that pre-peening examinations for RPVHPNs consist of volumetric examination of each nozzle, or surface examination of nozzle inside diameter surface and wetted nozzle outside diameter surface and J-groove weld; and a demonstrated volumetric or surface leak path assessment for the J-groove weld. The NRC staff evaluated these examinations and finds them to be acceptable because the proposed pre-peening examination requirements are consistent with ASME Code Case N-729-1 and 10 CFR 50.55a(g)(6)(ii)(D).

4.6.2 Follow-up Examinations

DMWs

The MRP proposed a volumetric and surface examination of all peened hot leg DMWs within 5 years and a second examination within 10 years following peening application. The MRP proposed a volumetric and surface examination of all peened cold leg DMWs once within 10 years of peening but no sooner than the third refueling outage following peening application. As previously described, the NRC staff finds that the follow-up examinations for cold leg DMWs are acceptable as proposed. Also as previously described, the NRC staff finds that the follow-up examinations for hot leg DMWs are not acceptable. The NRC staff has established Condition 5.3 to adjust the follow-up examination frequency of hot leg DMWs so as to provide reasonable assurance of structural integrity of the hot leg DMWs. These findings are based on the NRC staff's evaluation which finds that, given that the hot leg DMWs are peened and inspected, there will be at least an equal level of safety when compared to the unpeened DMWs inspected per current regulations.

RPVHPN

The MRP proposed that for RPVHPNs that had experienced equal to or greater than 8 total effective degradation years (EDY) at the time of peening, a volumetric examination or surface examination of nozzles; and a demonstrated volumetric or surface leak path assessment be performed in the first and second refueling outage after peening. The NRC staff finds that the proposed examination for RPVHPN ≥ 8 EDY during the first and second refueling outage after peening is acceptable because this inspection frequency is adequate to detect potential flaws, should they occur, after peening on RPVHPNs.

For RPVHPNs that have experienced less than 8 EDY at the time of peening, the MRP proposed a volumetric examination or surface examination; and a demonstrated volumetric or surface leak path assessment to be performed in the second refueling outage after peening. The NRC staff does not object to the proposed inspection requirement except that the NRC staff determines that a separate examination schedule should be implemented for this category of RPVHPNs (i.e., < 8 EDY) that contains pre-existing flaws.

For RPVHPNs and associated J-groove welds which, at the time of peening, have experienced < 8 EDYs and do not contain pre-existing flaws, the NRC staff finds that the proposed follow-up examination in the second refueling outage after peening is acceptable. This is because based

on the NRC staff's independent calculation, a flaw in the cold head (RPVHPN < 8 EDY) would not grow to a detectable size until second refueling outage after peening application.

For RPVHPN < 8 EDY containing pre-existing flaws, the NRC staff finds that the proposed follow-up examinations scheduled for the second refueling outage is inadequate. A RPVHPN that contains pre-existing flaw(s) needs to be examined more frequently than a RPVHPN without pre-existing flaws. To provide an equivalent level of safety to the current situation (i.e., inspect unpeened RPVHPNs per current regulations), the NRC staff finds that RPVHPNs and associated J-groove welds which, at the time of peening, have experienced < 8 EDYs and contain pre-existing flaws, must be inspected in the first and second refueling outage after peening as indicated in Condition 5.4.

4.6.3 ISI Examinations

DMWs

For ISI examinations, the MRP proposed that a volumetric and surface examination (eddy current) be performed on hot leg and cold leg DMWs once every 10 years beginning 10 years after peening application. The NRC staff finds that the proposed ISI examinations for DMWs are acceptable because there is reasonable assurance that new PWSCC cracks will not likely to initiate following peening and, based on NRC staff calculations, preexisting cracks which have not already been identified by the time ISI examinations begin will not grow from an undetectable size to through wall in less than 10 years.

RPVHPN

For the ISI examination, the MRP proposed a volumetric or surface examination of all peened RPVHPNs and a demonstrated volumetric or surface leak path assessment be performed each 10-year ISI interval beginning 10 years after peening application. In addition, the MRP proposed a bare metal visual examination and VT-2 examination be performed on all RPVHPNs as specified in Table 3 of this SE. The NRC staff finds that the proposed volumetric examinations are acceptable because they provide: defense in depth for the potential that a new PWSCC crack may initiate post-peening; crack detection capability for slow growing flaws which originate in the inspectable areas of the RPVHPN and were not identified in the follow-up examinations; and potential identification of cracks which originate in the uninspectable areas of the J-groove weld and grow into inspectable area of the RPVHPN.

The NRC staff finds that the proposed bare metal visual examinations for the RPVHPN are not acceptable. Due to the fact that the J-groove weld is not volumetrically inspectable, under both the current situation (no peening) and the proposed situation (peening) the bare metal visual examination is relied upon to identify cracking, which can originate and remain in uninspectable areas of the J-groove weld before significant corrosion of the head or RPVHPN ejection occur. The NRC staff has determined that in order to provide reasonable assurance of structural integrity of peened RPVHPN, it is necessary to perform bare metal visual examinations for all peened RPVHPNs every refueling outage. The NRC staff has created Condition 5.1 to address this issue.

Discovery of Cracks and/or Leakage Post-Peening

MRP-335R3 acknowledges that when peening is performed there may be some preexisting cracks that will grow from a size which is undetectable at the time of peening to a detectable size either within the time period of the follow-up examinations or, for slow growing cracks, during the period of ISI examinations. MRP-335R3 also acknowledges that there are very rare instances in which the proposed inspections may not identify a crack prior to leakage. The NRC staff finds MRP's assessment to be reasonable. However, the NRC staff notes that the discovery of a crack or leakage post-peening could indicate that the peening process was not effective. As a result, the NRC staff has a vested interest in ensuring that an adequate investigation into the crack or leak is conducted on the peened component and that the appropriate information is communicated to the NRC in a timely manner. To that end, the NRC has established Condition 5.2. Furthermore, the NRC staff has determined that the peened DMW or RPVHPN in which the flaw was identified shall be inspected in accordance with applicable current regulations (ASME Code Cases N-770-1 or N-729-1) or until a new alternative to the current regulation for that specific RPVHPN or DMW has been authorized by the NRC staff via a relief request as specified in Condition 5.2.

5.0 Conditions

As a compensating measure, the NRC staff imposes the following conditions for those licensees that wish to cite MRP-335R3 in plant-specific relief requests to deviate from the current regulatory inspection requirements for peened DMWs and RPVHPNs. The NRC authorized inspection requirements for peened DMWs and RPVHPNs are specified in Table 4 of this SE.

5.1 The bare metal visual examinations of all peened RPVHPNs and J-groove welds must be performed every refueling outage.

5.2 If a wetted surface-connected flaw, an unacceptable flaw based on the ASME Code, Section XI, or unacceptable flaw growth is observed in a peened DMW, RPVHPN, or J-groove weld, (a) a report summarizing the evaluation, including inputs, methodologies, assumptions, extent of conditions, and causes of the new flaw, unacceptable flaw, or flaw growth, must be submitted to the NRC prior to the plant entering into Mode 4. (b) A sample inspection of the peened components in the population must be performed to assess the extent of condition. (c) A final causal analysis report consistent with the licensee corrective action program including a description of corrective actions taken must be submitted to the NRC within six months of the discovery. (d) The inspection relaxation in MRP-335R3 is no longer applicable to the affected RPVHPN or DMW. The affected RPVHPN or DMW component shall be inspected in accordance with the requirements of 10 CFR 50.55a, unless an alternative is authorized.

5.3 The follow-up inspection for peened hot leg DMWs must be performed on the following schedule: (a) For hot leg DMWs above 625°F, perform a volumetric examination and a surface examination on the second refueling outage after the application of peening and a second examination within 10 years following the application of peening. (b) For hot leg DMWs equal to or less than 625°F, perform a volumetric examination and a surface examination within 5 years following the application of peening and a second examination within 10 years following the application of peening.

5.4 This condition applies to RPVHPNs and associated J-groove welds in a reactor vessel closure head that have experienced < 8 EDYs: (a) If all RPVHPNs in the reactor vessel closure head are free from pre-peening flaws, inspections shall be performed in accordance with the proposed inspection requirements, i.e., inspections shall be performed on each RPVHPN in the second refueling outage after peening; (b) If indications of cracking, attributed to PWSCC, has been identified in the RPVHPNs or associated J-groove welds, whether acceptable or not for continued service under Paragraphs -3130 or -3140 of ASME Code Case N-729-1, inspections shall be performed on each RPVHPN in the first and second refueling outage after peening.

Practical Considerations

The information below is beyond the scope of the MRP-335R3 review and, therefore, was not considered in assessing the acceptability of MRP-335R3. However, the information below is of significant interest to the NRC and may be of value to licensees preparing plant-specific relief requests to take advantage of inspection relaxation provided in MRP-335R3. This SE makes numerous assumptions regarding the process by which peening is conducted and qualified. If any of the assumptions below are not met, the use of MRP-335R3 and associated NRC SE are not permitted. Although not designed to be exhaustive, a list of issues significant to the NRC follows.

Peening Coverage – the extent to which peening must cover the areas of interest is specified in MRP-335R3. This SE assumes that these coverage areas are met. It is necessary that the required levels of surface compression are achieved in all areas for which coverage is required.

Residual Stresses at End of Plant Life – To use MRP-335R3 and this SE, it is necessary that the prescribed beneficial surface stresses be present at the end of plant life (i.e., the stresses that will prevent crack initiation and, to certain extent, minimize crack growth). The NRC notes that residual stresses resulting from peening degrade with time at temperature and due to thermal cycles. For this SE, the NRC has assumed that the beneficial stresses proposed will be present at the end of plant life.

Uncertainty of Residual Stress Measurements – For the purposes of this SE, the NRC staff has assumed that the precise residual stress measurement specified will be achieved. The NRC staff is aware of a substantial body of data which indicates that there is considerable uncertainty in residual stress measurements. The licensee needs to address this uncertainty in future plant-specific proposed alternative to ASME Code inspection requirements. As an example, if the performance criteria is a surface stress of 10 ksi under operating conditions, the licensee should consider the uncertainties associated with both the residual stress measurements and calculations to ensure compliance.

Use of X-Ray Diffraction to Determine Residual Stresses – The NRC staff is aware of substantial data which indicates that X-Ray diffraction has significant uncertainties associated in its measurements of surface residual stresses in welds. The licensee needs to address this issue in future plant-specific alternatives to the ASME Code inspection requirements for the peened DMWs and RPVHPNs.

6.0 CONCLUSION

The NRC staff finds that MRP-335R3 has adequately described the affected components, processes for peening, the supporting analyses of the peening application, testing used to verify the effectiveness of peening, and the proposed inspection requirements of peened components. The NRC staff also finds that the MRP has demonstrated that there is a beneficial effect from peening on the residual stress in the DMW and RPVHPN. The MRP has demonstrated by mockup testing as shown in MRP-267, Revision 1 and analyses in MRP-335R3 that the peening application will achieve a certain post-peening stress profile to minimize PWSCC initiation.

Based on information provided in MRP-335R3, and operating experience such as shot peening applied to steam generator tubes and abrasive water jet machining (peening) applied to repaired RPVHPNs, the NRC staff finds that peening application is a viable mitigation to minimize PWSCC initiation.

However, the NRC staff had questions regarding the details of the peening application, such as the adequacy of the post-peening stress field, the compression stress depth, and the potential for the small flaws that are not detected before peening that may grow after peening. The NRC staff finds that, given the input variables proposed in MRP-335R3, the analyses provided do not fully support the inspection intervals proposed in MRP-335R3. Therefore, the NRC staff has imposed conditions to ensure that the proposed inspection requirements in MRP-335R3 will provide adequate monitoring of the peened DMWs and RPVHPNs between required inspections.

The NRC staff concludes that the peening application, in combination with the proposed inspection requirements in MRP-335R3 and conditions imposed in this SE, will provide reasonable assurance of the adequate protection of public health and safety.

Attachment: MRP Tables

Principle Contributors: John Tsao, NRR/DE/EPNB
Jay Collins, NRR/DE/EPNB
Stephen Cumblidge, NRR/DE/EPNB
Robert Hardies, NRR/DE

Date: August 24, 2016

Table 1 MRP Proposed Performance Criteria (key criteria)

Affected Components	Operating Condition			
	Peened Area	Depth of Effect	Stress at Peened Surface	Stress At Peened Depth
Hot Leg DMW	full area of the susceptible material + 0.25 inches beyond susceptible material	Minimum nominal depth of 0.04 inch	Residual stress plus normal operating stress shall be < 0 ksi	Unspecified, tensile stresses allowed
Cold Leg DMW	full area of the susceptible material + 0.25 inches beyond susceptible material	Minimum nominal depth of 0.04 inch	Residual stress plus normal operating stress shall be < 0 ksi	Unspecified, tensile stresses allowed
Hot RPVHPN Head				
OD	Peened area defined in Figure 4-1through Figure 4-4 of MRP-335R3	0.04 inch	Residual stress plus normal operating stress < +10 ksi	Unspecified, tensile stresses allowed
ID		0.01 inch		Unspecified, tensile stresses allowed
J-groove weld		0.04 inch		Unspecified, tensile stresses allowed
Cold RPVHPN Head				
OD	Peened area defined in Figure 4-1through Figure 4-4 of MRP-335R3	0.04 inch	Residual stress plus normal operating stress < +10 ksi	Unspecified, tensile stresses allowed
ID		0.01 inch		Unspecified, tensile stresses allowed
J-groove weld		0.04 inch		Unspecified, tensile stresses allowed

Table 2 Inspection Requirements in Current Regulations

Components	Current ISI Volumetric & Surface Examination	Current ISI Bare Metal Visual Examination (VE)
RPVHPN EDY ≥ 8 years	Every 8 years or Prior to RIY ≥ 2.25, whichever is less Volumetric exam or surface exam; and a demonstrated volumetric or surface leak path assessment.	Each refueling outage (RFO)
RPVHPN EDY < 8 years	Every 8 years, or Prior to RIY ≥ 2.25, whichever is less Volumetric exam or surface exam; and a demonstrated volumetric or surface leak path assessment.	Each RFO If no flaws, VE every 3 rd RFO or 5 calendar years, whichever is less. VT-2 in outages that the VE is not performed
RPVHPN with indications of cracking, either acceptable or not for further operation.	Each RFO Volumetric exam or surface exam; and a demonstrated volumetric or surface leak path assessment.	Each RFO
Unmitigated DMW at hot leg with temperature > 625 degrees F	Volumetric exam every second refueling outage for uncracked DMWs	Each RFO
Unmitigated DMW at hot leg with temperature ≤ 625 degrees F	Volumetric exam every 5 years for uncracked DMWs	Each RFO
Unmitigated DMW at cold leg with temperature ≥ 525 degrees F and < 580 degrees F	Volumetric exam every second ISI period, not exceeding 7 years for uncracked DMWs	Each ISI interval

Notes:

1. The above table presents only key inspection requirements in the current regulations. The detailed ISI examination requirements for the unmitigated RPVHPN and DMWs without flaws are presented in ASME Code Cases N-729-1 and N-770-1, respectively. ASME Code Case N-722-1 also provide requirements for the bare metal visual examination of DMWs. Additional examination requirements are provided in 10 CFR 50.55a(g)(6)(ii)(D), 10 CFR 50.55a(g)(6)(ii)(E), and 10 CFR 50.55a(g)(6)(ii)(F).

Table 3 MRP Proposed Alternative Examination*1

Peened Components	Pre-Peening Examination	Follow-up Examination	ISI Examination	ISI Bare Metal Visual Exam (VE)
RPVHPNs with effective degradation years (EDYs) ≥ 8 years	Volumetric exam of each nozzle, or surface exam of nozzle ID surface and wetted surface of nozzle OD and J-groove weld. And, a demonstrated volumetric or surface leak path assessment thru J-groove weld	Volumetric exam or surface exam of nozzles; and a demonstrated volumetric or surface leak path assessment. Performed in the first and second refueling outage (RFO) after peening	Volumetric or surface exam of nozzles and a demonstrated volumetric or surface leak path assessment Each ISI interval (i.e., once every 10 years)	Each RFO
RPVHPNs with EDY < 8 years	Volumetric exam of each nozzle, or surface exam of nozzle ID surface and wetted surface of nozzle OD and J-groove weld. And, a demonstrated volumetric or surface leak path assessment thru J-groove weld	Volumetric exam or surface exam; and a demonstrated volumetric or surface leak path assessment. Performed in the second RFO after peening	Volumetric or surface exam and a demonstrated volumetric or surface leak path assessment Each ISI interval (i.e., once every 10 years)	Each RFO or, if VE is every 2 RFO before peening, after peening, VE is every 2nd RFO & VT-2 performed during VE is not performed If no flaw is found VE is every 3 rd RFO or 5 calendar years, whichever is less, & VT-2 performed during RFO in which VE is not performed
Hot leg DMWs with temperature ≤ 625 degrees F	Ultrasonic exam and eddy current testing (ET) on DMW ID surface	Volumetric and surface exam of all peened welds within 5 years and a second exam within 10 years following peening application	Surface and volumetric examination on all peened welds each 10-year ISI interval. Surface exam from ID surface and volumetric exam performed from either ID or OD surface	No VE or VT-2 specified
Cold leg DMWs with temperature ≥ 525 degrees F and < 580 degrees F	Ultrasonic exam and eddy current testing (ET) on DMW ID surface	Volumetric and surface exam of all peened welds once within 10 years of peening but no sooner than the 3 rd refueling outage following peening application	Surface and volumetric examination of all peened welds each 10-year ISI interval. Surface exam from ID surface and volumetric exam performed from either ID or OD surface	No VE or VT-2 specified

Footnotes-

- *1 "Materials Reliability Program: Topical Report for Primary Water Stress Corrosion Cracking Mitigation by Surface Stress Improvement (Revision 3)" (MRP-335R3), Table 4-1 and Table 4-3, provide detailed alternative examination requirements. The key examination requirements are presented above.

Table 4 NRC Authorized Inspections for Peened DMW and RPVHPN

Peened Components	Pre-Peening Examination	Follow-up Examination	ISI Examination	ISI Bare Metal Visual Exam (VE)
RPVHPNs with effective degradation years (EDYs) \geq 8 years	Volumetric exam of each nozzle, or surface exam of nozzle ID surface and wetted surface of nozzle OD and J-groove weld. And, a demonstrated volumetric or surface leak path assessment thru J-groove weld	Volumetric exam or surface exam of nozzles; and a demonstrated volumetric or surface leak path assessment. <i>Performed in the first and second refueling outage (RFO) after peening</i>	Volumetric or surface exam of nozzles and a demonstrated volumetric or surface leak path assessment Each ISI interval (i.e., once every 10 years)	Each RFO
RPVHPNs with EDY < 8 years	Volumetric exam of each nozzle, or surface exam of nozzle ID surface and wetted surface of nozzle OD and J-groove weld. And, a demonstrated volumetric or surface leak path assessment thru J-groove weld	Volumetric exam or surface exam; and a demonstrated volumetric or surface leak path assessment. <i>If all RPVHPNs are free from pre peening flaws, inspection is performed on each RPVHPN in the second refueling outage (RFO) after peening. If any RPVHPN has a PWSCC flaw, inspection is performed on each RPVHPN in the first and second RFO after peening.</i>	Volumetric or surface exam and a demonstrated volumetric or surface leak path assessment Each ISI interval (i.e., once every 10 years)	Each RFO
Hot leg DMWs with temperature > 625 degrees F	Ultrasonic exam and eddy current testing (ET) on DMW ID surface	Volumetric and surface exam of all peened welds performed in the 2 nd RFO and a second exam within 10 years following peening application	Surface and volumetric examination on all peened welds each 10-year ISI interval. Surface exam from ID surface and volumetric exam performed from either ID or OD surface	None
Hot leg DMWs with temperature \leq 625 degrees F	Ultrasonic exam and eddy current testing (ET) on DMW ID surface	Volumetric and surface exam of all peened welds performed within 5 years and a second exam within 10 years following peening application	Surface and volumetric examination on all peened welds each 10-year ISI interval. Surface exam from ID surface and volumetric exam performed from either ID or OD surface	None
Cold leg DMWs with temperature \geq 525 degrees F and < 580 degrees F	Ultrasonic exam and eddy current testing (ET) on DMW ID surface	Volumetric and surface exam of all peened welds once within 10 years of peening but no sooner than the 3 rd refueling outage following peening application	Surface and volumetric examination of all peened welds each 10-year ISI interval. Surface exam from ID surface and volumetric exam performed from either ID or OD surface	None

Table 5--NRC Staff's Disposition of EPRI's Comments on the Draft Safety Evaluation

No	Location in SE	Text in Question	Technical Error Misinterpretations Review Comments	NRC Disposition
1	Section 3.4.3 Page 10	For example, MRP reported that for a 1.3-percent deep circumferential flaw (0.040 inches),	The original text from Section 5.2.2.1 of MRP-335R3 is as follows: "Despite the bounding compressive residual stress profile that is assumed, Figure 5-6 and Figure 5-8 (initial through-wall fraction of 1.3% (0.9 mm)) show the effect peening can have on cracks with depths similar to the depth of the peening penetration depth..." 1.3% of 2.75 inches is 0.036 inches, and not 0.040 inches. The text should be corrected to: <i>"For example, MRP reported that for a 1.3-percent deep circumferential flaw (0.036 0.040-inches),"</i>	The NRC staff finds this comment to be an issue of fact. The NRC staff finds the comment to be correct. The NRC staff modified the safety evaluation accordingly. This modification has no bearing on the conclusions of the safety evaluation.
2	Section 3.4.3 Page 11	The MRP's sensitivity study shows that only three of 72 cases for peened DMWs result in leakage after the extension of the inspection interval whereas nine of 24 cases for unpeened DMWs result in leakage per the current inspection requirements.	The text incorrectly references the results presented in Section 5.2.3 and summarized in Table 5-3 of MRP-335R3. The text should be corrected to: <i>"The MRP's sensitivity study shows that only three of 72 cases for peened DMWs result in leakage after the extension of the inspection interval whereas 24 of 72 nine-of-24 cases for unpeened DMWs result in leakage per the current inspection requirements."</i>	The NRC staff finds this comment to be an issue of fact. The NRC staff finds the comment to be correct. The NRC staff modified the safety evaluation accordingly. This modification has no bearing on the conclusions of the safety evaluation.

3	Section 3.4.4 Pages 12 and 13	<p>The parameters that MRP sampled were the operating time, component temperature, and loads. MRP also analyzed uncertainty in crack initiation model, crack growth model, flaw inspection and detection model, and effect of peening on residual stress.</p>	<p>Operating time and effective loads were not sampled parameters for the DMW probabilistic assessment.</p> <p>The text should be corrected to:</p> <p>"The parameters that MRP sampled were the operating time, component temperature, and welding residual stress profiles, as well as model parameters for and loads. MRP also analyzed uncertainty in the crack initiation model, crack growth model, flaw inspection and detection model, and effect of peening on residual stresses."</p>	<p>The NRC staff finds this comment to be an issue of fact. The NRC staff finds the comment to be correct. The NRC staff modified the safety evaluation accordingly. This modification has no bearing on the conclusions of the safety evaluation.</p>
---	----------------------------------	---	--	--

4	Section 3.4.4 Page 13	Specifically, the cumulative leakage probability after peening is predicted to be reduced by a factor of 9 to 11, depending on when the follow-up inspection is performed.	<p>Section A.10 of MRP-335R3 states:</p> <p><i>"Specifically, the cumulative leakage probability after the hypothetical time of peening is predicted to be reduced by:</i></p> <ul style="list-style-type: none"> <i>• A factor of approximately 11 when the follow-up UT inspection is scheduled two cycles after peening and no subsequent UT inspections are scheduled after follow-up examinations are performed</i> <i>• A factor of approximately 12 when the follow-up UT inspection is scheduled three cycles after peening and no subsequent UT inspections are scheduled after follow-up examinations are performed</i> <i>• A factor of approximately 9 when the follow-up UT inspection is scheduled six cycles after peening and no subsequent UT inspections are scheduled after follow-up examinations are performed"</i> <p>As these resulting factors of reduction range from 9 to 12, the text should be corrected to:</p> <p><i>"Specifically, the cumulative leakage probability after peening is predicted to be reduced by a factor of 9 to 12 11, depending on when the follow-up inspection is performed."</i></p>	The NRC staff finds this comment to be an issue of fact. The NRC staff finds the comment to be correct. The NRC staff modified the safety evaluation accordingly. This modification has no bearing on the conclusions of the safety evaluation.
---	--------------------------	--	--	---

5	Section 3.4.6 Page 19	The sampled inputs include component geometry, operating time, RPVHPN operating temperature, welding residual stresses, and operating loading. MRP also treated uncertainties in the crack initiation model, crack growth model, flaw inspection and detection model, post-peening effects, and flaw stability model.	<p>Operating time and operating loading were not sampled parameters for the RPVHPN probabilistic assessment.</p> <p>The text should be corrected to:</p> <p><i>"The sampled inputs include component geometry, operating time, RPVHPN operating temperature, and welding residual stresses, as well as model parameters for and operating loading. MRP also treated uncertainties in the crack initiation model, crack growth model, flaw inspection and detection model, effect of peening on residual stresses post-peening effects, and flaw stability model."</i></p>	The NRC staff finds this comment to be an issue of fact. The NRC staff finds the comment to be correct. The NRC staff modified the safety evaluation accordingly. This modification has no bearing on the conclusions of the safety evaluation.
6	Section 4.2 Page 23	Cracks anywhere on RPVHPNs can lead to leakage. [two locations]	<p>This statement is incorrect. Circumferential flaws in RPVHPNs below the J-groove weld do not lead to leakage, as this portion of the CRDM nozzle tube is not part of the pressure boundary.</p> <p>These sentences should be modified to acknowledge this exception.</p>	The NRC staff finds this comment to be an issue of fact. The NRC staff finds the comment to be incorrect. The comment makes no reference to the orientation of a postulated crack. The NRC finds that the SE statement in question correctly states that there is no location on the RPVHPN at which at least an axial or circumferential crack could not originate and grow to a point at which leakage would not occur. The safety evaluation was not modified.

7	Section 4.2 Page 24	Section 5.2.1 of MRP-335R3 states that "the peening compressive stress at the RPVHPN inside diameter surface is set to result in a net tensile stress of 10 ksi, and a residual stress value that results in a net stress of 0 ksi is assumed for the peened surface of the RPVHPN outside diameter and J- groove weld because the operating stress in those regions is small."	<p>This is not a direct quotation of Section 5.2.1. Section 5.2.1 of MRP-335R3 states:</p> <p><i>"the peening compressive stress at the surface is set to result in a net tensile stress of +70 MPa (+10 ksi) in the direction of maximum operating stress for flaws on the nozzle ID surface, and a residual stress value that results in a net stress of 0 MPa (0 ksi) is assumed for the peened surface of the nozzle OD and weld since the operating stress in those regions is small."</i></p> <p>Note that as discussed in Comment 10 a net tensile surface stress of +10 ksi was assumed for RPVHPNs in the deterministic matrix in Section 5.2.3 of MRP-335R3.</p>	The NRC staff finds this comment to be an issue of fact. The NRC staff finds the comment to be correct. The NRC staff modified the safety evaluation accordingly. This modification has no bearing on the conclusions of the safety evaluation.
8	Section 4.2 Page 25	In that one set of tests, initiation occurred in two exposures at 360°C between 65,000-85,000 hours at a stress ratio as low as 0.78 between the applied stress and the test temperature yield stress. If these data are adjusted to account for lower temperature operation in service, the test exposures equate to greater than 222,000 hours of operation at hot leg temperatures.	<p>Results shown in Table 2-2 of MRP-335R3 are incorrectly referenced. The test duration for the Alloy 82 specimen with a stress ratio of 0.78 was 53,500 hours. This corresponds to a test duration of 418,200 hours at 325°C.</p> <p>The test duration for the Alloy 82 specimen with a stress ratio of 0.93 was 28,500 hours. This corresponds to a test duration of 222,900 hours at 325°C.</p> <p>The text should be corrected to:</p> <p><i>"In that one set of tests, initiation occurred in two exposures at 360°C between 28,500 and 53,500 45,000-85,000 hours at a stress ratio as low as 0.78 between the applied stress and the test temperature yield stress. If these data are adjusted to account for lower temperature operation in service, the test exposures equate to greater than 222,900 222,000 hours of operation at hot leg temperatures."</i></p>	The NRC staff finds this comment to be an issue of fact. The NRC staff finds the comment to be correct. The NRC staff modified the safety evaluation accordingly. This modification has no bearing on the conclusions of the safety evaluation.

9	Section 4.4 Page 31	<p>The NRC staff finds that the proposed inspection requirements for the hot leg DMWs unacceptable. For the hot leg DMWs, the NRC calculations support the timing of the first follow-up examination to follow the schedule described in ASME Code Case N-770-1, i.e. on the second refueling outage for hot leg temperatures above 625° F and by the fifth year for hot leg temperatures less than or equal to 625° F. This is reflected in Condition 5.3. In both cases the second follow-up examination would occur within ten years after peening.</p>	<p>The wording should be corrected to state that NRC finds the proposed inspection requirements for hot leg DMWs at operating temperatures less than or equal to 625°F to be acceptable. The current wording implies that this is not the case.</p> <p>An operating temperature of 625°F bounds the hot leg operating temperatures in U.S. PWRs. ASME Code Case N-770-1 describes pressurizer locations as hot leg locations with temperature greater than 625°F. Pressurizer locations of Alloy 82/182 piping butt welds are not considered to be candidates for peening. Therefore Condition 5.3 is expanding the applicability of MRP-335R3 beyond the intended bound of 625°F.</p>	<p>The NRC staff finds that this comment is not an issue of fact and not subject to revision in this process. The NRC staff chose to address all aspects of the definition of "hot leg" as contained in code case N-770-1 to ensure completeness. As a result, the proposed inspections were unacceptable in that they did not address temperatures above 625° F. The inspection requirements for hot leg conditions below 625° F are consistent between the proposed inspections and those required by the safety evaluation. The inclusion of higher temperatures ensures completeness but does not, in and of itself, expand the scope of the topical report. The safety evaluation was not changed.</p>
---	------------------------	--	--	---

10	Section 4.5 Page 31	However, the NRC staff finds that MRP's flaw analysis of RPVHPN in Section 5 of MRP-335R3 used a value for stress at operating conditions on RPVHPNs of 0 ksi on the outside diameter and J-groove weld surfaces, yet the performance criteria specified in Section 4.3 of MRP-335R3 indicate the stress at operating conditions may be up to +10 ksi for the inside and outside diameter surfaces of the RPVHPN and J-groove weld.	This statement is factually incorrect. For the deterministic matrix of analyses added to the report as Section 5.2.3 of Revision 3, the total stress at both the inner and outer RPVHPN surfaces (ID, OD below weld, and weld wetted surface) was set to +10 ksi tensile.	The NRC staff finds that this comment addresses the results of an NRC staff analysis and is therefore not a matter of fact and not subject to revision as a part of this process. The NRC staff notes that the safety evaluation statement in question is based on NRC independent calculations designed to confirm MRP calculations. The safety evaluation was not changed.
11	Section 4.5 Page 31	In addition, the period for small flaws to grow to 10% through-wall or leakage, as shown in the RPVHPN and the J-groove weld summary tables in Section 5 of MRP-335R3, do not seem to be consistent with operating stress profiles that range from 10 ksi tension on the inside diameter to a tensile stress of 30 to 60 ksi at depths of 0.01 to 0.04-inches.	This statement is not correct. An operating stress of 10 ksi tension on the inside diameter was applied by MRP in these calculations. The stress profile assumption for the MRP calculations being cited (Section 5.2.3.2) are shown in Figure 5-35 and Figure 5-36 of MRP-335R3.	The NRC staff finds that this comment addresses the results of an NRC staff analysis and is therefore not a matter of fact and not subject to revision as a part of this process. The NRC staff notes that the safety evaluation statement in question is based on NRC independent calculations designed to confirm MRP calculations. The safety evaluation was not changed.

12	Condition 5.2 Page 36	(c) A root cause analysis report must be submitted to the NRC within six months of the discovery.	<p>In Condition 5.2(c) the term "root cause analysis report" has very specific requirements associated with it in the industry. This should be changed as follows:</p> <p><i>"An appropriate causal analysis report consistent with the licensee corrective action program A-root cause analysis report must be submitted to the NRC within six months of the discovery."</i></p>	<p>The NRC staff finds this comment to be an issue of fact. The NRC staff finds the comment to be correct. The NRC staff modified the safety evaluation accordingly with an additional requirement to provide a description of corrective actions implemented as a result of the finding.</p>
13	Condition 5.2 Page 36	(d) The inspection relaxation in MRP-335R3 is no longer applicable to the affected component. The affected component shall be inspected in accordance with the requirements of 10 CFR 50.55a, unless an alternative is authorized.	<p>In Condition 5.2(d) the word "component" is unclear and should be "RPVHPN or DMW." This should be changed as follows:</p> <p><i>"The inspection relaxation in MRP-335R3 is no longer applicable to the affected RPVHPN or DMW component. The affected RPVHPN or DMW component shall be inspected in accordance with the requirements of 10 CFR 50.55a, unless an alternative is authorized."</i></p>	<p>The NRC staff finds this comment to be an issue of fact. The NRC staff finds the comment to be correct. The NRC staff modified the safety evaluation accordingly. This modification has no bearing on the conclusions of the safety evaluation.</p>
14	Table 2	"Volumetric exam every second refueling outage"	<p>The "Current ISI Volumetric & Surface Examination" entry for "Unmitigated DMW at hot leg with temperature > 625 degrees F" should be corrected to:</p> <p><i>"Volumetric exam every second refueling outage for uncracked DMWs"</i></p>	<p>The NRC staff finds this comment to be an issue of fact. The NRC staff finds the comment to be correct. The NRC staff modified the safety evaluation accordingly. This modification has no bearing on the conclusions of the safety evaluation.</p>

15	Table 3	<p>For "RPVHPNs with EDY < 8 years":</p> <p>"If no flaw is found VE is every 3rd RFO & VT-2 performed during VE is not performed"</p>	<p>This table should be corrected to indicate that the VE interval proposed for cold heads in MRP-335R3 is every 3rd RFO or 5 calendar years, whichever is less.</p> <p><i>"If no flaw is found VE is every 3rd RFO or 5 calendar years, whichever is less, & VT-2 performed during RFO in which VE is not performed"</i></p>	<p>The NRC staff finds this comment to be an issue of fact. The NRC staff finds the comment to be correct. The NRC staff modified the safety evaluation accordingly. This modification has no bearing on the conclusions of the safety evaluation.</p>
16	Table 4	<p>Row: <i>RPVHPNs with effective degradation years (EDYs) ≥ 8 years</i></p> <p>Column: <i>Follow-up Examination</i></p> <p>Row: <i>RPVHPNs with effective degradation years (EDYs) ≥ 8 years</i></p> <p>Column: <i>ISI Bare Metal Visual Exam (VE)</i></p> <p>Row: <i>Hot leg DMWs with temperature ≤ 625 degrees F</i></p> <p>Column: <i>Follow-up Examination</i></p>	<p>The items in these table entries are italicized, indicating that the draft NRC authorized inspection frequencies are different than those proposed in MRP- 335R3. However, these items in Table 4 are the same as those in Table 3, showing that there is no difference in these inspection requirements.</p> <p>Thus these entries in Table 4 should be un-italicized to show that they are not different from the inspection requirements proposed in MRP-335R3.</p>	<p>The NRC staff finds this comment to be an issue of fact. The NRC staff finds the comment to be correct. The NRC staff modified the safety evaluation accordingly. This modification has no bearing on the conclusions of the safety evaluation.</p>

17	Table 4	<p>For "RPVHPNs with EDY < 8 years":</p> <p><i>"Performed in the second RFO after peening if RPVHPN contains no flaw(s).</i></p> <p><i>Performed in the first and second refueling outage (RFO) after peening if RPVHPN contains flaw(s)"</i></p>	<p>This requirement of the draft SE is an unclear restatement of Condition 5.4 as written, and thus clarification is needed. The wording "contain flaw(s)" in Condition 5.4 is interpreted that the additional follow-up exam is only required for individual nozzle(s) that contain flaws that were not removed during a previous repair.</p>	<p>The NRC staff finds this comment to be an issue of fact. The NRC staff finds the comment concerning conflict between Condition 5.4 and Table 4 to be correct. The NRC staff finds the comment concerning follow up examinations for RPVHPNs with flaws to be inconsistent with regulation, code case N-729, and the NRC staff's intent for the condition and Table 4. The NRC staff clarified Condition 5.4 and Table 4 in the safety evaluation.</p>
----	---------	--	--	--

RECORD OF REVISIONS

Revision Number	Revision
MRP-335R3	<i>Original Report (MRP-335R3)</i>
MRP-335R3-A	<p><i>This report as originally published (MRP-335R3) was revised to incorporate changes provided by the MRP as recommended in the NRC Safety Evaluation (SE). All changes, except corrections to typographic errors, are marked with margin bars and summarized below. In accordance with a NRC request, the SE is included in the report and the report number includes an "A" indicating the version of the report accepted by the NRC staff.</i></p> <p>Abstract: <i>Included several editorial changes. These editorial changes do not change the meaning of the text.</i></p> <p>Executive Summary: <i>Added to reflect latest EPRI Report Guidelines. This new section only summarizes the existing report content.</i></p> <p>Record of Revisions: <i>Added to reflect changes from MRP-335R3.</i></p> <p>Section 1.2: <i>A minor editorial wording change was made for clarity. This editorial change does not change the meaning of the text.</i></p> <p>Table 1-1: <i>Updated Summary of Requirements for Section 3.9, Section 4.2.5.3, and 4.3.5.4 to reflect NRC Condition 5.2. Updated Summary of Requirements for Table 4-2 and Table 4-4 to reflect NRC Conditions 5.1, 5.2, 5.3, and 5.4.</i></p> <p>Section 2.5.3: <i>Included separate discussion for follow-up examinations for peened DMWs operating at reactor hot-leg temperatures above and below 625°F per NRC Condition 5.3.</i></p> <p>Section 2.5.5: <i>Updated discussion to reflect VE frequency of every refueling outage for all plants per NRC Condition 5.1.</i></p> <p>Section 3.6: <i>Updated to ensure that the intention of this section is clear with regard to qualification of ultrasonic testing for examination of peened RPVHPNs.</i></p> <p>Section 3.9: <i>Incorporated NRC Condition 5.2 by including NRC requirements in the case of a wetted surface-connected flaw, an</i></p>

Revision Number	Revision
	<p><i>unacceptable flaw based on Section XI of the ASME Code, or observation of unacceptable flaw growth.</i></p> <p>Section 4.2.3: <i>Included separate requirements for peened DMWs operating at hot-leg temperatures above and below 625°F per NRC Condition 5.3.</i></p> <p>Section 4.2.5: <i>Incorporated NRC Condition 5.2 by including NRC requirements in the case of a wetted surface-connected flaw, an unacceptable flaw based on Section XI of the ASME Code, or observation of unacceptable flaw growth. This section was also split into several subsections.</i></p> <p>Table 4-1: <i>Included separate requirements for peened DMWs operating at hot-leg temperatures above and below 625°F per NRC Condition 5.3.</i></p> <p>Table 4-2: <i>Updated reference to Section 4.2.5 to incorporate NRC Condition 5.2. Corrected references to -3132 of ASME Code Case N-770-1.</i></p> <p>Section 4.3.3: <i>Defined follow-up examinations for plants where RVPHPNs and associated J-groove welds in the reactor vessel head have experienced EDY<8 as per NRC Condition 5.4.</i></p> <p>Section 4.3.4: <i>Updated requirements to reflect VE frequency of every refueling outage for all plants per NRC Condition 5.1.</i></p> <p>Section 4.3.5: <i>Incorporated NRC Condition 5.2 by including NRC requirements in the case of a wetted surface-connected flaw, an unacceptable flaw based on Section XI of the ASME Code, or observation of unacceptable flaw growth. This section was also split into several subsections.</i></p> <p>Table 4-3: <i>Incorporated NRC Conditions 5.1 and 5.4.</i></p> <p>Table 4-4: <i>Updated reference to Section 4.3.5 to incorporate NRC Condition 5.2.</i></p> <p>Section 5.1: <i>Added wording to clarify the modeled stress conditions in the deterministic analyses and deterministic matrix for RPVHPNs subsequent to peening.</i></p> <p>Section 5.2.3.2: <i>Added wording to clarify the modeled stress condition in the deterministic matrix for RPVHPNs subsequent to peening.</i></p> <p>Section 7: <i>References [66] and [67] were updated due to revisions made in Section 3.6.</i></p> <p>Throughout Report: <i>Mentions of ASME Code Case N-729-5 were updated to also include ASME Code Case N-729-6, to reflect the latest revision of the code case. These code cases are not currently approved by NRC.</i></p>

ACRONYMS

AEF	Average Ejection Frequency
AHA	Auxiliary Head Adapter
ALF	Average Leakage Frequency
ASME	American Society of Mechanical Engineers
AWJ	Abrasive Water Jet
BAC	Boric Acid Corrosion
BMV	Bare Metal Visual
BPVC	[ASME] Boiler and Pressure Vessel Code
BWR	Boiling Water Reactor
CCDP	Conditional Core Damage Probability
CE	Combustion Engineering
CEDM	Control Element Drive Mechanism
CFR	Code of Federal Regulations
CGR	Crack Growth Rate
CPE	Cumulative Probability of Ejection
CPL	Cumulative Probability of Leakage
CRDM	Control Rod Drive Mechanism
DEI	Dominion Engineering, Inc.
DM	Dissimilar Metal [Weld]
DMW	Dissimilar Metal Weld
EDY	Effective Degradation Year
EFPY	Effective Full Power Year
EOC	End of Cycle
EPRI	Electric Power Research Institute
ET	Eddy Current Testing

FEA	Finite Element Analysis
ICI	In-Core Instrumentation
ID	Inner Diameter
IEF	Incremental Ejection Frequency
ILF	Incremental Leakage Frequency
ISI	In-Service Inspection
LP	Laser Peening
MC	Monte Carlo
MLE	Maximum Likelihood Estimator
MRP	[EPRI] Materials Reliability Program
NDE	Non-Destructive Examination
NRC	Nuclear Regulatory Commission
OD	Outer Diameter
PDI	Performance Demonstration Initiative
POD	Probability of Detection
PPRS	Post-Peening Residual Stress
PT	[Liquid] Penetrant Testing
PWR	Pressurized Water Reactor
PWSCC	Primary Water Stress Corrosion Cracking
QA	Quality Assurance
QC	Quality Control
RAI	Request for Additional Information
RCP	Reactor Coolant Pump
RIY	Re-Inspection Years, parameter defined by ASME Code Case N-729-1
RPVH	Reactor Pressure Vessel Head
RPVHPN	Reactor Pressure Vessel Head Penetration Nozzle
RVIN	Reactor Vessel Inlet Nozzle
RVON	Reactor Vessel Outlet Nozzle
SCC	Stress Corrosion Cracking
SSI	Surface Stress Improvement
TW	Through-Wall

UT	Ultrasonic Testing
VE	Direct visual examination of the external metal surface for evidence of leakage, as defined by ASME Code Case N-770-1 for Alloy 82/182 piping butt welds and ASME Code Case N-729-1 for reactor vessel upper heads
VT-2	Visual examination meeting the requirements of ASME Section XI IWA-2212
WJP	Water Jet Peening
WRC	Welding Research Council
WRS	Welding Residual Stress
xLPR	<u>E</u> xtremely <u>L</u> ow <u>P</u> robability of <u>R</u> upture [Software]
XRD	X-Ray Diffraction

CONTENTS

ACKNOWLEDGMENTS	III
ABSTRACT	V
EXECUTIVESUMMARY.....	VII
NRC SAFETY EVALUATION.....	IX
RECORD OF REVISIONS	LXVII
ACRONYMS	LXIX
CONTENTS	LXXIII
LIST OF FIGURES	LXXXIII
LIST OF TABLES	XCI
1 INTRODUCTION	1-1
1.1 Objective	1-1
1.2 Background.....	1-1
1.3 Approach	1-2
1.4 Locations and Peening Methods Addressed	1-3
1.5 Peening Requirements	1-3
1.6 Report Organization.....	1-5
2 BASES FOR PERFORMANCE CRITERIA	2-1
2.1 Quality Assurance Considerations.....	2-1
2.2 ASME Code Considerations Regarding Limitations on Peening and Need for Post-Peening Stress Relief	2-1
2.3 Magnitude, Depth, and Coverage of Compressive Stresses	2-2
2.3.1 Magnitude of Compressive Stresses	2-2
2.3.2 Compressive Stress Depth	2-2

2.3.3	Peening Coverage	2-4
2.3.4	Inhibition of PWSCC Initiation	2-6
2.3.4.1	Basis for Tensile Stress Threshold for PWSCC Initiation.....	2-7
2.3.4.1.1	Assessment of Laboratory PWSCC Initiation Data	2-7
2.3.4.1.2	Yield Strength for PWR Plant Applications of Alloys 600/82/182	2-10
2.3.4.1.3	Conclusion.....	2-10
2.3.5	Modeling of PWSCC Propagation.....	2-11
2.3.6	Characterizing Uncertainty in Residual Stress Measurements	2-11
2.4	Sustainability of Compressive Stresses for Plant Lifetime	2-12
2.5	Inspections and Inspectability of Peened Components	2-12
2.5.1	Pre-Peening Inspection.....	2-12
2.5.2	Follow-Up Inspection(s)	2-13
2.5.3	In-Service Inspections.....	2-13
2.5.4	Surface Examination Requirements.....	2-13
2.5.5	Benefit of the Requirement for Ongoing Visual Examinations for Evidence of Pressure Boundary Leakage of Top Head Nozzles	2-14
2.5.5.1	VT-2 Inspection Criteria	2-15
2.5.5.2	Technical Bases Supporting Increased VE Intervals for Cold Head Units.....	2-16
2.6	Verification of No Adverse Effects	2-18
3	EFFECTIVENESS OF CANDIDATE PEENING PROCESSES.....	3-1
3.1	Process Overview and Key Process Application Variables	3-1
3.2	Process Field Experiences	3-2
3.3	Attaining the Requisite Stress Improvement Effect.....	3-3
3.3.1	Geometric Limitations to Peening Process Application.....	3-3
3.3.2	Surface Condition Considerations.....	3-3
3.3.3	Effect of Pre-Peening Stress.....	3-4
3.4	Coverage Verification	3-5
3.5	Sustainability of the Stress Effect	3-5
3.6	Inspectability After Peening	3-6
3.7	Assessment of Potential Crack Growth During Operation after Peening.....	3-7
3.8	Basis for No Adverse Effects	3-7
3.9	Corrective Action Programs.....	3-8
4	EXAMINATION REQUIREMENTS.....	4-1

4.1	Summary of Technical Basis and Current Requirements for In-Service Examinations for Unmitigated Alloy 600/82/182 Components	4-2
4.1.1	Dissimilar Metal Butt Welds (DMWs) in Primary System Piping	4-2
4.1.2	Reactor Pressure Vessel Head Penetration Nozzles (RPVHPNs)	4-3
4.2	Requirements for Dissimilar Metal Butt Welds (DMWs) in Primary System Piping Mitigated by Peening.....	4-4
4.2.1	Summary of Performance Criteria of Section 4.2.8.....	4-4
4.2.2	Pre-Peening Inspection.....	4-5
4.2.3	Follow-Up Inspection.....	4-5
4.2.4	Subsequent ISI Program.....	4-5
4.2.5	Examination Coverage and Acceptance Criteria for Inspection Results.....	4-6
4.2.5.1	Examination Coverage	4-6
4.2.5.2	Acceptance Criteria for Item L of Table 4-1.....	4-6
4.2.5.3	Requirements for DMWs Subsequent to Flaw Detection or Observation of Flaw Growth	4-6
4.2.5.4	Requirement per 10 CFR 50.55a(g)(6)(ii)(F)(6)	4-7
4.2.6	NDE Qualification Requirements	4-7
4.2.7	Inspection Expansion	4-7
4.2.8	APPENDIX: Performance Criteria and Measurement or Quantification Criteria for Mitigation by Surface Stress Improvement (Peening) of Alloy 82/182 Piping Butt Welds in PWR Primary System Piping.....	4-8
4.2.8.1	Stress Effect.....	4-8
4.2.8.1.1	Magnitude of Surface Stress	4-9
4.2.8.1.2	Nominal Depth of Compressive Residual Stress.....	4-9
4.2.8.2	Sustainability	4-9
4.2.8.3	Inspectability	4-10
4.2.8.3.1	UT Inspectability	4-10
4.2.8.3.2	ET Inspectability	4-10
4.2.8.4	Lack of Adverse Effects.....	4-10
4.2.8.5	UT Qualification.....	4-10
4.2.8.6	Pre-Peening UT and ET	4-10
4.3	Requirements for Reactor Pressure Vessel Head Penetration Nozzles (RPVHPNs) Mitigated by Peening.....	4-14
4.3.1	Summary of Performance Criteria of Section 4.3.8.....	4-14
4.3.2	Pre-Peening Baseline Inspection	4-15
4.3.3	Follow-Up Inspection.....	4-15

4.3.4	Subsequent ISI Program.....	4-16
4.3.5	Examination Coverage and Acceptance Criteria for Inspection Results.....	4-16
4.3.5.1	Examination Coverage	4-16
4.3.5.2	Acceptance Criteria for Item B4.50 of Table 4-3	4-16
4.3.5.3	Acceptance Criteria for Item B4.60 of Table 4-3	4-17
4.3.5.4	Requirements for RPVHPNs Subsequent to Flaw Detection or Observation of Flaw Growth	4-17
4.3.6	NDE Qualification Requirements	4-17
4.3.7	Previously Repaired Top Head Nozzles Mitigated by Peening.....	4-18
4.3.8	APPENDIX: Performance Criteria and Measurement or Quantification Criteria for Mitigation by Surface Stress Improvement (Peening) of PWR Reactor Vessel Upper Head Penetrations and Attachment Welds	4-18
4.3.8.1	Stress Effect.....	4-19
4.3.8.1.1	Magnitude of Surface Stress	4-19
4.3.8.1.2	Nominal Depth of Compressive Residual Stress.....	4-20
4.3.8.2	Sustainability	4-20
4.3.8.3	UT Inspectability.....	4-20
4.3.8.4	Lack of Adverse Effects.....	4-20
4.3.8.5	NDE Qualification.....	4-21
5	SUPPORTING ANALYSES.....	5-1
5.1	Approach	5-1
5.2	Deterministic Analysis of Peening Effects.....	5-2
5.2.1	Effect of Peening on Stress Profile	5-2
5.2.2	Crack Growth	5-5
5.2.2.1	Dissimilar Metal Welds (DMWs).....	5-6
5.2.2.2	Reactor Pressure Vessel Head Penetration Nozzles (RPVHPNs).....	5-17
5.2.3	Deterministic Matrix of Crack Growth Rate Calculations	5-28
5.2.3.1	Dissimilar Metal Welds (DMWs).....	5-29
5.2.3.2	Reactor Pressure Vessel Head Penetration Nozzles (RPVHPNs).....	5-40
5.2.4	Validation Study for the Weight Function Method Stress Intensity Factor Calculation.....	5-52
5.3	Probabilistic Analysis of Peening Effects	5-53
5.3.1	Dissimilar Metal Welds (DMWs).....	5-53
5.3.1.1	Follow-Up and ISI Examination Intervals	5-53
5.3.1.2	Modeling and Inspection Scheduling Sensitivity Cases	5-54

5.3.2	Reactor Pressure Vessel Head Penetration Nozzles (RPVHPNs)	5-54
5.3.2.1	Follow-Up and ISI Examination Intervals	5-54
5.3.2.2	Modeling and Inspection Scheduling Sensitivity Cases	5-56
5.4	Conclusions	5-61
6	CONCLUSIONS	6-1
6.1	Bases for Effectiveness of Peening	6-1
6.2	Bases for Appropriate Relaxation of Inspection Requirements After Peening	6-2
6.3	Application-Specific Information Supporting Inspection Relief	6-3
6.4	Consideration for Pre-Mobilization	6-4
7	REFERENCES	7-1
 A PROBABILISTIC ASSESSMENT CASES FOR ALLOY 82/182 DISSIMILAR METAL WELDS IN PRIMARY SYSTEM PIPING		
A.1	Scope of Assessment	A-1
A.2	Probabilistic Modeling Methodology	A-1
A.3	Load and Stress Model	A-8
A.3.1	Internal Pressure and Piping Loads	A-8
A.3.2	Welding Residual Stress Before Peening	A-10
A.3.3	Residual Stress After Peening	A-11
A.3.4	Effect of Operating Temperature and Load Cycling	A-14
A.3.5	Summary of Load Model	A-15
A.4	Crack Initiation Model	A-15
A.4.1	Spatial Discretization of Crack Sites	A-16
A.4.2	Initiation Time for First Crack	A-16
A.4.3	Initiation Time for Multiple Cracks	A-17
A.4.4	Crack Initialization	A-18
A.5	Crack Growth Model	A-19
A.5.1	Stress Intensity Factor Calculation Using Influence Coefficient Method	A-20
A.5.2	Stress Intensity Factor Calculation Using the Weight Function Method	A-21
A.5.3	MRP-115 Crack Growth Rate Model for Alloy 82/182	A-23
A.5.4	Special Considerations for Crack Growth on a DM Butt Weld Geometry	A-24
A.5.5	Special Considerations for Crack Growth on a Peened Surface	A-26
A.6	Examination Model	A-29
A.6.1	Examination Scheduling	A-29

A.6.2	Inspection Modeling	A-30
A.6.3	Detection and Repair Modeling	A-31
A.7	Through-Wall Flaw (Leakage) Criterion	A-31
A.8	Probabilistic Model Inputs	A-32
A.8.1	Component Geometry, Operating Time, Temperature, and Loads	A-32
A.8.1.1	Component Geometry	A-33
A.8.1.2	Operating Time	A-33
A.8.1.3	Temperature	A-33
A.8.1.4	Loads	A-33
A.8.2	Crack Initiation Model	A-36
A.8.2.1	Industry Inspection Data used to Develop Initiation Model	A-36
A.8.2.2	Weibull Fitting Procedure for Time of First Initiation	A-37
A.8.2.3	Analysis Results for Time of First Initiation	A-39
A.8.2.4	Uncertainty in First Initiation Time Weibull Slope	A-39
A.8.2.5	Uncertainty in Anchor Point Time (t_1)	A-39
A.8.2.6	Uncertainty in the Multiple Flaw Weibull Model	A-40
A.8.2.7	Uncertainty in Flaw Orientation	A-40
A.8.2.8	Uncertainty in Initial Flaw Depth	A-40
A.8.2.9	Uncertainty in Flaw Aspect Ratio	A-41
A.8.2.10	Uncertainty in Temperature Effect	A-41
A.8.3	Crack Growth Model	A-46
A.8.3.1	Empirical Growth Parameters	A-46
A.8.3.2	Growth Variation Factors	A-46
A.8.3.3	Uncertainty in Temperature Effect	A-47
A.8.3.4	Correlation in Relating Flaw Initiation and Propagation	A-47
A.8.3.5	Crack Coalescence Factor	A-47
A.8.4	Flaw Inspection and Detection Model	A-50
A.8.4.1	Examination Scheduling	A-50
A.8.4.2	UT Probability of Detection	A-50
A.8.5	Effect of Peening on Residual Stress	A-51
A.8.5.1	Peening Application Scheduling	A-51
A.8.5.2	Post-Peening Residual Stresses	A-51
A.8.5.3	Thermal and Load Cycling	A-52
A.8.5.4	Effect of Peening on Growth	A-53
A.9	Results of Probabilistic Cases	A-54

A.9.1	Results for the Unmitigated Case	A-55
A.9.2	Results with Peening Mitigation	A-56
A.9.3	Results for Sensitivity Cases.....	A-56
A.10	Conclusions Regarding Appropriate In-Service Examination Requirements for DMWs in Primary System Piping Mitigated by Peening.....	A-77
A.11	References.....	A-78

B	PROBABILISTIC ASSESSMENT CASES FOR REACTOR PRESSURE VESSEL HEAD PENETRATION NOZZLES (RPVHPNS).....	B-1
B.1	Scope of Assessment	B-1
B.1.1	CRDM and CEDM Nozzles	B-1
B.1.2	Other RPVHPNs	B-1
B.2	Overall Modeling Methodology	B-3
B.2.1	Probabilistic Modeling Methodology.....	B-4
B.2.2	Definition of RPVHPN Cracking Modes	B-9
B.3	Load and Stress Model	B-11
B.3.1	Internal Pressure and Piping Loads	B-11
B.3.2	Welding Residual Stress Before Peening	B-12
B.3.3	Residual Stress After Peening	B-13
B.3.4	Effect of Operating Temperature and Load Cycling.....	B-14
B.3.5	Summary of Load Model.....	B-14
B.4	Crack Initiation Model	B-17
B.4.1	Spatial Discretization of Crack Sites	B-17
B.4.2	Initiation Time of First Crack	B-17
B.4.3	Initiation Times of Multiple Cracks	B-18
B.4.4	Crack Initialization	B-19
B.5	Crack Growth Model	B-19
B.5.1	Stress Intensity Factor Calculation Using Influence Coefficient Method.....	B-20
B.5.2	Stress Intensity Factor Calculation Using Weight Function Method	B-20
B.5.3	Stress Intensity Factor Calculation for Through-Wall Axial Cracks.....	B-21
B.5.4	Stress Intensity Factor Calculation for Through-Wall Cracks on the Weld Contour (i.e. Circumferential Cracks)	B-21
B.5.5	MRP-115 Crack Growth Rate Model for Alloy 82/182 (weld) and MRP-55 Crack Growth Rate Model for Alloy 600 (tube).....	B-22
B.5.6	Special Considerations for Crack Growth on RPVHPNs	B-23
B.5.7	Special Considerations for Crack Growth on a Peened Surface	B-24

B.6	Examination Model	B-25
B.6.1	Examination Scheduling.....	B-25
B.6.2	Inspection Modeling	B-26
B.6.3	Detection and Repair Modeling.....	B-27
B.7	Nozzle Ejection Criterion.....	B-27
B.8	Probabilistic Model Inputs	B-27
B.8.1	Reactor Vessel Head Geometry, Operating Time, Temperature, and Loads	B-28
B.8.1.1	Component Geometry.....	B-28
B.8.1.2	Operating Time	B-29
B.8.1.3	Temperature	B-29
B.8.1.4	Operational Loads.....	B-29
B.8.1.5	Welding Residual Stresses	B-30
B.8.2	Crack Initiation Model.....	B-41
B.8.2.1	Industry Inspection Data used to Develop Initiation Model	B-41
B.8.2.2	Weibull Fitting Procedure for Average Time of First Initiation.....	B-41
B.8.2.3	Analysis Results for Average Time of First Initiation.....	B-41
B.8.2.4	Uncertainty in First Initiation Time Weibull Slope.....	B-41
B.8.2.5	Uncertainty in Anchor Point Time (t_1).....	B-42
B.8.2.6	Uncertainty in the Multiple Flaw Weibull Slope	B-42
B.8.2.7	Uncertainty in Initial Flaw Location	B-42
B.8.2.8	Uncertainty in Initial Flaw Depth	B-43
B.8.2.9	Uncertainty in Flaw Aspect Ratio	B-43
B.8.2.10	Uncertainty in Temperature Effect	B-43
B.8.3	Crack Growth Model	B-51
B.8.3.1	Empirical Growth Parameters	B-51
B.8.3.2	Growth Variation Factors	B-51
B.8.3.3	Uncertainty in Temperature Effect	B-52
B.8.3.4	Correlation in Relating Flaw Initiation and Propagation	B-52
B.8.4	Flaw Inspection and Detection Model	B-56
B.8.4.1	Examination Scheduling	B-56
B.8.4.2	UT Probability of Detection	B-57
B.8.4.3	BMV Probability of Detection	B-57
B.8.5	Effect of Peening on Residual Stress.....	B-59
B.8.5.1	Peening Application Scheduling	B-59

B.8.5.2	Post-Peening Residual Stresses	B-59
B.8.5.3	Effect of Thermal and Load Cycling.....	B-60
B.8.5.4	Effect of Peening on Growth.....	B-60
B.8.6	Flaw Stability Model	B-60
B.9	Results of Probabilistic Cases	B-64
B.9.1	Results for the Unmitigated Case	B-65
B.9.2	Results with Peening Mitigation	B-66
B.9.3	Results for Sensitivity Cases.....	B-67
B.10	Conclusions Regarding Appropriate In-Service Examination Requirements for RPVHPNs Mitigated by Peening.....	B-94
B.11	References	B-96

C	TENSILE BALANCING STRESSES IN RESIDUAL STRESS PROFILE IN RESPONSE TO PEENING.....	C-1
C.1	Introduction	C-1
C.1.1	Deformation and Tensile Stress Response of Components to Peening	C-1
C.1.2	Purpose and Approach	C-1
C.1.3	Relevant Literature.....	C-2
C.2	ANSYS Model Description	C-3
C.2.1	Material Properties	C-4
C.2.2	Geometry	C-4
C.2.3	Boundary Conditions.....	C-5
C.2.4	Loading	C-6
C.3	ANSYS Model Cases.....	C-9
C.4	ANSYS Model Results	C-10
C.4.1	Validation of Exponential Form of Stress Source Function.....	C-10
C.4.2	Calculated Stress Profiles for Flat Plate and Thick-Wall Pipe Geometries	C-11
C.5	Model Validation Using Bilinear Stress Profile.....	C-19
C.6	Conclusions	C-21
C.7	References	C-22

LIST OF FIGURES

Figure 2-1 Distance Below Weld Toe on Nozzle Tube Where Stresses Remain Below 20 ksi Tensile	2-6
Figure 2-2 Example #1 of Boric Acid Deposits Observed During EPRI Mockup Testing: Leak Rate of 0.01 gpm (Duration of 32 Days) [60]	2-17
Figure 2-3 Example #2 of Boric Acid Deposits Observed During EPRI Mockup Testing: Leak Rate of 0.1 gpm (Duration of 29 Days) [59]	2-17
Figure 4-1 Required Peening Coverage Zone for RPVHPNs with Incidence Angle, θ , \leq 30 deg (Except Head Vent Nozzles) and for All RPVHPNs with Outer Diameter \geq 4.5 in. (115 mm)	4-24
Figure 4-2 Required Peening Coverage Zone for RPVHPNs with Incidence Angle, θ , $>$ 30 deg and Outer Diameter Less Than 4.5 in. (115 mm)	4-25
Figure 4-3 Required Peening Coverage Zone for J-Groove Head Vent Nozzles	4-26
Figure 4-4 Required Peening Coverage Zone for RPVHPNs with Outer Diameter \geq 4.5 in. (115 mm) for Which the End of the Nozzle is Parallel with the Head	4-27
Figure 5-1 Example Bounding Post-Peening Stress Profile for Circumferential Crack in a DMW Component	5-4
Figure 5-2 Example Bounding Post-Peening Stress Profile near Surface of Circumferential Crack in a DMW Component	5-5
Figure 5-3 Example of Crack Front Shapes Predicted in a Peened Component with: a) FEA, b) Classical Analytical Methods, or c) the Balloon Growth Approximation	5-10
Figure 5-4 Through-Wall Fraction vs. Time for Circumferential Crack on Unmitigated and Peened Component ($a_0/t=10\%$ [7.0 mm] and $2c_0/a_0=8.5$)	5-10
Figure 5-5 Through-Wall Fraction vs. Time for Axial Crack on Unmitigated and Peened Component ($a_0/t=10\%$ [7.0 mm] and $2c_0/a_0=4.5$)	5-11
Figure 5-6 Through-Wall Fraction vs. Time for Circumferential Crack on Unmitigated and Peened Component ($a_0/t=1.3\%$ [0.9 mm] and $2c_0/a_0=8.5$)	5-11
Figure 5-7 Stress Intensity Factor vs. Through-Wall Fraction for Circumferential Crack on Unmitigated and Peened Component ($a_0/t=1.3\%$ [0.9 mm] and $2c_0/a_0=8.5$)	5-12
Figure 5-8 Through-Wall Fraction vs. Time for Axial Crack on Unmitigated and Peened Component ($a_0/t=1.3\%$ [0.9 mm] and $2c_0/a_0=4.5$)	5-12
Figure 5-9 Time to Through-Wall Growth vs. Initial Crack Depth for Circumferential Cracks ($2c_0/a_0=8.5$)	5-13
Figure 5-10 Figure 5-9 (Circumferential Cracks with $2c_0/a_0=8.5$) Replotted Using Log-Scale Abscissa	5-13
Figure 5-11 Time to Through-Wall Growth vs. Initial Crack Depth for Axial Cracks (Log-Scale Abscissa and $2c_0/a_0=4.5$)	5-14

Figure 5-12 Comparing Differences due to Initial Aspect Ratio: Time to Through-Wall Growth vs. Initial Crack Depth for Circumferential Cracks	5-14
Figure 5-13 Time to Through-Weld Growth vs. Initial Crack Depth for Circumferential Crack on a RVIN ($T=563^{\circ}\text{F}$ and $2c_0/a_0=8.5$).....	5-15
Figure 5-14 Time to Through-Weld Growth vs. Initial Crack Depth for Circumferential Crack Subject to Example Representative Peening Compressive Residual Stresses ($2c_0/a_0=8.5$)	5-15
Figure 5-15 Time to Through-Weld Growth vs. Initial Crack Depth for Axial Crack Subject to Example Representative Peening Compressive Residual Stresses ($2c_0/a_0=4.5$)	5-16
Figure 5-16 Comparison of Stress Profiles used in Peening Stress Balance Study for Circumferential Cracking	5-16
Figure 5-17 Comparing Differences due to Concentration of Force Balance: Time to Through-Wall Growth vs. Initial Crack Depth for Circumferential Cracks.....	5-17
Figure 5-18 Through-Wall Percentage vs. Time for Uphill ID Axial Crack on Unmitigated and Peened Component ($a_0/t=1\%$ [0.16 mm] and $2c_0/a_0=4.5$)	5-21
Figure 5-19 Half-Length along Nozzle Surface vs. Time for Uphill OD Axial Crack on Unmitigated and Peened Component ($a_0/t=10\%$ [1.6 mm] and $2c_0/a_0=4.5$).....	5-21
Figure 5-20 Through-Weld Percentage vs. Time for Downhill Weld Radial Crack on Unmitigated and Peened Component ($a_0/t=5\%$ [1.2 mm] and $2c_0/a_0=4.5$).....	5-22
Figure 5-21 Time to Through-Wall Growth vs. Initial Crack Depth for Axial Crack on Uphill Penetration Nozzle ID (Log-Scale Abscissa, $2c_0/a_0=4.5$)	5-22
Figure 5-22 Time to Through-Wall Growth vs. Initial Crack Depth for Axial Crack on Downhill Penetration Nozzle ID (Log-Scale Abscissa, $2c_0/a_0=4.5$)	5-23
Figure 5-23 Time to OD Nozzle Annulus vs. Initial Crack Depth for Axial Crack on Uphill Penetration Nozzle OD ($2c_0/a_0=4.5$).....	5-23
Figure 5-24 Time to OD Nozzle Annulus vs. Initial Crack Depth for Axial Crack on Downhill Penetration Nozzle OD ($2c_0/a_0=4.5$)	5-24
Figure 5-25 Time to Through-Weld Growth vs. Initial Crack Depth for Weld Radial Crack on Uphill J-Groove Weld ($2c_0/a_0=4.5$)	5-24
Figure 5-26 Time to Through-Weld Growth vs. Initial Crack Depth for Weld Radial Crack on Downhill J-Groove Weld ($2c_0/a_0=4.5$).....	5-25
Figure 5-27 Time to Through-Weld Growth vs. Initial Crack Depth for Weld Crack on Downhill J-Groove Weld on a Cold Head RPVHPN ($2c_0/a_0=4.5$)	5-25
Figure 5-28 Time to Through-Weld Growth vs. Initial Crack Depth for Axial Crack on Uphill Penetration Nozzle ID Subject to More Compressive Peening Residual Stress Profile ($2c_0/a_0=4.5$)	5-26
Figure 5-29 Time to Through-Weld Growth vs. Initial Crack Depth for Weld Crack on Uphill Penetration Nozzle OD Subject to More Compressive Peening Residual Stress Profile ($2c_0/a_0=4.5$)	5-26
Figure 5-30 Time to Through-Weld Growth vs. Initial Crack Depth for Weld Crack on Downhill J-Groove Weld Subject to More Compressive Peening Residual Stress Profile ($2c_0/a_0=4.5$)	5-27
Figure 5-31 Half-Length along Nozzle Surface vs. Time for Uphill OD Axial Crack on Unmitigated and Peened Component Subject to More Compressive Peening Residual Stress Profile ($a_0/t=40\%$ [6.3 mm] and $2c_0/a_0=4.5$)	5-27

Figure 5-32 Circumferential Crack Length vs. Time for Through-Wall Cracks Along the Weld Contour for a Head Temperature of 605°F and an Assumed Environmental Crack Growth Factor of 2.0	5-28
Figure 5-33 Low, Median, and High Weld Residual Axial Stress Profiles Applied in Deterministic Matrix for DMWs.....	5-32
Figure 5-34 Low, Median, and High Weld Residual Hoop Stress Profiles Applied in Deterministic Matrix for DMWs.....	5-33
Figure 5-35 Low, Median, and High Pre-Peening Stress Profiles Applied in Deterministic Matrix for RPVHPNs (ID Uphill)	5-43
Figure 5-36 Low, Median, and High Pre-Peening Stress Profiles Applied in Deterministic Matrix for RPVHPNs (ID Downhill).....	5-43
Figure 5-37 Low, Median, and High Pre-Peening Stress Profiles Applied in Deterministic Matrix for RPVHPNs (OD Uphill).....	5-44
Figure 5-38 Low, Median, and High Pre-Peening Stress Profiles Applied in Deterministic Matrix for RPVHPNs (OD Downhill)	5-44
Figure 5-39 Results of Stress Intensity Factor Calculation Method Validation Study	5-53
Figure 5-40 Cumulative Probability of Leakage after Hypothetical Time of Peening vs. ISI Frequency for a RVON.....	5-56
Figure 5-41 Average Ejection Frequency after Hypothetical Time of Peening vs. ISI Frequency for Hot Reactor Vessel Head	5-57
Figure 5-42 Cumulative Probability of Leakage after Hypothetical Time of Peening vs. ISI Frequency for Hot Reactor Vessel Head	5-57
Figure 5-43 Cumulative Probability of Leakage for Stress Effect Performance Criteria Sensitivity Cases for RVON	5-58
Figure 5-44 Cumulative Probability of Leakage for Stress Effect Performance Criteria Sensitivity Cases for RVIN	5-58
Figure 5-45 Average Ejection Frequency for Stress Effect Performance Criteria Sensitivity Cases for Hot RPVHPN	5-59
Figure 5-46 Average Ejection Frequency for Stress Effect Performance Criteria Sensitivity Cases for Cold RPVHPN	5-59
Figure 5-47 Average Leakage Frequency for Stress Effect Performance Criteria Sensitivity Cases for Hot RPVHPN	5-60
Figure 5-48 Average Leakage Frequency for Stress Effect Performance Criteria Sensitivity Cases for Cold RPVHPN	5-60
Figure 5-49 Average Ejection Frequency for VE Interval Sensitivity Case for Cold RPVHPN	5-61
Figure A-1 DM Weld Probabilistic Model Flow Chart: Main Loop	A-6
Figure A-2 DM Weld Probabilistic Model Flow Chart: Detail of Time Loop.....	A-7
Figure A-3 Example Post-Peening Residual Stress Profile near Surface of Circumferential Crack in a DMW Component (Repeat of Figure 5-2).....	A-14
Figure A-4 Crack Location Relative to Bending Moment Assumed for Stress Intensity Factor Calculation [12]	A-21
Figure A-5 Example of Configurations Illustrating Impact of Coplanar Flaw Assumption.....	A-25

Figure A-6 Demonstration of Stresses Superposition for Partially Closed Crack	A-28
Figure A-7 Example of “Balloon” Crack Growth over Time Calculated with FEA Crack	A-28
Figure A-8 Example of Crack Front Shapes Predicted in a Peened Component with: a) FEA, b) Classical Analytical Methods, or c) the Balloon Growth Approximation (Repeat of Figure 5-3)	A-29
Figure A-9 Mean Assumed UT Inspection POD Curve for DMW Cracking from the ID	A-31
Figure A-10 Example MLE Weibull Probability Distribution for Alloy 82/182 Piping to Nozzle Butt Welds	A-45
Figure A-11 Result for DM Weld Numerical Study: Distribution of Number of Flaws per Component with at Least a Single Flaw	A-46
Figure A-12 MRP-115 Weld Factor f_{weld} Distribution [11] with Log-Normal Fit for Alloy 82/182/132	A-49
Figure A-13 MRP-115 Within-Weld Factor f_{ww} Distribution [11] with Log-Normal Fit for Alloy 82/182/132	A-49
Figure A-14 Experimental Data used to Estimate Thermal Residual Stress Relaxation Factor	A-53
Figure A-15 Post-Peening Total (Normal Operating Plus Residual) Axial Stress Profile for Circumferential Crack in an Alloy 82/182 Reactor Vessel Primary Nozzle Butt Weld Component (Azimuthal Position of Maximum Global Bending Stress)	A-63
Figure A-16 Prediction of Leakage vs. Time for RVON	A-64
Figure A-17 Prediction of Leakage vs. Time for RVIN	A-64
Figure A-18 Cumulative Probability of Leakage from Hypothetical Time of Peening to End of Operational Service Period vs. ISI Frequency for a RVON	A-65
Figure A-19 Cumulative Probability of Leakage from Hypothetical Time of Peening to End of Operational Service Period vs. ISI Frequency for a RVIN	A-65
Figure A-20 Incremental Leakage Frequency after Peening with Relaxed ISI Intervals	A-66
Figure A-21 Summary for Inspection Scheduling Sensitivity Results for RVON Probabilistic Model with Peening	A-67
Figure A-22 Summary of Model Sensitivity Results for RVON Probabilistic Model with Peening	A-68
Figure A-23 Summary of Model Sensitivity Results for RVON Probabilistic Model with Peening (continued)	A-69
Figure A-24 Summary of Model Sensitivity Results for RVON Probabilistic Model without Peening	A-70
Figure A-25 Summary of Model Sensitivity Results for RVON Probabilistic Model without Peening (continued)	A-71
Figure A-26 Summary for Inspection Scheduling Sensitivity Results for RVIN Probabilistic Model with Peening	A-72
Figure A-27 Summary of Model Sensitivity Results for RVIN Probabilistic Model with Peening	A-73
Figure A-28 Summary of Model Sensitivity Results for RVIN Probabilistic Model with Peening (continued)	A-74

Figure A-29 Summary of Model Sensitivity Results for RVIN Probabilistic Model without Peening	A-75
Figure A-30 Summary of Model Sensitivity Results for RVIN Probabilistic Model without Peening (continued)	A-76
Figure B-1 Summary of General RPVHPN Geometry	B-3
Figure B-2 RPVHPN Probabilistic Model Flow Chart: Main Loop	B-7
Figure B-3 RPVHPN Probabilistic Model Flow Chart: Time Loop	B-8
Figure B-4 Schematic of Modeled Cracking Modes for RPVHPN Probabilistic Assessment (Arrows Indicate Direction of Growth Toward Leakage)	B-10
Figure B-5 Depiction of Stress Profile Vectors for Each Crack Mode Location (six bold dotted lines) and Welding Residual Hoop Stress Contour Plot	B-15
Figure B-6 Scenarios for Excluding Peening Effects in RPVHPNs: a) Crack Extends Below Weld, Past Reduced-Stress Layer (top flaw); b) OD Crack Depth Reaches ID Reduced-Stress Layer (bottom flaw)	B-16
Figure B-7 Modeled Average Stress Intensity Factor vs. Crack Length for a Through-Wall Crack along the J-Groove Weld of a RPVHPN [10]	B-24
Figure B-8 Description of Weld Half-Width	B-25
Figure B-9 Normal Distribution Fit to Geometry Data Varying Across Penetration Nozzle Incidence Angles: Uphill Weld Path Length	B-37
Figure B-10 Normal Distribution Fit to Penetration Nozzle ID Hoop Stress Concentration Factors Predicted by FEA Study	B-37
Figure B-11 Stochastic Family (50 instances) of Curves and FEA Results for the Total Stress Profile between the Penetration Nozzle ID Above the Weld and the Penetration Nozzle OD Above the Weld, Uphill Side	B-38
Figure B-12 Stochastic Family (50 instances) of Curves and FEA Results for the Total Stress Profile between the Penetration Nozzle ID Above the Weld and the Penetration Nozzle OD Above the Weld, Downhill Side	B-38
Figure B-13 Stochastic Family (50 instances) of Curves and FEA Results for the Total Stress Profile between the Penetration Nozzle OD Below the Weld and the Penetration Nozzle ID Below the Weld, Uphill Side	B-39
Figure B-14 Stochastic Family (50 instances) of Curves and FEA Results for the Total Stress Profile between the Penetration Nozzle OD Below the Weld and the Penetration Nozzle ID Below the Weld, Downhill Side	B-39
Figure B-15 Stochastic Family (50 instances) of Curves and FEA Results for the Total Stress Profile between the Weld Center and the Weld Root, Uphill Side	B-40
Figure B-16 Stochastic Family (50 instances) of Curves and FEA Results for the Total Stress Profile between the Weld Center and the Weld Root, Downhill Side	B-40
Figure B-17 Example MLE Weibull Probability Distribution for Alloy 600 RPVHPNs with Alloy 82/182 J-groove Welds	B-48
Figure B-18 Result of RPVHPN Numerical Initiation Study: Distribution of Number of Flaws per Hot Head with at Least a Single Flaw	B-49
Figure B-19 Industry RPVHPN Flaw Initiation Data: Distribution of Normalized Number of Nozzles with PWSCC Indications per Head with at Least a Single Indication (23 Plants)	B-49

Figure B-20 Normal Distribution Fit to 80% Yield Stress Length on Uphill Side of Penetration Predicted by Different FEA Studies	B-50
Figure B-21 Normal Distribution Fit to 80% Yield Stress Length on Downhill Side of Penetration Predicted by Different FEA Studies	B-50
Figure B-22 Alloy 600 Crack Growth Rate Curves: MRP-55 ($K_{Ith}=9$) Curve and MRP-335 ($K_{Ith}=0$) Curve	B-55
Figure B-23 Heat Factor f_{heat} Distribution with Log-Normal Fit for MRP-55 Alloy 600 Data	B-55
Figure B-24 Within-Heat Factor f_{wh} Distribution with Log-Normal Fit for MRP-55 Alloy 600 Data.....	B-56
Figure B-25 Median Assumed UT Inspection POD Curve for Axial Cracking Initiating at the RPVHPN ID and OD	B-59
Figure B-26 Post-Peening Total (Normal Operating Plus Residual) Stress Profile for a Crack Initiating on the ID of an RPVHPN, Uphill Side.....	B-78
Figure B-27 Post-Peening Total (Normal Operating Plus Residual) Stress Profile for a Crack Initiating on the OD of an RPVHPN, Uphill Side.....	B-78
Figure B-28 Post-Peening Total (Normal Operating Plus Residual) Stress Profile for a Crack Initiating on the Weld of an RPVHPN, Uphill Side	B-79
Figure B-29 Post-Peening Total (Normal Operating Plus Residual) Stress Profile for a Crack Initiating on the ID of an RPVHPN, Downhill Side	B-79
Figure B-30 Post-Peening Total (Normal Operating Plus Residual) Stress Profile for a Crack Initiating on the OD of an RPVHPN, Downhill Side	B-80
Figure B-31 Post-Peening Total (Normal Operating Plus Residual) Stress Profile for a Crack Initiating on the Weld of an RPVHPN, Downhill Side	B-80
Figure B-32 Prediction of Ejection vs. Time for Hot RPVHPNs	B-81
Figure B-33 Prediction of Ejection vs. Time for Cold RPVHPNs	B-81
Figure B-34 Prediction of Leakage vs. Time for Hot RPVHPNs	B-82
Figure B-35 Prediction of Leakage vs. Time for Cold RPVHPNs	B-82
Figure B-36 Average Ejection Frequency from Hypothetical Time of Peening to End of Operational Service Period vs. ISI Frequency for Hot Reactor Vessel Head.....	B-83
Figure B-37 Average Ejection Frequency from Hypothetical Time of Peening to End of Operational Service vs. ISI Frequency for Cold Reactor Vessel Head	B-83
Figure B-38 Cumulative Probability of Leakage from Hypothetical Time of Peening to End of Operational Service Period vs. ISI Frequency for Hot Reactor Vessel Head	B-84
Figure B-39 Cumulative Probability of Leakage from Hypothetical Time of Peening to End of Operational Service Period vs. ISI Frequency for Cold Reactor Vessel Head	B-84
Figure B-40 Incremental Frequency of Leakage after Peening with Relaxed ISI Intervals.....	B-85
Figure B-41 Summary for Inspection Scheduling Sensitivity Results for Hot RPVHPN Probabilistic Model with Peening	B-86
Figure B-42 Summary of Model Sensitivity Results for Hot RPVHPN Probabilistic Model with Peening.....	B-87
Figure B-43 Summary of Model Sensitivity Results for Hot RPVHPN Probabilistic Model with Peening (continued).....	B-88

Figure B-44 Summary of Model Sensitivity Results for Hot RPVHPN Probabilistic Model without Peening.....	B-89
Figure B-45 Summary of Model Sensitivity Results for Hot RPVHPN Probabilistic Model without Peening (continued).....	B-90
Figure B-46 Summary for Inspection Scheduling Sensitivity Results for Cold RPVHPN Probabilistic Model with Peening	B-91
Figure B-47 Summary of Model Sensitivity Results for Cold RPVHPN Probabilistic Model with Peening.....	B-92
Figure B-48 Summary of Model Sensitivity Results for Cold RPVHPN Probabilistic Model without Peening.....	B-93
Figure B-49 Prediction of Nozzle Ejection vs. Time for Hot RPVHPNs with No Crack Detections to Date (Model Sensitivity Study 2)	B-94
Figure C-1 Example Mesh with Region of Application of Stress Source Function in Red (wall thickness = 63.5 mm).....	C-5
Figure C-2 Example Stress Source Function for $\sigma_{p,0} = -558$ MPa (-80.9 ksi) and $\delta_p = 1.09$ mm (0.043 in.)	C-7
Figure C-3 Example Equilibrium Stress Solution Contour Plot for the Length (Y) Direction Stress (SY) for Flat Plate Model (wall thickness = 63.5 mm)	C-8
Figure C-4 Validation of Exponential Form of Stress Source Function Using Through-Wall Stress Profile Measured by Hill et al. [5]	C-11
Figure C-5 Equilibrium Through-Wall Stress Profiles for Flat Plate for Common Stress Source Function	C-14
Figure C-6 Effect of Wall Thickness on Through-Wall Stress Profile for Plate Geometry for Same Equilibrium Surface Compressive Stress and Compressive Depth.....	C-15
Figure C-7 Effect of Wall Thickness on Through-Wall Axial Stress Profile for Constant Outer Diameter Pipe Geometry for Same Equilibrium Surface Compressive Stress and Compressive Depth.....	C-15
Figure C-8 Effect of Wall Thickness on Through-Wall Axial Stress Profile for Constant R_i / t Pipe Geometry for Same Equilibrium Surface Compressive Stress and Compressive Depth.....	C-16
Figure C-9 Effect of Wall Thickness on Through-Wall Hoop Stress Profile for Constant Outer Diameter Pipe Geometry for Same Equilibrium Surface Compressive Stress and Compressive Depth.....	C-16
Figure C-10 Effect of Wall Thickness on Through-Wall Hoop Stress Profile for Constant R_i / t Pipe Geometry for Same Equilibrium Surface Compressive Stress and Compressive Depth.....	C-17
Figure C-11 Effect of Wall Thickness on Peak Tensile Axial Stress for Same Equilibrium Surface Compressive Stress and Compressive Depth	C-17
Figure C-12 Effect of Wall Thickness on Peak Tensile Hoop Stress for Same Equilibrium Surface Compressive Stress and Compressive Depth	C-18
Figure C-13 Effect of Compressive Stress Depth on Through-Wall Axial Stress Profile for RVON Pipe Geometry (Surface Stress Held Constant)	C-18
Figure C-14 ANSYS Model Validation for Profile Measured by Hill et al. [5] Using Bilinear Stress Profile.....	C-20

Figure C-15 ANSYS Model Validation for Reactor Vessel Outlet Nozzle (RVON) Case
Using Bilinear Stress Profile..... C-20

LIST OF TABLES

Table 1-1 Requirements for Peening Mitigation of Alloy 600/82/182 Components in PWRs	1-3
Table 2-1 Evaluation of Stresses at Bottom Edge of Below-Weld Inspection Zone and Distance Below Weld Toe on Nozzle Tube Where Stresses Remain Below 20 ksi Tensile.....	2-5
Table 2-2 PWSCC Initiation Results for Alloy 82/132 for Relatively Small Stress Ratios ([34], [35]).....	2-9
Table 2-3 PWSCC Initiation Results for Alloy 600 for Relatively Small Stress Ratios.....	2-9
Table 2-4 ASME Code Section XI Requirements for VT-2 Visual Inspections [12]	2-15
Table 4-1 Inspection Requirements for Alloy 82/182 DMWs in Primary System Piping Mitigated by Peening.....	4-11
Table 4-2 List of Requirements in Section 4.2 within the Context of N-770-1	4-13
Table 4-3 Inspection Requirements for Alloy 600 RPVHPNs Mitigated by Peening.....	4-22
Table 4-4 List of Requirements in Section 4.3 within the Context of N-729-1	4-23
Table 5-1 Inputs for DMW Deterministic Calculations.....	5-9
Table 5-2 Inputs for RPVHPN Deterministic Calculations	5-20
Table 5-3 Summary of Deterministic Matrix for DMW and RPVHPN Crack Growth Calculations	5-29
Table 5-4 Inspection Schedule for Deterministic Matrix of Crack Growth Cases for Peened and Unpeened DMWs	5-32
Table 5-5 Matrix of Deterministic Crack Growth Calculations for Peened DMWs with Initial Flaw Depth of 0.010 in. (0.25 mm)	5-34
Table 5-6 Matrix of Deterministic Crack Growth Calculations for Peened DMWs with Initial Flaw Depth of 0.020 in. (0.50 mm)	5-35
Table 5-7 Matrix of Deterministic Crack Growth Calculations for Peened DMWs with Initial Flaw Depth of 0.039 in. (1.00 mm)	5-36
Table 5-8 Matrix of Deterministic Crack Growth Calculations for Unmitigated DMWs with Initial Flaw Depth of 0.010 in. (0.25 mm)	5-37
Table 5-9 Matrix of Deterministic Crack Growth Calculations for Unmitigated DMWs with Initial Flaw Depth of 0.020 in. (0.50 mm)	5-38
Table 5-10 Matrix of Deterministic Crack Growth Calculations for Unmitigated DMWs with Initial Flaw Depth of 0.039 in. (1.00 mm)	5-39
Table 5-11 Matrix of Deterministic Crack Growth Calculations for DMWs with Modified Crack Growth Rate Material Variability Factors	5-39
Table 5-12 Inspection Schedule for Deterministic Matrix of Crack Growth Cases for Peened and Unpeened RPVHPNs	5-42

Table 5-13 Matrix of Deterministic Crack Growth Calculations for Peened RPVHPNs with Initial Flaw Depth of 0.010 in. (0.25 mm)	5-45
Table 5-14 Matrix of Deterministic Crack Growth Calculations for Peened RPVHPNs with Initial Flaw Depth of 0.020 in. (0.50 mm)	5-46
Table 5-15 Matrix of Deterministic Crack Growth Calculations for Peened RPVHPNs with Initial Flaw Depth of 0.062 in. (1.58 mm)	5-47
Table 5-16 Matrix of Deterministic Crack Growth Calculations for Unmitigated RPVHPNs with Initial Flaw Depth of 0.010 in. (0.25 mm)	5-48
Table 5-17 Matrix of Deterministic Crack Growth Calculations for Unmitigated RPVHPNs with Initial Flaw Depth of 0.020 in. (0.50 mm)	5-49
Table 5-18 Matrix of Deterministic Crack Growth Calculations for Unmitigated RPVHPNs with Initial Flaw Depth of 0.062 in. (1.58 mm)	5-50
Table 5-19 Matrix of Deterministic Crack Growth Calculations for RPVHPNs with Modified Crack Growth Rate Material Variability Factors.....	5-51
Table A-1 Interpolation and Extrapolation Criteria for Influence Coefficient Lookup.....	A-21
Table A-2 Summary of General Inputs	A-35
Table A-3 Summary of Loading Inputs for DMW Model	A-36
Table A-4 Summary of Inputs for DM Weld Initiation Model	A-42
Table A-5 Summary of PWSCC Experience in U.S. PWR Piping Nozzle Dissimilar Metal Welds	A-44
Table A-6 Summary of PWSCC Experience in U.S. PWR Piping Nozzle Dissimilar Metal Welds Used to Define Initial Flaw Aspect Ratio	A-44
Table A-7 Summary of Weibull Distribution Parameter Fitting Results for DMW Analysis	A-44
Table A-8 Summary of Inputs for DM Weld Flaw Propagation Model	A-48
Table A-9 Summary of Inputs for DM Weld Examination Model.....	A-51
Table A-10 Summary of Peening-Specific Inputs for DM Weld Model	A-54
Table A-11 Description of Modified Inputs for DMW Model Sensitivity Cases.....	A-61
Table A-12 Summary of Modified Inputs for DMW Inspection Scheduling Sensitivity Cases	A-63
Table B-1 Summary of PWSCC Modes Modeled on RPVHPNs	B-10
Table B-2 Summary of General RPVHPN Inputs	B-31
Table B-3 Summary of Weld Geometry Inputs	B-32
Table B-4 Summary of Loading Inputs for RPVHPN Model	B-33
Table B-5 Summary of Inputs for RPVHPN Initiation Model	B-44
Table B-6 Inspection Data Through Fall 2013 Extrapolated Back to Predicted Time to First Crack/Leak (Based on Weibull slope $\beta = 3$) [3].....	B-46
Table B-7 Summary of Weibull Probability Distribution Parameter Fitting for RPVHPN Analysis.....	B-47
Table B-8 Summary of Inputs for RPVHPN Flaw Propagation Model	B-53
Table B-9 Summary of Inputs for RPVHPN Examination Model	B-58
Table B-10 Summary of Peening-Specific Inputs	B-61
Table B-11 Summary of Inputs for RPVHPN Stability Model.....	B-63

Table B-12 Summary of Modified Inputs for RPVHPN Model Sensitivity Cases	B-72
Table B-13 Summary of Modified Inputs for RPVHPN Inspection Scheduling Sensitivity Cases	B-77
Table C-1 Material Properties [9]	C-4

1

INTRODUCTION

1.1 Objective

The objective of this report is to present the technical bases for relaxation of inspection requirements based on the surface stress improvement (SSI) provided by peening applied for the purpose of mitigating primary water stress corrosion cracking (PWSCC). For any peening process meeting the applicable performance criteria, this report specifies appropriate inspection requirements and intervals for Alloy 600 reactor pressure vessel head penetration nozzles (RPVHPNs) and for Alloy 82/182 dissimilar metal butt welds (DMWs¹) in primary system piping that have been treated by SSI methods (that is, peening) for the purpose of mitigating PWSCC. The deterministic and probabilistic calculations herein show that, given an SSI process that meets the applicable performance criteria, relaxation of the inspection intervals for these components is justified after SSI treatment.

Because the inspection requirements for these components are prescribed by NRC regulations (based on ASME Boiler & Pressure Vessel Code Cases), NRC approval is required for relaxation of these inspection requirements following peening mitigation. Licensees may reference this topical report to provide part of the technical basis for site-specific relief requests. The relaxed inspection intervals and the performance criteria are developed to credit the performance of peening within the framework of the respective Code Cases upon which existing inspection requirements are based. This report may also serve as the technical basis for revision of the respective Code Cases to credit peening.

This topical report specifies requirements that apply in the case that relaxation of the applicable inspection requirements for unmitigated components is sought. The requirements of this report are generally not applicable in the case that peening is performed for asset management without request for inspection relief.

1.2 Background

PWSCC has occurred at PWR reactor coolant system DMW piping butt welds made with Alloys 82 and 182 and Alloy 600 RPVHPNs attached to the reactor vessel top head using Alloy 82/182 J-groove welds. In response to this cracking, Code Cases N-770-1 [1] and N-729-1 [2] have been issued by the American Society of Mechanical Engineers (ASME) and establish in-service inspection requirements for these components. These versions of the Code Cases have been made mandatory with conditions by the Nuclear Regulatory Commission (NRC) through 10 CFR 50.55a.³ Later versions of these Code Cases have been prepared but have not as yet been

¹ The term "DMW" is used throughout this report to refer specifically to Alloy 82/182 dissimilar metal butt welds located in PWR primary system piping and falling under the scope of Table 1 of ASME Code Case N-770-1 [1].

³ Code Case N-722-1 [3], which provides requirements for direct visual examinations for evidence of leakage at Alloy 600/82/182 PWR pressure boundary components, has also been made mandatory by NRC with conditions.

accepted by the NRC. Acceptance of this document is not predicated on the review or acceptance of updated versions of these Code Cases, and any mentions of the updated revisions are for information only. The most recent versions of the DMW code case (N-770-4) and of the RPVHPN code case (N-729-5 and N-729-6) cover the situation where PWSCC has been mitigated using surface stress improvement (SSI) by peening.

The inspection intervals specified in ASME Section XI and Code Cases N-770-1 and N-729-1 vary depending on the resistance to PWSCC of the specific component being considered. The intervals for components made with Alloys 600, 82, and/or 182 are the shortest, while intervals for components made with PWSCC-resistant materials are longer. Intervals for components made with Alloys 600, 82, and/or 182 that have had mitigation measures applied are also relaxed as compared to those for unmitigated components. Until relevant NRC regulations (10 CFR 50.55a) have been revised to accept peening as a mitigation method, this topical report may be used on a site-specific basis to request inspection relief from current requirements.

1.3 Approach

The basic approach taken in this report is to determine, through the use of deterministic and probabilistic safety analyses, the inspection requirements and intervals that are appropriate for Alloy 600/82/182 components that have had SSI applied by application of a peening technique meeting the specified performance criteria. The inspection requirements for unmitigated Alloy 600/82/182 PWR pressure boundary components were developed by MRP ([4], [5], [6], [7], [8], [9]) to maintain an acceptably low effect on nuclear safety of the PWSCC concern. These inspection requirements also result in low probability of through-wall cracking and leakage, ensuring defense in depth. The goal of this study was to develop inspection requirements for components mitigated via peening that maintain this acceptably low effect on nuclear safety of the PWSCC concern. As shown by probabilistic analyses, the requirements of this report actually result in an increased nuclear safety margin, plus a large reduction in the probability of leakage occurring. The leakage prevention benefit of peening performed in accordance with the requirements of this report is further demonstrated through a matrix of deterministic crack growth cases. In summary, peening mitigation implemented in accordance with the requirements of this topical report provides a substantial risk benefit for a risk that is already low.

Peening is effective in mitigating PWSCC by preventing PWSCC crack initiation at the treated surfaces. Any pre-existing flaws at the time of peening are addressed through the combination of a pre-peening examination and post-peening examinations. The post-peening examinations specifically address the small range of shallow flaw depths that are too small to be reliably detected during the pre-peening examination. Both deterministic and probabilistic approaches were taken to address the chance that shallow pre-existing flaws are not detected prior to the peening being performed. The deterministic and probabilistic analyses are performed using bounding stress conditions meeting the peening performance criteria.

N-722-1 explicitly does not address RPVHPNs, and the visual examination intervals under N-722-1 are identical to those of N-770-1 for unmitigated Alloy 82/182 piping butt welds. Code Case N-722-2, which was approved by ASME on September 8, 2011, excludes the primary piping Alloy 82/182 butt welds covered by N-770-1, but N-722-1 is the version made mandatory by NRC regulations as of the date of publication of this report.

Consequently, it is appropriate that longer inspection intervals be used for Alloy 600 RPVHPNs and Alloy 82/182 DMWs mitigated by peening in comparison to the current inspection intervals for unmitigated components.

1.4 Locations and Peening Methods Addressed

The inspection requirements in this report apply to any peening process meeting the performance criteria specified in Section 4 at the following locations:

- The inner diameter (ID) surfaces of DMW butt welds in PWR reactor coolant system piping.
- The susceptible surfaces of RPVHPNs:
 - The nozzle ID surfaces of RPVHPNs in the area with high weld residual stresses due to the presence of the J-groove attachment weld.
 - The nozzle outer diameter (OD) surfaces of RPVHPNs in the area with high weld residual stresses due to the presence of the J-groove attachment weld.
 - The J-groove weld surfaces of RPVHPNs, including the surfaces of the Alloy 82/182 weld filler metal and Alloy 82/182 weld butter metal that are normally wetted during operation.

1.5 Peening Requirements

The requirements for peening mitigation of Alloy 600/82/182 components in PWRs are summarized below in Table 1-1. The table includes the section number of the report and section title where requirements are located. These requirements apply in the case that relaxation of the applicable inspection requirements for unmitigated components is sought. These requirements are generally not applicable in the case that peening is performed for asset management without request for inspection relief.

Table 1-1
Requirements for Peening Mitigation of Alloy 600/82/182 Components in PWRs

Report Location	Report Section	Summary of Requirements
Section 2.1	Quality Assurance Considerations	This section requires SSI to be performed in accordance with a quality assurance program meeting the requirements of Appendix B to 10 CFR 50 (including the "Control of Special Processes" criterion) and the utility's plant specific commitments.

Table 1-1 (continued)
Requirements for Peening Mitigation of Alloy 600/82/182 Components in PWRs

Report Location	Report Section	Summary of Requirements
Section 3.9, Section 4.2.5.3, and Section 4.3.5.4	Corrective Action Programs, Requirements for DMWs Subsequent to Flaw Detection or Observation of Flaw Growth, and Requirements for RPVHPNs Subsequent to Flaw Detection or Observation of Flaw Growth	If a wetted surface-connected flaw, an unacceptable flaw based on the Section XI of the ASME Code, or unacceptable flaw growth is observed in a peened DMW, RPVHPN, or J-groove weld, (a) a report summarizing the evaluation, including inputs, methodologies, assumptions, extent of conditions, and causes of the new flaw, unacceptable flaw, or flaw growth, must be submitted to the NRC prior to the plant entering into Mode 4. (b) A sample inspection of the peened components in the population must be performed to assess the extent of condition. (c) A final causal analysis report consistent with the licensee corrective action program including a description of corrective actions taken must be submitted to the NRC within six months of the discovery. (d) The inspection relaxation per this report is no longer applicable to the affected RPVHPN or DMW. The affected RPVHPN or DMW component shall be inspected in accordance with the requirements of 10 CFR 50.55a, unless an alternative is authorized by the NRC.
Table 4-2	List of Requirements in Section 4.2 within the Context of N-770-1	Table 4-2 lists the requirements that are present within Section 4.2 and references Table 4-1. This includes incorporation of NRC Conditions 5.2 and 5.3. Table 4-1 defines the inspection requirements for Alloy 82/182 DMWs before and after application of peening per the performance criteria required by Section 4.2.8. The performance criteria specify the required minimum nominal depth of the compressive residual stress produced by the peening treatment as well as the analyses or demonstrations that are to be performed.
Table 4-4	List of Requirements in Section 4.3 within the Context of N-729-1	Table 4-4 lists the requirements that are present within Section 4.3 and references Table 4-3. This includes incorporation of NRC Conditions 5.1, 5.2, and 5.4. Table 4-3 defines the inspection requirements for RPVHPNs with Alloy 600/82/182 materials before and after application of peening per the performance criteria required by Section 4.3.8. The performance criteria specify the required minimum nominal depth of the compressive residual stress produced by the peening treatment as well as the analyses or demonstrations that are to be performed.
Section 6.3	Application-Specific Information Supporting Inspection Relief	Until NRC has generically approved inspection relief for peening within 10 CFR 50.55a (such as approval of ASME Code Cases N-729-5, N-729-6, or N-770-4), application-specific relief must be approved by NRC before implementing inspection relief for peening. Before implementing the inspection relief defined in Section 4, a relief request shall be submitted for NRC review and approval. This section lists technical information that shall be included in the relief request and lists additional technical information that shall be included in the peening qualification report. This section also requires a post-peening report to be produced documenting the performance of peening.

1.6 Report Organization

This report is organized as follows:

- This Section 1 describes the purpose of the report, the approach used, and how it is organized. It also includes a table identifying the locations where the specific requirements for crediting peening mitigation of Alloy 600/82/182 components in PWRs are located.
- Section 2 describes how the effectiveness of peening as a PWSCC mitigation measure, without adverse effects, is ensured by meeting the performance criteria contained in Section 4. It also provides requirements for the performance of peening under appropriate quality assurance programs.
- Section 3 supports the development of technical bases to demonstrate that peening processes such as those described in MRP-267R1⁴ [10] meet the performance criteria. The extensive test data and experience documented in MRP-267R1 [10] support the effectiveness of the laser peening and water jet (aka cavitation) peening methods described in that report to mitigate PWSCC.
- Section 4 defines appropriate inspection requirements and intervals for use with peening mitigation of Alloy 82/182 dissimilar metal butt welds in PWR primary system piping and Alloy 600 RPVHPNs. Section 4 also specifies the performance criteria that a peening process shall meet to permit use of the relaxed inspection intervals specified in this report.
- Section 5 presents the deterministic and probabilistic analyses that were used to establish appropriate inspection requirements and intervals for Alloy 82/182 DMWs and Alloy 600 RPVHPNs mitigated by peening. The deterministic analyses are based on PWSCC crack growth calculations, and the probabilistic analyses include the key aspects of the PWSCC degradation process including crack initiation, crack growth, and crack detection via NDE.
- Section 6 contains the main conclusions developed by this report. In this regard, this section summarizes the bases for concluding that a peening process meeting the specified performance criteria will be effective as a PWSCC mitigation measure without any adverse effects. It then summarizes the bases that support appropriate relaxation of inspection requirements for components that have been peened. Section 6.3 lists the application-specific information needed to support inspection relief.
- Section 7 lists the references that are cited in the body of this report.
- Appendix A and Appendix B describe detailed probabilistic safety assessments for DMWs and for RPVHPNs, respectively. These assessments show that the risks of leakage and pressure boundary rupture are reduced for mitigated components inspected at certain relaxed intervals in comparison to the risks for unmitigated components inspected at the currently required intervals for unmitigated components.

⁴ MRP-267R2 (EPRI 3002008083) was published in August 2016, subsequent to the NRC review of this report. MRP-267R2 is freely available at www.epri.com. This revision to MRP-267 includes updated and new information from individual peening vendors since MRP-267R1 (published in July 2012), a summary of NDE of peened coupons performed by EPRI, and a summary of additional detailed modeling including modeling of thermal stress relaxation effects for RPVHPNs.

Introduction

- Appendix C presents the methods and results of an investigation of the magnitude and distribution of tensile stresses developed in response to the peening compressive stresses produced at the treated surface. The technical literature on this subject and the analyses presented show that the peak residual tensile balancing stress is relatively small for the thick-wall components that are the subject of this report.

2

BASES FOR PERFORMANCE CRITERIA

This section describes how the effectiveness of peening as a PWSCC mitigation measure without adverse effects is assured by meeting the performance criteria specified in Section 4.2.8 and Section 4.3.8 of this report.

2.1 Quality Assurance Considerations

Since surface stress improvement by peening affects the performance of nuclear safety related systems and components, it shall be performed in accordance with a quality assurance program meeting the requirements of Appendix B to 10 CFR 50 and the utility's plant specific commitments. Further, since peening is a special process, it shall be controlled in a manner consistent with Criterion IX, "Control of Special Processes," of Appendix B and any applicable plant specific commitments. As stated in that criterion, this requires that the personnel and procedures involved need to be appropriately qualified. Since there are no industry standards that apply to peening, these qualifications shall be done to vendor requirements developed and documented per their 10 CFR 50 Appendix B quality assurance program and to utility requirements and commitments applicable at the plant site.

2.2 ASME Code Considerations Regarding Limitations on Peening and Need for Post-Peening Stress Relief

Section III [11] and Section XI [12] of the ASME Code have some limitations on application of peening to welds during the welding process and on the need for stress relief heat treatments after cold forming. As discussed in the following paragraphs, these limitations and requirements are not applicable to peening processes performed for the purpose of surface stress improvement.

Paragraph NB-4422, Peening, in Section III [11], Subsection NB, of the ASME Code reads: "Controlled peening may be performed to minimize distortion. Peening shall not be used on the initial layer, root of the weld metal, or on the final layer unless the weld is post weld heat treated." This limitation in the Code is clearly directed at control of the type of peening that is sometimes used to control distortion during the welding process (while the weld is cooling) [13], and is not applicable to the superficial type of peening being considered here that will be applied on finished parts. This conclusion has been confirmed by the ASME Section III Standards Committee in an inquiry response letter (Interpretation III-1-13-03) dated August 22, 2012 [14]:

"Question (1): Does NB-4422 apply when peening is performed for the purpose of introducing compressive stress on a weld or base metal surface after all welding, heat treating, and examinations have been completed?

Reply (1): No."

IWA-4650, Butter Bead - Temper Bead Welding for Class MC and for Class CC Metallic Liners, Sub-section IWA-4651(g) [12] states that "Controlled peening of welds may be performed to

minimize distortion, provided it is also used on the welds made to qualify the welding procedure and the production test assembly. Peening shall not be used on the initial layer of the weld or on the final layer. If peening is used, it shall be considered as an essential variable in the welding procedure." IWA-4620, Temper Bead Welding of Similar Materials, Sub-section IWA-4621(c) [12] identifies that "Peening may be used except on the initial and final weld layers." These limitations are not applicable to peening for the purpose of SSI for the same reason as Paragraph NB-4422. This conclusion has been confirmed by the ASME Section XI Standards Committee in an inquiry response letter (Interpretation XI-1-13-07) dated November 8, 2012 [15]:

“Question: Does the prohibition of peening in IWA-4621(c) and IWA-4651(g) apply to peening of austenitic alloys?

Answer: No.”

Paragraph NB-4652 in Section III [11] of the ASME Code indicates that heat treatment of formed carbon steel or austenitic stainless steel parts may be required following bending or forming. This paragraph is not considered applicable to the type of peening considered here since the proposed peening is so superficial that it causes negligible distortions of the heavy wall parts involved and thus does not constitute bending or forming.

2.3 Magnitude, Depth, and Coverage of Compressive Stresses

The performance criteria of Section 4.2.8 and of Section 4.3.8 specify the minimum magnitude and depth of compressive stresses that must be met by a peening process in order to apply the relaxed inspection intervals for peened components. A concise summary of the required stress effect is provided by Section 4.2.1 and Section 4.3.1.

2.3.1 Magnitude of Compressive Stresses

The performance criteria include the requirement that the peening result in a steady-state surface stress within the region required to be peened including the effect of normal operating stress that is either compressive in the case of DMWs or no greater than +10 ksi (tensile) (+70 MPa) in the case of RPVHPNs. Because these stress levels are well below the threshold stress necessary for PWSCC initiation over plant time scales [16], peening meeting the performance criteria prevents subsequent PWSCC initiation. The deterministic and probabilistic analyses in Section 5 credit the lack of future PWSCC initiation. These analyses assumed the limiting surface stress condition of compression (0 ksi) for DMWs and +10 ksi (tensile) for RPVHPNs based on the range of capabilities of peening mitigation processes available for these components. These analyses demonstrate that the peening residual plus normal operating surface stress conditions and the compressive residual stress depths specified in the performance criteria are effective and sufficient to justify the relaxed inspection intervals of Section 4.

2.3.2 Compressive Stress Depth

The compressive residual stress depth of the peened surface of the RPVHPN nozzle ID required by Section 4.3.8 is shallower than that required at other locations. The specific requirement for the nozzle ID is for a nominal compressive residual stress depth of at least 0.01 inch (0.25 mm). The requirement for RPVHPN outer surfaces and for DMWs is for a nominal compressive residual stress depth of at least 0.04 inch (1.0 mm). The effectiveness of the shallower

compressive residual stress depth for the RPVHPN nozzle ID to prevent crack initiation is supported by both laboratory testing and plant experience:

- Experience with the abrasive water jet conditioning process since it was qualified in the late 1990s shows that the compressive stresses it develops are sufficient to mitigate against the initiation of PWSCC. Abrasive water jet (AWJ) conditioning uses abrasive particles in a high-pressure water jet to remove a small layer of material and impart compressive residual stresses to a depth of about 0.010 inch (0.25 mm) in Alloy 600 base material and about 0.003 inch (0.08 mm) in Alloy 82/182 weld material [17]. In laboratory testing using thick-wall ring specimens of Alloy 600 [17], zero of six high stressed regions treated with AWJ were found with SCC after accelerated corrosion testing in simulated primary water at 399°C (750°F). Four regions were exposed for 2001 hours while two other regions were exposed for 1403 hours. This compares to eight of 30 untreated regions (control specimens) with SCC initiation exposed to 1300-2200 hours of accelerated corrosion testing. More than 123 RPVHPNs have been repaired using the ID temper bead technique since 2001—which includes abrasive water jet conditioning of the new mid-wall weldment—and 26 of these were still in service as of July 2010 (the rest were taken out of service by head replacement) [18]. Periodic UT examination of the repaired region is required to monitor the integrity of the repaired area (e.g., [19]). The ID temper bead process has been used extensively in the U.S. to repair CRDM nozzles, and no such cases have been identified in which new leaks or cracks were detected (see Section C.7 of MRP-110 [4]).
- Several hundred thousand steam generator tubes have been peened with experience extending more than 30 years, with generally satisfactory results [10]. The typical compressive residual stress depths generated ($< 150\text{ }\mu\text{m}$) are less than that required for the ID of RPVHPNs. Newly detectable cracks occurred in steam generators that had operated prior to peening (most likely due to low POD for flaws less than 500 μm in depth at the time of peening), but only small numbers of PWSCC cracks developed in units peened prior to service (in some cases, due to plastic strain from denting, but possibly due to manufacturing flaws in cases where denting was not present).

The use of a reduced nominal compressive residual stress depth for the inside surface of RPVHPNs is also supported by the plant experience that shows a low frequency of PWSCC indications detected at that location. This experience supports the lack of a requirement for a pre-peening surface examination on the nozzle ID surfaces (see also Section 2.5.4), as well. Plant experience with RPVHPNs [20] has demonstrated a low frequency of PWSCC on the nozzle ID, even for the most susceptible temperature and material conditions. PWSCC has been detected on the ID of CRDM/CEDM nozzles for only 3 of the 23 heads in the U.S. with reported PWSCC. Only about 15 of the approximate 184 CRDM/CEDM nozzles with detected PWSCC in the U.S. were reported to have PWSCC that originated on the nozzle ID. Furthermore, the deterministic and probabilistic calculations explicitly model the possibility of pre-existing flaws that were too shallow at the time of the pre-peening UT to be detected, and none of the probabilistic analysis cases of Section 5 (as detailed in Appendix A and Appendix B) take credit for any eddy current examinations.

2.3.3 Peening Coverage

The performance criteria require coverage of the entire wetted surface of Alloy 82/182 material (filler weld and butter), plus Alloy 600 base material if present, for DMWs and of the wetted surfaces of the attachment weld, butter, and nozzle base material for RPVHPNs. Similar to the approach in ASME Code Case N-729-1 for defining the required inspection coverage, the extent of RPVHPN nozzle base material required to be peened is defined by a series of figures within the performance criteria (Figure 4-1 through Figure 4-4). The difference in the specification of the RPVHPN base material coverage for NDE versus that for peening coverage is the result of the difference in the purpose of these two activities. The purpose of the NDE is to determine whether there is a grown PWSCC flaw inside the nozzle examination *volume*, whereas the peening is performed to prevent PWSCC initiation on a particular *surface*.

The technical basis for the RPVHPN inspection coverage (defined in Figure 2 of ASME Code Case N-729-1 [2]) is provided by MRP-95R1 [16]. This technical basis includes results from weld residual stress calculations for representative head geometries and plant experience with the region in which cracking has been detected in RPVHPNs. The weld residual stress analyses show that the region of elevated tensile stresses that may lead to initiation of PWSCC on the nozzle ID (where the residual plus normal operating stress exceeds +20 ksi (tensile) (+138 MPa) (see Section 2.3.4.1 below)) generally extends below the weld toe to a much greater extent on the uphill side compared to the downhill side of the nozzle. The weld shrinkage on the downhill side of the nozzle ovalizes the tube ([21], [22]) and influences the stresses on the opposite side of the tube, creating high tensile hoop stresses at the tube ID. For large nozzle penetration angles, the weld shrinkage puts the region below the weld on the uphill side into a through-wall bending stress state. The through-wall bending tends to put the outside surface of the nozzle into compression, limiting the distance below the weld where there are significant tensile stresses on the nozzle OD. The effect of the through-wall bending can also be seen in the difference in stresses between the inside and outside surfaces of the nozzle below the weld ([21], [22]).

The peening coverage required for RPVHPNs was also established using the stress results in MRP-95R1 and the stress limit of +20 ksi (tensile) (+138 MPa). The distance above the weld where the surface of the RPVHPN nozzle tube ID is required to be peened is the same as for the examination volume and surface above the weld. Table 2-1 and Figure 2-1 show the distance below the weld on the RPVHPN nozzle tube OD and ID for the downhill, sidehill, and uphill azimuths where the total (residual plus normal operating) surface stress is greater than +20 ksi (+138 MPa). This figure and table indicate that the distance where the total surface stresses remain above +20 ksi is much shorter on the nozzle OD than on the nozzle ID. Additionally, Table 2-1 includes the total (residual plus normal operating) surface stress at the edge of the inspection zone.

Given the limited distance below the weld where OD stresses remain above +20 ksi and the fact that the region below the weld is not part of the pressure boundary, it is appropriate to define a peening coverage zone below the weld on the OD that differs from the NDE coverage specified by N-729-1. Above the weld, where that portion of the nozzle is part of the pressure boundary, the peening coverage zone is defined to cover the surface of the examination volume. The peening coverage zone required by the performance criteria ensures that all surfaces that are susceptible to PWSCC initiation are mitigated. In contrast, the inspection coverage zone defines a volume that is regularly inspected for PWSCC indications. The benefit of defining the required

peening coverage in this manner is to avoid the application time associated with peening areas below the weld that are not susceptible to PWSCC initiation and that are not part of the pressure boundary.

Section 4.3.8.1 requires that the peening coverage region defined in Figure 4-1 through Figure 4-4 be extended a suitable distance to ensure a high confidence of coverage in the intended area, considering the particular peening method being applied.

Table 2-1
Evaluation of Stresses at Bottom Edge of Below-Weld Inspection Zone and Distance
Below Weld Toe on Nozzle Tube Where Stresses Remain Below 20 ksi Tensile

Plant	Type	Pen. Angle (°)	MRP-95 R1 Figures	Location	Inspection Zone Distance from Weld (in.)	Stresses at Edge of Inspection Zone Below Weld (ksi)				Distance from Bottom of Weld to 20 ksi (in.)	
						ID Hoop	OD Hoop	ID Axial	OD Axial	OD	ID
Plant A	B&W	38	A-1	Downhill	1.00	-24.9	-13.2	-1.5	0.2	0.21	-0.02
			through	Sidehill	3.07	9.5	-7.9	4.4	-9.5	0.91	1.72
			A-6	Uphill	5.08	-16.0	-0.2	-1.3	-0.9	0.63	2.95
Plant A	B&W	26	A-7	Downhill	1.50	-31.0	-20.5	1.8	-3.5	0.32	0.47
			through	Sidehill	2.77	-4.9	-9.9	4.8	-9.5	0.66	1.73
			A-12	Uphill	4.02	-10.8	-5.6	0.6	-5.2	0.61	2.48
Plant A	B&W	18	A-13	Downhill	1.50	-25.1	-19.8	5.8	-7.6	0.48	0.78
			through	Sidehill	2.34	-13.5	-14.0	8.1	-11.7	0.57	1.71
			A-18	Uphill	3.18	-12.3	-11.8	5.4	-9.9	0.63	2.27
Plant A	B&W	0	A-19	Downhill	1.50	-23.0	-28.4	6.8	-11.0	0.48	1.02
			through	Sidehill	1.50	-23.0	-28.4	6.8	-11.0	0.49	1.02
			A-24	Uphill	1.50	-23.0	-28.4	6.8	-11.0	0.49	1.02
Plant B	W 2-loop	43	A-25	Downhill	1.00	5.5	13.1	20.0	-18.5	0.78	1.00
			through	Sidehill	2.62	8.3	-12.3	17.2	-21.2	0.88	2.48
			A-30	Uphill	4.19	-14.6	-2.2	1.0	-1.3	0.22	2.70
Plant B	W 2-loop	30	A-31	Downhill	1.50	-8.4	-10.6	15.7	-15.5	0.63	1.29
			through	Sidehill	2.42	-1.9	-11.9	13.2	-15.7	0.62	2.03
			A-36	Uphill	3.32	-10.4	-6.4	2.9	-7.3	0.38	2.26
Plant B	W 2-loop	13	A-37	Downhill	1.50	-0.1	-13.1	18.8	-20.5	0.60	1.39
			through	Sidehill	1.78	-10.3	-14.3	18.2	-19.7	0.51	1.63
			A-42	Uphill	2.07	-10.1	-17.2	14.2	-17.2	0.38	1.82
Plant B	W 2-loop	0	A-43	Downhill	1.50	-27.8	-33.2	8.1	-12.4	0.50	1.10
			through	Sidehill	1.50	-27.8	-33.2	8.1	-12.4	0.49	1.10
			A-48	Uphill	1.50	-27.8	-33.2	8.1	-12.4	0.50	1.09
Plant C	W 4-loop	48	A-49	Downhill	1.00	-8.9	9.0	14.9	-7.8	0.54	0.20
			through	Sidehill	3.30	12.6	-12.4	9.9	-18.9	0.56	2.10
			A-54	Uphill	5.52	-12.1	-0.9	2.7	1.5	0.51	2.99
Plant D	CE	49	A-55	Downhill	1.00	2.3	7.5	15.8	-5.4	0.50	0.13
			through	Sidehill	3.55	4.2	-9.8	9.1	-18.1	1.54	2.59
			A-60	Uphill	5.99	-10.8	-0.4	-0.2	3.2	0.48	3.94
Plant D	CE	8	A-61	Downhill	1.50	6.3	-4.4	20.3	-20.6	0.53	1.52
			through	Sidehill	1.82	2.3	-7.7	18.6	-19.8	0.56	1.76
			A-66	Uphill	2.13	-1.4	-10.4	16.2	-17.9	0.54	1.95

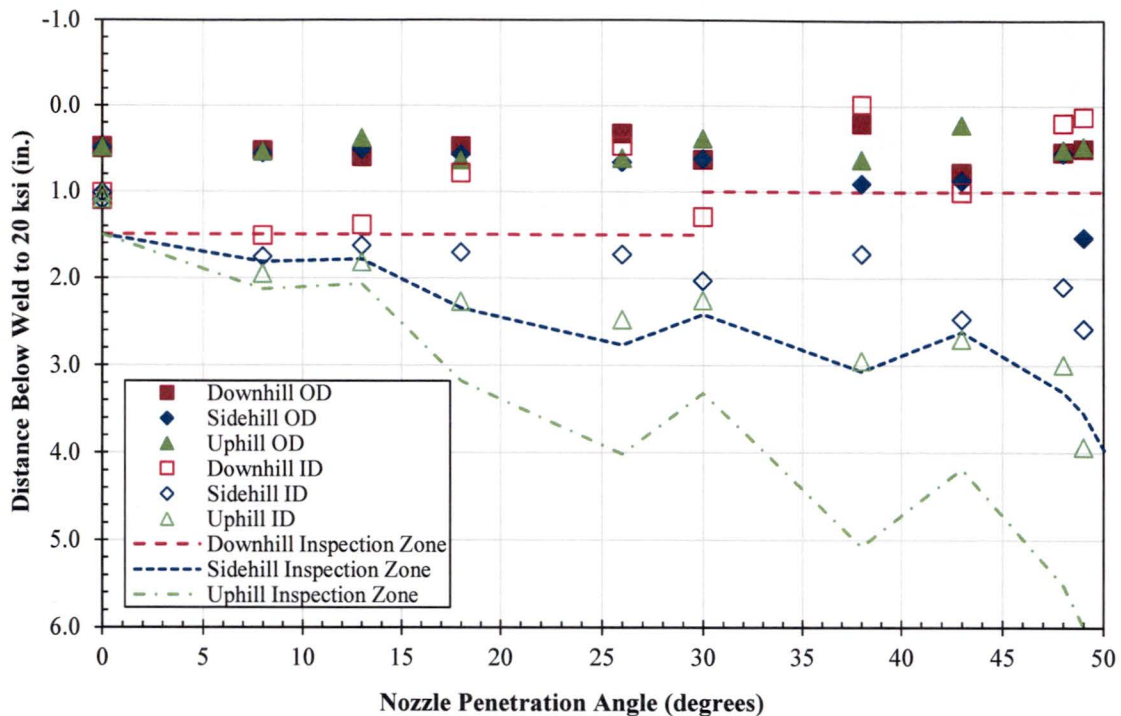


Figure 2-1
Distance Below Weld Toe on Nozzle Tube Where Stresses Remain Below 20 ksi Tensile

2.3.4 Inhibition of PWSCC Initiation

In order to prevent the initiation of new PWSCC, the application of peening has to result in the peak tensile stresses at the wetted surface of PWSCC material being less than the “threshold” stress for initiation of PWSCC. While it is considered that there is no firm “threshold” below which PWSCC will never occur, from a practical experience perspective a tensile stress of +20 ksi (+140 MPa) is a conservative lower bound of the stress level below which PWSCC initiation will not occur during plant lifetimes [16].⁵ This applies to steady-state stresses during normal operation as SCC initiation is a long-term process, and does not apply to transient stresses that occur only for short periods of time. The basis for a +20 ksi tensile stress threshold for PWSCC initiation is further described in Section 2.3.4.1.

The following discusses the magnitude of operating stresses that are expected at the surface of each component, for which the compressive residual stress needs to account:

- The peak applied stresses will rarely be more than 30 ksi (207 MPa) at DMW butt weld surfaces, and in the extreme are very likely to be limited to 50 ksi (345 MPa), which is approximately equal to 3 times the Code allowable stress parameter S_m for stainless steel pipe material at a design temperature of 650°F (based on Equation 10 of ASME Section III Division 1 NB-3600 [11]).

⁵ The 20 ksi (140 MPa) threshold stress corresponds to about 80% of the lower bound yield strength for Alloy 600 materials at operating temperatures.

- Based on extensive previous weld residual stress FEA work performed by the authors for CRDM/CEDM nozzles in many PWRs (see, e.g. [22]):
 - The peak applied stresses at the ID surfaces of RPVHPNs are relatively low, approximately between 15 and 25 ksi (103-172 MPa) or less.
 - The peak applied stresses at the OD surfaces of RPVHPNs, at either the weld or base material, are relatively low, 5 ksi (35 MPa) or less.

2.3.4.1 Basis for Tensile Stress Threshold for PWSCC Initiation

2.3.4.1.1 Assessment of Laboratory PWSCC Initiation Data

Research data obtained on PWSCC initiation in Alloys 600/82/182/132 has shown that initiation is very unlikely below the yield strength of the material. This section provides a literature review for these materials, particularly for data from specimens that were stressed near or below the conventional yield point at the test temperature. Troyer [23] presented a comprehensive review for Alloys 82/182/132, and this section supplements that work with the inclusion of data for Alloy 600 with low stress ratios. Consistent with the yield strength range known to be applicable to J-groove nozzles fabricated from Alloy 600 wrought material, laboratory testing for Alloy 600 materials with yield strengths up to 65 ksi (448 MPa) were considered.

In 1999, Amzallag [24] reported that the time to PWSCC initiation in Alloy 600 is proportional to stress to the negative fourth power:

$$\frac{1}{t} = B\sigma^{-4} \quad [2-1]$$

It was suggested by Amzallag that a stress threshold of approximately the yield strength of the material, 36 ksi (250 MPa) for Alloy 600, could be applicable at all temperatures, while a higher threshold may be valid for the weld metal, perhaps 51 ksi (350 MPa) [25]. The maximum specimen exposure time in this research was about 10^5 hours (adjusted to 325°C).

Troyer [23] calculated the stress exponent using a compilation from several other investigations, including some described below. He determined that the best estimate value was -5 for Alloys 82/182/132. This is similar to the -4 identified by Amzallag [24] for Alloy 600, and -4 is used for both the wrought and the weld metals in the remainder of this section.

Vaillant [26] presented additional constant load testing results for weld metal up to 1.6×10^5 hours (adjusted to 325°C), and he also concluded that an apparent stress threshold of about 51 ksi (350 MPa) is suitable for Alloy 182. He determined that the threshold for Alloy 82 may be even higher. Richey [27] and Amzallag [25] have indicated that plastic strain may be a better parameter than applied stress for predicting PWSCC initiation. This suggests that stresses below yield would not be responsible for PWSCC initiation.

Le Hong [28] reported on tests of Alloy 600 tubing where no cracking was observed for stresses at or below the yield strength of the bulk material, even with a cold-worked surface. In the capsule tests at 64 ksi (441 MPa) and 360°C, cracks were initiated in specimens with at-temperature yield strengths of 42 ksi (290 MPa) and 52 ksi (359 MPa), but not in specimens with

a yield strength of 64 ksi (441 MPa). The duration of the non-initiating tests was over 13,000 hours, which corresponds to over 100,000 hours adjusted to 325°C.

Benhamou and Amzallag [29] introduced a Monte Carlo modeling approach developed by AREVA and EdF. The model form is similar to that previously reported by Amzallag [24], with the time to initiation being inversely proportional to σ^4 . However, for illustrative purposes, if it is assumed that Alloy 600 with a yield strength of 35 ksi (241 MPa) initiates PWSCC in 100,000 hours when stressed at the yield stress, then the σ^{-4} relationship indicates that initiation would not occur for over 105 years at 20 ksi (138 MPa) (57% of yield), or over 1700 years at 10 ksi (69 MPa) (29% of yield). Based on industry experience, as documented in EPRI's *Materials Handbook for Nuclear Plant Pressure Boundary Applications* [30], initiation of PWSCC at the yield strength is unlikely, so the assumption of PWSCC initiating at 100,000 hours is conservative.

Couvant [31] proposed a model of the same form as Benhamou and Amzallag [29], but with a stress exponent of -6.8. It was reported that for an applied stress of the at-temperature yield strength, 51 ksi (350 MPa), at 290°C, the predicted time to initiation of Alloy 182 is expected to be 730,000 hours (83 years). Converting this to 20 ksi (138 MPa) (40% of yield) using the -4 stress exponent and 325°C using an activation energy of 44.2 kcal/mol (185 kJ/mol), the predicted time to initiation is 325 years. Using the stress exponent of -4 is conservative relative to higher exponent absolute values; using -6.8 would result in an initiation time of over 4200 years.

Extrapolation of a figure by Yonezawa [32] indicates that the time to failure at a 0.2% offset yield stress value of 38 ksi (262 MPa) was 29,000 hours at 360°C. Adjusting to 325°C and a stress level of 80% of the yield (30.4 ksi (210 MPa)) using the -4 stress exponent, the time to SCC initiation increases to 554,000 hours, or approximately 63 years. At 20 ksi (53% of yield), initiation is not expected for 337 years.

MHI [33] tested Alloy 600 with a reported room-temperature yield strength of 346 MPa (50.2 ksi). The specimens, which have an at-temperature yield strength of approximately 284 MPa (41.2 ksi), have not initiated in 80,000 hours at 360°C, stressed to 102-108% of the at-temperature yield stress. This is equivalent to almost 71 years at 325°C. Additional tests [34] of Alloy 600 resulted in some cracking of specimens loaded to 97% of the room-temperature yield strength after 1×10^5 hours. However, compared to the at-temperature yield stress, the applied stress level was 118% of yield.

On the other hand, high temperature and long exposure time results indicate PWSCC initiation could potentially occur at applied stresses slightly below the at-temperature yield stress in the weld metals corresponding to Alloy 600. Failures in tests by MHI [35] occurred at estimated stress ratios of 78% and 93% of yield in Alloy 82 in 418,000 hours and 223,000 hours, respectively (failure times adjusted to 325°C). Nevertheless, converting the applied stress values of 35.2 ksi and 41.8 ksi to 20 ksi (44% of the at-temperature yield stress) increases the time to cracking to 457 years and 492 years, respectively, assuming a negative fourth power dependence on stress. Note that the reported room-temperature yield strength for the Alloy 82 weld metal specimen with initiation observed for a stress ratio estimate of 78% is 57 ksi (394 MPa). This strength is close to the manufacturer's catalog value of 57 ksi (394 MPa) for Alloy 82 [36]. Because the weld metal is designed to have a yield strength well above the minimum strength for Alloy 600 wrought material, a stress of 20 ksi in Alloy 82 or 182 weld metal is very likely to

represent a stress ratio of less than 50%, which is substantially less than the 78% value cited above.

Table 2-2 lists the results of the MHI testing of Alloys 82 and 132, and Table 2-3 provides a summary of Alloy 600 testing cited above. All of the initiation testing listed in these tables were performed at 360°C. The time to initiation (or test duration if no initiation was observed) has been adjusted to 325°C for ease of comparison using an activation energy of 185 kJ/mol [37]. The stress ratio shown in the tables are based on the stress and estimated yield strength under test conditions.

Table 2-2
PWSCC Initiation Results for Alloy 82/132 for Relatively Small Stress Ratios ([34], [35])

Alloy	Stress Ratio, %	Applied Stress, ksi (MPa)	At-Temperature Yield Strength,* ksi (MPa)	Test Duration, h	Adjusted Test Duration,** h	Initiation
132	67	28.5 (196)	42.2 (291)	69,100	540,000	—
	82	34.5 (238)	42.2 (291)	84,300	659,200	—
	100	42.4 (292)	42.2 (291)	5000	38,700	X
	117	49.3 (340)	42.2 (291)	4700	36,600	X
82	63	28.2 (194)	45.1 (311)	64,400	503,500	—
	78	35.2 (243)	45.1 (311)	53,500	418,200	X
	93	41.8 (288)	45.1 (311)	28,500	222,900	X

* Yield strength at 360°C; estimated as 82% of the room-temperature yield strength reported by MHI

** 325°C equivalent; adjusted using an activation energy of 185 kJ/mol

Table 2-3
PWSCC Initiation Results for Alloy 600 for Relatively Small Stress Ratios

Stress Ratio, %	Applied Stress, ksi (MPa)	At-Temperature Yield Strength,* ksi (MPa)	Test Duration, h	Adjusted Test Duration,** h	Initiation	Reference
89	37.4 (258)	42.1 (290)	5335	41,700	—	[28]
100	63.8 (440)	63.8 (440)	13,000	101,600	—	
122	63.8 (440)	52.2 (360)	2800	21,900	X	
130	82.7 (570)	63.8 (440)	680	5,300	X	
152	63.8 (440)	42.1 (290)	2160	16,900	X	
158	82.7 (570)	52.2 (360)	950	7,400	X	
80	64.5 (445)	80.8 (557)	12,800	100,400	—	[32]
100	34.4 (237)	34.4 (237)	9500	74,300	—	
100	64.1 (442)	64.1 (442)	3700	29,000	X	
100	64.1 (442)	64.1 (442)	5800	45,100	X	
102	41.9 (289)	41.2 (284)	79,300	619,800	—	[33], [34]
108	44.7 (308)	41.2 (284)	81,000	633,100	—	
118	48.7 (336)	41.2 (284)	16,700	130,400	X	

* Yield strength at 360°C (350°C for Le Hong data); yield strengths for MHI data were estimated as 82% of the room-temperature yield strength reported by MHI

** 325°C equivalent; adjusted using an activation energy of 185 kJ/mol

It is concluded from this extensive literature review that for stresses approaching that of the at-temperature yield stress, PWSCC initiation will not occur over plant service periods (i.e., at least 80 years). Based on theoretical considerations, this apparent stress threshold is related to the presence of plasticity and thus the yield strength at operating temperature.

2.3.4.1.2 Yield Strength for PWR Plant Applications of Alloys 600/82/182

The 1988 Inconel product handbook for annealed Alloy 600 lists the room-temperature yield strength as 35.5 ksi (245 MPa) [38]. The most recent version [36] of the manufacturer's catalog expands the range for the typical room-temperature yield strength for a cold-drawn annealed tube to 25-50 ksi (172-345 MPa). Itoh [39] measured the yield strengths of Alloy 600 tubing and piping at multiple temperatures, and he reported room-temperature yield strengths of 41.3 and 35.5 ksi (285 and 245 MPa), respectively. Additionally, reports from eight ([40], [41], [42], [43], [45]) PWRs that have not replaced the Alloy 600 RPVHNS indicate that the yield strengths of their CRDM nozzles are in the range 36-60 ksi (248-414 MPa), in comparison to the minimum allowable room-temperature yield strength of 30 or 35 ksi (207 or 241 MPa) per the ASME Boiler and Pressure Vessel Code for the large majority of Alloy 600 PWR plant applications.

The effect of higher temperatures on Alloy 600 yield strength is available from the manufacturer's catalog, laboratory measurements, and the ASME Code. From these references, the 618°F (325°C) yield strength values are 76-86% of the room-temperature yield strength values. The ASME Code, for example, specifies a minimum yield strength of 24.2 ksi (167 MPa), which is 81% of the room temperature value.

For the weld metals, the manufacturer's catalog [36] for Alloy 82 lists the room-temperature yield strength as 57.1 ksi (394 MPa) and the high-temperature (618°F (325°C)) yield strength as 46.7 ksi (322 MPa), or 82% of the room-temperature yield point. Alloy 182 has a room-temperature yield strength of 55.1 ksi (380 MPa) and a high-temperature (618°F (325°C)) yield strength of 46.2 ksi (319 MPa), or 84% of the room-temperature yield point.

Thus, 80% is an appropriate factor to determine the yield strength of Alloys 600, 82, and 182 at 618°F (325°C) from that at room temperature. Determined similarly, 82% is appropriate for calculating the yield strength at 360°C, the temperature at which the laboratory testing was performed.

2.3.4.1.3 Conclusion

By applying yield strength values applicable to plant applications to the laboratory results detailed above, the level of conservatism of the +10 ksi (tensile) stress limit can be shown. In this conservative approach, it is assumed that PWSCC initiation can occur in the absence of plasticity effects (i.e., at stresses well below the conventional yield point) and that the stress dependence developed for higher stress levels can be applied to stresses well below yield. Using a very conservative room-temperature yield strength value of 30 ksi (207 MPa), the yield stress at 618°F (325°C) is estimated to be 24 ksi (165 MPa). The 10 ksi limit is approximately 42% of this latter value. Laboratory data can subsequently be extrapolated using this stress ratio to provide an estimated time to initiation.

The two Alloy 82 specimens that exhibited indications at stress levels below yield in laboratory tests were at 78% and 93% of the 360°C (680°F) yield stress estimate of 45.1 ksi (311 MPa). Adjustment of the measured initiation times of 53,500 hours and 28,500 hours to 325°C (618°F)

using an activation energy of 185 kJ/mol (44.2 kcal/mol) results in times of 47.7 years and 25.4 years, respectively, for the equivalent time at the stress levels applied in the test. After further adjustment to a stress ratio of 42% of the high-temperature yield strength (19 ksi (131 MPa)) using a stress exponent of -4, the predicted initiation time is 568 and 611 years, respectively, much longer than the remaining service period.

It is concluded from this extensive literature review that for stresses approaching that of the at-temperature yield stress, PWSCC initiation will not occur over plant service periods (i.e., at least 80 years). In the large majority of cases, the room-temperature yield stresses for PWR plant Alloy 600 materials are in the range 35-60 ksi (248-414 MPa). Applying a factor of 0.8 to obtain the at-temperature yield stress and an 80% conservative margin factor, the stresses required for initiation are 22-38 ksi. The basis for the required coverage area for peening and examination is +20 ksi, which is a conservatively low limit for the stress level required for PWSCC initiation over plant service periods. A limit of +10 ksi provides substantial additional margin for post-peening stresses to prevent initiation.

2.3.5 Modeling of PWSCC Propagation

With regard to inhibiting crack growth due to PWSCC, the important parameter is the stress intensity factor at the tip of any cracks that are present on the peened surface. If this stress intensity factor is less than the threshold stress intensity factor for SCC, K_{ISCC} , then crack growth will not occur. The threshold stress intensity factor for growth of PWSCC is generally thought to be about 5 to 9 MPa-m^{1/2} (5 to 8 ksi-in^{1/2}) but is not well known (see MRP-115 [44]). For simplicity and to be conservative, K_{ISCC} is taken as zero in this report. Thus, crack growth due to PWSCC will not occur if the stress intensity factor at the tip of the deepest crack present in the peened location is shown to be zero or less. The stress intensity factor is calculated considering peening induced residual stresses plus the applied stresses that occur during normal full power operation, including the effects of any stress concentration factors that act at the location being considered. If the steady-state stress intensity factor becomes positive at any location on the crack, then PWSCC-driven growth is modeled to occur.

2.3.6 Characterizing Uncertainty in Residual Stress Measurements

The performance criteria of this topical report require that the uncertainty in residual stress measurement be considered when assessing the surface stress after peening.

Techniques that are applied for measuring residual stresses include X-ray diffraction (XRD), hole drilling, neutron diffraction, microhardness mapping, photo-stress coatings, and eddy current measurements. XRD, often implemented as a non-destructive technique, has commonly been applied for peening qualification work. XRD stress measurements can be successfully applied to weld metals ([46], [47], [48], [49]), including Alloy 82/182 [50], although care must be taken as grain sizes of Alloy 82/182 welds can vary significantly. For example, Reference [51] presents XRD measurements of the maximum residual stresses in an Alloy 82 welded joint between a ferritic steel and a stainless steel, both with and without a buttering layer. It is concluded that X-ray diffraction residual stress measurements can provide accurate estimates of the effectiveness of peening processes.

2.4 Sustainability of Compressive Stresses for Plant Lifetime

Section 4.2.8.2 and Section 4.3.8.2 require that the residual plus operating stress be maintained below a specified limit for at least the remaining service life of the component. As discussed above in Section 2.3, initiation of PWSCC will not occur during plant lifetimes if the peak stress at the wetted surface during normal operation is below the conservative "threshold" tensile stress of +20 ksi (+140 MPa). The performance criteria require that the peening process results in a stress during steady-state operation (i.e., the residual stress plus normal operating stress) within the area required to be peened that remains well below this conservative measure of the threshold for at least the remaining service life of the component. The performance criteria require that the effects of both thermal stress relaxation and load cycling (i.e., shakedown) be considered.

Consequently, the compressive residual stresses produced by peening meeting the performance criteria are sufficient to prevent PWSCC crack initiation subsequent to peening for the remaining service life of the component.

2.5 Inspections and Inspectability of Peened Components

Surface stress improvement using peening coupled with examinations using performance demonstrated UT at relaxed schedules specified in Section 4 results in a reduced nuclear safety risk, as well as reduced probability of leakage, compared to the corresponding case for unmitigated components inspected according to standard inspection requirements and intervals. This is demonstrated by the deterministic and probabilistic analyses summarized in Section 5. Subsequent to peening mitigation, follow-up UT examinations and ongoing in-service UT examinations are required. Thus, the performance criteria include the requirement to maintain UT inspectability following peening. The same UT qualification requirements applicable to the unmitigated components also apply to the UT performed subsequent to peening.

The sensitivity of UT inspection methods as applied to DMWs in primary system piping and RPVHPNs is discussed in Section A.6 and B.6. Probability of detection (POD) curves for UT developed on the basis of statistically rigorous analyses of Performance Demonstration data are available for DMWs for the circumferential flaw orientation in MRP-262R1 [52]. This report shows median POD values of at least about 95% for circumferential flaw depths of 10% of the wall thickness or deeper. In the absence of similarly rigorous data for axial flaws in DMWs and circumferential and axial flaws in RPVHPN tubes, conservatively low UT POD curves were developed for use in the probabilistic analyses of Appendix A and Appendix B based on current Performance Demonstration requirements.

2.5.1 Pre-Peening Inspection

It is required that performance demonstrated UT methods will be applied to RPVHPN tube base metal and to DMWs in conjunction with peening applications. It is also required that the ID surfaces of DMWs be examined by ET. A pre-peening non-destructive examination has the benefit of reducing the probability of any flaws being left in service at the time of peening. Detected flaws are to be addressed prior to peening, as permitted by the requirements of Section 4.2 and Section 4.3. The post-peening examinations specifically address the possibility of growth of pre-existing flaws not detected during the pre-peening examination.

2.5.2 Follow-Up Inspection(s)

Nevertheless, there is the possibility that some undetected flaws may remain after the pre-peening inspection. Growth of these cracks is controlled by the stress intensity factor at the crack tip, as discussed above in Section 2.3. The stress intensity factor at the crack tip is a function of the depth and shape of the crack and the crack loading (operating stress and residual stress after shakedown and thermal relaxation). Probabilistic analyses using appropriate uncertainty distributions for all key modeling inputs have been performed to address this concern for growth of pre-existing flaws, as described in Section 5.3 and in Appendix A and Appendix B. A matrix of deterministic investigations have also been performed to evaluate the growth of flaws with sizes at the time of peening that are at or below detectability limits, as described in Section 5.2. Under the conservative assumption that the residual plus normal operating stress is at the limit meeting the performance criteria of Section 4.2.8 or Section 4.3.8, a pre-existing flaw of any depth would be modeled to grow via PWSCC. The analyses of this report show that the required follow-up inspections, in combination with the ongoing in-service inspections, are effective to address this possibility. As concluded in Section 5, the safety risks associated with growth of cracks in mitigated components inspected at the relaxed schedules specified in Section 4 are less than those for unmitigated components inspected at currently required schedules.

2.5.3 In-Service Inspections

The deterministic matrix of crack growth calculations in Section 5.2.3 and the probabilistic safety analyses summarized in Section 5.3 form the bases for the in-service inspection intervals and examination requirements of Table 4-1 and Table 4-3. These analyses show that peening meeting the applicable performance criteria in combination with the inspection requirements defined in Section 4 results in a reduced nuclear safety risk and a reduced probability of throughwall cracking and leakage compared to the case for unmitigated components examined per the requirements of 10 CFR 50.55a. Note that the timing of the first follow-up examination for peened DMWs operating at reactor hot-leg temperature but at or below 625°F (within 5 years after peening) was set on the basis of the deterministic approach. The timing of the follow-up examination for peened DMWs operating at reactor hot-leg temperatures above 625°F (second refueling outage after peening) was set to be consistent with the schedule for unmitigated DMWs defined in Code Case N-770-1. The sooner initial follow-up examination is justified given the fact that pre-existing PWSCC flaws grow more quickly at higher operating temperatures.

2.5.4 Surface Examination Requirements

Surface (ET or PT) examinations are not credited in the probabilistic safety analyses described in Section 5 and Appendix A and Appendix B. Nevertheless, Table 4-1 specifies performance of an ET examination during the pre-peening inspection of DMWs as a secondary method providing additional assurance of flaw detection and removal. As a secondary method intended to provide additional assurance of flaw detection and removal, Section 4 specifies that the ET of the DMW inside surface be performed in accordance with IWA-2223 of ASME Section XI.

The reasons for not using ET at the J-groove welds of RPVHPNs are (1) rupture of the head or nozzle ejection due to instability of a flaw located exclusively in the J-groove weld is not a credible concern, (2) experience has shown that PWSCC flaws located in the weld metal often extend into the base metal and are thus detectable via UT from the nozzle ID, (3) surface

examinations of the wetted surface of the J-groove weld of RPVHPNs are not required as part of the current inspection requirements for unmitigated RPVHPNs, and (4) plant owners find ET surface examinations of J-groove welds to be impractical considering the potential for false calls, detection of acceptable fabrication flaws, and high radiation worker dose associated with supplemental PT examinations to characterize ET indications, imposing unnecessary and unwarranted radiation dose to NDE inspection and repair personnel who prepare surfaces for examination and implement repairs. The main safety concerns for RPVHPNs are nozzle ejection due to a very large circumferential flaw in the nozzle tube located at or above the top of the J-groove weld and structurally significant boric acid corrosion of the low-alloy steel head material due to significant pressure boundary leakage. The probabilistic calculations in Appendix B for RPVHPNs conservatively assume that flaws that initiate in the weld are not detectable by volumetric UT examinations and that a 30° through-wall circumferential flaw initiates immediately in the nozzle tube upon growth of the weld flaw to cause leakage. The results of these analyses demonstrate that the examinations developed for use with peening, including direct visual examinations for evidence of pressure boundary leakage, are sufficient to address these concerns without the use of surface examination, resulting in a sufficiently small effect of PWSCC on nuclear safety. It is further noted that the probabilistic analysis does not credit the performance of a surface or volumetric leak path examination which would further increase the likelihood that a leaking penetration is detected by the in-service inspections and that the inspection requirements of Section 4 maintain the same basic direct visual examination (VE) intervals as required by Code Case N-729-1 [2] (as conditioned by 10 CFR 50.55a) for unmitigated heads. Finally, it is emphasized that a flaw exclusively located in the J-groove weld metal is unlikely to produce a leak rate of sufficient magnitude to result in significant boric acid corrosion of the head.

2.5.5 Benefit of the Requirement for Ongoing Visual Examinations for Evidence of Pressure Boundary Leakage of Top Head Nozzles

The requirements specified in Table 4-3 include periodic direct bare-metal visual examinations (VE) for all RPVHs with Alloy 600 nozzles that have implemented peening mitigation. The VE interval is required to be each refueling outage for all peened heads. The VE examination has the benefit of detecting leakage that could potentially lead to significant boric acid corrosion (BAC) of the low-alloy steel head material if the leak rate were to increase to the point that substantial local cooling and sustained moisture on the head could be produced.

The VE examination also supplements the periodic volumetric or surface examinations as a means to detect leakage due to PWSCC before significant circumferential cracking in the nozzle tube located outboard of the J-groove weld may be produced. The analyses in MRP-395 [20] and in Figure 5-32 of this report demonstrate that the time for a circumferential nozzle crack to grow to critical size is much longer than the time between VE examinations required by Section 4. Note that this crack growth time is even longer (i.e., factor of at least about 3) for heads operating at reactor cold-leg temperature.

The remainder of this Section 2.5.5 discusses the benefit of a VT-2 examination under the insulation through multiple access points as an opportunity for precluding significant BAC. This type of examination is currently required for unmitigated heads with Alloy 600 nozzles in refueling outages in which a VE examination is not required (in cases in which a VE is not required every refueling outage). Because a VE examination is required during every refueling

outage for all peened heads, this approved topical report does not include a requirement for a VT-2 examination under the insulation through multiple access points. Thus, the remainder of this Section 2.5.5 is included for information only.

2.5.5.1 VT-2 Inspection Criteria

The original intent of the VT-2 inspection as stated in Article IWA-2212 of the ASME Code Section XI [12] is to “detect evidence of leakage from pressure retaining components.” The application of VT-2 inspections to cold head RPVHs was established previously in Note 4 of ASME Code Case N-729-1 [2] with the primary purpose of mitigating the risk of BAC of the RPVH associated with a leak that initiates shortly after completion of the most recent VE.

As a reference, Table 2-4 lists the specific requirements associated with a VT-2 inspection as they are written in Article IWA-5240 of the ASME Code [12].

Table 2-4
ASME Code Section XI Requirements for VT-2 Visual Inspections [12]

<i>IWA-5240 Ref.</i>	<i>Requirement</i>	<i>Applicable to RPVH?</i>
(a)	“The VT-2 visual examination shall be conducted by examining the accessible external exposed surfaces of pressure retaining components for evidence of leakage.”	Yes
(b)	“For components whose external surfaces are inaccessible for direct VT-2 visual examination, only the examination of the surrounding area (including floor areas or equipment surfaces located underneath the components) for evidence of leakage shall be required.”	Yes (see "h")
(c)	“Components within rooms, vaults, etc., where access cannot be obtained, may be examined using remote visual equipment or installed leakage detection systems.”	Yes (see "h")
(d)	“Essentially vertical surfaces need only be examined at the lowest elevation where leakage may be detected.”	No
(e)	“Discoloration or residue on surfaces shall be examined for evidence of boric acid accumulations from borated reactor coolant leakage.”	Yes
(f)	“For insulated components in systems borated for the purpose of controlling reactivity, insulation shall be removed from pressure retaining bolted connections for VT-2 visual examination...”	No (no bolts)
(g)	“Essentially horizontal surfaces of insulation shall be examined at each insulation joint if accessible for direct VT-2 examination.”	Yes
(h)	“When examining insulated components, the examination of the surrounding area (including floor areas or equipment surfaces located underneath the components) for evidence of leakage, or other areas to which such leakage may be channeled, shall be required.”	Yes

The application of VT-2 inspections to cold head RPVHs as described in Table 4-3 is subject to the requirements of Note 4 of N-729-1 [2]. This requires that the examination be performed under the head and through multiple access points (meaning through multiple openings in the head shroud). Thus, the VT-2 examination required by N-729-1 and described in this topical report has much greater sensitivity to detect leakage due to PWSCC of RPVHPNs than the

standard VT-2 examination that is required every refueling outage. EPRI 1007842 [53] provides industry guidance regarding visual examinations for evidence of leaking RPVHPNs, including example photographs of leaking nozzles.

2.5.5.2 Technical Bases Supporting Increased VE Intervals for Cold Head Units

There are several technical considerations that support an increase in the VE interval for cold head units up to the lesser of three 18-month fuel cycles or 5 calendar years, provided that a VT-2 inspection as described in Section 2.5.5.1 is performed during refueling outages when a VE is not performed:

1. The PWR plant experience for PWSCC of Alloy 600 J-groove nozzles, including that for reactor vessel top head nozzles, shows that periodic visual examinations performed under the insulation at appropriate intervals are highly effective in detecting leakage caused by PWSCC before discernible material loss is produced via boric acid corrosion of carbon or low-alloy steel pressure boundary components. This experience is documented in detail in the EPRI BAC Guidebook [54] and is summarized in both a 2013 industry paper [55] and in a presentation given at an NRC public meeting [56]. The most significant cases of BAC due to PWSCC all occurred prior to the requirement for periodic visual examinations under the insulation for evidence of leakage.
2. As discussed in MRP-110 [4] and the EPRI BAC Guidebook [54], there have been more than 55 leaking CRDM nozzles and many more cases of leakage detected in other Alloy 600 J-groove nozzles. The limited number of cases with significant BAC have been accompanied by substantial amounts of boric acid deposits that are expected to be readily detectable via the type of VT-2 examination required by Code Case N-729-1 and described in this topical report. A majority of the leaking CRDM nozzles were repaired using a method that would have revealed discernible BAC of the penetration bore surface.
3. Results of mockup testing and analyses documented in MRP-308 [57] and presented at NRC public meetings ([58], [59], [60], [61])—including photographs of deposit buildup on test mockups (e.g., Figure 2-2 and Figure 2-3)—show that: a) the leak rate is the key parameter for determining whether relatively rapid and sustained BAC may occur and b) substantial volumes of boric acid deposits accompany the leakage necessary to produce significant BAC damage to RPVHs. These large volumes of deposits are expected to be readily visible during the VT-2 examinations required by N-729-1 and described in this topical report.



Figure 2-2
Example #1 of Boric Acid Deposits Observed During EPRI Mockup Testing: Leak Rate of 0.01 gpm (Duration of 32 Days) [60]



Figure 2-3
Example #2 of Boric Acid Deposits Observed During EPRI Mockup Testing: Leak Rate of 0.1 gpm (Duration of 29 Days) [59]

4. Changes in temperature at the crack location have a consistent and well characterized effect on the PWSCC crack growth rate ([62], [44]). In the U.S., cold head units operate with a head temperature within the range of about 547°F to 561°F compared to a typical non-cold head temperature of 600°F. Based on the Arrhenius relationship for the effect of temperature on the PWSCC crack growth rate with the standard activation energy value of 31 kcal/mol [62], the crack growth rate for cold heads relative to a head operating at 600°F is lower by a factor of 2.8 to 4.0. Consequently, the maximum temperature-equivalent operating time between VEs for U.S. cold head units—all of which operate with 18-month fuel cycles—

would be no more than $4.5 / 2.8 = 1.6$ equivalent years.⁶ In comparison, non-cold head units are permitted to operate for up to 24 months between VEs. Accordingly, the risk that leakage substantial enough to produce significant BAC would occur between VEs at cold head units is comparable to or less than the risk at the typical non-cold head units—even without crediting the required VT-2 examinations under the insulation through multiple access points.

5. In addition to periodic visual examinations for leakage, there are several other potential indicators of pressure boundary leakage or corrosion prior to structurally significant head material loss occurring. These include tracking of unidentified primary system leakage, boric acid deposits on containment building surfaces, and clogging/plugging of containment air coolers and containment radiation monitor filters [4]. Another approach that has been applied is on-line monitoring of the tritium concentrations in containment. This concentration is proportional to the RCS leak rate.

In view of the above, it is clear that VT-2 inspections completed in accordance with N-729-1 [2] would yield a substantial reduction in the risk that (hypothetical) undetected flaws which begin to leak shortly after completion of a VE would grow to the point where structurally significant BAC could occur without detection prior to the subsequent VE (up to three fuel cycles later). Given the benefit of the VT-2 examination under the insulation through multiple access points, a VE interval of every third refueling outage (or 5 calendar years if sooner) is appropriate for cold heads. The substantially lower crack growth rate for cold heads compared to heads operating at temperatures near hot-leg temperature results in a much greater time for increase of the leak rate to the point that relatively rapid BAC may occur. Furthermore, as shown in this topical report, peening yields a large reduction in the probability of leakage, including through the J-groove weld. The much lower probability of leakage reduces the risk for BAC.

2.6 Verification of No Adverse Effects

Section 4.2.8.4 and Section 4.3.8.4 require that analysis or testing be performed to verify that peening will not degrade the peened component or other components in the system or cause undesirable adverse effects. Degradation would include initiating cracks or causing growth of any pre-existing flaws. The relevant undesirable effects are erosion of surfaces, undesirable surface roughening, or detrimental effects in the transition regions adjacent to the peened regions. High tensile surface stresses at the transition regions could promote PWSCC degradation during subsequent operation.

Introducing hardness at the peened surface is not an adverse effect. The somewhat elevated surface hardness resulting from peening reflects the mechanism of peening. The surface hardness is not adverse because the compressive residual stresses at the surface prevent PWSCC degradation in the area of elevated hardness. In addition, the thick-wall components that are the subject of this topical report are not susceptible to large plastic strains that could reverse the compressive residual stress field developed by peening (see Section 4.6.3 of MRP-267R1 [10]).

As discussed in MRP-267R1 [10], neither plant experience nor laboratory tests have identified any adverse effects to parts that have been peened with the peening methods being considered in

⁶ This value is calculated based on the maximum cold head temperature of 561°F and a typical hot head temperature of 600°F.

this report. However, as noted in MRP-267R1, vibration problems have occurred to adjacent small-diameter, thin-walled nozzles and instrument lines in BWRs. The performance criteria require that vibration effects during application be considered when assessing the potential for adverse effects.

3

EFFECTIVENESS OF CANDIDATE PEENING PROCESSES

An application-specific qualification report is required to demonstrate that a given peening process will meet the performance criteria in Section 4.2.8 and Section 4.3.8 of this report. In addition, a post-peening report is required to verify that the intended peening effect was achieved and that any relevant non-conformances are acceptable. Section 3 describes in more general terms how the candidate water jet and laser peening processes covered in MRP-267R1 [10] are capable of meeting the performance criteria, including the required stress improvement effect and lack of adverse effects. Peening is effective to mitigate PWSCC if the intended stress effect is achieved regardless of the details of the process. Thus, it is expected that there are surface stress improvement techniques beyond those covered in MRP-267R1 that are capable of meeting the performance criteria.

3.1 Process Overview and Key Process Application Variables

Laser peening and water jet peening (also known as cavitation peening) operate by impact of a pressure shock wave, leaving the treated surface in a compressive residual stress state. The shock wave may be produced via laser energy (laser peening, LP) or via collapse of vapor bubbles due to a water jet impinging on the surface (water jet peening, WJP). Detailed descriptions of these peening methods and the relevant physical mechanisms are contained in MRP-267R1 [10], but a brief description of the operating principle for each is provided below:

- The LP process uses the laser energy to create plasma that is confined by the inertia of surrounding water and reaches very high pressures and temperatures. This rapid rise in surface pressure creates a shock wave with pressure above the yield strength of the substrate. The shock wave propagates through the ablative layer and into the metal, plastically deforming it as it propagates inward. After the passage of the shock wave, the reaction of the metal surrounding the treated surface leaves the surface in a compressive residual stress state. Different processes vary in energy level, spot size, and beam delivery method.
- Cavitation bubbles are produced in a submerged water jet. The cavitation bubbles are produced by the strong shear force that acts on the boundary between the high-speed jet and the surrounding stationary water, and the bubbles are carried by the high-speed water jet to the material surface. The collapse of the cavitation bubbles generates a large shock pressure that causes local plastic deformation. In the same manner as for laser peening, after the passage of the shock wave, the reaction of the metal surrounding the treated surface leaves the surface in a compressive residual stress state.

Peening is controlled as a special process, as discussed in Section 2.1. The key process application variables for a given peening process as applied to the target component will be established and will be demonstrated by qualification testing to meet the peening performance

criteria. Examples of the key process application variables for WJP and LP are described in Section 3 of MRP-267R1 [10] and are summarized below:

- Water Jet Peening (WJP)
 - Nozzle diameter
 - Jet stand-off distance and nozzle offset in ID applications
 - Water flow rate
 - Water jet traverse time
 - Impingement angle
 - Restricted stationary peening time
 - Water level and water temperature
- Laser Peening (LP)
 - Laser type (wavelength)
 - Pulse energy
 - Pulse repetition rate
 - Pulse duration
 - Laser spot footprint dimensions
 - Pulse number density

3.2 Process Field Experiences

The many locations in numerous plants that have been peened in Japanese BWRs and PWRs using LP and WJP are described in detail in MRP-267R1 [10]. The main locations in Japanese PWRs that have been peened using these techniques are as follows:

- Reactor vessel outlet nozzle DMWs: WJP at 17 PWRs
- Reactor vessel inlet nozzle DMWs: WJP at 18 PWRs, and LP at 2 PWRs
- Reactor vessel safety injection nozzle DMWs: WJP at 6 PWRs, and LP at 2 PWRs
- Bottom mounted instrument nozzle ID surfaces: WJP at 20 PWRs, and LP at 2 PWRs.
- Bottom mounted instrument J-groove weld and adjacent nozzle OD base material: WJP at 21 PWRs, and LP at 2 PWRs.

Peening in Japanese PWRs for PWSCC mitigation started in 2001. There have been no reports of problems or PWSCC detected subsequent to peening in the PWRs. However, there have been no reports of subsequent in-service volumetric or surface inspections of the peened parts in PWRs to date. In-service inspections have been performed on peened BWR components, including enhanced visual examinations. To date, no service-related cracking has been reported in the peened components.

3.3 Attaining the Requisite Stress Improvement Effect

MRP-267R1 [10] describes in detail the magnitude and the depth of the compressive residual stresses that are generated by candidate WJP and LP processes and that are substantially deeper and more compressive than the bounding stress effect required by the performance criteria. WJP and LP methods generally produce compressive residual stress fields with depths of at least 1 mm (0.04 in.) [10], although reduced compressive depths may be expected in restricted geometries such as on the inside surface of RPVHPNs in the case that a thermal sleeve is present within the nozzle.

The following subsections discuss potential limitations on the stress effect of peening.

3.3.1 Geometric Limitations to Peening Process Application

Demonstration of the ability of a peening process to meet the performance criteria of this report over the area of material susceptible to PWSCC initiation is required for use of the relaxed inspection requirements. For the WJP and LP methods considered in MRP-267R1 [10], the following geometric limitations have been identified for DMWs and RPVHPNs:

- No access or other geometric limitations have been identified for peening the ID surface of DMWs.
- No access limitations have been identified for peening the weld wetted surface and wetted surface of the tube OD for RPVHPNs.
- For the region of the RPVHPN tube ID surface to be peened, the limited access because of the presence of the thermal sleeve located inside some nozzles may result in a reduced depth of the compressive stress field for some peening methods.
- In addition, due to geometry, some peening techniques of interest cannot be used to peen the threaded areas that are present in some cases near the bottom of the RPVHPN tube (either on the nozzle OD or nozzle ID). Because any such threaded areas are located below the weld toward the end of the nozzle and are not part of the pressure boundary, the performance criteria do not require that peening be performed of the threaded regions when present.

The processes considered in MRP-267R1 for each geometry have demonstrated an ability to meet the applicable performance criteria.

3.3.2 Surface Condition Considerations

There are no known limitations imposed by surface conditions on the peening applications considered in MRP-267R1 [10]. The successful use of the WJP and LP methods for many BWR and PWR applications confirms that the surface conditions of the Alloy 600/82/182 and stainless steel materials present at the peening locations are compatible with the peening processes.

While there are no known limitations imposed by surface conditions, conceptually there are conditions that one could conceive of as limiting the effectiveness of peening in the applications considered in MRP-267R1:

- Areas with unusually high levels of local cold work (e.g., due to aggressive grinding) could conceivably reduce the effectiveness of the peening process. Appendix A of MRP-267R1 [10] documents successful application of laser peening to a 20% cold worked stainless steel,

which shows that the levels of cold work present on plant parts are unlikely to interfere with peening. In addition, as also discussed in Appendix A of MRP-267R1, water jet peening and laser peening of heavily ground U-bends of Alloy 182 successfully inhibited initiation of PWSCC, while non-peened specimens cracked when exposed to aggressive PWSCC conditions. It is also noted that the ASM Handbook volume on surface engineering [63] notes that surface condition and surface hardness are generally not limitations for shot peening. Further, shot peening mitigation of PWSCC of Alloy 600 steam generator tubes in areas that were significantly cold worked, e.g., roll overlaps and roll transitions, has been observed to be highly effective as discussed in Section 4.6.5 of MRP-267R1 [10]. Consequently, peening methods are expected not to be subject to surface condition or surface hardness limitations.

- One could envision surface oxides as possibly limiting peening effectiveness by providing a hard shell that prevents plastic deformation of the underlying metal. However, this effect has not been noted in either laboratory tests or service applications. Further, oxide thicknesses on plant materials are in the neighborhood of 1 μm thick, and thus are much too thin and too structurally weak to interfere with peening, which involves dimensions on the order of 1 mm, i.e., 1000 times larger.

3.3.3 Effect of Pre-Peening Stress

The peening effect is self-normalizing as the effect is enhanced for areas with relatively high tensile initial residual stress and attenuated for areas with compressive initial residual stress. The stress measurements below illustrate the relative insensitivity to the initial residual stress state and illustrate that the largest post-peening surface compressive stress corresponds to the point of maximum tensile initial residual stress.

Although it is not necessary that the compressive stresses from peening be uniform for peening to be effective, the peening compressive stresses do tend to be relatively uniform due to this self-normalizing behavior.

As described in Section 4.5 of MRP-267R1 [10], a surface that is in high tension relaxes more when it is peened vs. a surface that has low tension. Likewise a material that is already in compression does not relax as much when it is peened. The conclusion is peening on a material has about the same final result regardless of the initial residual stress state of the material.

The pre-peening through-wall stress profile does dominate the post-peening stress profile in the region beyond the peening compressive residual stress layer near the treated surface. In this regard, a conservative stress condition is assumed in the analyses of Section 5 and Appendix A for the Alloy 82/182 piping butt weld cases based on the effect of a deep ID weld repair. High tensile weld residual stresses are predicted for RPVHPNs regardless of the presence of weld repairs because of the constraint of the J-groove geometry.

The following is a description of X-ray diffraction measurements of the residual stress state of a bottom mounted nozzle OD test block before and after peening [64]. The surface axial stresses on the Alloy 82/182 material ranged from -64 ksi to +68 ksi (-441 MPa to +469 MPa). Two locations (A7 and A9) also had depth residual stress measurements taken:

- Location A7 was at -64 ksi (-441 MPa) before peening and went to -74 ksi (-510 MPa) after peening.

- Location A8 was at -29 ksi (-200 MPa) before peening and went to -63 ksi (-434 MPa) after peening.
- Location A9 was at +68 ksi (469 MPa) before peening and went to -81 ksi (-558 MPa) after peening.
- Location A10 was at -22 ksi (-152 MPa) before peening and went to -80 ksi (-552 MPa) after peening.

The data show the greatest peening response occurred with the highest amount of initial tension. Regardless of the initial state, high tension or high compression, the final compressive stresses ended up within a -63 ksi to -81 ksi (-434 MPa to -558 MPa) range.

3.4 Coverage Verification

Examples of the approaches taken to ensure 100% coverage of the areas being peened for WJP and LP are described in Sections 5.3.2, 3.1.3.1, and 5.4.2 of MRP-267R1 [10]. In summary, they are as follows:

- Complete coverage of the areas designated for peening are assured by use of overlapping passes and by extending the peening out to beyond the edge of the designated area (or to the nozzle end as applicable).
- Process controls are used to ensure that the desired area is peened and that it is peened for the desired length of time or for the desired number of pulses per unit area, as applicable.
- After the peening is completed, the records are given a QA/QC or an independent review to ensure that 100% coverage was achieved. Alternatively, verification of complete coverage may be performed automatically by use of a 3D computer model with as-built dimensions, in which the main process parameters are recorded for each successful laser firing.
- In addition, a visual inspection of laser peened surfaces may be performed to ensure that all of the desired surface shows visible signs of peening (LP changes the surface enough to make obvious the difference between peened and unpeened areas).

3.5 Sustainability of the Stress Effect

A detailed evaluation is contained in Section 4 of MRP-267R1 [10] that describes the experimental and analytical evaluations that show that the required stress effect will be sustained for extended operating periods to ensure the long-term effectiveness of the mitigation of PWSCC. The experiments involve measurement of residual stresses in samples after exposure to periods of high temperature and to numerous stress cycles, and show that the stresses decrease moderately during the first few cycles, but then remain relatively constant with time and cycles. An analytical evaluation was performed using a thermal activation energy approach that concludes that the results of these experiments show that the peening will remain effective for more than 60 years of operation.

Detailed finite-element stress relaxation analyses as applied to RPVHPNs have shown that substantial compressive residual stresses at the peened surface are sustained for 1,000,000 hours (114 years) at operating pressure and temperature [65].

As discussed in Section 3 of MRP-267R1 [10], plant experience with shot peened steam generator tubes also demonstrates that compressive stresses remain high after long periods of operation.

3.6 Inspectability After Peening

General background information regarding the effects of peening on inspectability is provided in Section A.4.1 of MRP-267R1 [10]. As discussed in that report, tests were performed of a flat plate specimen of Alloy 600 welded to Type 304 stainless steel using Alloy 182 in which cracks had been induced using potassium tetrathionate. These tests showed that the detectability of the cracks by phased array ultrasonic testing (UT) was not adversely affected by water jet peening. These tests were performed with the UT probe located on the peened surface. The extensive experience for more than 20 years with inspections by ET and UT of steam generator tubes that have been shot peened in the tube expansion and tube expansion transition regions, as described in MRP-267R1, has also demonstrated that inspectability is not adversely affected by peening. Again, the probes in steam generator tubes are applied to the peened surface.

In the U.S., NDE studies have been completed or are planned to determine if peening has an effect on the results from the UT and ET methods typically applied to Alloy 82/182 dissimilar metal butt welds in primary system piping (i.e., DMWs) and from the UT methods typically applied to RPVHPNs from the inside of the nozzle. These NDE studies are intended to address the peening performance criteria for inspectability and NDE qualification (Sections 4.2.8.3 and 4.2.8.5 for DMWs and Sections 4.3.8.3 and 4.3.8.5 for RPVHPNs):

- *Inspectability of Peened DMWs.* Tests of the inspectability by UT and ET of dissimilar metal butt welds were performed by EPRI as described in EPRI report 3002008359 [66]. These tests used coupons with dissimilar metal welds, e.g., an Alloy 82/182 butt weld between stainless steel and carbon steel. Essentially identical sets of cracks were thermally and mechanically induced in each coupon. The cracks, which were not electrodischarge-machined (EDM) notches, are representative of PWSCC cracks in terms of flaw response. EPRI NDE personnel performed UT and ET of the coupons before and after peening. The UT procedure employed conventional UT techniques (i.e., single-angle, frequency, and focal depth probes). These tests show that UT and ET qualified for use on unmitigated DMWs are reliable for use on peened DMWs. The reader should consult Reference [66] to confirm its applicability prior to applying it as the basis for meeting the performance criteria in Sections 4.2.8.3 and 4.2.8.5.

This EPRI test program included coupons peened using water jet/cavitation methods and using laser methods. The following peening vendors participated in the study by peening coupons:

- AREVA: water jet/cavitation method
- Hitachi-GE Nuclear Energy (HGNE): water jet/cavitation method
- Toshiba-Westinghouse: laser method
- Metal Improvement Company: laser method
- Mitsubishi Heavy Industries/ Mitsubishi Nuclear Energy Systems (MNES): water jet/cavitation method

- *Inspectability of Peened RPVHPNs.*
 - In early 2016, AREVA completed a study [67] to evaluate the effect of cavitation peening on procedures qualified for UT of RPVHPNs. The evaluation consisted of performing ultrasonic examinations of a CRDM nozzle both pre and post cavitation peening. The mockup was provided by EPRI and contained thermal fatigue cracks that are representative of PWSCC cracks in terms of flaw response. The examinations were performed in accordance with the qualified examination procedures. The techniques evaluated included time-of-flight diffraction (TOFD) and pulse-echo angle beam. The ultrasonic data were analyzed in accordance with qualified procedures and the responses obtained with the examination technique were evaluated and compared. The results demonstrated that a CRDM nozzle peened in the same manner as was performed on this mockup would not invalidate AREVA's ultrasonic examination procedure qualification. As both the peening method and the ultrasonic examination procedures used were specific to AREVA's processes and were specific to a peening methodology planned for use at a site, the reader should consult Reference [67] to confirm its applicability prior to applying it as the basis for meeting the performance criteria in Sections 4.3.8.3 and 4.3.8.5.
 - UT qualification testing for underwater laser peening of RPVHPNs is also anticipated in the near future and will be performed by WesDyne International in cooperation with EPRI. As such, utilities should review both the peening methodology and the ultrasonic examination procedures used to determine the applicability of this study to their own planned applications. EPRI will perform a review of the technical justification and provide an independent assessment of the vendor's results.

3.7 Assessment of Potential Crack Growth During Operation after Peening

Tests have been performed to determine if flaws that are present at the time of peening will grow after peening. The tests performed, and the results, are covered in Appendix A of MRP-267R1 [10]. These tests involved developing cracks in stressed specimens of sensitized Alloy 600 using tetrathionate or polythionic acid or in specimens of stainless steel using boiling magnesium chloride, peening some of the specimens, and subjecting them to further exposures in the cracking environment. These tests showed that flaws with depths less than the depth of the compressive stress field did not grow in the peened specimens, while those in non-peened specimens did grow. Flaws with depths that significantly exceeded the depth of the compressive stress field appeared to grow unaffected by the effect of the peening. The deterministic and probabilistic analyses in Section 5 and Appendix A and Appendix B are used to develop a post-peening inspection regimen (follow-up and in-service inspections) that addresses any pre-existing flaws in the event they are not detected during the pre-peening inspection. In particular, Section 5.2 presents a matrix of deterministic analyses that evaluates the growth of flaws with sizes at the time of peening that are at or below reliably detectable values.

3.8 Basis for No Adverse Effects

The following discussion provides evidence that there will not be adverse effects in U.S. PWRs associated with peening for PWSCC mitigation:

- WJP and LP have been used extensively in Japanese PWRs and BWRs for over 10 years with no reported adverse effects to the peened parts. However, in Japanese BWRs, there have been vibration-induced failures of small-diameter, thin-wall nozzles and instrument lines with pre-existing flaws and located close to the peened areas, as discussed in MRP-267R1 [10] and further in MRP 2014-027 (response to NRC Request for Additional Information No. 4-4) [64]. In response to this experience, the Japanese have instituted pre-peening evaluations to ensure that such problems do not occur and have also instituted post-peening inspections to verify that problems did not occur. Based on industry review there are no thin-wall lines near the areas to be peened in PWRs. However, when vibration effects are present, the performance criteria of Section 4.2.8.4 and Section 4.3.8.4 require analysis or testing to verify that the mitigation process does not result in vibration-induced degradation, including when peening RPVHPNs to any thermal sleeves present inside the nozzle.
- Extensive qualification testing, including examination of many peened samples and test blocks, has been performed of the WJP and LP processes as described in MRP-267R1 [10]. No adverse effects have been identified in this testing. For example, testing showed that peening did not affect the structural integrity of the treated component by introducing flaws into the component, or by causing growth of pre-existing cracks.
- Shot peening has been widely used as a PWSCC mitigation method in steam generator tubes since the mid-1980s, with no adverse effects being identified. The peened surfaces have not experienced unusual corrosion nor have they interfered with normal eddy current test inspections and occasional ultrasonic inspections.

3.9 Corrective Action Programs

In most cases, the pre-peening and follow-up examinations will address the potential for a PWSCC indication detected subsequent to peening. The residual risk of having a pre-existing flaw that is not detected is addressed by the ISI examinations, as discussed in Section 5. An investigation is required per the existing plant corrective action program if PWSCC indications are detected subsequent to the last follow-up examination. The purpose of the follow-up investigation is to assess any evidence that PWSCC initiation occurred subsequent to the peening.

As part of the licensing process, 10 CFR 50.34 [68] requires that every utility provide a description of a plant-specific QA program meeting the requirements of 10 CFR 50 Appendix B [69], including Criterion XVI, "Corrective Action," which states the following:

Measures shall be established to assure that conditions adverse to quality, such as failures, malfunctions, deficiencies, deviations, defective material and equipment, and nonconformances are promptly identified and corrected. In the case of significant conditions adverse to quality, the measures shall assure that the cause of the condition is determined and corrective action taken to preclude repetition. The identification of the significant condition adverse to quality, the cause of the condition, and the corrective action taken shall be documented and reported to appropriate levels of management.

The "NQA-1" ASME standards include requirements and guidance for establishing and executing QA programs in accordance with 10 CFR 50 Appendix B [69]. With NRC approval, several plants use NQA-1-1994 [70] as the basis for establishing the necessary measures and governing procedures to promptly identify, control, document, classify, and correct conditions adverse to

quality during plant operation ([71], [72], [73], [74], [75]). In addition to committing to perform an investigation in the case of a significant condition adverse to quality and identify a corrective action to prevent recurrence of the event, each licensee has agreed to analyze the results of evaluations of conditions adverse to quality to identify trends. Both significant conditions adverse to quality and significant adverse trends are reported to responsible management. The plant corrective action program can be reviewed by NRC inspectors to ensure that problems are identified, evaluated, and resolved in a manner commensurate with their safety significance.

Upon detection of PWSCC indications in a peened component at a plant subsequent to all follow-up inspections, the plant-specific corrective action program would trigger an assessment documenting the number of indications detected, including the size, location, and orientation for each indication. Depending on the particular circumstances, the following types of activities could be included as part of the evaluation:

- Review prior NDE records and indication morphology to investigate whether the indication is pre-existing or newly initiated. In particular, the surface length of the flaw in comparison to the flaw depth may indicate that some crack growth occurred prior to peening.
- Review industry operating experience to investigate whether the cracking morphology is consistent with cracking that has occurred in unmitigated components.
- Determine if the indication is in a location with high weld residual stress or high operating stresses. Consider the expected stresses subsequent to peening at the relevant location.
- Review latest industry operating experience regarding any other cases of indications being detected subsequent to peening.
- Review application-specific post-peening report to verify that the peening was performed as expected (i.e., no problems or unusual events occurred during the peening, especially for the affected nozzle and indication location). Review the peening essential variable values used where the indication is located.
- Crack growth calculations considering the operating temperature and expected material susceptibility to estimate the most likely time of initiation.

Furthermore, a wetted surface-connected flaw, an unacceptable flaw based on Section XI of the ASME Code, or unacceptable flaw growth is observed in a peened DMW, RPVHPN, or J-groove weld, could indicate a potential problem with the peening. A pre-existing flaw may have either been too small to be detected, or the peening may have not been effective. If such a flaw is observed, the following shall be performed:

- A report summarizing the evaluation, including inputs, methodologies, assumptions, extent of conditions, and causes of the new flaw, unacceptable flaw, or flaw growth, must be submitted to the NRC prior to the plant entering into Mode 4.
- A sample inspection of the peened components in the population must be performed to assess the extent of the condition.
- A final causal analysis report consistent with the licensee corrective action program including a description of corrective actions taken must be submitted to the NRC within six months of the discovery.

- The inspection relaxation per this report is no longer applicable to the affected RPVHPN or DMW. The affected RPVHPN or DMW component shall be inspected in accordance with the requirements of 10 CFR 50.55a, unless an alternative is authorized by the NRC.

4

EXAMINATION REQUIREMENTS

Section XI of the ASME Boiler and Pressure Vessel Code specifies periodic in-service inspections of safety-significant light water reactor components including primary system pressure boundary components. Because of the concern for PWSCC of Alloy 600/82/182 pressure boundary components in PWRs, augmented inspection requirements have been developed for such locations. These augmented inspection requirements are currently defined in ASME Code Cases that are made mandatory with conditions by U.S. NRC regulations, specifically in 10 CFR 50.55a. The inspection requirements identify the nondestructive examination (NDE) inspection method, inspection frequency, inspection coverage, and flaw acceptance standards. In general, these items are based on the location, configuration, and historical condition of the component.

In the context of the current inspection requirements for key Alloy 600/82/182 locations in PWRs, this section defines appropriate inspection requirements for Alloy 82/182 piping DMWs⁷ and Alloy 600 RPVHPNs mitigated by surface stress improvement (SSI) (i.e., peening). Given the demonstrated effectiveness of the SSI techniques, relaxation of the inspection requirements for these components is appropriate after SSI treatment. As discussed in Section 5, the specific inspection requirements developed for use with peening are supported by detailed deterministic and probabilistic modeling. Because the inspection requirements for these components are prescribed by NRC regulations, NRC approval is required for relaxation of current inspection requirements following peening mitigation.

Section 4.1 contains a summary of the current inspection requirements for DMWs and RPVHPNs with unmitigated Alloy 600/82/182 materials as specified by Code Cases N-770-1 [1] and N-729-1 [2], respectively, as conditioned by 10 CFR 50.55a(g)(6)(ii). Appropriate requirements for inspections to be performed on these components before and after application of peening, as well as the required minimum nominal depth of the compressive residual stress produced by the peening treatment, are defined in Section 4.2 for DMWs and in Section 4.3 for RPVHPNs.

For peened components, three different categories of inspection requirements are defined:

- The pre-mitigation inspection is performed in the same outage during which peening is applied. The pre-peening inspection is considered to be the pre-service baseline inspection.
- A follow-up examination is performed a certain number of cycles after the peening application to address the possibility of flaws that were not detected in the pre-peening examination of the DMW or the RPVHPN tube base metal. The required timing of the

⁷ The term DMW is used here to refer specifically to Alloy 82/182 dissimilar metal butt welds located in PWR primary system piping and falling under the scope of Table 1 of ASME Code Case N-770-1 [1].

follow-up inspection(s) was established on the basis of the detailed deterministic and probabilistic calculations.

- Finally, in-service inspections (ISIs) are required to be performed regularly at the intervals prescribed in Table 4-1 for DMWs and Table 4-3 for RPVHPNs. The long-term in-service inspections address the residual potential for pre-existing flaws that are not detected by the pre-peening or follow-up examination(s).

Further inspection requirements for Alloy 600/82/182 PWR primary pressure boundary components are specified by ASME Code Case N-722-1 [3] as conditioned by 10 CFR 50.55a(g)(6)(ii)(E). This code case requires periodic direct visual examinations of the exterior metal surface of Alloy 600/82/182 components for evidence of pressure boundary leakage. Code Case N-722-1 excludes the reactor vessel top head nozzles in deference to Code Case N-729-1. For the case of Alloy 82/182 piping butt welds, the requirements of Code Case N-770-1 (as conditioned by 10 CFR 50.55a) generally bound the requirements of Code Case N-722-1 (as conditioned by 10 CFR 50.55a).

4.1 Summary of Technical Basis and Current Requirements for In-Service Examinations for Unmitigated Alloy 600/82/182 Components

The basic inspection regimes currently required — for the Alloy 600/82/182 components that are the focus of this report — are described below for information only.

4.1.1 Dissimilar Metal Butt Welds (DMWs) in Primary System Piping

ASME Code Case N-770-1 [1] (dated December 25, 2009) provides inspection requirements for visual, volumetric, and surface inspections of piping butt welds in the primary system that are made of Alloys 82 and/or 182, which are considered to be susceptible to PWSCC. This code case has been made mandatory by the U.S. NRC through regulation 10 CFR 50.55a(g)(6)(ii)(F), subject to the conditions detailed in this regulation.⁸ The conditions applied by the NRC cover topics such as how to treat welds that have had PWSCC mitigation measures applied. Note that the inspection requirements, including inspection frequencies for Alloy 82/182 piping and nozzle butt welds, were previously defined in MRP-139R1 [5].

The volumetric re-inspection interval per N-770-1 for components not treated by a qualified mitigation method depends on the operating temperature of the component in consideration of the strong dependence of PWSCC susceptibility to temperature. The volumetric inspection frequency for unmitigated Alloy 82/182 DMWs operating at hot-leg temperature (Category A-2) is every 5 years. The volumetric inspection frequency for unmitigated Alloy 82/182 DMWs operating at cold-leg temperature (Category B) is every second inspection period (as defined in ASME Section XI), not to exceed 7 years.

Code Case N-770-1 includes specific categories to address inspection methods and frequencies for piping DMW locations mitigated against PWSCC using specific methods. These requirements are currently not directly applicable to SSI treatments. The SSI treatment methods

⁸ An update of N-770-1 (Code Case N-770-4, May 7, 2014) has been prepared and issued by ASME, but the version that is currently made mandatory by the NRC regulations is still N-770-1 as of summer 2015. N-770-4 incorporates inspection requirements for components mitigated using SSI. N-770-1 is the only version of this code case currently accepted by U.S. NRC.

described in this report are not addressed by Code Case N-770-1, although SSI treatment is similar to mechanical stress improvement without welding, which is addressed in N-770-1. For stress improvement methods for which the N-770-1 requirements are currently applicable, the volumetric inspection requirement following mitigation of an uncracked DMW (Category D) is a single examination within 10 years following mitigation, followed by a program of periodic inspections in which the component is placed into a population to be examined on a sample basis, provided that no indications of cracking are found.

4.1.2 Reactor Pressure Vessel Head Penetration Nozzles (RPVHPNs)

ASME Code Case N-729-1 [2] (dated March 28, 2006) provides the current inspection requirements for RPVHPNs attached using partial-penetration (i.e., J-groove) welds, including CRDM/CEDM nozzles. It bases the frequency of inspection in part on two calculated parameters — the Effective Degradation Years (EDY) and the Reinspection Years (RIY) of the head — each of which is a function of the time and temperature history of the head. The code case provides acceptance criteria for visual examinations that detect evidence of reactor coolant leakage or boric acid corrosion and for volumetric or surface examinations that detect indications of planar flaws. The technical bases for the requirements of N-729-1 are documented in MRP-117 [6], the top-level safety assessment report MRP-110 [4], and lower-level safety assessment reports MRP-103 [76], MRP-104 [77], and MRP-105 [7]. In the fall of 2014, the technical basis for inspections of unmitigated heads with Alloy 600 nozzles was updated by MRP [20] to consider the most recent set of plant experience, including part-depth PWSCC indications detected in several heads operating at reactor cold-leg temperature. MRP-395 [20] concluded that the current inspection requirements for unmitigated heads with Alloy 600 nozzles remain valid. This code case has been made mandatory by the U.S. NRC through regulation 10 CFR 50.55a(g)(6)(ii)(D), subject to the conditions detailed in this regulation.⁹ The conditions applied by the NRC generally cover issues related to performance of ultrasonic inspections and required re-inspection intervals.

For heads with Alloy 600 nozzles, the volumetric inspection intervals (between examinations of all nozzles) per N-729-1 are based on the Reinspection Years (RIY) parameter, which is a measure of operating time normalized to a head temperature of 600°F using the consensus temperature dependence of the PWSCC crack growth rate. The required interval is every 8 calendar years or before $RIY = 2.25$, whichever is less.

As of the beginning of 2016, there are heads with Alloy 600 nozzles in service at 24 U.S. PWRs. The heads at 41 currently operating U.S. PWRs have been replaced with heads using PWSCC-resistant nozzles made of Alloy 690. Of the 24 Alloy 600 heads remaining in service, 19 heads operate at the reactor cold-leg temperature and are typically referred to as “cold” heads. The others generally operate at temperatures closer to the reactor hot-leg temperature.

The effect of the inspection regime per N-729-1 is that the non-cold heads with Alloy 600 nozzles remaining in service must generally perform volumetric examinations for indications of

⁹ Updates of N-729-1 (through Code Case N-729-6, March 3, 2016) have been prepared and issued by ASME, but the version that is currently made mandatory by the NRC regulations is still N-729-1 as of August 2016. N-729-5 and N-729-6 incorporate inspection requirements for components mitigated using SSI and revised volumetric or surface examination intervals for heads with Alloy 690 nozzles. N-729-1 is the only version of this code case currently accepted by U.S. NRC.

PWSCC every one or two refueling outages. The corresponding interval for the cold heads with Alloy 600 nozzles is typically every four or five 18-month fuel cycles, or three or four 24-month fuel cycles. More frequent volumetric or surface examinations may be required if PWSCC has previously been detected in the subject head.

4.2 Requirements for Dissimilar Metal Butt Welds (DMWs) in Primary System Piping Mitigated by Peening

Item L of Table 4-1 defines alternative inspection requirements for uncracked Alloy 82/182 dissimilar metal piping butt welds mitigated by a peening mitigation technique meeting the performance criteria of Section 4.2.8. The inspection requirements in Table 4-1 include a pre-peening inspection (Section 4.2.2), follow-up inspection (Section 4.2.3), and long-term in-service inspections (Section 4.2.4). Within the context of this section, the term “uncracked” refers to a component examined in accordance with the requirements of N-770-1-2500 with no planar surface-connected flaws in contact with the reactor coolant environment during normal operation.

Within the context of Section 4.2, references to portions of ASME Code Case N-770-1 are indicated using a hyphen followed by the relevant location within this code case (e.g. -2000). Section 4.2 defines inspection requirements relevant to peening by specifying additions to ASME Code Case N-770-1. A listing of such additions and other requirements in this section is provided by Table 4-2.

4.2.1 Summary of Performance Criteria of Section 4.2.8

The performance criteria of Section 4.2.8 shall be satisfied. For information only, brief summaries of the requirements of Section 4.2.8 are provided below.

Peening Coverage

The required coverage is the full area of the susceptible material along the entire wetted surface under steady-state operation. Susceptible material includes the weld, butter, and base material, as applicable. The coverage shall be extended at least 0.25 in. (0.64 cm) beyond the susceptible material.

Stress Magnitude

The residual stress plus normal operating stress is compressive on all peened surfaces.

Depth of Effect

The compressive residual stress field extends to a minimum nominal depth of 0.04 in. (1.0mm) on the susceptible material along the wetted surface.

Sustainability of Effect

The mitigation process is effective for at least the remaining service life of the component, i.e., the residual plus normal operating surface stress state after considering the effects of thermal relaxation and load cycling (i.e., shakedown) must remain compressive.

Inspectability

The capability to perform ultrasonic examinations of the relevant volume of the component is not adversely affected, and the relevant volume is inspectable using a qualified process. The capability to perform eddy current examinations of the relevant surface of the component is not adversely affected.

Lack of Adverse Effects

As verified by analysis or testing, the mitigation process is not to have degraded the component, caused detrimental surface conditions, or adversely affected other components in the system.

4.2.2 Pre-Peening Inspection

Prior to performance of peening but during the same outage, the following examinations are to be performed in accordance with the requirements in Table 4-1.

- An ultrasonic examination is to be performed of the weld.
- An eddy current (ET) inspection is also to be performed of the weld inner surface.

It is emphasized that the surface examination that is required in this report for use prior to peening is not credited in the probabilistic safety analyses described in Section 5 and Appendix A.

4.2.3 Follow-Up Inspection

During the follow up inspection(s), volumetric examination of the required volume and surface examination of the required area are performed in accordance with the requirements in Table 4-1. The follow-up inspection schedule depends on the operating temperature of the weld:

- For hot leg piping with normal operating temperature above 625°F (including pressurizer locations), the follow-up inspections are during the second refueling outage after the application of peening and a second examination within 10 years following the application of peening.
- For hot leg piping with normal operating temperature equal to or below 625°F, the follow-up inspections are once within 5 years following the application of peening and a second examination within 10 years following the application of peening.
- For cold leg piping, the follow-up inspection is once within 10 years but no sooner than the third refueling outage following the application of peening.

4.2.4 Subsequent ISI Program

The in-service inspection requirements for peened welds after completion of the follow-up inspection(s) are shown in Table 4-1.

100% of the peened welds are to be examined once each Section XI inspection interval (nominally 10 years).

4.2.5 Examination Coverage and Acceptance Criteria for Inspection Results

4.2.5.1 Examination Coverage

The required examination volume is defined by volume C-D-E-F of Figure 1 in ASME Code Case N-770-1. The required examination surface shall be surface E-F in the same figure.

In accordance with 10 CFR 50.55a(g)(6)(ii)(F)(4) and for U.S. plants, essentially 100% coverage is required for the examination for axial flaws instead of the requirements in -2500(c).

4.2.5.2 Acceptance Criteria for Item L of Table 4-1

The volumetric acceptance standards for Item L of Table 4-1 are in accordance with Paragraph -3130 of N-770-1 with the addition of the following requirements:

Added to Subparagraph -3132.2:

- (d) If examinations of weld volumes or areas reveal unacceptable flaws in accordance with -3132.3(e) in a weld that has been previously mitigated by peening, the weld is unacceptable for continued service until corrected in accordance with (a). If corrected by a mitigation technique in Table 1 of ASME Code Case N-770-1, the weld shall be placed in the Inspection Item for the repair/replacement activity or corrective measure used for acceptance of the flaw.
- (e) As an alternative to the -3132.3(e) reclassification of a weld previously mitigated by peening containing acceptable flaws, the weld shall be corrected by repair/replacement activity in accordance with IWA-4000 or by other mitigation techniques in accordance with the requirements of Table 1 of ASME Code Case N-770-1 during the outage in which the flaw was identified. If corrected by a mitigation technique in Table 1 of ASME Code Case N-770-1, the weld shall be placed in the Inspection Item for the repair/replacement activity or corrective measure used for acceptance in the flaw.

Added to Subparagraph -3132.3:

- (e) If volumetric or surface examination of the weld previously mitigated by peening detects new planar surface flaws in the butt weld or base metal inside surface, the weld is acceptable for continued service without additional repair/replacement activity or corrective measures, provided an analytical evaluation meets the requirements of IWB-3600, and the additional examinations of -2430 are performed in the current outage. In this analytical evaluation, the beneficial effects of peening shall not be considered, the weld shall not be considered mitigated; and the weld shall be reclassified as Inspection Items A-1, A-2, or B, as applicable, and re-examined in accordance with Note (5) of Table 1 of ASME Code Case N-770-1.

4.2.5.3 Requirements for DMWs Subsequent to Flaw Detection or Observation of Flaw Growth

If a wetted surface-connected flaw, an unacceptable flaw based on the ASME Code, Section XI, or unacceptable flaw growth is observed in a peened DMW,

- (a) A report summarizing the evaluation, including inputs, methodologies, assumptions, extent of conditions, and causes of the new flaw, unacceptable flaw, or flaw growth, must be submitted to the NRC prior to the plant entering into Mode 4.
- (b) A sample inspection of the peened components in the population must be performed to assess the extent of condition.
- (c) A final causal analysis report consistent with the licensee corrective action program including a description of corrective actions taken must be submitted to the NRC within six months of the discovery.
- (d) The inspection relaxation per this report is no longer applicable to the affected DMW. The affected DMW component shall be inspected in accordance with the requirements of 10 CFR 50.55a, unless an alternative is authorized by the NRC.

4.2.5.4 Requirement per 10 CFR 50.55a(g)(6)(ii)(F)(6)

In accordance with 10 CFR 50.55a(g)(6)(ii)(F)(6) and for U.S. plants, for any mitigated weld for which volumetric examination detects growth of existing flaws in the required examination volume that exceed the previous ASME Section XI IWB-3600 flaw evaluations or new flaws, a report summarizing the evaluation, along with inputs, methodologies, assumptions, and causes of the new flaw or flaw growth is to be provided to the NRC prior to the weld being placed in service other than modes 5 or 6.

4.2.6 NDE Qualification Requirements

Volumetric examinations shall be qualified to the performance demonstration requirements of ASME Section XI, Mandatory Appendix VIII per Note (4) of Table 1 in ASME Code Case N-770-1.

Eddy current examinations shall be performed in accordance with Section XI IWA-2223 and Section 4.2.8.3.2.

4.2.7 Inspection Expansion

Examinations performed in accordance with Table 4-1 that reveal unacceptable flaws shall be extended to include examinations of additional welds during the current outage. The use of IWB-3514 is for the purpose of determination of scope expansion and not the purpose of determining acceptability of the flaws. Acceptability of flaws is determined in accordance with -3132.

The specific requirements are defined in -2430 of ASME Code Case N-770-1 (specifically -2430(a), -2430(a)(5), the unnumbered paragraph below -2430(a)(6), and -2430(b)) with the addition of the following bullet:

- For Table 4-1 Inspection Item L and the examination volume of Figure 1 of N-770-1, additional mitigated welds from the same Inspection Item and using the same peening method shall be examined during the current outage, if planar surface flaws are revealed in the butt weld or base metal inside surface.

For other than the flaws in -2430(a)(1), (2), (3), (4), (5), or the above bullet, the additional examination requirements of IWB-2430 apply.

4.2.8 APPENDIX: Performance Criteria and Measurement or Quantification Criteria for Mitigation by Surface Stress Improvement (Peening) of Alloy 82/182 Piping Butt Welds in PWR Primary System Piping

It is noted that Section 2.1 discusses quality assurance considerations with regard to implementation of peening mitigation:

“Since surface stress improvement by peening affects the performance of nuclear safety related systems and components, it shall be performed in accordance with a quality assurance program meeting the requirements of Appendix B to 10 CFR 50 and the utility’s plant specific commitments. Further, since peening is a special process, it shall be controlled in a manner consistent with Criterion IX, ‘Control of Special Processes,’ of Appendix B and any applicable plant specific commitments. As stated in that criterion, this requires that the personnel and procedures involved need to be appropriately qualified. Since there are no industry standards that apply to peening, these qualifications shall be done to vendor requirements developed and documented per their 10 CFR 50 Appendix B quality assurance program and to utility requirements and commitments applicable at the plant site.”

Thus peening shall be performed and qualified per requirements meeting the quality assurance criteria of 10 CFR 50 Appendix B. As such, the analysis and demonstration testing required below are performed in accordance with these quality assurance requirements, which provide adequate controls.

4.2.8.1 Stress Effect

To minimize the likelihood of crack initiation, the process shall have resulted in a compressive stress in the full area of the susceptible UNS N06600, UNS N06082, and UNS W86182 material along the entire wetted surface under steady-state operation. Susceptible material includes the weld, butter, and base material, as applicable. The residual stress plus normal operating stress on surfaces required to be peened shall be included in the evaluation. The boundaries of the area required to be effectively peened shall be extended at least 0.25 in. (0.64 cm) beyond the PWSCC susceptible area to provide high assurance that the areas susceptible to PWSCC receive the required peening effect.

A combination of demonstration testing and analysis shall be performed to demonstrate the required capability of the peening method to produce the required post-mitigation stress state:

- (a) Demonstration testing shall be performed to determine the residual stress state at the surface to be peened. Specimens representative of the geometry, accessibility, and surface condition of the component to be peened shall be used. For peening of main loop piping welds, it is acceptable to use welded flat plate specimens. The nominal wall thickness of the specimen shall be no greater than that of the component to be peened.
- (b) Analysis shall be performed to determine the effect of normal operating loads on the steady-state operating axial and hoop direction stresses.

The testing shall be used to demonstrate the critical process parameters and define acceptable ranges of the parameters needed to ensure that the required residual stress field (exclusive of normal operating stresses) has been produced on the mitigated surface.

The uncertainty in measurement of the surface residual stress shall be considered in the analysis to determine the surface stress including operating and residual stress. The basis for that consideration shall be documented in the relief request.

4.2.8.1.1 Magnitude of Surface Stress

The combination of demonstration testing and analysis shall show that the steady-state operating axial and hoop direction stresses combined with residual stresses are compressive at the inside surface of susceptible material.¹⁰

4.2.8.1.2 Nominal Depth of Compressive Residual Stress

The testing shall demonstrate that the nominal depth of the compressive surface residual stress field produced by the peening technique is at least 0.04 in. (1.0 mm).¹¹ The nominal depth refers to the depth of the compressive residual stress that is reliably obtained in demonstration testing, i.e., for at least 90% of the locations measured.

4.2.8.2 Sustainability

Analysis or testing shall be performed to verify that the peening process maintains the compressive surface stress condition (normal operating and residual stress) for at least the remaining service life of the component. The analysis or demonstration test plan shall include startup and shutdown stresses, normal operating pressure stress, thermal cyclic stresses, transient stresses, and residual stresses. The analysis or demonstration test shall account for:

- (a) load combinations that could relieve stress due to shakedown
- (b) any material properties related to stress relaxation over time

¹⁰ Some advanced peening processes result in a very thin surface layer (i.e., within 0.001 to 0.002 inch (25 to 50 μm) from the surface) where the residual stress is tensile or not as compressive as the residual stress deeper into the material. For example, see Figures A-14, A-42, and A-43 of MRP-267R1 [10]. The underlying compressive residual stresses prevent development of significant PWSCC cracks at the surface. Thus, the residual stresses in this very thin surface layer may be excluded when showing that the requirement of Section 4.2.8.1.1 is met. The combination of demonstration testing and analysis shall show that the steady-state operating axial and hoop direction stresses combined with residual stresses are compressive immediately beyond the very thin surface zone of elevated residual stress.

¹¹ Some advanced peening processes result in a very thin surface layer (i.e., within 0.001 to 0.002 inch (25 to 50 μm) from the surface) where the residual stress is tensile. The tensile residual stresses in this very thin surface layer may be excluded when showing that the requirement of Section 4.2.8.1.2 is met. The testing shall demonstrate that the nominal depth of the compressive surface residual stress field, excluding the very thin layer of tensile stress at the surface, is at least 0.04 in. (1.0 mm). The depth measurement shall be from the surface to the point where the compressive residual stress becomes neutral.

4.2.8.3 Inspectability

4.2.8.3.1 UT Inspectability

The capability to perform ultrasonic examinations of the relevant volume of the component shall not be adversely affected. Nondestructive examination qualified to Section XI, Mandatory Appendix VIII, performance demonstration requirements using representative weld specimens shall have been performed to demonstrate that a qualified examination of the relevant volume of the mitigated component can be accomplished subsequent to the mitigation including changes to component geometry, material properties, or other factors.

4.2.8.3.2 ET Inspectability

The capability to perform eddy current examinations of the relevant surface of the component shall not have been adversely affected.

4.2.8.4 Lack of Adverse Effects

Analysis or testing shall be performed to verify the following:

- (a) The mitigation process, including any vibration effects during application, does not degrade the component or adversely affect other components in the system.
- (b) The mitigation process does not cause erosion of surfaces, undesirable surface roughening, or detrimental effects in the transition regions adjacent to the peened regions.

4.2.8.5 UT Qualification

The mitigated weld shall be inspectable by a qualified process. An evaluation shall be performed to confirm that the required examination volume of the mitigated configuration is within the scope of a Section XI, Mandatory Appendix VIII, supplement or supplements and that the examination procedures to be used have been qualified in accordance with Mandatory Appendix VIII. The evaluation shall confirm that the geometric limitations (e.g., weld crown, nozzle contour) of a Mandatory Appendix VIII qualification are not exceeded for the mitigated weld.

4.2.8.6 Pre-Peening UT and ET

A volumetric examination qualified to Section XI Mandatory Appendix VIII, performance demonstration requirements and a surface examination in accordance with IWA-2223 shall have been performed in accordance with Table 4-1 to assure the absence of planar surface flaws before the application of the peening mitigation.

Table 4-1
Inspection Requirements for Alloy 82/182 DMWs in Primary System Piping Mitigated by Peening

EXAMINATION CATEGORIES						
CLASS 1 PWR PRESSURE RETAINING DISSIMILAR METAL PIPING AND VESSEL NOZZLE BUTT WELDS CONTAINING ALLOY 82/182						
Item No.	Parts Examined	Examination Requirements/ Fig. No.	Examination Method	Acceptance Standard	Extent and Frequency of Examination	Deferral of Examination to End of Interval
L	Uncracked butt weld mitigated by peening (19)	Figure 1 of N-770-1	Volumetric (4), (19), (21); Surface (19), (20)	Section 4.2.5	Perform a volumetric examination (21) and a surface examination (20) of all hot leg welds above 625°F the second refueling outage following the application of peening and a second examination within 10 yr following the application of peening. Perform a volumetric examination (21) and a surface examination (20) of all hot leg welds at or below 625°F within 5 yr following the application of peening and a second examination within 10 yr following the application of peening. Subsequently, 100% of these welds shall be examined once each inspection interval. A surface examination (20) shall be performed from the weld inside surface and a volumetric examination (21) shall be performed from either the inside or outside surface. Perform a volumetric examination (21) and a surface examination (20) of all cold leg welds once within 10 yr but no sooner than the third refueling outage following application of peening. Subsequently, 100% of these welds shall be examined once each inspection interval. A surface examination (20) shall be performed from the weld inside surface and a volumetric examination (21) shall be performed from either the inside or outside surface.	(11)

NOTES: (1) through (5) and (10) are identical to those in ASME Code Case N-770-1 [1]. Notes (6) through (9) and notes (12) through (18) are not applicable. Note (11) modifies Note (11) in N-770-1, and the other notes below are in addition to those in N-770-1.

(11) Deferral of Examinations

- (a) Examinations of welds originally classified Table IWB-2500-1, Category B-J welds prior to mitigation are not permitted to be deferred to the end of the interval.
- (b) Examinations of welds originally classified Table IWB-2500-1, Category B-F welds, Item Numbers B5.10, and B5.20 prior to mitigation, may be deferred following peening, as follows:
 - (1) Not applicable.
 - (2) The first examinations following peening for Inspection Item L shall be performed as specified. The second examination of hot leg welds of Inspection Item L shall be performed as specified. Subsequent examinations for Inspection Item L may be performed coincident with the vessel nozzle examinations required by Category B-D.
 - (3) For successive inspection intervals following peening, subsequent examinations may be deferred to the end of the interval, provided no additional repair/replacement activities have been performed on the examination item, and no flaws or relevant conditions requiring successive examination in accordance with Table 4-1 are contained in the mitigated weld.
- (c) Welds that were classified in accordance with Nonmandatory Appendix R, prior to mitigation shall be reclassified based on the configuration of each piping structural element and the postulated degradation mechanisms if any remaining after the mitigation. Deferral of examinations shall be according to (a) and (b), above.
- (d) Not applicable

Examination Requirements

- (19) If peening techniques are used, the following shall be met:
- (a) Volumetric (21) examination from either the inside or outside surface and surface (20) examinations from the inside surface shall be performed on these welds prior to the application of peening techniques and as a pre-service examination in accordance with -2220. The pre-peening examination shall be conducted in the same outage as the application of peening. The examination volume of Figure 1 in N-770-1 and examination surface defined by points E-F of Figure 1 in N-770-1 apply. Eddy current examination in accordance with IWA-2223 is required.
 - (b) The pre-peening examination shall be considered the pre-service baseline examination. The following acceptance standards apply:
 - (1) No planar surface flaws are acceptable for Inspection Item L welds. If any planar surface flaws are detected, the requirements of (c) shall be met.
 - (2) Flaws other than planar surface flaws detected in the butt weld or base metal inside surface shall be acceptable for continued service in accordance with the requirements of -3132.1(b).
 - (c) A weld with a planar surface flaw shall be acceptable for continued service in accordance with -3132.2(a) or -3132.3(a) and be categorized by Inspection Item in accordance with Table 4-1 or Table 1 of N-770-1 as follows:
 - (1) If the flaw is removed by repair/replacement activity in accordance with IWA-4000 prior to the application of peening, the weld may be peened and be placed into Inspection Item L.
 - (2) If the flaw is not removed, the weld may be peened while acceptability for continued service in accordance with -3132.3(a) is determined. If the weld is acceptable for continued service in accordance with -3132.3(a), the weld shall be placed into Inspection Items A-1, A-2, or B, and shall be re-examined in accordance with Note (5) of Table 1 of N-770-1. The flaw may subsequently be made acceptable for continued service in a subsequent outage in accordance with (3).
 - (3) If the flaw will be made acceptable for continued service in accordance with -3132.2(a), Table 4-1, and Table 1 of N-770-1, peening may be performed over the flaw prior to or following the repair/replacement activity or corrective measure. The weld shall be placed in the Table 1 of N-770-1 Inspection Item category for the repair/replacement activity or corrective measure used for acceptance of the flaw.
- (20) In-service Surface Examination for Peening
- (a) Surface examinations shall be performed on the examination area defined by points E-F in Figure 1 of N-770-1. Surface examinations shall be performed using eddy current examination in accordance with IWA-2223.
 - (b) If new surface flaws are detected, the weld shall be reclassified as Inspection Items A-1, A-2, or B, as applicable, and shall be re-examined in accordance with Note (5) of Table 1 of N-770-1. Alternatively, the flaw may be made acceptable by a repair/replacement activity or other mitigation techniques in accordance with -3132.2(e), as stated in Section 4.2.5.
- (21) In-service Volumetric Examination for Peening
- (a) The examination volume of Figure 1 of N-770-1 shall be ultrasonically examined.
 - (b) The acceptance standards of -3000 apply for the peened dissimilar metal weld.
 - (c) If in-service examinations of (a) reveal new cracking, the surface examination [Note (20)] shall be performed to confirm that the flaw is not surface-connected. If the flaw is not surface-connected, the weld shall be re-examined during each of the next three refueling outages.
 - (d) If the examinations required by (c) reveal that the flaw remains essentially unchanged for three successive examinations, the weld schedule may revert to the schedule of examinations identified in Table 4-1.
 - (e) If an indication is found to be surface-connected, the weld shall be reclassified as Inspection Items A-1, A-2, or B, as applicable, and shall be re-examined in accordance with Note (5) of Table 1 of N-770-1. Alternatively, the flaw may be made acceptable by a repair/replacement activity or other mitigation techniques in accordance with -3132.2(e), as stated in Section 4.2.5.

Table 4-2
List of Requirements in Section 4.2 within the Context of N-770-1

Report Section	Referenced Part of N-770-1	Insertion / Replace N-770-1 Material	Summary of Requirement
4.2.5.1	[Caption of Figure 1]	Insertion	Defines examination surface
4.2.5.1	-2500(c)	Modification	Changes inspection coverage in accordance with 10 CFR 50.55a(g)(6)(ii)(F)(4)
4.2.5.2	-3132.2(d) -3132.2(e)	Insertion	Provides requirements for flaw acceptance by repair/replacement activity or corrective measures for a weld previously mitigated by peening upon subsequent detection of planar surface flaws on the inside surface, including weld reclassification
4.2.5.2	-3132.3(e)	Insertion	Provides requirements for flaw acceptance by evaluation for a weld previously mitigated by peening upon subsequent detection of planar surface flaws on the inside surface, including weld reclassification
4.2.5.3		Insertion	Incorporation of NRC Condition 5.2
4.2.5.4		Insertion	Incorporation of 10 CFR 50.55a(g)(6)(ii)(F)(6)
4.2.7	-2430(a)	Insertion	Specifies inspection expansion requirement for peened components
Subsections of 4.2.8	Mandatory Appendix I	Insertion	Provides the performance criteria that a peening method must meet to use the inspection requirements of Table 4-1
Table 4-1	Table 1	Insertion, Except modification of Note (11)	Specifies inspection requirements for uncracked butt welds mitigated by peening

4.3 Requirements for Reactor Pressure Vessel Head Penetration Nozzles (RPVHPNs) Mitigated by Peening

Items B4.50 and B4.60 of Table 4-3 define alternative inspection requirements for Alloy 600 reactor pressure vessel head penetration nozzles and Alloy 82/182 partial-penetration welds mitigated by a peening mitigation technique meeting the performance criteria of Section 4.3.8. The inspection requirements in Table 4-3 include a pre-peening inspection (Section 4.3.2), follow-up inspection(s) (Section 4.3.3), and long-term in-service inspections (Section 4.3.4).

Within the context of Section 4.3, references to portions of ASME Code Case N-729-1 are indicated using a hyphen followed by the relevant location within this code case (e.g. -2000). Section 4.3 defines inspection requirements relevant to peening by specifying additions to ASME Code Case N-729-1. A listing of such additions and other requirements in this section is provided by Table 4-4.

4.3.1 Summary of Performance Criteria of Section 4.3.8

The performance criteria of Section 4.3.8 shall be satisfied. For information only, brief summaries of the requirements of Section 4.3.8 are provided below.

Peening Coverage

The required coverage is the full wetted surfaces of the attachment weld, butter, and nozzle base material in the region defined in Figure 4-1 through Figure 4-4. As discussed in Section 2.3.3, these coverage figures were specified to ensure that areas susceptible to PWSCC initiation are mitigated. Section 4.3.8.1 requires that the boundaries of the area required to be effectively peened in Figure 4-1 through Figure 4-4 be extended a suitable distance for the specific peening method to provide high assurance that the areas susceptible to PWSCC receive the required peening effect.

Due to geometry, some peening techniques of interest cannot be used to peen the threaded areas that are present in some cases near the bottom of the nozzle tube. Because any such threaded areas are located below the weld toward the end of the nozzle and are not part of the pressure boundary, it is not necessary that peening be performed of the threaded regions when present.

Stress Magnitude

The stress prior to consideration of operating stresses must be compressive on all peened surfaces. The residual stress plus normal operating stress on peened surfaces must not exceed +10 ksi (+70 MPa) tensile stress.

Depth of Effect

The compressive residual stress field extends a nominal minimum depth of:

- 0.04 in. (1.0 mm) on the susceptible area of the nozzle outside surface and weld surface
- 0.01 in. (0.25 mm) on the susceptible area of the nozzle inside surface

Sustainability of Effect

The mitigation process is effective for at least the remaining service life of the component, i.e., the residual plus normal operating surface stress state after considering the effects of thermal

relaxation and load cycling (i.e., shakedown) must remain no greater than +10 ksi (+70 MPa) tensile.

Inspectability

The capability to perform ultrasonic examinations of the relevant volume of the component is not adversely affected, and the relevant volume or surface is inspectable using a qualified process.

Lack of Adverse Effects

As verified by analysis or testing, the mitigation process is not to have degraded the component, caused detrimental surface conditions, or adversely affected other components in the system.

4.3.2 Pre-Peening Baseline Inspection

Prior to performance of peening but during the same outage, the following examinations are to be performed in accordance with the requirements in Table 4-3:

- A volumetric examination of each nozzle tube is to be performed as the baseline inspection. As an alternative, surface examination of the nozzle inner surface and the wetted surface of the nozzle outside and weld may be performed and considered the baseline inspection.
- Additionally, a demonstrated volumetric or surface leak path assessment through all J-groove welds is to be performed.

The leak path examination detects through-wall cracking by checking for areas at the interface between the nozzle tube and low-alloy steel head material where leakage has caused a loss of interference fit. The analyses in Section 5 and Appendix B conservatively do not take credit for the leak path examination.

4.3.3 Follow-Up Inspection

During the follow-up inspection(s), a volumetric examination of 100% of the required volume or equivalent surfaces of the nozzle tube is to be performed and a leak path examination is also to be performed. The follow-up inspection requirements are contained in Table 4-3, which provides different inspection schedules depending on the value of the EDY parameter (defined in N-729-1) at the time of peening:

- For plants where RPVHPNs and associated J-groove welds in a reactor vessel closure head have experienced $EDY \geq 8$, a follow-up inspection is to be performed in the first and second refueling outages subsequent to peening.
- For plants where RVPHPNs and associated J-groove welds in a reactor vessel closure head have experienced $EDY < 8$, if all RPVHPNs in the reactor vessel closure head are free from pre-peening flaws, inspections shall be performed on each RPVHPN in the second refueling outage subsequent to peening.
- For plants where RVPHPNs and associated J-groove welds in a reactor vessel closure head have experienced $EDY < 8$, if indications of cracking, attributed to PWSCC, have been identified in the RPVHPNs or associated J-groove welds, whether acceptable or not for continued service under Paragraphs -3130 or -3140 of ASME Code Case N-729-1,

inspections shall be performed on each RPVHPN in the first and second refueling outage subsequent to peening.

4.3.4 Subsequent ISI Program

The in-service inspection requirements are shown in Table 4-3 and are summarized as follows:

Visual Examinations

A VE visual examination for evidence of leakage shall be performed each refueling outage.

Volumetric or Surface Examinations

The following ISI program occurs after completion of the follow-up inspection(s):

- Volumetric or surface examinations of peened penetrations are to be performed at an interval not to exceed one inspection interval (nominally 10 years).
- A demonstrated volumetric or surface leak path assessment through all J-groove welds is performed each time the periodic volumetric or surface examination is performed.

4.3.5 Examination Coverage and Acceptance Criteria for Inspection Results

4.3.5.1 Examination Coverage

The required examination volume and the required examination surface (as applicable) are defined in Figure 2 of ASME Code Case N-729-1. In accordance with 10 CFR 50.55a(g)(6)(ii)(D)(6) and for U.S. plants, implementation of Note (5) of Table 4-3 requires prior NRC approval.

4.3.5.2 Acceptance Criteria for Item B4.50 of Table 4-3

The visual examination acceptance standards for Item B4.50 of Table 4-3 are in accordance with Subsubarticle -3140 of N-729-1 with the addition of the following to Paragraph -3141:

- (d)(1) For examinations performed prior to application of peening mitigation, flaws exceeding the criteria of -3142 of N-729-1 shall be considered defects and shall be corrected in accordance with IWA-4000 prior to the application of peening mitigation.
- (d)(2) For examinations performed following application of peening mitigation, indications exceeding the acceptance criteria of -3142 of N-729-1 are unacceptable. If an indication is identified, the indication shall be evaluated under -3142 of N-729-1 and the head shall be identified as Item B4.10 of N-729-1 until the indication has been corrected in accordance with IWA-4000. Following repair/replacement activities, the corrected area of the nozzle, plus 0.5 in. (12.7 mm) beyond the corrected area, may be re-peened. The preservice examination required by IWA-4000 for the repair/replacement activity may be performed prior to or after re-peening. If no relevant indications are identified, or are corrected prior to subsequent re-peening, the head may be returned to Examination Category Item B4.50. Follow-up volumetric or surface examinations in accordance with Note (11) of Table 4-3 are required for the re-peened nozzle.

4.3.5.3 Acceptance Criteria for Item B4.60 of Table 4-3

The surface and volumetric examination acceptance standards for Item B4.60 of Table 4-3 are in accordance with Subsubarticle -3130 of N-729-1 with the addition of the following to Paragraph -3131:

- (d)(1) For examinations performed prior to the application of peening mitigation, flaws exceeding the criteria of -3132 of N-729-1 shall be considered defects and shall be corrected in accordance with IWA-4000 prior to the application of peening mitigation.
- (d)(2) For examinations performed following the application of peening mitigation, flaws exceeding the criteria of -3132 of N-729-1 shall be considered defects and shall be corrected in accordance with IWA-4000. If an acceptable flaw is found, the nozzle shall be identified as Item B4.20 of N-729-1 until the flaw has been corrected in accordance with IWA-4000. Following repair/replacement activities, the corrected area of the nozzle, plus 0.5 in. (12.7 mm) beyond the corrected area, may be re-peened. The preservice examination required by IWA-4000 for the repair/replacement activity may be performed prior to or after re-peening. If no relevant indications are identified, or are corrected prior to subsequent re-peening, the nozzle may be identified as Item B4.60. Follow-up volumetric or surface examinations in accordance with Note (11) of Table 4-3 are required for the re-peened nozzle.

Additionally, the phrase “of the 2004 Edition” is omitted from the second to last sentence of paragraph -3132.3 of N-729-1.

4.3.5.4 Requirements for RPVHPNs Subsequent to Flaw Detection or Observation of Flaw Growth

If a wetted surface-connected flaw, an unacceptable flaw based on the ASME Code, Section XI, or unacceptable flaw growth is observed in a peened RPVHPN or J-groove weld,

- (a) A report summarizing the evaluation, including inputs, methodologies, assumptions, extent of conditions, and causes of the new flaw, unacceptable flaw, or flaw growth, must be submitted to the NRC prior to the plant entering into Mode 4.
- (b) A sample inspection of the peened components in the population must be performed to assess the extent of condition.
- (c) A final causal analysis report consistent with the licensee corrective action program including a description of corrective actions taken must be submitted to the NRC within six months of the discovery.
- (d) The inspection relaxation per this report is no longer applicable to the affected RPVHPN. The affected RPVHPN component shall be inspected in accordance with the requirements of 10 CFR 50.55a, unless an alternative is authorized by the NRC.

4.3.6 NDE Qualification Requirements

Ultrasonic examinations shall be performed using personnel, procedures, and equipment that have been qualified by blind demonstration on representative mockups using a methodology that meets the conditions specified in 10 CFR 50.55a(g)(6)(ii)(D)(4).

Visual examinations for evidence of leakage shall be performed in accordance with IWA-2200 and Notes (1) and (2) of Table 1 in ASME Code Case N-729-1.

If performed, surface examinations shall be performed in accordance with Section XI IWA-2200 and Section 4.3.8.5.

4.3.7 Previously Repaired Top Head Nozzles Mitigated by Peening

If the requirements of this Section 4.3 are satisfied, a top head nozzle with flaws that have been corrected may be subsequently peened using a process meeting the performance criteria of Section 4.3.8. In that case, the head and nozzle may be identified as Item B4.50 and Item B4.60, respectively, in Table 4-3.

From the perspective of susceptibility to PWSCC degradation, a penetration repaired using the embedded flaw repair technique (i.e., with an Alloy 52 weld overlay applied to the outer and/or inner penetration surfaces) and subsequently peened is bounded by the analyses of Section 5 and Appendix B for unrepaired penetrations. Subsequent to peening, the areas with Alloy 600/82/182 material in contact with reactor coolant will have a residual plus normal operating surface stress well below that necessary to initiate PWSCC flaws. Even if exposed areas of Alloy 52 weld metal are not peened, the improved PWSCC resistance of Alloy 52 material in comparison to Alloys 600/82/182 conservatively supports the nominal 10-year interval for volumetric or surface examinations of Item B4.60 in Table 4-3 (based on the assessments in MRP-375 [78]). It is also noted that at least one follow-up volumetric or surface examination is required within the first two refueling outages subsequent to the peening outage. Follow-up inspections have the benefit of checking the condition of any previously repaired nozzles.

4.3.8 APPENDIX: Performance Criteria and Measurement or Quantification Criteria for Mitigation by Surface Stress Improvement (Peening) of PWR Reactor Vessel Upper Head Penetrations and Attachment Welds

It is noted that Section 2.1 discusses quality assurance considerations with regard to implementation of peening mitigation:

“Since surface stress improvement by peening affects the performance of nuclear safety related systems and components, it shall be performed in accordance with a quality assurance program meeting the requirements of Appendix B to 10 CFR 50 and the utility’s plant specific commitments. Further, since peening is a special process, it shall be controlled in a manner consistent with Criterion IX, ‘Control of Special Processes,’ of Appendix B and any applicable plant specific commitments. As stated in that criterion, this requires that the personnel and procedures involved need to be appropriately qualified. Since there are no industry standards that apply to peening, these qualifications shall be done to vendor requirements developed and documented per their 10 CFR 50 Appendix B quality assurance program and to utility requirements and commitments applicable at the plant site.”

Thus peening shall be performed and qualified per requirements meeting the quality assurance criteria of 10 CFR 50 Appendix B. As such, the analysis and demonstration testing required below are performed in accordance with these quality assurance requirements, which provide adequate controls.

4.3.8.1 Stress Effect

To minimize the likelihood of crack initiation, the process shall have resulted in a compressive stress in the full area of the susceptible UNS N06600, UNS N06082, and UNS W86182 material as defined by Figure 4-1 through Figure 4-4 prior to consideration of operating stresses. The susceptible material locations are the attachment weld, butter, and nozzle base material, including the inside surface region of nozzle penetrations in areas adjacent to the attachment weld, as applicable. The residual stress plus normal operating stress on surfaces required to be peened shall be included in the evaluation and shall not exceed +10 ksi (+70 MPa).

The boundaries of the area required to be effectively peened shall be extended beyond the PWSCC susceptible area defined in Figure 4-1 through Figure 4-4 a suitable distance to provide high assurance that the areas susceptible to PWSCC receive the required peening effect. Due to geometry, some peening techniques of interest cannot be used to peen the threaded areas that are present in some cases near the bottom of the nozzle tube. Because any such threaded areas are located below the weld toward the end of the nozzle and are not part of the pressure boundary, it is not necessary that peening be performed of the threaded regions when present.

A combination of demonstration testing and analysis shall be performed to demonstrate the required capability of the peening method to produce the required post-mitigation stress state:

- (a) Demonstration testing shall be performed to determine the residual stress state at the surfaces required to be peened. Test sections representative of the geometry, accessibility, and surface condition of the component to be peened shall be used. Each test section shall include a cylindrical tube representative of the nozzle tube and a thick-wall section representative of the low-alloy steel head material. The nominal wall thickness of the thick-wall section shall be no greater than that of the actual head. Multiple test sections shall be used to bound the range of nozzle incidence angles.
- (b) Analysis shall be performed to determine the effect of normal operating loads on the steady-state operating stresses at the surfaces required to be peened.

The testing shall be used to demonstrate the critical process parameters and define acceptable ranges of the parameters needed to ensure that the required residual stress field (exclusive of normal operating stresses) has been produced on the mitigated surface.

The uncertainty in measurement of the surface residual stress shall be considered in the analysis to determine the surface stress including operating and residual stress. The basis for that consideration shall be documented in the relief request.

4.3.8.1.1 Magnitude of Surface Stress

The combination of demonstration testing and analysis shall show that the steady-state operating stresses combined with residual stresses do not exceed +10 ksi (+70 MPa) (tensile) on the required application surface.¹²

¹² Some advanced peening processes result in a very thin surface layer (i.e., within 0.001 to 0.002 inch (25 to 50 μm) from the surface) where the residual stress is tensile or not as compressive as the residual stress deeper into the material. For example, see Figures A-14, A-42, and A-43 of MRP-267R1 [10]. The underlying compressive residual stresses prevent development of significant PWSCC cracks at the surface. Thus, the residual stresses in this very thin surface layer may be excluded when showing that the requirement of Section 4.3.8.1.1 is met. The combination of

4.3.8.1.2 Nominal Depth of Compressive Residual Stress

The testing shall demonstrate that the nominal depth of the compressive surface residual stress field produced by the peening technique is at least:¹³

- a) 0.04 in. (1.0 mm) on the outside surface of the nozzle and wetted surface of the attachment weld and butter susceptible to PWSCC initiation as defined in Section 4.3.8.1.
- b) 0.01 in. (0.25 mm) on the inside surface of the nozzle susceptible to PWSCC initiation as defined in Section 4.3.8.1.

The nominal depth refers to the depth of the compressive residual stress that is reliably obtained in demonstration testing, i.e., for at least 90% of the locations measured.

4.3.8.2 Sustainability

Analysis or testing shall be performed to verify that the peening process maintains the surface stress state no greater than +10 ksi (+70 MPa) tensile (normal operating and residual stress) for at least the remaining service life of the component. The analysis or demonstration test plan shall include startup and shutdown stresses, normal operating pressure stress, thermal cyclic stresses, transient stresses, and residual stresses. The analysis or demonstration test shall account for:

- (a) load combinations that could relieve stress due to shakedown
- (b) any material properties related to stress relaxation over time

4.3.8.3 UT Inspectability

The capability to perform ultrasonic examinations of the relevant volume of the component shall not be adversely affected. Ultrasonic examinations shall be performed using personnel, procedures, and equipment qualified by blind demonstration on representative mockups that meet the requirements of the ASME Code Case N-729-1 requirements of -2500 and the conditions in 10 CFR 50.55a(g)(6)(ii)(D)(4). Testing shall be performed to demonstrate that the examination volume of the mitigated component can be examined subsequent to mitigation, including changes to component geometry, material properties, or other factors.

4.3.8.4 Lack of Adverse Effects

Analysis or testing shall be performed to verify the following:

- (a) The mitigation process, including any vibration effects during application, does not degrade the component or adversely affect other components in the system, including but

demonstration testing and analysis shall show that the steady-state operating stresses combined with residual stresses do not exceed +10 ksi (+70 MPa) (tensile) immediately beyond the very thin surface zone of elevated residual stress.

¹³ Some advanced peening processes result in a very thin surface layer (i.e., within 0.001 to 0.002 inch (25 to 50 μ m) from the surface) where the residual stress is tensile. The tensile residual stresses in this very thin surface layer may be excluded when showing that the requirement of Section 4.3.8.1.2 is met. The testing shall demonstrate that the nominal depth of the compressive surface residual stress field, excluding the very thin layer of tensile stress at the surface, is at least 0.04 in. (1.0 mm) or 0.01 in. (0.25 mm) as defined in Section 4.3.8.1.2. The depth measurement shall be from the surface to the point where the compressive residual stress becomes neutral.

not limited to any thermal sleeve present within the nozzle or funnel directly attached to the end of the nozzle.

- (b) The mitigation process does not cause erosion of surfaces, undesirable surface roughening, or detrimental effects in the transition regions adjacent to the peened regions.

4.3.8.5 NDE Qualification

The relevant volume or surface shall be inspectable using a qualified process. An evaluation shall be performed to confirm that the required examination volume and surfaces of the mitigated configuration are within the scope of the qualification.

Examination Requirements

Table 4-3
Inspection Requirements for Alloy 600 RPVHPNs Mitigated by Peening

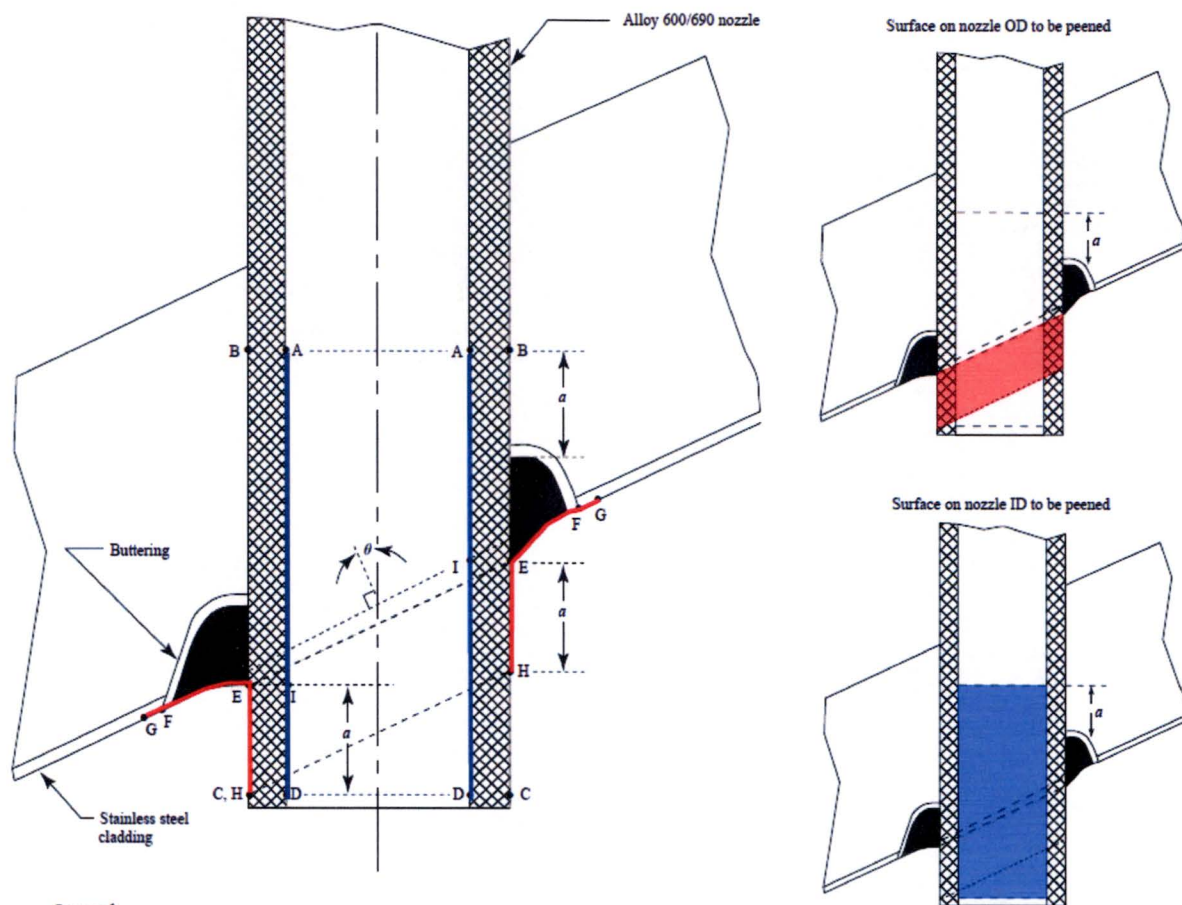
EXAMINATION CATEGORIES						
CLASS 1 PWR REACTOR VESSEL UPPER HEAD						
Item No.	Parts Examined	Examination Requirements/ Fig. No.	Examination Method	Acceptance Standard	Extent and Frequency of Examination	Deferral of Examination to End of Interval
B4.50	Head with UNS N06600 nozzles and UNS N06082 or UNS W86182 partial-penetration welds mitigated by peening qualified in accordance with Section 4.3.8	Figure 1 of N-729-1	Visual, VE (1), (2)	Section 4.3.5	Each refueling outage (3), (12), (13)	Not permissible
B4.60	UNS N06600 nozzles and UNS N06082 or UNS W86182 partial-penetration welds mitigated by peening in accordance with Section 4.3.8	Figure 2 of N-729-1 (5)	Volumetric (6) Surface (6)	Section 4.3.5	All Nozzles, not to exceed one inspection interval (nominally 10 calendar years) (9), (11), (12), (13)	Not permissible

NOTES: (1) through (5) and (7) are identical to those in ASME Code Case N-729-1 [2]

- (6) Volumetric or surface examinations shall be performed on essentially 100% of the required volume or equivalent surfaces of the nozzle tube, as identified by Figure 2 of N-729-1. A demonstrated volumetric or surface leak path assessment through all J-groove welds shall be performed. For leaking penetrations, the meandering fluid stream pattern of the ultrasonic data display represents the leak path of the primary coolant from the pressure vessel to the atmosphere. If a surface examination is being substituted for a volumetric examination on a portion of a penetration nozzle that is below the toe of the J-groove weld (Point E in Figure 2 of N-729-1) the surface examination shall be on the penetration nozzle inside and outside wetted surface.
- (8) If flaws are attributed to PWSCC, whether or not acceptable for continued service in accordance with -3130 or -3140 of N-729-1, the re-inspection interval shall be each refueling outage. Additionally, repaired areas shall be examined during the next refueling outage following the repair.
- (9) Includes essentially 100% of surface or volume.
- (10) Not used.
- (11) After peening application, a follow-up examination meeting the inspection requirements of Note 6 shall be performed:
- in the first and second refueling outages following peening mitigation, for plants with EDY ≥ 8 at the time of peening.
 - in the first and second refueling outages following peening mitigation, for plants with EDY < 8 at the time of peening, if indications of cracking, attributed to PWSCC, have been identified in the RPVHPNs or associated J-groove welds, whether acceptable or not for continued service under Paragraphs -3130 or -3140 of N-729-1.
 - in the second refueling outage following peening mitigation, for plants with EDY < 8 at the time of peening, if all RPVHPNs in the reactor vessel closure head are free from pre-peening flaws.
- (12) If flaws are detected that are unacceptable for continued service in accordance with -3132.3 or -3142.3(a), they shall be corrected by repair/replacement activity of -3132.2 or -3142.3(b). The head or nozzle shall be identified as item B4.10 or item B4.20 of N-729-1. If peening mitigation is subsequently performed, the head or nozzle may be again identified as item B4.50 or item B4.60.
- (13) If peening mitigation techniques qualified in accordance with Section 4.3.8 are used, the following shall be met:
- Volumetric examination of the volume (A-B-C-D) as identified in Figure 2 of N-729-1 shall be performed prior to application of peening mitigation techniques. This examination shall be considered the pre-service baseline examination.
 - Prior to peening mitigation, a documented leak path evaluation shall be performed of each penetration capable of being examined by the leak path evaluation method.
 - As an alternative to (a) and (b), a surface examination of A-D and C-G may be performed and considered the pre-service examination.
 - A documented evaluation shall be completed demonstrating that the peening mitigation techniques meet the performance criteria in Section 4.3.8.
 - Prior to peening, flaws detected during the pre-mitigation inspection shall be corrected by a repair/replacement activity of -3132.2.
 - The surfaces to be mitigated shall include the regions of the J-groove attachment weld and penetration tubing (outside and inside) defined in Figure 4-1 through Figure 4-4.

Table 4-4
List of Requirements in Section 4.3 within the Context of N-729-1

Report Section	Referenced Part of N-729-1	Insertion / Replace N-729-1 Material	Summary of Requirement
4.3.5.1	Note (5) of Table 4-3	Modification	Incorporation of the NRC condition specified in 10 CFR 50.55a(g)(6)(ii)(D)(6)
4.3.5.2	-3141(d)(1) -3141(d)(2)	Insertion	Visual examination acceptance standards, and requirements for returning a penetration to inspection per Item B4.50 following detection of an indication subsequent to peening
4.3.5.3	-3131(d)(1) -3131(d)(2)	Insertion	Surface and volumetric examination acceptance standards, and requirements for returning a penetration to inspection per Item B4.60 following detection of an indication subsequent to peening
4.3.5.3	-3132.3	Modification	Omittance of the phrase "of the 2004 Edition" from the second to last sentence of paragraph -3132.3
4.3.5.4		Insertion	Incorporation of NRC Condition 5.2
4.3.6	-2500	Modification	Incorporation of the NRC condition specified in 10 CFR 50.55a(g)(6)(ii)(D)(4)
4.3.6	-2500	Insertion	Provides performance requirements for any surface examinations performed
Subsections of 4.3.8	Mandatory Appendix II	Insertion	Provides the performance criteria that a peening method must be performed in accordance with to use the inspection requirements of Table 4-3
Table 4-3	Table 1	Insertion, Except modification of Notes (6), (8), (9), (10)	Specifies inspection requirements for Alloy 600 RPVHPNs mitigated by peening



Legend:

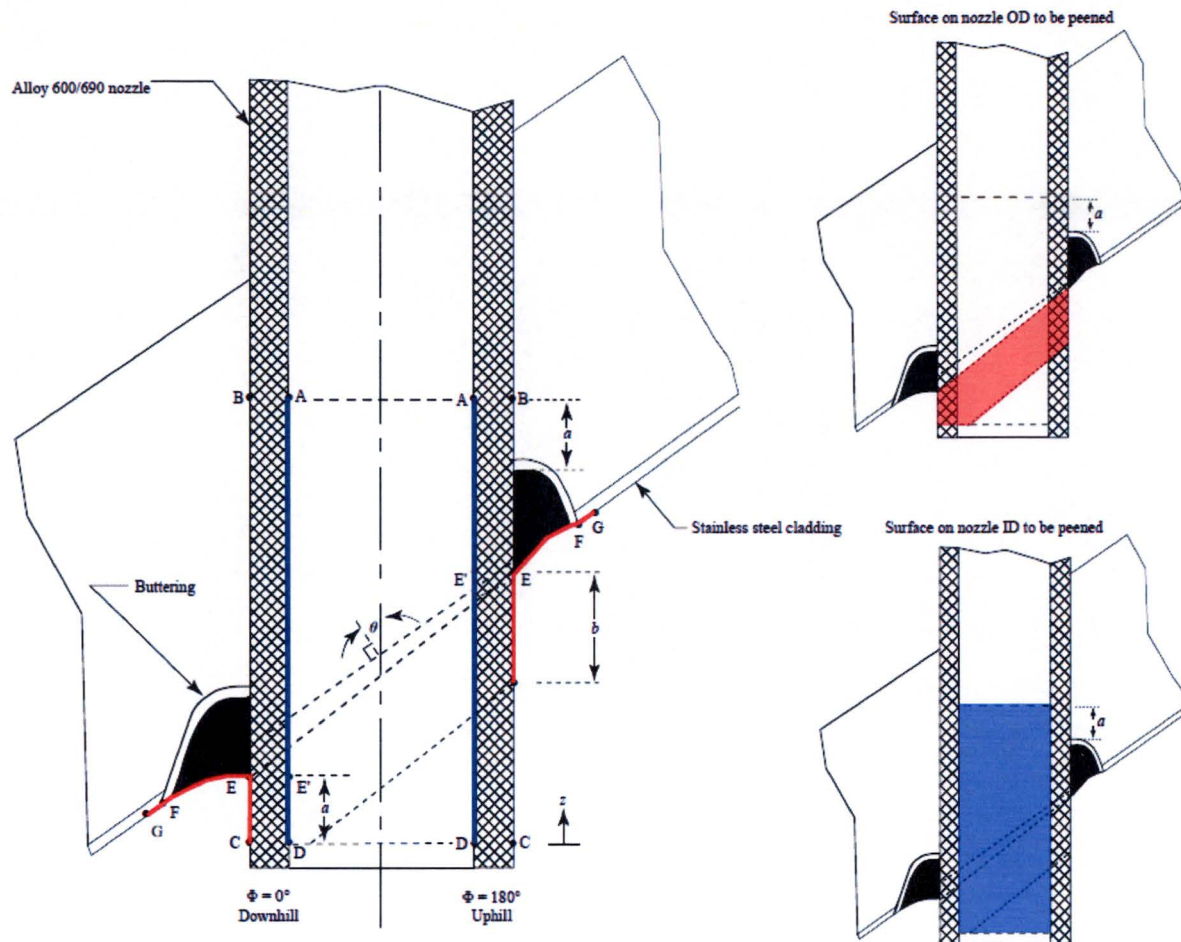
$a = 1.5$ in. (38 mm), or to the end of the tube, whichever is less

$G-F = 0.25$ in. (6 mm) from the theoretical point "F" in accordance with the design drawings, including tolerances, unless the point "F" can be physically determined

Surface on the penetration outer surfaces required to be peened = H-E-F-G, excluding any threaded region on the nozzle OD

Surface on the penetration ID required to be peened = A-D, excluding any threaded region on the nozzle ID

Figure 4-1
Required Peening Coverage Zone for RPVHPNs with Incidence Angle, θ , ≤ 30 deg (Except Head Vent Nozzles) and for All RPVHPNs with Outer Diameter ≥ 4.5 in. (115 mm)



Legend:

$a = 1.0$ in. (25 mm), or to the end of the tube, whichever is less

$b = 1.5$ in. (38 mm)

$z =$ elevation above C-C plane

$\Phi =$ azimuthal angle from downhill position

$\Phi_1, \Phi_2 =$ two azimuthal positions where the horizontal C-C plane is 1.5 in. (38 mm) below the toe of the weld on the nozzle OD

$$z(\Phi) = \begin{cases} 0 & \text{if } \Phi < \Phi_1, \text{ or } \Phi > \Phi_2 \\ 1.5 \text{ in. (38 mm) below toe of weld} & \text{if } \Phi_1 \leq \Phi \leq \Phi_2 \end{cases}$$

$G-F = 0.25$ in. (6 mm) from the theoretical point "F" in accordance with the design drawings, including tolerances, unless the point "F" can be physically determined

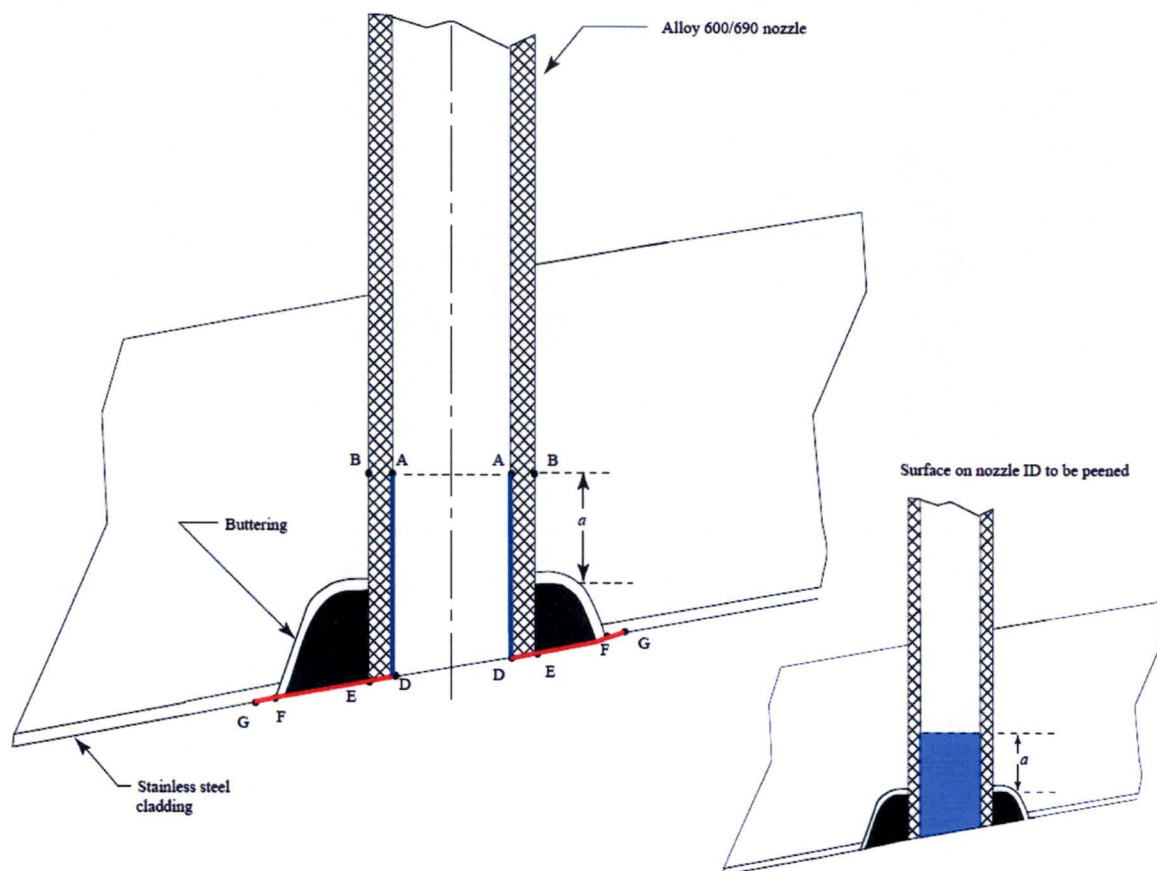
Surface on the weld required to be peened = E-F-G

Surface on the nozzle OD required to be peened = full height between elevation $z(\Phi)$ and toe of weld on nozzle OD, excluding any threaded region

Surface on the penetration ID required to be peened = A-D, excluding any threaded region

Figure 4-2

Required Peening Coverage Zone for RPVHPNs with Incidence Angle, θ , > 30 deg and Outer Diameter Less Than 4.5 in. (115 mm)



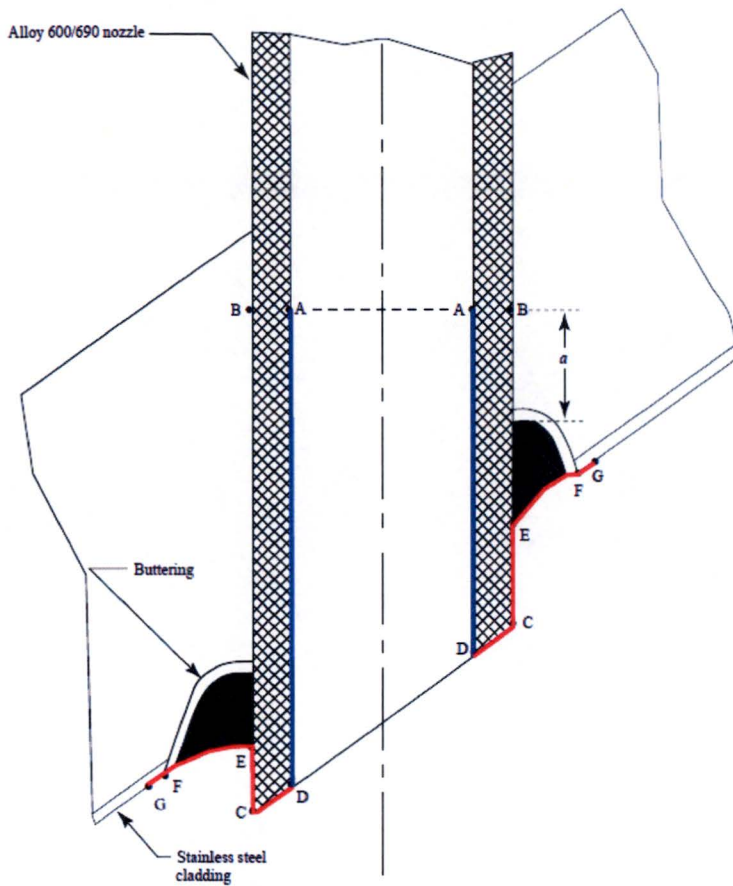
Legend:

$a = 1.5 \text{ in. (38 mm)}$

$G-F = 0.25 \text{ in. (6 mm)}$ from the theoretical point "F" in accordance with the design drawings, including tolerances, unless the point "F" can be physically determined

Surface on the penetration required to be peened = A-D-E-F-G

Figure 4-3
Required Peening Coverage Zone for J-Groove Head Vent Nozzles



Legend:

 $a = 1.5 \text{ in. (38 mm)}$

E = toe of the weld on the OD of the tube at every azimuthal position

G-F = 0.25 in. (6 mm) from the theoretical point "F" in accordance with the design drawings, including tolerances, unless the point "F" can be physically determined

Surface on the penetration required to be peened = A-D-C-E-F-G

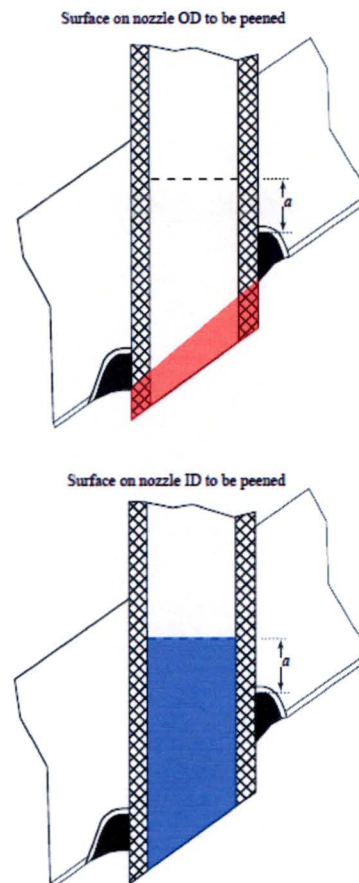


Figure 4-4
Required Peening Coverage Zone for RPVHPNs with Outer Diameter ≥ 4.5 in. (115 mm) for Which the End of the Nozzle is Parallel with the Head

5

SUPPORTING ANALYSES

5.1 Approach

To demonstrate the benefit of peening on PWSCC of Alloy 600/82/182 components, this section presents deterministic and probabilistic analyses that factor in surface stress improvement and its effects on the PWSCC degradation process. This section, in conjunction with the additional detail provided in Appendix A and Appendix B, provides the technical bases for the inspection requirements of Section 4.

The deterministic analyses specifically investigate the effect of the surface stress improvement on PWSCC crack growth versus time. These analyses predict crack growth versus time, at various assumed crack locations, from various initial crack sizes. Stress profiles representative of those present in components before peening and after peening are considered. Peening mitigation is effective because it prevents initiation of new PWSCC flaws. Peening also has the potential to affect growth of pre-existing flaws because of its influence on the residual stress field. The deterministic crack growth analyses demonstrate that flaws significantly deeper than the peening compressive residual stress layer tend to grow in depth at a rate similar to that for the unmitigated case. A matrix of deterministic crack growth cases is applied to demonstrate the effectiveness of the peening inspection requirements (pre-peening, follow-up, and long-term ISI examinations) to detect pre-existing PWSCC before through-wall penetration and leakage occurs. As the deterministic calculations investigate crack growth versus time from an assumed initial flaw size at the time of peening until the time that leakage predicted, and as cracks can initiate at any time during plant operation prior to peening, the deterministic results are generally applicable to any plant service lifetime. As shown by plant experience ([54], [55]), any leakage calculated to occur in the deterministic matrix is expected to be small and represent no direct safety concern, including for boric acid corrosion and unstable rupture.

The deterministic crack growth calculation methodology is also implemented within the probabilistic framework for the purpose of assessing the effectiveness of follow-up and ongoing ISI examinations in addressing the potential effects of any pre-existing flaws not detected in the pre-peening examination. The probabilistic analyses take a more comprehensive approach to predicting the effect of surface stress improvement on PWSCC, incorporating detailed probabilistic models for component loading, crack initiation, crack growth, and crack detection. The integrated probabilistic model, which unites the various models into a probabilistic simulation framework, allows the prediction of PWSCC throughout the operating lifetime of the PWR. The probabilistic analyses show that the application of peening coupled with the required post-peening inspection schedules results in reduced safety risk as compared to that associated with unpeened components inspected at the currently required schedules.

The benefit of peening in the deterministic and probabilistic analyses is modeled on the basis of the compressive residual stress field assumed to be induced at the treated surface by peening.

The main analysis cases apply the bounding stress conditions meeting the performance criteria of Section 4, i.e., the minimum acceptable nominal depth of the compressive residual stress layer and the limiting magnitude of the residual plus normal operating stress at the peened surface. For the deterministic analysis results for RPVHPNs in Section 5.2.2.2, the peening compressive stress at the surface is set to result in a net tensile stress of +70 MPa (+10 ksi) in the direction of maximum operating stress for flaws on the nozzle ID surface, and a residual stress value that results in a net stress of 0 MPa (0 ksi) is assumed for the peened surface of the nozzle OD and weld since the operating stress in those regions is small. For the deterministic matrix results for RPVHPNs in Section 5.2.3.2, the total (residual plus normal operating) stresses on the nozzle tube OD and weld were modeled to be +10 ksi (different from Section 5.2.2.2) subsequent to peening. The total (residual plus normal operating) stresses on the nozzle tube ID were modeled to be +10 ksi (as in Section 5.2.2.2) subsequent to peening.

5.2 Deterministic Analysis of Peening Effects

This section focuses on deterministic growth calculations for cracks in unmitigated and peened components.

For reference, Section 5.2.1 describes the stress profiles assumed before and after peening. The bounding peening stress effect meeting the performance criteria of Section 4 is used in the main calculation cases.

Section 5.2.2 gives deterministic growth calculations for cracks assumed to remain active after an outage in which inspection and peening occur. In addition to the bounding cases meeting the performance criteria, cases are shown for stress profiles reflecting a larger peening stress effect based on stress measurements documented in MRP-267R1 [10].

Similarly, the matrix of deterministic growth calculations in Section 5.2.3 evaluates the timing of follow-up and in-service inspections relative to the growth of median and bounding (using 5th and 95th percentile crack growth rate material behavior) cases with initial crack sizes smaller than those detectable by the pre-peening examinations. The deterministic matrix of cases demonstrates the effectiveness of the peening inspection requirements to detect pre-existing PWSCC flaws not detected in the pre-peening inspection prior to leakage being produced.

Section 5.2.4 documents a validation study demonstrating congruity of stress intensity factors calculated with an analytical weight function method and with a high-fidelity finite element approach.

Section 5.4 discusses the conclusions of the supporting analyses, including the deterministic growth calculations of Section 5.2.2 and the matrix of deterministic growth calculations demonstrating the effectiveness of the required inspections to prevent through-wall penetration and leakage in Section 5.2.3.

5.2.1 Effect of Peening on Stress Profile

The modeled post-peening residual stress profile is characterized by a thin compressive region near the peened surface followed by a rapid transition to the pre-peening residual stresses. The key attributes of this stress profile are the compressive residual stress magnitude at the surface and the penetration depth – the depth to which peening imparts compressive residual stresses. These attributes are assumed to be the same in orthogonal directions (i.e. hoop and axial

stresses). An example post-peening stress profile is shown in Figure 5-1 and is repeated for the region near the peened surface in Figure 5-2 (the details of which are given in Appendix A). The quantities given in the remainder of this subsection are assumed for the deterministic crack growth analyses in Section 5.2.2. Input values corresponding to the bounding performance criteria for the post-peening residual stress are assumed for the deterministic crack growth analyses.

Bounding Peening Stress Profile

The magnitude of the peening compressive residual stress on the peened surfaces is chosen to obtain the bounding surface stress allowed in Section 4:

- For piping dissimilar metal butt welds (DMWs), the residual plus normal operating stress remains compressive for all wetted surfaces along the susceptible material. Thus, the peening compressive stress at the surface is set to result in a total (operating plus residual) stress of zero at the circumferential location and for the principal stress direction with the maximum operating stress.
- For reactor pressure vessel head penetration nozzles (RPVHPNs), the residual plus normal operating stress on the peened surface does not exceed +70 MPa (+10 ksi), and the residual stress on the peened surface is compressive. Thus, the peening compressive stress at the surface is set to result in a net tensile stress of +70 MPa (+10 ksi) in the direction of maximum operating stress for flaws on the nozzle ID surface, and a residual stress value that results in a net stress of 0 MPa (0 ksi) is assumed for the peened surface of the nozzle OD and weld since the operating stress in those regions is small.

The penetration depth of peening is expected to vary depending on the component and location being peened. The depths of the peening compressive residual stress layer in the analyses are assumed to be commensurate with the bounding performance criteria meeting the minimum acceptable stress effect described in Section 4:

- For the ID of a DMW component, a 1.0 mm (0.04 inch) deep layer of compressive residual stress is assumed.
- For the ID of a RPVHPN, a 0.25 mm (0.01 inch) deep layer of compressive residual stress is assumed.
- For the nozzle OD and weld wetted surfaces of a RPVHPN, a 1.0 mm (0.04 inch) deep layer of compressive residual stress is assumed.

After the superposition of operational loads (e.g., pressure loads) with the residual stresses, the stresses at the surface tend to become less compressive and more tensile. For the bounding deterministic calculations in Section 5.2.2, the stress profile (residual and operating stress) is modeled as 0 or 10 ksi tensile at the surface and increasingly tensile into the material in the surface region. The performance criteria modeled in the bounding deterministic calculations require that the peening process results in a stress during steady-state operation (residual stress plus normal operating stress) within the full area required to be peened that remains below this conservative measure of the threshold for at least the remaining service life of the peened component. The performance criteria require that the effects of load cycling (i.e., shakedown) and thermal stress relaxation be considered.

Example Representative Peening Stress Profile

In addition to the bounding case based on the bounding stress effect meeting the performance criteria, cases are also evaluated using a peening residual stress profile representative of stress measurements documented in MRP-267R1 [10]:

- For all components, a compressive residual stress magnitude at the surface of 689.5 MPa (100 ksi) is assumed. Data and other information from peening vendors suggest that a compressive surface stress magnitude between 400 and 1000 MPa (58.0 to 145 ksi) can be achieved by peening. While thermal and load cycling may reduce the compressive stress magnitude over the operating lifetime of the plant (with a large majority of relaxation occurring during the first operational cycle after peening), the stress magnitude for these cases is chosen to demonstrate the crack growth behavior in components where peening induces a highly compressive residual stress.
- For the ID of a DMW component, a compressive residual stress depth of approximately 1.0 mm (0.04 inch) is assumed, based on the expected capability of applicable peening techniques.
- For the ID of a RPVHPN, a compressive residual stress depth of approximately 0.5 mm (0.02 inch) is assumed.
- For the outer surface locations (weld and nozzle OD) of a RPVHPN, the compressive residual stress depth is assumed to be approximately 3.0 mm (0.12 inch).

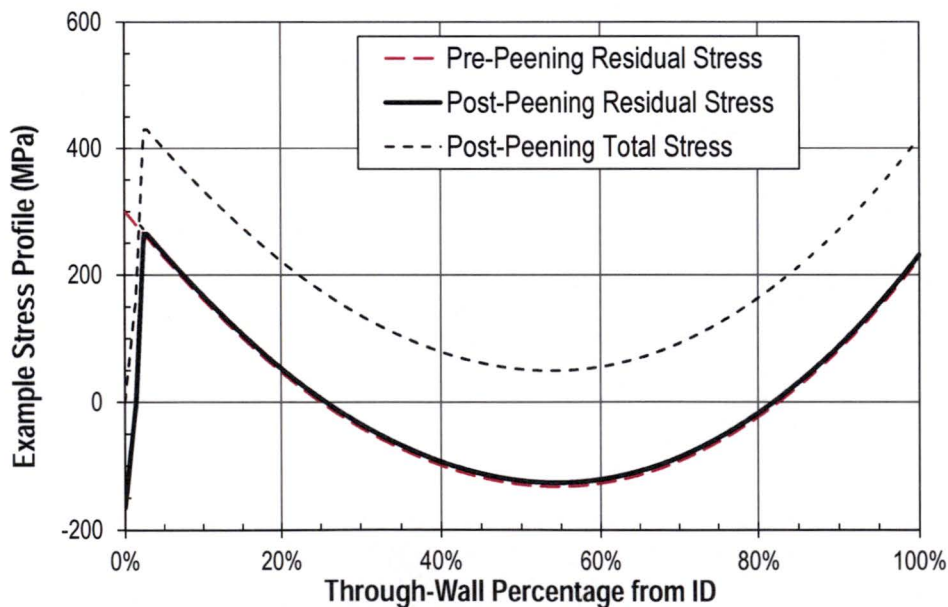


Figure 5-1
Example Bounding Post-Peening Stress Profile for Circumferential Crack in a DMW Component

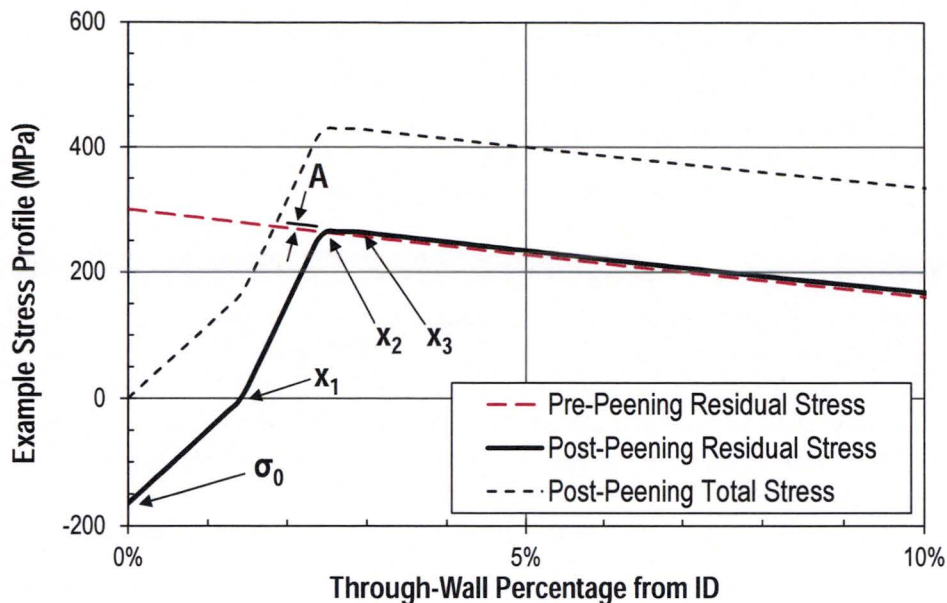


Figure 5-2
Example Bounding Post-Peening Stress Profile near Surface of Circumferential Crack in a DMW Component

5.2.2 Crack Growth

This section presents predictions for crack growth in unmitigated and peened components so as to demonstrate the effects of peening. Growth predictions are given for cracks on the inner diameter of DMW components (Section 5.2.2.1) and at various locations on reactor vessel head penetrations (Section 5.2.2.2). For growth in peened components (i.e., components with a thin compressive residual stress layer near the surface), three prediction types are presented:

- The first uses the more classical weight function method (detailed in appendix Section A.5.2) to predict the stress intensity factors at the crack surface and deepest point locations.
- The second disregards the effect of peening on the growth of the crack surface point locations. This convention, which is further explained in appendix Section A.5.5, is used to approximate the realistic “balloon”-type growth of the crack front below the surface layer with reduced stress due to peening. Figure 5-3 demonstrates the crack front shapes predicted with FEA, the classical approach, and the “balloon” growth approximation, when the crack has reached the same depth. Numerical studies have demonstrated that the depth growth of a realistic crack is generally bounded by the classical approach and balloon growth approximation.
- The third accounts for the effects of partial crack closure. When partial crack closure occurs, contact stresses are produced over the area of closure that are equal and opposite to the compressive stresses over the same area. This results in a balancing of some of the compressive load. So, if partial crack closure is not accounted for, a larger benefit to peening may be predicted. Accounting for crack closure has no effect when the surface stress is modeled to be tensile during operation, as is the case for the bounding stress conditions

meeting the performance criteria of Section 4. This effect is further detailed in appendix Section A.5.5.

The component loading models that are used to determine the stresses on the crack in each analysis are detailed in appendix Sections A.3 and B.3 for DMWs and RPVHPNs, respectively. The crack growth models (including the stress intensity factor calculations) are detailed in appendix Sections A.5 and B.5.

In general, the inputs used for the deterministic calculations in this section are taken to be the median of the respective distributed inputs for the analogous, hot component, probabilistic analyses in the following section. One exception is that the 75th percentile of material variability is used to model the crack growth rates, in line with MRP-55 [62] and MRP-115 [44]. For the reader's benefit, these deterministic inputs are given in Table 5-1 (for the DMW calculations) and Table 5-2 (for the RPVHPN calculations), and instances in which they do not match the median of their analogous distributed input are bolded. The selection and/or derivation of the distributed inputs, and effectively the deterministic inputs, are detailed in appendix Sections A.8 and B.8.

5.2.2.1 Dissimilar Metal Welds (DMWs)

Two distinct DMW crack morphologies were studied deterministically: a circumferential crack located at the point of maximum tensile bending and an axial crack (of arbitrary location). The average growth rates of other crack locations/orientations are bounded by these predictions.

The weld-to-weld variation factor for crack growth is set to its 75th percentile value (1.49) to generate these results. The temperature of the component is set to 625°F for the deterministic crack growth calculations, corresponding to bounding reactor vessel outlet nozzle operating conditions.

For reference in converting between through-wall fraction and absolute depth, the component thickness in these studies is 69.9 mm. This is representative of a Westinghouse reactor vessel nozzle geometry.

Bounding Peening Stress Profile

For a flaw with an initial through-wall fraction of 10% (7.0 mm), Figure 5-4 shows the calculated growth vs. time for a circumferential crack, and Figure 5-5 shows the equivalent calculation for an axial crack. This initial through-wall fraction is the threshold below which the POD is conservatively assumed to be zero. At this initial through-wall fraction, peening has a small effect on the rate of growth, delaying through-wall growth by approximately 7 months for the circumferential crack and by less than 1 month for the axial crack.

Peening has a greater effect on the through-wall growth rates of cracks that are smaller at the time of peening. Despite the bounding compressive residual stress profile that is assumed, Figure 5-6 and Figure 5-8 (initial through-wall fraction of 1.3% (0.9 mm)) show the effect peening can have on cracks with depths similar to the depth of the peening penetration depth, nearly doubling (70% longer for circumferential flaw and about 100% longer for axial flaw) the time to through-wall growth. Figure 5-7 shows the stress intensity factor at the deepest crack point vs. through-wall fraction for the circumferential crack as it goes through-wall. The reduced tensile stresses

near the treated surface resulting from peening bias the stress intensity factor lower, and this acts to slow PWSCC growth.

Figure 5-6 through Figure 5-8 also include the growth predictions on the peened component when the balloon crack growth approximation is allowed and when partial crack closure is accounted for. As expected, approximating balloon growth reduces the benefit of the peening because the crack is modeled to grow in length along the surface under the influence of the residual stresses existing prior to peening. The greater crack length increases the stress intensity factor at the deepest point on the crack (as demonstrated in Figure 5-7). Accounting for partial crack closure has a minor effect for this weakly compressive peening stress profile; it has a greater effect for highly compressive peening residual stress profiles but still only effects growth when the crack depth is similar to the peening penetration depth.

The subsequent figures, Figure 5-9 through Figure 5-11, present the results for a range of initial crack sizes by plotting the calculated time for a crack to grow through-wall as a function of the initial through-wall fraction. Figure 5-10 and Figure 5-11 provide a log-scale presentation to better detail the initial through-wall fractions for which peening has a greater effect.

Figure 5-12 gives the predictions of time to through-wall growth vs. initial through-wall fraction for cracks of two different initial aspect ratios. In this particular case, the longer crack, with the same initial depth, is predicted to grow through-wall 0% to 40% faster than the shorter crack.

Figure 5-13 shows that the lower operating temperature of a reactor vessel inlet nozzle (RVIN) results in a much greater period of growth before a crack penetrates through-wall. As expected, the results scale directly with the Arrhenius factor for crack growth (changing from 625°F to 563°F scales the time to leakage by a factor of 4.8).

Example Representative Peening Stress Profile

Using the example representative peening compressive residual stress profile with a compressive residual stress maximum value of 689.5 MPa (100 ksi) and compressive residual stress layer depth of 1.0 mm, the analysis results are more consistent with experimental data and other information provided by vendors. In Figure 5-14 and Figure 5-15, peening is predicted to arrest growth for circumferential DMW cracks less than or somewhat (up to 50%) deeper than the compressive residual stress layer depth, depending on the calculation method for stress intensity factor. Peening can be beneficial for slowing the growth of cracks significantly (~50%-2000%) deeper than the compressive residual stress layer depth, but the effective depth depends on the nature of the stresses beyond the peening affected zone. As modeled, peening has a greater effect on the growth rate of initially deep flaws with circumferential orientation than on that of flaws with axial orientation because the pre-peening axial residual stresses are compressive in the center of the wall while axial flaws are subject to tensile pre-peening hoop residual stresses for the entire thickness.

Approximating balloon crack growth reduces the predicted effect of peening on the CGR for cracks significantly (>50%) deeper than the compressive residual layer depth but does not affect whether a crack arrests. As mentioned earlier, the actual crack growth is expected to fall somewhere between the results of the classical and balloon approximation approaches. For all base case probabilistic analyses, the balloon growth approximation is used.

Accounting for crack closure influences growth predictions for cracks of a similar (within about 30%) depth to the compressive residual stress layer depth. As demonstrated in Figure 5-14, accounting for partial crack closure can be the difference between predicting the total arrestment of a crack rather than the continuation of slow growth. Because accounting for partial crack closure requires a substantial computational effort and because the bounding peening stress profile for probabilistic base cases is not influenced by crack closure, it is not applied for base case probabilistic analyses, but is included for a sensitivity case.

Stress Profile with Alternate Stress Balance

As is discussed in appendix Section A.3.3, residual stress after peening is modeled under the assumption that any tensile stresses removed near the surface of application are redistributed such that total axial and hoop forces remain unchanged, before and after peening. For the prior deterministic cases, this force balance is achieved by distributing tensile stresses removed near the surface uniformly over the remaining thickness of the component. To test this convention, a set of deterministic calculations were redone for circumferential cracking with a post-peening stress profile that balances both the force and the moment imparted by the peening affected zone. This effect is obtained by introducing a linear offset term to the stress profile beyond the peening affected zone in addition to the constant offset that is shown in Figure 5-2. The modified stress profile, shown in Figure 5-16, results in slightly (less than 8%) more tensile stresses near the inner surface and more compressive stresses near the outer surface. Results for these calculations are compared with the standard approach (force balanced) in Figure 5-17. As expected, the effect is small with less than 7% difference in time to leakage between the two re-balancing conventions.

The same base modeling convention in Section 5.2.1 of balancing the axial and hoop force imparted by peening using a constant offset of the residual stress profile beyond the peening affected zone is used for the probabilistic modeling. The base modeling simplification in Section 5.2.1 is appropriate for the relatively large wall thickness of reactor vessel outlet and inlet nozzles in comparison to the depth of the peening compressive residual stress layer. This behavior was confirmed by the sensitivity case that considered the effect of the balancing through-wall bending moment on the tensile stress profile. A small difference in the crack-tip stress intensity factor and crack growth time ($< 7\%$ in time) resulted versus the base case. Furthermore, it is emphasized that the time for through-wall crack growth is not a key factor for the effectiveness of peening mitigation.

Table 5-1
Inputs for DMW Deterministic Calculations

Symbol	Description	Units	Value	Units	Value
General Component Inputs					
t	Component wall thickness	in	2.750	m	0.0699
D_o	Component outer diameter	in	35.500	m	0.9017
w	DM weld width	in	1.752	m	0.0445
T	Operating temperature - Hot Case	°F	625	°C	329
	Operating temperature - Cold Case		563		295
P_{op}	Normal operating pressure	ksi	2.25	MPa	15.5
F_x	Effective loads for Westinghouse RVON / RVIN (including deadweight, thermal expansion, and thermal stratification loading)	kips	100	kN	444.8
M_x		in-kips	0	kN-m	0
M_y		in-kips	40000	kN-m	4519.4
M_z		in-kips	0	kN-m	0
Growth Rate Inputs					
Q_g	Thermal activation energy for PWSCC flaw propagation	kcal/mole	31.1	kJ/mole	130.0
f_{weld}	Weld-to-weld factor (75 th percentile value)	Nondim	1.49	Nondim	1.49
f_{wvw}	Within weld factor (median value)	Nondim	1.00	Nondim	1.00
α	Flaw propagation rate equation power law constant	(in/hr)(ksi-in ^{0.5}) ^{-1.6}	1.62E-07	(m/s)(MPa-m ^{0.5}) ^{-1.6}	9.82E-13
b	Flaw propagation rate equation power law exponent	Nondim	1.6	Nondim	1.6
$K_{I,th}$	K_I Stress intensity factor threshold	ksi-in ^{0.5}	0.0	MPa-m ^{0.5}	0.0
$T_{ref,g}$	Absolute reference temperature to normalize PWSCC flaw propagation data	°F	617	°C	325
Δt	Time step size for crack increment	yr	1/20	yr	1/20
Residual Stress Inputs					
σ_{0WRSa}	Weld residual axial stress on ID surface	ksi	43.6	MPa	300.3
X_c	Fractional through-thickness at which weld residual axial stress profile crosses zero	Nondim	0.25	Nondim	0.25
f_{WRSa}	Scaling factor for weld residual axial stress on OD surface	Nondim	0.75	Nondim	0.75
$\sigma_{0WRS h}$	Weld residual hoop stress on ID surface	ksi	43.6	MPa	300.3
X_{min}	Fractional through-thickness at which weld residual hoop stress is minimum	Nondim	0.5	Nondim	0.5
$f_{WRS h 1}$	Scaling factor for minimum weld residual hoop stress	Nondim	0.5	Nondim	0.5
$f_{WRS h 2}$	Scaling factor for weld residual hoop stress on OD surface	Nondim	1.0	Nondim	1.0
$\sigma_{0,PPRS}$	Sum of residual plus normal operating stress at the peened surfaces	ksi	0.0	MPa	0.0
$x_{1,PPRS}$	Penetration depth (depth beyond which residual stress is tensile)	in	0.04	mm	1.0
$f_{1,PPRS}$	Ratio of minimally-affected depth to penetration depth (See Section A.3.3)	Nondim	2.0	Nondim	2.0
$f_{2,PPRS}$	Fraction of depth between penetration depth and minimally affected depth where peening results in no effect (See Section A.3.3)	Nondim	0.7	Nondim	0.7

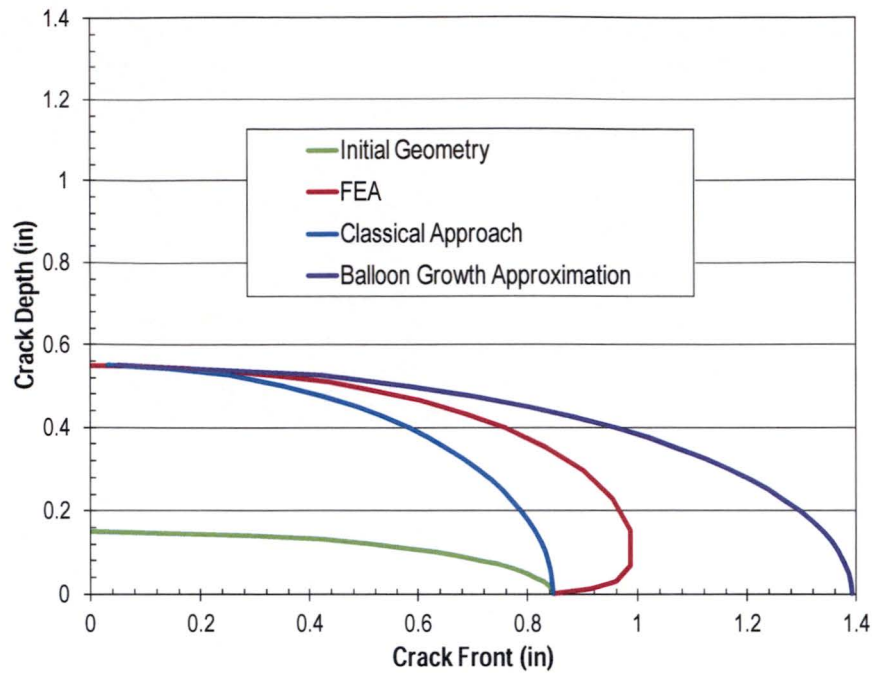


Figure 5-3
Example of Crack Front Shapes Predicted in a Peened Component with: a) FEA, b) Classical Analytical Methods, or c) the Balloon Growth Approximation

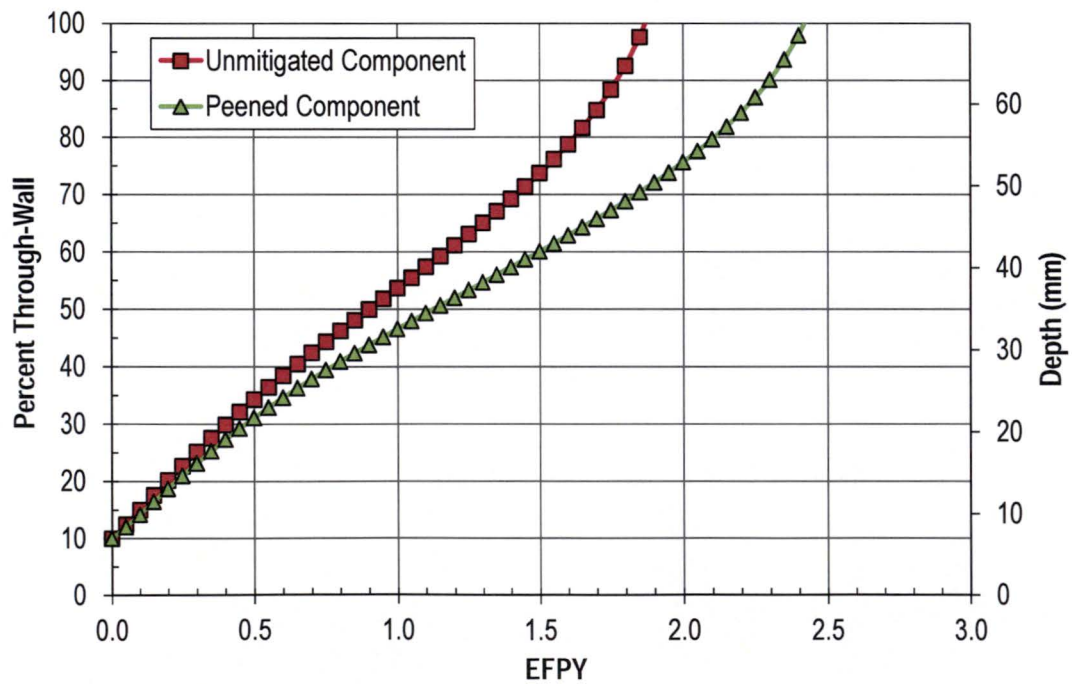


Figure 5-4
Through-Wall Fraction vs. Time for Circumferential Crack on Unmitigated and Peened Component ($a_0/t=10\%$ [7.0 mm] and $2c_0/a_0=8.5$)

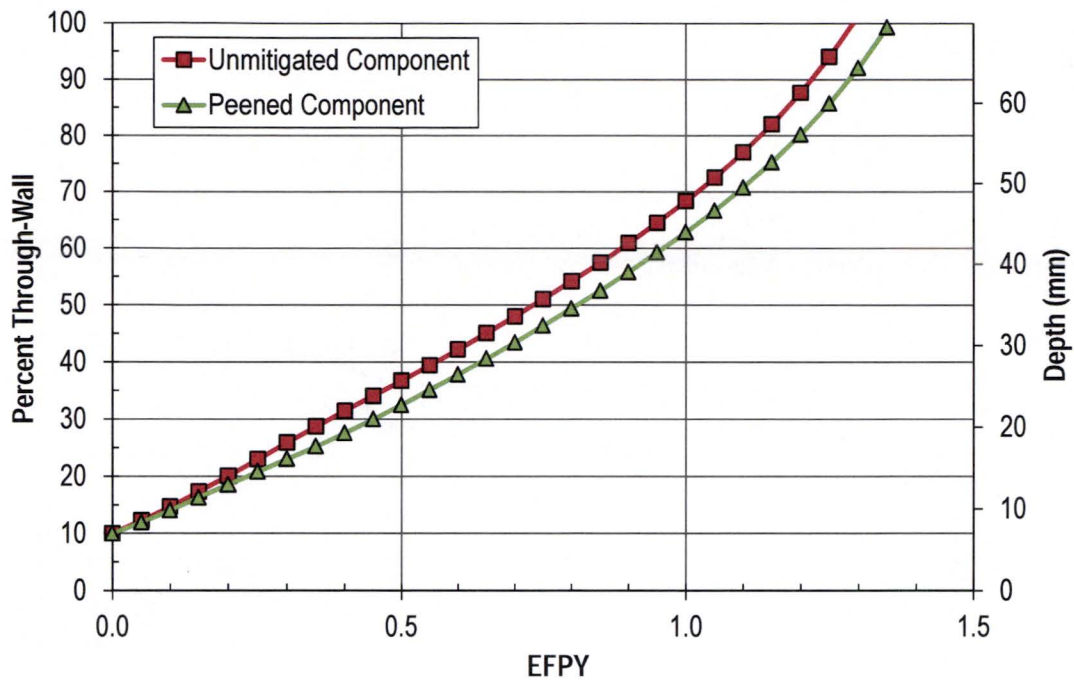


Figure 5-5
Through-Wall Fraction vs. Time for Axial Crack on Unmitigated and Peened Component
($a_0/t=10\%$ [7.0 mm] and $2c_0/a_0=4.5$)

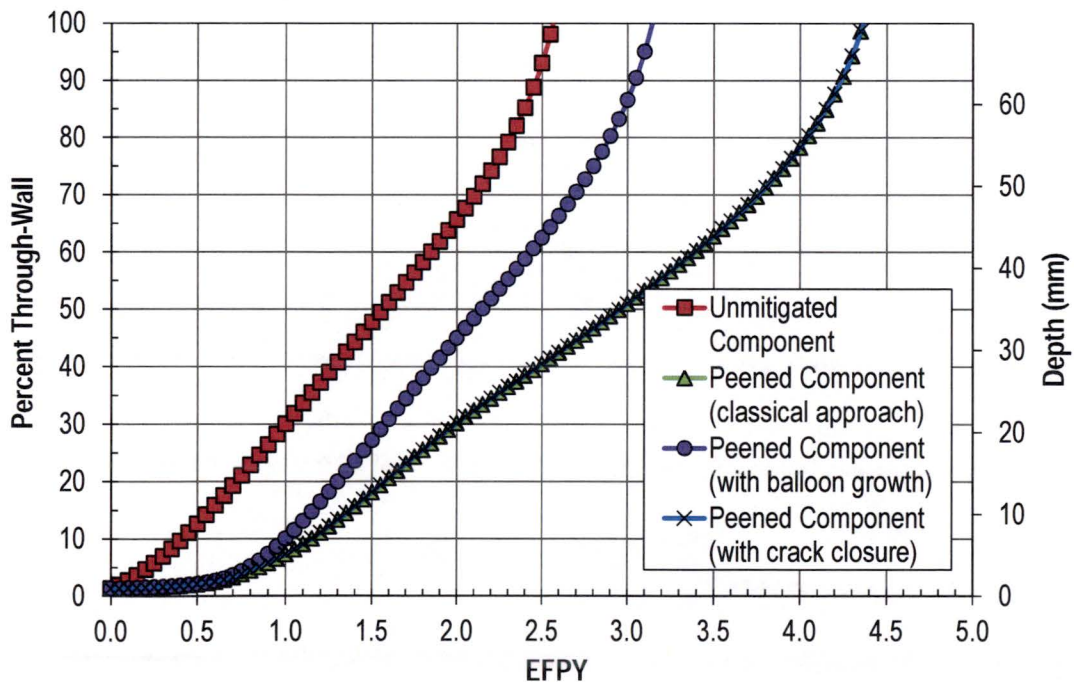


Figure 5-6
Through-Wall Fraction vs. Time for Circumferential Crack on Unmitigated and Peened Component
($a_0/t=1.3\%$ [0.9 mm] and $2c_0/a_0=8.5$)

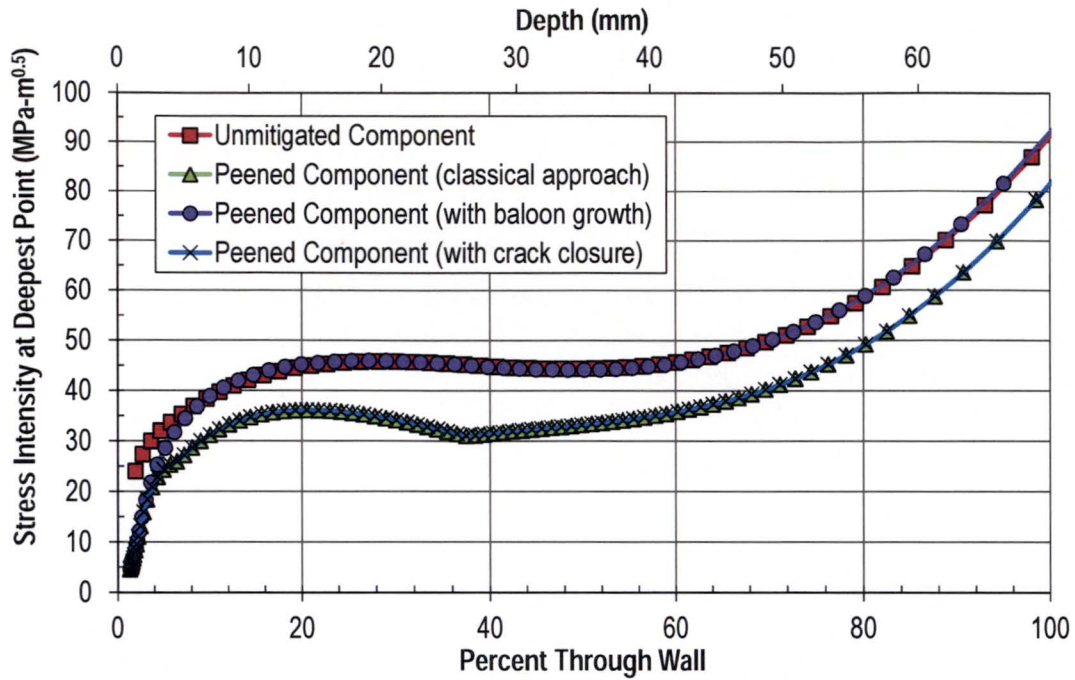


Figure 5-7
Stress Intensity Factor vs. Through-Wall Fraction for Circumferential Crack on Unmitigated and Peened Component ($a_0/t=1.3\%$ [0.9 mm] and $2c_0/a_0=8.5$)

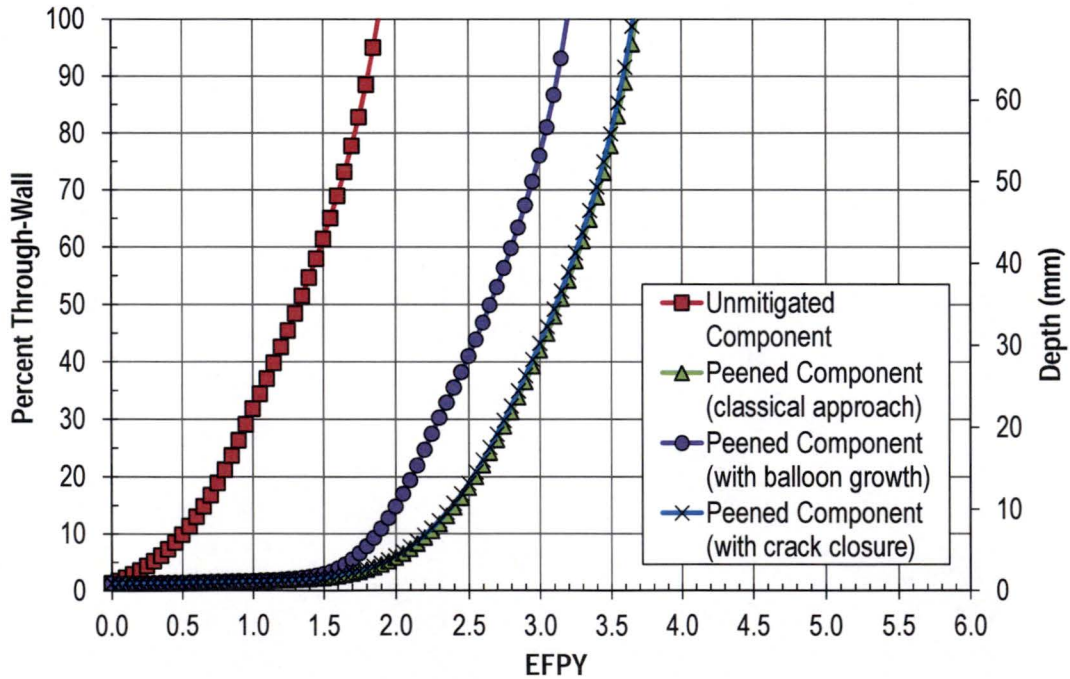


Figure 5-8
Through-Wall Fraction vs. Time for Axial Crack on Unmitigated and Peened Component ($a_0/t=1.3\%$ [0.9 mm] and $2c_0/a_0=4.5$)

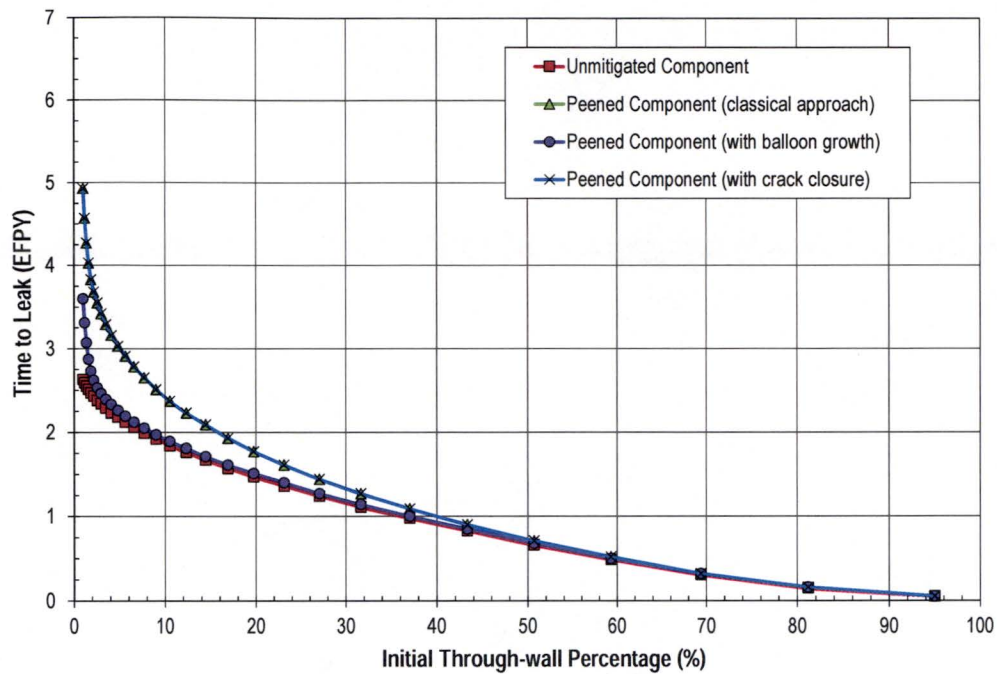


Figure 5-9
Time to Through-Wall Growth vs. Initial Crack Depth for Circumferential Cracks
($2c_0/a_0=8.5$)

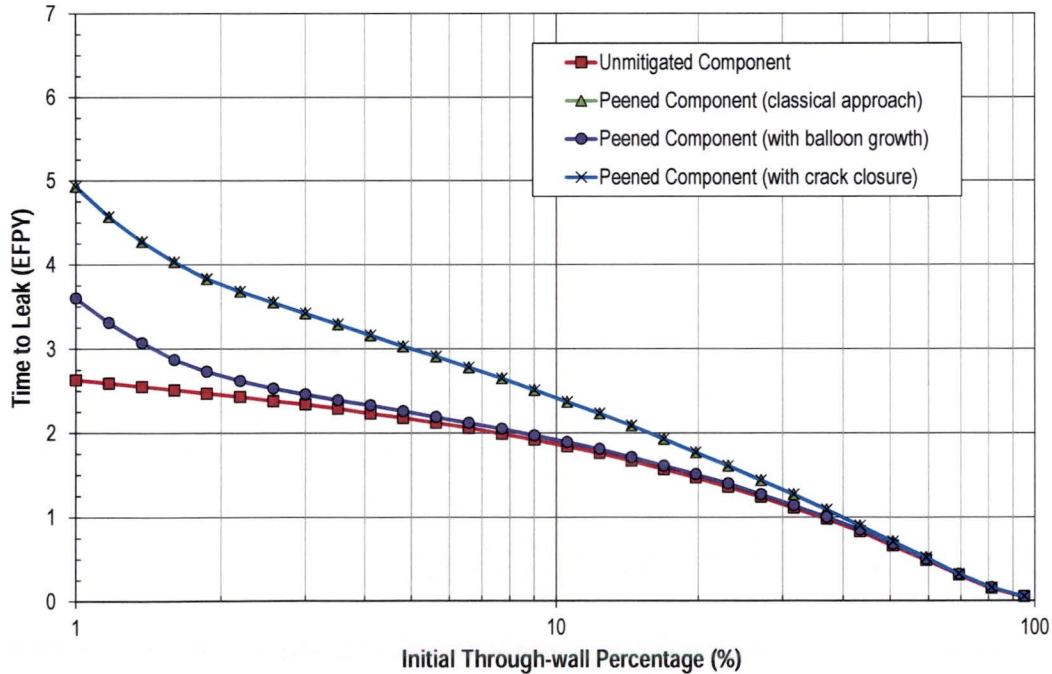


Figure 5-10
Figure 5-9 (Circumferential Cracks with $2c_0/a_0=8.5$) Replotted Using Log-Scale Abscissa

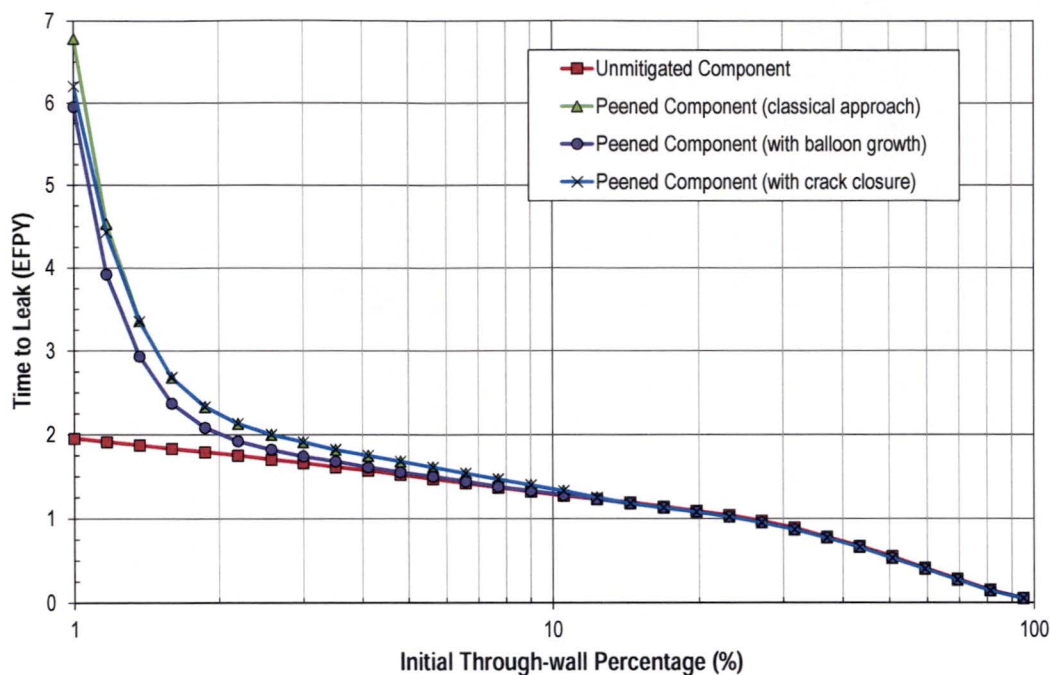


Figure 5-11
Time to Through-Wall Growth vs. Initial Crack Depth for Axial Cracks (Log-Scale Abscissa and $2c_0/a_0=4.5$)

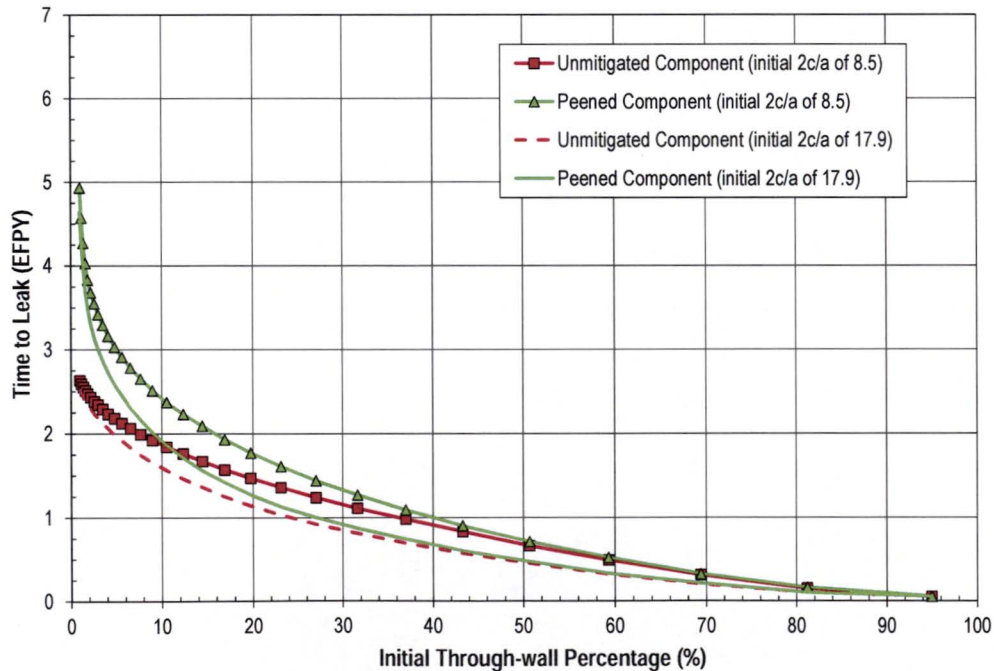


Figure 5-12
Comparing Differences due to Initial Aspect Ratio: Time to Through-Wall Growth vs. Initial Crack Depth for Circumferential Cracks

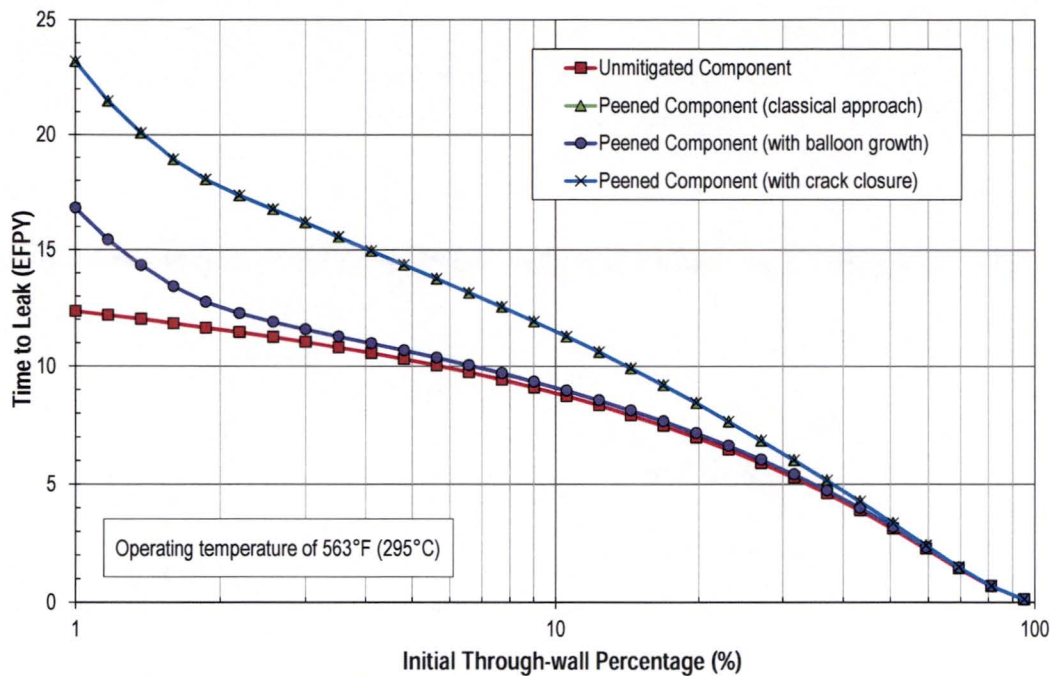


Figure 5-13
Time to Through-Weld Growth vs. Initial Crack Depth for Circumferential Crack on a RVIN
($T=563^{\circ}\text{F}$ and $2c_0/a_0=8.5$)

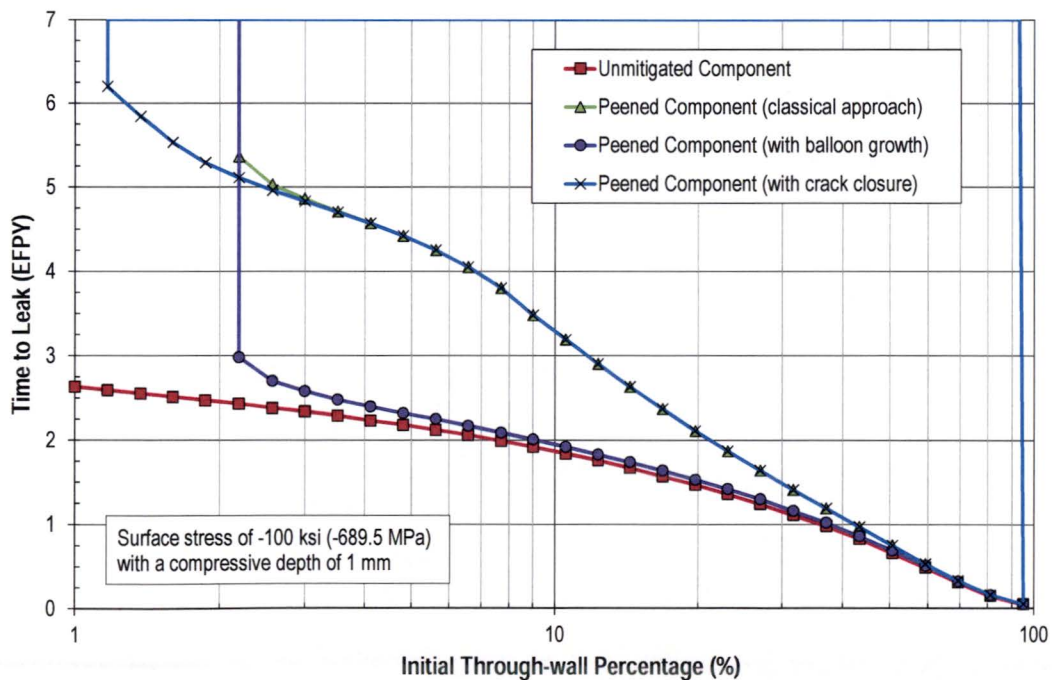


Figure 5-14
Time to Through-Weld Growth vs. Initial Crack Depth for Circumferential Crack Subject to
Example Representative Peening Compressive Residual Stresses ($2c_0/a_0=8.5$)

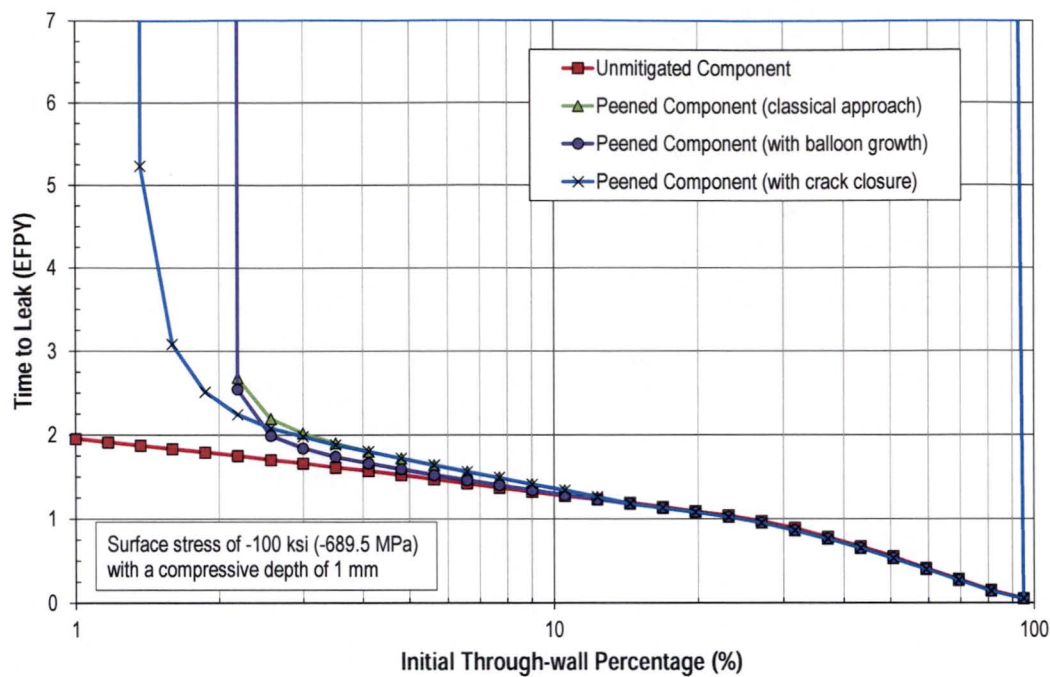


Figure 5-15
Time to Through-Weld Growth vs. Initial Crack Depth for Axial Crack Subject to Example Representative Peening Compressive Residual Stresses ($2c_0/a_0=4.5$)

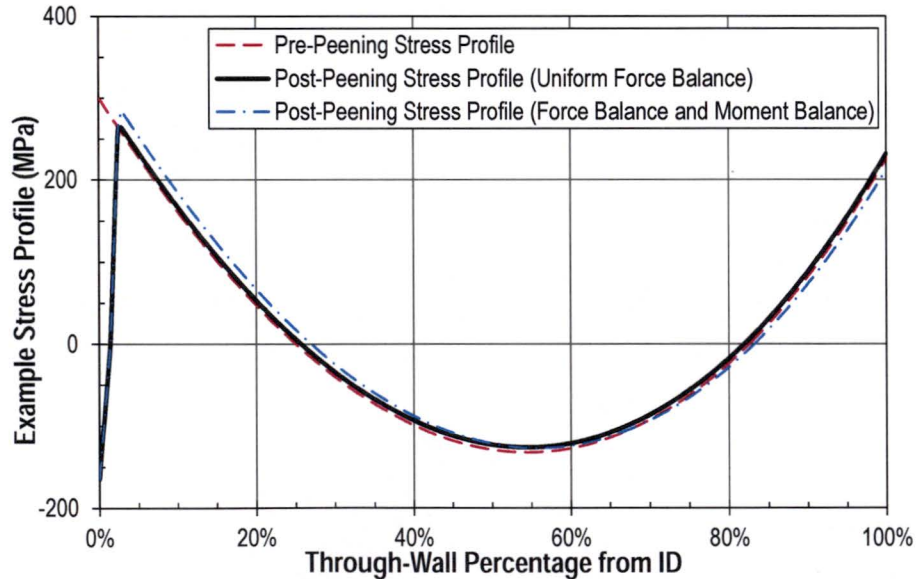


Figure 5-16
Comparison of Stress Profiles used in Peening Stress Balance Study for Circumferential Cracking

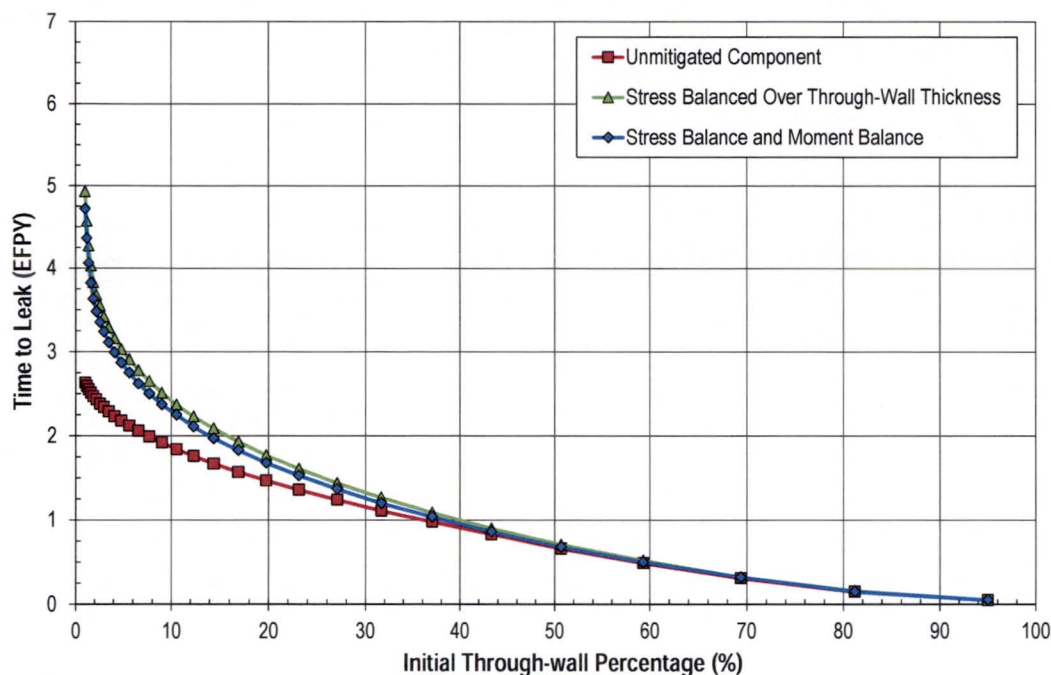


Figure 5-17
Comparing Differences due to Concentration of Force Balance: Time to Through-Wall Growth vs. Initial Crack Depth for Circumferential Cracks

5.2.2.2 Reactor Pressure Vessel Head Penetration Nozzles (RPVHPNs)

Growth of four distinct RPVHPN crack types were studied deterministically: an axial crack on the penetration nozzle ID initiating above the J-groove weld, an axial crack on the penetration nozzle OD initiating below the J-groove weld, a crack initiating on the J-groove weld, and a circumferential through-wall crack growing along the weld contour. For the first three crack types, growth is predicted from a part-depth flaw until the time of leakage; for the fourth crack type, growth is predicted from an initially through-wall flaw until the time of ejection.

Growth predictions for each crack type can be made for the uphill and downhill locations on the penetration by using stress profiles that are representative of each location (as detailed in appendix Section B.3).

The weld-to-weld and heat-to-heat growth variation factors were set to their 75th percentile values (1.49 and 1.98, respectively) to generate these results. The temperature of the component was set to 605°F, and cases also were run at 561°F for comparison with typical cold head operating conditions.

For reference in converting between through-wall fraction and absolute depth, the component thickness in these studies is 15.8 mm. This is representative of typical CRDM nozzle geometry.

Crack Growth Prior to Leakage: Bounding Peening Stress Profile

Figure 5-18 shows the growth vs. time calculation for an axial crack on the penetration nozzle ID with an initial through-wall fraction of 1% (0.16 mm). At this initial through-wall fraction, the

effect of peening is predicted to be considerable, delaying through-wall growth by approximately 5 EFPY.

Unlike ID cracks above the weld, growth of axial cracks on the penetration nozzle OD through the wall does not cause leakage. Instead, leakage occurs once an OD axial crack grows in length to reach the OD nozzle annulus beyond the weld root. Figure 5-19 shows the calculated time history for the crack length parallel to the nozzle surface for an axial crack on the penetration nozzle OD with an initial nozzle through-wall fraction of approximately 10%. In this case the effect of peening on growth of shallow flaws is large, delaying leakage by 1-4 EFPY for flaws up to about 30% (5 mm) through-wall at the time of peening.

Figure 5-20 shows the growth vs. time calculation for a weld crack with an initial through-wall fraction of 5%. In this particular case, there is significant reduction in time to grow through-wall with peening, delaying the through-weld growth time by a factor of approximately two.

Figure 5-21 through Figure 5-26 give time to leakage vs. initial crack through-wall fraction, for each of the three partial crack types, at the uphill and downhill sides of the penetration. The downhill locations tend to grow to leak faster because of characteristically more tensile weld residual stresses.

Figure 5-25 demonstrates some initial crack depths for which the peened component results in leakage earlier than the unmitigated component. This occurs for relatively deep cracks and is due to the modeling assumption that the effective forces on the cross-section of the peened component balance; i.e., tensile stresses are displaced from the peened surface and are redistributed to deeper locations.

Figure 5-27 shows that the lower operating temperature of RPVHPNs in a head operating near the cold leg temperature results in a greater period of growth before a crack grows through-wall. As expected, the results scale directly with the Arrhenius factor for crack growth (changing from 605°F to 561°F scales the time to leakage by a factor of 3.1).

Crack Growth Prior to Leakage: Example Representative Peening Stress Profile

Figure 5-28 through Figure 5-30 present results for an example (not bounding) peening stress profile. As in the DMW deterministic analyses, peening is predicted to arrest growth for cracks less than or somewhat (up to 80%) deeper than the compressive layer depth. Peening is predicted to be beneficial for slowing the growth of cracks significantly (~80-300%) deeper than the compressive residual stress layer depth, but the potency of this effect depends on the nature of the operating stresses and residual stresses beyond the peening compressive layer (i.e. the pre-peening stresses); the effect of peening on the crack growth time rapidly fades for weld cracks deeper than the compressive layer depth. It is emphasized that the main deterministic and probabilistic cases apply the bounding peening stress profile meeting the performance criteria, and thus the conclusions of this assessment regarding appropriate inspection requirements and intervals for peened components are not dependent on the benefit of these representative stress profiles in slowing growth of sufficiently shallow flaws.

Generally speaking, because penetration nozzles are thinner-walled than DMW components, the effect of peening on crack growth times is observed for cracks of greater through-wall percentages.

At the nozzle OD and weld locations, where the peening penetration depth is assumed to be 3.0 mm, cracks less than approximately 15%-35% through-wall may be arrested upon the application of peening. Figure 5-31 presents the time history for the calculated length parallel to the nozzle surface of an uphill nozzle OD flaw, demonstrating how balloon crack growth permits growth in crack length along the nozzle surface while the compressive surface stress for the example representative (i.e., non-bounding) stress profile pins the crack length using the classical and crack closure approaches to stress intensity factor calculation. In the classical approach, the effect of peening to reduce the tensile surface stress at the surface is credited when calculating the increase in crack length based on the stress intensity factor at the surface tips of the crack. Once the crack penetrates through-wall, the effect of peening is conservatively not credited for through-wall crack growth. Balloon crack growth is modeled in the probabilistic analysis base cases.

As with DMW components, the effect of peening on the growth of cracks that are deeper than the compressive residual stress layer depth is predicted to be small when balloon crack growth is approximated. The effect of the balloon growth approximation is not observed at weld locations, where crack surface length growth is constrained by the width of the weld.

Circumferential Through-Wall Crack Growth

Circumferential through-wall crack growth along the weld contour of penetration nozzles is a significant concern when assessing PWSCC risk in reactor vessel heads because, if such cracks grow large enough, they can result in nozzle ejection. In the RPVHPN probabilistic model, circumferential through-wall cracks initiate instantly after leakage (due to any of the crack locations discussed in the previous section). Applying the growth model detailed in appendix Section B.5.4, this section provides crack growth predictions for circumferential through-wall cracks, from initiation until nozzle ejection. Peening has no modeled effect on the growth of circumferential through-wall cracks.

The initial flaw angle is assumed to be 30° (per the convention in MRP-105 [7]). A flaw angle of 300° is conservatively taken to be the size at which nozzle ejection occurs, per the calculations in MRP-110 [4]. To generate results for circumferential through-wall cracks, the heat-to-heat growth variation factor was set to its 75th percentile value (1.98), the temperature of the component was set to 605°F, and the environmental growth factor was set to 2.0. No multiplier was applied to the FEA predicted average stress intensity factors (presented in Figure B-7 in Appendix B) that are used to predict the crack growth.

Figure 5-32 shows the growth vs. time prediction for circumferential through-wall cracks initiating on the uphill and downhill side of the penetration nozzle. It is noted that peening stresses are conservatively neglected for the growth of circumferential through-wall cracks such that these predictions do not vary after peening.

With the deterministic parameters used for this study, which are more aggressive than the median case in the probabilistic model, downhill cracks are predicted to cause ejection approximately 18 EFPY after initiation and uphill cracks are predicted to cause ejection approximately 23 EFPY after initiation. In the rare case in which two circumferential through-wall cracks initiate—one from the uphill location and one from the downhill location—ejection is predicted approximately 9.5 EFPY after initiation.

Table 5-2
Inputs for RPVHPN Deterministic Calculations

Symbol	Description	Units	Value	Units	Value
General Component Inputs					
t	Nozzle thickness	in	0.622	m	0.0158
D_o	Nozzle outer diameter	in	4	m	0.1016
t_{head}	Reactor head thickness	in	5.984	m	0.152
T	Operating temperature - Hot Case	°F	605.0	°C	318
	Operating temperature - Cold Case		561.0		294
P_{op}	Normal operating pressure	ksi	2.25	MPa	15.5
$f_{oper,ID}$	Penetration nozzle ID hoop stress concentration factor	Nondim	3.48	Nondim	3.48
N/A	J-groove weld geometries used to simulate crack growth of crack initiation on weld	See mean values given in Table B-3			
Growth Rate Inputs					
Q_g	Thermal activation energy for PWSCC flaw propagation	kcal/mole	31.1	kJ/mole	130.0
f_{weld}	Weld-to-weld factor (75 th percentile value)	Nondim	1.49	Nondim	1.49
f_{ww}	Within weld factor (median value)	Nondim	1.00	Nondim	1.00
f_{heat}	Heat-to-heat factor (75 th percentile value)	Nondim	1.98	Nondim	1.98
f_{wh}	Within heat factor (median value)	Nondim	1.00	Nondim	1.00
α_{weld}	Flaw propagation rate equation power law constant for Alloy 182	(in/hr)(ksi-in ^{0.5}) ^{-1.6}	1.62E-07	(m/s)/(MPa-m ^{0.5}) ^{-1.6}	9.82E-13
α_{heat}	Flaw propagation rate equation power law constant for Alloy 600	(in/hr)(ksi-in ^{0.5}) ^{-1.6}	3.25E-08	(m/s)/(MPa-m ^{0.5}) ^{-1.6}	1.97E-13
b	Flaw propagation rate equation power law exponent	Nondim	1.6	Nondim	1.6
$K_{I,th}$	K _I Stress intensity factor threshold	ksi-in ^{0.5}	0.0	MPa-m ^{0.5}	0.0
$T_{ref,g}$	Absolute reference temperature to normalize PWSCC flaw propagation data	°F	617.0	°C	325
$K_{circ,mult}$	Circumferential through-wall crack K curve multiplier	Nondim	1.0	Nondim	1.0
$c_{circ,mult}$	Circumferential through-wall crack environmental factor	Nondim	2.0	Nondim	2.0
N/A	Distance below weld toe of OD crack location	in	0.13	mm	3.2
Δt	Time step size for crack increment	yr	1/20	yr	1/20
Residual Stress Inputs					
N/A	Weld residual stress profile parameters	See mean values given in Table B-4			
$\sigma_{0,PPRS,ID}$	Sum of residual plus normal operating stress on nozzle ID surfaces	ksi	10.0	MPa	69.0
$x_{1,PPRS,ID}$	Penetration depth for peening performed on nozzle ID surfaces	in	0.01	mm	0.25
$\sigma_{0,PPRS,ext}$	Sum of residual plus normal operating stress on nozzle OD and weld surfaces	ksi	0.0	MPa	0.0
$x_{1,PPRS,ext}$	Penetration depth for peening performed on nozzle OD and weld surfaces	in	0.04	mm	1.0
$f_{1,PPRS}$	Ratio of minimally-affected depth to penetration depth (See Section B.3.3)	Nondim	2.0	Nondim	2.0
$f_{2,PPRS}$	Fraction of depth between penetration depth and minimally affected depth where peening results in no effect (See Section B.3.3)	Nondim	0.7	Nondim	0.7
Stability Inputs					
$\theta_{circ,init}$	Initial angle for circumferential through-wall cracks immediately following leaks	degrees	30.0	degrees	30.0
$\theta_{circ,crit}$	Critical flaw angle for nozzle ejection	degrees	300.0	degrees	300.0

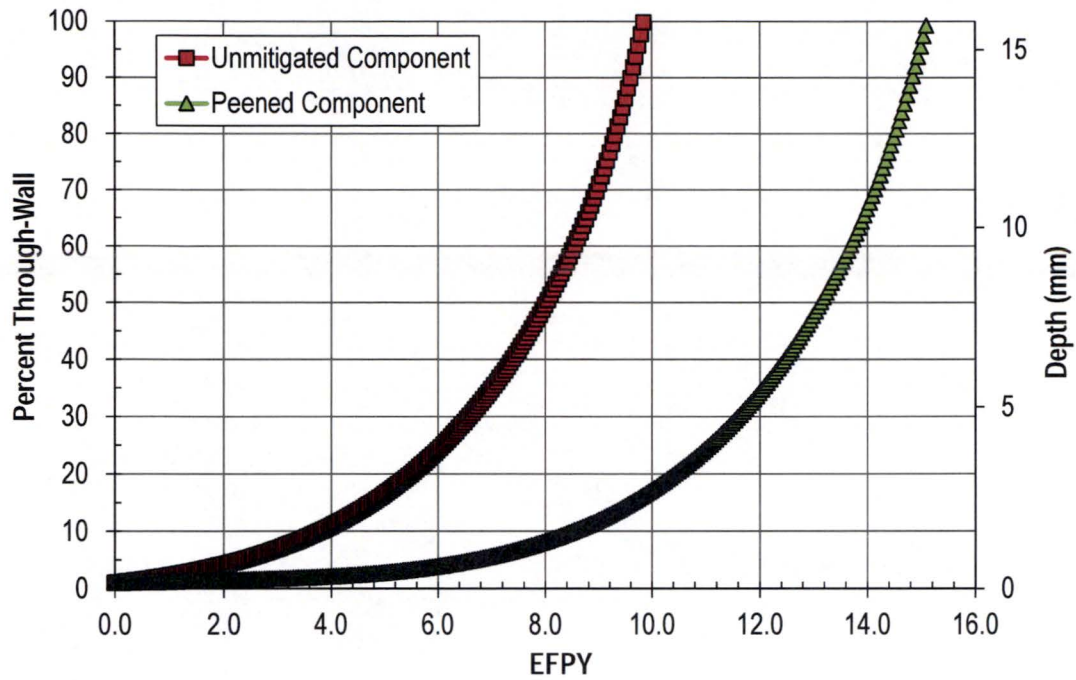


Figure 5-18
Through-Wall Percentage vs. Time for Uphill ID Axial Crack on Unmitigated and Peened Component ($a_0/t=1\%$ [0.16 mm] and $2c_0/a_0=4.5$)

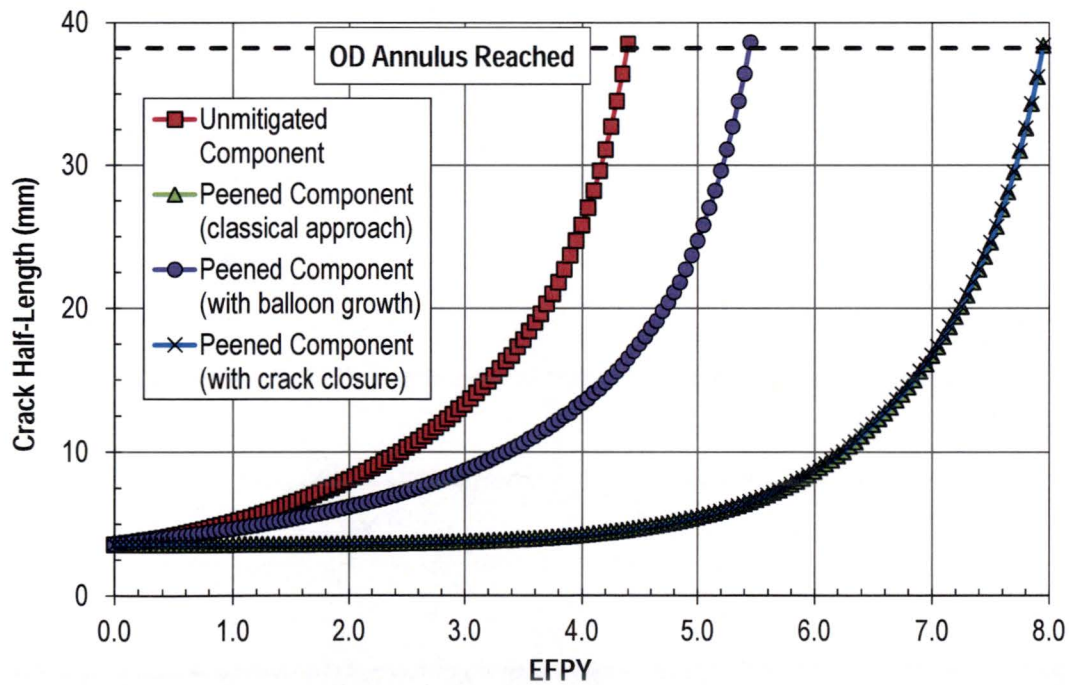


Figure 5-19
Half-Length along Nozzle Surface vs. Time for Uphill OD Axial Crack on Unmitigated and Peened Component ($a_0/t=10\%$ [1.6 mm] and $2c_0/a_0=4.5$)

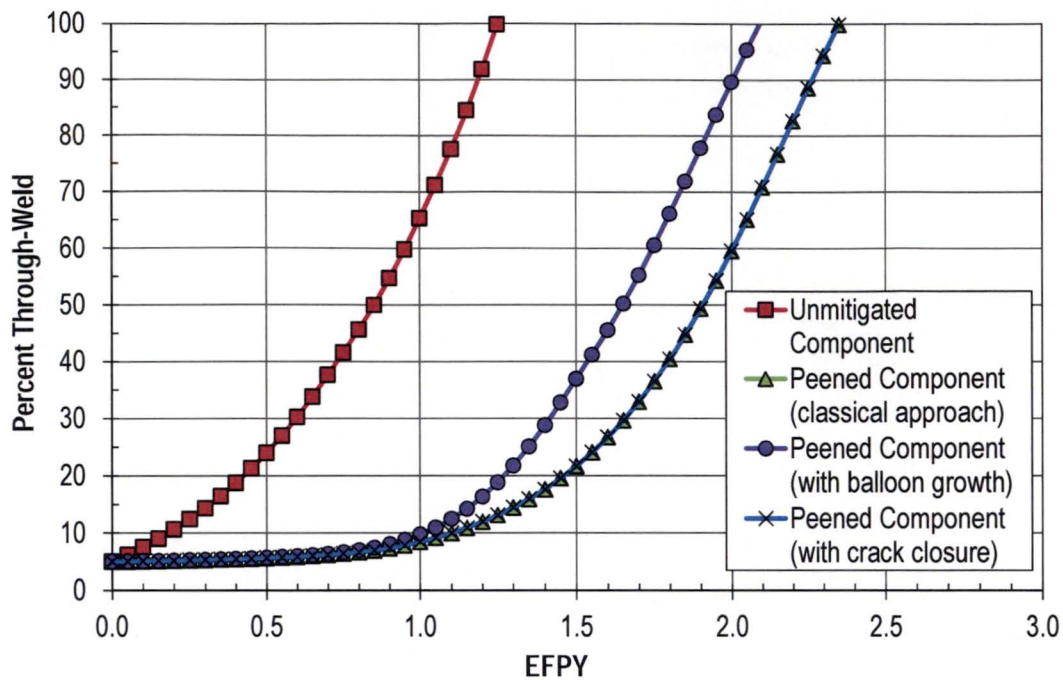


Figure 5-20
Through-Weld Percentage vs. Time for Downhill Weld Radial Crack on Unmitigated and Peened Component ($a_0/t=5\%$ [1.2 mm] and $2c_0/a_0=4.5$)

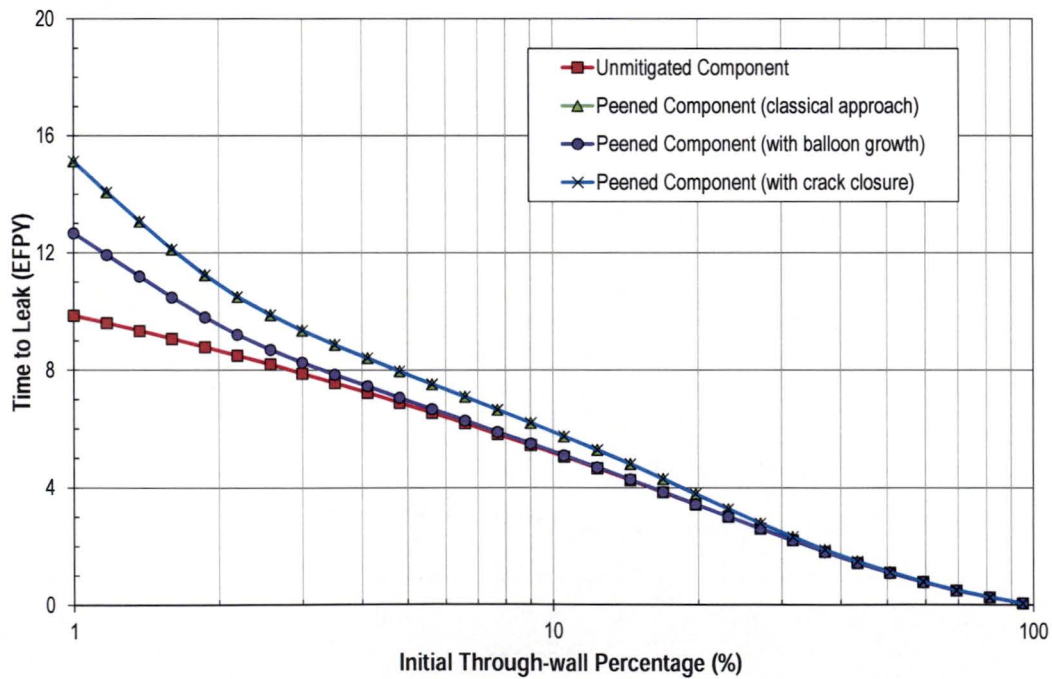


Figure 5-21
Time to Through-Wall Growth vs. Initial Crack Depth for Axial Crack on Uphill Penetration Nozzle ID (Log-Scale Abscissa, $2c_0/a_0=4.5$)

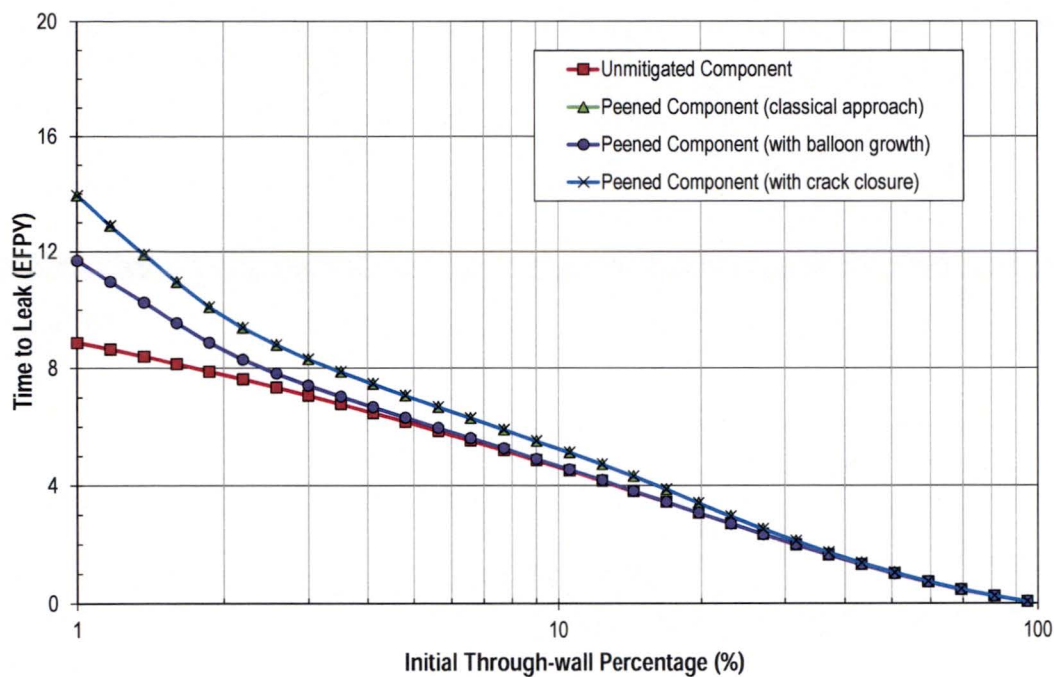


Figure 5-22
Time to Through-Wall Growth vs. Initial Crack Depth for Axial Crack on Downhill Penetration Nozzle ID (Log-Scale Abscissa, $2c_0/a_0=4.5$)

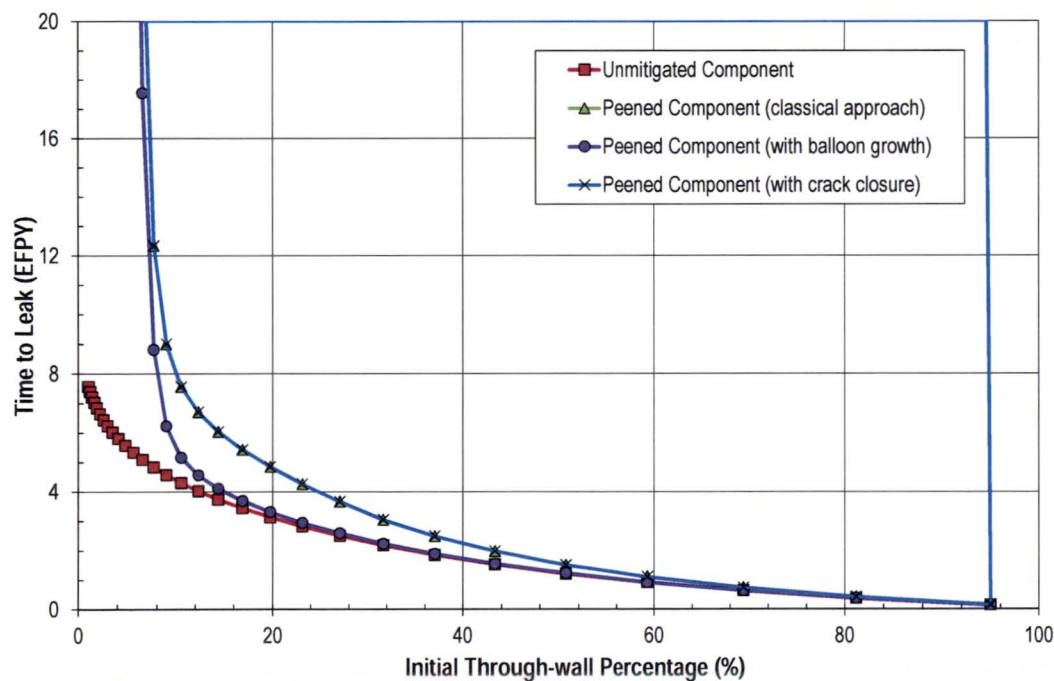


Figure 5-23
Time to OD Nozzle Annulus vs. Initial Crack Depth for Axial Crack on Uphill Penetration Nozzle OD ($2c_0/a_0=4.5$)

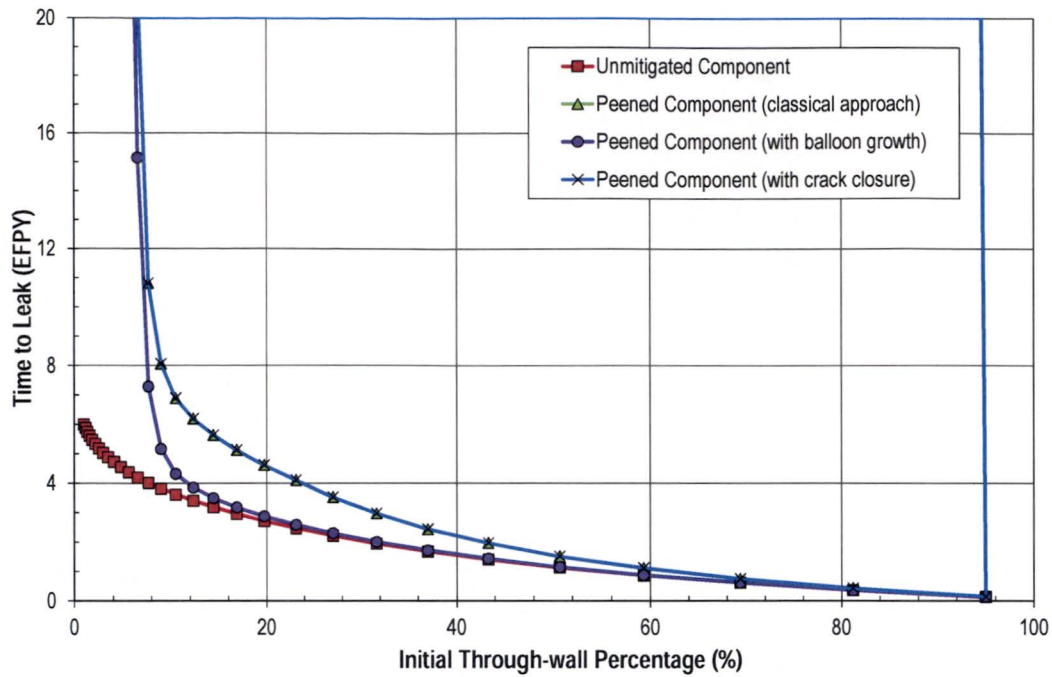


Figure 5-24
Time to OD Nozzle Annulus vs. Initial Crack Depth for Axial Crack on Downhill Penetration
Nozzle OD ($2c_0/a_0=4.5$)

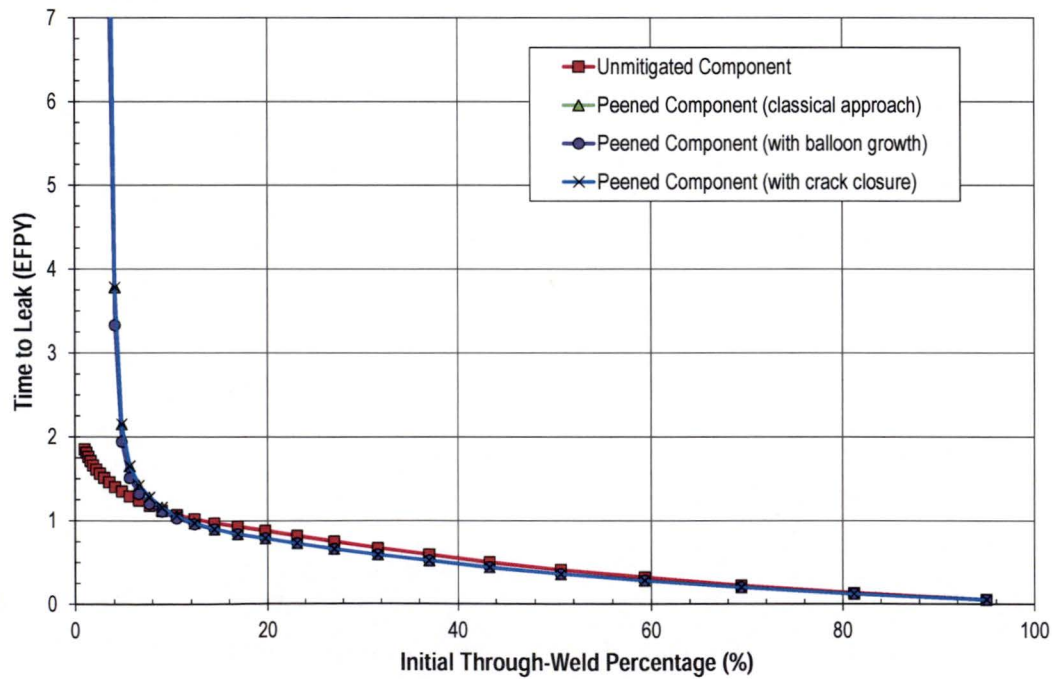


Figure 5-25
Time to Through-Weld Growth vs. Initial Crack Depth for Weld Radial Crack on Uphill J-Groove Weld ($2c_0/a_0=4.5$)

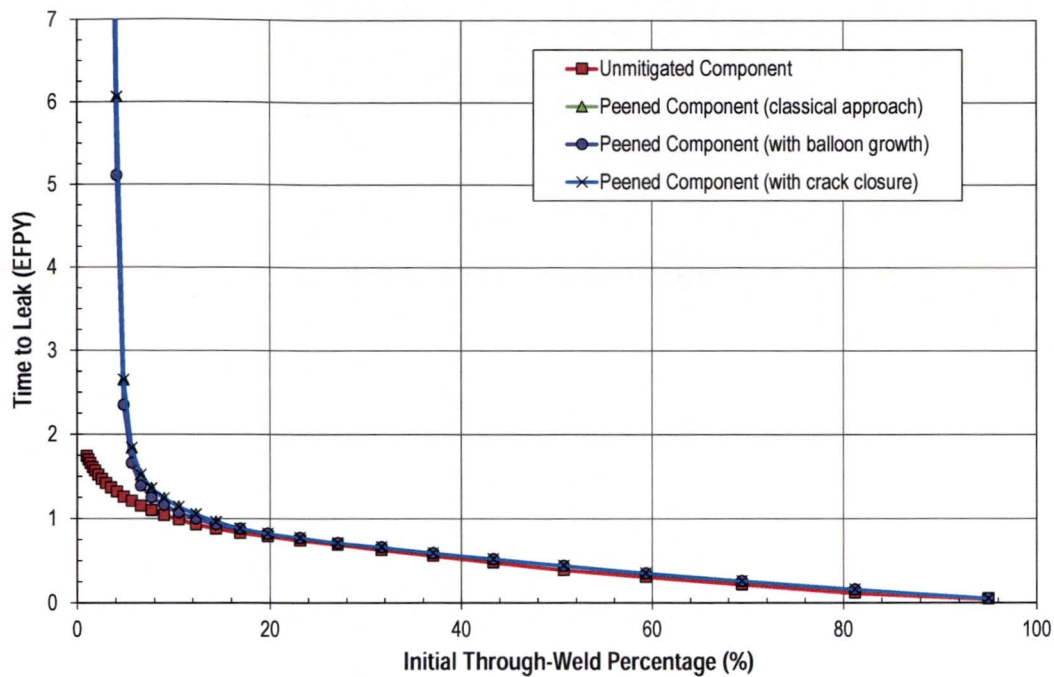


Figure 5-26
Time to Through-Weld Growth vs. Initial Crack Depth for Weld Radial Crack on Downhill J-Groove Weld ($2c_0/a_0=4.5$)

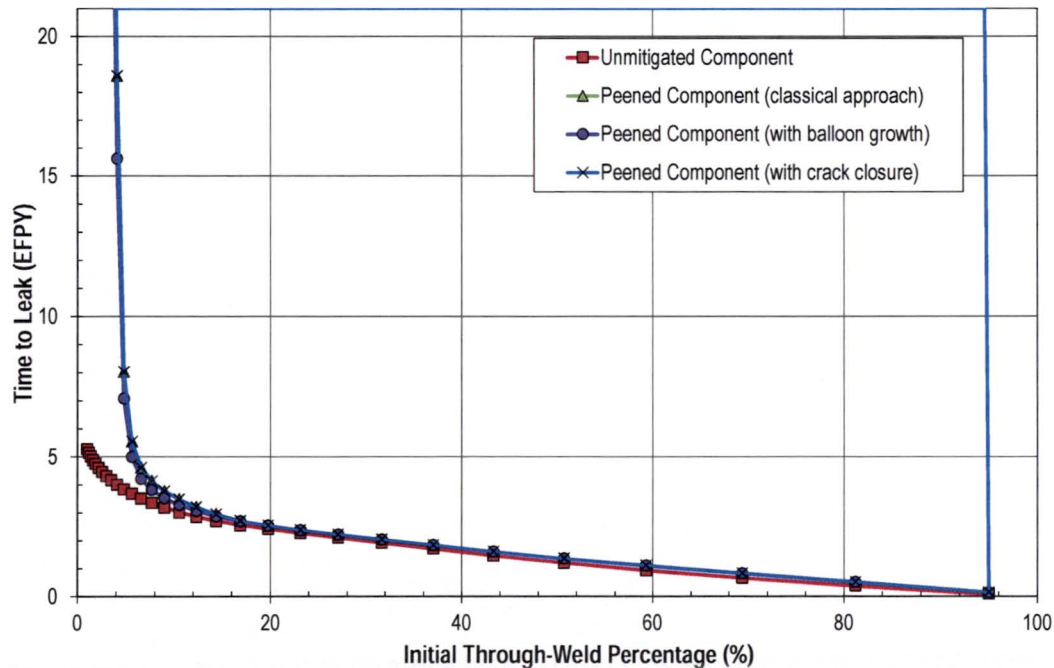


Figure 5-27
Time to Through-Weld Growth vs. Initial Crack Depth for Weld Crack on Downhill J-Groove Weld on a Cold Head RPVHPN ($2c_0/a_0=4.5$)

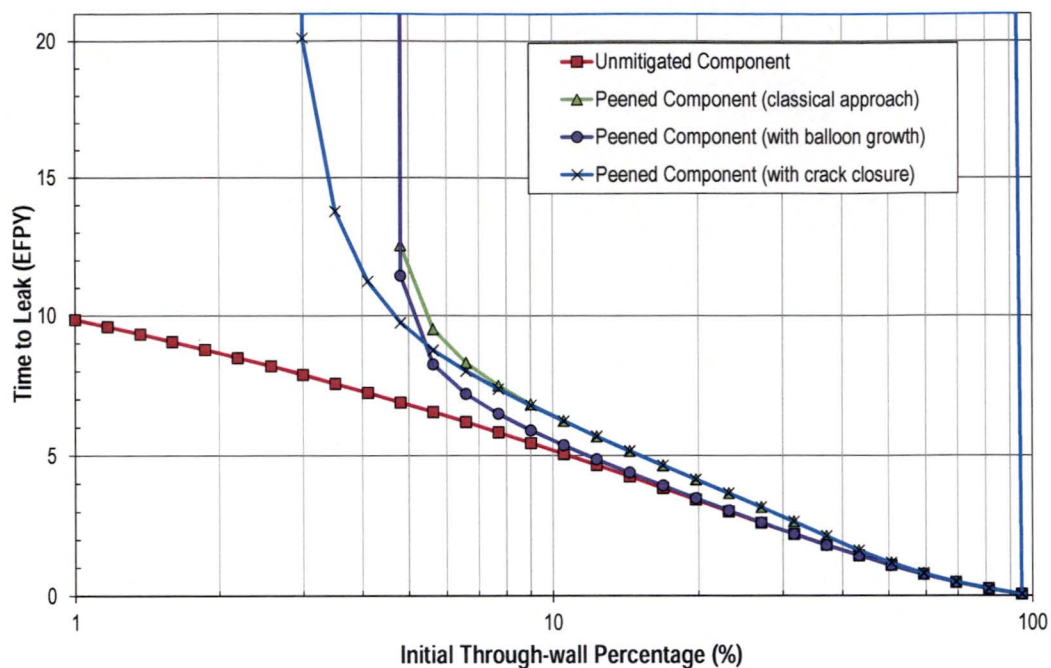


Figure 5-28
Time to Through-Weld Growth vs. Initial Crack Depth for Axial Crack on Uphill Penetration Nozzle ID Subject to More Compressive Peening Residual Stress Profile ($2c_0/a_0=4.5$)

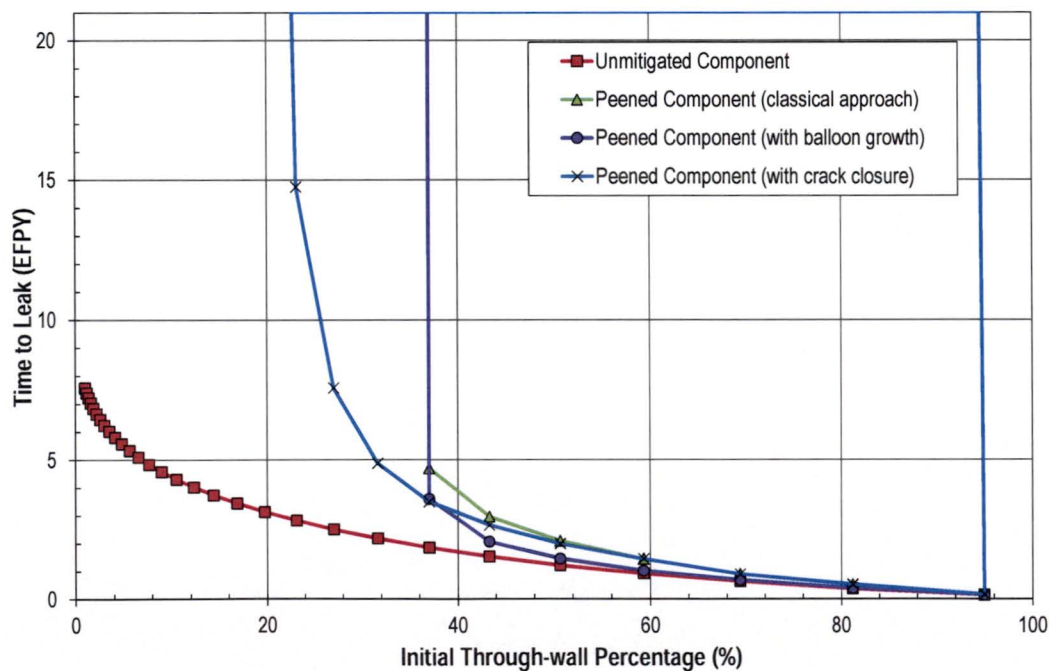


Figure 5-29
Time to Through-Weld Growth vs. Initial Crack Depth for Weld Crack on Uphill Penetration Nozzle OD Subject to More Compressive Peening Residual Stress Profile ($2c_0/a_0=4.5$)

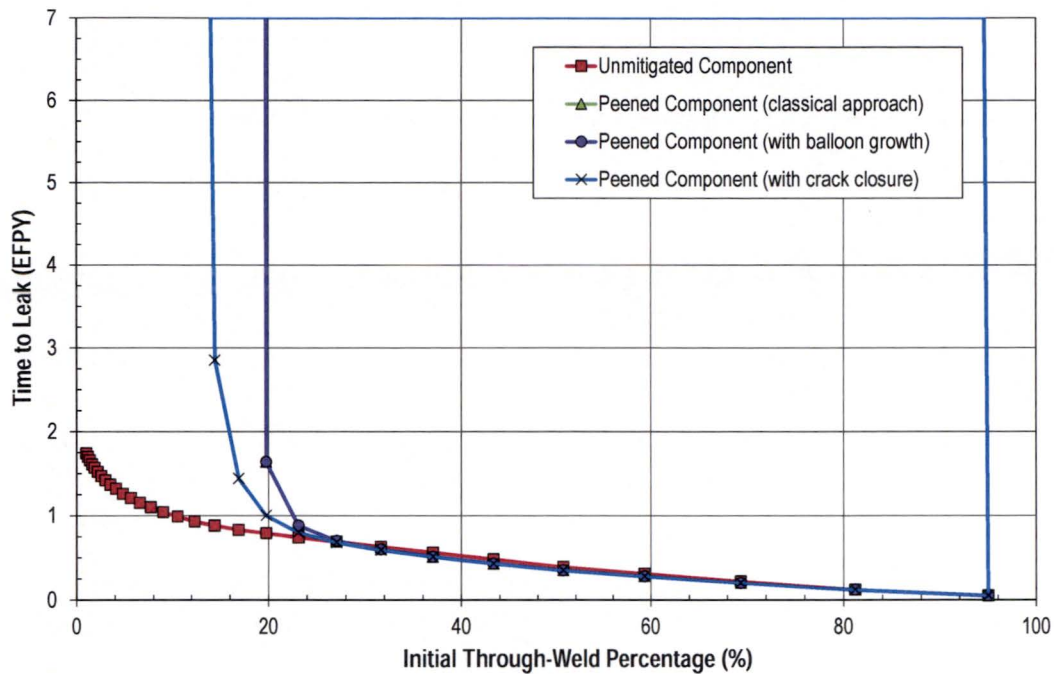


Figure 5-30
Time to Through-Weld Growth vs. Initial Crack Depth for Weld Crack on Downhill J-Groove Weld Subject to More Compressive Peening Residual Stress Profile ($2c_0/a_0=4.5$)

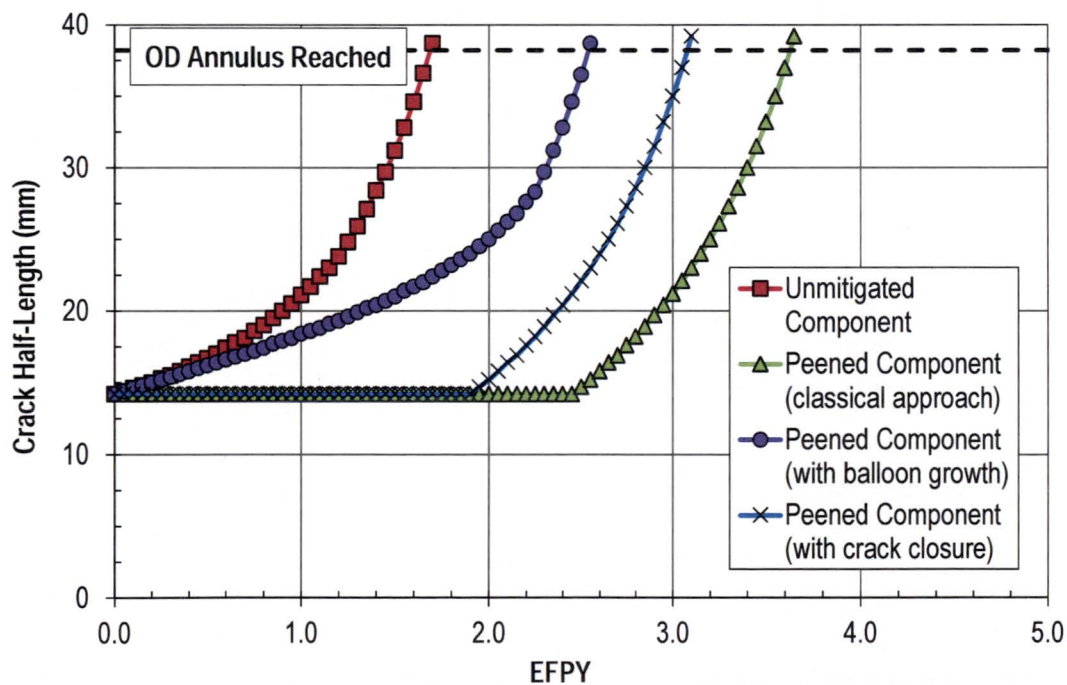


Figure 5-31
Half-Length along Nozzle Surface vs. Time for Uphill OD Axial Crack on Unmitigated and Peened Component Subject to More Compressive Peening Residual Stress Profile ($a_0/t=40\%$ [6.3 mm] and $2c_0/a_0=4.5$)

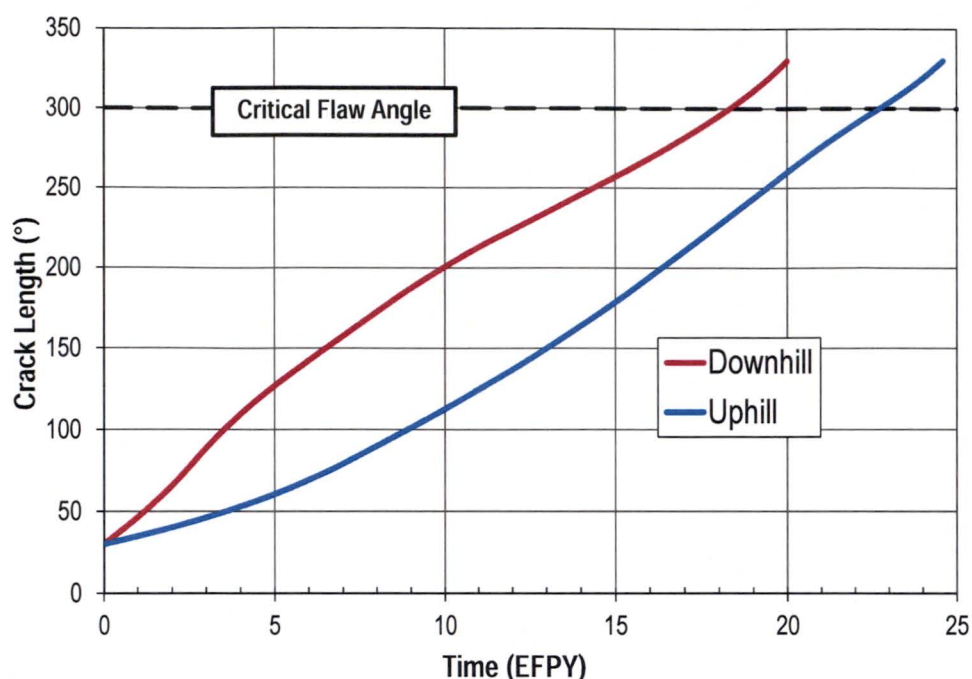


Figure 5-32
Circumferential Crack Length vs. Time for Through-Wall Cracks Along the Weld Contour for a Head Temperature of 605°F and an Assumed Environmental Crack Growth Factor of 2.0

5.2.3 Deterministic Matrix of Crack Growth Rate Calculations

Sections 5.2.3.1 and 5.2.3.2 present a matrix of deterministic crack growth calculations that demonstrates the effectiveness of the schedule of peening follow-up and ISI examinations to detect any pre-existing PWSCC indications not detected in the pre-peening inspection prior to through-wall penetration and leakage occurring. These calculations model crack growth for a range of initial flaw depths up to the NDE detectability limit for DMWs and RPVHPNs.

In this deterministic approach, dozens of cases of different combinations of key input variables are considered in order to investigate the effect of input variability. Wide ranges of key input variables were selected to cover the range of potential behavior, including 5th and 95th percentile values of the standard statistical distributions representing the material heat-to-heat variability in PWSCC crack growth rate for Alloy 600 and for Alloys 82/182. These low and high cases are combined with low and high values of weld residual stress and initial crack aspect ratio in order to further cover the range of potential crack growth rates. This deterministic approach necessarily does not cover every combination of possible inputs, and each analysis case is not weighted by its likelihood of being realized in actual plant behavior. Hence, this deterministic approach complements the probabilistic analyses of Appendices A and B, which more fully consider the range of potential combinations of modeling inputs and which consider the likelihood of occurrence of each such combination.

Table 5-3 presents a summary of the results, which further supports that performing peening and inspecting per the relaxed inspection requirements of Section 4 provides a lower likelihood of

leakage than inspecting unmitigated components per the current inspection requirements. As discussed below, it is emphasized that all but one of the peened cases that are predicted to result in leakage assume the combination of a high tensile weld residual stress profile, the highest operating temperature for their category, and 95th percentile crack growth rate behavior. There is a very low probability of cases like this occurring in practice.

Table 5-3
Summary of Deterministic Matrix for DMW and RPVHPN Crack Growth Calculations¹⁴

Disposition	DMW – Peened		DMW – No Peening		RPVHPN – Peened		RPVHPN – No Peening	
Never Leaks, Never Detected	10 of 72	14%	0 of 72	0%	28 of 72	39%	10 of 72	14%
Detected in Follow-Up Exam	31 of 72	43%	N/A	N/A	30 of 72	42%	N/A	N/A
Detected in ISI Exam	20 of 72	28%	48 of 72	67%	12 of 72	17%	52 of 72	72%
Leaks Before Extension of Intervals	8 of 72	11%	24 of 72	33%	0 of 72	0%	10 of 72	14%
Leaks After Extension of Intervals	3 of 72	4%		N/A	2 of 72	3%		

5.2.3.1 Dissimilar Metal Welds (DMWs)

For peened hot-leg DMWs, the follow-up examinations are scheduled at an interval equal to the volumetric/surface examination interval for unmitigated DMWs. Any leakage that would occur prior to the extension of examination intervals for the peened DMWs would not be prevented had the DMWs not been mitigated. For peened cold-leg DMWs, the follow-up examination can be scheduled at an interval longer than the volumetric/surface inspection interval required for unmitigated DMWs. Thus, inspection credit for cold-leg DMWs is taken at the time of peening. As such, each case in the matrix is assessed as to whether leakage occurs subsequent to the time that inspection relief is taken.

Base case inputs for the deterministic crack growth rate calculations are defined in Table 5-1. The deterministic cases presented in the matrix below include variations of these inputs that are shown in Table 5-5 through Table 5-11 and are summarized below:

- Operating temperatures are based on the minimum and maximum hot and cold leg temperatures for reactor vessel primary nozzles at U.S. PWRs considered to be peening candidates (i.e., plants with Alloy 82/182 piping butt welds on reactor vessel primary nozzles that have not yet been mitigated using another stress improvement or weld overlay method).
- Crack growth rate material variability factors corresponding to 5th percentile, 50th percentile, and 95th percentile crack growth rates are applied.
- Weld residual stress profiles corresponding to the median and $\pm 1\sigma$ for the normally distributed variables $\sigma_{WRS,a}$ and $\sigma_{WRS,h}$ in Table A-3 are applied. Varying these inputs effectively scales the magnitude of the WRS profile. The low (-1σ), median, and high ($+1\sigma$) weld residual stress profiles applied are shown in Figure 5-33 and Figure 5-34.

¹⁴ The likelihood of each deterministic case occurring varies such that the fraction of cases showing leakage is only a relative indicator of, and is not equal to, the probability of leakage.

- The base-case bending loads, as well as bending loads for the high and low bending sensitivity cases (Model Sensitivity Case 7 and Model Sensitivity Case 9 defined in Table A-11) are applied.
- An axial effective load (F_x) of 250 kips (1112 kN) is applied for the low bending moment case. An effective axial load of 100 kips (444.8 kN) is applied for base-case bending loads and for the high bending moment case. This ensures that the crack orientation evaluated for each case corresponds to the orientation with the greatest operating stress, resulting in the bounding stress profile for each orientation.
- Initial crack aspect ratios ($2c/a$) of 6, 8, and 10 are applied.
- Initial crack depths of 0.010 in. (0.25 mm), 0.020 in. (0.5 mm), and 0.039 in. (1.0 mm) are applied. The initial crack depth of 0.010 in. was selected on the basis of the thickness of the cold-worked surface layer that is known to be a key susceptibility factor for PWSCC.

For the range of cases evaluated, the time to grow to leakage is compared against the relevant inspection schedule. The effect of inspections is modeled using the following inputs:

- A detectability limit of a 1.0 mm flaw depth is applied given the requirement for ET examinations. A maximum crack depth of 1.0 mm is required by Supplement 2 of Appendix IV of ASME Section XI [12] for ET qualification. Section 4.2 requires that the ET examinations of the Alloy 82/182 piping butt welds be performed in accordance with Section XI IWA-2223, which requires that the ET be conducted in accordance with Section XI Appendix IV.
- The representative inspection schedule modeled for hot-leg and cold-leg DMWs is shown in Table 5-4. For hot-leg DMWs, follow-up inspections are modeled 5 and 10 years after peening. For cold-leg DMWs, follow-up inspections are modeled 10 years after peening. Subsequent ISI examinations are modeled every 10 years. For the cases in Table 5-8 through Table 5-10 and those in Table 5-11 without peening, inspections are modeled to occur every 5 years for hot-leg DMWs and every 7 years for cold-leg DMWs. Inspections are scheduled assuming an operating capacity factor of 0.97.

Results of the crack growth rate calculations are shown in Table 5-5 through Table 5-11 below. Each table includes the time, crack depth, and aspect ratio of the crack when it reaches the detectability limit. Furthermore, the time required for the crack to grow from the detectability limit to leakage is included, and the follow-up or ISI examination during which a crack would be detected is assessed. If a crack is not detected and does not leak prior to the end of the plant operational service period (i.e., more than 80 years), that crack is marked as "Never Leaks." If a crack on a mitigated nozzle leaks prior to inspection credit being taken for peening, it is labeled as "Leaks before extension of interval", and if a crack leaks subsequent to inspection credit, it is labeled as "Leaks." For unmitigated cases, all cracks that leak are labeled as "Leaks." As shown by plant experience ([54], [55]), any leakage calculated to occur in the deterministic matrix is expected to be small and represent no direct safety concern, including for boric acid corrosion and unstable rupture.

Table 5-5 through Table 5-7 show crack growth rate results for mitigated cases with initial flaw depths up to the modeled limit of detectability for peened components. These tables indicate during which follow-up or ISI examination a flaw would be detected, or if a modeled flaw would

be expected to leak. Although the majority of the flaws are detected in a follow-up examination, some flaws are modeled to be detected during the long-term ISI examinations. These cases result in no leakage subsequent to the extension of inspection intervals.

Some (eight of 72) cases in Table 5-5 through Table 5-7 are shown to leak before the extension of the inspection interval, i.e., they occurred during the first 5 years after peening of a hot-leg DMW when the inspection interval is the same as if peening was not performed. Not peening the DMW would not have prevented these hypothetical leaks. Thus, these eight cases are not relevant to granting inspection credit for peening, as the leakage occurs before any extension of inspection intervals. There are only three of 72 cases in Table 5-5 through Table 5-7 that show leakage after the extension of the inspection interval. This is a small proportion of the full set of cases. In addition, the number of cases in which this occurs is greatly reduced compared to the number of cases with leakage for unpeened components (24 of 72) inspected per the current requirements (defined in ASME Code Case N-770-1 as conditioned by NRC), as shown in Table 5-8 through Table 5-10. Furthermore, most of the cases showing leakage assume a high tensile weld residual stress profile combined with the highest operating temperature for their category, and 95th percentile crack growth rate behavior. There is a very low probability of cases like this occurring in practice. Note that the deterministic PWSCC crack growth rates for Alloys 600, 82, and 182 included in Appendix C of ASME Section XI are based on the 75th percentile of crack growth rate behavior recognizing both the structural factors that are applied in allowable flaw size calculations and the importance of structural integrity of the pressure boundary to resist unstable rupture ([62], [44]).

These results are consistent with the probabilistic assessment in Appendix A, which shows a large leakage prevention benefit of peening. The results of Appendix A show that peening mitigation with assumed inspections based on those specified in Section 4 results in a large reduction in the probability/frequency of leakage when compared to unpeened components inspected per the current requirements.

Table 5-11 investigates modifications to the crack growth rate material variability factor for cases in Table 5-5, Table 5-7, and Table 5-10. These supplemental results further illustrate the leakage prevention benefit of peening with relaxed inspection intervals in comparison to the situation for unmitigated DMWs.

Table 5-4
Inspection Schedule for Deterministic Matrix of Crack Growth Cases for Peened and Unpeened DMWs

Inspection	Inspection Time (yr)	
	Hot-Leg DMW	Cold-Leg DMW
Pre-Peening	every 5	every 7
1st Follow Up	5	10
2nd Follow Up	10	N/A
1st ISI	20	20
2nd ISI	30	30
3rd ISI	40	40
4th ISI	50	50
5th ISI	60	60
6th ISI	70	70
Never Leaks	80	80

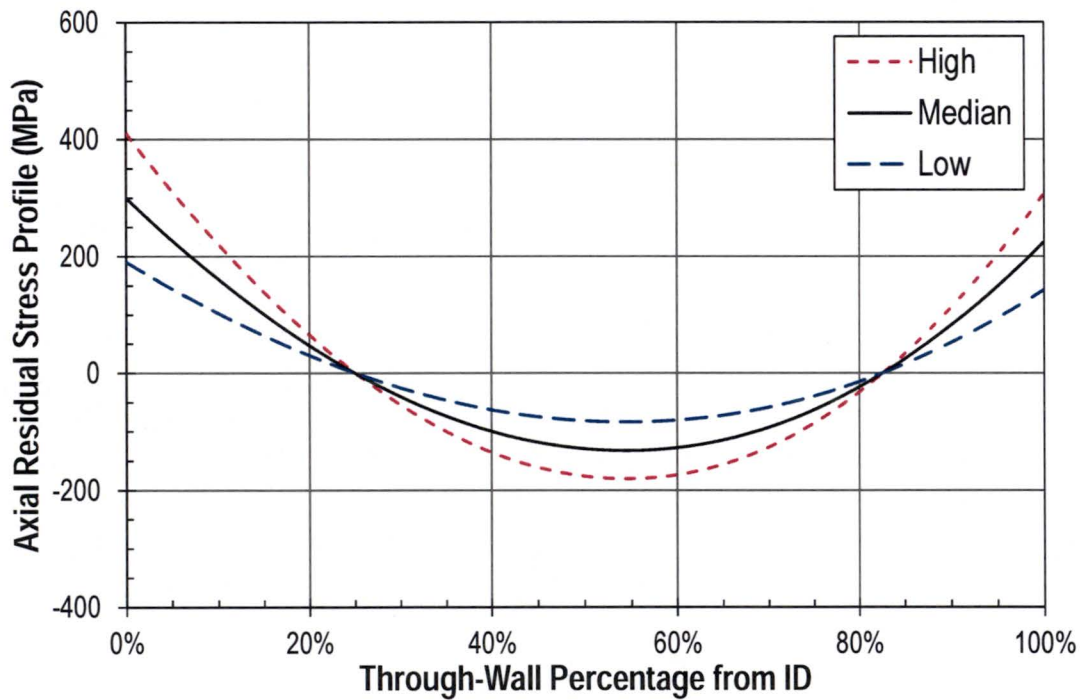


Figure 5-33
Low, Median, and High Weld Residual Axial Stress Profiles Applied in Deterministic Matrix for DMWs

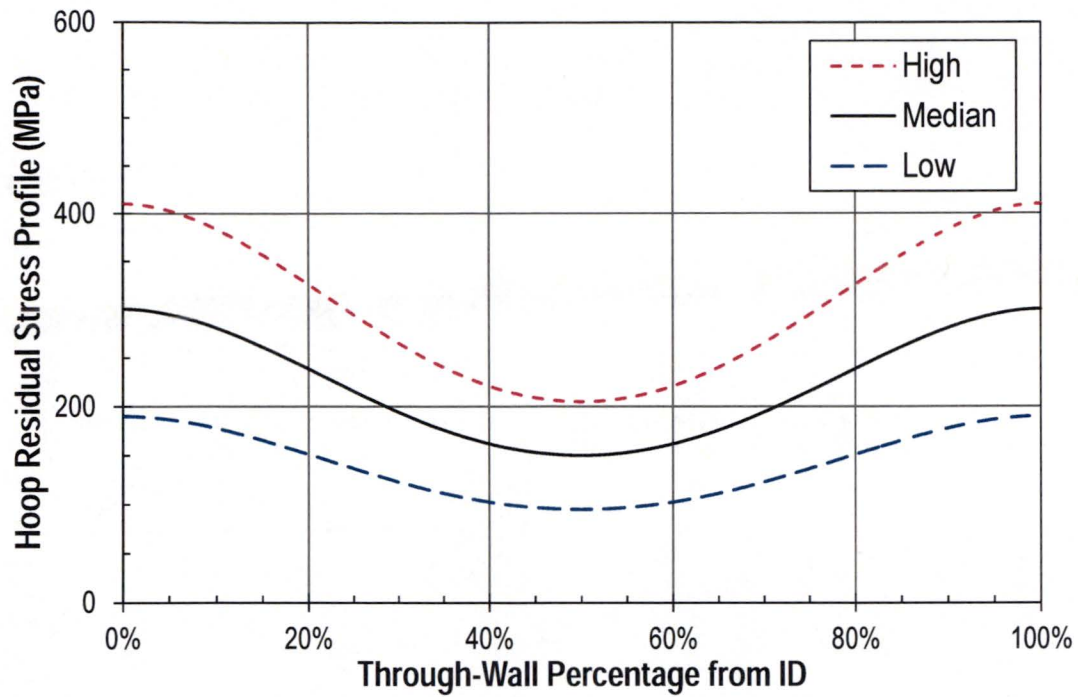


Figure 5-34
Low, Median, and High Weld Residual Hoop Stress Profiles Applied in Deterministic Matrix for DMWs

Table 5-5
Matrix of Deterministic Crack Growth Calculations for Peened DMWs with Initial Flaw Depth of 0.010 in. (0.25 mm)

Case Number	Crack Orient. Axial/Circ	Detect. Limit (%TW)	Weld Residual Stress Profile	MRP-115 A182 CGR %ile	Temp. (°F)	Initial Depth (in.)	Initial Depth (mm)	Initial Aspect Ratio ($2c/a_0$)	Bending Moment	Growth Time to Detect Limit (yr)	Growth Time from Detect Limit to Leak (yr)	Detection Time	Aspect Ratio at Detect Limit ($2c/a$)	Total Length at Detect Limit (in.)	Total Length at Detect Limit (mm)
1	Axial	1.4%	Low	5%	593	0.010	0.25	6.0	N/A	63.0	40.1	6th ISI	1.9	0.076	1.94
2	Axial	1.4%	Median	50%	605.5	0.010	0.25	8.0	N/A	15.8	7.7	1st ISI	2.4	0.093	2.37
3	Axial	1.4%	High	95%	618	0.010	0.25	10.0	N/A	4.2	1.6	1st Follow Up	2.8	0.111	2.82
4	Circ	1.4%	Low	5%	593	0.010	0.25	6.0	Base Case	62.2	48.2	6th ISI	1.6	0.065	1.65
5	Circ	1.4%	Median	50%	605.5	0.010	0.25	8.0	Base Case	15.8	11.5	1st ISI	2.1	0.084	2.13
6	Circ	1.4%	High	95%	618	0.010	0.25	10.0	Base Case	4.2	2.9	1st Follow Up	2.6	0.103	2.62
7	Circ	1.4%	Low	5%	593	0.010	0.25	6.0	Low	82.7	83.9	Never Leaks	1.8	0.073	1.85
8	Circ	1.4%	Median	50%	605.5	0.010	0.25	8.0	Low	20.8	19.7	2nd ISI	2.3	0.091	2.30
9	Circ	1.4%	High	95%	618	0.010	0.25	10.0	Low	5.5	4.9	2nd Follow Up	2.8	0.108	2.76
10	Circ	1.4%	Low	5%	593	0.010	0.25	6.0	High	44.8	27.6	4th ISI	1.6	0.061	1.55
11	Circ	1.4%	Median	50%	605.5	0.010	0.25	8.0	High	11.6	6.8	Leaks	2.0	0.080	2.04
12	Circ	1.4%	High	95%	618	0.010	0.25	10.0	High	3.1	1.7	Leaks before extension of interval	2.5	0.100	2.54
13	Axial	1.4%	Low	5%	538	0.010	0.25	6.0	N/A	274.5	174.9	Never Leaks	1.9	0.076	1.94
14	Axial	1.4%	Median	50%	548.5	0.010	0.25	8.0	N/A	70.4	34.4	Never Leaks	2.4	0.093	2.37
15	Axial	1.4%	High	95%	559	0.010	0.25	10.0	N/A	18.8	7.4	1st ISI	2.8	0.111	2.82
16	Circ	1.4%	Low	5%	538	0.010	0.25	6.0	Base Case	271.0	209.9	Never Leaks	1.6	0.065	1.65
17	Circ	1.4%	Median	50%	548.5	0.010	0.25	8.0	Base Case	70.4	51.3	Never Leaks	2.1	0.084	2.13
18	Circ	1.4%	High	95%	559	0.010	0.25	10.0	Base Case	19.0	13.0	1st ISI	2.6	0.103	2.62
19	Circ	1.4%	Low	5%	538	0.010	0.25	6.0	Low	360.2	365.6	Never Leaks	1.8	0.073	1.85
20	Circ	1.4%	Median	50%	548.5	0.010	0.25	8.0	Low	92.5	87.4	Never Leaks	2.3	0.091	2.30
21	Circ	1.4%	High	95%	559	0.010	0.25	10.0	Low	24.8	22.1	2nd ISI	2.8	0.108	2.76
22	Circ	1.4%	Low	5%	538	0.010	0.25	6.0	High	195.2	120.4	Never Leaks	1.6	0.061	1.55
23	Circ	1.4%	Median	50%	548.5	0.010	0.25	8.0	High	51.5	30.4	5th ISI	2.0	0.080	2.04
24	Circ	1.4%	High	95%	559	0.010	0.25	10.0	High	14.0	7.8	1st ISI	2.5	0.100	2.54

Table 5-6
Matrix of Deterministic Crack Growth Calculations for Peened DMWs with Initial Flaw Depth of 0.020 in. (0.50 mm)

Case Number	Crack Orient. Axial/ Circ	Detect. Limit (%TW)	Weld Residual Stress Profile	MRP-115 A182 CGR %aile	Temp. (°F)	Initial Depth (in.)	Initial Depth (mm)	Initial Aspect Ratio ($2c/a_0$)	Bending Moment	Growth Time to Detect Limit (yr)	Growth Time from Detect Limit to Leak (yr)	Detection Time	Aspect Ratio at Detect Limit ($2c/a$)	Total Length at Detect Limit (in.)	Total Length at Detect Limit (mm)
25	Axial	1.4%	Low	5%	593	0.020	0.50	6.0	N/A	21.1	38.6	2nd ISI	3.2	0.126	3.20
26	Axial	1.4%	Median	50%	605.5	0.020	0.50	8.0	N/A	5.4	7.2	2nd Follow Up	4.2	0.164	4.16
27	Axial	1.4%	High	95%	618	0.020	0.50	10.0	N/A	1.4	1.5	Leaks before extension of interval	5.1	0.202	5.14
28	Circ	1.4%	Low	5%	593	0.020	0.50	6.0	Base Case	15.7	47.2	1st ISI	3.1	0.121	3.08
29	Circ	1.4%	Median	50%	605.5	0.020	0.50	8.0	Base Case	4.1	11.1	1st Follow Up	4.1	0.160	4.06
30	Circ	1.4%	High	95%	618	0.020	0.50	10.0	Base Case	1.1	2.8	Leaks before extension of interval	5.1	0.199	5.06
31	Circ	1.4%	Low	5%	593	0.020	0.50	6.0	Low	25.6	82.1	2nd ISI	3.2	0.124	3.16
32	Circ	1.4%	Median	50%	605.5	0.020	0.50	8.0	Low	6.6	18.9	2nd Follow Up	4.1	0.162	4.12
33	Circ	1.4%	High	95%	618	0.020	0.50	10.0	Low	1.8	4.7	1st Follow Up	5.1	0.201	5.12
34	Circ	1.4%	Low	5%	593	0.020	0.50	6.0	High	9.3	27.2	2nd Follow Up	3.0	0.120	3.04
35	Circ	1.4%	Median	50%	605.5	0.020	0.50	8.0	High	2.4	6.6	1st Follow Up	4.0	0.159	4.03
36	Circ	1.4%	High	95%	618	0.020	0.50	10.0	High	0.7	1.7	Leaks before extension of interval	5.0	0.198	5.03
37	Axial	1.4%	Low	5%	538	0.020	0.50	6.0	N/A	91.8	168.2	Never Leaks	3.2	0.126	3.20
38	Axial	1.4%	Median	50%	548.5	0.020	0.50	8.0	N/A	23.9	32.2	2nd ISI	4.2	0.164	4.16
39	Axial	1.4%	High	95%	559	0.020	0.50	10.0	N/A	6.5	6.9	1st Follow Up	5.1	0.202	5.14
40	Circ	1.4%	Low	5%	538	0.020	0.50	6.0	Base Case	68.6	205.8	6th ISI	3.1	0.121	3.08
41	Circ	1.4%	Median	50%	548.5	0.020	0.50	8.0	Base Case	18.1	49.5	1st ISI	4.1	0.160	4.06
42	Circ	1.4%	High	95%	559	0.020	0.50	10.0	Base Case	4.9	12.5	1st Follow Up	5.1	0.199	5.06
43	Circ	1.4%	Low	5%	538	0.020	0.50	6.0	Low	111.5	357.7	Never Leaks	3.2	0.124	3.16
44	Circ	1.4%	Median	50%	548.5	0.020	0.50	8.0	Low	29.3	84.2	2nd ISI	4.1	0.162	4.12
45	Circ	1.4%	High	95%	559	0.020	0.50	10.0	Low	8.0	21.3	1st Follow Up	5.1	0.201	5.12
46	Circ	1.4%	Low	5%	538	0.020	0.50	6.0	High	40.6	118.5	4th ISI	3.0	0.120	3.04
47	Circ	1.4%	Median	50%	548.5	0.020	0.50	8.0	High	10.8	29.4	1st ISI	4.0	0.159	4.03
48	Circ	1.4%	High	95%	559	0.020	0.50	10.0	High	3.0	7.5	1st Follow Up	5.0	0.198	5.03

Table 5-7
Matrix of Deterministic Crack Growth Calculations for Peened DMWs with Initial Flaw Depth of 0.039 in. (1.00 mm)

Case Number	Crack Orient. Axial/Circ	Detect. Limit (%TW)	Weld Residual Stress Profile	MRP-115 A182 CGR %ile	Temp. (°F)	Initial Depth (in.)	Initial Depth (mm)	Initial Aspect Ratio ($2c/a_0$)	Bending Moment	Growth Time to Detect Limit (yr)	Growth Time from Detect Limit to Leak (yr)	Detection Time	Aspect Ratio at Detect Limit ($2c/a$)	Total Length at Detect Limit (in.)	Total Length at Detect Limit (mm)
49	Axial	1.4%	Low	5%	593	0.039	1.00	6.0	N/A	0.0	36.2	1st Follow Up	6.0	0.236	6.00
50	Axial	1.4%	Median	50%	605.5	0.039	1.00	8.0	N/A	0.0	6.8	1st Follow Up	8.0	0.315	8.00
51	Axial	1.4%	High	95%	618	0.039	1.00	10.0	N/A	0.0	1.4	Leaks before extension of interval	10.0	0.394	10.00
52	Circ	1.4%	Low	5%	593	0.039	1.00	6.0	Base Case	0.0	45.2	1st Follow Up	6.0	0.236	6.00
53	Circ	1.4%	Median	50%	605.5	0.039	1.00	8.0	Base Case	0.0	10.6	1st Follow Up	8.0	0.315	8.00
54	Circ	1.4%	High	95%	618	0.039	1.00	10.0	Base Case	0.0	2.6	Leaks before extension of interval	10.0	0.394	10.00
55	Circ	1.4%	Low	5%	593	0.039	1.00	6.0	Low	0.0	78.6	1st Follow Up	6.0	0.236	6.00
56	Circ	1.4%	Median	50%	605.5	0.039	1.00	8.0	Low	0.0	18.2	1st Follow Up	8.0	0.315	8.00
57	Circ	1.4%	High	95%	618	0.039	1.00	10.0	Low	0.0	4.5	Leaks before extension of interval	10.0	0.394	10.00
58	Circ	1.4%	Low	5%	593	0.039	1.00	6.0	High	0.0	26.0	1st Follow Up	6.0	0.236	6.00
59	Circ	1.4%	Median	50%	605.5	0.039	1.00	8.0	High	0.0	6.3	1st Follow Up	8.0	0.315	8.00
60	Circ	1.4%	High	95%	618	0.039	1.00	10.0	High	0.0	1.6	Leaks before extension of interval	10.0	0.394	10.00
61	Axial	1.4%	Low	5%	538	0.039	1.00	6.0	N/A	0.0	157.7	1st Follow Up	6.0	0.236	6.00
62	Axial	1.4%	Median	50%	548.5	0.039	1.00	8.0	N/A	0.0	30.1	1st Follow Up	8.0	0.315	8.00
63	Axial	1.4%	High	95%	559	0.039	1.00	10.0	N/A	0.0	6.4	Leaks	10.0	0.394	10.00
64	Circ	1.4%	Low	5%	538	0.039	1.00	6.0	Base Case	0.0	196.9	1st Follow Up	6.0	0.236	6.00
65	Circ	1.4%	Median	50%	548.5	0.039	1.00	8.0	Base Case	0.0	47.2	1st Follow Up	8.0	0.315	8.00
66	Circ	1.4%	High	95%	559	0.039	1.00	10.0	Base Case	0.0	11.9	1st Follow Up	10.0	0.394	10.00
67	Circ	1.4%	Low	5%	538	0.039	1.00	6.0	Low	0.0	342.3	1st Follow Up	6.0	0.236	6.00
68	Circ	1.4%	Median	50%	548.5	0.039	1.00	8.0	Low	0.0	81.1	1st Follow Up	8.0	0.315	8.00
69	Circ	1.4%	High	95%	559	0.039	1.00	10.0	Low	0.0	20.5	1st Follow Up	10.0	0.394	10.00
70	Circ	1.4%	Low	5%	538	0.039	1.00	6.0	High	0.0	113.2	1st Follow Up	6.0	0.236	6.00
71	Circ	1.4%	Median	50%	548.5	0.039	1.00	8.0	High	0.0	27.9	1st Follow Up	8.0	0.315	8.00
72	Circ	1.4%	High	95%	559	0.039	1.00	10.0	High	0.0	7.2	Leaks	10.0	0.394	10.00

Table 5-8
Matrix of Deterministic Crack Growth Calculations for Unmitigated DMWs with Initial Flaw Depth of 0.010 in. (0.25 mm)

Case Number	Crack Orient. Axial/Circ	Detect. Limit (%TW)	Weld Residual Stress Profile	MRP-115 A182 CGR %ile	Temp. (°F)	Initial Depth (in.)	Initial Depth (mm)	Initial Aspect Ratio (2c/a ₀)	Bending Moment	Growth Time to Detect Limit (yr)	Growth Time from Detect Limit to Leak (yr)	Detected/Leaks	Aspect Ratio at Detect Limit (2c/a)	Total Length at Detect Limit (in.)	Total Length at Detect Limit (mm)
1 - NP	Axial	1.4%	Low	5%	593	0.010	0.25	6.0	N/A	3.2	27.7	Detected	2.7	0.105	2.66
2 - NP	Axial	1.4%	Median	50%	605.5	0.010	0.25	8.0	N/A	0.5	4.9	Detected	3.0	0.117	2.96
3 - NP	Axial	1.4%	High	95%	618	0.010	0.25	10.0	N/A	0.1	1.0	Leaks	3.5	0.137	3.49
4 - NP	Circ	1.4%	Low	5%	593	0.010	0.25	6.0	Base Case	2.6	30.2	Detected	2.7	0.105	2.66
5 - NP	Circ	1.4%	Median	50%	605.5	0.010	0.25	8.0	Base Case	0.4	6.8	Detected	2.9	0.114	2.90
6 - NP	Circ	1.4%	High	95%	618	0.010	0.25	10.0	Base Case	0.1	1.6	Leaks	3.5	0.137	3.49
7 - NP	Circ	1.4%	Low	5%	593	0.010	0.25	6.0	Low	3.3	49.7	Detected	2.7	0.106	2.68
8 - NP	Circ	1.4%	Median	50%	605.5	0.010	0.25	8.0	Low	0.5	11.0	Detected	3.0	0.118	2.99
9 - NP	Circ	1.4%	High	95%	618	0.010	0.25	10.0	Low	0.1	2.6	Leaks	3.5	0.137	3.48
10 - NP	Circ	1.4%	Low	5%	593	0.010	0.25	6.0	High	1.9	18.3	Detected	2.6	0.104	2.64
11 - NP	Circ	1.4%	Median	50%	605.5	0.010	0.25	8.0	High	0.4	4.2	Leaks	3.0	0.119	3.03
12 - NP	Circ	1.4%	High	95%	618	0.010	0.25	10.0	High	0.1	1.0	Leaks	3.4	0.134	3.39
13 - NP	Axial	1.4%	Low	5%	538	0.010	0.25	6.0	N/A	13.8	120.6	Detected	2.7	0.105	2.66
14 - NP	Axial	1.4%	Median	50%	548.5	0.010	0.25	8.0	N/A	2.3	21.6	Detected	3.0	0.117	2.96
15 - NP	Axial	1.4%	High	95%	559	0.010	0.25	10.0	N/A	0.4	4.4	Leaks	3.5	0.137	3.49
16 - NP	Circ	1.4%	Low	5%	538	0.010	0.25	6.0	Base Case	11.2	131.5	Detected	2.7	0.105	2.66
17 - NP	Circ	1.4%	Median	50%	548.5	0.010	0.25	8.0	Base Case	2.0	30.0	Detected	2.9	0.114	2.90
18 - NP	Circ	1.4%	High	95%	559	0.010	0.25	10.0	Base Case	0.4	7.3	Detected	3.5	0.137	3.49
19 - NP	Circ	1.4%	Low	5%	538	0.010	0.25	6.0	Low	14.5	216.7	Detected	2.7	0.106	2.68
20 - NP	Circ	1.4%	Median	50%	548.5	0.010	0.25	8.0	Low	2.4	48.9	Detected	3.0	0.118	2.99
21 - NP	Circ	1.4%	High	95%	559	0.010	0.25	10.0	Low	0.5	11.9	Detected	3.5	0.137	3.48
22 - NP	Circ	1.4%	Low	5%	538	0.010	0.25	6.0	High	8.2	79.6	Detected	2.6	0.104	2.64
23 - NP	Circ	1.4%	Median	50%	548.5	0.010	0.25	8.0	High	1.6	18.8	Detected	3.0	0.119	3.03
24 - NP	Circ	1.4%	High	95%	559	0.010	0.25	10.0	High	0.3	4.6	Leaks	3.4	0.134	3.39

Supporting Analyses

Table 5-9
Matrix of Deterministic Crack Growth Calculations for Unmitigated DMWs with Initial Flaw Depth of 0.020 in. (0.50 mm)

Case Number	Crack Orient. Axial/Circ	Detect. Limit (%TW)	Weld Residual Stress Profile	MRP-115 A182 CGR %ile	Temp. (°F)	Initial Depth (in.)	Initial Depth (mm)	Initial Aspect Ratio ($2c/a_0$)	Bending Moment	Growth Time to Detect Limit (yr)	Growth Time from Detect Limit to Leak (yr)	Detected/Leaks	Aspect Ratio at Detect Limit ($2c/a$)	Total Length at Detect Limit (in.)	Total Length at Detect Limit (mm)
25 - NP	Axial	1.4%	Low	5%	593	0.020	0.50	6.0	N/A	1.5	27.2	Detected	3.6	0.142	3.61
26 - NP	Axial	1.4%	Median	50%	605.5	0.020	0.50	8.0	N/A	0.2	4.7	Leaks	4.5	0.178	4.51
27 - NP	Axial	1.4%	High	95%	618	0.020	0.50	10.0	N/A	0.0	0.9	Leaks	6.0	0.236	5.99
28 - NP	Circ	1.4%	Low	5%	593	0.020	0.50	6.0	Base Case	1.2	29.6	Detected	3.7	0.145	3.69
29 - NP	Circ	1.4%	Median	50%	605.5	0.020	0.50	8.0	Base Case	0.2	6.6	Detected	4.4	0.174	4.42
30 - NP	Circ	1.4%	High	95%	618	0.020	0.50	10.0	Base Case	0.0	1.6	Leaks	6.3	0.247	6.26
31 - NP	Circ	1.4%	Low	5%	593	0.020	0.50	6.0	Low	1.6	49.1	Detected	3.6	0.142	3.62
32 - NP	Circ	1.4%	Median	50%	605.5	0.020	0.50	8.0	Low	0.3	10.8	Detected	4.6	0.179	4.56
33 - NP	Circ	1.4%	High	95%	618	0.020	0.50	10.0	Low	0.0	2.6	Leaks	5.9	0.231	5.87
34 - NP	Circ	1.4%	Low	5%	593	0.020	0.50	6.0	High	0.9	18.0	Detected	3.6	0.142	3.61
35 - NP	Circ	1.4%	Median	50%	605.5	0.020	0.50	8.0	High	0.2	4.1	Leaks	4.9	0.193	4.91
36 - NP	Circ	1.4%	High	95%	618	0.020	0.50	10.0	High	0.0	1.0	Leaks	6.7	0.265	6.73
37 - NP	Axial	1.4%	Low	5%	538	0.020	0.50	6.0	N/A	6.5	118.3	Detected	3.6	0.142	3.61
38 - NP	Axial	1.4%	Median	50%	548.5	0.020	0.50	8.0	N/A	1.1	21.0	Detected	4.5	0.178	4.51
39 - NP	Axial	1.4%	High	95%	559	0.020	0.50	10.0	N/A	0.2	4.2	Leaks	6.0	0.236	5.99
40 - NP	Circ	1.4%	Low	5%	538	0.020	0.50	6.0	Base Case	5.3	129.1	Detected	3.7	0.145	3.69
41 - NP	Circ	1.4%	Median	50%	548.5	0.020	0.50	8.0	Base Case	1.0	29.3	Detected	4.4	0.174	4.42
42 - NP	Circ	1.4%	High	95%	559	0.020	0.50	10.0	Base Case	0.2	7.2	Detected	6.3	0.247	6.26
43 - NP	Circ	1.4%	Low	5%	538	0.020	0.50	6.0	Low	6.9	214.0	Detected	3.6	0.142	3.62
44 - NP	Circ	1.4%	Median	50%	548.5	0.020	0.50	8.0	Low	1.1	48.2	Detected	4.6	0.179	4.56
45 - NP	Circ	1.4%	High	95%	559	0.020	0.50	10.0	Low	0.2	11.8	Detected	5.9	0.231	5.87
46 - NP	Circ	1.4%	Low	5%	538	0.020	0.50	6.0	High	3.9	78.4	Detected	3.6	0.142	3.61
47 - NP	Circ	1.4%	Median	50%	548.5	0.020	0.50	8.0	High	0.7	18.3	Detected	4.9	0.193	4.91
48 - NP	Circ	1.4%	High	95%	559	0.020	0.50	10.0	High	0.1	4.5	Leaks	6.7	0.265	6.73

Table 5-10
Matrix of Deterministic Crack Growth Calculations for Unmitigated DMWs with Initial Flaw Depth of 0.039 in. (1.00 mm)

Case Number	Crack Orient. Axial/Circ	Detect. Limit (%TW)	Weld Residual Stress Profile	MRP-115 A182 CGR %ile	Temp. (°F)	Initial Depth (in.)	Initial Depth (mm)	Initial Aspect Ratio ($2c/a_0$)	Bending Moment	Growth Time to Detect Limit (yr)	Growth Time from Detect Limit to Leak (yr)	Detection/Leak	Aspect Ratio at Detect Limit ($2c/a$)	Total Length at Detect Limit (in.)	Total Length at Detect Limit (mm)
49 - NP	Axial	1.4%	Low	5%	593	0.039	1.00	6.0	N/A	0.0	26.1	Detected	6.0	0.236	6.00
50 - NP	Axial	1.4%	Median	50%	605.5	0.039	1.00	8.0	N/A	0.0	4.5	Leaks	8.0	0.315	8.00
51 - NP	Axial	1.4%	High	95%	618	0.039	1.00	10.0	N/A	0.0	0.9	Leaks	10.0	0.394	10.00
52 - NP	Circ	1.4%	Low	5%	593	0.039	1.00	6.0	Base Case	0.0	28.8	Detected	6.0	0.236	6.00
53 - NP	Circ	1.4%	Median	50%	605.5	0.039	1.00	8.0	Base Case	0.0	6.4	Detected	8.0	0.315	8.00
54 - NP	Circ	1.4%	High	95%	618	0.039	1.00	10.0	Base Case	0.0	1.5	Leaks	10.0	0.394	10.00
55 - NP	Circ	1.4%	Low	5%	593	0.039	1.00	6.0	Low	0.0	48.0	Detected	6.0	0.236	6.00
56 - NP	Circ	1.4%	Median	50%	605.5	0.039	1.00	8.0	Low	0.0	10.6	Detected	8.0	0.315	8.00
57 - NP	Circ	1.4%	High	95%	618	0.039	1.00	10.0	Low	0.0	2.5	Leaks	10.0	0.394	10.00
58 - NP	Circ	1.4%	Low	5%	593	0.039	1.00	6.0	High	0.0	17.3	Detected	6.0	0.236	6.00
59 - NP	Circ	1.4%	Median	50%	605.5	0.039	1.00	8.0	High	0.0	4.0	Leaks	8.0	0.315	8.00
60 - NP	Circ	1.4%	High	95%	618	0.039	1.00	10.0	High	0.0	1.0	Leaks	10.0	0.394	10.00
61 - NP	Axial	1.4%	Low	5%	538	0.039	1.00	6.0	N/A	0.0	113.9	Detected	6.0	0.236	6.00
62 - NP	Axial	1.4%	Median	50%	548.5	0.039	1.00	8.0	N/A	0.0	20.0	Detected	8.0	0.315	8.00
63 - NP	Axial	1.4%	High	95%	559	0.039	1.00	10.0	N/A	0.0	4.0	Leaks	10.0	0.394	10.00
64 - NP	Circ	1.4%	Low	5%	538	0.039	1.00	6.0	Base Case	0.0	125.5	Detected	6.0	0.236	6.00
65 - NP	Circ	1.4%	Median	50%	548.5	0.039	1.00	8.0	Base Case	0.0	28.5	Detected	8.0	0.315	8.00
66 - NP	Circ	1.4%	High	95%	559	0.039	1.00	10.0	Base Case	0.0	7.0	Leaks	10.0	0.394	10.00
67 - NP	Circ	1.4%	Low	5%	538	0.039	1.00	6.0	Low	0.0	209.2	Detected	6.0	0.236	6.00
68 - NP	Circ	1.4%	Median	50%	548.5	0.039	1.00	8.0	Low	0.0	47.2	Detected	8.0	0.315	8.00
69 - NP	Circ	1.4%	High	95%	559	0.039	1.00	10.0	Low	0.0	11.5	Detected	10.0	0.394	10.00
70 - NP	Circ	1.4%	Low	5%	538	0.039	1.00	6.0	High	0.0	75.5	Detected	6.0	0.236	6.00
71 - NP	Circ	1.4%	Median	50%	548.5	0.039	1.00	8.0	High	0.0	17.7	Detected	8.0	0.315	8.00
72 - NP	Circ	1.4%	High	95%	559	0.039	1.00	10.0	High	0.0	4.4	Leaks	10.0	0.394	10.00

Table 5-11
Matrix of Deterministic Crack Growth Calculations for DMWs with Modified Crack Growth Rate Material Variability Factors

Case Number	Crack Orient. Axial/Circ	Detect. Limit (%TW)	Weld Residual Stress Profile	MRP-115 A182 CGR %ile	Temp. (°F)	Initial Depth (in.)	Initial Depth (mm)	Initial Aspect Ratio ($2c/a_0$)	Bending Moment	Growth Time to Detect Limit (yr)	Growth Time from Detect Limit to Leak (yr)	Detection Time	Aspect Ratio at Detect Limit ($2c/a$)	Total Length at Detect Limit (in.)	Total Length at Detect Limit (mm)
11	Circ	1.4%	Median	60%	605.5	0.010	0.254	8.0	High	10.0	5.9	2nd Follow Up	2.0	0.080	2.0
11	Circ	1.4%	Median	44%	605.5	0.010	0.254	8.0	High	12.6	7.4	1st ISI	2.0	0.080	2.0
63	Axial	1.4%	High	81%	559	0.039	1.00	10.0	N/A	0.0	10.0	1st Follow Up	10.0	0.394	10.0
63 - NP	Axial	1.4%	High	75%	559	0.039	1.00	10.0	N/A	0.0	7.0	Next ISI per N-770-1	10.0	0.394	10.0
72	Circ	1.4%	High	86%	559	0.039	1.00	10.0	High	0.0	10.0	1st Follow Up	10.0	0.394	10.0
72 - NP	Circ	1.4%	High	80%	559	0.039	1.00	10.0	High	0.0	7.0	Next ISI per N-770-1	10.0	0.394	10.0

5.2.3.2 Reactor Pressure Vessel Head Penetration Nozzles (RPVHPNs)

For peened RPVHPNs, the follow-up examination(s) are scheduled after a period shorter than or equal to the volumetric or surface examination interval for the unmitigated RPVHPNs. Thus, any leakage that would occur prior to the follow-up examinations for the peened RPVHPNs would not be prevented had the RPVHPNs not been mitigated.

Base case inputs for the deterministic crack growth rate calculations are defined in Table 5-2. The deterministic cases presented in the matrix below include variations of these inputs that are shown in Table 5-13 through Table 5-19 and are summarized below:

- Operating temperatures applied are based on the range of head temperatures for the remaining U.S. with Alloy 600 RPVHPNs and Alloy 82/182 J-groove welds.
- Crack growth rate material variability factors corresponding to 5th percentile, 50th percentile, and 95th percentile crack growth rates are applied.
- Total (residual plus normal operating) stresses on the nozzle tube OD and weld were modeled to be +10 ksi (different from Table 5-2). The total (residual plus normal operating) stresses on the nozzle tube ID were modeled to be +10 ksi (as in Table 5-2).
- Weld residual stress profiles corresponding to the median and $\pm 1\sigma$ for the normally distributed $\sigma_{0,tot}$ variables in Table B-4 are applied. Varying these inputs effectively scales the magnitude of the WRS profile. In addition, the ID operating stress input (in terms of the factor $f_{oper,ID}$) is varied with the WRS; the low (-1σ), median, and high ($+1\sigma$) values of $f_{oper,ID}$ are applied in combination with the corresponding low, median, and high WRS profiles. The low (-1σ), median, and high ($+1\sigma$) stress profiles (WRS plus operating stress) applied are shown in Figure 5-35 through Figure 5-38.
- Initial crack aspect ratios ($2c/a$) of 2, 3, and 4 are applied.
- Initial crack depths of 0.010 in. (0.25 mm), 0.020 in. (0.5 mm), and 0.062 in. (1.58 mm) are applied. The initial crack depth of 0.010 in. was selected on the basis of the thickness of the cold-worked surface layer that is known to be a key susceptibility factor for PWSCC.

For the range of cases evaluated, the time to grow to leakage is compared against the relevant inspection schedule. The effect of inspections is modeled using the following inputs:

- A UT detectability limit of 10% TW (0.062 in.) is applied. This is based on the UT detectability threshold applied for the probabilistic assessment in Appendix B (as shown in Table B-9).
- The representative inspection schedule modeled for hot head and cold head RPVHPNs is shown in Table 5-12. For non-cold heads, follow-up inspections are modeled 2 and 4 years after peening. For cold-heads, follow-up inspections are modeled 3 years (two 18-month cycles) after peening. Subsequent ISI examinations are modeled every 10 years. For the cases in Table 5-16 through Table 5-18 without peening, inspections are modeled to occur every 8 years or before $RIY = 2.25$, whichever is less. Inspections are scheduled assuming an operating capacity factor of 0.97.

Axial cracks are modeled in this section because they are the predominant concern for producing leakage due to base metal PWSCC, as shown by plant experience [20] and stress analyses [16].

Circumferential flaws above the weld can potentially be produced after the nozzle OD annulus region is wetted. The analyses in MRP-395 [20] and in Figure 5-32 of this report demonstrate a substantial time period for a circumferential nozzle crack to grow to critical size. The combination of ongoing volumetric (UT) and visual (VE and VT-2 under the insulation through multiple access points) examinations addresses the concerns for circumferential nozzle cracking located above the weld, as well as for boric acid corrosion of the low-alloy steel head material. For this analysis, ID axial cracks are assumed to initiate in the region above the weld such that they immediately result in leakage if they penetrate through-wall into the OD nozzle annulus. OD axial cracks are modeled to cause leakage if they grow in length upward to reach the nozzle OD annulus.

For unmitigated RPVHPNs, any weld cracking is addressed by bare metal visual examinations for leakage. Peening reduces the probability of leakage due to weld cracking by preventing future PWSCC initiation, and Section 4 maintains the same basic visual examination schedule as is currently required for unmitigated RPVHPNs.

Results of the crack growth rate calculations are shown in Table 5-13 through Table 5-19 below. Each table includes the time, crack depth, and aspect ratio of the crack when it reaches the detectability limit. Furthermore, the time required for the crack to grow from the detectability limit to leakage is included, and the follow-up or ISI examination during which a crack is detected is assessed. If a crack is not detected and does not leak prior to the end of the plant operational service period (i.e., more than 80 years), that crack is marked as "Never Leaks," and if a crack leaks subsequent to inspection credit, it is labeled as "Leaks."

Table 5-13 through Table 5-15 show crack growth rate results for mitigated cases with initial flaw depths up to the modeled limit of detectability. These tables indicate during which follow-up or ISI examination a flaw would be detected, or if a modeled flaw would be expected to leak. Although the majority of the flaws are detected in a follow-up examination, some of the modeled flaws are modeled to be detected during the long-term ISI examinations. Only two cases out of 72 are calculated to result in leakage, consistent with the probabilistic analysis results that show a low probability of leakage with peening. Both of these leakage cases assume an unlikely combination of conditions leading to upper end crack growth rates, and both of these leakage cases assume initiation on the nozzle ID surface. As discussed near the end of Section 2.3.2, operating experience shows a very low probability of PWSCC initiation on the nozzle ID surface. The large majority of PWSCC indications in RPVHPNs have been located on the nozzle outer surfaces.

Table 5-16 through Table 5-18 show crack growth results for unmitigated cases with initial flaw depths up to the modeled limit of detectability. Of the 72 modeled cases, leakage is calculated for 10 cases. This provides a comparison between the unmitigated component per the current inspection requirements (defined in ASME Code Case N-729-1 [2], as conditioned by NRC) and the inspection requirements for peened components defined in Section 4. A direct comparison between Table 5-15 and Table 5-18 shows that peening mitigation in combination with the inspection schedule of Section 4.3 results in a much lower number of cases that produce leaks.

Table 5-19 investigates both increases and decreases to the crack growth rate material variability factor for the two cases out of 72 in Table 5-13 that show leakage after implementing inspection relief. This table illustrates that there is only a narrow range of crack growth rate material behavior that could result in leakage given the other input parameters represented by these cases

with peening mitigation. Both of the cases in Table 5-13 that show leakage assume a high tensile weld residual stress profile combined with the highest operating temperature for their category, and 95th percentile crack growth rate behavior. There is a very low probability of cases like this occurring in practice. Furthermore, the deterministic PWSCC crack growth rates for Alloys 600, 82, and 182 included in Appendix C of ASME Section XI are based on the 75th percentile of crack growth rate behavior recognizing both the structural factors that are applied in allowable flaw size calculations and the importance of structural integrity of the pressure boundary to resist unstable rupture ([62], [44]). These supplemental results further illustrate the leakage prevention benefit of peening with relaxed inspection intervals in comparison to the situation for unmitigated RPVHPNs.

Table 5-12
Inspection Schedule for Deterministic Matrix of Crack Growth Cases for Peened and Unpeened RPVHPNs

Inspection	Inspection Time (yr)	
	Hot Head	Cold Head
Pre-Peening	min(RIY=2.25, 8yr)	
1st Follow Up	2	3
2nd Follow Up	4	N/A
1st ISI	14	13
2nd ISI	24	23
3rd ISI	34	33
4th ISI	44	43
5th ISI	54	53
6th ISI	64	63
7th ISI	74	73
Never Leaks	80	80

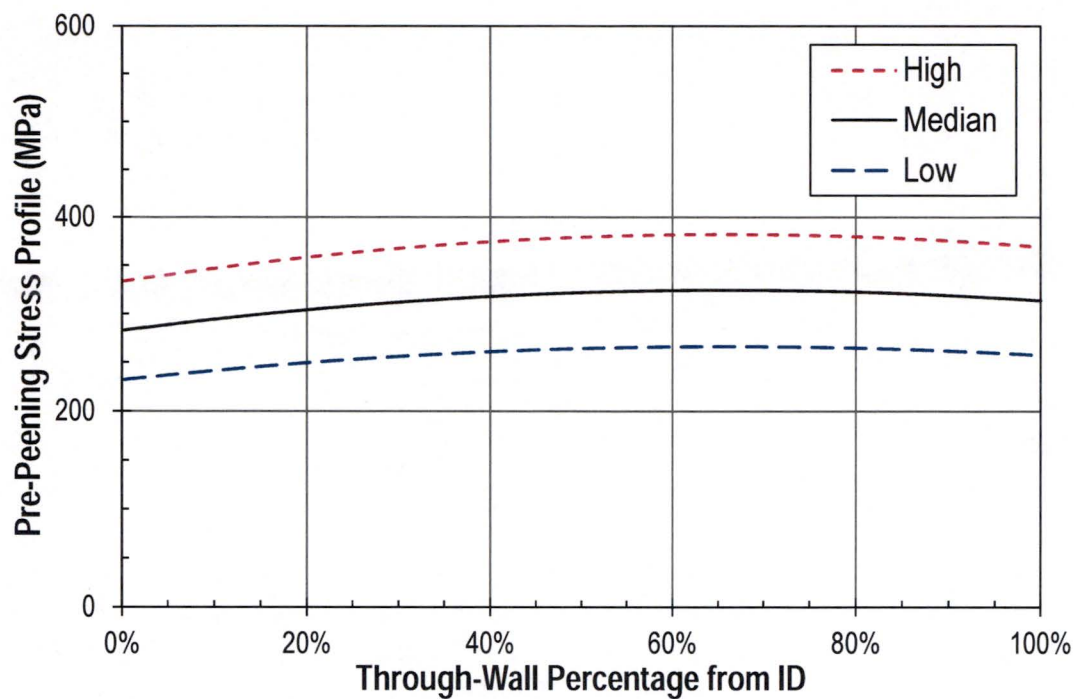


Figure 5-35
Low, Median, and High Pre-Peening Stress Profiles Applied in Deterministic Matrix for RPVHPNs (ID Uphill)

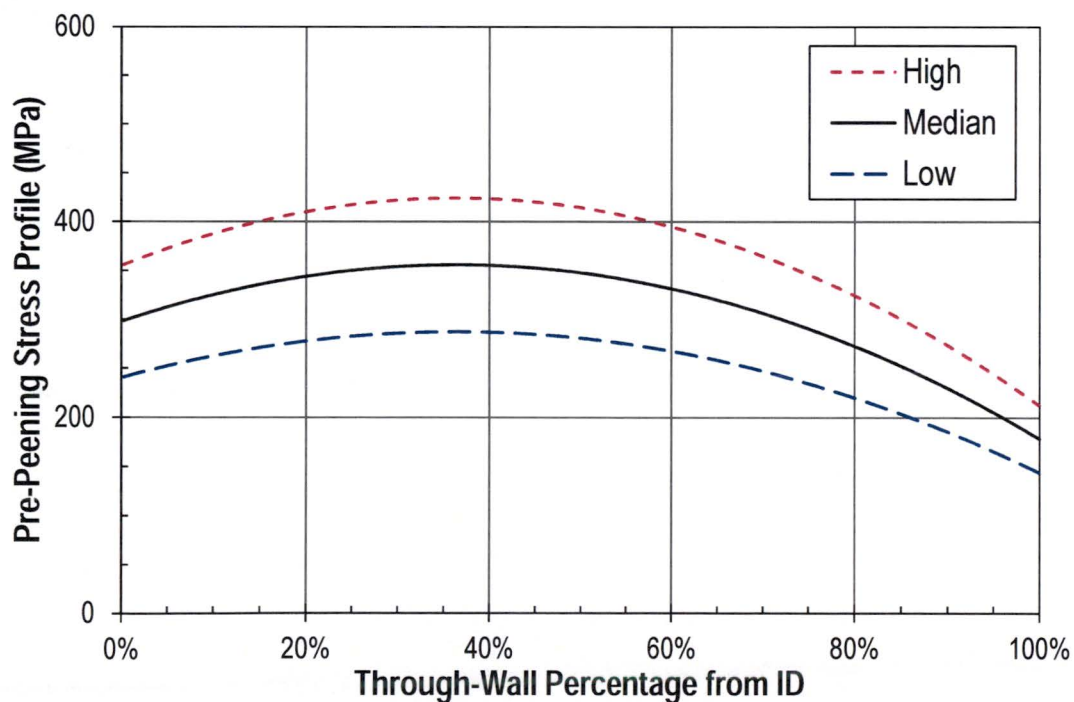


Figure 5-36
Low, Median, and High Pre-Peening Stress Profiles Applied in Deterministic Matrix for RPVHPNs (ID Downhill)

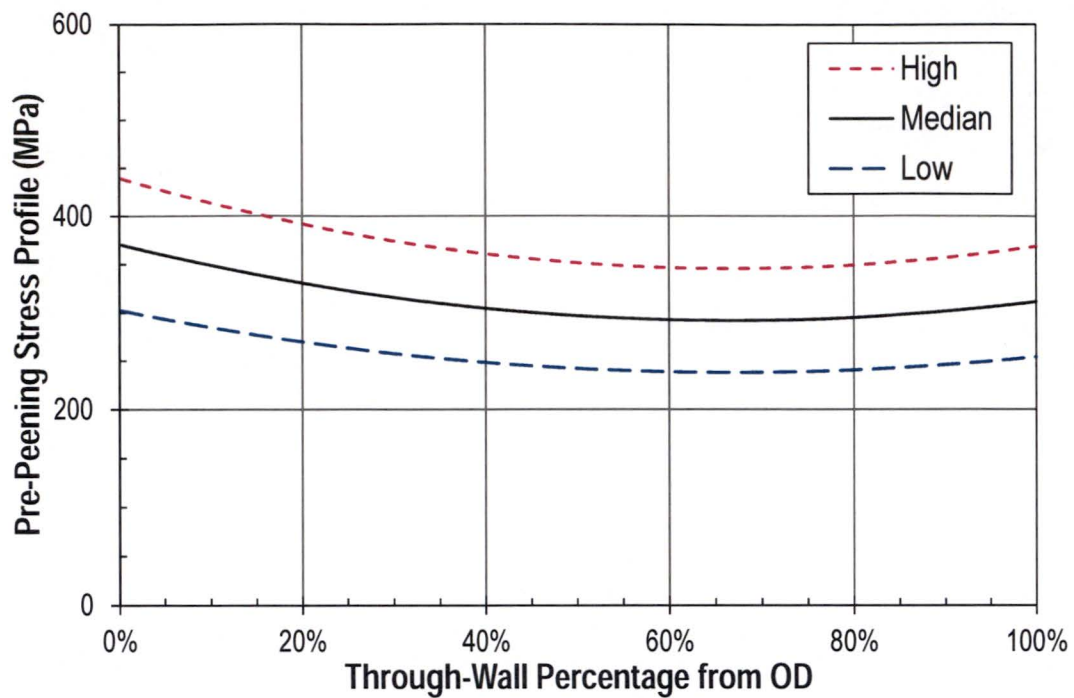


Figure 5-37
Low, Median, and High Pre-Peening Stress Profiles Applied in Deterministic Matrix for RPVHPNs (OD Uphill)

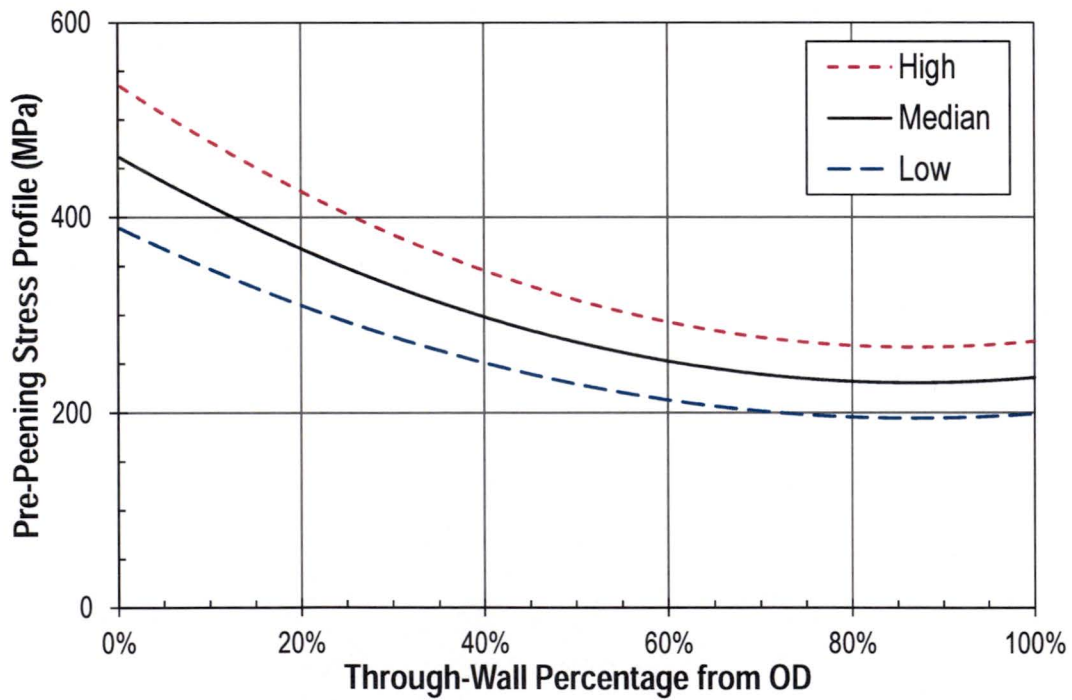


Figure 5-38
Low, Median, and High Pre-Peening Stress Profiles Applied in Deterministic Matrix for RPVHPNs (OD Downhill)

Table 5-13
Matrix of Deterministic Crack Growth Calculations for Peened RPVHPNs with Initial Flaw Depth of 0.010 in. (0.25 mm)

Case Number	Nozzle Tube Location ID/OD	Nozzle Tube Location UH/DH	Stress Profile	MRP-55 A600 CGR %ile	Temp. (°F)	Initial Depth (in.)	Initial Depth (mm)	Initial Aspect Ratio ($2c/a_0$)	Growth Time to 10%TW (yr)	Growth Time from 10% to Leak (yr)	Detection Time	Aspect Ratio at 10%TW ($2c/a$)	Total Length at 10%TW (in.)	Total Length at 10%TW (mm)
1	ID	UH	Low	5%	586	0.010	0.25	2.0	154.6	157.8	Never Leaks	1.1	0.069	1.7
2	ID	UH	Median	50%	590.5	0.010	0.25	3.0	18.1	19.7	2nd ISI	1.2	0.072	1.8
3	ID	UH	High	95%	595	0.010	0.25	4.0	2.3	2.6	2nd Follow Up	1.2	0.078	2.0
4	ID	DH	Low	5%	586	0.010	0.25	2.0	146.5	142.8	Never Leaks	1.1	0.066	1.7
5	ID	DH	Median	50%	590.5	0.010	0.25	3.0	16.9	17.4	2nd ISI	1.1	0.070	1.8
6	ID	DH	High	95%	595	0.010	0.25	4.0	2.1	2.3	2nd Follow Up	1.2	0.075	1.9
7	OD	UH	Low	5%	586	0.010	0.25	2.0	>80	>80	Never Leaks	-	-	-
8	OD	UH	Median	50%	590.5	0.010	0.25	3.0	>80	>80	Never Leaks	-	-	-
9	OD	UH	High	95%	595	0.010	0.25	4.0	>80	>80	Never Leaks	-	-	-
10	OD	DH	Low	5%	586	0.010	0.25	2.0	>80	>80	Never Leaks	-	-	-
11	OD	DH	Median	50%	590.5	0.010	0.25	3.0	>80	>80	Never Leaks	-	-	-
12	OD	DH	High	95%	595	0.010	0.25	4.0	>80	>80	Never Leaks	-	-	-
13	ID	UH	Low	5%	547	0.010	0.25	2.0	437.9	446.9	Never Leaks	1.1	0.069	1.7
14	ID	UH	Median	50%	554	0.010	0.25	3.0	47.5	51.6	5th ISI	1.2	0.072	1.8
15	ID	UH	High	95%	561	0.010	0.25	4.0	5.5	6.3	Leaks	1.2	0.078	2.0
16	ID	DH	Low	5%	547	0.010	0.25	2.0	415.0	404.4	Never Leaks	1.1	0.066	1.7
17	ID	DH	Median	50%	554	0.010	0.25	3.0	44.3	45.7	5th ISI	1.1	0.070	1.8
18	ID	DH	High	95%	561	0.010	0.25	4.0	5.1	5.5	Leaks	1.2	0.075	1.9
19	OD	UH	Low	5%	547	0.010	0.25	2.0	>80	>80	Never Leaks	-	-	-
20	OD	UH	Median	50%	554	0.010	0.25	3.0	>80	>80	Never Leaks	-	-	-
21	OD	UH	High	95%	561	0.010	0.25	4.0	>80	>80	Never Leaks	-	-	-
22	OD	DH	Low	5%	547	0.010	0.25	2.0	>80	>80	Never Leaks	-	-	-
23	OD	DH	Median	50%	554	0.010	0.25	3.0	>80	>80	Never Leaks	-	-	-
24	OD	DH	High	95%	561	0.010	0.25	4.0	>80	>80	Never Leaks	-	-	-

Table 5-14
Matrix of Deterministic Crack Growth Calculations for Peened RPVHPNs with Initial Flaw Depth of 0.020 in. (0.50 mm)

Case Number	Nozzle Tube Location ID/OD	Nozzle Tube Location UH/DH	Stress Profile	MRP-55 A600 CGR %ile	Temp. (°F)	Initial Depth (in.)	Initial Depth (mm)	Initial Aspect Ratio ($2c_0/a_0$)	Growth Time to 10%TW (yr)	Growth Time from 10% to Leak (yr)	Detection Time	Aspect Ratio at 10%TW ($2c/a$)	Total Length at 10%TW (in.)	Total Length at 10%TW (mm)
25	ID	UH	Low	5%	586	0.020	0.51	2.0	73.3	157.5	7th ISI	1.2	0.077	2.0
26	ID	UH	Median	50%	590.5	0.020	0.51	3.0	8.7	19.7	1st ISI	1.5	0.093	2.4
27	ID	UH	High	95%	595	0.020	0.51	4.0	1.0	2.6	1st Follow Up	1.7	0.108	2.7
28	ID	DH	Low	5%	586	0.020	0.51	2.0	67.4	142.7	7th ISI	1.2	0.075	1.9
29	ID	DH	Median	50%	590.5	0.020	0.51	3.0	7.8	17.4	1st ISI	1.5	0.091	2.3
30	ID	DH	High	95%	595	0.020	0.51	4.0	0.9	2.2	1st Follow Up	1.7	0.106	2.7
31	OD	UH	Low	5%	586	0.020	0.51	2.0	3574.2	171.0	Never Leaks	1.6	0.097	2.5
32	OD	UH	Median	50%	590.5	0.020	0.51	3.0	493.6	26.7	Never Leaks	1.7	0.108	2.7
33	OD	UH	High	95%	595	0.020	0.51	4.0	72.0	3.5	7th ISI	1.9	0.120	3.1
34	OD	DH	Low	5%	586	0.020	0.51	2.0	3512.2	185.8	Never Leaks	1.5	0.095	2.4
35	OD	DH	Median	50%	590.5	0.020	0.51	3.0	486.2	24.1	Never Leaks	1.7	0.106	2.7
36	OD	DH	High	95%	595	0.020	0.51	4.0	71.1	3.3	7th ISI	1.9	0.120	3.0
37	ID	UH	Low	5%	547	0.020	0.51	2.0	207.8	446.2	Never Leaks	1.2	0.077	2.0
38	ID	UH	Median	50%	554	0.020	0.51	3.0	22.7	51.6	2nd ISI	1.5	0.093	2.4
39	ID	UH	High	95%	561	0.020	0.51	4.0	2.5	6.3	1st Follow Up	1.7	0.108	2.7
40	ID	DH	Low	5%	547	0.020	0.51	2.0	191.1	404.1	Never Leaks	1.2	0.075	1.9
41	ID	DH	Median	50%	554	0.020	0.51	3.0	20.4	45.6	2nd ISI	1.5	0.091	2.3
42	ID	DH	High	95%	561	0.020	0.51	4.0	2.3	5.5	1st Follow Up	1.7	0.106	2.7
43	OD	UH	Low	5%	547	0.020	0.51	2.0	10125.1	484.3	Never Leaks	1.6	0.097	2.5
44	OD	UH	Median	50%	554	0.020	0.51	3.0	1293.9	70.0	Never Leaks	1.7	0.108	2.7
45	OD	UH	High	95%	561	0.020	0.51	4.0	174.9	8.5	Never Leaks	1.9	0.120	3.1
46	OD	DH	Low	5%	547	0.020	0.51	2.0	9949.7	526.3	Never Leaks	1.5	0.095	2.4
47	OD	DH	Median	50%	554	0.020	0.51	3.0	1274.5	63.1	Never Leaks	1.7	0.106	2.7
48	OD	DH	High	95%	561	0.020	0.51	4.0	172.7	7.9	Never Leaks	1.9	0.120	3.0

Table 5-15
Matrix of Deterministic Crack Growth Calculations for Peened RPVHPNs with Initial Flaw Depth of 0.062 in. (1.58 mm)

Case Number	Nozzle Tube Location ID/OD	Nozzle Tube Location UH/DH	Stress Profile	MRP-55 A600 CGR %ile	Temp. (°F)	Initial Depth (in.)	Initial Depth (mm)	Initial Aspect Ratio ($2c/a_0$)	Growth Time to 10%TW (yr)	Growth Time from 10% to Leak (yr)	Detection Time	Aspect Ratio at 10%TW ($2c/a$)	Total Length at 10%TW (in.)	Total Length at 10%TW (mm)
49	ID	UH	Low	5%	586	0.062	1.58	2.0	0.0	157.8	1st Follow Up	2.0	0.124	3.2
50	ID	UH	Median	50%	590.5	0.062	1.58	3.0	0.0	19.0	1st Follow Up	3.0	0.187	4.7
51	ID	UH	High	95%	595	0.062	1.58	4.0	0.0	2.4	1st Follow Up	4.0	0.249	6.3
52	ID	DH	Low	5%	586	0.062	1.58	2.0	0.0	142.7	1st Follow Up	2.0	0.124	3.2
53	ID	DH	Median	50%	590.5	0.062	1.58	3.0	0.0	16.8	1st Follow Up	3.0	0.187	4.7
54	ID	DH	High	95%	595	0.062	1.58	4.0	0.0	2.1	1st Follow Up	4.0	0.249	6.3
55	OD	UH	Low	5%	586	0.062	1.58	2.0	0.0	213.4	1st Follow Up	2.0	0.124	3.2
56	OD	UH	Median	50%	590.5	0.062	1.58	3.0	0.0	25.7	1st Follow Up	3.0	0.187	4.7
57	OD	UH	High	95%	595	0.062	1.58	4.0	0.0	3.2	1st Follow Up	4.0	0.249	6.3
58	OD	DH	Low	5%	586	0.062	1.58	2.0	0.0	184.2	1st Follow Up	2.0	0.124	3.2
59	OD	DH	Median	50%	590.5	0.062	1.58	3.0	0.0	23.1	1st Follow Up	3.0	0.187	4.7
60	OD	DH	High	95%	595	0.062	1.58	4.0	0.0	3.0	1st Follow Up	4.0	0.249	6.3
61	ID	UH	Low	5%	547	0.062	1.58	2.0	0.0	447.1	1st Follow Up	2.0	0.124	3.2
62	ID	UH	Median	50%	554	0.062	1.58	3.0	0.0	49.9	1st Follow Up	3.0	0.187	4.7
63	ID	UH	High	95%	561	0.062	1.58	4.0	0.0	5.8	1st Follow Up	4.0	0.249	6.3
64	ID	DH	Low	5%	547	0.062	1.58	2.0	0.0	404.4	1st Follow Up	2.0	0.124	3.2
65	ID	DH	Median	50%	554	0.062	1.58	3.0	0.0	44.1	1st Follow Up	3.0	0.187	4.7
66	ID	DH	High	95%	561	0.062	1.58	4.0	0.0	5.0	1st Follow Up	4.0	0.249	6.3
67	OD	UH	Low	5%	547	0.062	1.58	2.0	0.0	604.5	1st Follow Up	2.0	0.124	3.2
68	OD	UH	Median	50%	554	0.062	1.58	3.0	0.0	67.3	1st Follow Up	3.0	0.187	4.7
69	OD	UH	High	95%	561	0.062	1.58	4.0	0.0	7.8	1st Follow Up	4.0	0.249	6.3
70	OD	DH	Low	5%	547	0.062	1.58	2.0	0.0	521.8	1st Follow Up	2.0	0.124	3.2
71	OD	DH	Median	50%	554	0.062	1.58	3.0	0.0	60.6	1st Follow Up	3.0	0.187	4.7
72	OD	DH	High	95%	561	0.062	1.58	4.0	0.0	7.3	1st Follow Up	4.0	0.249	6.3

Table 5-16
Matrix of Deterministic Crack Growth Calculations for Unmitigated RPVHPNs with Initial Flaw Depth of 0.010 in. (0.25 mm)

Case Number	Nozzle Tube Location ID/OD	Nozzle Tube Location UH/DH	Stress Profile	MRP-55 A600 CGR %ile	Temp. (°F)	Initial Depth (in.)	Initial Depth (mm)	Initial Aspect Ratio ($2c/a_0$)	Growth Time to 10%TW (yr)	Growth Time from 10% to Leak (yr)	Detected/Leaks	Aspect Ratio at 10%TW ($2c/a$)	Total Length at 10%TW (in.)	Total Length at 10%TW (mm)
1 - NP	ID	UH	Low	5%	586	0.010	0.25	2.0	88.3	145.4	Never Leaks	2.2	0.137	3.5
2 - NP	ID	UH	Median	50%	590.5	0.010	0.25	3.0	10.1	18.1	Detected	2.3	0.140	3.6
3 - NP	ID	UH	High	95%	595	0.010	0.25	4.0	1.2	2.4	Detected	2.3	0.143	3.6
4 - NP	ID	DH	Low	5%	586	0.010	0.25	2.0	82.0	133.8	Never Leaks	2.2	0.135	3.4
5 - NP	ID	DH	Median	50%	590.5	0.010	0.25	3.0	9.1	16.3	Detected	2.2	0.138	3.5
6 - NP	ID	DH	High	95%	595	0.010	0.25	4.0	1.1	2.1	Detected	2.3	0.141	3.6
7 - NP	OD	UH	Low	5%	586	0.010	0.25	2.0	61.0	122.3	Detected	2.3	0.142	3.6
8 - NP	OD	UH	Median	50%	590.5	0.010	0.25	3.0	6.9	15.1	Detected	2.3	0.144	3.7
9 - NP	OD	UH	High	95%	595	0.010	0.25	4.0	0.8	2.0	Detected	2.4	0.147	3.7
10 - NP	OD	DH	Low	5%	586	0.010	0.25	2.0	42.8	96.2	Detected	2.3	0.145	3.7
11 - NP	OD	DH	Median	50%	590.5	0.010	0.25	3.0	5.1	12.5	Detected	2.4	0.146	3.7
12 - NP	OD	DH	High	95%	595	0.010	0.25	4.0	0.6	1.7	Detected	2.4	0.149	3.8
13 - NP	ID	UH	Low	5%	547	0.010	0.25	2.0	250.1	411.9	Never Leaks	2.2	0.137	3.5
14 - NP	ID	UH	Median	50%	554	0.010	0.25	3.0	26.4	47.5	Detected	2.3	0.140	3.6
15 - NP	ID	UH	High	95%	561	0.010	0.25	4.0	3.0	5.8	Detected	2.3	0.143	3.6
16 - NP	ID	DH	Low	5%	547	0.010	0.25	2.0	232.2	379.0	Never Leaks	2.2	0.135	3.4
17 - NP	ID	DH	Median	50%	554	0.010	0.25	3.0	23.9	42.7	Detected	2.2	0.138	3.5
18 - NP	ID	DH	High	95%	561	0.010	0.25	4.0	2.7	5.1	Detected	2.3	0.141	3.6
19 - NP	OD	UH	Low	5%	547	0.010	0.25	2.0	172.7	346.4	Never Leaks	2.3	0.142	3.6
20 - NP	OD	UH	Median	50%	554	0.010	0.25	3.0	18.0	39.7	Detected	2.3	0.144	3.7
21 - NP	OD	UH	High	95%	561	0.010	0.25	4.0	2.0	4.8	Detected	2.4	0.147	3.7
22 - NP	OD	DH	Low	5%	547	0.010	0.25	2.0	121.2	272.5	Never Leaks	2.3	0.145	3.7
23 - NP	OD	DH	Median	50%	554	0.010	0.25	3.0	13.3	32.6	Detected	2.4	0.146	3.7
24 - NP	OD	DH	High	95%	561	0.010	0.25	4.0	1.6	4.1	Leaks	2.4	0.149	3.8

Table 5-17
Matrix of Deterministic Crack Growth Calculations for Unmitigated RPVHPNs with Initial Flaw Depth of 0.020 in. (0.50 mm)

Case Number	Nozzle Tube Location ID/OD	Nozzle Tube Location UH/DH	Stress Profile	MRP-55 A600 CGR %ile	Temp. (°F)	Initial Depth (in.)	Initial Depth (mm)	Initial Aspect Ratio ($2c_0/a_0$)	Growth Time to 10%TW (yr)	Growth Time from 10% to Leak (yr)	Detected/Leaks	Aspect Ratio at 10%TW ($2c/a$)	Total Length at 10%TW (in.)	Total Length at 10%TW (mm)
25 - NP	ID	UH	Low	5%	586	0.020	0.51	2.0	59.1	145.8	Detected	2.2	0.136	3.5
26 - NP	ID	UH	Median	50%	590.5	0.020	0.51	3.0	6.4	18.0	Detected	2.3	0.145	3.7
27 - NP	ID	UH	High	95%	595	0.020	0.51	4.0	0.8	2.3	Detected	2.5	0.156	4.0
28 - NP	ID	DH	Low	5%	586	0.020	0.51	2.0	54.5	134.4	Detected	2.2	0.134	3.4
29 - NP	ID	DH	Median	50%	590.5	0.020	0.51	3.0	5.8	16.2	Detected	2.3	0.143	3.6
30 - NP	ID	DH	High	95%	595	0.020	0.51	4.0	0.7	2.1	Detected	2.5	0.154	3.9
31 - NP	OD	UH	Low	5%	586	0.020	0.51	2.0	41.1	122.4	Detected	2.3	0.141	3.6
32 - NP	OD	UH	Median	50%	590.5	0.020	0.51	3.0	4.4	15.0	Detected	2.4	0.149	3.8
33 - NP	OD	UH	High	95%	595	0.020	0.51	4.0	0.5	1.9	Detected	2.6	0.159	4.0
34 - NP	OD	DH	Low	5%	586	0.020	0.51	2.0	29.0	96.3	Detected	2.3	0.143	3.6
35 - NP	OD	DH	Median	50%	590.5	0.020	0.51	3.0	3.3	12.4	Detected	2.4	0.151	3.8
36 - NP	OD	DH	High	95%	595	0.020	0.51	4.0	0.4	1.7	Detected	2.6	0.160	4.1
37 - NP	ID	UH	Low	5%	547	0.020	0.51	2.0	167.5	413.1	Never Leaks	2.2	0.136	3.5
38 - NP	ID	UH	Median	50%	554	0.020	0.51	3.0	16.8	47.1	Detected	2.3	0.145	3.7
39 - NP	ID	UH	High	95%	561	0.020	0.51	4.0	1.8	5.7	Detected	2.5	0.156	4.0
40 - NP	ID	DH	Low	5%	547	0.020	0.51	2.0	154.5	380.7	Never Leaks	2.2	0.134	3.4
41 - NP	ID	DH	Median	50%	554	0.020	0.51	3.0	15.1	42.4	Detected	2.3	0.143	3.6
42 - NP	ID	DH	High	95%	561	0.020	0.51	4.0	1.6	5.0	Detected	2.5	0.154	3.9
43 - NP	OD	UH	Low	5%	547	0.020	0.51	2.0	116.4	346.7	Never Leaks	2.3	0.141	3.6
44 - NP	OD	UH	Median	50%	554	0.020	0.51	3.0	11.6	39.3	Detected	2.4	0.149	3.8
45 - NP	OD	UH	High	95%	561	0.020	0.51	4.0	1.3	4.7	Leaks	2.6	0.159	4.0
46 - NP	OD	DH	Low	5%	547	0.020	0.51	2.0	82.1	272.8	Never Leaks	2.3	0.143	3.6
47 - NP	OD	DH	Median	50%	554	0.020	0.51	3.0	8.6	32.6	Detected	2.4	0.151	3.8
48 - NP	OD	DH	High	95%	561	0.020	0.51	4.0	1.0	4.1	Leaks	2.6	0.160	4.1

Table 5-18
Matrix of Deterministic Crack Growth Calculations for Unmitigated RPVHPNs with Initial Flaw Depth of 0.062 in. (1.58 mm)

Case Number	Nozzle Tube Location ID/OD	Nozzle Tube Location UH/DH	Stress Profile	MRP-55 A600 CGR %ile	Temp. (°F)	Initial Depth (in.)	Initial Depth (mm)	Initial Aspect Ratio ($2c/a_0$)	Growth Time to 10%TW (yr)	Growth Time from 10% to Leak (yr)	Detected/Leaks	Aspect Ratio at 10%TW ($2c/a$)	Total Length at 10%TW (in.)	Total Length at 10%TW (mm)
49 - NP	ID	UH	Low	5%	586	0.062	1.58	2.0	0.0	148.4	Detected	2.0	0.124	3.2
50 - NP	ID	UH	Median	50%	590.5	0.062	1.58	3.0	0.0	17.1	Detected	3.0	0.187	4.7
51 - NP	ID	UH	High	95%	595	0.062	1.58	4.0	0.0	2.1	Detected	4.0	0.249	6.3
52 - NP	ID	DH	Low	5%	586	0.062	1.58	2.0	0.0	136.1	Detected	2.0	0.124	3.2
53 - NP	ID	DH	Median	50%	590.5	0.062	1.58	3.0	0.0	15.2	Detected	3.0	0.187	4.7
54 - NP	ID	DH	High	95%	595	0.062	1.58	4.0	0.0	1.8	Leaks	4.0	0.249	6.3
55 - NP	OD	UH	Low	5%	586	0.062	1.58	2.0	0.0	124.8	Detected	2.0	0.124	3.2
56 - NP	OD	UH	Median	50%	590.5	0.062	1.58	3.0	0.0	14.4	Detected	3.0	0.187	4.7
57 - NP	OD	UH	High	95%	595	0.062	1.58	4.0	0.0	1.8	Leaks	4.0	0.249	6.3
58 - NP	OD	DH	Low	5%	586	0.062	1.58	2.0	0.0	98.5	Detected	2.0	0.124	3.2
59 - NP	OD	DH	Median	50%	590.5	0.062	1.58	3.0	0.0	12.0	Detected	3.0	0.187	4.7
60 - NP	OD	DH	High	95%	595	0.062	1.58	4.0	0.0	1.5	Leaks	4.0	0.249	6.3
61 - NP	ID	UH	Low	5%	547	0.062	1.58	2.0	0.0	420.4	Detected	2.0	0.124	3.2
62 - NP	ID	UH	Median	50%	554	0.062	1.58	3.0	0.0	44.7	Detected	3.0	0.187	4.7
63 - NP	ID	UH	High	95%	561	0.062	1.58	4.0	0.0	5.1	Leaks	4.0	0.249	6.3
64 - NP	ID	DH	Low	5%	547	0.062	1.58	2.0	0.0	385.7	Detected	2.0	0.124	3.2
65 - NP	ID	DH	Median	50%	554	0.062	1.58	3.0	0.0	39.9	Detected	3.0	0.187	4.7
66 - NP	ID	DH	High	95%	561	0.062	1.58	4.0	0.0	4.5	Leaks	4.0	0.249	6.3
67 - NP	OD	UH	Low	5%	547	0.062	1.58	2.0	0.0	353.6	Detected	2.0	0.124	3.2
68 - NP	OD	UH	Median	50%	554	0.062	1.58	3.0	0.0	37.9	Detected	3.0	0.187	4.7
69 - NP	OD	UH	High	95%	561	0.062	1.58	4.0	0.0	4.3	Leaks	4.0	0.249	6.3
70 - NP	OD	DH	Low	5%	547	0.062	1.58	2.0	0.0	278.9	Detected	2.0	0.124	3.2
71 - NP	OD	DH	Median	50%	554	0.062	1.58	3.0	0.0	31.5	Detected	3.0	0.187	4.7
72 - NP	OD	DH	High	95%	561	0.062	1.58	4.0	0.0	3.8	Leaks	4.0	0.249	6.3

Table 5-19
Matrix of Deterministic Crack Growth Calculations for RPVHPNs with Modified Crack Growth Rate Material Variability Factors

Case Number	Nozzle Tube Location ID/OD	Nozzle Tube Location UH/DH	Stress Profile	MRP-55 A600 CGR %tile	Temp. (°F)	Initial Depth (in.)	Initial Depth (mm)	Initial Aspect Ratio ($2c_0/a_0$)	Growth Time to 10%TW (yr)	Growth Time from 10% to Leak (yr)	Detection Time	Aspect Ratio at 10%TW ($2c/a$)	Total Length at 10%TW (in.)	Total Length at 10%TW (mm)
15	ID	UH	High	99%	561	0.010	0.25	4.0	3.0	3.4	1st Follow Up	1.2	0.078	2.0
15	ID	UH	High	94%	561	0.010	0.25	4.0	6.0	7.0	1st ISI	1.2	0.078	2.0
18	ID	DH	High	98%	561	0.010	0.25	4.0	3.0	3.2	1st Follow Up	1.2	0.075	1.9
18	ID	DH	High	92%	561	0.010	0.25	4.0	6.2	6.8	1st ISI	1.2	0.075	1.9

5.2.4 Validation Study for the Weight Function Method Stress Intensity Factor Calculation

The weight function method for the calculation of crack stress intensity factors is detailed in appendix sections A.5 and B.5; especially section A.5.2. Like the classic influence coefficient method, this method relies on the superposition method of linear elastic fracture mechanics and a parameterized set of finite element results. However, the weight function method is more general than the influence coefficient method, allowing for the calculation of stress intensity factor in the presence of a stress profile with a general functional form (i.e., the functional form is not required to be a polynomial of some degree).

The weight function method demands substantial implementation effort and complexity, including numerical quadrature routines (or alternatively, analytical indefinite integration leading to complicated algebraic routines). To validate the weight function method implementation that is used to generate results in this report, the stress intensity factor calculation at the deepest crack point, for various crack sizes in the presence of a stress profile typical of a peened component (thickness of 69.9 mm; compressive residual stress depth of 1 mm; surface stress of -600 MPa), was performed and compared to FEA Crack [79] solutions for identical cracks in the presence of identical stress profiles. The results of this validation study are depicted in Figure 5-39.

As shown, as the crack depth gets closer to the compressive layer depth, the classical weight function method (i.e., no accounting for the balancing effects of partial crack closure) underestimates the stress intensity factor at the deepest crack point. When partial crack closure is accounted for, the largest observed relative error (as compared to the FEA solution) is 3.9% across cracks between 2.5% and 30% through-wall with aspect ratios of 2 or 40. This degree of agreement between the analytical methods and FEA results is considered adequate for the purposes of this report.

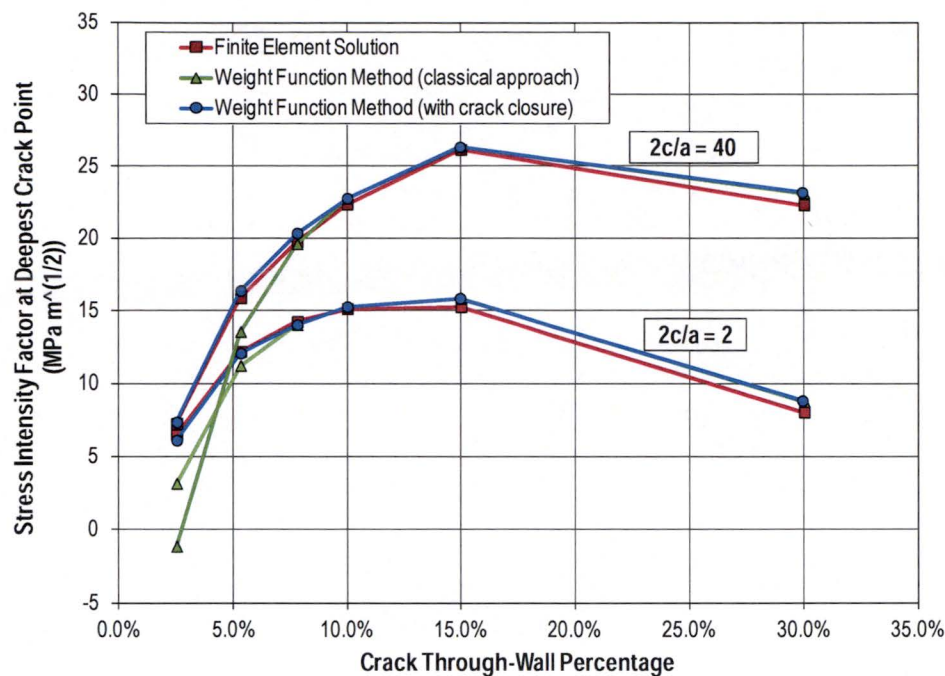


Figure 5-39
Results of Stress Intensity Factor Calculation Method Validation Study

5.3 Probabilistic Analysis of Peening Effects

The probabilistic analyses of PWSCC in DMWs and RPVHPNs are discussed in the following sections. For both component types, a unique integrated probabilistic model has been developed that is capable of accepting plant- and industry-specific inputs (distributed or deterministic), conducting lifetime analysis of PWSCC manifesting in various forms at various locations, and returning statistics to describe the risks of key failure modes (e.g., leakage and/or ejection).

The integrated probabilistic models include modules for simulating component loading and stress, PWSCC initiation, PWSCC growth, flaw examination, etc. All modules have been augmented to include special considerations for peening such that failure risks may be predicted, compared, and contrasted for unmitigated and peened components.

5.3.1 Dissimilar Metal Welds (DMWs)

The reader is directed to Appendix A for a detailed description of the DMW PWSCC integrated probabilistic model, including example analyses and results. Figure A-1 and Figure A-2 give flow diagrams to concisely describe the DMW probabilistic model.

5.3.1.1 Follow-Up and ISI Examination Intervals

Figure 5-40 provides an important example result depicting cumulative probability of leakage versus post-peening inspection schedule characteristics (i.e., the number of cycles between peening and the follow-up inspection; the in-service inspection frequency) for a hot leg DMW component (RVON). When calculating the cumulative probability of leakage after the

hypothetical time of peening, realizations in which leakage occurs prior to the time of peening are discarded and not included in the reported statistic.

For both the hot and cold DMW components, the predicted likelihood of cracks existing on a given weld after the pre-peening inspection was low; less than 3×10^{-3} for the base cases. The cumulative probability of leakage after the follow-up inspection was predicted to be lower; less than 1.6×10^{-4} per year for the base cases. This result predicted that the vast majority (>90%) of the leakage risk would be incurred between the application of peening and the follow-up inspection.

For the RVON, it was predicted that the cumulative probability of leakage after peening would be reduced by a factor between 60 and 150 (compared to cumulative probabilities of leakage on the same span of time for an unmitigated RVON), depending on the post-peening follow-up and ISI scheduling. While there is some small trend with respect to follow-up time, in general the degree of improvement was not significantly influenced by the follow-up time or the ISI frequency. The former is the result of the fact that most of the cracks that go undetected at the pre-peening inspection are small, and accordingly grow slowly after peening (see deterministic calculations that demonstrate this in Section 5.2); the latter is a result of the fact that nearly all cracks are detected during the pre-peening or follow-up inspection and no new cracks are expected to initiate after peening.

For the RVIN, it was predicted that the cumulative probability of leakage after peening would be reduced by a factor between 8 and 24 (compared to cumulative leakage probabilities on the same span of time for an unmitigated RVIN), depending on the post-peening follow-up and ISI scheduling. This degree of improvement is smaller than that predicted for the hot leg component because the inspection schedule for an unmitigated cold leg component conservatively takes little credit for its reduced temperature in comparison to that for hot-leg locations.

5.3.1.2 Modeling and Inspection Scheduling Sensitivity Cases

Modeling and inspection scheduling sensitivity cases investigated variations to key input parameters. These sensitivity cases show that conclusions drawn from the base case results are robust and not highly sensitive to the precise input values used. Specifically, sensitivity cases that examined sensitivity to the magnitude and depth of the peening stress effect (as shown in Figure 5-43 and Figure 5-44) showed only minimal risk benefit for peened DMWs with increased depth of the peening stress effect or with more compressive stresses at the peened surface. Further discussion of sensitivity case results for DMWs is included in Section A.9.3.

5.3.2 Reactor Pressure Vessel Head Penetration Nozzles (RPVHPNs)

The reader is directed to Appendix B for a detailed description of the RPVHPN PWSCC integrated probabilistic model, including example analyses and results. Figure B-2 and Figure B-3 give flow diagrams to concisely describe the RPVHPN probabilistic model.

5.3.2.1 Follow-Up and ISI Examination Intervals

Figure 5-41 provides an important example result depicting average ejection frequency (AEF) versus post-peening inspection schedule characteristics (i.e., the number of cycles between peening and the follow-up inspection; the in-service inspection frequency) for a hot reactor

vessel head. Figure 5-42 provides an important example result depicting cumulative leakage probability versus post-peening inspection schedule characteristics for a hot reactor vessel head.

The RPVHPN results demonstrated a larger trend with respect to the ISI frequency than the DMW results. This is due in large part to the higher likelihood of cracks existing after the pre-peening inspection. It was predicted that, on average, approximately two nozzles in each hot head and one nozzle in approximately two cold heads would have unrepaired cracks after the pre-peening inspection.

For both the hot and cold heads, the cumulative probability of leakage after peening was predicted to be reduced by a factor between 3.5 and 6.0 times, depending on the post-peening examination schedule. For example, using a 10-year (one interval) UT inspection frequency, the cumulative probability of leakage after peening was predicted to decrease by a factor of approximately five for both hot and cold heads. It is emphasized that the leakage probability as calculated is greatly influenced by the conservative assumptions that one third of the crack initiations occur on the wetted surface of the weld metal and that the weld flaws grow to cause leakage with no chance of becoming detectable via UT performed from the nozzle inside surface. In the probabilistic modeling, 75% to 90% or more of leaks that occur after peening occur due to weld-initiated cracks. On the contrary, plant experience shows that most CRDM nozzles leaks have been accompanied by cracking of the nozzle tube base metal detectable via UT from the nozzle inside surface. The assumptions made in the modeling conservatively increase the chance of developing circumferential cracks in the nozzle tube above the weld elevation since a 30° through-wall circumferential crack is assumed to be produced immediately upon leakage. The probability of leakage due to base metal cracking is also a more relevant measure to assess the benefit of periodic UT examinations because such examinations are not qualified to detect weld flaws.

For the hot head, using a post-peening ISI interval of 10 years (one interval), combined with a follow-up examination either one or two cycles after peening resulted in somewhat higher ejection risks compared to the unmitigated case: 182% and 147% of the unmitigated reactor vessel head risk, respectively. However, the same interval with a follow-up inspection both one and two cycles after peening resulted in an ejection risk lower than (83% of) the unmitigated case.

For the cold head, the AEF after peening was predicted to improve compared to the unmitigated case when a post-peening ISI frequency of every 10 years (one interval) was used. A post-peening ISI of one interval resulted in somewhat lower ejection risks compared to the unmitigated case: 79%, 45%, and 66% of the unmitigated risk for follow-up inspections scheduled one, two, and three cycles after peening, respectively. This result suggests that it may be beneficial to delay the follow-up inspection to the second cycle after peening to allow more significant cracks to grow such that they are more easily detected at the follow-up inspection, i.e., before entering the ISI schedule.

It is important to consider the maximum incremental frequency of ejection (IEF) for any cycle, in addition to the AEF, in order to understand how concentrated the risk may be over particular spans of time and if there are particular cycles with considerably higher risk. For instance, for a peened hot head (with a follow-up inspection the first and second cycle after peening and an ISI interval of 5 cycles), the ratio of maximum IEF to AEF was 3.12. The same ratio for the unmitigated hot head was 1.42. For a peened cold head (with a follow-up inspection two cycles

after peening and an ISI interval of 10 cycles), the ratio of maximum IEF to AEF was 4.00. The same ratio for the unmitigated cold head was 3.60. The risk concentration was not substantially worse for the peened case than for the unmitigated case. Moreover, these ratios are considered modest in absolute terms.

5.3.2.2 Modeling and Inspection Scheduling Sensitivity Cases

Modeling and inspection scheduling sensitivity cases investigated variations to key input parameters. These sensitivity cases show that conclusions drawn from the base case results are robust and not highly sensitive to the precise input values used. Specifically, sensitivity cases that examined sensitivity to the magnitude and depth of the peening stress effect (as shown in Figure 5-45 through Figure 5-48) showed minimal risk benefit for peened RPVHPNs with increased depth of the peening stress effect or with more compressive stresses at the peened surface. Sensitivity cases that model a range of bare metal visual (VE) examination frequencies indicate that performing VE examinations at an interval nominally equivalent to the examination frequency for unmitigated heads is effective in reducing the risk of nozzle ejection. Bare metal visual examinations performed more frequently than for unmitigated heads only provide a limited additional risk benefit for nozzle ejection (as shown in Figure 5-49). Further discussion of sensitivity case results for RPVHPNs is included in Section B.9.3.

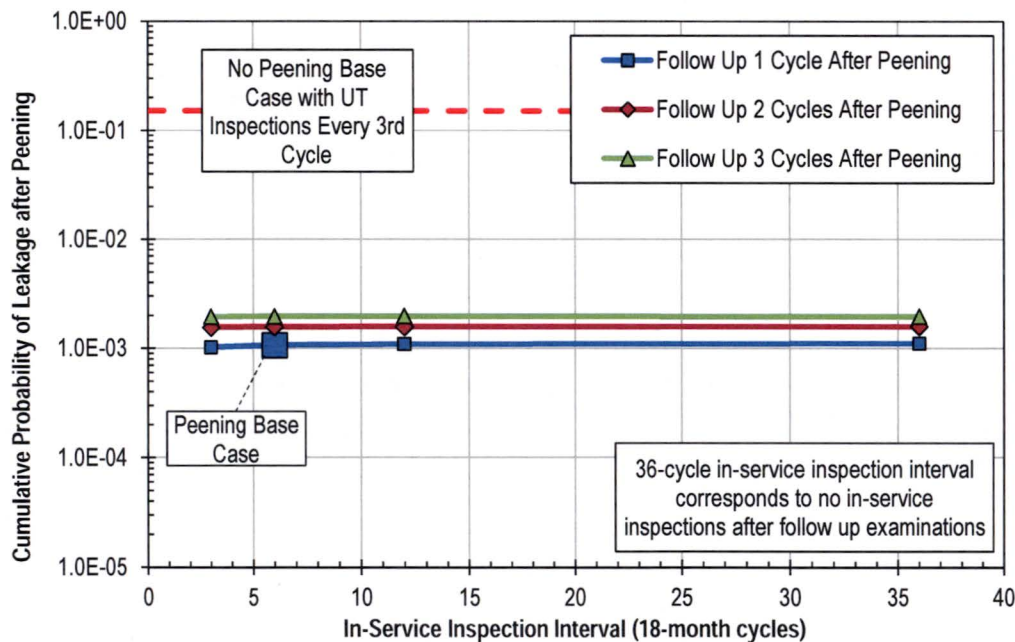


Figure 5-40
Cumulative Probability of Leakage after Hypothetical Time of Peening vs. ISI Frequency for a RVON

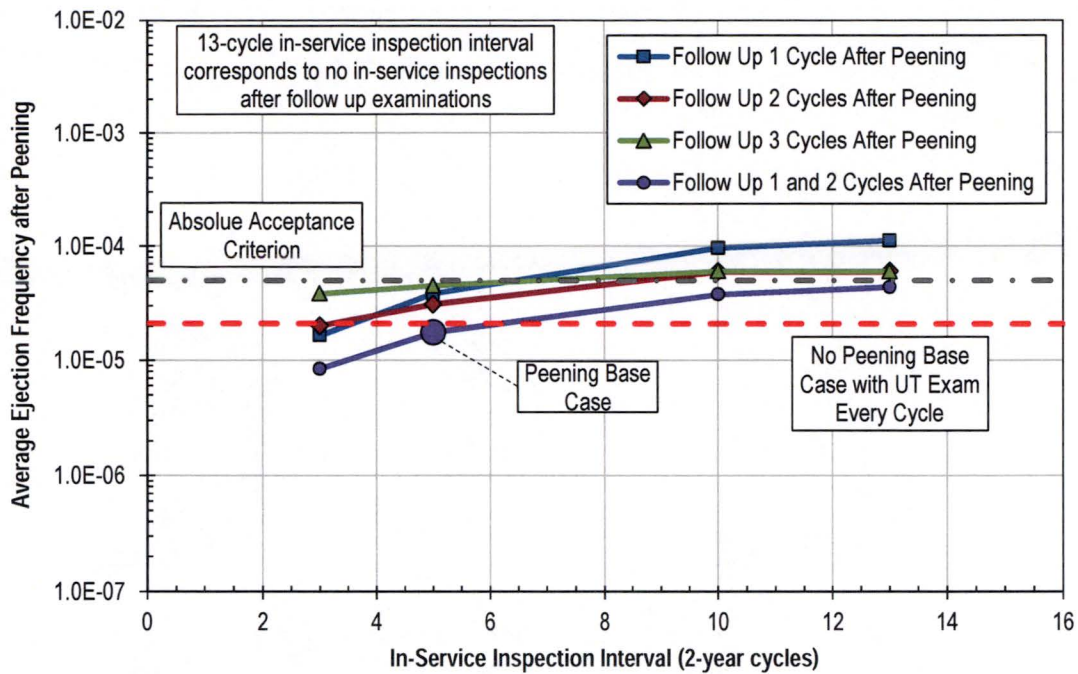


Figure 5-41
Average Ejection Frequency after Hypothetical Time of Peening vs. ISI Frequency for Hot Reactor Vessel Head

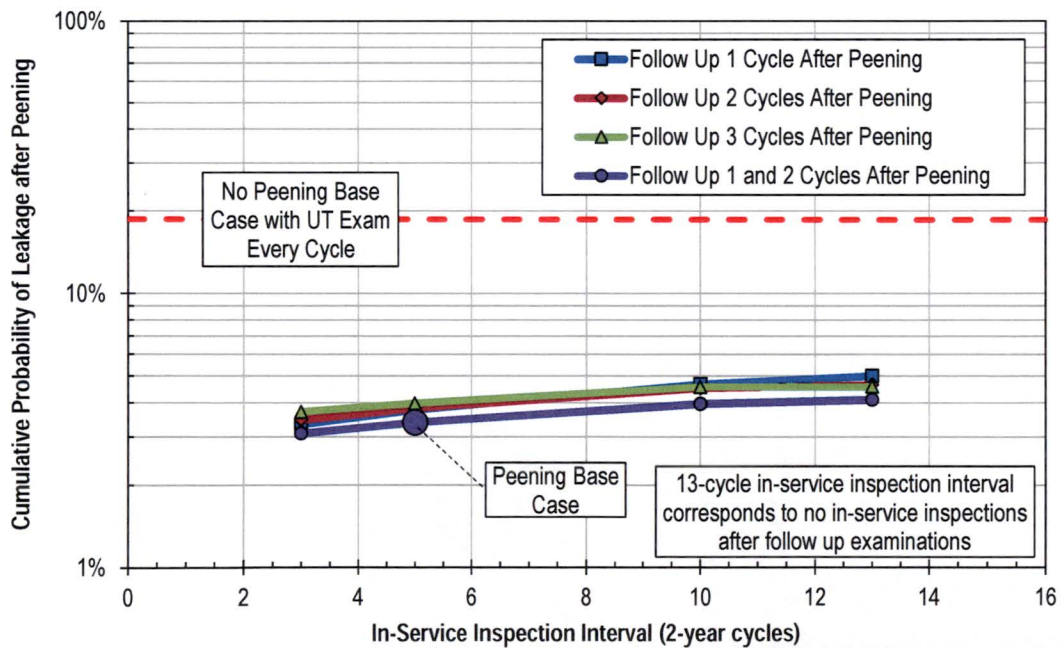


Figure 5-42
Cumulative Probability of Leakage after Hypothetical Time of Peening vs. ISI Frequency for Hot Reactor Vessel Head

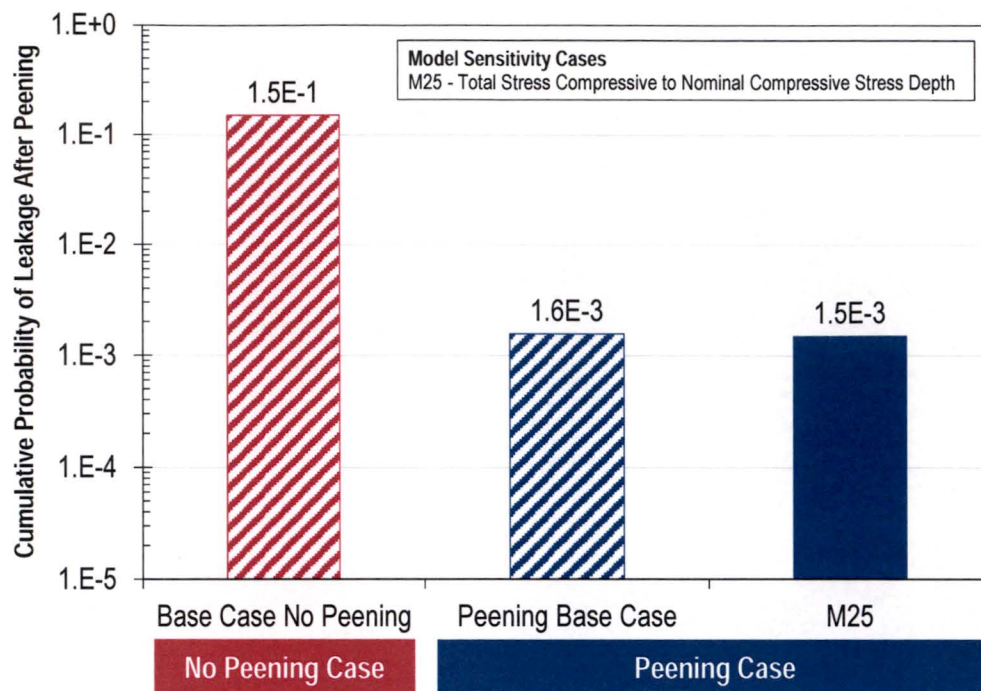


Figure 5-43
Cumulative Probability of Leakage for Stress Effect Performance Criteria Sensitivity Cases for RVON

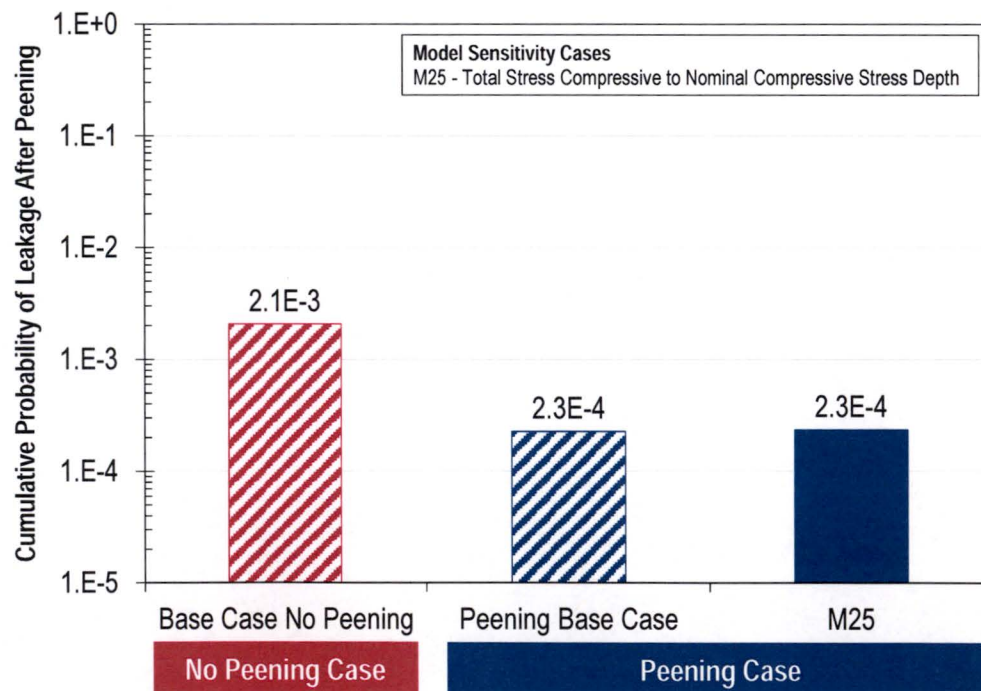


Figure 5-44
Cumulative Probability of Leakage for Stress Effect Performance Criteria Sensitivity Cases for RVIN

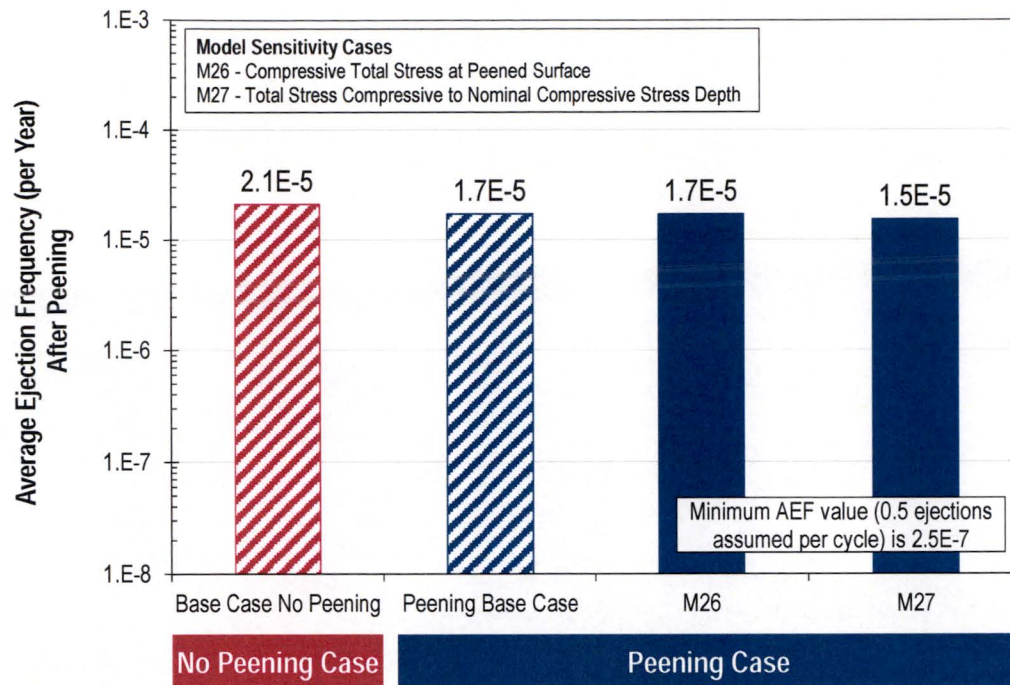


Figure 5-45
Average Ejection Frequency for Stress Effect Performance Criteria Sensitivity Cases for Hot RPVHPN

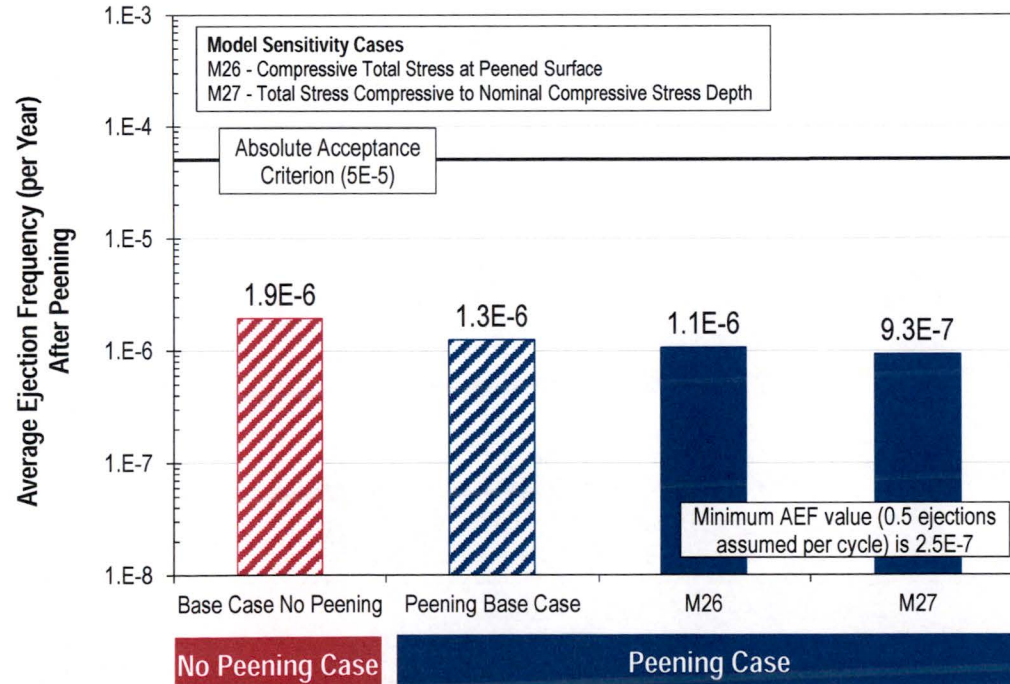


Figure 5-46
Average Ejection Frequency for Stress Effect Performance Criteria Sensitivity Cases for Cold RPVHPN

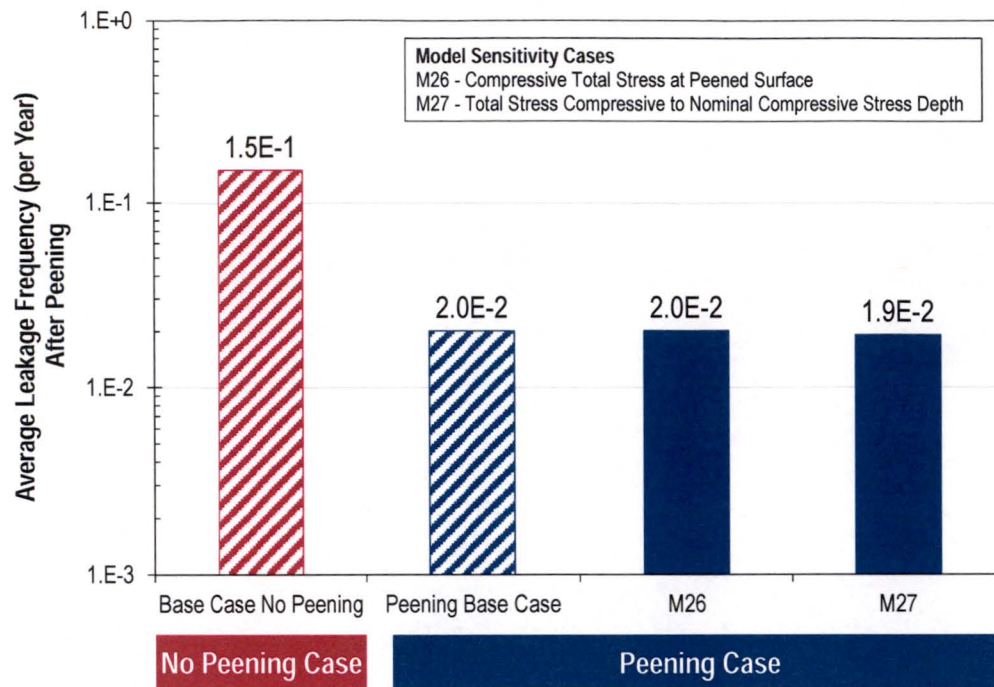


Figure 5-47
Average Leakage Frequency for Stress Effect Performance Criteria Sensitivity Cases for Hot RPVHPN

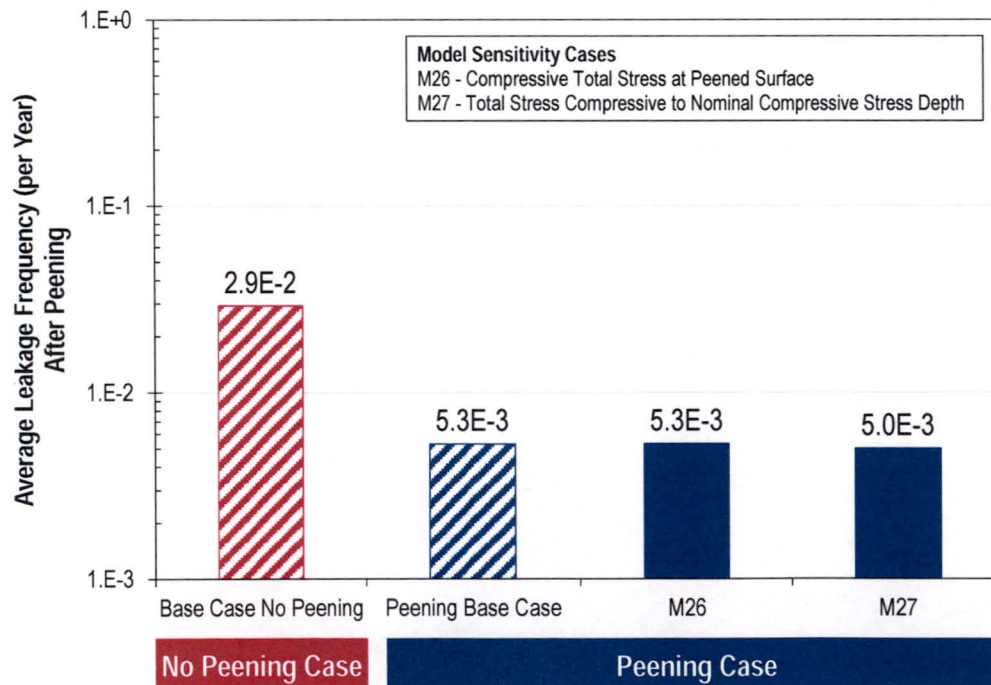


Figure 5-48
Average Leakage Frequency for Stress Effect Performance Criteria Sensitivity Cases for Cold RPVHPN

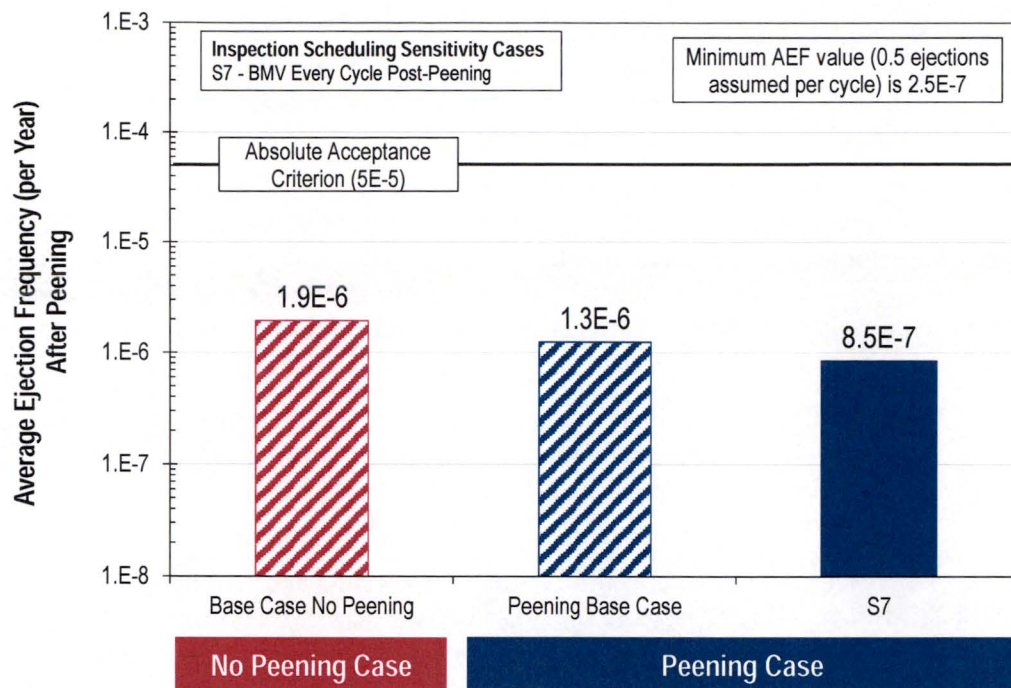


Figure 5-49
Average Ejection Frequency for VE Interval Sensitivity Case for Cold RPVHPN

5.4 Conclusions

Peening imparts a compressive residual stress layer at the surface where it is applied. The effect of this compressive residual stress layer on PWSCC has been studied using deterministic and probabilistic analyses.

The effect of peening on PWSCC of Alloy 600/82/182 components is modeled in the following key ways:

- No new PWSCC initiation is allowed to occur on a surface after peening application. Per the performance criteria of Section 4, the residual plus normal operating stress at the peened surface during future operation of the peened component is no greater than +10 ksi (+70 MPa) (tensile) for RPVHPNs and no greater than 0 ksi (0 MPa) for DMWs. These bounding stress levels are conservatively less than the tensile stress required for PWSCC initiation of an engineering scale flaw to occur over plant time scales. Laboratory testing demonstrates that a tensile stress that is at least a large fraction of the yield stress is necessary for PWSCC initiation [16]. A tensile stress of +10 ksi is clearly below the threshold.

The deterministic and probabilistic calculations of this report investigate the growth of flaws on a component where peening has the bounding stress effect meeting the performance criteria in Section 4.

- The integrated probabilistic modeling framework is used to investigate the appropriate degree of relaxation in the inspection interval following peening.

The deterministic analyses presented in this chapter investigate the effect of the surface stress improvement on PWSCC crack growth versus time. The deterministic results show that flaws significantly deeper than the reduced-stress region below the treated surface tend to grow in depth at a rate similar to that for the unmitigated case.

A set of deterministic crack growth rate calculations that apply a range of deterministic inputs demonstrate that a large fraction of cases with peening show no leakage subsequent to the extension of inspection intervals. Although a few cases do show leakage subsequent to peening, the frequency of cases with leakage is greatly reduced versus that for unpeened components inspected per the current inspection requirements. Furthermore, these deterministic results remain consistent with the probabilistic assessment.

The results predicted with the probabilistic models presented in this chapter, and detailed in Appendix A and Appendix B, support the inspection requirements listed in Section 4 for use with peened Alloy 82/182 DMWs and peened RPVHPNs in primary system piping:

- Alloy 82/182 DMWs: The results of Appendix A show that peening mitigation with assumed inspections consistent with those specified in Section 4 results in a relatively large reduction in the probability/frequency of leakage (i.e., through-wall crack penetration). The benefit shown is greater for the case of DMWs operating at reactor hot-leg temperature. The probability of leakage is an appropriate surrogate for the rupture frequency because, as is the case for leakage, relatively large flaws must be produced in order for a rupture to occur. Similarly, leakage is a necessary precursor for any concern for boric acid corrosion of the outside of the primary pressure boundary. The large reduction in leakage probability with peening (approximately between a factor of 10 and 100 for the probabilistic base cases per Section 4) supports the conclusion that rupture frequency (and boric acid wastage potential) is also reduced through the program of peening with the reduced frequency inspections specified in Section 4.
- Alloy 600 RPVHPNs: The results of Appendix B show that peening mitigation with assumed inspections consistent with those specified in Section 4 results in an average nozzle ejection frequency (roughly 1.7×10^{-5} per reactor year or less) that is well below the level resulting in a core damage frequency of 1×10^{-6} per reactor year, the criterion of NRC Regulatory Guide 1.174 [80] for permanent changes in plant equipment, etc. (see appendix Section B.7). In addition, the ratio of the maximum incremental nozzle ejection frequency to the time average nozzle ejection frequency calculated in Appendix B is of an acceptable magnitude (only a factor of 3-4). Thus, the peening mitigation in combination with the inspection requirements defined in Section 4 is concluded to result in an acceptably small effect of PWSCC on nuclear safety. Furthermore, the probabilistic results in Appendix B show a reduced average nozzle ejection frequency with peening and the inspection intervals of Section 4 compared to the case of no mitigation and inspection performed per the requirements of 10 CFR 50.55a and N-729-1. Peening reduces the nuclear safety risk. Thus, the inspection requirements developed for use with peening mitigation are acceptable from both absolute and relative risk perspectives.

Lastly, cumulative probability of nozzle leakage (after peening) is reduced by about a factor of 5 to 8 for the case of peening mitigation compared to the no mitigation case. This demonstrates that the concern for boric acid corrosion of the low-alloy steel head material is addressed by, and defense-in-depth is supported by, the required program of peening

mitigation and inspections defined in Section 4, which maintains the same basic intervals for periodic direct visual examinations for evidence of leakage as prior to peening.

Furthermore, a large number of modeling and inspection scheduling sensitivity studies show that the probabilistic model results are robust and are independent of the precise values selected for the model inputs. All sensitivity cases for peened components result in a cumulative probability of leakage substantially below that of the equivalent sensitivity case for an unmitigated component. The sensitivity results show that there would be minimal benefit to requiring a more compressive stress effect than that specified by the performance criteria in Section 4 for both DMWs and RPVHPNs.

The probabilistic modeling generally reflects a best-estimate approach with uncertainties treated using statistical distributions. However, with regard to some detailed aspects of the modeling, conservative simplifications were necessary to make the simulation tractable. The following modeling simplifications include conservatisms that tend to make the analysis results and the above conclusions conservative:

- For deterministic analyses of DMWs, circumferential flaws are assumed to be centered at the location of maximum bending tensile stress.
- For RPVHPNs, no credit is given to peening for slowing the growth of through-wall circumferential cracks along the weld contour.
- For RPVHPNs, a through-wall 30° circumferential flaw located at the top of the weld is assumed to be produced immediately upon nozzle leakage (i.e., through-wall cracking to the nozzle annulus). This assumption was maintained from the approach taken in MRP-105 [7] as part of the technical basis for the inspection requirements for unmitigated RPVHPNs in N-729-1 [2]. In most cases, circumferential cracking in the nozzle tube at or near the top of the weld has not been detected for leaking RPVHPNs [4].
- For RPVHPNs, no credit is given to peening for slowing the growth of axial through-wall cracks growing toward the OD annulus from the below the J-groove weld.
- For both DMWs and RPVHPNs in the probabilistic analysis, growth under the peening layer, which may manifest as balloon crack growth, is given full credit by neglecting peening stresses for the calculation of surface growth of cracks.
- For DMWs in the probabilistic analysis, realizations in which leakage occurs prior to the time of peening are not credited in the reported statistics. In other words, the statistics reflect cases in which leakage has not occurred by the time of peening.
- The RVON analysis cases conservatively enter the relaxed ISI schedule immediately while a second follow-up examination within 10 years is specified by the inspection requirements.
- For both the deterministic and probabilistic analyses, cracks up to 10% of the through-wall extent are assumed to have a POD of zero via UT.
- For DMWs in the probabilistic analysis, the detection of flaws by ET is not credited.

6

CONCLUSIONS

This report describes the technical bases for relaxation of inspection requirements based on the surface stress improvement provided by peening. Given that the applicable requirements outlined in Table 1-1 (including the peening performance criteria) are met, this report defines appropriate inspection requirements and intervals for Alloy 82/182 DMWs and Alloy 600 RPVHPNs that have been treated by SSI methods for the purpose of mitigating PWSCC. The deterministic and probabilistic calculations show that, given an SSI process that meets the applicable performance criteria, inspection of the peened components at the schedules specified in Table 4-1 and Table 4-3 is appropriate after SSI treatment.

The deterministic and probabilistic analyses discussed in Section 5 and Appendix A and Appendix B conservatively model the effects of peening on PWSCC. These analyses show that the peening provides large benefits in terms of preventing initiation of new PWSCC and that any cracks that could be present after pre-peening inspections and repairs are effectively addressed by inspections subsequent to peening. Section 6.1 and Section 6.2 summarize the main bases for the effectiveness of peening mitigation and for the relaxed in-service inspection requirements. Section 6.3 lists the application-specific information needed to support inspection relief.

6.1 Bases for Effectiveness of Peening

An application-specific qualification report is used to demonstrate that peening of a specific set of Alloy 82/182 DMWs or Alloy 600 RPVHPNs will be effective to mitigate PWSCC. From a general perspective, the water jet and laser peening processes described in MRP-267R1 are concluded to be effective based on the following:

- There is extensive industrial experience that shows that peening of many types is effective at inhibiting the initiation of both fatigue and stress corrosion cracks. For this reason, peening of many types is used in various industrial applications to improve resistance to these modes of cracking.
- Over 25 years of service experience with shot peening of steam generator tubes has shown that the peening provides large benefits with regard to mitigation of PWSCC of the tubes.
- As described in MRP-267R1 [10], extensive laboratory tests have been performed of samples exposed to peening processes being considered for use on DMWs and RPVHPNs. These tests, for example, have shown that these peening processes do not result in growth of any pre-existing flaws during peening.
- Extensive testing, including examination of many peened samples and test blocks, has been performed of peening processes as described in MRP-267R1 [10]. No adverse effects have been identified in this testing. Peening has been extensively used in Japanese PWRs and BWRs for 14 years with no reported adverse effects to the peened components. Additionally,

shot peening has been widely used since the mid-1980s in steam generator tubes as a PWSCC mitigation method, with no adverse effects being identified.

6.2 Bases for Appropriate Relaxation of Inspection Requirements After Peening

The inspection requirements for unmitigated Alloy 600/82/182 PWR pressure boundary components were developed by MRP ([4], [5], [6], [7], [8], [9]) to maintain an acceptably low effect on nuclear safety of the PWSCC concern. These inspection requirements also result in low probability of through-wall cracking and leakage, ensuring defense in depth. The goal of this study was to develop inspection requirements for components mitigated via peening that maintain this acceptably low effect on nuclear safety of the PWSCC concern. As shown by probabilistic analyses, the requirements of this report actually result in an increased nuclear safety margin, plus a large reduction in the probability of leakage occurring. The leakage prevention benefit of peening performed in accordance with the requirements of this report is further demonstrated through a matrix of deterministic crack growth cases.

Appropriate relaxed in-service inspection requirements for Alloy 82/182 DMWs and Alloy 600 RPVHPNs that have been mitigated by peening are shown in Table 4-1 and Table 4-3, respectively. The main bases for concluding that the defined relaxations of the in-service inspection requirements are appropriate are as follows:

- The deterministic and probabilistic analyses discussed in Section 5 and Appendix A and Appendix B show that risks of leakage and nozzle ejection are reduced for mitigated components inspected at the relaxed schedule in comparison to the risks for unmitigated components inspected at currently required schedules.
- A set of deterministic crack growth rate calculations using a range of deterministic inputs demonstrate that a large fraction of cases with peening show no leakage subsequent to the extension of inspection intervals. Although some cases do show leakage, the frequency of cases with leakage is greatly reduced versus that for unpeened components inspected per the current inspection requirements. Most of the cases that do show leakage represent very unlikely combinations of conditions resulting in crack growth rates near the upper bound of credible behavior. These deterministic results are consistent with the probabilistic assessment.
- The probabilistic analyses show reduced nuclear safety risk and reduced leakage risks with peening and the relaxed inspection schedules (as well as acceptably low risks) in comparison to unmitigated components inspected per the standard required intervals. The probabilistic analyses include significant conservatisms such that the benefits of peening tend to be under predicted. Among other conservatisms, the nominal input values for peening bases cases correspond to the bounding performance criteria for the peening residual stress effect. These conservatisms provide high confidence that the combination of SSI using peening coupled with the relaxed schedule for inspections will ensure that nuclear safety, as well as defense in depth, is maintained. In summary, peening mitigation implemented in accordance with the requirements of this topical report provides a substantial risk benefit for a risk that is already low.

- Sensitivity cases for the probabilistic assessment investigate sensitivity to modeling and input assumptions, such as the stress effect or inspection intervals for visual examinations. These sensitivity studies showed that the probabilistic model produces robust results which are independent of the precise values of the input parameters. The sensitivity results show that there would be minimal benefit to requiring a more compressive stress effect than that specified by the performance criteria in Section 4 for both DMWs and RPVHPNs.

6.3 Application-Specific Information Supporting Inspection Relief

Until NRC has generically approved inspection relief for peening within 10 CFR 50.55a (such as approval of ASME Code Cases N-729-5, N-729-6, or N-770-4), application-specific relief must be approved by NRC before implementing inspection relief for peening. Before implementing the inspection relief defined in Section 4, a relief request shall be submitted for NRC review and approval. The licensee shall provide the following technical information to support requests for inspection relief based on peening surface stress improvement meeting the applicable performance criteria:

- Identification of the components to be given surface stress improvement peening treatments, together with identification of the specific areas to be treated.
- Identification of the specific equipment and processes that will be used for each area of each component.
- Identification of any limitations in the accessibility of the treated surface for the peening equipment and process.
- Identification of the specific changes in inspection requirements that are requested based on application of surface stress improvement by peening.
- A reference to the peening process qualification report.
- Discussion of how uncertainty in the measurements of the surface residual stress subsequent to peening were addressed in the assessment of the peening stress effect.

The peening process shall be qualified and the qualification shall be documented in a qualification report. In accordance with applicable QA requirements (Section 2.1), the qualification report shall be reviewed by the licensee as part of the pre-implementation approval for peening mitigation.

The following technical information shall be included in the peening process qualification report:

- Discussion of how the specific processes that will be used have been demonstrated to be effective per the criteria discussed in this report, including surface stress magnitude, compressive residual stress depth, and sustainability of the stress effect. Included shall be a description of the demonstration testing of peening of specimens or test sections representative of the geometry, accessibility, and surface condition of the component to be peened.
- Discussion of how the specific processes that will be used have been demonstrated to result in no adverse effects.

Conclusions

- Essential variables with associated ranges of acceptable values for the specific application, plus a description of the process controls to ensure that the essential variables will be within their acceptable ranges.
- Discussion of the specific process or controls that will ensure that the coverage requirements are met with a high degree of confidence, including what overlap of peening beyond the susceptible material is required.
- Description of plans for addressing contingencies, such as equipment failure, during performance of peening.

An application- specific post-peening report shall be developed to document the performance of peening and verification that the peening effect met the applicable performance criteria. The following information shall be included in the post-peening report:

- Description of the components that were peened.
- Identification of personnel and equipment used for the peening, together with qualification information for the equipment and personnel.
- Results of the pre-peening NDE.
- Description of any repairs or other disposition of reported indications made in response to the pre-peening inspections.
- Verification that the required peening coverage was obtained and that the peening process essential variables were maintained within their acceptable ranges.
- Listing and descriptions of any problems or unusual events that occurred during the peening, and how these were handled.
- Dispositioning of any criteria that were not met as a corrective action.

6.4 Consideration for Pre-Mobilization

It may be prudent to pre-mobilize a response to a flaw detection in the pre-peening inspection, depending on industry and plant-specific experience. If there is a reasonable likelihood that shallow flaws could be present, preparations may be made to remove them if they are detected, e.g., by grinding and polishing. If there is a reasonable likelihood of flaws being present that are too deep to be removed by grinding and polishing, other mitigation measures may be considered or preparations may be made for local removal and repair of such flaws (e.g., by grinding and welding).

7

REFERENCES

1. ASME Code Case N-770-1, "Alternative Examination Requirements and Acceptance Standards for Class 1 PWR Piping and Vessel Nozzle Butt Welds Fabricated With UNS N06082 or UNS W86182 Weld Filler Material With or Without Application of Listed Mitigation Activities," Section XI, Division 1, American Society of Mechanical Engineers, New York, Approval Date: December 25, 2009.
2. ASME Code Case N-729-1, "Alternative Examination Requirements for PWR Reactor Vessel Upper Heads With Nozzles Having Pressure-Retaining Partial-Penetration Welds," Section XI, Division 1, American Society of Mechanical Engineers, New York, Approval Date: March 28, 2006.
3. ASME Code Case N-722-1, "Additional Examinations for PWR Pressure Retaining Welds in Class 1 Components Fabricated with Alloy 600/182/82 Materials," Section XI, Division 1, American Society of Mechanical Engineers, New York, Approval Date: January 26, 2009.
4. *Materials Reliability Program: Reactor Vessel Closure Head Penetration Safety Assessment for U.S. PWR Plants (MRP-110NP): Evaluations Supporting the MRP Inspection Plan*, EPRI, Palo Alto, CA: 2004. 1009807-NP. [NRC ADAMS Accession No.: ML041680506]
5. *Materials Reliability Program: Primary System Piping Butt Weld Inspection and Evaluation Guidelines (MRP-139, Revision 1)*, EPRI, Palo Alto, CA: 2008. 1015009. [Freely Available at www.epri.com]
6. *Materials Reliability Program: Inspection Plan for Reactor Vessel Closure Head Penetrations in U.S. PWR Plants (MRP-117)*, EPRI, Palo Alto, CA: 2004. 1007830. [Freely Available at www.epri.com]
7. *Materials Reliability Program: Probabilistic Fracture Mechanics Analysis of PWR Reactor Pressure Vessel Top Head Nozzle Cracking (MRP-105NP)*, EPRI, Palo Alto, CA: 2004. 1007834. [NRC ADAMS Accession No.: ML041680489]
8. *Materials Reliability Program: Alloy 82/182 Pipe Butt Weld Safety Assessment for U.S. PWR Plant Designs (MRP-113)*, EPRI, Palo Alto, CA: 2005. 1009549.
9. *Materials Reliability Program: Inspection and Evaluation Guidelines for Reactor Vessel Bottom Mounted Nozzles in U.S. PWR Plants (MRP-206)*. EPRI, Palo Alto, CA: 2009. 1016594. [Freely Available at www.epri.com]
10. *Materials Reliability Program: Technical Basis for Primary Water Stress Corrosion Cracking Mitigation by Surface Stress Improvement (MRP-267, Revision 1)*, EPRI, Palo Alto, CA: 2012. 1025839. [Freely Available at www.epri.com]
11. ASME Boiler and Pressure Vessel Code 2013, Section III, ASME, 2013.
12. ASME Boiler and Pressure Vessel Code 2013, Section XI, ASME, 2013.

References

13. Section titled "Peening," page 891, *ASM Metals Handbook*, Ninth Edition, Volume 6, "Welding, Brazing and Soldering," ASM, 1983.
14. Letter from A. Byk (ASME) to D. Weakland (Ironwood Consulting, LLC), "ASME BPVC, Section III, Division 1, NB-4422, Peening (1968 Edition through the 2011 Addenda)," 12-1192, dated August 22, 2012.
15. Letter from R. Crane (ASME) to D. Weakland (Ironwood Consulting, LLC), "ASME BPVC, Section XI, IWA-4621(c) and IWA-4651(g), 1989 Edition through the 2013 Edition," 12-1238, dated November 8, 2012.
16. *Materials Reliability Program Generic Evaluation of Examination Coverage Requirements for Reactor Pressure Vessel Head Penetration Nozzles, Revision 1 (MRP-95R1)*, EPRI, Palo Alto, CA: 2004. 1011225. [Freely Available at www.epri.com]
17. *Materials Reliability Program: An Assessment of the Control Rod Drive Mechanism (CRDM) Alloy 600 Reactor Vessel Head Penetration PWSCC Remedial Techniques (MRP-61)*, EPRI, Palo Alto, CA: 2003. 1008901. [Freely Available at www.epri.com]
18. R. Smith, "Reactor Vessel Head CRDM Nozzle Repairs with Abrasive Water Jet Remediation," AREVA presentation at *Industry – NRC 2010 Meeting on PWSCC Mitigation*, Rockville, MD, July 13, 2010. [NRC ADAMS Accession No.: ML102020677]
19. Letter from U.S. Nuclear Regulatory Commission to G. Hamrick, "Shearon Harris Nuclear Power Plant, Unit 1 -Relief Request 13R-11 For Reactor Vessel Closure Head Penetration Nozzles Repair Inservice Inspection Program -Third 10-Year Interval (TAC No. MF1876)," dated September 13, 2013. [NRC ADAMS Accession No.: ML13238A154]
20. *Materials Reliability Program: Reevaluation of Technical Basis for Inspection of Alloy 600 PWR Reactor Vessel Top Head Nozzles (MRP-395)*. EPRI, Palo Alto, CA: 2014. 3002003099. [Freely Available at www.epri.com]
21. *PWSCC of Alloy 600 Materials in PWR Primary System Penetrations*. EPRI, Palo Alto, CA: 1994. TR-103696. [Freely Available at www.epri.com]
22. D. Rudland, J. Broussard, et al., "Comparison of Welding Residual Stress Solutions for Control Rod Drive Mechanism Nozzles," *Proceedings of the ASME 2007 Pressure Vessels & Piping Division Conference: PVP2007*, San Antonio, Texas, July 2007.
23. G. Troyer, S. Fyfe, K. Schmitt, G. White, and C. Harrington, "Dissimilar Metal Weld PWSCC Initiation Model Refinement for xLPR Part I: A Survey of Alloy 82/182/132 Crack Initiation Literature," *Proceedings of the 17th International Conference on Environmental Degradation of Materials in Nuclear Power Systems – Water Reactors*, 2015.
24. C. Amzallag, S. Le Hong, C. Pages, and A. Gelpi, "Stress Corrosion Life Assessment of Alloy 600 PWR Components," *Proceedings of the 9th International Conference on Environmental Degradation of Materials in Nuclear Power Systems – Water Reactors*, 1999.
25. C. Amzallag, J. M. Boursier, C. Pages, and C. Gimond, "Stress Corrosion Life Assessment of 182 and 82 Welds Used in PWR Components," *Proceedings of the 10th International Conference on Environmental Degradation of Materials in Nuclear Power Systems – Water Reactors*, 2001.

26. F. Vaillant, J. M. Boursier, C. Amzallag, C. Bibollet, and S. Pons, "Environmental Behaviour and Weldability of Ni-Base Weld Metals in PWRs," *Proceedings of Fontevraud 6, Contribution of Materials Investigations to Improve the Safety and Performance of LWRs*, 2006.
27. E. Richey, D. S. Morton, and M. K. Schurman, "SCC Initiation Testing of Nickel-Based Alloys Using In-Situ Monitored Uniaxial Tensile Specimens," *Proceedings of the 12th International Conference on Environmental Degradation of Materials in Nuclear Power Systems – Water Reactors*, 2005.
28. S. Le Hong, "Influence of Surface Condition on Primary Water Stress Corrosion Cracking Initiation of Alloy 600," *Corrosion*, Vol. 57, No. 4, pp. 323-333, 2001.
29. C. Benhamou and C. Amzallag, "Prediction of Stress Corrosion Initiation Time of Alloy 600 PWR Components," *Proceedings of the 14th International Conference on Environmental Degradation of Materials in Nuclear Power Systems – Water Reactors*, 2009.
30. *Materials Handbook for Nuclear Plant Pressure Boundary Applications (2010)*. EPRI, Palo Alto, CA: 2010. 1022344.
31. T. Couvant, M. Wehbi, C. Duhamel, and J. Crepin, "Initiation of PWSCC of Weld Alloy 182," *Proceedings of the 16th International Conference on Environmental Degradation of Materials in Nuclear Power Systems*, 2013.
32. T. Yonezawa, K. Onimura, H. Itoh, I. Saito, H. Takamatsu, and T. Fujitani, "Effect of Cold Working and Applied Stress on the Stress Corrosion Cracking Resistance of Nickel-Chromium-Iron Alloys," *Proceedings: 1991 EPRI Workshop on PWSCC of Alloy 600 in PWRs*, 1991.
33. K. Sakima, T. Maeguchi, K. Sato, K. Fujimoto, Y. Nagoshi, and M. Nakano, "An Update on Alloys 690/52/152 PWSCC Initiation Testing," *Proceedings of the 17th International Conference on Environmental Degradation of Materials in Nuclear Power Systems*, 2015.
34. H. Itoh, Y. Kutomi, M. Mukai, and K. Sakai, "Long Term PWSCC Susceptibility of Alloy 600 in Constant Load Testing," *Proceedings of ICON 5: 5th International Conference on Nuclear Engineering*, 1997.
35. T. Maeguchi, K. Fujimoto, I. Hongo, M. Nishimura, and S. Hirano, "PWSCC Long-Term Reliability of Alloy 690 and Its Weld Metals," *Alloy 690/52/152 Primary Water Stress Corrosion Cracking Research Collaboration Meeting*, 2011.
36. "Inconel Alloy 600," Publication SMC-027, ©Special Metals Corporation, 2008.
37. C. Amzallag, et al., "Stress Corrosion Life Assessment of Alloy 600 PWR Components," *Ninth International Symposium on Environmental Degradation of Materials in Nuclear Power Systems – Water Reactors*, Edited by F.P. Ford et al., The Minerals, Metals & Materials Society (TMS), 1999.
38. "Product Handbook," Publication No. IAI-38, © Inco Alloys International, Inc., 1988.
39. H. Itoh, E. Otsuka, T. Yonezawa, and K. Sakai, "Effect of Pipe Making Process on SCC Resistance of Alloy 600," *Proceedings: 1994 EPRI Workshop on PWSCC of Alloy 600 in PWRs*. TR-105406.

References

40. Topical Report CE NPSD-1085, "CEOG Response to NRC Generic Letter 97-01: 'Degradation of CEDM Nozzle and Other Vessel Closure Head Penetrations,'" Combustion Engineering Owners Group, July 1997. Nonproprietary Report.
41. "Millstone Nuclear Power Station, Unit No. 3: Response to Generic Letter 97-01," Letter from M. H. Brothers to U.S. NRC, B16601, July 28, 1997.
42. "Vogtle Electric Generating Plant – Response to Generic Letter 97-01 Degradation of Control Rod Drive Mechanism Nozzle and other Vessel Closure Head Penetrations," Letter from C. K. McCoy to U.S. NRC, LCV-1015-A, July 24, 1997.
43. "Sequoyah Nuclear Plant (SQN), Watts Bar Nuclear Plant (WBN), and Bellefonte Nuclear Plant (BLN) 120-Day Response to NRC Generic Letter (GL) 97-01, "Degradation of Control Rod Drive Mechanism (CRDM) Nozzle and other Vessel Closure Head Penetrations (VHP)," Dated April 1, 1997," Letter from M. J. Burzynski to U.S. NRC, July 30, 1997.
44. *Materials Reliability Program Crack Growth Rates for Evaluating Primary Water Stress Corrosion Cracking (PWSCC) of Alloy 82, 182, and 132 Welds (MRP-115)*, EPRI, Palo Alto, CA: 2004. 1006696. [Freely Available at www.epri.com]
45. "Comanche Peak Steam Electric Station (CPSES) Docket Nos. 50-445 and 50-446, Response to Generic Letter 97-01, 'Degradation of Control Rod Drive Mechanism Nozzle and other Vessel Closure Head Penetrations,'" Letter from C. L. Terry to U.S. NRC, Log #TXX-97163, July 29, 1997.
46. Section titled "X-Ray Diffraction Residual Stress Measurement in Failure Analysis," page 484–497, *ASM Handbook*, Volume 11, "Failure Analysis and Prevention," ASM, 2002.
47. J.A. Pineault, M.E. Brauss, and J.S. Eckersley, "Residual Stress Characterization of Welds Using X-Ray Diffraction Techniques," *Welding Mechanics and Design*, American Welding Society, 1996.
48. M. Belassel, M.E. Brauss, and J.A. Pineault, "Residual Stress Characterization Using X-ray Diffraction Techniques, Applications on Welds," *Proceedings 2001 ASME PV&P Conference*, PVP-Vol. 429, 2001.
49. L. Zhang, Y.K. Zhang, et al., "Effects of Laser Shock Processing on Electrochemical Corrosion Resistance of ANSI 304 Stainless Steel Weldments after Cavitation Erosion," *Corrosion Science*, vol. 66, pp. 5–13, January 2013.
50. J. J. Wall, K. J. Krzywosz, et al., "Residual Stress Measurement in Alloy 182," *Proceedings of the Seventh International Conference on NDE in Relation to Structural Integrity for Nuclear and Pressurised Components. 12-14 May 2009 - Yokohama, Japan*, Publications Office of the European Union, 2009.
51. A. Joseph, S. K. Rai, T. Jayakumar, and N. Murugan, "Evaluation of Residual Stresses in Dissimilar Weld Joints," *International Journal of Pressure Vessels and Piping*, vol. 82, no. 9, pp. 700–705, September 2005.
52. *Materials Reliability Program: Development of Probability of Detection Curves for Ultrasonic Examination of Dissimilar Metal Welds (MRP-262, Revision 1) – Typical PWR Leak-Before-Break Line Locations*, EPRI, Palo Alto, CA: 2009. 1020451. [Freely Available at www.epri.com]

53. *Visual Examination for Leakage of PWR Reactor Head Penetrations: Revision 2 of 1006296, Includes 2002 Inspection Results and MRP Inspection Guidance*, EPRI, Palo Alto, CA: 2003. 1007842. [freely available on www.epri.com]
54. *Materials Reliability Program: Boric Acid Corrosion Guidebook, Revision 2: Managing Boric Acid Corrosion Issues at PWR Power Stations (MRP-058, Rev 2)*, EPRI, Palo Alto, CA: 2012. 1025145.
55. G. White, R. Jones, J. Gorman, C. Marks, J. Collin, and R. Reid, "Revision 2 of the EPRI Boric Acid Corrosion Guidebook," *16th International Conference on Environmental Degradation of Materials in Nuclear Power Systems—Water Reactors*, 2013.
56. R. Jones and G. White, "Boric Acid Corrosion: Revision to BAC Guidebook," Presented at NRC Public Meeting, February 29, 2012. [NRC ADAMS Accession No. ML120690185]
57. *Materials Reliability Program: Boric Acid Corrosion Testing: Implications and Assessment of Test Results (MRP-308)*, EPRI, Palo Alto, CA: 2011. 1022853. [freely available on www.epri.com]
58. R. Jones and G. White, "Boric Acid Corrosion: Implications Assessment of BAC Test Programs," Presented at NRC Public Meeting, February 29, 2012. [NRC ADAMS Accession No. ML120690182]
59. R. Reid, "Boric Acid Corrosion Testing Program Overview," Presented at NRC Public Meeting, February 29, 2012. [NRC ADAMS Accession No. ML120690174]
60. W. Sims, "Boric Acid Corrosion Testing Program: Industry Perspective," Presented at NRC Public Meeting, February 29, 2012. [NRC ADAMS Accession No. ML120690171]
61. S. Stuchell, "Summary of April 23, 2013, Public Meeting Regarding Volumetric Examination of Bottom Mounted J-Groove Welded Nozzles," Memorandum to A. Mendiola et al., May 9, 2013. [NRC ADAMS Accession No. ML13119A207]
62. *Materials Reliability Program (MRP) Crack Growth Rates for Evaluating Primary Water Stress Corrosion Cracking (PWSCC) of Thick-Wall Alloy 600 Materials (MRP-55) Revision 1*, EPRI, Palo Alto, CA: 2002. 1006695. [Freely Available at www.epri.com]
63. Section titled "Shot Peening," page 131, *ASM Handbook*, Volume 5, "Surface Engineering," ASM, 1994.
64. Letter from B. C. Rudell (Exelon) and A. Demma (EPRI) to U.S. NRC, "Response to the NRC Request for Additional Information (RAI) related to Electric Power Research Institute (EPRI) MRP-335, Revision 1, "Topical Report for Primary Water Stress Corrosion Cracking Mitigation by Surface Stress Improvement [Peening]" (TAC No. MF2429)," MRP 2014-027, dated October 10, 2014. [NRC ADAMS Accession No.: ML14288A370]
65. *Materials Reliability Program: Prediction of Relaxation of Peening Residual Stresses in Alloy 600 (MRP-397)*. EPRI, Palo Alto, CA: 2014. 3002003955. [Freely available at www.epri.com]
66. *Pressurized Water Reactor Materials Reliability Program: Effects of Surface Peening on the Inspectability of Nondestructive Evaluation*, EPRI, Palo Alto, CA: 2016. 3002008359. [Freely Available at www.epri.com]

References

67. *Evaluation of the Effect of Cavitation Peening on Ultrasonic Examination of Reactor Head Penetration Nozzles*, AREVA, Document No.: 51-9251566-000, dated February 29, 2016. Proprietary to AREVA Inc.
68. 10 CFR 50.34, *Contents of Applications; Technical Information*, dated December 31, 2015.
69. 10 CFR 50 Appendix B, *Quality Assurance Criteria for Nuclear Power Plants and Fuel Reprocessing Plants*, dated December 2, 2015.
70. NQA-1-1994, *Quality Assurance Requirements for Nuclear Facility Applications*, American Society of Mechanical Engineers, dated July 29, 1994.
71. Letter from J. Heffley to U.S. Nuclear Regulatory Commission, "Calvert Cliffs Nuclear Power Plant Unit Nos. I & 2; Docket Nos. 50-317 & 50-318, Nine Mile Point Nuclear Station Unit Nos. 1 & 2; Docket Nos. 50-220 & 50-410, R.E. Ginna Nuclear Power Plant Docket No. 50-244, Request for Approval of a Common Quality Assurance Program for Constellation Generation Group. LLC," dated December 5, 2005. [NRC ADAMS Accession No.: ML053470094]
72. Letter from M. Sartain to U.S. Nuclear Regulatory Commission, "Dominion Energy Kewaunee, Inc., Dominion Nuclear Connecticut, Inc., Virginia Electric and Power Company., Kewaunee Power Station and ISFSI, Millstone Power Station Units 1, 2 & 3 and ISFSI, North Anna Power Station Units 1 & 2 and ISFSI, Surry Power Station Units 1 & 2 and ISFSI, Submission of Revisions 17, 18, and 19 of the Quality Assurance Topical Report," dated June 23, 2015. [NRC ADAMS Accession No.: ML15204A605]
73. Letter from M. Gallagher to U.S. Nuclear Regulatory Commission, "Request for Approval of Quality Assurance Program Changes for Exelon Generation Company, LLC, and AmerGen Energy Company, LLC, Nuclear Power Plants," dated April 9, 2002. [NRC ADAMS Accession No.: ML021070541]
74. Letter from J. Stall to U.S. Nuclear Regulatory Commission, "Florida Power and Light Company St. Lucie Units 1 and 2 Docket Nos. 50-335 and 50-389, Turkey Point Units 3 and 4 Docket Nos. 50-250 and 50-251, FPL Energy Seabrook, LLC Seabrook Station Docket No. 50-443. FPL Energy Duane Arnold, LLC Duane Arnold Energy Center Docket No. 50-331, Request for Approval of FPL Quality Assurance Topical Report," dated March 31, 2006. [NRC ADAMS Accession No.: ML060950329]
75. Letter from C. Pierce to U.S. Nuclear Regulatory Commission, "Joseph M. Farley Nuclear Plant; Edwin I. Hatch Nuclear Plant; Vogtle Electric Generating Plant Quality Assurance Topical Report," dated November 21, 2013. [NRC ADAMS Accession No.: ML13325B080]
76. *Materials Reliability Program: Reactor Vessel Head Nozzle and Weld Safety Assessment (MRP-103NP)*, EPRI, Palo Alto, CA: 2004. 1009402. [NRC ADAMS Accession No.: ML041680477]
77. *Materials Reliability Program: RV Head Nozzle and Weld Safety Assessment for Westinghouse and Combustion Engineering Plants (MRP-104NP)*, EPRI, Palo Alto, CA: 2004. 1009403. [NRC ADAMS Accession No.: ML041680483]

78. *Materials Reliability Program: Technical Basis for Reexamination Interval Extension for Alloy 690 PWR Reactor Vessel Top Head Penetration Nozzles (MRP-375)*. EPRI, Palo Alto, CA: 2014. 3002002441. [Freely Available at www.epri.com]
79. *3-D Finite Element Software for Cracks: User's Manual v2.7*. Structural Reliability Technology – FEA Crack.
80. U.S. NRC, Regulatory Guide 1.174, “An Approach for Using Probabilistic Risk Assessment in Risk-Informed Decisions on Plant-Specific Changes to the Licensing Basis,” Revision 2, May 2011.

A

PROBABILISTIC ASSESSMENT CASES FOR ALLOY 82/182 DISSIMILAR METAL WELDS IN PRIMARY SYSTEM PIPING

A.1 Scope of Assessment

The probabilistic modeling presented in this appendix explicitly considers two example large-diameter Alloy 82/182 dissimilar metal welds in PWR primary system piping: a reactor vessel outlet nozzle operating at reactor hot-leg temperature and a reactor vessel inlet nozzle operating at reactor cold-leg temperature. The reactor vessel outlet and inlet nozzles are considered to be the main candidates for peening where access limitations may preclude other types of mitigation from the exterior (i.e., mechanical stress improvement and weld overlay). However, considering the range of sensitivity cases included (including the effect of variability in pipe loads), it is concluded that the examination requirements of Section 4 are also valid for other Alloy 82/182 piping butt weld locations, including large-diameter reactor coolant pump suction and discharge nozzles in B&W- and CE-designed plants, reactor vessel safety injection nozzles in two-loop Westinghouse-designed plants, and reactor vessel core flood nozzles in B&W-designed plants. These other cited locations operate at or below reactor cold-leg temperature. The calculations presented in this appendix showed large improvement in the leakage probability versus the case without peening and with inspections performed per intervals applicable to unmitigated welds.

A.2 Probabilistic Modeling Methodology

The integrated probabilistic modeling framework that is used to study the effect of peening DMW components on PWSCC combines the individual models discussed in Sections A.3 through A.6. Namely, this integrated probabilistic modeling framework is used to predict leakage criterion statistics, which are discussed in Section A.7, over the operating lifetime of the unit. Results generated with this model are given in Section A.9, using the inputs and uncertainties discussed in Section A.8.

The DMW probabilistic model described in this appendix applies a framework similar to those applied in MRP-373 [2] to assess depth-sizing uncertainty of flaws in large-diameter piping welds and by the xLPR probabilistic software tool ([4], [5]), which is currently under development under sponsorship of NRC and EPRI. The approach taken for the DMW probabilistic model is also similar in form to other models applied over the last 12 years to assess PWSCC of RPVHPNs in MRP-105 [1] and MRP-395 [3] or of BMNs in the analyses summarized in MRP-206 [6]. For example:

- Uncertainty propagation is handled by sampling input and parameter values from appropriately selected probability distributions (with appropriately selected bounds) in the main model loop, prior to the time looping structure. It is noted that for simplicity the model

discussed in this report does not treat differently epistemic (i.e., due to incomplete knowledge) and aleatory (i.e., due to random variation) uncertainties.

- Event scheduling for a given weld, including operating, mitigation, inspection, and PWSCC initiation times, is developed in the main loop prior to entering the time looping structure.
- If one or more of the predicted PWSCC initiation times, adjusted for differences in stress and temperature, are less than the final operating time and the peening time (if applied), the time looping structure is entered. Each active flaw is allowed to grow until it coalescences with another active flaw, it achieves through-wall crack growth, it is detected and repaired, or it reaches the end of the operation partially through-wall.
- Initiations, leaks, repairs, among other events, are tracked as a function of operating cycle for each Monte Carlo realization and summary statistics are compiled at the end of each Monte Carlo run.

It is noted that there are several key differences between the DMW probabilistic model and xLPR Version 2.0:

- The DMW model described in this report takes a simplified approach of modeling through-wall penetration but not pressure boundary rupture. Growth after through-wall penetration, crack opening displacement and leak rate, and component stability are not explicitly modeled. However, by demonstrating a greatly reduced probability of through-wall penetration, the results demonstrate a reduced risk of large flaws that could compromise structural integrity.
- As the cracking degradation concern in Alloy 82/182 piping butt welds is dominated by PWSCC initiation and growth, fatigue initiation and growth are not modeled in the DMW model described in this report. xLPR Version 2.0 predictions are expected to confirm the marginal effect of fatigue on leakage risks in piping butt weld components.
- xLPR Version 2.0 includes treatment for accident conditions, such as seismic loading. These accident conditions are of interest in xLPR primarily for their contribution to stability risks. As stated above, the DMW probabilistic model presented in this report does not consider stability risks explicitly and therefore modeling of accident loads is not critical.
- PWSCC initiation modeling is similar between both probabilistic models. Both utilize semi-empirical model forms with key coefficients calibrated with field data for PWSCC detections in butt weld components in domestic plants. Both utilize circumferential discretization in order to model multiple flaw formation. However, in addition to the Weibull initiation model, the xLPR Version 2.0 model includes two additional initiation model forms. Furthermore, the xLPR initiation model factors in temporal variation using a Miner's rule approximation for damage accumulation. This approach enables the treatment of changing surface stresses or temperature. The DMW probabilistic model described in this report treats only one key temporal change—the change in surface stresses at the time of peening—but otherwise does not treat temporal variation. Studies with temporal variation were not of importance for this report.
- The probabilistic model discussed in this report utilizes the weld residual stress profile model form from the xLPR Pilot Study—third or fourth order polynomials fit to a set of constraints on the value of stresses at various through-wall positions. In xLPR Version 2.0, the weld

residual stress profile progressed to a piecewise linear model with stress defined at up to 26 points through the component thickness. While the xLPR Version 2.0 model affords more flexibility in the definition of weld residual stress, the primary characteristics of the weld residual stress (i.e., ID surface stress, OD surface stress, tensile-compressive crossover point, and force balance in the case of axial stresses) are well captured in the DMW model.

- The DMW model described in this report includes more detail for modeling peening stress profiles. This includes explicit definition of the peening stress profile with surface compressive stress and penetration characteristics, treatment of stress redistribution, and implementation of a partial crack closure methodology. xLPR Version 2.0 allows the specification of a surface stress component with the capability to mimic the effect of peening on PWSCC initiation, but stress profiles have not been developed within xLPR to mimic the penetration of the peening stress effect into the component thickness.
- The probabilistic model discussed in this report has the added capability (relative to the xLPR tool) of allowing correlation of selected input parameters during runtime. Specifically, multi-dimensional normal deviates are computed using a covariance matrix Cholesky-decomposition-based approach as discussed in *Numerical Recipes* [7]. For a given pair of correlated input parameters, a Pearson product-moment correlation coefficient, which provides a measure of the strength of the linear relationship between two variables, is specified and the pair of correlated random deviates is then used to sample the relevant input parameter distributions. The Pearson coefficient provides a measure of the strength of the linear relationship between two variables where a value of 1 indicates a perfect positive correlation (i.e., a perfect linear correlation with a positive slope), a value of -1 indicates a perfect negative correlation (i.e., a perfect linear correlation with a negative slope), and a value of 0 indicates that there is no linear relationship between the given variables.
- It is noted that for convenience of analysis, the probabilistic model described in this report has been designed to simulate up to three distinct DMWs (i.e., welds with different geometries, temperatures, inspection and mitigation schedules, etc.) during a single Monte Carlo run.

The probabilistic model is made up of a main loop with an internal time looping structure. Inside the time looping structure, a flaw looping structures are included to account for multiple flaws and their potential interaction. A high level presentation of the main loop of the probabilistic model for a given weld is presented in Figure A-1 and a more detailed presentation of the time looping structure is given in Figure A-2. The remainder of this section provides an end-to-end description of a DMW Monte Carlo run.

The initial conditions for the run are defined prior to entering the main loop. These initial conditions include all input parameters that remain constant throughout the run, such as the number and length of operating cycles, the frequency of inspections, certain weld geometry attributes, and the times of mitigation.

Following the definition of the initial conditions the main loop is entered. The main loop is cycled for each Monte Carlo realization and is exited once all of the user-specified Monte Carlo realizations have been completed. After exiting the main loop, the program evaluates the results of the run, outputs certain information relevant to the study, and terminates the run.

At the beginning of each Monte Carlo realization, the values of the distributed inputs (detailed in Section A.8) are determined by random sampling. The distributions for each of the distributed inputs are user-defined. The program then calls the load models (detailed in Section A.3) to determine the relevant circumferential or axial loads (including peening loads if peening is scheduled before the end of the plant operational period).

Once all stresses have been determined from the load model, the program invokes the initiation model (detailed in Section A.4) to predict the initiation times at all potential flaw sites. The flaw initiation times are compared to the "initiation end time": the final operating time or, if peening is scheduled, the peening application time. It is assumed that flaws may not initiate on the component surface after the application of peening. The current Monte Carlo realization is terminated if all of the predicted initiation times exceed the "initiation end time". If not, the initiation model assigns initiation conditions to each flaw with an initiation time occurring before the "initiation end time." These flaws are "scheduled to initiate". Subsequently, the Monte Carlo realization enters the time looping structure.

The time looping structure is composed of an outer cycle-by-cycle loop with a nested within-cycle loop. The cycle-by-cycle loop may be terminated if all flaws that have been "scheduled to initiate" have been repaired. If this occurs, the program exits the time loop structure, stores relevant information, and cycles to the next Monte Carlo realization.

The within-cycle loop is entered if there is an active flaw whose initiation time is less than the time of the end of the current operating cycle. Immediately prior to entering the within-cycle loop, any peening application that is scheduled for the current cycle is invoked resulting in new stress profiles utilized to predict crack growth.

If no flaw initiations occur prior to the end of the current sub-step in the within-cycle loop, the sub-step is skipped. Otherwise, at the beginning of each sub-step, the stress intensity factor for each active flaw is calculated based on the geometry of the flaw and the stress profile at the beginning of the sub-step. During each sub-step, all active flaws are grown using the flaw propagation model (detailed in Section A.5) that determines the flaw propagation rate and increases the depth and length of the flaw at a constant rate for the duration of the sub-step.

Before completing a given sub-step, the program checks if any flaw has reached through-wall, and if so, the cycle number is stored for a statistical summary generated at the end of Monte Carlo run. The exception to this is if a flaw achieves through-wall crack growth before a user-defined past inspection time for which it is assumed that no flaws have leaked or been detected (i.e., credit is taken for the fact that the modeled DM weld has not leaked or had detected cracks up to a user defined time); in this case, the Monte Carlo realization is restarted with newly sampled values. For DM welds, when through-wall growth occurs (and its timing does not contradict the results of the assumed past inspection), the current realization is terminated and the program returns to the start of the main loop (contrary to RPVHPNs whose simulation continues to check for nozzle ejection).

At the end of each sub-step, if multiple flaws are active, the coalescence model (detailed in Section A.5.4) is used to consolidate circumferential flaws that are determined to be close enough to coalesce.

When all sub-steps during a given cycle have been completed, the program determines if an ultrasonic examination (UT) is to be performed at the end of the current cycle. If so, the UT

inspection models (detailed in Section A.6) are called appropriately. If a flaw is detected, and its detection time does not contradict the results of the assumed past inspection, the flaw is repaired and the cycle number is stored for a statistical summary generated at the end of the Monte Carlo simulation; the examination continues to any other active flaws. In a similar fashion to a through-wall occurrence, if any flaw detection result contradicts the results of the assumed past inspection, the code exits the time looping structure without saving any results and restarts the current Monte Carlo realization from the beginning of the main loop. If a flaw is not detected, it remains active. After all scheduled inspections, the code returns to the cycle-by-cycle loop and continues to the next cycle or returns to the main loop if the cycle-by-cycle loop is complete.

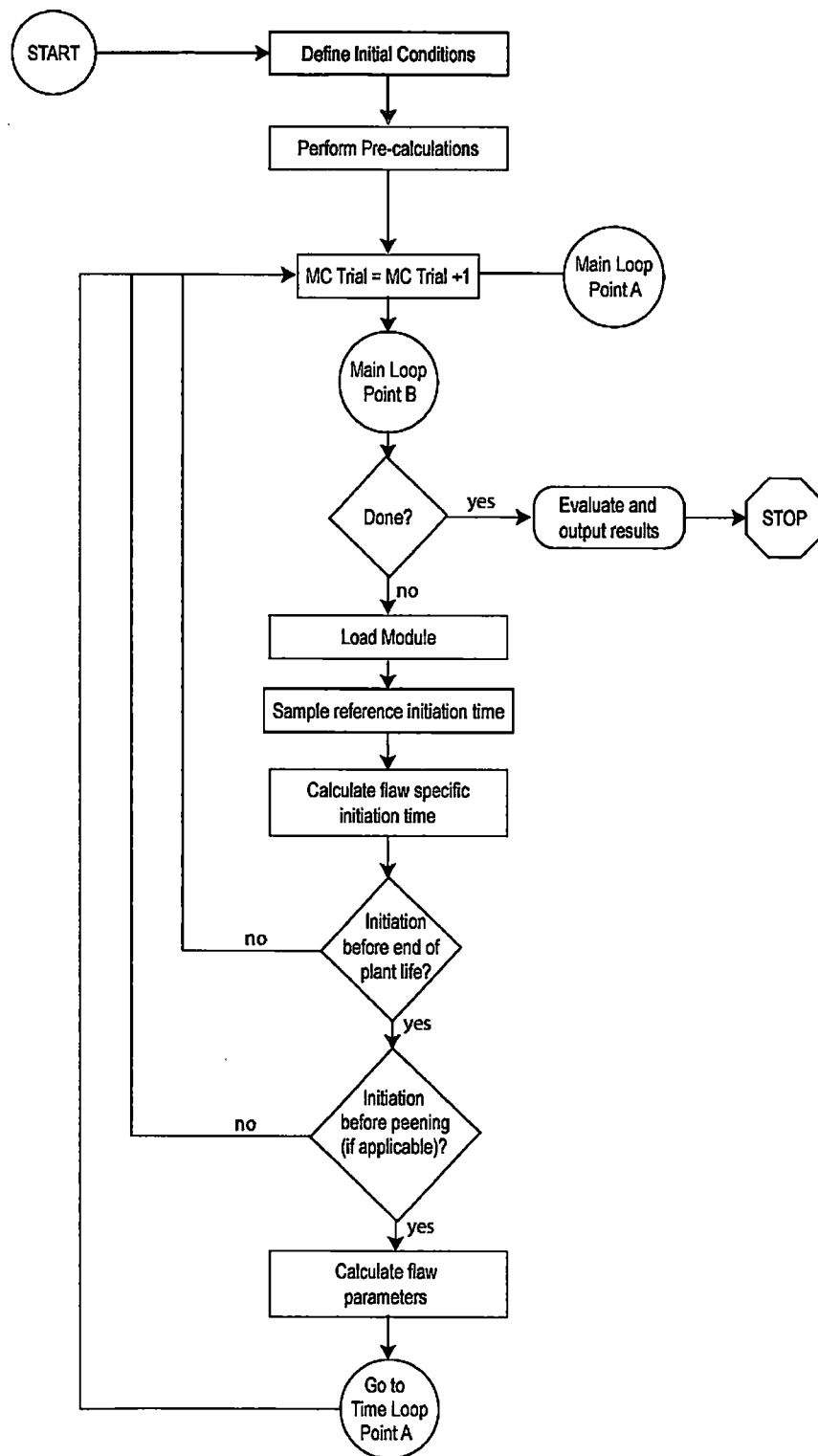


Figure A-1
DM Weld Probabilistic Model Flow Chart: Main Loop

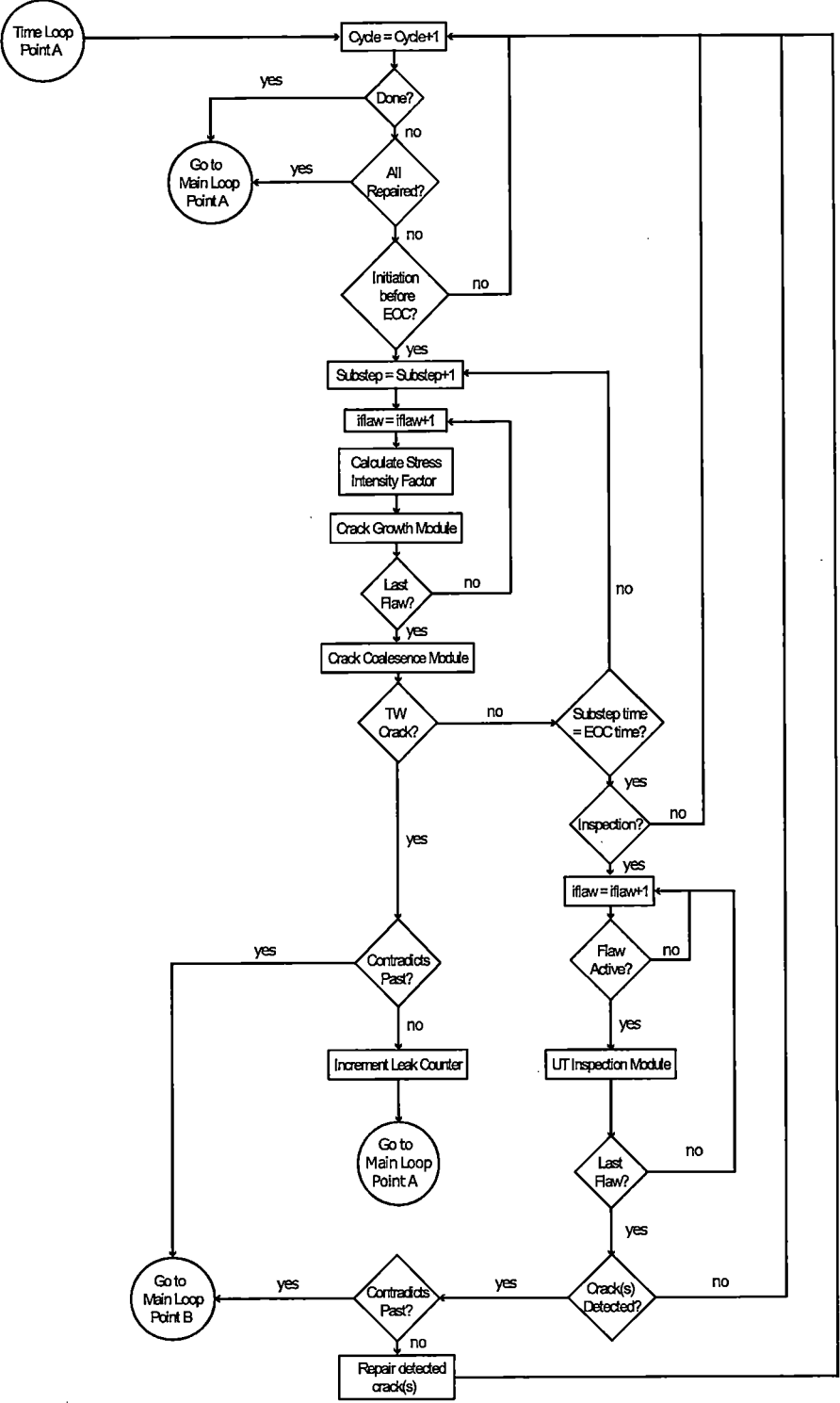


Figure A-2
DM Weld Probabilistic Model Flow Chart: Detail of Time Loop

A.3 Load and Stress Model

Load models are used to calculate the stress in the DM weld component during each Monte Carlo realization. The crack initiation and crack growth models utilize this information. Separate load models are used for hoop stresses (driving axial cracks) and axial stresses (driving circumferential cracks).¹⁵

The load models account for welding residual stresses, internal pressure, and piping loads (dead weight, thermal expansion, and thermal stratification, if applicable). In addition, a peening residual stress model is introduced for modeling crack growth during cycles after a peening application. The load models differentiate between residual stress and operational stress (which can all be combined to obtain total stress) as well as membrane stress and bending stress; the initiation and growth models use these differentiations at various steps.

The DM weld load models described in this report use general methodologies that are similar to those used by the xLPR Pilot Study program [5]. Significant differences between the models used in this study and those used in the xLPR Pilot Study include the following:

- Both axial and circumferential cracks are considered in this analysis. Because this study concentrates on the probability of through-wall crack growth and leakage rather than the probability of rupture, it was necessary to include axial flaws in the analysis.
- Peening residual stresses are modeled. The peening models are based on the bounding stress conditions meeting the performance criteria of Section 4. These models are pertinent because the main goal of this report is to assess the impact of peening on component performance with respect to leak mitigation (and ejection mitigation for RPVHPNs).
- No seismic loads (which affect crack stability but not subcritical crack growth) are considered in the analysis reported here. For simplicity, the failure criterion in the current study was selected to be a through-wall crack. Therefore, demonstrated crack stability during seismic events is not relevant.
- Thermal stratification loads are not included in this study. The xLPR Pilot Study investigated PWSCC degradation for a pressurizer surge nozzle, and thus included thermal stratification loads.

Similarly to the xLPR Pilot Study, it is assumed that the residual stress profile does not vary around the circumference (i.e., all residual stresses are axisymmetric).

The methodologies for calculating stresses due to internal pressure and piping loads (operational loads), component welding, and peening are discussed in Sections A.3.1, A.3.2, A.3.3, respectively. Considerations for the effects of temperature and load cycling are discussed in Section A.3.4. The load model for initiation and growth is summarized fully in Section A.3.5.

A.3.1 Internal Pressure and Piping Loads

Pipe stresses due to internal pressure, in the hoop and axial directions, are calculated using thin-walled cylindrical shell equations:

¹⁵ The subscripts “h” and “a” will be used to differentiate between hoop and axial stresses.

$$\sigma_{P,h} = \frac{PD_i}{2t} \quad [A-1]$$

$$\sigma_{P,a} = \frac{PD_i^2}{(D_i + 2t)^2 - D_i^2} \quad [A-2]$$

where P is the normal operating pressure, D_i is the pipe inner diameter, and t is the pipe thickness.

For both axial and circumferential cracks, a crack face pressure stress equal to the operating pressure, P , is superimposed after initiation.

Other piping loads include dead weight and pipe thermal expansion. These loads act to create a longitudinal force component, torsion, and two orthogonal bending moments. These loads do not affect the hoop stress.

The axial membrane stresses due to deadweight and normal thermal expansion are calculated:

$$\sigma_{DW,a} = \frac{F_{DW}}{A} \quad [A-3]$$

$$\sigma_{NTE,a} = \frac{F_{NTE}}{A} \quad [A-4]$$

where F_{DW} and F_{NTE} are the axial loads due to dead weight and normal thermal expansion, respectively, and A is the cross-sectional area of the pipe.

The bending stress is calculated using the bending moment and torsion components of the dead weight and normal thermal expansion piping loads (i.e., M_x (torsion) and M_y and M_z (bending)). The load model determines an effective moment (M_{eff}) as a Von Mises combination of the bending and torsional loads:

$$M_{eff} = \sqrt{M_y^2 + M_z^2 + \left[\frac{\sqrt{3}}{2} M_x \right]^2} \quad [A-5]$$

(For the calculation results presented in this appendix, the effective pipe moment acting on the weld cross section is an assumed input rather than calculated from components through this equation. Sensitivity cases are used to assess the effect of the magnitude of the effective moment, given its variability for actual plant components.)

Then, using the effective moment, the OD bending stress at any azimuthal angle (ϕ) is approximated as:

$$\sigma_B(\phi) = \frac{M_{eff} R_o}{I} \cos(\phi) \quad [A-6]$$

$$I = \frac{\pi(R_o^4 - R_i^4)}{4} \quad [A-7]$$

where R_o is the pipe outer diameter and I is the moment of inertia of the pipe cross-sectional area. Given this definition, $\varphi=0^\circ$ is the location of maximum tensile stress due to bending and $\varphi=180^\circ$ is the location of maximum compressive stress due to bending.

A.3.2 Welding Residual Stress Before Peening

The through-thickness residual stress profile is affected by local weld repairs and weld starts and stops. Thus, these processes can affect the susceptibility of the weld to initiation of PWSCC and the growth of PWSCC flaws through the weld, and as such must be modeled. In this analysis of DM welds, welding residual stress profiles are assumed to be axisymmetric and varying through-wall. The through-wall WRS profiles in the axial and hoop directions are detailed in the remainder of this section.

The axial load model uses a third-order polynomial function of through-wall fraction to approximate the axial WRS profile:

$$\sigma_{WRS,a} \left(\frac{x}{t} \right) = \sigma_{0,WRS,a} + \sigma_{1,WRS,a} \left(\frac{x}{t} \right) + \sigma_{2,WRS,a} \left(\frac{x}{t} \right)^2 + \sigma_{3,WRS,a} \left(\frac{x}{t} \right)^3 \quad [A-8]$$

where x is through-wall depth from the inner diameter, $\sigma_{0,WRS,a}$ is the ID axial WRS stress, and $\sigma_{1,WRS,a}$, $\sigma_{2,WRS,a}$, and $\sigma_{3,WRS,a}$ are curve-fit parameters.

The model solves for the three curve-fit parameters using three constraints resulting in a system of three linear equations:

1. The OD axial WRS ($\sigma_{OD,WRS,a}$) is defined:

$$\sigma_{WRS,a}(1) = \sigma_{OD,WRS,a} \quad [A-9]$$

2. A through-wall fraction at which axial WRS is zero (X_c) is defined:

$$\sigma_{WRS,a}(X_c) = 0 \quad [A-10]$$

3. The axial WRS is constrained to equilibrate through the thickness of the wall considering the effect of curvature. Using the axisymmetric assumption, that is:

$$\int_0^t \sigma_{WRS,a} \left(\frac{x}{t} \right) (R_i + x) dx = 0 \quad [A-11]$$

The circumferential load model uses a fourth-order polynomial function of through-wall percentage to approximate the hoop WRS profile:

$$\sigma_{WRS,h} \left(\frac{x}{t} \right) = \sigma_{0,WRS,h} + \sigma_{1,WRS,h} \left(\frac{x}{t} \right) + \sigma_{2,WRS,h} \left(\frac{x}{t} \right)^2 + \sigma_{3,WRS,h} \left(\frac{x}{t} \right)^3 + \sigma_{4,WRS,h} \left(\frac{x}{t} \right)^4 \quad [A-12]$$

where $\sigma_{0,WRS,h}$ is the ID hoop WRS stress, and $\sigma_{1,WRS,h}$, $\sigma_{2,WRS,h}$, $\sigma_{3,WRS,h}$ and $\sigma_{4,WRS,h}$ are curve-fit parameters.

The model solves for the four curve-fit parameters using four constraints resulting in a system of four linear equations:

1. The OD hoop WRS ($\sigma_{OD,WRS,h}$) is defined:

$$\sigma_{WRS,h} (1) = \sigma_{OD,WRS,h} \quad [A-13]$$

2. The location of minimum hoop WRS (X_{min}) is defined:

$$\left[\frac{d}{dx} \sigma_{WRS,h} \left(\frac{x}{t} \right) \right]_{\frac{x}{t} = X_{min}} = 0 \quad [A-14]$$

3. The minimum hoop WRS ($\sigma_{min,WRS,h}$) is defined:

$$\sigma_{WRS,h} (X_{min}) = \sigma_{min,WRS,h} \quad [A-15]$$

4. The derivative of hoop WRS is assumed to be zero at the ID, effectively:

$$\sigma_{1,WRS,h} = 0 \quad [A-16]$$

A.3.3 Residual Stress After Peening

As discussed in the body of this report, peening has the effect of adding a thin region of compressive residual stress at the surface of its application. For modeling purposes, a single outage in the operating life of the plant can be selected for the application of peening. After the application, it is assumed that no new cracks initiate and the growth of existing cracks occurs in the presence of normal operating stresses and the post-peening residual stress (PPRS) profile described below.

As with WRS, the peening stress profile is assumed to be axisymmetric and varying through-wall. The through-wall PPRS, in both the hoop and axial directions, is modeled using a piecewise stress equation that captures the minimum depth of the compressive residual stress layer and the limiting magnitude of the residual plus normal operating stress as detailed in Section 4. The assumed PPRS profile shape is depicted in Figure A-3 and is described in the remainder of this section (using the symbols presented in the figure).

For modeling purposes, the post-peening profile is separated into four general regions: the compressive region (nearest to the peened surface), the first transition region, the second transition region, and the "minimally affected" region (farthest from the peened surface). These regions are presented out of spatial order below for pedagogical reasons:

Region 1: The Compressive Region

The compressive region is the thin region near the application surface where the hoop and axial residual stresses are compressive. This region is characterized by a surface stress ($\sigma_{0,PPRS}$) and a penetration depth ($x_{1,PPRS}$). In this region, the PPRS profile varies linearly from the surface stress at the application surface to neutral stress at the penetration depth, as is reflected in the following equation:

$$\sigma_{PPRS}(x) = \sigma_{0,PPRS} - \left(\frac{\sigma_{0,PPRS}}{x_{1,PPRS}} \right) x \quad 0 \leq x \leq x_{1,PPRS} \quad [A-17]$$

Note that the argument to the PPRS equations is absolute depth as opposed to the non-dimensional depth used by the WRS equations. This reflects the notion that the peening profile is insensitive to the thickness of the peening component (for thicknesses characteristic of components studied here).

The same surface stress and peening depth are applied to the axial and hoop directions. This reflects the assumption that the peening-induced pressure waves travel without dependence on their orientation to the peened component. Vendor-supplied data, including orthogonal stress profiles from the same peened component, support this assumption.

It is noted that the peening profile data from vendors uncovered a slight trend between the residual surface stress after peening and the residual surface stress prior to peening. This effect, described in Section 3.3.3, can be included in the model as a linear adjustment to the sampled PPRS surface stress value that is dependent on the residual surface stress before the peening application. This effect is not included for base case results because the bounding stress effect meeting the performance criteria is used.

Region 4: The “Minimally Affected” Region

The “minimally affected” region is the portion of the PPRS profile that is far enough (greater than the “minimally affected depth”, $x_{3,PPRS}$) from the application surface that it does not experience a stress improvement. This region takes up the majority of the thickness of the component and is described by the following equations:

$$\begin{aligned} \sigma_{PPRS,a}(x) &= \sigma_{WRS,a} \left(\frac{x}{t} \right) + A_a & x_{3,PPRS} < x \leq t \\ \sigma_{PPRS,h}(x) &= \sigma_{WRS,h} \left(\frac{x}{t} \right) + A_h & x_{3,PPRS} < x \leq t \end{aligned} \quad [A-18]$$

The additive terms A_a and A_h are force balance terms included to ensure the effective residual force on the peened through-wall element does not change due to peening (accounting for curvature for the axial stress case). Under the axisymmetric assumption, that is:

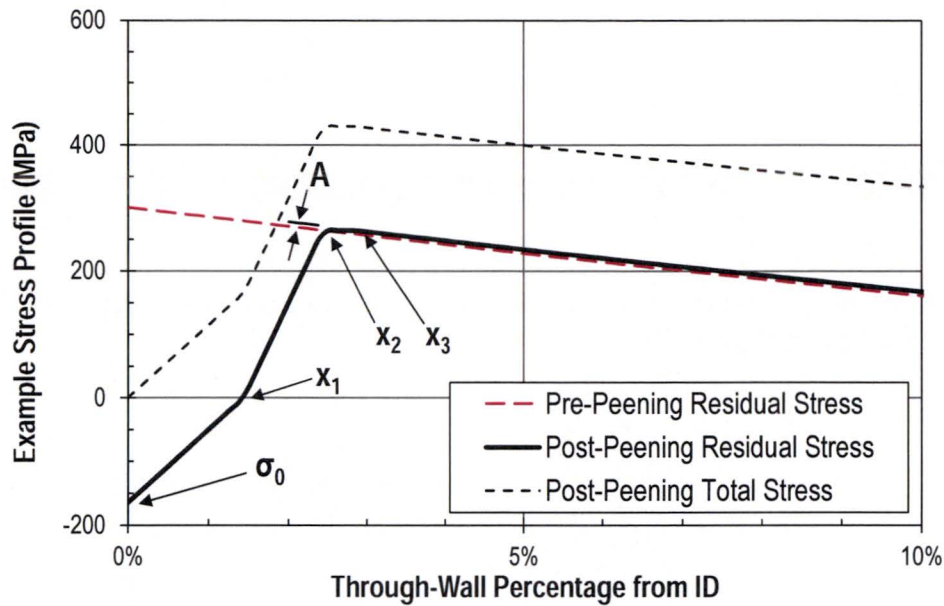


Figure A-3
Example Post-Peening Residual Stress Profile near Surface of Circumferential Crack in a DMW Component (Repeat of Figure 5-2)

A.3.4 Effect of Operating Temperature and Load Cycling

Residual stress relaxation can occur in reactor components due to temperature and load cycling effects. This relaxation is characterized by a reduction of residual stress magnitudes as a function of operating time. As the bounding stress profile defined in Section 4 is applied to this analysis, no stress relaxation effects are applied to the base-case probabilistic model. The performance criteria of Section 4.2.8 require that the effects of thermal relaxation and load cycling (shakedown) be considered when demonstrating that the bounding stress effect meeting the performance criteria will be obtained for the remaining service life of the component.

A best-fit time-dependent model is applied to peening and welding residual stresses in a sensitivity case presented later to quantify the dependence of predicted results on the stress relaxation model:

$$\sigma_{PPRS,d}(x, \Delta t_{peen}) = \sigma_{PPRS,d}(x, \Delta t = 0) \cdot \exp[-m \cdot \Delta t_{peen}] \quad [A-22]$$

where Δt_{peen} is the time elapsed since peening (in EFPYs) and m is the empirical stress relaxation exponent.

The final (relaxed) surface stress is based on the minimum acceptable peening performance criteria defined in Section 4. The relaxation factor is based on vendor-supplied data for peened samples subjected to strain cycling and/or elevated temperatures [8]. These analyses are detailed in Section A.8.5. Using the model form described in Equation [A-22], the initial surface stress is then evaluated by back-extrapolating the final (relaxed) stress state to the stress state just after peening.

$$\int_0^t \sigma_{WRS,a} \left(\frac{x}{t} \right) (R_i + x) dx = \int_0^t \sigma_{PPRS,a} (x) (R_i + x) dx = 0$$

$$\int_0^t \sigma_{WRS,h} \left(\frac{x}{t} \right) dx = \int_0^t \sigma_{PPRS,h} (x) dx$$
[A-19]

This modeling convention assumes that any residual tension removed near the application surface is redistributed through the wall-thickness of the peened component. Validation of this assumption is included in Appendix C.

Regions 2 and 3: The Transition Regions

The two transition regions are used to connect the compressive region stresses with the “minimally affected” region stresses, preserving stress continuity through-wall. Because little information is available to describe this transition, a simple approach is taken.

The first transition region uses a linear equation to connect the neutral stress location at the penetration depth to the pre-peening residual stress at the “transition depth” ($x_{2,PPRS}$). The general equation for this is:

$$\sigma_{PPRS,d} (x) = \left(\frac{x - x_{1,PPRS}}{x_{2,PPRS} - x_{1,PPRS}} \right) \cdot \sigma_{WRS,d} \left(\frac{x_{2,PPRS}}{t} \right) \quad x_{1,PPRS} < x \leq x_{2,PPRS}$$
[A-20]

where the subscript d indicates a placeholder for the subscript a (axial) or the subscript h (hoop).

The second transition region uses a linear equation to connect the pre-peening residual stress at the “transition depth” to the “minimally affected” region at the “minimally affected depth”. The general equation for this is:

$$\sigma_{PPRS,d} (x) = \left(\sigma_{WRS,d} \left(\frac{x_{3,PPRS}}{t} \right) + A_d - \sigma_{WRS,d} \left(\frac{x_{2,PPRS}}{t} \right) \right) \cdot \left(\frac{x - x_{2,PPRS}}{x_{3,PPRS} - x_{2,PPRS}} \right) + \sigma_{WRS,d} \left(\frac{x_{2,PPRS}}{t} \right) \quad x_{2,PPRS} < x \leq x_{3,PPRS}$$
[A-21]

- The within-weld variation factor for the resulting cracks is calculated using a depth-weighted average of cracks A and B :

$$f_{ww,i} = \frac{a_A f_{ww,A} + a_B f_{ww,B}}{a_A + a_B} \quad [A-42]$$

The within-weld variation is thought to be a function of varying material and chemical conditions. During coalescence, the resultant within-weld variation factor is considered to be dependent on the within-weld factors of the original cracks. This is because the resultant crack will grow in a combination of the material and chemical conditions of the original cracks. The depth-weighted average in Equation [A-42] gives preference toward the deeper crack, which on average is expected to have the higher of the two within-weld factors.

The coalescence of cracks is repeated until there are no active cracks close enough to one another (although it would be extremely rare for more than two cracks to coalescence during a given sub-cycle given the initiation rates discussed previously).

A.5.5 Special Considerations for Crack Growth on a Peened Surface

This section discusses special considerations made for predicting growth in a component with a stress profile characteristic of a peened component, i.e., with a compressive stress region near the surface. The traditional stress intensity factor calculation methods discussed in Sections A.5.1 and A.5.2 assume a crack that is fully-open and semi-elliptical, while in fact, given a compressive stress region near the surface, these assumptions may not be realistic. Two deviations from these assumptions, and how they are addressed from a modeling standpoint, are discussed in this section; they are crack closure and sub-surface, often resembling a “balloon” shape, crack growth. Both of these topics have been investigated in detail in other empirical, numerical, and analytical studies.

As has been emphasized throughout this report, peening produces a compressive residual stress layer near the surface that prevents crack initiation and tends to reduce the growth rate of shallow cracks. During operation after the application of peening, the depths of the compressive layer, when present, in the axial and hoop directions, $x_{comp,a}$ and $x_{comp,h}$, are given by the following equations:

$$\begin{aligned} x_{comp,a} &= x_{1,PPRS} \left(1 - \frac{\sigma_{oper,a}}{\sigma_{0,PPRS}} \right) \\ x_{comp,h} &= x_{1,PPRS} \left(1 - \frac{\sigma_{oper,h}}{\sigma_{0,PPRS}} \right) \end{aligned} \quad [A-43]$$

where $\sigma_{oper,a}$ and $\sigma_{oper,h}$ are terms that include all the operational stresses on the peened location of interest; if the operational stress is tensile, it has the effect of moving the compressive layer depth nearer to the surface, or eliminating it entirely.

Cracks loaded with a combination of compressive and tensile stress have the possibility of partial closure, i.e., open at their deepest point, but closed near the surface due to the compressive layer (see Figure A-6). At locations where crack closure occurs, a contact stress is created that is equal

cracks may grow more quickly than the other. However, given the large variability in weld residual stress and crack growth rates assumed in the probabilistic analyses, the coplanar simplification is appropriate. It is assumed that axial cracks do not interact with each other, or with circumferential cracks.

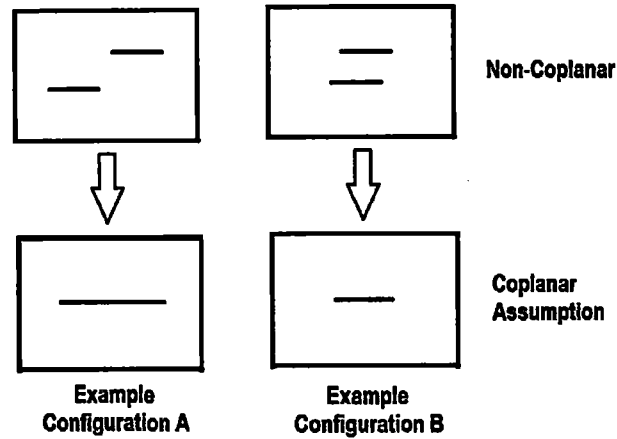


Figure A-5
Example of Configurations Illustrating Impact of Coplanar Flaw Assumption

Given the coplanar assumption for circumferential cracks, it was necessary to develop a coalescence model, or a set of coalescence rules, to describe the crack interaction on this plane. These are described in the remainder of this section.

Coalescence is modeled at the completion of each sub-cycle growth prediction, if multiple circumferential cracks are active. Coalescence is considered to occur if, at the completion of a given sub-cycle, two adjacent cracks (call them cracks *A* and *B*) overlap or are close enough such that the dividing section of weld material collapses. While the phenomena of weld section collapse is highly complex, the collapse distance, $\Delta C_{threshold}$, is modeled here as a user-defined ratio, $1/F_{coalescence}$, of the maximum depth of cracks *A* and *B*:

$$\Delta C_{threshold} = \frac{\max\{a_A, a_B\}}{F_{coalescence}} \quad [A-41]$$

where the subscripts *A* and *B* denote the two adjacent cracks. The same methodology is discussed in ASME Section XI [16], where $F_{coalescence}$ is defined as 2.0.

If coalescence occurs, the following rules are used to consolidate the original cracks into a single resulting crack:

- The resulting crack is assumed to take on a semi-elliptical shape immediately following coalescence, with a depth equal to the maximum depth of cracks *A* and *B* and a length such that the original cracks *A* and *B* are fully circumscribed.

The estimation of crack growth versus time requires the solution of the above ordinary differential equation. This is achieved numerically by discretizing each plant operating cycle into many sub-cycles and advancing growth linearly over each sub-cycle, using the crack geometry and stress profile at the beginning of each sub-cycle to predict growth rate (i.e., a forward Euler method). The use of 12 sub-cycles per calendar year has been demonstrated to converge sufficiently to actual solution (e.g., a solution that uses twice as many sub-cycles) for a variety of initial conditions, temperatures, and stress profiles.

Various parameters in the above equation are empirical in nature and their derivation for crack growth in Alloy 82/182 is described in Section A.8.3. These include the absolute reference temperature T_{ref} , the growth activation energy Q_g , the power-law coefficient α , the crack-tip stress intensity factor threshold K_{Ith} , and the stress intensity factor exponent b .

Two additional factors, f_{weld} and f_{ww} , are included in the crack growth model to describe the aleatory uncertainty in the crack growth rate model (i.e., uncertainty due to the unknowns that differ each time we run the same experiment). The within-weld variation, f_{ww} , is a value sampled for each flaw site from a distribution reflective of the growth rate variation observed in laboratory studies of cracks in a controlled weld. Similarly, the weld-to-weld growth rate variation, f_{weld} , is a value sampled for each weld from a distribution reflective of the growth rate variation observed in laboratory studies of cracks in identically controlled welds, after accounting for the within-weld variation. The derivation of these distributions is described in Section A.8.3.

As discussed in Section A.4.4, the sampled growth variation terms may be correlated with sampled initiation times to simulate the premise that components and locations that are more susceptible to PWSCC initiation tend to have higher flaw propagation rates.

A.5.4 Special Considerations for Crack Growth on a DM Butt Weld Geometry

This section discusses the special constraints and interactions applied to cracks growing on a DM weld component. These constraints and interactions are imposed by a set of modeling “rules” used to approximate known physical behaviors. While these physical behaviors are complex in nature, the simple set of rules is applied in the probabilistic model in order to capture the most essential growth characteristics.

As discussed in Section A.4.1, both axial and circumferential cracks are allowed to initiate on the inner diameter of the DM weld. Axial cracks are constrained such that they cannot grow beyond the defined width of the weld geometry. Circumferential cracks are constrained such that they cannot grow beyond the defined inner circumference of the weld geometry. In the case that an axial, or circumferential, crack grows beyond the defined maximum length (weld width or inner circumference of the weld) before growing through-wall in the depth direction, its length is truncated.

All initiated circumferential cracks are assumed to initiate and grow on the same axial plane. For cracks with little to no circumferential overlap (Example Configuration A in Figure A-5), this assumption will lead to a single large flaw at the expense of two axially offset flaws, slightly increasing the probability of leakage and susceptibility to rupture. For cracks with substantial circumferential overlap (Example Configuration B in Figure A-5), this assumption would tend to result in a slightly reduced probability of leakage and susceptibility to rupture as one of two

due to axisymmetric membrane stresses. Accordingly, for circumferential cracks, Equation [A-36] becomes:

$$K = \int_0^a h(x, a) \sigma(x) dx + G_{gb} \sigma_{gb} \sqrt{a\pi} \quad [A-39]$$

A.5.3 MRP-115 Crack Growth Rate Model for Alloy 82/182

The model selected in this study to estimate PWSCC crack growth in Alloy 182 weld metal is the model presented in MRP-115 [11].

The crack growth model provides a way to predict the extension of crack length and depth due to PWSCC. The model is relatively simple and incorporates the major factors affecting flaw growth rate: temperature and stress intensity factor. Temperature effects are incorporated through a widely accepted Arrhenius term and stress effects are incorporated through a standard power-law dependence, as presented below:

$$\frac{\delta}{\delta t}(d) = e^{\frac{Q_g}{R} \left(\frac{1}{T} - \frac{1}{T_{ref}} \right)} \alpha f_{weld} f_{ww} (K_I - K_{Ith})^b \quad [A-40]$$

where

- d = general crack dimension (e.g., depth or length)
- Q_g = thermal activation energy for crack growth
- R = universal gas constant
- T = absolute temperature at location of crack
- T_{ref} = absolute reference temperature used to normalize data
- α = power-law coefficient
- f_{weld} = common factor applied to all specimens fabricated from the same weld to account for weld wire/stick heat processing and for weld fabrication
- f_{ww} = "within weld" factor that accounts for the variability in crack growth rate for different specimens fabricated from the same weld
- K_I = crack-tip stress intensity factor at location of interest
- K_{Ith} = crack-tip stress intensity factor threshold, below which the crack growth rate is zero
- b = stress intensity factor exponent

This model is analogously applied to predict depth growth (substituting the K_{90} stress intensity factor term for the K_I term above) and length growth (substituting the K_0 stress intensity factor term for the K_I term above).

the location on the crack although this is not demonstrated explicitly by its argument list for the sake of conciseness.)

For the purpose of predicting crack growth under the semi-elliptical crack shape assumption, the two points of interest on the crack are the deepest point (denoted by the subscript 90) and the surface tip points (denoted by the subscript 0). The general weight functions for these two points, respectively, are:

$$h_{90} = \frac{2}{\sqrt{2\pi(a-x)}} \left[1 + M_1 \left(1 - \frac{x}{a} \right)^{1/2} + M_2 \left(1 - \frac{x}{a} \right) + M_3 \left(1 - \frac{x}{a} \right)^{3/2} + M_4 \left(1 - \frac{x}{a} \right)^2 \right] \quad [\text{A-37}]$$

$$h_0 = \frac{2}{\sqrt{\pi x}} \left[1 + N_1 \left(\frac{x}{a} \right)^{1/2} + N_2 \left(\frac{x}{a} \right) + N_3 \left(\frac{x}{a} \right)^{3/2} + N_4 \left(\frac{x}{a} \right)^2 \right] \quad [\text{A-38}]$$

where the M and N terms are simple algebraic equations of the influence coefficients discussed in the previous section [14].

The weight function method is powerful because it allows the estimation of stress intensity factors for an arbitrary through-wall stress profile function. This capability is required in this study because the post-peening stress profile cannot accurately be represented by a polynomial.

There are several approaches to evaluating the integral in Equation [A-36]. If the functional form of the stress profile is available, the integral may be solvable analytically. This approach has been implemented for the four-region piecewise polynomial stress profile defined for post-peening in this study (Equations [A-27] and [A-28]). This method is similar to approximating any arbitrary stress profile with piecewise linear equation, resulting in a closed-form solution [14].

To experiment with different stress profiles, without having to derive the analytical weight function indefinite integral for each, a numerical integration procedure is also available. An adaptive, open, degree-2, Newton-Cotes integration algorithm with a 1% convergence termination criteria is employed to estimate the weight function integral numerically (see Section 4.1 of *Numerical Recipes* [7]). The use of an integral transformation discussed in Section 4.4 of *Numerical Recipes* [7] accelerates convergence by concentrating the integrand evaluations in areas with the most rapid change (i.e., near the vertical asymptotes of the weight functions given in Equations [A-37] and [A-38]).

Due to the mathematical and programming complexities of the implemented weight function solution modules, verification studies were performed to compare stress intensity factor solutions against FEA Crack [15], for various crack geometries and stress profiles.

It is noted that the weight function method cannot be applied accurately for estimating stress intensity factors due to bending because the bending stress profile is by definition not uniform along the crack length. So, after the application of peening, the contribution of the global bending load to the stress intensity factor continues to be evaluated with the influence coefficient method (as discussed in the previous section) and is superimposed with those stress intensities

Table A-1
Interpolation and Extrapolation Criteria for Influence Coefficient Lookup

	R_i / t	c / a	a / t
Lower Bound	1	1	0
Lower Truncation Protocol	Error message is given. Extrapolation is not reliable below $R_i/t=1$.	Value of $c/a=1$ is used. Extrapolation is not reliable below $c/a=1$.	Error message is given. Negative depth indicates error.
Upper Bound	1000	16	0.8
Upper Truncation Protocol	User is instructed to use $R_i/t=1000$. Solution is converged to a flat plate	Value of $c/a=16$ is used. Extrapolation is not reliable above $c/a=16$.	Linear extrapolation of look-up table is executed.

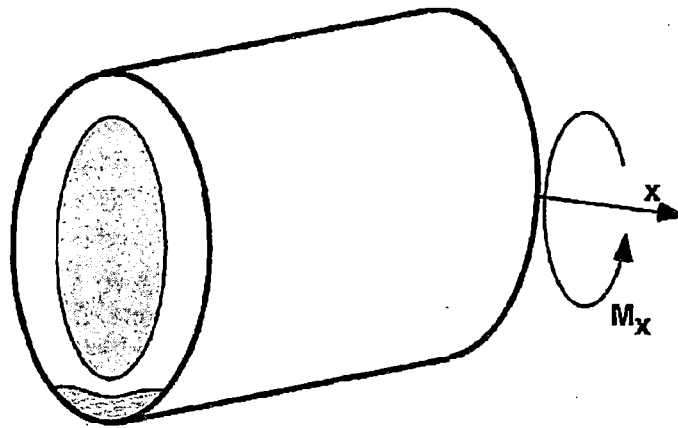


Figure A-4
Crack Location Relative to Bending Moment Assumed for Stress Intensity Factor Calculation [12]

A.5.2 Stress Intensity Factor Calculation Using the Weight Function Method

Section 6 in WRC Bulletin 471 [12] describes the calculation of stress intensity factor, K , for a circumferentially or axially oriented surface crack on a pipe of arbitrary size using the weight function method, a generalization of the influence coefficient method discussed in the previous section. The weight function method may be applied to a crack subjected to a stress profile acting orthogonally to the crack face (i.e., axial stresses for circumferential cracks and hoop stresses for axial cracks) that is defined by an arbitrary function in the direction of the crack depth and is uniform along the crack length.

The general form of the stress intensity factor calculation by way of the weight function method is:

$$K = \int_0^a h(x, a) \sigma(x) dx \quad [A-36]$$

where x is the distance from the surface, $h(x, a)$ is the weight function, and $\sigma(x)$ is the stress profile function. (The weight function is dependent on the crack and component geometries and

A.5.1 Stress Intensity Factor Calculation Using Influence Coefficient Method

Welding Research Council (WRC) Bulletin 471 [12] describes the calculation of stress intensity factor, K , for a circumferentially or axially oriented surface crack on a pipe of arbitrary size using the influence coefficient method. The method described may be applied to a crack subjected to: a) a stress profile acting orthogonally to the crack face (i.e., axial stresses for circumferential cracks and hoop stresses for axial cracks) that is defined by a polynomial function in the direction of the crack depth and is uniform along the crack length, and/or b) stresses due to global bending loads, which are by definition not uniform over the crack length. (In this study, global bending loads are only considered for the growth of circumferential cracks.)

Before the application of peening, the axial and hoop residual stresses may be approximated by polynomial functions, as demonstrated in Equations [A-25] and [A-26], and so the influence coefficient method is used due to its simplicity and computational efficiency. After peening, the more general weight function method, which is described in the next section, must be employed.

The general form of the stress intensity factor calculation (for a surface crack with depth a on a pipe with thickness t) by way of the influence coefficient method is:

$$K = \left[\sigma_0 G_0 + \sigma_1 G_1 \left(\frac{a}{t} \right) + \sigma_2 G_2 \left(\frac{a}{t} \right)^2 + \sigma_3 G_3 \left(\frac{a}{t} \right)^3 + \sigma_4 G_4 \left(\frac{a}{t} \right)^4 + G_{gb} \sigma_{gb} \right] \sqrt{a\pi} \quad [\text{A-35}]$$

where the G terms are the influence coefficients specific to the crack and component geometries and the point on the crack, σ_0 through σ_4 are the polynomial coefficients of the through-wall stress profile (in units of stress), and σ_{gb} is the nominal bending stress due to a bending moment acting in the direction indicated in Figure A-4 (i.e., the bending moment is assumed to be directed such that the crack center is at the azimuthal location of maximum tensile or compressive stress). While the bending direction indicated in Figure A-4 only applies to two distinct azimuthal locations on a pipe, stress intensity factors at all locations are calculated with Equation [A-35] using bending stress approximated as a function of azimuthal angle per Equation [A-6].

The influence coefficients are interpolated from tables built by way of linear-elastic finite element parametric analyses. Table 15 and 39 in Marie, et al. [13] provides such look-up tables for the surface tip and deepest points of cracks of interest to the study of PWSCC in DM weld components: semi-elliptical, axial or circumferential surface cracks on the inner diameter of a pipe. Higher order influence coefficients (e.g., G_2 , G_3 , and G_4) may be calculated with weight function coefficients as discussed in Section 6.3 in WRC Bulletin 471 [12].

The look-up tables for the crack types of interest require three non-dimensional terms: the ratio of the pipe inner radius to pipe thickness (R/t), the ratio of crack half-length to crack depth (c/a), and the ratio of crack depth to pipe thickness (a/t). Table A-1 describes the lower and upper bounds of the look-up tables provided in Marie, et al. [13] and the protocol used for extrapolation of the look-up tables.

possible for finite crack sizes. Initial crack lengths are attained by scaling the initial depth by a sampled aspect ratio.

Crack center location, ϕ_i , which is important in this study for modeling growth and coalescence of *circumferential* cracks only, is sampled uniformly on the arc length of each initiated crack, defined in Section A.4.1.

Finally, growth capacity for each crack is modeled using sampled growth variation terms, f_{weld} and $f_{ww,i}$, discussed in more detail in Section A.5.3. It is generally accepted by PWSCC experts that components and locations that are more susceptible to PWSCC initiation tend to have higher flaw propagation rates, even after normalizing for temperature and stress effects [11]. This tendency is modeled by correlating the weld-to-weld growth variation, f_{weld} , with the reference time of first PWSCC initiation, t_{ref} , and similarly by correlating the within-weld variation for each crack, $f_{ww,i}$, with the corresponding multiple flaw reference initiation time, $t_{ref,i}$.

A.5 Crack Growth Model

This study employs a model to allow the prediction of PWSCC growth rate as a function of crack geometry, component loading, and other conditions. Assuming that cracks maintain a semi-elliptical shape as they grow through-wall, the model predicts growth rates of the surface tips (in the length direction) and the deepest point (in the depth direction) of the crack.

The model predicts growth rates for partially through-wall cracks. As discussed in Section A.7, a through-wall growth (i.e., leakage) event is treated as the end condition in this study of DM welds, so growth prediction does not proceed to necessitate a through-wall crack growth model (contrary to the analysis of RPVHPNs).

Growth is simulated by integrating the crack growth rates over time. This integration is done numerically by discretizing each cycle into many sub-cycles and advancing growth linearly over each sub-cycle, using the crack geometry and stress profile at the beginning of each sub-cycle to predict growth rate (i.e., a forward Euler method).

The dependence of PWSCC on component loading (i.e., stresses near and orthogonal to the crack) requires the calculation of stress intensity factors at the crack points of interest. Sections A.5.1 and A.5.2 discuss the stress intensity factor calculation methods for a crack subject to a polynomial stress profile and a crack subject to a general stress profile, respectively. These solutions are based on the results of finite element parametric analyses for circumferential and axial cracks; these analyses are based on the superposition method of linear-elastic fracture mechanics.

The crack growth rate model, which factors in stress intensity factor, temperature, and various other effects, is discussed in Section A.5.3.

Finally, Sections A.5.4 and A.5.5 discuss special considerations made for predicting growth given geometry characteristics specific to a DM weld component and a stress profile characteristic of a peened component (i.e., with a compressive stress region near the surface), respectively.

The shape parameter for the multiple flaw Weibull model, θ_{mult} , is calculated from β_{mult} , t_f , and F_{1st} above using Equation [A-30]. Then, an initiation time for each remaining crack site, $t_{ref,i,d}$, is sampled from the resulting Weibull distribution. Sampled initiation times are truncated at t_f such that no cracks form prior to the crack at the site experiencing the largest tensile surface stress (i.e., if the initiation time sampled from the multiple flaw model is less than that of the first flaw, it is resampled).

Employing the surface stresses calculated by the load model (Equations [A-23] and [A-24]), each initiation time is adjusted for surface stress effects using an empirical stress-dependent factor ($S_{factor,i}$):

$$t_{f,i,d} = \frac{t_{ref,i,d}}{S_{factor,i,d}} \quad [A-33]$$

$$S_{factor,i,a} = \left(\frac{\sigma_{ID,a}(\hat{\phi}_i)}{\sigma_{ref}} \right)^n$$
$$S_{factor,i,h} = \left(\frac{\sigma_{ID,h}}{\sigma_{ref}} \right)^n \quad [A-34]$$

where the stress exponent n and reference stress σ_{ref} are empirical parameters. Note that initiation times for sites with a compressive (negative) surface stress are not modeled with the above equations and instead the stress adjustment factor is considered to be zero; i.e., the initiation times are set to infinity; i.e., cracks are not allowed to initiate orthogonal to a compressive stress field.

By convention, the reference stress, σ_{ref} , is set equal to the stress at the site of maximum tensile stress. This constrains the stress adjustment factor in Equation [A-34] to be less than or equal to one, across all crack sites, and effectively shifts initiation times for sites with lower stresses further into the future. This normalizing convention has been selected over using a constant reference stress across all Monte Carlo realizations (as has been done in other studies) because it is assumed that the variation in the multiple flaw Weibull initiation models already includes the effects due to varying surface stresses throughout in-service DM welds. Thus, to apply Equation [A-33] with a *constant* reference stress would be to “double-count” the variation due to component surface stress and, furthermore, would require an arbitrary selection of σ_{ref} .

A.4.4 Crack Initialization

In this context, crack initialization refers to assigning of initial conditions to each crack at its initiation time. These conditions include size, location, and capacity for growth. Orientation of an initiated crack, which has been part of initialization in other studies, is inherently addressed in the spatial discretization procedure discussed in Section A.4.1.

Initial crack depth is sampled from a distribution of positive, non-zero, crack through-wall percentages. This reflects both that the Weibull initiation models discussed above were fit to industry data recording first detection of crack indications and that crack detection is only

The process by which β , F_1 , and t_1 are fit to existing data for first crack initiation in DM welds is discussed in Section A.8.2.

Once β and θ are known for the current Monte Carlo realization, they can be used to sample a reference initiation time in EDY (t_{ref}). This sampled initiation time can be adjusted to account for temperature, material condition, and feedwater chemistry. In this study, the initiation time is adjusted for temperature (to convert to EFPY) using the widely accepted Arrhenius relationship:

$$t_f = t_{ref} \times e^{\left(\frac{Q_i}{R}\right)\left(\frac{1}{T} - \frac{1}{T_{ref}}\right)} \quad [A-31]$$

where T is the absolute operating temperature, Q_i is the apparent thermal activation energy for crack initiation, R is the universal gas constant, and T_{ref} is the Arrhenius model absolute reference temperature.

The result, t_f , is the time of the first PWSCC on the component for the current Monte Carlo realization. As a convention, this time is attributed to the crack located at the point of maximum tensile stress. If this point happens to be at a circumferential crack site, it will be at the location maximum tensile bending stress; if this point happens to be at an axial crack site, all of which experience the same tensile stress, the crack site is arbitrary (and the axial crack site located at 0° is selected). As described in the next section, the multiple flaw initiation model uses the first initiation time to predict the initiation times of the remaining crack sites.

A.4.3 Initiation Time for Multiple Cracks

A Weibull model has been selected for use in predicting times of initiation of multiple PWSCC cracks in a single DM weld component. The use of this statistical model reflects systematic and statistical variations in material properties and environmental conditions from location to location on a single component. An adjustment is made for surface stress at each location to capture the known dependence of PWSCC initiation susceptibility on surface stress.

The multiple crack initiation Weibull model uses a new Weibull slope, β_{mult} , or a new rate at which PWSCC degradation spreads to multiple sites on a component after the first crack initiation. This rate, when used to predict a time of initiation at each crack site independently, results in more rapid crack initiation than the time to first initiation model. This reflects the premise that there may be a distinct, but random, event or condition that, after its onset, promotes more rapid PWSCC. This behavior has been observed in industry. The selection of a value for β_{mult} is discussed in Section A.8.2.6.

As in the previous section, a defined cumulative fraction at a defined time is necessary to complete the Weibull model. Since the time provided by Equation [A-31] is indicative of the time of first PWSCC initiation across all $2N_{crack}$ crack sites, it is associated with the cumulative probability (F_{1st}) given in Equation [A-32] below:

$$F_{1st} = \frac{1 - 0.3}{2N_{crack} + 0.4} \quad [A-32]$$

significant for crack initiation prediction. Furthermore, the model allows for initiation of multiple flaws with axial or circumferential orientations.

A.4.1 Spatial Discretization of Crack Sites

To account for the possibility of multiple cracks, the DM weld component is divided into a 19 (N_{crack}) crack initiation locations. Because this study also analyzes axial cracks, each of the 19 crack *locations* is given both an axial and circumferential crack *site*. This results in 38 total crack sites at which initiation is modeled.

The program sets the crack locations simply by dividing the 360 degrees of the pipe ID into N_{crack} equal arc lengths. By convention, the first crack location is centered at zero degrees, resulting in the following equation for the arc length centers (in radians):

$$\hat{\phi}_i = \frac{2\pi}{N_{crack}}(i-1) \quad i = 1, \dots, N_{crack} \quad [A-29]$$

where the subscript i will be used throughout the remainder of this appendix to denote the different crack locations.

After initiation, crack location is randomly sampled within its respective arc length.

A.4.2 Initiation Time for First Crack

A Weibull model has been selected for use in predicting the time of first initiation of PWSCC in DM welds. The use of this statistical model reflects systematic and statistical variations in material properties and environmental conditions from part to part. Furthermore, this statistical model captures the fact that the time between PWSCC initiation, for the population's first DM weld component and its last DM weld component, is quite long (several decades and even centuries). A number of distributions can be used to model failures, but the Weibull distribution is one of the most commonly used in reliability engineering since it can model a variety of data and life characteristics [10].

The two-parameter Weibull cumulative distribution function is given as follows:

$$F(t) = 1 - e^{-\left(\frac{t}{\theta}\right)^\beta} \quad [A-30]$$

where F is the cumulative fraction of components with a PWSCC initiation and t is the corresponding operating time. The Weibull slope, or shape parameter, β , is related to the rate at which degradation spreads through a given component population such as steam generator tubing. The Weibull characteristic time parameter, θ , provides a measure of the time scale for the degradation mode of interest. Specifically, the Weibull characteristic time is the time required to reach a cumulative failure fraction of 0.632 (i.e., the time required for 63.2% of the items in a given population to fail).

The Weibull slope, β , an arbitrary failure fraction, F_1 , (e.g., 0.1%, 1%, 10%, 63.2%, etc.), and the time at which this arbitrary failure fraction is reached, t_1 , are provided as inputs to the probabilistic model. The value of θ is then determined during runtime using Equation [A-30].

A.3.5 Summary of Load Model

The models discussed in the previous sections can be combined to obtain total stress applicable to crack initiation or crack growth, before or after peening, and applicable to axial or circumferential cracks.

The DM weld *initiation* model considers only the surface (ID) stress and does not include crack face pressure. Prior to peening, this results in the following equations for axial and circumferential cracks:

$$\sigma_{ID,a}(\varphi) = \sigma_{P,a} + \sigma_{DW,a} + \sigma_{NTE,a} + \sigma_{0,WRS,a} + \frac{R_i}{R_o} \sigma_B(\varphi) \quad [A-23]$$

$$\sigma_{ID,h} = \sigma_{P,h} + \sigma_{0,WRS,h} \quad [A-24]$$

After peening, it is assumed that initiation cannot occur. That is, it is assumed that the compressive residual surface stress introduced by peening is sufficient to prevent the total surface stress during operation from reaching approximately +20 ksi (+140 MPa) tensile (which is a conservative threshold for initiation of PWSCC [9]).

The growth model requires total stress as a function of through-wall depth. Prior to peening, the total stresses for axial and circumferential cracks are:

$$\sigma_{tot,a}(x, \varphi) = \sigma_{P,a} + \sigma_{DW,a} + \sigma_{NTE,a} + \frac{R_i + x}{R_o} \sigma_B(\varphi) + \sigma_{WRS,a} \left(\frac{x}{t} \right) + P \quad [A-25]$$

$$\sigma_{tot,h}(x) = \sigma_{P,h} + \sigma_{WRS,h} \left(\frac{x}{t} \right) + P \quad [A-26]$$

After peening, the total stresses for axial and circumferential cracks are:

$$\sigma_{tot,a}(x, \varphi) = \sigma_{P,a} + \sigma_{DW,a} + \sigma_{NTE,a} + \frac{R_i + x}{R_o} \sigma_B(\varphi) + \sigma_{PPRS,a}(x) + P \quad [A-27]$$

$$\sigma_{tot,h}(x) = \sigma_{P,h} + \sigma_{PPRS,h}(x) + P \quad [A-28]$$

Note that at most azimuthal locations on the pipe, the pressure and thermal loads that occur during operation result in a tensile contribution to stress. Superimposing these tensile operating stresses with the post-peening residual stress profile results in a less compressive and more tensile stress near the peened surface stress. This is effectively captured in the equations above.

A.4 Crack Initiation Model

This study employs a statistical Weibull approach for predicting crack initiation and allows adjustments for operating temperature and surface stress, two factors commonly considered

and opposite to the local stresses. If the stress required to keep the crack closed is superimposed with the contact stresses (as in Figure A-6) it can be shown that the only stresses that contribute to crack stress intensity factor are those acting in regions where the crack remains open. As a corollary, if closure is not accounted for, stress intensity factors may be underestimated, and in some cases they may be predicted to be negative or zero when in fact they are positive.

Beghini and Bertini [17] present a methodology for accounting for crack closure under the assumption of elastic deformation of the crack face. This methodology has been implemented in this study. Because the methodology is iterative in nature and requires a substantial computational effort, it is not applied for the simulation base case. A sensitivity study is presented later to demonstrate the effect of crack closure on leakage probability.

A second special consideration for crack growth near a compressive surface stress is “balloon” crack growth: growth of PWSCC below the treated surface where the flaw is modeled to grow in length along the surface under the influence of the residual stresses existing prior to peening. In this manner, the tendency of the crack to change shape and grow in length a greater extent below the surface may be investigated while still using the standard semi-elliptical surface flaw shape.

To assess balloon-shaped growth, analyses were conducted using the finite element software FEA Crack to produce high fidelity predictions for crack growth, allowing for non-semi-elliptical growth (e.g., growth resembling a balloon), as seen in Figure A-7. (While the FEA Crack program simulates fatigue crack growth, advancing the crack front over load cycles instead of time, the resultant shape progression is reflective of the advancement of a PWSCC flaw.) The crack shape results of these analyses were compared to two limiting cases; the first case did not allow crack length growth while the second allowed crack length growth uninhibited by peening. An example comparison of crack front shapes predicted using the different methods is shown in Figure A-8. As expected, the balloon growth approximation bounds the length of the FEA predicted crack shape, given the same crack depth.

In a related study [18], it is demonstrated that crack growth below a PWSCC resistant weld inlay may be closely approximated by assuming a semi-elliptical shape below the inlay, driving growth with the deepest and surface points of sub-inlay portion of the crack (referred to as “idealized crack growth”). The idealized crack growth results in accurate time to through-wall crack growth relative to the actual crack growth predicted with FEA.

Considering these results, the “balloon” crack growth phenomenon is approximated conservatively by allowing crack length growth independent of peening (i.e., using only the pre-peening stresses). A sensitivity study is presented later to demonstrate the effect of this alternative crack growth approach.

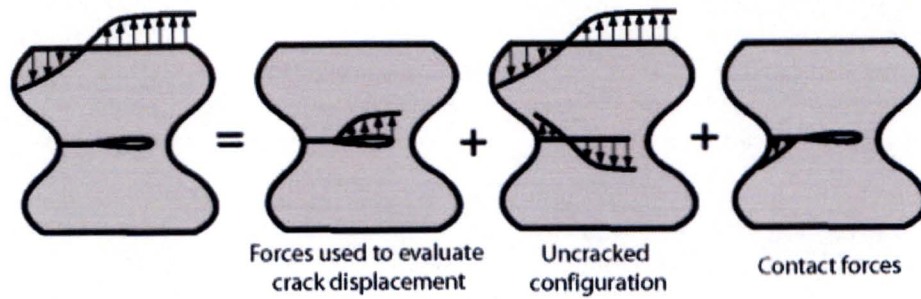


Figure A-6
Demonstration of Stresses Superposition for Partially Closed Crack

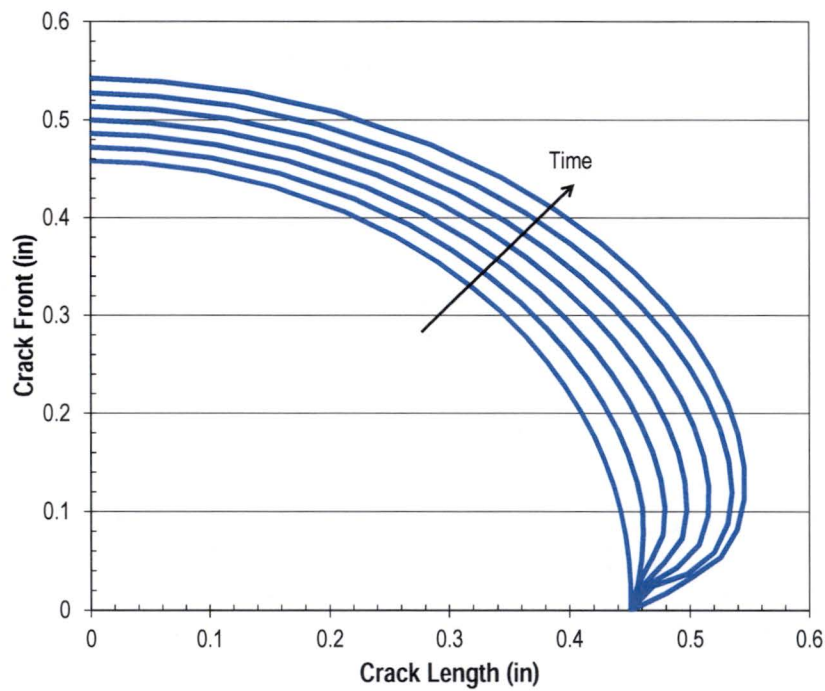


Figure A-7
Example of "Balloon" Crack Growth over Time Calculated with FEA Crack

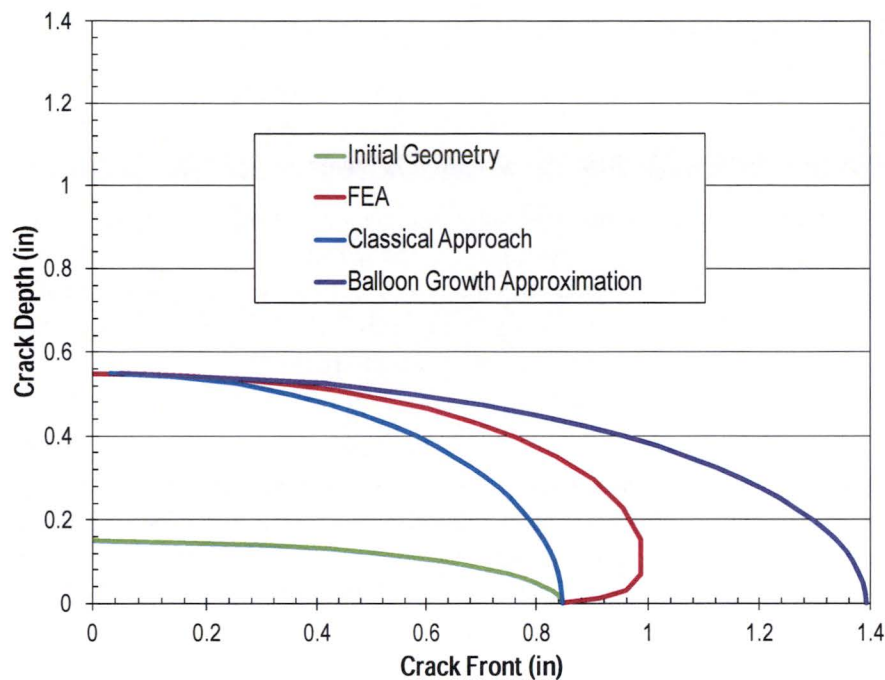


Figure A-8
Example of Crack Front Shapes Predicted in a Peened Component with: a) FEA, b)
Classical Analytical Methods, or c) the Balloon Growth Approximation (Repeat of Figure
5-3)

A.6 Examination Model

This section describes the models applied to simulate ultrasonic examinations of DM welds. This study uses probability of detection (POD) curves to estimate the likelihood of a crack being detected, given its size. These models are essential for predicting leakage probabilities since cracks that lead to leaks are often those that go undetected during one or more scheduled examinations.

Section A.6.1 discusses how examinations are scheduled, before and after peening. Section A.6.2 describes the inspection models, i.e., how POD is calculated, factoring for the geometry of the crack. Finally, Section A.6.3 describes the detection and repair modeling rules.

A.6.1 Examination Scheduling

UT examination scheduling for DM welds (prior to peening) is required per ASME Code Case N-770-1 [19]. Specifically, a Performance Demonstration Initiative (PDI) qualified volumetric inspection is required once every five years for unmitigated hot leg DM welds and once every seven years for hot leg cold leg DM welds. The time of the first modeled UT inspection is set by the user.

When peening is applied, different examination scheduling requirements and options are included in the model. First, during the peening application outage, immediately prior to peening, a UT inspection can be modeled to simulate a pre-peening inspection.

A follow-up UT examination is included before entering the relaxed in-service inspection (ISI) schedule. In the comparative studies presented later, the follow-up inspection time is varied between 1, 2, or 3 cycles after the peening application for the RVON and 1, 2, 3, or 6 cycles after the peening application for the RVIN. Conservatively, the second follow-up UT examination for the RVON is not credited, and the new ISI schedule is entered after the first follow-up.

After the follow-up examination, a new ISI schedule is used. The central goal of this probabilistic modeling effort is to demonstrate that the ISI inspection interval after peening can be elongated compared to N-770-1 requirements without increasing the probability of leakage over the entire plant service life. Accordingly, several different ISI intervals will be tested after peening and compared to predictions for unmitigated components.

A.6.2 Inspection Modeling

For modeling UT inspections of cracks in DM welds, a modified version of the POD model from MRP-262R1 [20] will be used. This model is based on POD data for inspections of realistic DMW mockups containing well-characterized, representative cracks. However, the POD model applied in this probabilistic assessment assumes a POD of zero for flaws less than 10% through-wall.

The modified MRP-262R1 model from is comprised by a POD curve that is a function of the through-wall fraction of the crack, as given in the following equation:

$$POD\left(\frac{a}{t}\right) = \begin{cases} 0 & 0 \leq \frac{a}{t} < 0.1 \\ \frac{e^{\beta_1 + \beta_2\left(\frac{a}{t}\right)}}{1 + e^{\beta_1 + \beta_2\left(\frac{a}{t}\right)}} & 0.1 \leq \frac{a}{t} \leq 1 \end{cases} \quad [A-44]$$

where β_1 and β_2 are fit parameters determined by regression analysis of inspection data from the mockups containing circumferential flaws. The specific values of these fit parameters are given in Section A.8.4. The resulting set of POD curves is demonstrated in Figure A-9.

The model defined in Equation [A-44] is based on experiments which included circumferential cracks only. Experience gathered during UT detection qualification suggests that POD may be lower in general for axial cracks. Accordingly, for axial cracks, an optional POD reduction factor, $f_{UT,axial}$, may be applied to the POD predicted by Equation [A-44].

The model defined in Equation [A-44] is based on experiments including cracks ranging from 10% to 100% through-wall. As the data documented in MRP-262R1 do not include flaws shallower than 10% of the wall thickness, a POD of zero is conservatively applied for cracks with depths less than 10% through-wall. (The model also includes the ability to linearly extrapolate the POD between the origin, i.e. 0% POD for an infinitesimal crack, and the POD given by Equation [A-44] for a 10% through-wall crack; this option is invoked in a sensitivity case.)

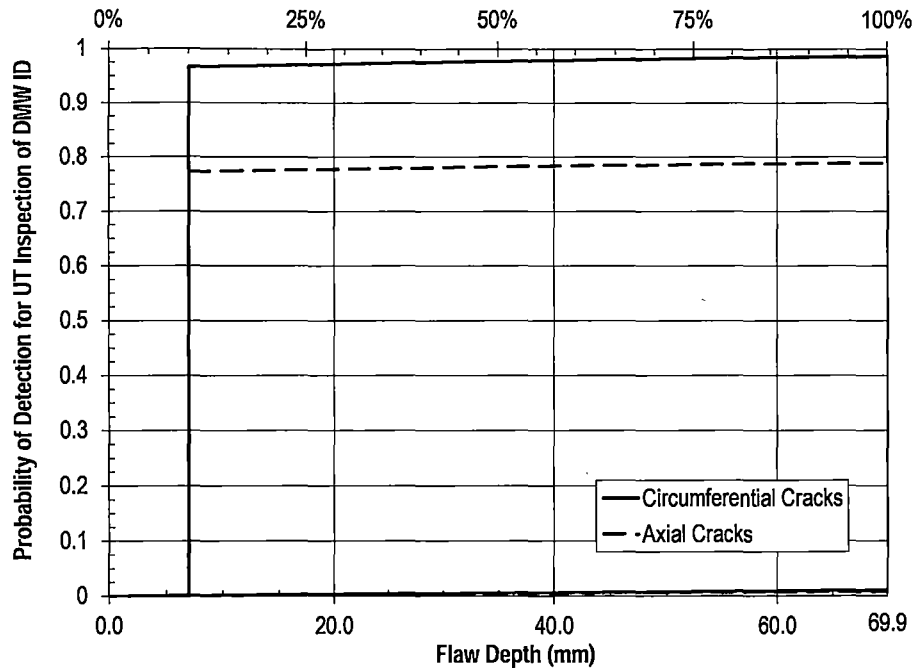


Figure A-9
Mean Assumed UT Inspection POD Curve for DMW Cracking from the ID

A.6.3 Detection and Repair Modeling

After a POD has been calculated, given the size of the crack of interest, detection may be simulated by sampling a random value between zero and one, referred to as the detection sample. If the detection sample is less than or equal to the POD, the crack is predicted to be detected; if not, the crack is predicted to be undetected for the current examination.

If the detection sample is sampled independently of previous samples, it reflects the premise that inspection success is uncorrelated, from examination to examination. Alternatively, the examination model allows for the correlation of successive detection samples for a given flaw. This is equivalent to assuming that each crack has some ambiguous features which may make it harder or easier to detect than the general population.

Credit can be taken for the condition that the unit(s) of interest have had no flaw detections before some user-defined past inspection time. If a flaw is predicted to be detected before this user-defined past inspection time, the Monte Carlo realization is rejected and repeated with newly sampled inputs. If a flaw is predicted to be detected after this past inspection time, that flaw is repaired (removed entirely from the flaw site), but the DM weld component stays in service and other flaws remain active.

A.7 Through-Wall Flaw (Leakage) Criterion

At the end of each Monte Carlo realization, the probabilistic model discussed in this report stores a limited number of metrics related to the extent of flaw growth and the repair status of the weld, including the timing of related events. Most importantly, during each realization, the code tracks

if at least one flaw reaches through-wall crack growth (i.e., leakage) and, if so, the number of the cycle of the first through-wall crack growth.

Similar to detection, credit can be taken for the condition that the unit(s) of interest have had no leakages before some user-defined past inspection time. If a flaw is predicted to grow through-wall before this user-defined past inspection time, the Monte Carlo realization is rejected and repeated with newly sampled inputs, and the leak is not counted toward the metric discussed above.

Flaws modeled using the xLPR tool are able to reach through-wall crack growth either by propagating through the entire thickness of the component wall or by net section collapse of a critical surface flaw. Specifically, if the xLPR tool determines that the bending load on a given surface flaw exceeds the calculated net section collapse bending load, the surface flaw will transition to a through-wall flaw. For simplicity, the probabilistic model described in this report does not address the net section collapse failure mode and a given flaw may only reach through-wall crack growth if it propagates through the entire thickness of the wall before it is repaired.

A.8 Probabilistic Model Inputs

The probabilistic modeling framework for DMWs accepts both deterministic and distributed inputs. The values of the deterministic inputs are constant for every Monte Carlo realization. The values of the distributed inputs are determined by sampling probability distributions (e.g., normal distribution, log-normal distribution, triangular distribution, etc.) during each Monte Carlo realization. The probabilistic model accepts an array of eight inputs that is used to define the distribution of each distributed input. Each input array contains the following information:

- The value of the parameter to be used when conducting deterministic assessments;
- The distribution type to be sampled during probabilistic assessments (e.g., normal distribution);
- Parameter values defining the distributions (up to four, e.g., the mean and standard deviation of a normal distribution);
- Lower and upper truncation limits used to impose bounds on the sampled values.

The inputs selected for use in the probabilistic model are discussed in Section A.8.1 through A.8.5. All inputs to the probabilistic model for the reactor vessel outlet nozzle (hot leg, RVON) and reactor vessel inlet nozzle (cold leg, RVIN) are tabulated in this section.

A.8.1 Component Geometry, Operating Time, Temperature, and Loads

The choice of inputs for component geometry, operating time, temperature, and component loading are discussed in this section. These inputs are given for two component cases for which results will be presented: a reactor vessel outlet nozzle (hot leg) in a Westinghouse plant and a reactor vessel inlet nozzle (cold leg) in a Westinghouse plant. These inputs are tabulated in Table A-2.

A.8.1.1 Component Geometry

The component specific parameters (i.e., wall thickness, outer diameter, and weld width) were taken as deterministic inputs. The values selected are for the outer diameter and the wall thickness are based on information provided in MRP-44, Part 1 [21] and are given in Table A-2.

A.8.1.2 Operating Time

Both DM weld components are simulated from plant startup until the end of the plant operational service period. This is considered to occur approximately 80 years after startup (i.e., a 40-yr original license and two 20-yr license renewals). Cumulative statistics are provided at the end of the plant operational service period.

Both DM weld components are simulated with 18-month operating cycles at a capacity factor of 0.97. These values are representative of U.S. PWRs.

As discussed in the modeling sections, credit can be taken for the fact that the simulated component has not experienced leaks or repairs before some user-defined outage. Monte Carlo realizations that predict leaks or repairs before the user-defined outage are rejected and rerun with new samples. As defined in Section A.9, average leakage frequencies and cumulative probabilities of leakage are averaged over the total number of Monte Carlo realizations that are active (have not yet leaked) following the hypothetical time of peening.

As a sensitivity case, a user-defined outage (before which no leaks or repairs have occurred) will be set. All statistics presented in this study apply conditionally to Alloy 182 reactor vessel outlet/inlet nozzles that have experienced no leaking or repairs to date, but otherwise have characteristics similar to those defined in Table A-2. For this sensitivity case, the number of rejected and rerun Monte Carlo realizations is reported, which provides further insight on this modeling assumption.

A.8.1.3 Temperature

Uncertainty in the component temperature is incorporated into the model by using a normal distribution. The temperature distributions used for the RVON and RVIN base cases are included in Table A-2. The means of these distributions reflect bounding reactor hot-leg and cold-leg temperatures for U.S. PWRs. The uncertainty in the temperatures represents a number of factors including temperature streaming and measurement uncertainty. The standard deviations have been selected such that the 95% confidence band is $\pm 5.1^{\circ}\text{C}$ ($\pm 9.2^{\circ}\text{F}$) for the RVON and $\pm 1^{\circ}\text{C}$ ($\pm 1.8^{\circ}\text{F}$) for the RVIN.

A.8.1.4 Loads

The input parameters specific to the DM weld loading are summarized in Table A-3 and are further discussed below.

Relevant operational loads are taken as deterministic inputs. The values selected are considered to be representative of the loads in the actual components as described in MRP-307 [22]. Additionally, a tensile axial load of 100 kips (445 kN) was assumed (in addition to the axial pressure stresses). The loads applied to DM welds documented in this report bound those

documented in a NRC hot leg flaw evaluation summary [23]. Sensitivity studies are included to explore more extreme loading conditions.

Welding residual stresses are modeled stochastically. Uncertainty is incorporated into the calculation of welding residual stresses by setting distributions for parameters used to characterize and constrain the WRS profiles (Equations [A-9] through [A-16] present the constraint equations for the axial and circumferential WRS profiles). For the axial stress profile, the distributed inputs are the ID stress, the through-wall depth where the stress changes sign (from tensile to compressive) and ratio of the OD stress to ID stress. For the hoop stress profile, the distributed inputs are the ID stress, the location of the minimum stress, the ratio of the minimum stress to the ID stress, and the ratio of the OD stress to the ID stress.

The distributions for the parameters of the axial and hoop stress profiles are included in Table A-3. The distributions for the axial stress profile parameters are taken from the xLPR pilot study. The distributions for the hoop stress profile parameters were determined iteratively by using random sampling to generate a family of curves which adequately captured the uncertainty in the data as well as uncertainty due to missing data [22]. The truncation limits are used to prevent the use of unrealistic stress profiles.

Table A-2
Summary of General Inputs

Symbol	Description	Source	Units	Parameter Type	DMW Base Case
	Total number of trials	Convergence Study	# trials		1.00E+07
	Number of operating cycles	Selected to yield desired cumulative operating time	-	RVON	53
				RVIN	53
	Nominal cycle length	Representative cycle length at Westinghouse plant	years	RVON	1.5
				RVIN	1.5
CF	Operating capacity factor	Representative capacity factor for U.S. PWR	-	RVON	0.97
				RVIN	0.97
	Cycle of first UT inspection	Based on typical operating reactor service histories	Cycle number	RVON	14
				RVIN	15
	Pre-peening UT inspection interval	ASME Code Case N-770-1	# cycles	RVON	3
				RVIN	4
T	Operating temperature of RVON-DMW	Maximum Westinghouse hot leg operating temperature	°F	type	Normal
				mean	625.0
				stdev	4.6
				min	597.4
				max	652.6
	Operating temperature of RVIN-DMW	Maximum Westinghouse cold leg operating temperature	°F	type	Normal
				mean	563.0
				stdev	0.9
				min	557.5
				max	568.5
t	Wall thickness of RVON-DMW	Representative component thickness for Westinghouse plants	in.	RVON	2.75
	Wall thickness of RVIN-DMW			RVIN	2.75
D _o	Outer diameter of RVON-DWM	Representative component OD for Westinghouse plants	in.	RVON	35.5
	Outer diameter of RVIN-DWM			RVIN	35.5
w	Width of RVON-DMW	Representative weld width for Westinghouse plants	in.	RVON	1.75
	Width of RVIN-DMW			RVIN	1.75

Table A-3
Summary of Loading Inputs for DMW Model

Symbol	Description	Source	Units	Parameter Type	DMW Base Case
P_{op}	Normal operating pressure	Representative of U.S. PWRs	ksi		2.248
F_x	Effective loads for RVON-DMW (including deadweight, thermal expansion, and thermal stratification loading)	Representative reactor vessel nozzle loads for Westinghouse plant	kips		100
M_x			in-kips		0
M_y			in-kips		40000
M_z			in-kips		0
F_x	Effective loads for RVIN-DMW (including deadweight, thermal expansion, and thermal stratification loading)	Representative reactor vessel nozzle loads for Westinghouse plant	kips		100
M_x			in-kips		0
M_y			in-kips		40000
M_z			in-kips		0
σ_{0WRsa}	Weld residual axial stress on ID surface	xLPR Pilot Study	ksi	type	Normal
				mean	43.55
				stdev	15.95
				min	21.75
				max	79.91
X_c	Fractional through-thickness at which weld residual axial stress profile crosses zero	xLPR Pilot Study	-	type	Normal
				mean	0.25
				stdev	0.05
				min	0.125
				max	0.50
f_{WRsa}	Random scaling factor for weld residual axial stress on OD surface	xLPR Input	-	type	Uniform
				min	0.5
				max	1.0
σ_{0WRsh}	Weld residual hoop stress on ID surface	xLPR Pilot Study	ksi	type	Normal
				mean	43.55
				stdev	15.95
				min	21.75
				max	79.91
f_{WRsh1}	Random scaling factor for minimum weld residual hoop stress	Iterative random sampling, see Section A.8.1.4	-	type	Normal
				mean	0.50
				stdev	0.10
				min	0.25
				max	0.75
f_{WRsh2}	Random scaling factor for weld residual hoop stress on OD surface	Iterative random sampling, see Section A.8.1.4	-	type	Normal
				mean	1.00
				stdev	0.075
				min	0.80
				max	1.20
X_{min}	Fractional through-thickness at which weld residual hoop stress is minimum	Iterative random sampling, see Section A.8.1.4	-	type	Normal
				mean	0.50
				stdev	0.075
				min	0.40
				max	0.75

A.8.2 Crack Initiation Model

The set of inputs for the DM weld PWSCC initiation model is described in Table A-4 at the end of this section. Various inputs are detailed in the following subsections.

A.8.2.1 Industry Inspection Data used to Develop Initiation Model

The following plant inspection data for piping to nozzle DM welds fabricated from Alloys 82 and 182 were used in the Weibull initiation model development:

- Pressurizer safety/relief nozzles, spray nozzles, surge nozzles;
- Reactor hot leg piping surge nozzles, decay heat nozzles, drain nozzles, reactor vessel outlet nozzles, steam generator inlet nozzles, and shutdown cooling nozzles;
- Reactor cold leg piping letdown drain nozzles, core flood nozzles, high-pressure injection nozzles, reactor coolant pump (RCP) suction and discharge nozzles, inlet nozzles, and safety injection nozzles.

Table A-5 shows the list of PWR piping DM welds in which indications of cracking were detected that was used for this analysis. The data were compiled from industry documents (primarily documents from the NRC website such as LERs) using Table E-1 of MRP-216 [24] as a guide. Please note the following regarding Table A-5:

- All of the data are for U.S. plants
- No exhaustive effort was made to include all inspections of PWR piping DM welds that resulted in no indications being reported. This conservatively results in a higher probability of crack initiation than would have been the case if additional inspections were considered.
- The 20 welds given in Table A-5 were evaluated in detail and are considered either to be representative of service-induced cracking or it was not possible to rule out the presence of service-induced cracking (as opposed to fabrication-related defects, etc.). The remaining nozzles without indications are treated as suspended items [10] in the Weibull analysis.

Size data for PWSCC indications presented in Table A-5 were collected from the following sources:

- Table E-1 in MRP-216R1 [24]
- Licensee Event Reports to the NRC
- Other documents from the NRC (such as ASME Code Section Flaw Evaluations, Special Inspections, Issuance of Relief from Code Requirements, etc.)

Operating EFPYs at the time of inspection were taken from the EPRI steam generator degradation database, and operating temperatures were based on various sources.

Some of the welds inspected were without indications of cracking and are treated as suspended items. Specifically, a given weld that was found not to have any indications of cracking during its most recent inspection is modeled to have been removed from the statistical population at the time of the most recent inspection. The inspection data given in Table A-5 represent a summary of the detected flaws, which are part of what is known as a censored sample. For a Weibull distribution with a censored sample (i.e., failure data plus suspension data), it is necessary to account for the suspension times within the data set. Using the censored data set, it is possible to include the effect of the effective operating times of the uncracked components.

A.8.2.2 Weibull Fitting Procedure for Time of First Initiation

After adjusting the operating time data for the effect of operating temperature using the Arrhenius adjustment, the values of the Weibull parameters, β and θ , were determined using a maximum likelihood estimator (MLE) statistical procedure [10] fit to the PWR dissimilar metal

weld experience. The MLE procedure is preferred over a least-squares fitting procedure in the case that limited cracking experience is available.

For the particular case of a Weibull distribution with a censored sample (i.e., failure data plus suspension data), the maximum likelihood estimates of the Weibull parameters β and θ may be determined by simultaneously solving the following equations:

$$\frac{\sum_{i=1}^n x_i^{\beta^*} \ln x_i}{\sum_{i=1}^n x_i^{\beta^*}} - \frac{1}{r} \sum_{i=1}^r \ln x_i - \frac{1}{\beta^*} = 0 \quad [\text{A-45}]$$

$$\theta^* = \left(\frac{\sum_{i=1}^n x_i^{\beta^*}}{r} \right)^{\frac{1}{\beta^*}} \quad [\text{A-46}]$$

where

- β^* = maximum likelihood estimate of β
- θ^* = maximum likelihood estimate of θ
- x_i = operating time of component i
- n = number of components in the population
- r = number of failures

Components censored at times t_i are assigned values $x_{r+i}=t_i$. Thus, the second term in Equation [A-45] sums the logarithms of the failure times only. The values of β^* and θ^* may be found using an iterative procedure.

A least squares fitting procedure may also be used to determine the values of the Weibull slope and characteristic time parameters. This procedure consists of fitting the available data to the linearized representation of the Weibull distribution (see Equation [A-47]) using a least squares analysis.

$$\ln(-\ln(1-F)) = \beta \ln(t) - \beta \ln(\theta) \quad [\text{A-47}]$$

$$y = mx + c$$

Specifically, a plot of F versus t on a double log-log plot yields a line with slope β . The value of θ may then be determined using the values of β and the vertical intercept (referred to here as c) obtained from the fit.

A.8.2.3 Analysis Results for Time of First Initiation

Figure A-10 shows an example MLE Weibull distribution fit to the industry experience with DM welds fabricated from Alloys 82 and 182 given in Table A-5. The failure and suspension times were adjusted to a common reference temperature of 600°F (315°C) using a thermal activation energy of 44.0 kcal/mole (184 kJ/mole) (the mean value given in Section A.8.2.10).

Table A-7 summarizes the MLE fit parameters of the Weibull analysis. Also included in Table A-7 are the standard errors in the Weibull fit parameter, β , and the vertical intercept of the linearized model determined from the linear least squares fit (which is used to determine the value of θ).

It is noted that for simplicity, the standard errors of the linear least squares parameters are presented instead of the MLE parameter values. It is also noted that the standard error in the vertical intercept of the linearized Weibull fit (referred to here as σ_c) is presented because it is used during runtime to account for the uncertainty in the value of the anchor point time, t_1 , as discussed later.

A.8.2.4 Uncertainty in First Initiation Time Weibull Slope

The uncertainty in the Weibull slope, β , is modeled with a normal distribution having the mean and standard deviation given in Table A-7. The mean was selected as the value calculated using the MLE fitting procedure and for simplicity, the standard deviation was selected as the standard parameter error determined using the least squares fitting procedure. Based on the similarity of the Weibull slopes calculated using the two methods, this simplification is considered reasonable.

A.8.2.5 Uncertainty in Anchor Point Time (t_1)

Based on data presented in Figure A-10, a value of 0.01 was selected as the value of the arbitrary failure fraction, F_1 . Figure A-10 shows that this failure fraction provides a reasonable representation of the earlier failures observed in the field, which will provide a more realistic set of Weibull curves defined by random sampling during the Monte Carlo analysis. That is, appropriately selecting the value of F_1 (which in combination with the Weibull slope and characteristic life determines the mean value of the anchor point time, t_1) will reduce the probability that the initiation model will greatly under-predict or over-predict (relative to observed plant experience) the initiation time of the first flaw during a given Monte Carlo realization.

The value of t_1 is determined by solving Equation [A-30] for time at a failure fraction of F_1 and the mean values of the Weibull parameters, β and θ , given in Table A-7.

Uncertainty in the anchor point time is incorporated for each Monte Carlo realization using the following procedure:

- Determine the characteristic time, θ , using the value of F_1 and the deterministic values of β and t_1 .
- Determine the mean intercept parameter, c , using the deterministic value of β and the value of θ determined in the previous step.

- Sample the value of c from a normal distribution using the mean intercept parameter determined in the previous step and the standard error (σ_c) given in Table A-7.
- Determine the anchor point time for the current trial using the sampled value from the previous step and the deterministic value of β .

A.8.2.6 Uncertainty in the Multiple Flaw Weibull Model

As discussed in the modeling section, a second Weibull model is used to predict the initiation of multiple flaws on a single component. The key inputs to this model are the Weibull slope and the empirical stress exponent.

Based on analysis of laboratory data, an empirical stress exponent, n , of about 4 is often assumed to describe the stress dependence of the initiation of PWSCC in Alloy 600 [25]. For this study, this exponent value is inherited for modeling PWSCC initiation in Alloy 82/182. A normal distribution with a mean of 4.0 standard deviation of 1.0 is employed to incorporate the uncertainties due to material and manufacturing disparities. A lower truncation bound of 0.0 is used to prevent the unphysical trend of earlier initiation for lower tensile surface stresses.

The Weibull slope of the multiple flaw model, β_{flaw} , quantifies the rate at which flaws occur after the initiation of the first flaw. An analytical data fitting procedure, as done for the first initiation time model, was not considered appropriate to fit β_{flaw} given the modeling complexities involved in sampling multiple flaw initiation times. Instead, a mean value of 2.0 was selected for β_{flaw} . This value has a precedent in probabilistic modeling of SCC in steam generators [25]. A normal distribution with a mean of 2.0 and a standard deviation of 0.5 is employed to incorporate uncertainties due to material and manufacturing disparities. A lower truncation bound of 1.0 was selected to prevent a multiple flaw Weibull model in which the PWSCC initiation rate decreases over all time.

A numerical experiment was run with a value of 2.0 for β_{flaw} in order to demonstrate the resulting number of cracks per component, given the parameter and stress distributions discussed throughout this Section A.8. Figure A-11 depicts the resulting distribution of number of flaws in components with at least a single flaw, at 20 EFPY, given an operating temperature of 625°F. The average number of flaws at 20 EFPY, given that at least a single flaw exists, is 3.3.

Industry experience listed in Table A-5 shows that there have been up to five detected cracking indications on a single hot leg DMW component, with the average close to 1.5 indications per component with at least a single flaw. These values are regarded as low given the existence of small cracks that have not been identified. Accordingly, the results given in the numerical study are not considered excessively conservative.

A.8.2.7 Uncertainty in Flaw Orientation

Flaw orientation is not directly controlled with a probability distribution. Rather, the stress adjustment together with the surface stress distributions dictates the ratio of flaw orientations.

A.8.2.8 Uncertainty in Initial Flaw Depth

The initial flaw modeled within the simulation is assumed to be of engineering scale. The initial flaw is the result of both initiation processes and early growth processes (for which growth is

driven by stress intensity factor). This approach bypasses the early stages of growth when coalescence of micro-fissures is especially important. Moreover, the initiation predictions are based on empirical plant experience for detected flaws, which are all of engineering scale, i.e., at least 1 to 2 millimeters in depth.

A log-normal distribution with a median of 5% of through-wall was selected to model the uncertainty in the initial flaw depth. The log-normal distribution conservatively provides greater weight for the upper end of the initial depth distribution (i.e., a long tail). The 95% confidence bound of the distribution was set to an initial depth of 9% through-wall. The log-normal standard deviation was determined using the median and 95% confidence bound values specified above.

A lower truncation limit was defined to prevent the initiation of very small flaws for which the stress intensity factor (based on the input distributions of the surface welding residual stress and other sources of normal operating stress) would be significantly less than the lower bound of stress intensity factors (about $20 \text{ MPa}\cdot\text{m}^{1/2}$ or $18 \text{ ksi}\cdot\text{in}^{1/2}$) evaluated in the laboratory studies used to define the flaw propagation models given in MRP-115 [11] for Alloys 82 and 182.

The sensitivity results section presents a study in which the flaw through-wall fraction distribution is scaled down such that cracks initiate approximately 10 times smaller. This is included to assess the potential effect on leakage probability of smaller cracks not being identified during inspections prior to entering the relaxed inspection schedule after peening.

A.8.2.9 Uncertainty in Flaw Aspect Ratio

The distributions of the initial aspect ratios of axial and circumferential flaws were determined from the population of in-service inspection data discussed in A.8.2.1. The aspect ratio of a given flaw was calculated by dividing its total length by its depth. These data were used to determine approximate distributions of the axial and circumferential initial aspect ratios.

A log-normal distribution was selected to model the uncertainty in the initial aspect ratio of both circumferential and axial flaws because they provide reasonable fits to the aspect ratio data given in Table A-6. The parameter values defining these distributions are given in Table A-4.

A.8.2.10 Uncertainty in Temperature Effect

Uncertainty in the apparent activation energy for PWSCC crack initiation is treated by defining a distributed input. As shown in Table A-4, a normal distribution is assumed to describe the uncertainty in the activation energy.

An activation energy of 209.4 kJ/mole is a standard value applied for the initiation of PWSCC in Alloy 600 components [26]. This value is based on evaluations of PWSCC in Alloy 600 steam generator tubing [27]. A lower, experimentally determined value of 184.2 kJ/mole (44 kcal/mole) was determined for Alloy 600 CRDM nozzle (i.e., thick-wall) material [28]. Activation energies ranging from 125.6 kJ/mole (30 kcal/mole) to 201.0 kJ/mole (48 kcal/mole) were reported in a review of laboratory and field data [27]. Due to similarities in the compositions of Alloy 82/182 and Alloy 600 wrought material, 184.2 kJ/mole was selected as the mean of the distribution and the standard deviation was selected such that the 95% confidence bound of the distribution would be 209.4 kJ/mole (50 kcal/mole).

Table A-4
Summary of Inputs for DM Weld Initiation Model

Symbol	Description	Source	Units	Parameter Type	DMW Base Case
t_1	Time at which failure fraction F_1 is reached	See Section A.8.2.5	EDY	type	Normal
				mean	11.40
				stdev	0.304
				min	3.14
				max	41.10
σ_c	Standard error in intercept of linearized Weibull fit	See Section A.8.2.3	ln(EDY)		0.304
F_1	Arbitrary failure fraction selected to define Weibull PWSCC initiation function	See Section A.8.2.5	-		0.010
β	Weibull slope for PWSCC flaw initiation	See Section A.8.2.3	-	type	Normal
				mean	1.419
				stdev	0.082
				min	0.927
				max	1.911
N_{crack}	Number of circumferential locations for crack initiation	xLPR Pilot Study	-		19
β_{flaw}	Weibull slope for PWSCC multiple flaw initiation	Based on representative value for formation of PWSCC at multiple locations in industry SGs	-	type	Normal
				mean	2.0
				stdev	0.5
				min	1.0
				max	5.0
ρ_{weld}	Correlation coefficient between PWSCC initiation and propagation rates for all cracks in Alloy 82/182 weld	xLPR Input	-		0.0
ρ_{wv}	Correlation coefficient between PWSCC initiation and propagation rates for individual crack	xLPR Input	-		0.0

Table A-4 (continued)
Summary of Inputs for DM Weld Initiation Model

Symbol	Description	Source	Units	Parameter Type	DMW Base Case
Q_i	Thermal activation energy for PWSCC flaw initiation	Distribution based on laboratory data and experience with Weibull analysis	kcal/mole	type	Normal
				mean	44.03
				stdev	3.06
				min	25.65
				max	62.41
$T_{ref,i}$	Reference temperature to normalize PWSCC flaw initiation data	Temperature used to adjust flaw initiation data assessed in this report	°R		1060
n	Exponent for surface stress adjustment to initiation time	EPRI TR-104030	-	type	Normal
				mean	4.0
				stdev	1.0
				min	0.0
				max	10.0
a_0/t	Initial depth assigned to newly initiated flaw	Based on expected performance of UT inspection technique	-	type	Log-Normal
				linear μ	0.053
				median	0.050
				log-norm μ	-3.00
				log-norm σ	0.35
				min	0.01
AR_{circ}	Initial aspect ratio assigned to newly initiated circumferential flaw	Flaw initiation data from operating experience	-	max	0.42
				type	Log-Normal
				linear μ	11.28
				median	8.66
				log-norm μ	2.159
				log-norm σ	0.727
AR_{ax}	Initial aspect ratio assigned to newly initiated axial flaw	Flaw initiation data from operating experience	-	min	0.110
				max	679.7
				type	Log-Normal
				linear μ	3.44
				median	1.74
				log-norm μ	0.554
				log-norm σ	1.167
				min	0.0016
				max	1912.2

Table A-5
Summary of PWSCC Experience in U.S. PWR Piping Nozzle Dissimilar Metal Welds

Plant	Component Type	Inspection Operating Time (EFPY)	Operating Temp. (°F)	Orientation	Wall Thickness (in.)	Number of Axial PWSCC Indications	Largest Axial PWSCC Indication				Number of Circ PWSCC Indications	Largest Circumferential PWSCC Indication			
							Axial Indication Depth (a, in.)	Axial Indication Total Length (2c, in.)	Axial Indication a/t	Axial Indication Aspect Ratio (2c/a)		Circ Indication Depth (a, in.)	Circ Indication Total Length (2c, in.)	Circ Indication a/t	Circ Indication Aspect Ratio (2c/a)
Plant A	Safety Relief	23.1	653	Axial	1.3	1	0.10	0.60	8%	6.00					
Plant B	Safety Relief	19.2	653	Axial	1.40	1	1.23	0.40	88%	0.32					
Plant C	Surge	21.9	653	Axial+Circ	1.5	1	0.31	0.50	20%	1.61	1	0.51	~3	33.0%	5.88
Plant D	Spray	13.9	653	Axial	0.89	1	0.21	0.25	24%	1.17					
Plant E	Relief (Note 1)	10.0	643	Circ	0.44						1	0.44	3.50	100.0%	7.99
Plant F	Surge	17.9	653	Circ	1.5						3	0.45	4.03	31.0%	8.97
Plant F	Safety Relief	17.9	653	Circ	1.3						1	0.30	2.51	22.5%	8.44
Plant F	Safety Relief	17.9	653	Circ	1.4						1	0.34	7.69	25.8%	22.61
Plant A	HL Surge	23.1	597	Circ	1.6						1	0.40	2.40	25.0%	6.00
Plant G	HL Surge	19.2	601	Axial	1.3	1	0.59	(Note 2)	45%	(Note 2)					
Plant A	HL Drain	23.1	597	Circ	0.5						1	0.10	0.45	19.0%	4.50
Plant H	HL Drain	21.7	597	Axial	0.6	2	0.39	(Note 3)	70%	(Note 3)					
Plant I	Decay Heat	21.6	601	Circ	1.3						1	0.90	10.00	68.6%	11.11
Plant J	Decay Heat	19.2	605	Axial	1.3	1	1.25	1.75	100%	1.40					
Plant K	RPV Outlet	20.2	605	Circ	2.62						1	0.63	2.06	24.2%	3.25
Plant L	RPV Outlet	16.5	621	Axial	2.9	2	0.6	0.96	21%	1.6					
Plant M	RPV Outlet	15.6	621	Axial	~2.5	1	2.5	2.5	100%	1.0	1	0.20	2.00	8%	10.00
Plant N	SG Inlet	26.6	620	Axial	4.66	5	4.1	2.0	88%	0.5					
Plant H	CL Drain	21.7	545	Circ	0.6						1	0.06	0.63	10%	11.21
Plant J	CL Drain	17.6	555	Axial	0.6	1	0.06	≥ 0.25	7%	≥ 4.46					

Notes:

(1) PWSCC indication was located in heat affected zone of an Alloy 600 safe end.

(2) Indication reported to extend over the width of weld metal.

(3) Indication length not available.

Table A-6
Summary of PWSCC Experience in U.S. PWR Piping Nozzle Dissimilar Metal Welds Used to Define Initial Flaw Aspect Ratio

Plant	Component Type	Inspection Operating Time (EFPY)	Operating Temp. (°F)	Orientation	Wall Thickness (in.)	Number of PWSCC Indications	Indication Depth (a, in.)	Indication Total Length (2c, in.)	Indication a/t	Indication Aspect Ratio (2c/a)
Plant A	Safety Relief	23.1	653	Axial	1.3	1	0.10	0.60	8%	6.00
Plant C	Surge	21.9	653	Circ	1.5	1	0.51	~3	33.0%	5.88
Plant D	Spray	13.9	653	Axial	0.89	1	0.21	0.25	24%	1.17
Plant F	Surge	17.9	653	Circ	1.5	3 (1)	0.45	4.03	31.0%	8.97
Plant F	Surge	17.9	653	Circ	1.5	3 (2)	0.36	2.22	25.0%	6.17
Plant F	Safety Relief	17.9	653	Circ	1.3	1	0.30	2.51	22.5%	8.44
Plant F	Safety Relief	17.9	653	Circ	1.4	1	0.34	7.69	25.8%	22.61
Plant A	HL Surge	23.1	597	Circ	1.6	1	0.40	2.40	25.0%	6.00
Plant I	Decay Heat	21.6	601	Circ	1.3	1	0.90	10.00	68.6%	11.11
Plant L	RPV Outlet	16.5	621	Axial	2.9	2	0.6	0.96	21%	1.6
Plant M	RPV Outlet	15.6	621	Circ	~2.5	1	0.20	2.00	8%	10.00
Plant H	CL Drain	21.7	545	Circ	0.6	1	0.06	0.63	10%	11.21

Table A-7
Summary of Weibull Distribution Parameter Fitting Results for DMW Analysis

Fitting Method	β	θ (EDY)	Standard Error in Weibull Slope	Standard Error in Vertical Intercept (ln(EDY))
Maximum Likelihood	1.42	291		
Linearized Least Squares	1.32	331	0.082	0.304

All inspection data adjusted to 600 °F ($Q = 44$ kcal/mole)

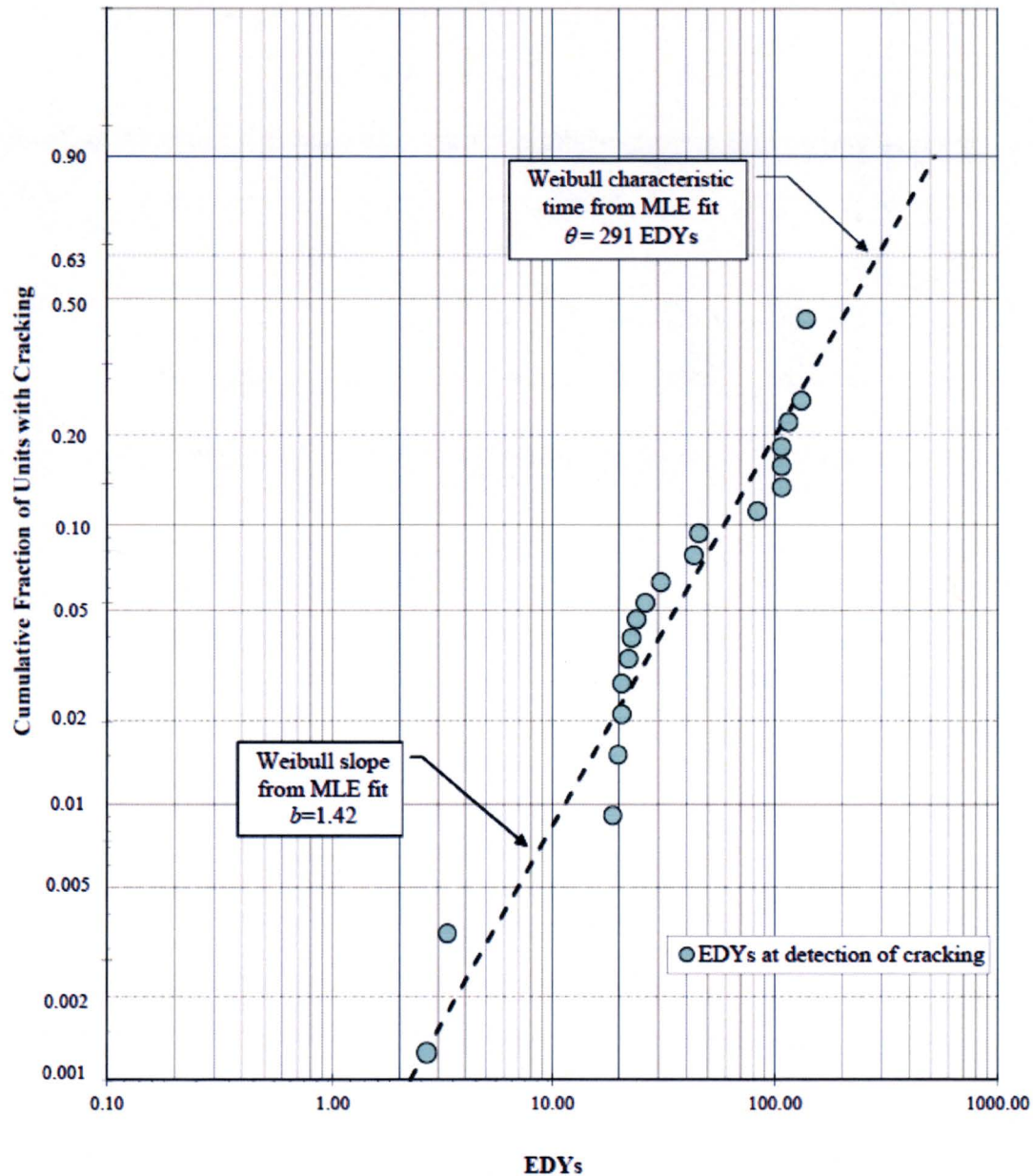


Figure A-10
Example MLE Weibull Probability Distribution for Alloy 82/182 Piping to Nozzle Butt Welds

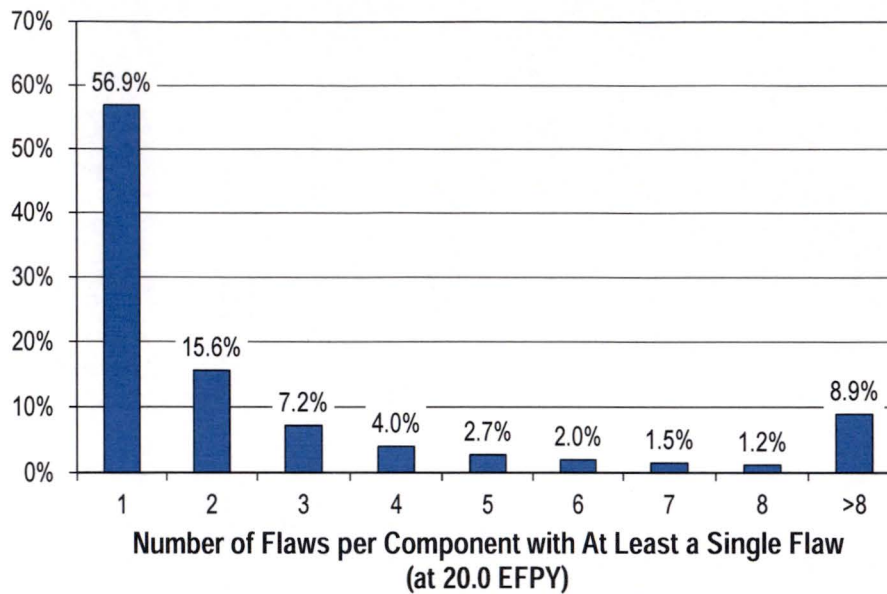


Figure A-11

Result for DM Weld Numerical Study: Distribution of Number of Flaws per Component with at Least a Single Flaw

A.8.3 Crack Growth Model

The set of inputs for the PWSCC propagation model is described in Table A-8 at the end of this section, including deterministic and distributed inputs. Various inputs are detailed in the following subsections.

A.8.3.1 Empirical Growth Parameters

The general flaw propagation rate equation used in this study is given in Equation [A-40]. The flaw propagation rate constant for growth in Alloy 82/182, α_{weld} , is based on MRP-115 and is taken as a deterministic input. Likewise, the stress intensity factor threshold and propagation rate stress intensity factor exponent (for growth in Alloy 82/182) are based on MRP-115 and are taken as deterministic inputs.

A.8.3.2 Growth Variation Factors

The uncertainty in the probabilistically calculated flaw propagation is principally characterized by the f_{weld} and f_{ww} parameters in the MRP-115 flaw propagation rate equations described Section A.5.3.

The f_{weld} parameter is a common factor applied to all specimens fabricated from the same weld to account for effects of the weld wire/stick heat processing and of weld fabrication. For this study, the log-normal distribution fit to the weld factors for the set of laboratory test welds assessed in MRP-115 is used (see Figure A-12).

A “within weld factor” (f_{ww}) is included to describe the variability in flaw propagation rate for different weld specimens fabricated from the same test weld. Log-normal distributions were

developed and are shown in Figure A-13 to describe the variability in f_{ww} observed for the data generated in MRP-115. The f_{ww} distribution describes the scatter in the flaw propagation rate model that remains after all effects addressed by the model are considered including the particular f_{weld} parameter calculated for each test weld.

Because there is a physical upper limit to the rate at which PWSCC crack propagation can proceed, an upper truncation limit is applied when sampling f_{weld} or f_{ww} . The f_{weld} or f_{ww} upper bound is set to the maximum of: the 95th percentile of the respective distribution and the maximum calculated f_{weld} or f_{ww} , respectively. The lower bound is imposed in a similar manner as the minimum of the 5th percentile of the respective distribution and the minimum calculated f_{weld} or f_{ww} , respectively.

Note that when an f_{ww} factor is applied in addition to the f_{weld} factor, the product of the two corresponding upper truncation limits proscribes the maximum flaw propagation rate that can be applied within the flaw propagation model. That maximum flaw propagation rate is assured to be greater than the maximum flaw propagation rate actually observed in any of the laboratory tests used to develop the f_{weld} and f_{ww} distributions when the conditions for each test are applied to the applicable flaw propagation rate equation.

A.8.3.3 Uncertainty in Temperature Effect

The temperature dependence of the flaw propagation process is modeled using a thermal activation energy. As shown in Table A-8, a normal distribution is used to describe the uncertainty in the activation energy. The standard deviation assumed corresponds to 5 kJ/mole, relative to the 130 kJ/mole mean activation energy value for PWSCC growth, and is based on the range of PWSCC flaw propagation activation energy values reported by various investigators for Alloy 600 wrought material [11].

A reference temperature of 617°F is chosen as the reference temperature for the crack growth model. The uncertainty in the activation energy accounts for the uncertainty in the temperature effect between 617°F and the operating temperature.

A.8.3.4 Correlation in Relating Flaw Initiation and Propagation

As discussed in A.5.3, it is generally accepted by PWSCC experts [11] that components that are more susceptible to PWSCC flaw initiation than other components tend to have higher flaw propagation rates than those other components. The main challenge in correlating the time to initiation and the flaw propagation rate in a probabilistic PWSCC assessment is that there is a general lack of data with which to choose an appropriate correlation coefficient. In the absence of data to select an appropriate correlation coefficient, this correlation is examined in a sensitivity study. The correlation coefficient was therefore set to zero for the base case analysis.

A.8.3.5 Crack Coalescence Factor

Crack coalescence modeling requires a distance threshold at which coalescence occurs. In this study, this threshold is modeled by some deterministic ratio of the maximum depth of the two cracks for which coalescence is assessed (that ratio being $1/F_{coalescence}$). For the base case result, the $F_{coalescence}$ parameter is inputted as an arbitrarily large number such that cracks must abut for coalescence to occur.

Table A-8
Summary of Inputs for DM Weld Flaw Propagation Model

Symbol	Description	Source	Units	Parameter Type	DMW Base Case
$1/\Delta t$	Number of time steps per year for crack size increment	The value chosen provides sufficient convergence	1/yr		12
f_{weld}	Weld-to-weld factor: common factor applied to all specimens fabricated from the same weld to account for weld wire/stick heat processing and for weld fabrication	Fit to weld-to-weld variation data from MRP-115	-	type	Log-Normal
				linear μ	1.19
				median	1.00
				75%ile	1.49
				log-norm μ	0.000
				log-norm σ	0.589
				min	0.313
f_{ww}	Within-weld factor: factor accounting for the variability in crack growth rate for different specimens fabricated from the same weld	Fit to within-weld variation from MRP-115 data after normalizing for weld-to-weld variation factor	-	max	2.64
				type	Log-Normal
				linear μ	1.12
				median	1.00
				log-norm μ	0.000
				log-norm σ	0.481
				min	0.309
α_{weld}	Flaw propagation rate equation power law constant for Alloy 182 weld	MRP-115	$(\text{in/hr})/(\text{ksi}\cdot\text{in.})^{0.5,1.6}$	max	3.24
					1.62E-07
Q_g	Thermal activation energy for PWSCC flaw propagation	MRP-115	kcal/mole	type	Normal
				mean	31.07
				stdev	1.20
				min	23.90
				max	38.24
$T_{ref,g}$	Absolute reference temperature to normalize PWSCC flaw propagation data	MRP-115	$^{\circ}\text{R}$		1077
$K_{I,th}$	K_I Stress intensity factor threshold	MRP-115	$\text{ksi}\cdot\text{in.}^{0.5}$		0.0
$K_{I,min}$	Minimum allowable value for K_I	No technical basis for non-zero value	$\text{ksi}\cdot\text{in.}^{0.5}$		0.0
b	Flaw propagation rate equation power law exponent for Alloy 82/182 weld	MRP-115	-		1.6
$1/F_{coalescence}$	Ratio of maximum crack depth that is used to evaluate the critical separation distance for coalescence	Set arbitrarily small such that coalescence occurs only once two cracks overlap	-		1.0E-06
	Flag indicating if crack growth will be predicted considering the effect of crack closure	Crack closure effects are neglected for base case	Logical		FALSE
	Flag indicating if cracks may grow in length without the effect of peening stresses	Sub-surface balloon growth of crack conservatively included for base case	Logical		TRUE

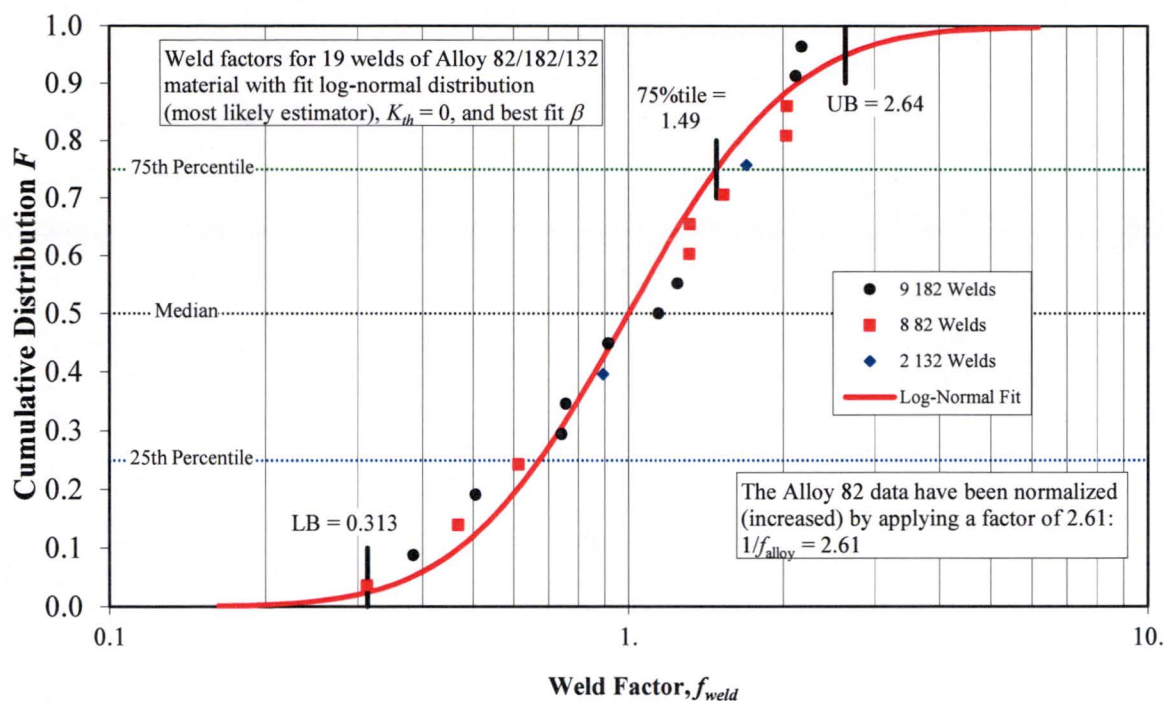


Figure A-12
MRP-115 Weld Factor f_{weld} Distribution [11] with Log-Normal Fit for Alloy 82/182/132

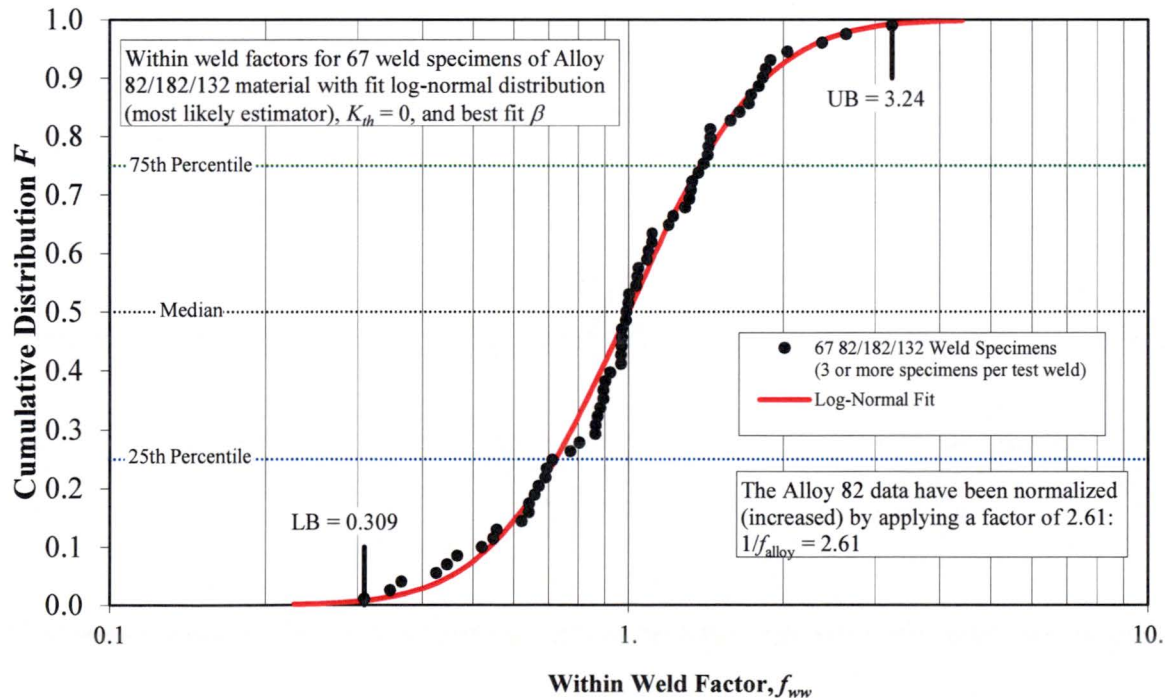


Figure A-13
MRP-115 Within-Weld Factor f_{ww} Distribution [11] with Log-Normal Fit for Alloy 82/182/132

A.8.4 Flaw Inspection and Detection Model

The set of inputs for the flaw examination models is described in Table A-9 at the end of this section, including deterministic and distributed inputs. Various inputs are detailed in the following subsections.

A.8.4.1 Examination Scheduling

As mentioned in the modeling section, UT inspection scheduling prior to peening for DM welds is based on ASME Code Case N-770-1 [19]. Accordingly, a UT inspection is simulated once every three cycles for the RVON and once every four cycles for the RVIN. The first PDI qualified UT inspection is modeled as occurring after the 14th simulated cycle for the RVON and after the 15th simulated cycle for the RVIN. These dates correspond with the units that were used to develop the operating timeline, and geometry inputs discussed in Section A.8.1.

In cases where peening is scheduled, the follow-up and in-service inspection intervals are varied to generate comparative results. The follow-up interval is varied between 1, 2, or 3 cycles for the RVON and between 1, 2, 3, or 6 cycles for the RVIN. The in-service inspection interval is varied from 3 cycles (same as the unmitigated component ISI) to the total plant service life for the RVON and from 4 cycles to the total plant service life for the RVIN.

A.8.4.2 UT Probability of Detection

The UT POD model for DM welds is described by Equation [A-44]. Based on the study of UT qualification data published in MRP-262R1 [20], the uncertainty of the detection model parameters, β_1 and β_2 , can be accurately captured using a bivariate normal distribution. The distribution parameters for POD of DM weld cracking on RVONs from this study are given in Table A-9. Note that these parameters are also applied for the RVIN case given that the two nozzles have a similar geometry in Westinghouse plants.

As discussed in the modeling section, the study used to derive the UT POD curve discussed above did not include axial cracks. Experience indicates a decreased capability to detect axial cracks relative to circumferential cracks using UT. Accordingly, a deterministic reduction factor of 0.8 is conservatively applied to the POD predicted by the model from MRP-262R1 [20] in order to model detection of axial flaws by UT. This assumption is examined in a sensitivity study, in which both axial and circumferential POD curves are decreased by an additional 20%.

A correlation coefficient relating the results of the next inspection to the results of the previous inspection can be included to take into account the increasing likelihood of non-detection if a crack has already been missed in a previous inspection. Because this value has not been experimentally determined, a modest correlation coefficient of 0.5 is used for the base case input.

Table A-9
Summary of Inputs for DM Weld Examination Model

Symbol	Description	Source	Units	Parameter Type	DMW Base Case
	The through-wall fraction below which the small-flaw contingency (POD = 0) is used	Smallest flaw size used in UT mockup testing			0.10
ρ_{msp}	Correlation coefficient for successive UT inspection	Conservative assumption	-		0.50
$\beta_1 (B1)$	POD model for 0th order logistic equation parameter for Category B1 components: RV Inlet and Outlet	Table 12-3 of MRP-262	-	type	Normal
				mean	3.244
				stdev	0.549
$\beta_2 (B1)$	POD model for 1st order logistic equation parameter for Category B1 components: RV Inlet and Outlet	Table 12-3 of MRP-262	-	type	Normal
				mean	1.06
				stdev	1.32
$\rho_{\beta (B1)}$	Correlation coefficient for Category B1 component POD model parameters	MRP-262 Appendix B Wald Model Results	-		-0.8698
$f_{UT,axial}$	Reduction factor applied to POD predicted from circumferential crack detection data	See Section A.8.4.2	-		0.80

A.8.5 Effect of Peening on Residual Stress

The set of inputs related to peening considerations is described in Table A-10 at the end of this section, including deterministic and distributed inputs. Various inputs are detailed in the following subsections.

A.8.5.1 Peening Application Scheduling

For both the RVON and RVIN base cases, the peening application is scheduled for the outage coinciding with the second UT inspection. Given the first inspection times and inspection intervals defined in Section A.8.1.2, the time of peening application for the RVON is EOC 17 and the time of peening application for the RVIN is EOC 19.

A.8.5.2 Post-Peening Residual Stresses

The parameterized model for post-peening residual stress profiles are described in Equations [A-17] through [A-21].

For piping DM welds, the residual plus normal operating stress is modeled to remain compressive for all wetted surfaces along the susceptible material, as defined in Section 4. Thus, the peening compressive stress at the surface is set to result in a total (operating plus residual) stress of zero at the circumferential location and for the principal stress direction with the maximum operating stress.

The peening compressive residual stress depth for the DM weld ID is modeled with a normal distribution. This distribution is given a mean of 1.0 mm (0.039 inch). This value is the minimum allowable compressive residual stress depth defined in Section 4. A standard deviation of 0.25 mm (0.010 inch) is conservatively assumed. The non-realistic case of negative penetration depth is prevented by using a lower truncation bound of 0.0 mm (0.0 inch).

To define the transition from the compressive surface layer to the pre-peening stress profile, two characteristic lengths are required (as detailed in Section A.3.3 and Figure A-3). The first length, $x_{2,PPRS}$, defines the distance from the peened surface to the point where the pre-peening WRS profile is regained. The second length, $x_{3,PPRS}$, defines the distance from the peened surface to the point where the post-peening, stress-balanced WRS profile is regained. These lengths are defined with deterministic ratios:

$$\begin{aligned}x_{3,PPRS} &= f_{1,PPRS} x_{1,PPRS} \\x_{2,PPRS} &= x_{1,PPRS} + f_{2,PPRS} (x_{3,PPRS} - x_{1,PPRS})\end{aligned}\tag{A-48}$$

These ratios were defined based on a review of the peening residual stress profiles in MRP-267R1 [8]. Their values are given in Table A-8.

A.8.5.3 Thermal and Load Cycling

The base case probabilistic inputs do not include any stress relaxation effects; the peening residual stress inputs are based on the bounding stresses permitted by the performance criteria of Section 4 for the remaining service life of the component. The inputs described in this section are used in a sensitivity case.

To estimate the stress relaxation occurring in a peened component over a plant service life, experimental data monitoring residual surface stress measurements on a peened surface as a function of time were analyzed. Specifically, measurements were available for three Alloy 182 specimens treated with WJP by Hitachi-GE [8]. These data are shown in Figure A-14.

To accelerate the stress relaxation, the experiments were performed at a temperature of 842°F (450°C) for 1000 hr, which is much higher than typical component temperatures during operation. This temperature and duration were converted to an equivalent operating time at 625°F (329°C) using an Arrhenius relationship with an activation energy of 188 kJ/mol (44.9 kcal/mol), which corresponds to the lower bound of an activation energy range for creep of Alloy 600 in primary water determined by Was et al. [29]. This results in a total equivalent operating time of approximately 59.5 EFPY at 625°F (329°C).

After linearizing the exponential model defined in Section A.3.4, a best-fit value of the stress relaxation exponent was calculated with linear least squares regression. A value of 5.1×10^{-3} EFPY⁻¹ was estimated. This results in a stress relaxation vs. time that is nearly linear between 0 and 80 years (77.6 EFPY).

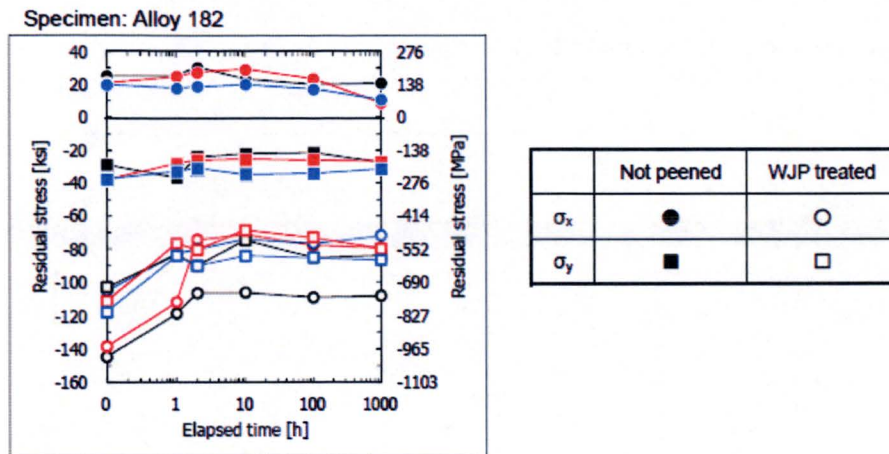


Figure A-14
Experimental Data used to Estimate Thermal Residual Stress Relaxation Factor

A.8.5.4 Effect of Peening on Growth

For the base case probabilistic model results, growth of cracks is simulated without consideration for crack closure. This effect is considered as a sensitivity case.

Also for the baseline results, full credit is given to growth of the length of a crack under the peening surface. As discussed in Section A.5.5, this is done by using the “balloon” growth approximation – neglecting peening stresses for the calculation of length growth. The “balloon” growth approximation is lifted for a sensitivity study.

Table A-10
Summary of Peening-Specific Inputs for DM Weld Model

Symbol	Description	Source	Units	Parameter Type	DMW Base Case
	Outage of peening application	Scheduled at next outage coinciding with a UT inspection	Cycle number	RVON	17
				RVIN	19
	Number of cycles between peening application and follow-up	Section 4	# cycles	RVON	2
				RVIN	6
	Inspection interval after peening	Section 4	# cycles	RVON	6
				RVIN	None
	Flag indicating if a UT pre-peening exam is performed	Section 4	-		TRUE
$\sigma_{0,PPRS}(t=0)$	Sum of post-peening residual plus normal operating stress on ID surface	Bounds minimum value from performance criteria (Section 4)	ksi		0.0
$x_{1,PPRS}$	Depth of compressive residual stress layer from ID surface	Bounds minimum value from performance criteria (Section 4)	in.	type	Normal
				mean	0.039
				stdev	0.010
				min	0.000
				max	0.098
$f_{1,PPRS}$	Ratio of minimally-affected depth to peening penetration depth	See Section A.3.3	-		2.0
$f_{2,PPRS}$	Fraction of depth between peening penetration depth and minimally-affected depth where peening results in no effect	See Section A.3.3	-		0.7
m	Empirical stress relaxation exponent	Unused in base case, sensitivity case using best-fit value; Section A.8.5.3	EFPY ⁻¹		0.0

A.9 Results of Probabilistic Cases

This section presents results generated using the integrated probabilistic model described in Sections A.2 through A.6, with particular focus on the prediction of the leakage criterion described in Section A.7. Using the inputs described in Section A.8, this section presents predictions for the RVON and RVIN base cases without peening mitigation (Section A.9.1) and with peening mitigation (Section A.9.2).

Section A.9.3 presents the results of sensitivity studies wherein one or more inputs or modeling methodologies were varied from those described in Sections A.2 through A.8. The aim of these sensitivity studies is to demonstrate the relative change in the predicted leakage risk for a DM weld component when an input or modeling assumption is varied.

The primary statistics used to assess and compare the results of the probabilistic model are defined below:

- Incremental leakage frequency (ILF) is defined as the average number of new leaking reactor vessel outlet/inlet nozzles per year. A simulated flaw causes leakage if it propagates through the entire material thickness before it is detected and repaired. This statistic is derived for any given operational cycle by averaging the predicted number of new leaking nozzles for that operational cycle across all MC realizations. This is adjusted to a probability per year by dividing by the number of calendar years per cycle.

$$ILF = \frac{(\text{Number of new leaks predicted during cycle across all realizations})}{(\text{Number of realizations})(\text{Calendar years per cycle})} \quad [A-49]$$

- Average leakage frequency (ALF) is the time-average of the ILFs following the hypothetical time of peening until the end of the operational service period of the plant. This statistic is averaged over the number of MC realizations that are active (have not yet leaked) following the hypothetical time of peening. Using this subset of realizations provides no credit to realizations where the component leaks and is removed from the modeled population prior to the hypothetical time of peening.

$$ALF = \frac{\sum_{i=i_{peen}}^{N_{cycle}} (\text{Number of new leaking nozzles predicted during cycle across all realizations})}{(\text{Number of realizations})(\text{Calendar years per cycle})(N_{cycle} - i_{peen})} \quad [A-50]$$

where:

N_{cycle} = number of cycles in operational service period
 i_{peen} = cycle number associated with the hypothetical time of peening

- Cumulative probability of leakage (CPL) is defined as the fraction of reactor vessel inlet/outlet nozzles with a predicted leak across all active MC realizations across all cycles of interest. This document reports two versions of this statistic: (1) cumulated from the start of operation to a given cycle and (2) cumulated from the hypothetical time of peening to the end of plant operation. When calculating the CPL after the hypothetical time of peening, realizations in which leakage occurs prior to the time of peening are discarded and are not included in the reported statistic.

$$CPL = \frac{(\text{Total number of realizations with at least one predicted leak})}{(\text{Number of realizations})} \quad [A-51]$$

These probabilistic results are used to compare the risk associated with peened welds examined on a relaxed schedule versus the risk for unmitigated welds examined per the standard intervals. This comparative approach has the advantage of minimizing any potential for bias introduced by the various modeling assumptions.

A.9.1 Results for the Unmitigated Case

Using the inputs specified in Section A.8, predictions were made for the RVON and RVIN base cases without any peening mitigation; leakage probability vs. time predictions are given in Figure A-16 and Figure A-17, respectively. For these cases, inspections were scheduled based on N-770-1 for unmitigated components.

For reference, the hypothetical time of peening is shown on these plots. As discussed in the inputs section, this time of peening has been set to coincide with the second modeled UT inspection. Between the hypothetical time of peening and 80 calendar years (77.6 EFPY), the model predicts a cumulative probability of leakage of 1.5×10^{-1} for the RVON and 2.1×10^{-3} for

the RVIN. These values will be important for assessing the performance of peening with respect to leakage mitigation in the following section.

A.9.2 Results with Peening Mitigation

As discussed previously, a follow-up inspection is expected to be conducted either one, two, three, or six cycles after peening, and after the follow-up inspection, a new in-service inspection interval is expected to be utilized through the end of plant service life. Various combinations of follow-up inspection time and in-service inspection frequency were used to make leakage risk predictions after peening. These results are summarized in Figure A-18 and Figure A-19 for the RVON and RVIN, respectively. It is emphasized that no surface examinations are modeled at the pre-peening inspection for these results.

For both the hot and cold DM weld components, the predicted likelihood of cracks existing after the pre-peening inspection is very low; less than 2.6×10^{-3} .

For the RVON, it was predicted that the cumulative probability of leakage after peening would be reduced by a factor between 60 and 150, (compared to cumulative leakage probabilities on same span of time for an unmitigated RVON), depending on the post-peening follow-up examination and ISI scheduling. While there is some small trend with respect to follow-up time, in general the degree of improvement is not significantly influenced by the follow-up time or the ISI frequency. The former is the result of the fact that most of the cracks that go undetected at the pre-peening inspection are small, and accordingly grow slowly after peening (see deterministic calculations that demonstrate this in Section 5.2); the latter is a result of the fact that nearly all cracks are detected during the pre-peening or follow-up inspection and no new cracks are expected to initiate after peening.

For the RVIN, it was predicted that the cumulative probability of leakage after peening is reduced by a factor between 8 and 24, (compared to cumulative leakage probabilities on same span of time for an unmitigated RVIN), depending on the post-peening follow-up examination and ISI scheduling. This degree of improvement is smaller than that predicted for the RVON because the inspection schedule for an unmitigated RVIN conservatively takes little credit for its reduced temperature in comparison to that for hot-leg locations.

For both the RVON and RVIN peening base cases, the probability of leaking after the follow-up inspection is very low, as can be seen in Figure A-16 and Figure A-17. Furthermore, Figure A-20 demonstrates the decaying nature of leakage probability vs. time after peening, for both the hot and cold components with relaxed UT inspection intervals.

A.9.3 Results for Sensitivity Cases

Various sensitivity studies were conducted with the DM weld probabilistic model in order to demonstrate the relative change in the predicted results given one or more changes to modeling or input assumptions. Each sensitivity case has been classified as either a Model Sensitivity (in which an approximated input or model characteristic is varied) or an Inspection Scheduling Sensitivity (in which a controllable inspection option is varied). These sensitivity cases are described in Table A-11 and Table A-12.

Figure A-21 (RVON) and Figure A-26 (RVIN) compare the cumulative probability of leakage from the hypothetical time of peening to end of plant operation for peened and unmitigated components for Inspection Scheduling Sensitivity cases.

Figure A-22 through Figure A-25 compare the cumulative probability of leakage from the hypothetical time of peening to the end of the operational service period of the plant for peened (Figure A-22 and Figure A-23) and unmitigated (Figure A-24 and Figure A-25) RVON Model Sensitivity cases, respectively. Figure A-27 through Figure A-30 provide the equivalent comparison for RVIN cases.

All sensitivity cases for peened components result in a cumulative probability of leakage substantially below that of the equivalent sensitivity case for an unmitigated component.

The cases of greatest interest are discussed below:

DMW Inspection Scheduling Sensitivity Cases 1 and 2: Skipping Pre-Peening or Follow-Up UT Inspections

The base case included a volumetric (UT) inspection during the pre-peening examination, as well as a follow-up inspection before entering a relaxed in-service inspection schedule. Under the conservative assumption that no credit is taken for the required ET examinations, both the pre-peening and follow-up inspections are key for detecting significant cracks before entering the relaxed inspection schedule. Skipping UT follow-up examinations (Inspection Scheduling Sensitivity Case 1) results in a CPL of 2.5×10^{-3} for the RVON and a CPL of 5.4×10^{-4} for the RVIN. Skipping UT pre-peening inspections (Inspection Scheduling Sensitivity Case 2) results in a CPL of 1.1×10^{-2} for the RVON and a CPL of 9.4×10^{-4} for the RVIN. These sensitivity cases emphasize the importance of pre-peening and follow-up inspections, such that pre-existing cracks of detectable size are corrected.

DMW Model Sensitivity Case 6 – Decreasing UT POD Curves by 20%

The base case POD curves shown in Figure A-9 are a conservatively modified version of the POD model from MRP-262R1 [20], with a zero POD assumed for flaws less than 10% through-wall. This sensitivity study decreases both UT POD curves by 20%, which results in an increased cumulative probability of leakage. The scaled POD curve results in a CPL of 4.5×10^{-3} for the peened RVON, a CPL of 1.9×10^{-1} for the unmitigated RVON, a CPL of 6.3×10^{-4} for the peened RVIN, and a CPL of 3.7×10^{-3} for the unmitigated RVIN. However, this sensitivity case results in a maximum POD just under 80% for near-through-wall circumferential flaws, which is significantly lower than the best-estimate POD curve derived from personnel and equipment qualification data representative of NDE methods applied in the field. Furthermore, the POD curve for axial flaws applied in this sensitivity case falls below the minimum detection rates (between 0.68 and 0.82) defined in Appendix VIII of ASME Section XI [30] for specimens with a mixture of circumferential and axial flaws.

DMW Model Sensitivity Cases 7 and 8 – NB-3600 [31] Bending Loads

To study the effect of worst-case bending loads on leakage, the high and extreme loads calculated with NB-3600 [31] equations were applied to RVON in DMW Model Sensitivity Case 7.

The extreme bending load calculated using NB-3600 equations is approximately 90% larger than the load used in the base case. These modified loads result in a CPL of 1.1×10^{-3} for the peened RVON, a CPL of 1.9×10^{-1} for the unmitigated RVON, a CPL of 1.6×10^{-4} for the peened RVIN, and a CPL of 2.6×10^{-3} for the unmitigated RVIN. While this resulted in a modest increase in the probability of the leakage for the unmitigated component, it counter-intuitively reduced the probability of leakage for the peened component. This is partially due to the fact that the higher bending results in faster crack growth prior to peening, and thus higher probabilities of detection at the pre-peening inspection.

To compensate for this effect (in Model Sensitivity Case 8), a reduction factor is applied to t_1 of the first crack initiation time model.

$$t_1' = f_{adjust} t_1 \quad [A-52]$$

This results in earlier first crack initiation to counteract the reduction in the mean arrival time of multiple crack initiation. The reduction factor is calculated to normalize the initiation times of the extreme bending case:

$$f_{adjust} = \left(\frac{\sigma_{surf,base}}{\sigma_{surf,extreme}} \right)^n \quad [A-53]$$

where $\sigma_{surf,base}$ and $\sigma_{surf,extreme}$ are the nominal surface stresses at the point of maximum bending for the base case and the extreme loading case, respectively. The modified loads and initiation model result in a CPL of 3.2×10^{-3} for the peened RVON, a CPL of 3.7×10^{-1} for the unmitigated RVON, a CPL of 5.7×10^{-4} for the peened RVIN, and a CPL of 9.0×10^{-3} for the unmitigated RVIN. This suggests that the faster rate of growth due to the larger bending load outweighs the larger POD at the pre-peening inspection.

DMW Model Sensitivity Case 10: Time-Dependent Residual Stress Relaxation

As an alternative to the bounding peening performance criteria defined in Section 4, an example peening surface stress was combined with a time-dependent residual stress relaxation for DMW Model Sensitivity Case 10.

As demonstrated in Figure A-22, the relative change caused by applying this model was negligible. The modified stress profile results in a CPL of 1.6×10^{-3} for the peened RVON, and a CPL of 2.2×10^{-4} for the peened RVIN. Both of these results are statistically equivalent to the respective peening base cases. This case shows that the results are insensitive to the assumed stress profile.

DMW Model Sensitivity Case 13: Earlier Initiation of First PWSCC

This model sensitivity case explored the effect of shifting the initiation time model such that initiations are predicted earlier in general. This provides an alternative approach to accounting for the fact that the initiation model used for the base case was fit to data for detected cracks; hypothetically, if undetected cracks could be included to fit the initiation model, the initiation time distribution would be shifted toward earlier times. (On the other hand, some detections used to fit the initiation model may not reflect actual PWSCC.) Conservatively, the parameter t_1 of the

first crack initiation model, which quantifies the time at which 1% of DM weld components are expected to initiate PWSCC, was reduced by a factor 3 for this sensitivity case.

The modified initiation model results in a CPL of 6.2×10^{-3} for the peened RVON, a CPL of 3.2×10^{-1} for the unmitigated RVON, a CPL of 1.4×10^{-3} for the peened RVIN, and a CPL of 1.2×10^{-2} for the unmitigated RVIN. This sensitivity case results in the largest CPL of all modeling sensitivity cases for the mitigated RVON, mitigated RVIN, and unmitigated RVIN.

It is noted that cumulative probability of leakage for an unmitigated RVON, predicted at 23 EPFY, for this sensitivity case, was approximately 28%. This is a higher probability than indicated by the incidence rate in U.S. PWRs.

DMW Model Sensitivity Case 15: Correlation of Initiation and Growth

DMW Model Sensitivity Case 15 explored the generally accepted tendency for cracks that initiate earlier to grow faster; specifically it explored this tendency's impact on the leakage probability predictions. This tendency is implemented by adding a negative correlation between the time of first crack initiation on DM weld component, t_{ref} , and the weld-to-weld variation factor, f_{weld} , as well as between each multiple crack initiation time, $t_{ref,i}$, and the sampled within-weld variation, $f_{ww,i}$, for each crack. The base case used zero correlation because cases in which relative material susceptibility to both initiation and growth are available are rare, precluding development of a proper correlation coefficient. Instead, this sensitivity case uses a medium/strong (-0.8) correlation coefficient for the correlations described above.

Applying a correlation between initiation and growth results in a CPL of 7.7×10^{-4} for the peened RVON, a CPL of 2.7×10^{-1} for the unmitigated RVON, a CPL of 1.2×10^{-4} for the peened RVIN, and a CPL of 1.0×10^{-2} for the unmitigated RVIN. For the peened component, adding correlation results in a decrease in the probability of leakage after peening because it causes generally larger cracks at the time of the pre-peening inspection which fosters detection before the relaxed inspection scheduled. However, for the unmitigated component, adding correlation results in an increase in probability of leakage because cracks that initiate during the operating lifetime of a DM weld component are considered early (for the corresponding chemical and material conditions) and thus grow faster.

DMW Model Sensitivity Cases 18 and 19: Reduced Initial Crack Depth

The base case inputs used to make predictions for the RVON assumed an initial crack depth with a 5th percentile of roughly 2 mm (3% TW), a median of 3.5 mm (5% TW), and a 95th percentile of roughly 6 mm (9% TW). In reality, the initiation depth of PWSCC can be on the micro- or nano-scale, arising from manufacturing processes, other forms of corrosion, cavitation, etc. The rationale behind selecting a much larger initiation depth is that the initiation time model is based on data for detected cracks, and so it does not account for micro- or nano-scale cracks, of which there are likely many more incidences. Furthermore, the prediction of crack growth rate with the methods presented in the modeling section is compromised as the depth of the crack to be analyzed becomes smaller than approximately 0.1 mm.

Because of the importance of detection during the pre-peening and follow-up inspections, it may be non-conservative to assume cracks with large initial depths. Such cracks may more easily be detected at the pre-peening or follow-up inspections, resulting in fewer active cracks during the post-peening ISI schedule. DMW Model Sensitivity Cases 18 and 19 assessed this possibility by

using an initial crack depth distribution with a median depth 10 times less than that used for the base case, resulting in an initial crack depth with a 5th percentile of roughly 0.2 mm (0.3% TW), a median of 0.35 mm (0.5% TW), and a 95th percentile of roughly 0.6 mm (0.9% TW). This is investigated in combination with utilizing crack closure methodology (Model Sensitivity Case 18) and by applying a minimum K_I value (Model Sensitivity Case 19).

Applying a reduced initial crack depth and imposing a minimum stress intensity factor (Model Sensitivity Case 19) results in a CPL of 2.8×10^{-3} for the peened RVON, a CPL of 1.4×10^{-1} for the unmitigated RVON, a CPL of 4.8×10^{-4} for the peened RVIN, and a CPL of 2.0×10^{-3} for the unmitigated RVIN. The reduction in initial depth with a minimum K_I results in increased leakage likelihood for DMWs. Nonetheless, the leakage likelihood for peened DMWs with a relaxed in-service inspection schedule remains well below that predicted for unpeened components inspected in accordance with the applicable requirements for unmitigated DMWs.

Applying a reduced initial crack depth and crack closure (Model Sensitivity Case 18) results in a CPL of 3.1×10^{-3} for the peened RVON, a CPL of 1.4×10^{-1} for the unmitigated RVON, a CPL of 4.9×10^{-4} for the peened RVIN, and a CPL of 2.0×10^{-3} for the unmitigated RVIN.

The application of the partial crack closure methodology with the reduction in initial depth has a rather small effect on the leakage predictions. This is because pre-existing flaws are often appreciably deeper (e.g., two times or more) than the surface region with reduced tensile stresses induced by peening and therefore largely unaffected. Partial crack closure has been found to be more important for deeper stress improvement methods like mechanical stress improvement.

DMW Model Sensitivity Case 25: Total Stress Compressive to Nominal Compressive Residual Stress Depth

The base case, which models the peening performance requirements defined in Section 4, includes a compressive total (residual plus operating) stress at the peened surface, and a compressive residual stress at the nominal compressive residual stress depth of 0.04 in. (1.0 mm). DMW Model Sensitivity Case 25 investigates the effect of a compressive total (residual plus operating) stress at the nominal compressive residual stress depth. To do so, this sensitivity case is modeled by assigning a greater value for the compressive residual stress depth and a more compressive peening surface residual stress compared to the base cases. The stress profile used in this sensitivity case is compared to the base case peened stress profile in Figure A-15.

Setting the total (residual plus operating) stress to be compressive from the surface to the nominal compressive residual stress depth results in a CPL of 1.5×10^{-3} for the peened RVON, and a CPL of 2.3×10^{-4} for the peened RVIN. When compared to the base case results for the mitigated components (a CPL of 1.6×10^{-3} for the RVON, and a CPL of 2.3×10^{-4} for the RVIN), there is only a minimal reduction in the cumulative probability of leakage for this sensitivity case. These results show that there would be very limited benefit to requiring a more compressive stress effect than that specified by the performance criteria in Section 4.2.8.1 for DMWs.

Table A-11
Description of Modified Inputs for DMW Model Sensitivity Cases

Sensitivity Case	Description	Symbol	Units	Parameter Type	Base Case Value	Sensitivity Case Value
M1	Reduce Operating Capacity Factor	CF	-	RVON	0.97	0.92
				RVIN	0.97	0.92
M2	Reject trials with detections before given cycle		Cycle number	RVON	0	16
				RVIN	0	18
M3	Halve growth integration time step	$1/\Delta t$	1/yr		12	24
M4	Remove correlation between UT inspections	ρ_{insp}	-		0.5	0.0
M5	Linearly extrapolate POD to zero below 10% TW		-		Assume POD = 0 below 10% TW	Linearly extrapolate
M6	Decrease POD by 20%	$\beta_1(B1)$	-	mean	3.244	1.242
				stdev	0.549	0.210
		$\beta_2(B1)$	-	mean	1.06	0.055
				stdev	1.32	0.069
M7	Increase effective bending load per NB-3600 Eq. 10	M_y	in.-kips	RVON	40000	75987
		M_y	in.-kips	RVIN	40000	75987
M8	Increase effective bending load per NB-3600 Eq. 10 and decrease initiation characteristic time	M_y	in.-kips	RVON	40000	75987
		M_y	in.-kips	RVIN	40000	75987
		t_1	EDY	type	Normal	Normal
				mean	11.40	5.18
				stdev	0.304	0.304
				min	3.14	1.43
M9	Decrease effective load to match Case C of ML112160169	M_y	in.-kips	RVON	40000	14721
		M_y	in.-kips	RVIN	40000	14721
M10	Include time-dependent stress relaxation	$\sigma_{0,PPRS}(t=0)$	ksi		Normal operating plus residual stress is zero ksi	Residual stress is 30.75 ksi compressive
		m	EFPY ⁻¹		0	5.10E-03
M11	Double standard deviation of peening penetration depth	$x_{1,PPRS}$	in.	type	Normal	Normal
				mean	0.039	0.039
				stdev	0.010	0.020
				min	0.000	0.000
				max	0.098	0.157
M12	Increase peening compressive surface stress and penetration depth	$x_{1,PPRS}$	in.	type	Normal operating plus residual stress is zero ksi	Residual stress is 100 ksi compressive
				mean	Normal	Normal
				stdev	0.039	0.118
				min	0.010	0.059
				max	0.000	0.000
M13	Decrease initiation characteristic time by factor of 3	t_1	EDY	type	Normal	Normal
				mean	11.40	3.80
				stdev	0.304	0.304
				min	3.14	1.047
				max	41.10	13.70
M14	Increase multiple flaw initiation model slope	β_{flaw}	-	type	Normal	Normal
				mean	2.0	3.0
				stdev	0.5	0.5
				min	1.0	1.0
				max	5.0	6.0
M15	Include initiation-growth correlation	ρ_{weld}	-		0.0	-0.8
		ρ_{wv}	-		0.0	-0.8

Table A-11 (continued)
Description of Modified Inputs for DMW Model Sensitivity Cases

Sensitivity Case	Description	Symbol	Units	Parameter Type	Base Case Value	Sensitivity Case Value
M16	Increase initiation activation energy to N-729-1 value	Q_i	kcal/mole	type	Normal	Normal
				mean	44.03	50.00
				stdev	3.06	3.06
				min	25.65	31.62
				max	62.41	68.38
M17	Remove stress adjustment of initiation times	n	-	type	Normal	Constant
				mean	4.0	0.0
				stdev	1.0	-
				min	0.0	-
				max	10.0	-
M18	Utilize crack closure methodology and decrease initial flaw depth	a_0/t	-	type	Do not utilize crack closure	Utilize crack closure
				linear μ	Log-Normal	Log-Normal
				median	0.053	0.0053
				log-norm μ	0.050	0.0050
				log-norm σ	-3.00	-5.30
				min	0.35	0.35
				max	0.01	0.001
M19	Decrease median initial crack depth and impose minimum K value	a_0/t	-	type	0.42	0.42
				linear μ	Log-Normal	Log-Normal
				median	0.053	0.005
				log-norm μ	0.050	0.005
				log-norm σ	-3.00	-5.30
				min	0.35	0.35
				max	0.01	0.001
M20	Increase growth activation energy	Q_g	kcal/mole	type	0.42	0.42
				linear μ	Log-Normal	Log-Normal
				median	0.053	0.005
				log-norm μ	0.050	0.005
				log-norm σ	-3.00	-5.30
M21	Increase coalescence distance threshold	$1/F_{coalescence}$	-	type	0.35	0.35
M22	Utilize crack closure methodology		-	linear μ	0.01	0.001
M23	Prevent balloon growth		-	log-norm σ	0.42	0.42
M24	Increase peening compressive surface stress and penetration depth	$\sigma_{0,PPRS}(t=0)$	ksi	type	0.00	10.9
				mean	Normal	Normal
				stdev	31.07	33.46
				min	1.195	1.195
				max	23.90	26.29
M25	Total stress compressive to nominal compressive stress depth	$x_{1,PPRS}$	in.	type	38.24	40.63
				mean	Normal operating plus residual stress is zero ksi	Residual stress is 100 ksi compressive
				stdev	Normal	Normal
				min	0.039	0.118
				max	0.010	0.059
M26	Utilize crack closure methodology	$\sigma_{0,PPRS}(t=0)$	ksi	type	0.000	0.000
				mean	0.098	0.295
				stdev	Do not utilize crack closure	Utilize crack closure
				min	Prevent balloon growth	Allow balloon growth
				max	Normal operating plus residual stress is zero ksi	Residual stress is 180.9 ksi compressive
M27	Prevent balloon growth	$x_{1,PPRS}$	in.	type	Normal	Constant
				mean	0.039	0.079
				stdev	0.010	-
				min	0.000	-
				max	0.098	-
M28	Total stress compressive to nominal compressive stress depth	$f_{1,PPRS}$	-	type	2	1.5
				mean	2	1.5
				stdev	2	1.5
				min	2	1.5
				max	2	1.5

Table A-12
Summary of Modified Inputs for DMW Inspection Scheduling Sensitivity Cases

Sensitivity Case	Description	Symbol	Units	Parameter Type	Base Case Value	Sensitivity Case Value
S1	Skip follow-up inspection and enter post peening ISI schedule		-	RVON	Perform follow-up UT 2nd cycle after peening	Skip follow-up UT inspection; first ISI after 6 cycles
				RVIN	Perform follow-up UT 6th cycle after peening	Do not perform UT inspection after peening
S2	Skip UT during pre-peening inspection		-		Perform UT during pre-peening inspection	Skip UT during pre-peening inspection

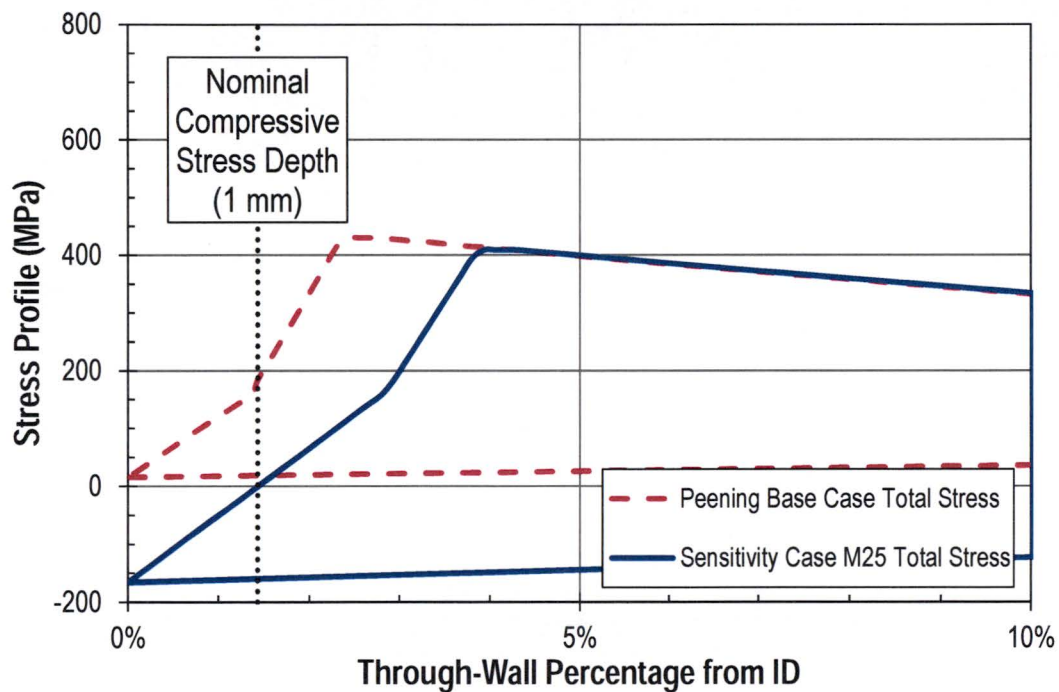


Figure A-15
Post-Peening Total (Normal Operating Plus Residual) Axial Stress Profile for Circumferential Crack in an Alloy 82/182 Reactor Vessel Primary Nozzle Butt Weld Component (Azimuthal Position of Maximum Global Bending Stress)

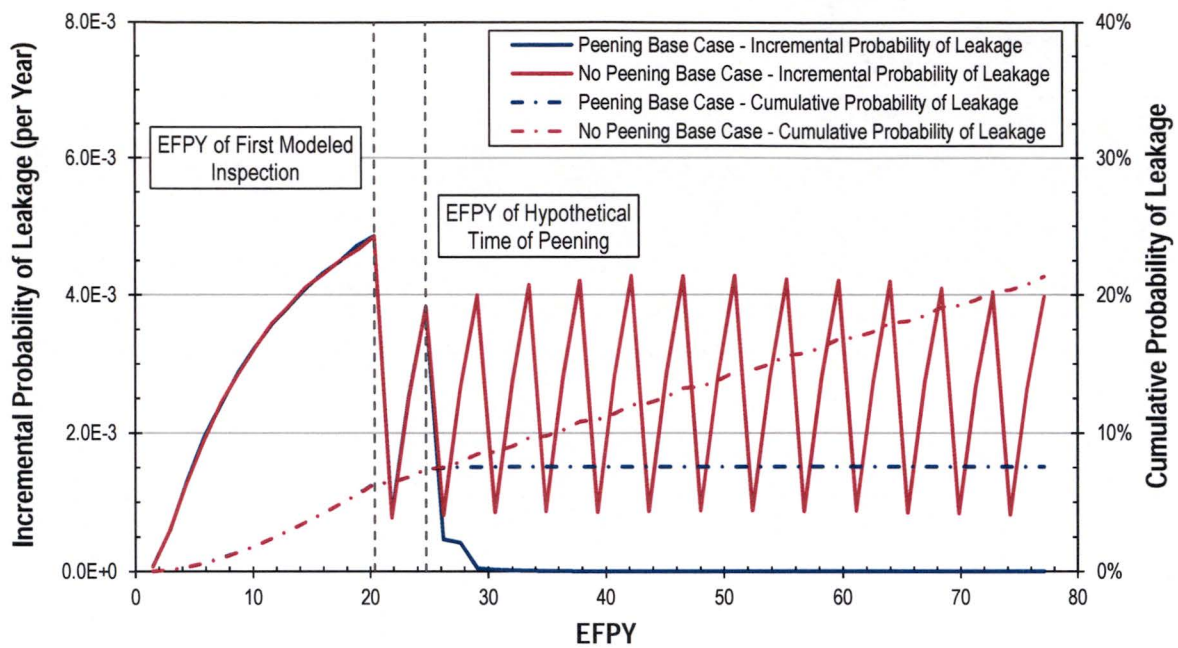


Figure A-16
Prediction of Leakage vs. Time for RVON

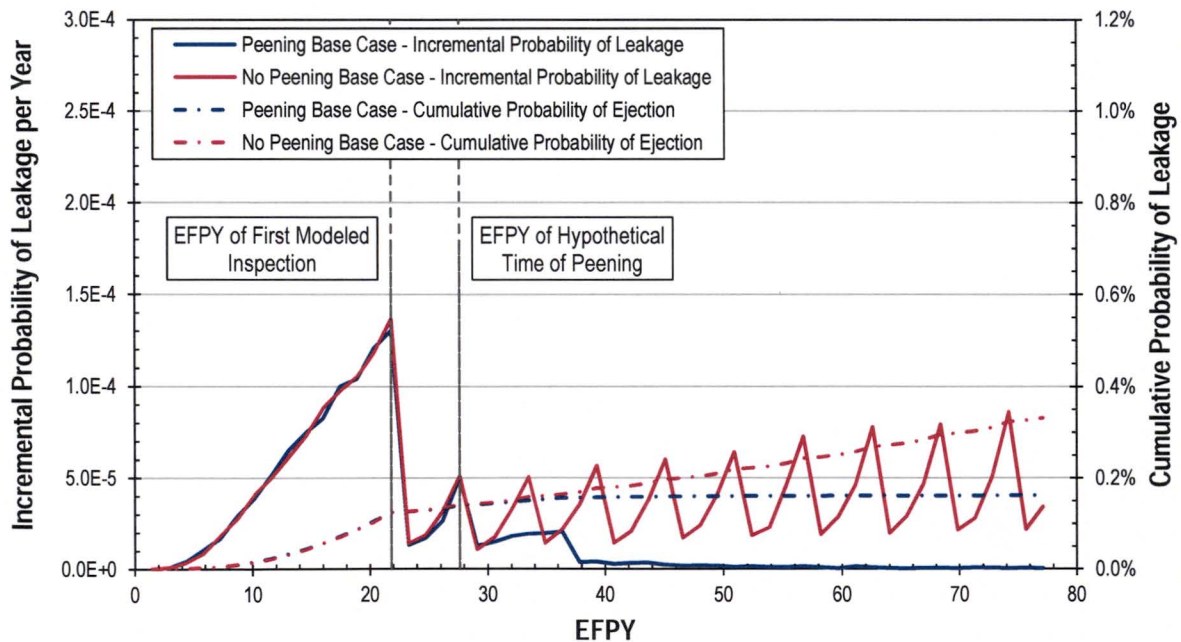


Figure A-17
Prediction of Leakage vs. Time for RVIN

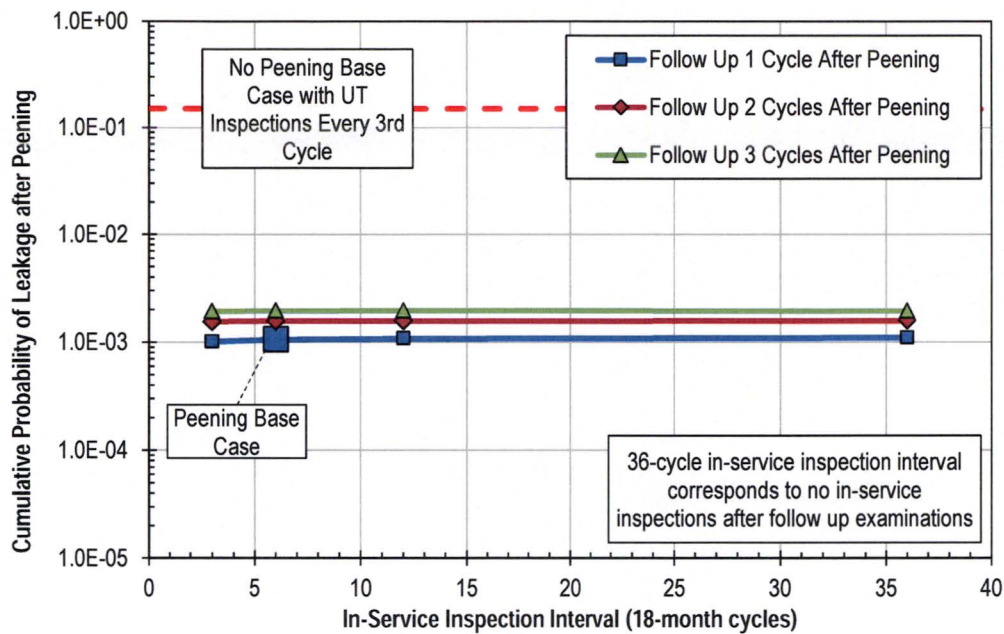


Figure A-18
Cumulative Probability of Leakage from Hypothetical Time of Peening to End of Operational Service Period vs. ISI Frequency for a RVON

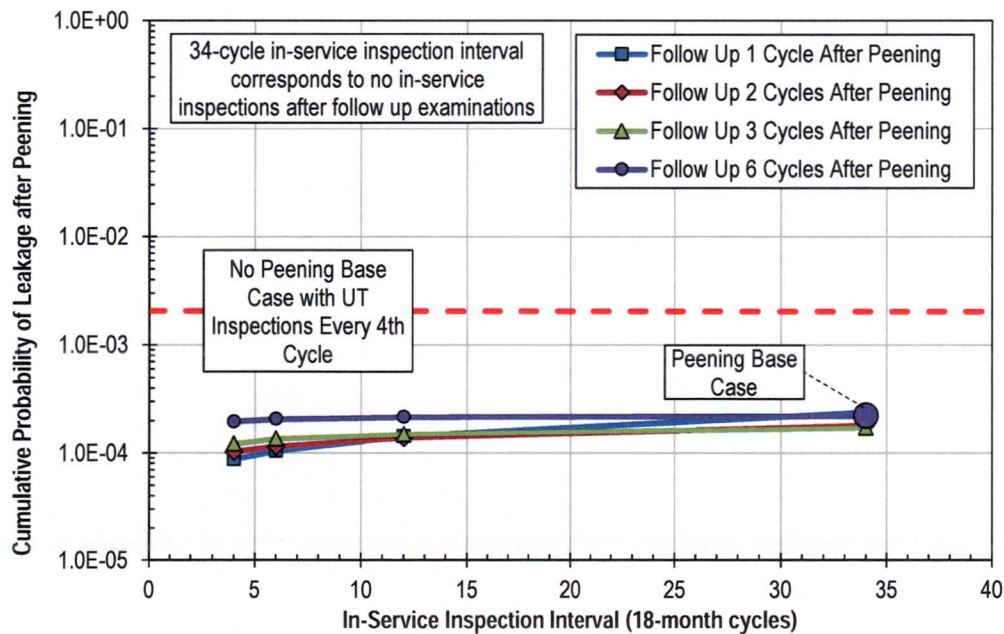


Figure A-19
Cumulative Probability of Leakage from Hypothetical Time of Peening to End of Operational Service Period vs. ISI Frequency for a RVIN

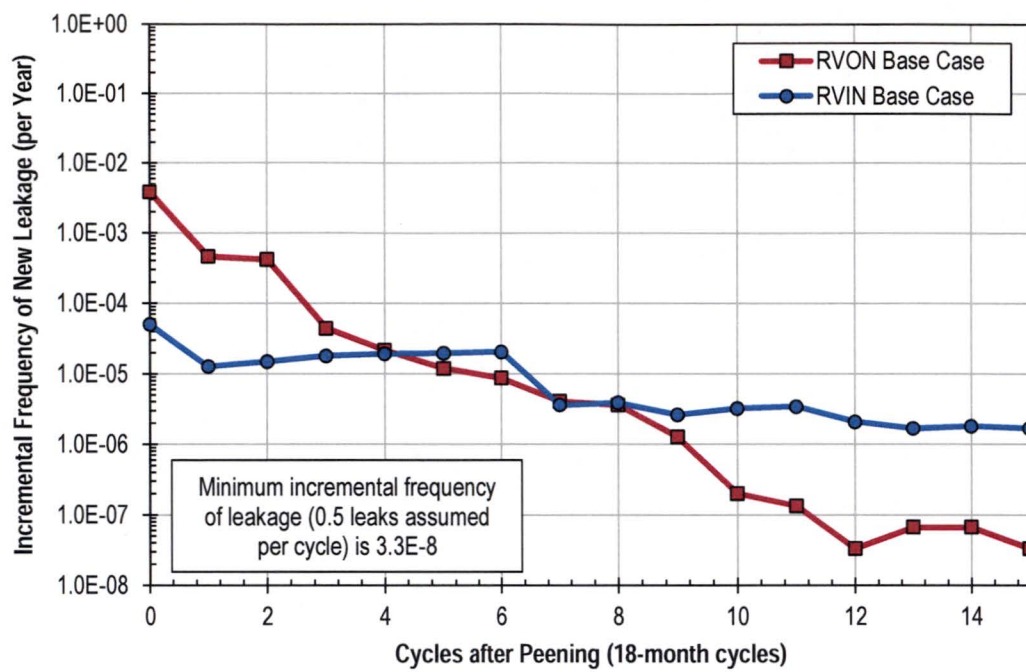


Figure A-20
Incremental Leakage Frequency after Peening with Relaxed ISI Intervals

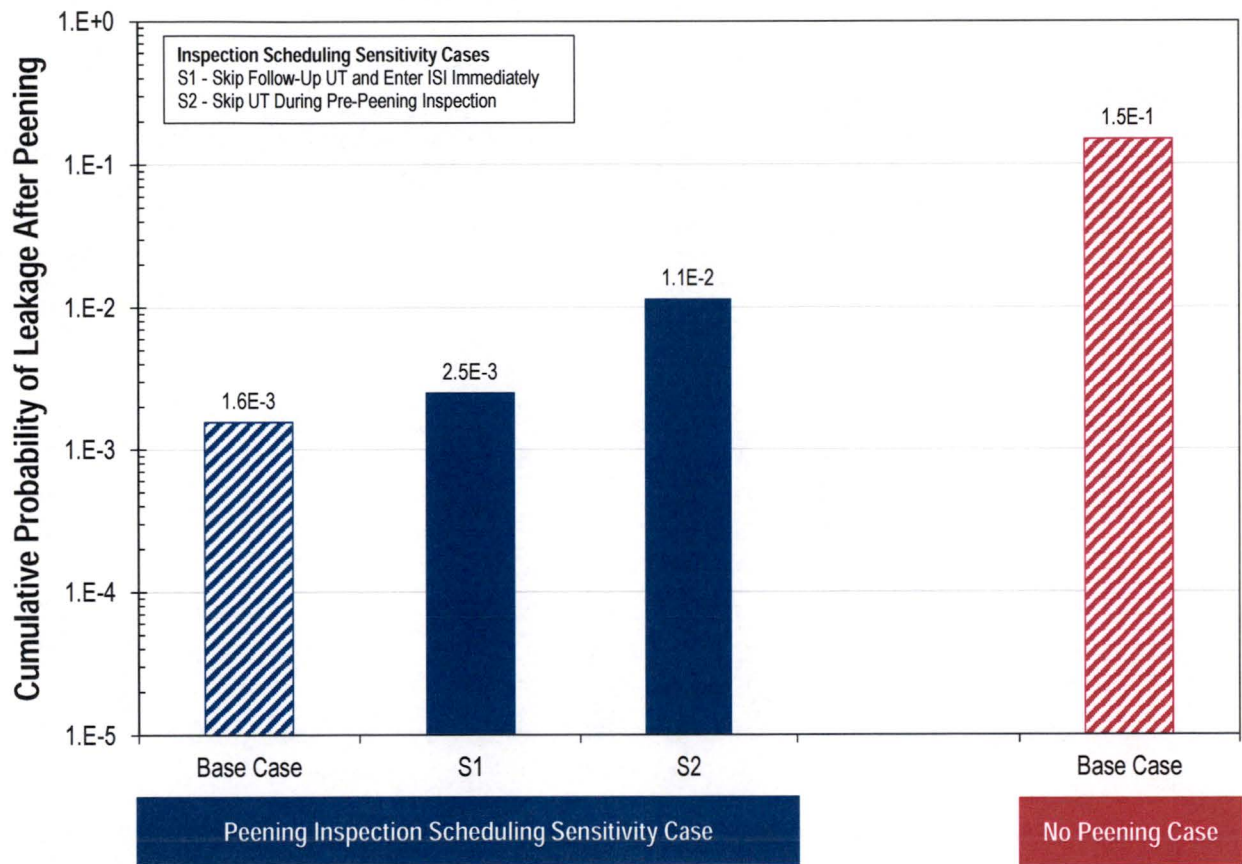


Figure A-21
Summary for Inspection Scheduling Sensitivity Results for RVON Probabilistic Model with Peening

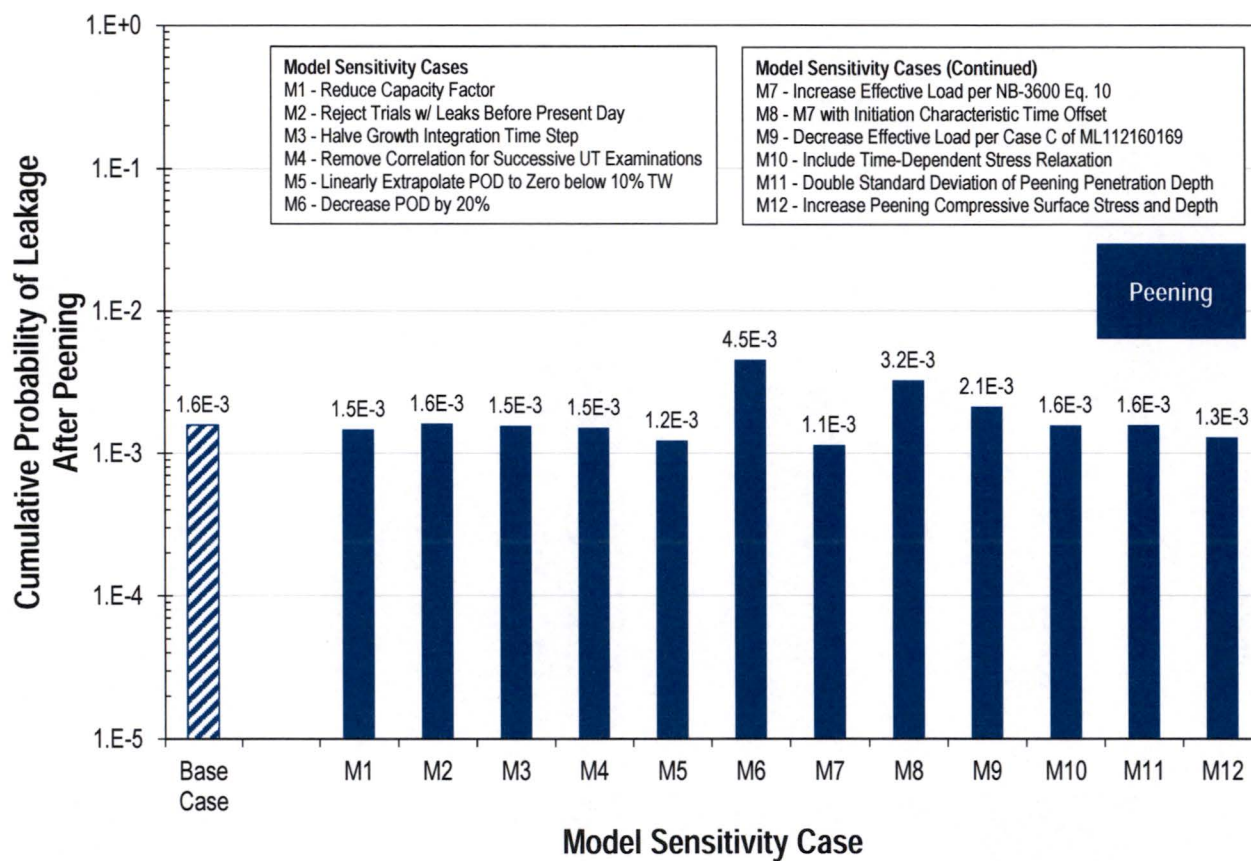


Figure A-22
Summary of Model Sensitivity Results for RVON Probabilistic Model with Peening

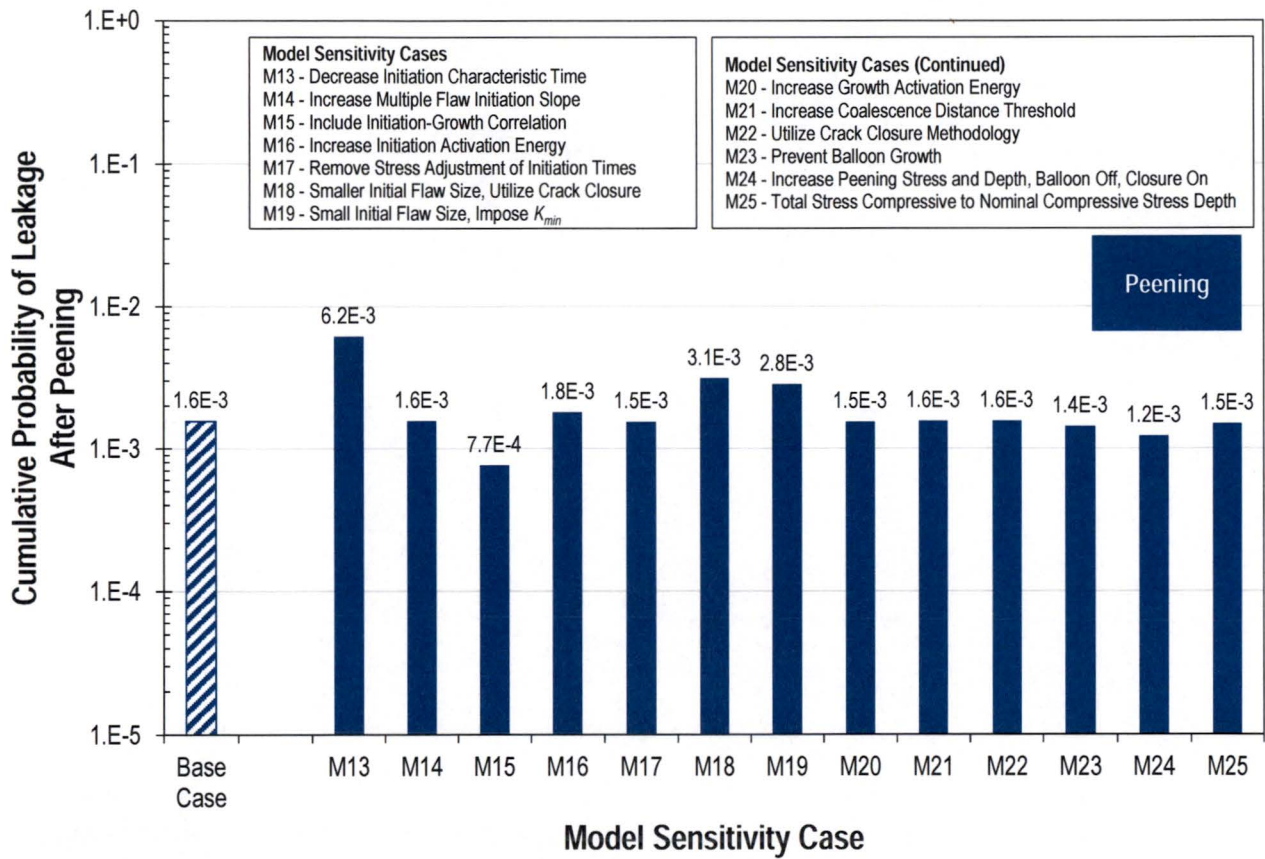


Figure A-23
Summary of Model Sensitivity Results for RVON Probabilistic Model with Peening (continued)

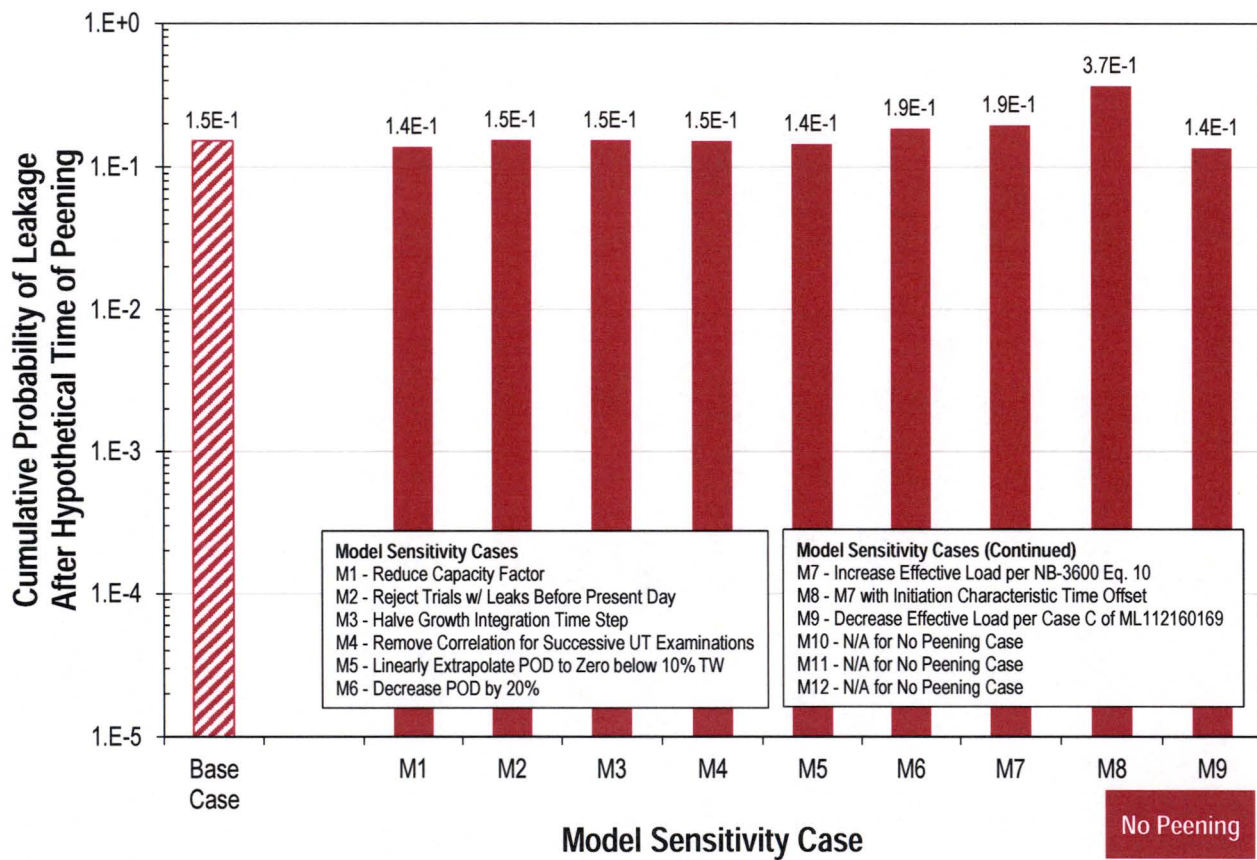


Figure A-24
Summary of Model Sensitivity Results for RVON Probabilistic Model without Peening

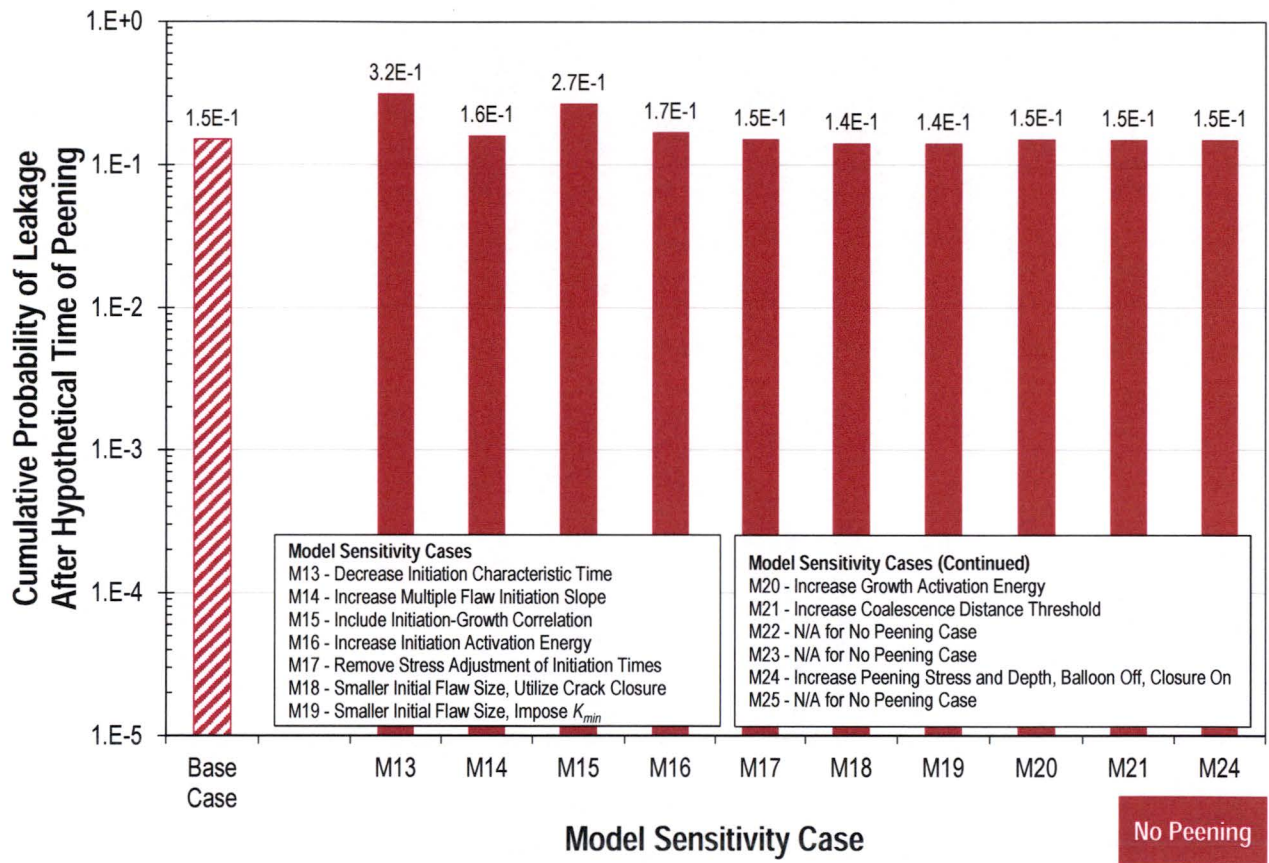


Figure A-25
Summary of Model Sensitivity Results for RVON Probabilistic Model without Peening (continued)

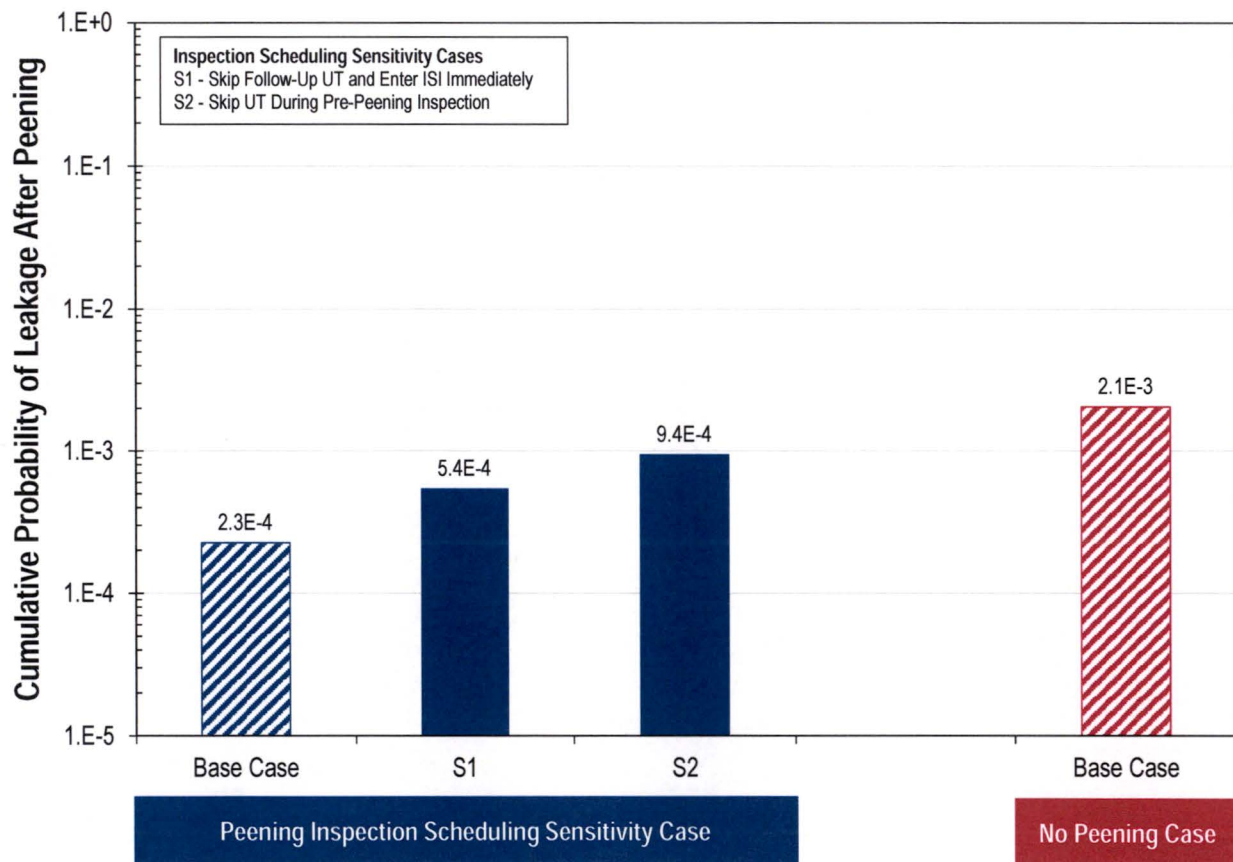


Figure A-26
 Summary for Inspection Scheduling Sensitivity Results for RVIN Probabilistic Model with Peening

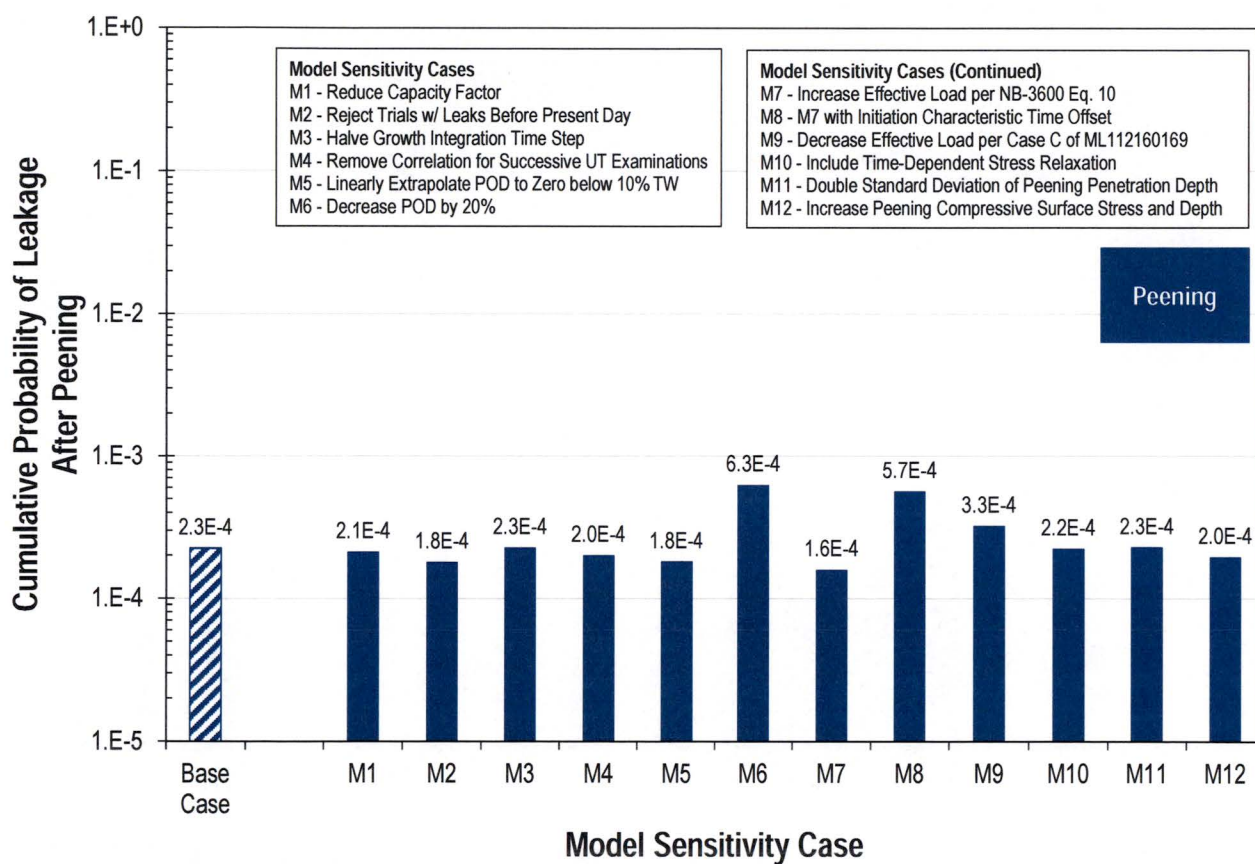


Figure A-27
Summary of Model Sensitivity Results for RVIN Probabilistic Model with Peening

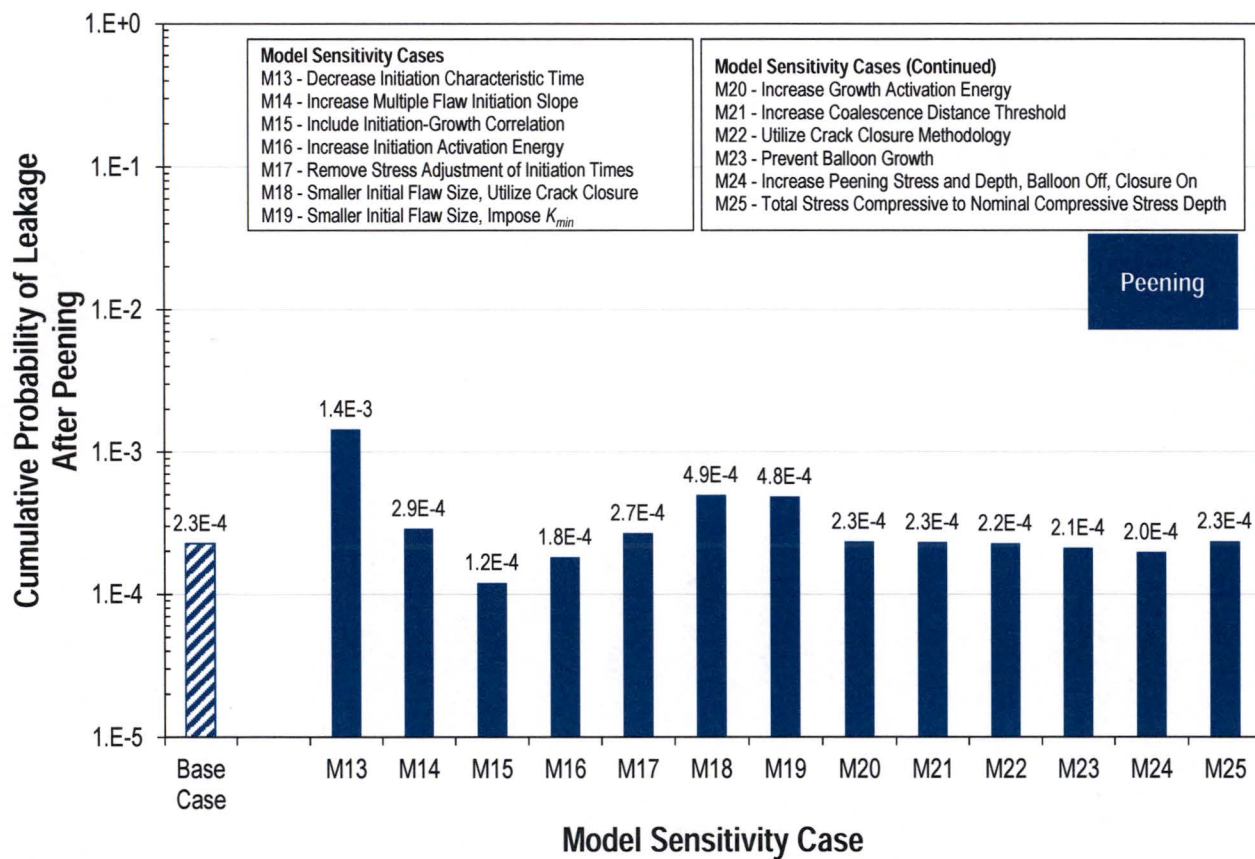


Figure A-28
Summary of Model Sensitivity Results for RVIN Probabilistic Model with Peening (continued)

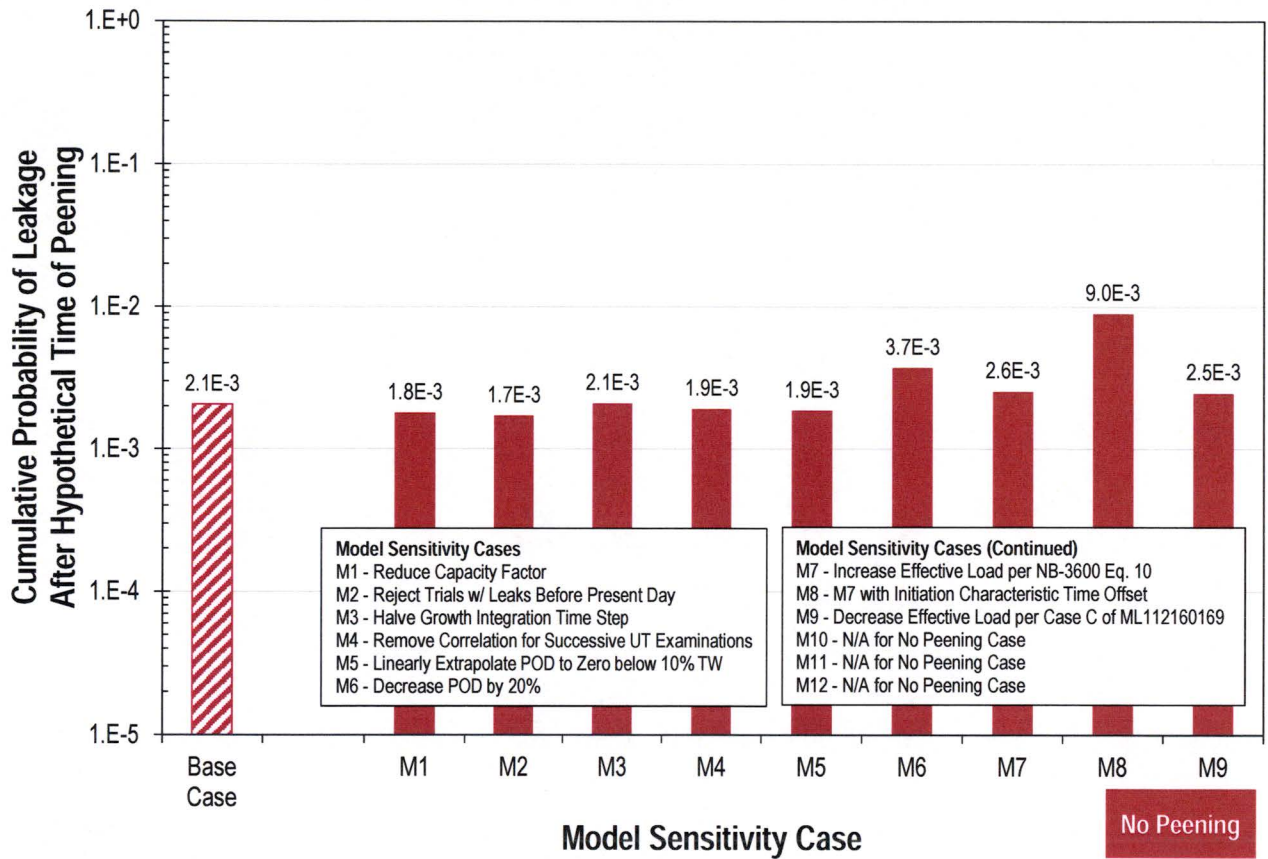


Figure A-29
Summary of Model Sensitivity Results for RVIN Probabilistic Model without Peening

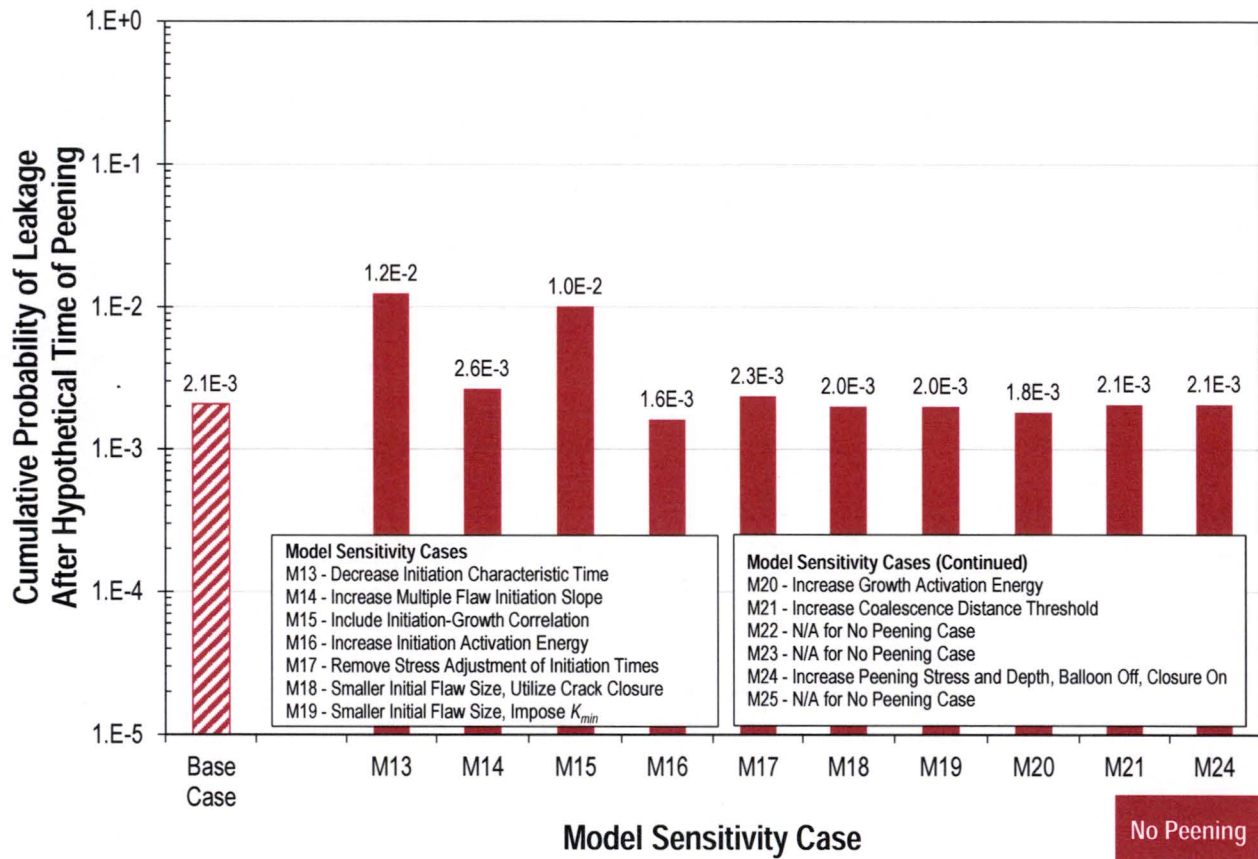


Figure A-30
Summary of Model Sensitivity Results for RVIN Probabilistic Model without Peening (continued)

A.10 Conclusions Regarding Appropriate In-Service Examination Requirements for DMWs in Primary System Piping Mitigated by Peening

The results of the probabilistic analysis of PWSCC on a general RVON support the relaxed UT inspection schedules prescribed in Section 4 of this report. Specifically, the cumulative leakage probability after the hypothetical time of peening is predicted to be reduced by:

- A factor of approximately 142 when the follow-up UT inspection is scheduled one cycle after peening and subsequent UT inspections are scheduled every 10 years (every interval)
- A factor of approximately 97 when the follow-up UT inspection is scheduled two cycles after peening and subsequent UT inspections are scheduled every 10 years (every interval)

The results of the probabilistic analysis of PWSCC on a general RVIN support the relaxed UT inspection schedules prescribed in Section 4 of this report. Specifically, the cumulative leakage probability after the hypothetical time of peening is predicted to be reduced by:

- A factor of approximately 11 when the follow-up UT inspection is scheduled two cycles after peening and no subsequent UT inspections are scheduled after follow-up examinations are performed
- A factor of approximately 12 when the follow-up UT inspection is scheduled three cycles after peening and no subsequent UT inspections are scheduled after follow-up examinations are performed
- A factor of approximately 9 when the follow-up UT inspection is scheduled six cycles after peening and no subsequent UT inspections are scheduled after follow-up examinations are performed

Many key input or modeling assumptions have been varied for Model Sensitivity Cases. While the leakage probability predictions are shown to vary for many of these cases, no case negates the prediction that a peened RVON or RVIN can maintain a lower probability of leakage with a relaxed inspection schedule (as compared to the unmitigated component). This is due primarily to the large margin of improvement predicted for the base cases.

Two Inspection Scheduling Sensitivity Cases investigate the impact of optional alterations to the inspection schedule/scope. Inspection Scheduling Sensitivity Case 2 demonstrates the importance of a pre-peening UT inspection.

A.11 References

1. *Materials Reliability Program: Probabilistic Fracture Mechanics Analysis of PWR Reactor Vessel Top Head Nozzle Cracking (MRP-105NP)*, EPRI, Palo Alto, CA: 2004. 1007834. [NRC ADAMS Accession No.: ML041680489]
2. *Materials Reliability Program: Technical Basis for Change to American Society of Mechanical Engineers (ASME) Section XI Appendix VIII Root-Mean-Square Error (RMSE) Requirement for Qualification of Depth-Sizing for Ultrasonic Testing (UT) Performed for the Inner Diameter (ID) of Large-Diameter Thick-Wall Supplement 2, 10, and 14 Piping Welds (MRP-373)*. EPRI, Palo Alto, CA: 2013. 3002000612. [Freely Available at www.epri.com]
3. *Materials Reliability Program: Reevaluation of Technical Basis for Inspection of Alloy 600 PWR Reactor Vessel Top Head Nozzles (MRP-395)*. EPRI, Palo Alto, CA: 2014. 3002003099. [Freely Available at www.epri.com]
4. D. Rudland, et al., "Development of Computational Framework and Architecture for Extremely Low Probability of Rupture (xLPR) Code," *Proceedings of the ASME 2010 Pressure Vessels & Piping Division / K-PVP Conference: PVP2010*, Bellevue, Washington, July 2010.
5. *xLPR Pilot Study Report*. U.S. NRC-RES, Washington, DC, and EPRI, Palo Alto, CA: NUREG-2110 and EPRI 1022860. 2012. [NRC ADAMS Accession No.: ML12145A470]
6. *Materials Reliability Program: Inspection and Evaluation Guidelines for Reactor Vessel Bottom Mounted Nozzles in U.S. PRW Plants (MRP-206)*. EPRI, Palo Alto, CA: 2009. 1016594. [Freely Available at www.epri.com]
7. W. H. Press, S. A. Teukolsky, W. T. Vetterling, B. P. Flannery, *Numerical Recipes. The Art of Scientific Computing. Third Edition*. Cambridge University Press, Cambridge, MA, 2007.
8. *Materials Reliability Program: Technical Basis for Primary Water Stress Corrosion Cracking Mitigation by Surface Stress Improvement (MRP-267, Revision 1)*, EPRI, Palo Alto, CA: 2012. 1025839. [Freely Available at www.epri.com]
9. *Materials Reliability Program Generic Evaluation of Examination Coverage Requirements for Reactor Pressure Vessel Head Penetration Nozzles, Revision 1 (MRP-95R1)*, EPRI, Palo Alto, CA: 2004. 1011225. [Freely Available at www.epri.com]
10. R. B. Abernethy, *The New Weibull Handbook, Second Edition*, Robert B. Abernethy, North Palm Beach, Florida, 1996.
11. *Materials Reliability Program: Crack Growth Rates for Evaluating Primary Water Stress Corrosion Cracking (PWSCC) of Alloy 82, 182, and 132 Welds (MRP-115)*, EPRI, Palo Alto, CA: 2004. 1006696. [Freely Available at www.epri.com]
12. T. L. Anderson, et al., "Development of Stress Intensity Factor Solutions for Surface and Embedded Cracks in API 579," *Welding Research Council Bulletin 471*, May 2002.
13. S. Marie, et al., "French RSE-M and RCC-MR code appendices for flaw analysis: Presentation of the fracture parameters calculation – Part III: Cracked Pipes," *International Journal of Pressure Vessels and Piping*, 84, pp. 614-658, 2007.

14. S. Xu, et al., "Technical Basis for Proposed Weight Function Method for Calculation of Stress Intensity Factor for Surface Flaws in ASME Section XI Appendix A," *Proceedings of the ASME 2011 Pressure Vessels & Piping Division / K-PVP Conference: PVP2011*, Baltimore, Maryland, July 2011.
15. *3-D Finite Element Software for Cracks: User's Manual v2.7*. Structural Reliability Technology – FEA Crack.
16. *ASME Boiler and Pressure Vessel Code 2011, Section XI, IWA-3330*, ASME, 2011.
17. M. Beghini and L. Bertini, "Fatigue Crack Propagation Through Residual Stress Fields with Closure Phenomena," *Engineering Fracture Mechanics*, Vol. 36, No. 3, pp. 379-387, 1990.
18. D. Rudland, et al., "PWSCC Crack Growth Mitigation with Inlay," *Proceedings of the ASME 2011 Pressure Vessels & Piping Division Conference: PVP2011*, Baltimore, Maryland, July 2011.
19. Case N-770-1, "Alternative Examination Requirements and Acceptance Standards for Class 1 PWR Piping and Vessel Nozzle Butt Welds Fabricated With UNS N06082 or UNS W86182 Weld Filler Material With or Without Application of Listed Mitigation Activities," Section XI, Division 1, American Society of Mechanical Engineers, New York, Approval Date: December 25, 2009.
20. *Materials Reliability Program: Development of Probability of Detection Curves for Ultrasonic Examination of Dissimilar Metal Welds (MRP-262, Revision 1) – Typical PWR Leak-Before-Break Line Locations*, EPRI, Palo Alto, CA: 2009. 1020451. [Freely Available at www.epri.com]
21. *PWR Materials Reliability Project, Interim Alloy 600 Safety Assessments for US PWR Plants (MRP-44): Part 1: Alloy 82/182 Pipe Butt Welds*, EPRI, Palo Alto, CA: 2001. TP-1001491, Part 1.
22. *Materials Reliability Program: Probabilistic Assessment of Chemical Mitigation of Primary Water Stress Corrosion Cracking in Nickel-Base Alloys (MRP-307), Zinc Addition and Hydrogen Optimization Mitigate Primary Water Stress Corrosion Cracking in Westinghouse Reactor Vessel Outlet Nozzles and Babcock & Wilcox Reactor Coolant Pump Nozzles*, EPRI, Palo Alto, CA: 2011. 1022852. [Freely Available at www.epri.com]
23. Memo from A. Csontos (NRC-NRR) to T.R. Lupold (NRC-NRR), "Hot Leg Flaw Evaluation Summary" dated August 18, 2011. [NRC ADAMS Accession No.: ML112160169]
24. *Materials Reliability Program: Advanced FEA Evaluation of Growth of Postulated Circumferential PWSCC Flaws in Pressurizer Nozzle Dissimilar Metal Welds (MRP-216, Rev. 1): Evaluations Specific to Nine Subject Plants*, EPRI, Palo Alto, CA: 2007. 1015400. [Freely Available at www.epri.com]
25. *PWSCC Prediction Guidelines*, EPRI, Palo Alto, CA: 1994. TR-104030. [Freely Available at www.epri.com]
26. J. A. Gorman, et al., "Correlation of Temperature with Steam Generator Tube Corrosion Experience," *Fifth International Symposium on Environmental Degradation of Materials in Nuclear Power Systems – Water Reactors*, E. Simonen and D. Cubicciotti, eds., American Nuclear Society, LaGrange Park, Illinois, 1992.

27. *Statistical Analysis of Steam Generator Tube Degradation*, EPRI, Palo Alto, CA: 1991. NP-7493. [Freely Available at www.epri.com]
28. C. Amzallag, et al., "Stress Corrosion Life Assessment of Alloy 600 PWR Components," *Ninth International Symposium on Environmental Degradation of Materials in Nuclear Power Systems – Water Reactors*, Edited by F.P. Ford et al., The Minerals, Metals & Materials Society (TMS), 1999.
29. Y. Yi and G. S. Was, "Stress and Temperature Dependence of Creep in Alloy 600 in Primary Water," *Metallurgical and Materials Transactions A*, Vol. 32, No. 10, pp. 2553-2560, 2001.
30. ASME Boiler and Pressure Vessel Code 2013, Section XI, Mandatory Appendix VIII, ASME, 2013.
31. ASME Boiler and Pressure Vessel Code 2011, Section III, Division 1, NB-3600, ASME, 2011.

B

PROBABILISTIC ASSESSMENT CASES FOR REACTOR PRESSURE VESSEL HEAD PENETRATION NOZZLES (RPVHPNS)

B.1 Scope of Assessment

There is currently a subpopulation of 24 reactor vessel top heads with Alloy 600 penetration nozzles operating in the U.S. that are potential candidates for peening mitigation. Currently, there are 41 replacement heads with PWSCC-resistant Alloy 690 nozzles in operation at U.S. PWRs, with two additional plants planning to perform head replacement by 2017. Of the 24 remaining Alloy 600 heads in operation, 19 operate at cold-leg temperature (i.e., cold heads) and five operate at a temperature significantly above cold-leg temperature (i.e., non-cold heads).

The probabilistic calculations presented in this section are designed to bound the conditions for all 24 of these heads, such that the conclusions of the probabilistic model are applicable to all U.S. PWRs that may perform peening mitigation of RPVHPNs. As described below, probabilistic calculations are performed for a non-cold head case (i.e., hot head) with an assumed head temperature (605°F) bounding that for the five candidate non-cold heads and for a cold head case with an assumed head temperature (561°F) bounding that for the 19 candidate cold heads.

B.1.1 CRDM and CEDM Nozzles

The design information tabulated in MRP-48 [1] shows that the large majority of RPVHPNs in the 24 heads with Alloy 600 penetration nozzles (1822 of 1890) are CRDM or CEDM nozzles. The basic geometry of CRDM/CEDM nozzles is illustrated in Figure B-1. All CRDM nozzles have the same basic nozzle tube dimensions (OD = 4.00 inches, ID = 2.75 inches, and wall thickness = 0.625 inch), while CEDM nozzles have roughly similar dimensions that vary among different plants designed by Combustion Engineering. The base case calculations presented in this section are based on the standard CRDM nozzle dimensions, while sensitivity cases are used to investigate the specific CEDM nozzle dimensions for two CE-designed heads.

B.1.2 Other RPVHPNs

A relatively small number of the Alloy 600 RPVHPNs currently operating in U.S. PWRs are nozzle types other than CRDM or CEDM nozzles (68 of 1890):

- 16 in-core instrumentation (ICI) nozzles in two CE-designed heads
- 22 J-groove head vent nozzles in 22 heads
- 8 J-groove auxiliary head adapter (AHA) nozzles in two Westinghouse-designed cold heads

- 2 “butt-weld” type head vent nozzles in two Westinghouse-designed heads
- 20 “butt-weld” type auxiliary head adapter (AHA) nozzles in five Westinghouse-designed cold heads

MRP-44 Part 2 [2] includes sketches illustrating each of these nozzles types. Because of their relatively small number, these other nozzles types were not explicitly included in the probabilistic calculations. Furthermore, the last two “butt-weld” type nozzles are not within the scope of Code Case N-729-1 [4] because they are not attached to the head with a partial-penetration (i.e., J-groove) weld. The conclusions of the probabilistic calculations are considered to extend to the full set of RPVHPNs attached using J-groove (i.e., partial penetration) welds for the following reasons:

- The greater diameter of the ICI nozzles results in a larger crack growth distance required for nozzle ejection compared to the case for a CRDM nozzle. Furthermore, there have not been any reported cases of PWSCC detected in ICI nozzles [3]. Thus, the ICI nozzles are conservatively represented with CRDM nozzle dimensions in the probabilistic calculations.
- For the same reasons as for the case of ICI nozzles, the J-groove type AHA nozzles are represented by CRDM nozzle dimensions in the probabilistic calculations.
- As was the case for the MRP-105 [5] probabilistic calculations forming a key part of the basis for inspection requirements for unmitigated RPVHPNs, the J-groove type head vent nozzles are not included in the probabilistic modeling. There is no more than one such nozzle in each head, it represents a much smaller potential break size than CRDM nozzles (about 1-inch diameter break compared to 2.75-inch ID typical for CRDM nozzles), and an ejection of a head vent nozzle would not result in an ejected control rod. It is considered that the head vent nozzle has a negligible effect on the probabilistic assessment of the set of RPVHPNs in a particular head.

Finally, the small number of “butt-weld” type nozzles noted above were not assessed as part of the analyses of RPVHPNs in this appendix. These nozzles explicitly fall outside of the scope of ASME Code Case N-729-1 [4].

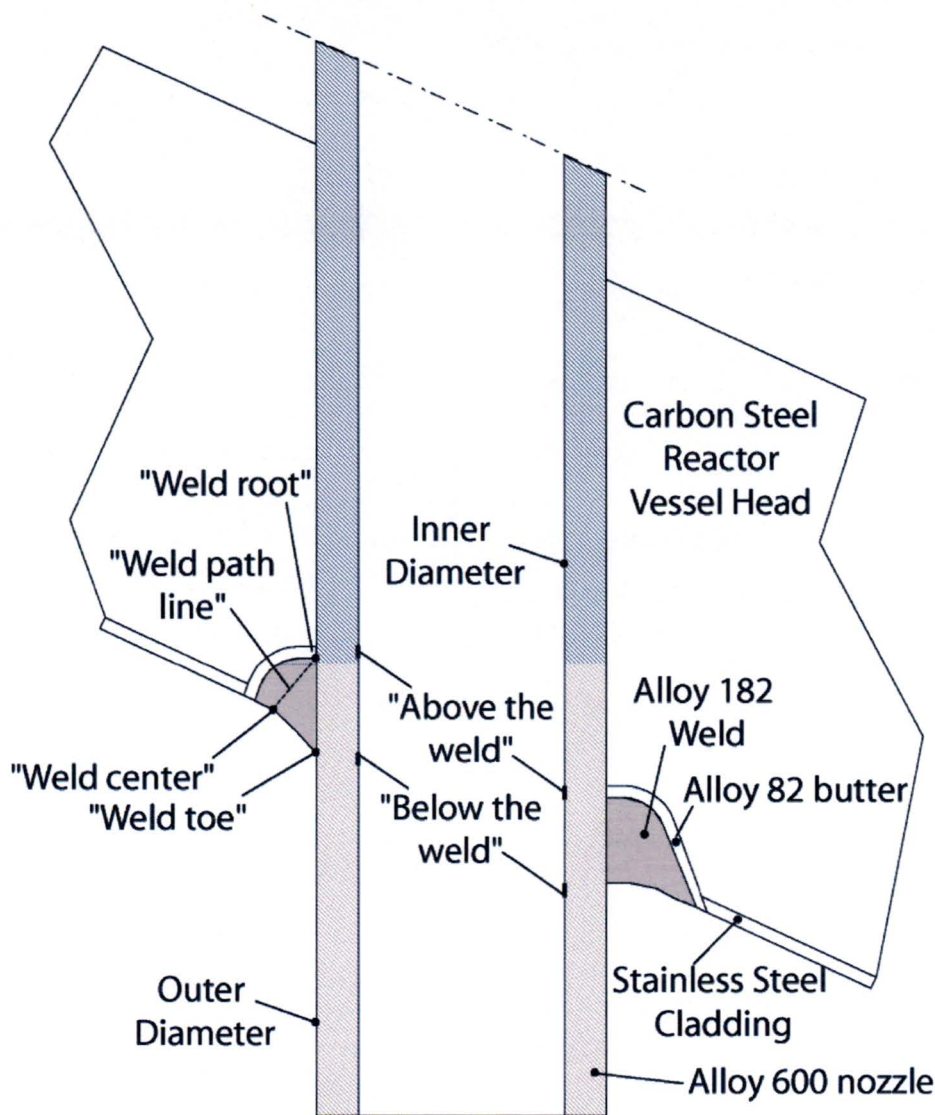


Figure B-1
Summary of General RPVHPN Geometry

B.2 Overall Modeling Methodology

The probabilistic model that was developed to study PWSCC in RPVHPNs was derived from the DM weld probabilistic model that is fully detailed in Appendix A. While the two models share a similar simulation framework, and several sub-models, there are many significant differences that will be discussed in this appendix. For conciseness, this appendix will reference portions of Appendix A where large overlap exists between the two models. To facilitate comprehension, this appendix has been organized analogously to Appendix A, in as much as possible.

A full description of the RPVHPN probabilistic modeling framework is given in the Section B.2.1. This is followed by Section B.2.2, which introduces the specific cracking modes (e.g., type, location, orientation, etc.) for which PWSCC initiation and growth are modeled; these modes will be referenced frequently throughout this appendix.

B.2.1 Probabilistic Modeling Methodology

The integrated probabilistic modeling framework that is used to study the effect of peening on RPVHPN PWSCC combines the individual models discussed in Sections B.3 through B.6. Namely, the probabilistic modeling framework is used to predict ejection criterion statistics, as discussed in Section B.7. Results generated with this model, using the inputs and uncertainties discussed in Section B.8, are given in Section B.9.

The RPVHPN probabilistic model applies a framework similar to the DM weld probabilistic model. In summary:

- Uncertainty propagation is handled by sampling input and parameter values from appropriately selected probability distributions (with appropriately selected bounds) in the main model loop, prior to the time looping structure. Important correlations are included.
- Event scheduling for a given weld, including operating, mitigation, inspection, and PWSCC initiation times, is developed in the main loop prior to entering the time looping structure.
- If one or more of the predicted PWSCC initiation times, adjusted for differences in temperature, are less than the final operating time and the time of peening (if applied), the time looping structure is entered. Each active flaw is allowed to grow until it reaches the end of the operation, its penetration is repaired, or its penetration nozzle is ejected.
- Initiations, ejections, repairs, among other events, are tracked as a function of operating cycle for each Monte Carlo realization and summary statistics are compiled at the end of each Monte Carlo run.

The central differences between the DM weld and RPVHPN models include:

- The RPVHPN model accounts for flaw initiation and growth on multiple penetrations (between 54 and 98 in a reactor vessel head), while the DM weld model only accounts for a single component, per Monte Carlo realization. Accordingly, a penetration loop exists inside the main loop and contains the time looping structure.
- The RPVHPN model accounts for several diverse modes of PWSCC initiation and growth (as detailed in Section B.2.2) as opposed to just axial and circumferential ID cracks. In fact, the majority of the model augmentation required for the RPVHPN model was to address new crack types and locations.
- In the case of DM welds, through-wall growth (i.e., leakage) is considered the end criteria (at which point simulation ends and summary statistics are compiled). For RPVHPNs, the end criteria is nozzle ejection; when leakage occurs due to a flaw at any location, it is assumed that this flaw immediately transitions to through-wall circumferential crack that grows along the top of the J-groove weld contour until it is repaired or it becomes large enough to fulfill the ejection criterion.
- Visual examination for leakage is modeled.
- There are other technical augmentations or logical revisions to be disclosed fully in the following sections.

A high level presentation of the main loop of the probabilistic model for a given weld is presented in Figure B-2 and a more detailed presentation of the time looping structure is given in

Figure B-3. The remainder of this section provides an end-to-end description of a single RPVHPN Monte Carlo run. Contrary to the rest of this appendix, this description is comprehensive and may have substantial overlap with Appendix A.

The initial conditions for the run are defined prior to entering the main loop. These initial conditions include all input parameters that remain constant throughout the run, such as the number and length of operating cycles, the frequency of inspections, certain weld geometry attributes, and the times of mitigation.

Following the definition of the initial conditions, the main loop is entered. The main loop is cycled for each Monte Carlo realization and is exited once all of the user-specified Monte Carlo realizations have been completed. After exiting the main loop, the program evaluates the results of the run, outputs certain information relevant to the study, and terminates the run.

At the beginning of each Monte Carlo realization, the values of reactor vessel head-specific distributed inputs are determined by random sampling. The distributions for each of the distributed inputs are user-defined. Then, the first flaw initiation model (detailed in Section B.4) is called to predict the initiation reference time for the reactor vessel head; the average time of the first PWSCC initiation in the head.

Following the definition of the head-specific values, the penetration loop is entered. This loop is cycled until PWSCC initiation and growth has been simulated for each penetration in the head. Upon exiting the penetration loop, the penetration results are cumulated to form penetration-specific and head-specific results.

At the beginning of each penetration cycle, penetration-specific distributed inputs are determined by random sampling. Then, the program invokes the multiple flaw initiation model (detailed in Section B.4) to predict the initiation times at all potential flaw sites. The flaw initiation times are compared to the "initiation end time": the final operating time, or, if peening is scheduled, the peening application time. The current penetration cycle is terminated if all of the predicted initiation times exceed the "initiation end time." If not, the initiation model assigns initiation conditions to each flaw with an initiation time occurring before the "initiation end time".

After determining that there are flaws that will initiate during the initiation time window in the current penetration, the program calls the load models (detailed in Section B.3) to determine the relevant loads at the various crack sites (including peening loads if peening is scheduled before the end of plant operation). This is different from, and more computationally efficient than, the DM weld model, which calculates load prior to initiation. The DM weld initiation model utilizes load information to incorporate a functional dependence of initiation time versus surface stress; the RPVHPN model does not; i.e., it is assumed that all locations on a given nozzle are equally likely to initiate PWSCC.

After attaining the stresses at locations of interest, the program enters the time looping structure for the current penetration.

The time looping structure is composed of an outer cycle-by-cycle loop with a nested within-cycle loop. The cycle-by-cycle loop may be terminated if the penetration is repaired or ejected. If this occurs, the program stores relevant information and cycles to the next penetration.

The within-cycle loop is entered if there is an active flaw on the current penetration whose initiation time is less than the time of the end of the current operating cycle. Immediately prior to

entering the within-cycle loop, any peening application that is scheduled for the current cycle is invoked resulting in new stress profiles utilized to predict crack growth.

If no flaw initiations occur prior to the end of the current sub-step in the within-cycle loop, the sub-step is skipped. Otherwise, at the beginning of the sub-step, the stress intensity factor for each active flaw is calculated based on the location of the flaw, the geometry of the flaw and its respective stress profile at the beginning of the sub-step. During each sub-step, all active flaws are grown using the flaw propagation model (detailed in Section B.5) that determines the flaw propagation rate and increases the depth and length of the flaw at a constant rate for the duration of the sub-step.

Before completing a given sub-step, the program checks if any flaw has reached through-wall (or through-weld in the case of the weld location), and if so, the cycle number is stored for a statistical summary generated at the end of the Monte Carlo run. Flaws that grow through-wall may or may not cause a leak (e.g., flaws that grow through-wall below the weld do not produce a leak). If a flaw does cause a leak, it is assumed to transition immediately to a circumferential through-wall crack that grows along the top of the J-groove weld contour. Flaws that are below the weld must grow in length to the nozzle OD annulus (i.e., the weld toe) before they are considered to leak.

At the end of each sub-step, any through-wall circumferential flaws are evaluated to predict if, cumulatively, they occupy enough of the nozzle circumference to cause ejection (detailed in B.7). The user can define an operating time at which an inspection has been performed by which time no nozzle ejections and no nozzle repairs had occurred. If ejection is predicted to occur (and the ejection time does not contradict the results of a user-defined assumed past inspection), the penetration is removed from service, the cycle number is stored for a statistical summary generated at the end of the Monte Carlo simulation, the current penetration simulation is terminated, and the program moves on to the next penetration. If the ejection result does contradict the results of the assumed past inspection, the code exits the penetration loop without saving any results and restarts the current Monte Carlo realization from the beginning of the main loop.

When all sub-steps of a given cycle have been completed, the program determines if an examination is to be performed at the end of the current cycle, and if the examination is to be ultrasonic (UT), bare-metal visual (BMV), or some combination of the two. If so, the inspection models (discussed in Section B.6) are called appropriately. If any flaw is detected (and its detection time does not contradict the results of an assumed user-defined past inspection) it is repaired, the cycle number is stored for a statistical summary generated at the end of the Monte Carlo simulation, the current penetration simulation is terminated, and the program moves on to the next penetration. In a similar fashion to an ejection occurrence, if the detection result contradicts the results of the assumed past inspection, the code exits the penetration loop without saving any results and restarts the current Monte Carlo realization from the beginning of the main loop. If a flaw is not detected, it remains active. After all scheduled inspections, the code returns to the cycle-by-cycle loop and continues to the next cycle or returns to the penetration loop if the cycle-by-cycle loop is complete.

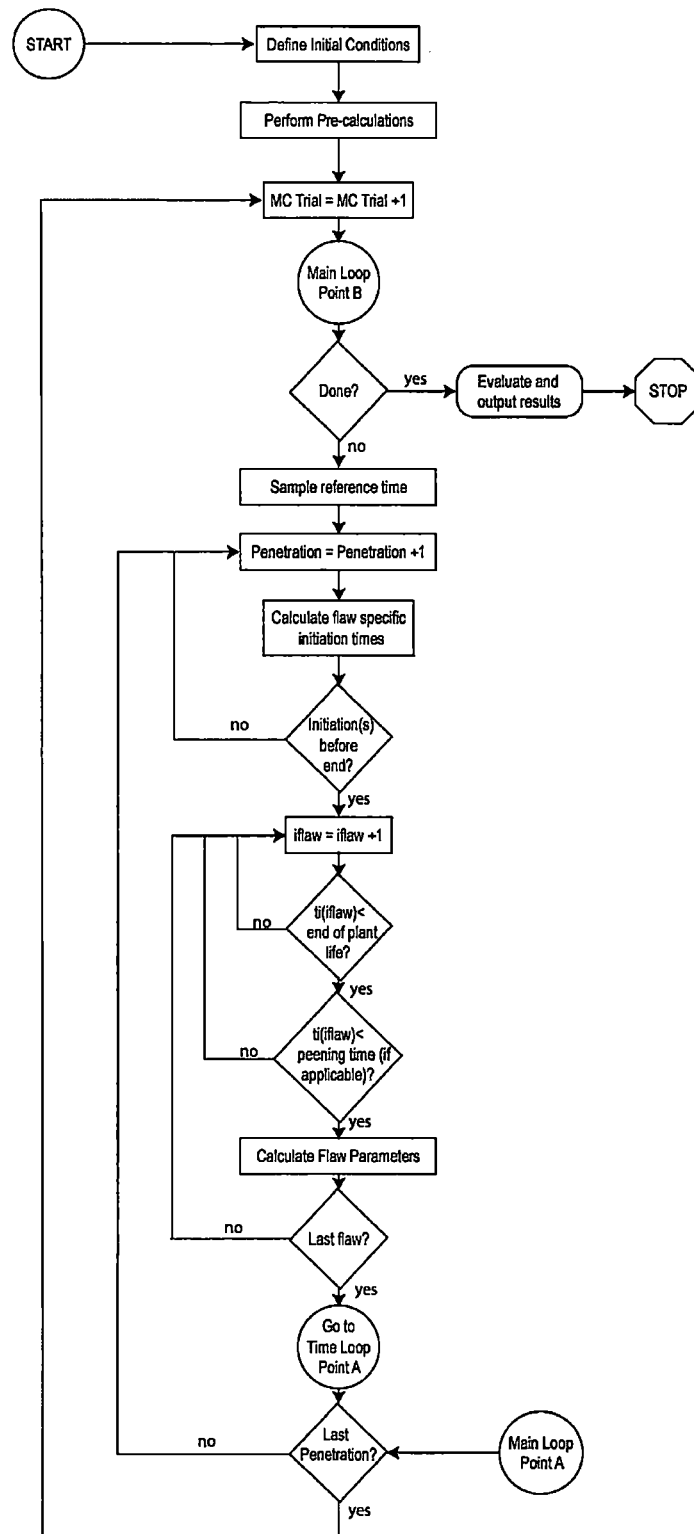


Figure B-2
RPVHPN Probabilistic Model Flow Chart: Main Loop

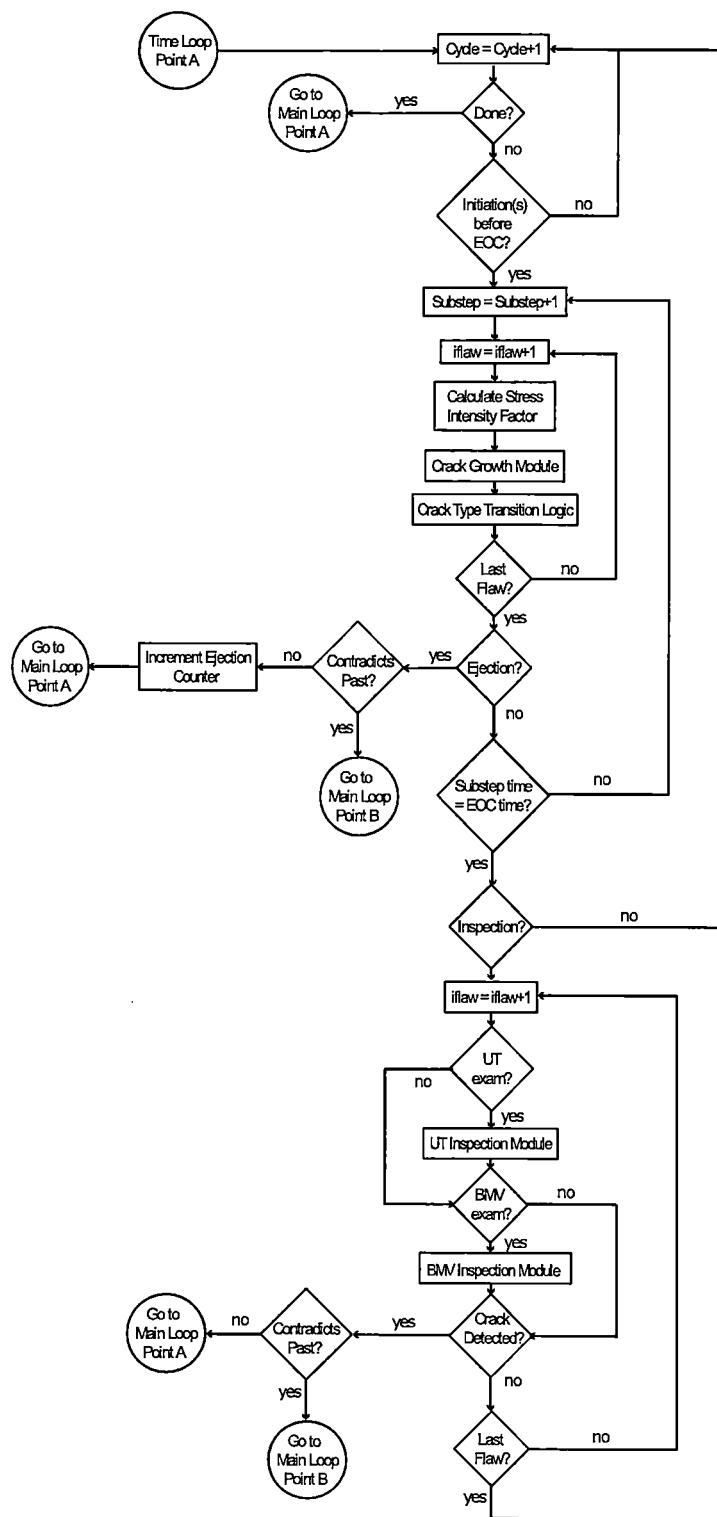


Figure B-3
RPVHPN Probabilistic Model Flow Chart: Time Loop

B.2.2 Definition of RPVHPN Cracking Modes

This section introduces the spatial discretization used to model PWSCC in RPVHPNs and, subsequently, the different cracking modes modeled at the various locations. Each cracking mode reflects a cracking type observed on reactor vessel heads in industry. Due to varying geometry, accessibility, material condition, etc., each mode is modeled with a unique set of initiation, load, growth, and examination techniques. It is important to distinguish each mode, as they will be referenced frequently throughout this appendix. Table B-1 summarizes each mode. Figure B-4 provides a schematic of a general RPVHPN and indicates the primary growth direction (i.e., the direction that leads to leakage) of each modeled PWSCC mode.

For the purpose of this study, each RPVHPN is divided into an uphill and downhill side. Each cracking mode may initiate on either the uphill or downhill sides, both of which have their own unique loading conditions. The downhill and uphill sides are selected as the only circumferential locations for crack initiation. This convention is based on the fact that the downhill and uphill locations are the locations of highest tensile weld residual stresses (due to nozzle ovalization).

The key characteristics of the cracking modes modeled in this study are given below:

- **ID axial cracks (Mode 1)** – partial through-wall cracks located on the penetration nozzle ID. These cracks are conservatively assumed to initiate in the region above the weld such that they immediately result in leakage if they penetrate through-wall into the OD nozzle annulus. These cracks are opened by hoop stresses in the penetration nozzle.
- **OD axial cracks (Mode 2)** – partial through-wall cracks located on the penetration nozzle OD located below the weld. These cracks cause leakage if they grow in length to reach the nozzle OD annulus; they may transition to through-wall axial cracks if they grow through-wall before reaching the annulus. These cracks are opened by hoop stresses in the penetration nozzle.
- **Radially-oriented weld cracks (Mode 3)** – cracks located on the J-groove weld that grow toward the weld toe. These cracks cause leakage if they reach the weld toe. These cracks are opened by hoop stresses in the J-groove weld.
- **Through-wall axial cracks (Mode 4)** – through-wall cracks located below the weld. These cracks may only form if an OD axial crack reaches through-wall before reaching the nozzle OD annulus. These cracks cause leakage if they grow long enough to reach the nozzle OD annulus. These cracks are opened by hoop stresses in the penetration nozzle.
- **Circumferential through-wall cracks (Mode 5)** – through-wall cracks located on the weld contour above the weld. These cracks are assumed to occur immediately following leakage caused by any of the preceding crack modes, either by branching of the flaw causing the leakage or by initiation of a new flaw on the OD surface of the nozzle. These cracks are opened by a complex stress field acting orthogonally to the weld contour.

Table B-1
Summary of PWSCC Modes Modeled on RPVHPNs

Mode ID	Orientation	Shape	Material Characteristics	Location	Transitions to...
1	Axial	Semi-elliptical, part-through-wall	Alloy 600	Top of weld, inner diameter	Mode 5 upon growing through-wall
2	Axial	Semi-elliptical, part-through-wall	Alloy 600	Bottom of weld, outer diameter	Mode 5 upon growing to weld root, or mode 4 upon growing through-wall
3	Radially-oriented	Semi-elliptical, part-through-weld	Alloy 82/182	On weld	Mode 5 upon growing to weld root
4	Axial	Rectangular, through-wall	Alloy 600	Bottom of weld	Mode 5 upon growing to weld root
5	Circumferential	Through-wall	Alloy 600	Along upper weld contour	Ejection upon growing past stability threshold

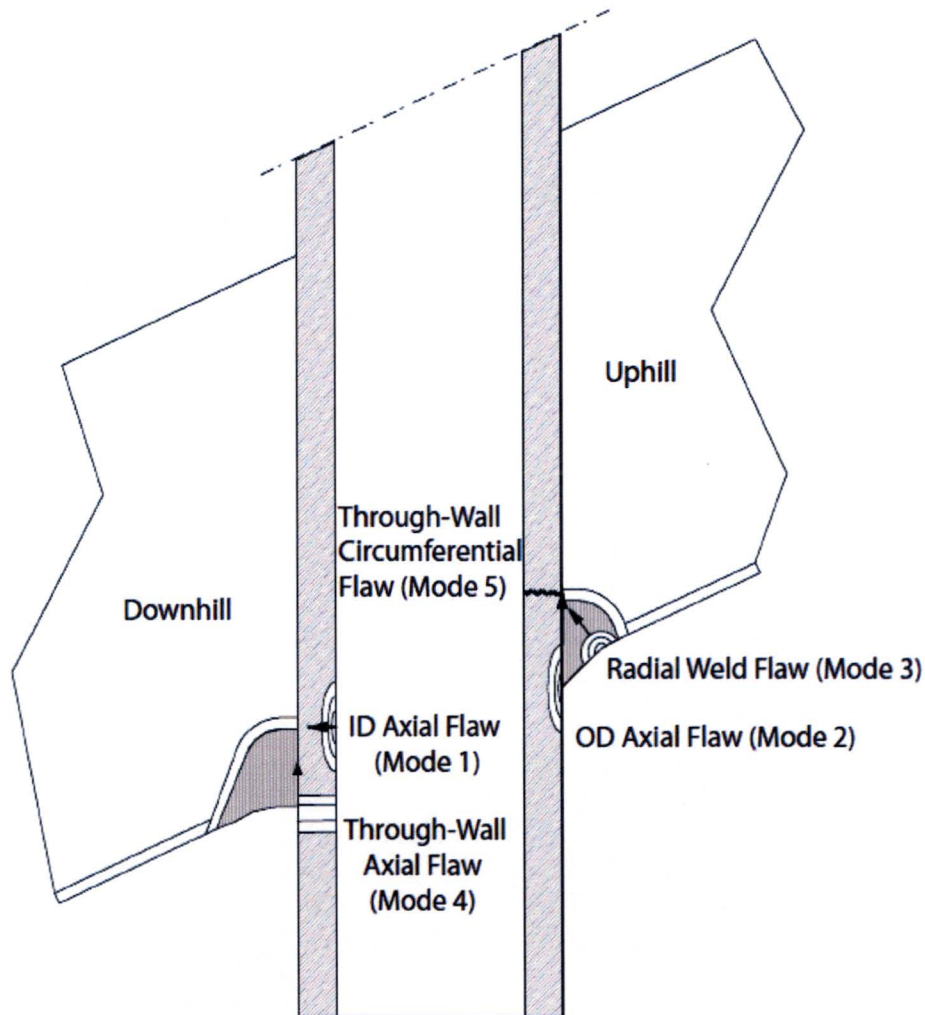


Figure B-4
Schematic of Modeled Cracking Modes for RPVHPN Probabilistic Assessment (Arrows Indicate Direction of Growth Toward Leakage)

B.3 Load and Stress Model

Load models are used to calculate stresses at the different locations of interest for PWSCC on RPVHPNs. The crack growth model uses this stress information; it is noted, however, that the RPVHPN crack initiation model does not explicitly account for stress dependence.

The load models account for welding residual stresses as well as operational loads. In addition, a peening residual stress model is introduced for modeling crack growth during cycles after a peening application, if applicable.

The methodologies for calculating stresses due to operational loads, penetration welding, and peening are discussed in Sections B.3.1, B.3.2, and B.3.3, respectively. Considerations for the effects of temperature and load cycling are discussed in Section B.3.4. The loads used for crack growth at the various locations are summarized in Section B.3.5.

B.3.1 Internal Pressure and Piping Loads

The operational stresses, which are due predominantly to internal pressure, are separated from the residual stresses in this analysis (as they were for the DM weld load models). This separation serves a practical purpose in modeling peening because it allows for peening effects to be applied to existing residual stresses, without altering operational stresses. The operational stresses can be superimposed with post-peening residual stresses to provide the total stresses used to estimate crack growth.

Unlike DM welds, the complex geometry of a reactor vessel head penetration precludes the accurate estimation of operational stresses at the various locations of interest by way of analytical, or textbook, approaches. Accordingly, operational stresses at each location have been ascertained from the results of various J-groove weld finite element analyses (the general methodology of such RPVHPN FEA studies is outlined in [6]). Specifically, operational stresses are attained by subtracting stress states predicted by FEA during operation from those predicted during shutdown (i.e., operational = total – residual).

Operational stress at each location of interest is treated as being constant through-wall (or through-weld), with a magnitude equal to the *surface* operational stress predicted by FEA results. This convention accurately accounts for the separation of residual and operational stresses near the peened surface. Careful separation of the residual and operational stresses away from the peened surface is not necessary; the total stress profile after peening is largely insensitive to the way residual and operational stresses are separated away from the surface (as becomes apparent after reviewing the peening modeling methodology in Section A.3.3).

The FEA results reveal that operational stresses are negligible at the OD and weld surfaces (in comparison to the welding residual stresses at these surfaces). As with DM welds, pressure acting to open a crack face is included after crack formation such that the operational stresses become:

$$\begin{aligned}\sigma_{oper,OD} &= P \\ \sigma_{oper,weld} &= P\end{aligned}\tag{B-1}$$

Hoop operational stresses at the ID surface are modeled using a stress concentration that is applied to the nominal hoop stress estimated with thin-walled cylinder theory:

$$\sigma_{oper,ID} = F_{oper,ID} \frac{PD_i}{2t} + P \quad [B-2]$$

where $F_{oper,ID}$ is the ID hoop stress concentration factor, P is the normal operating pressure, D_i is the penetration nozzle inner diameter, and t is the penetration nozzle thickness. The ID stress concentration factor has been derived from FEA results as is detailed in Section B.8.1. Note that this equation also includes the pressure acting to open the crack face after crack formation.

B.3.2 Welding Residual Stress Before Peening

The J-groove welding residual stress profiles at six locations/directions (vectors) of interest are derived from the same set of FEA results used for operational stresses in the previous section. Specifically, six vectors are relevant for predicting the crack growth modes discussed in Section B.2.2: hoop stress from the penetration nozzle ID to the OD above the weld (uphill/downhill), hoop stresses from the penetration nozzle OD to the ID below the weld (uphill/downhill), and hoop stresses from the weld surface to the weld toe (uphill/downhill). These vectors are depicted in Figure B-5.

For all six vectors, a second-order polynomial function of through-wall (or through-weld) fraction is used to model the total stress profile. These polynomials are fit to FEA results during operational loading (and the residual stresses are attained by subtracting the operational stresses discussed in the previous section). This is different from the third- and fourth-order curves used for welding residual stresses in DM welds, but is considered accurate for capturing the essential gradient and curvature characteristics observed in RPVHPN FEA results [6]. The resulting general equation form is:

$$\sigma_{tot,loc} \left(\frac{x}{D} \right) = \sigma_{0,FEA,loc} + \sigma_{1,FEA,loc} \left(\frac{x}{D} \right) + \sigma_{2,FEA,loc} \left(\frac{x}{D} \right)^2 + P \quad [B-3]$$

where the *loc* subscript is a placeholder for the various locations of interest, D is a general dimension equal to the penetration nozzle thickness for ID and OD locations and equal to the weld path length for weld locations, and $\sigma_{0,FEA,loc}$, $\sigma_{1,FEA,loc}$, and $\sigma_{2,FEA,loc}$ are sampled parameters based on curve-fits to FEA results. Note that the standard superposition approach is applied to consider the crack face pressure by adding it to the membrane stress term in the equation above.

The fit parameters are calculated such that they give the second-order polynomial stress profile defined by the following three points:

1. The stress at the initiation surface:

$$\sigma_{tot,loc} (0) = \sigma_{0,FEA,loc} + P \quad [B-4]$$

2. The stress at the opposite surface (or the weld root for weld locations):

$$\sigma_{tot,loc}(1) = R_{1,loc} \sigma_{0,FEA,loc} + P \quad [B-5]$$

3. The stress at the mid-radius (or the mid-point between the weld center and the weld root for weld locations):

$$\sigma_{tot,loc}(0.5) = R_{0.5,loc} \left(\frac{\sigma_{0,FEA,loc} + R_{1,loc} \sigma_{0,FEA,loc}}{2} \right) + P \quad [B-6]$$

The $R_{1,loc}$ and $R_{0.5,loc}$ terms are indicative of the average gradient and curvature of the resulting stress profile, respectively. Together with the surface stress at the location/direction of interest ($\sigma_{0,WRS,loc}$), these terms have been fit to FEA results, as detailed in Section B.8.1.

For completeness, the general welding residual stress equation is given below:

$$\sigma_{WRS,loc} \left(\frac{x}{D} \right) = \sigma_{0,FEA,loc} + \sigma_{1,FEA,loc} \left(\frac{x}{D} \right) + \sigma_{2,FEA,loc} \left(\frac{x}{D} \right)^2 - \sigma_{oper,loc} \quad [B-7]$$

B.3.3 Residual Stress After Peening

As discussed previously, peening has the effect of adding a thin region of compressive stress in all three principal directions near the surface of its application. This compressive residual stress region prevents crack initiation and affects the stress field that influences growth of pre-existing flaws. Hence, peening is required to be captured in this modeling effort.

At all locations of interest for each penetration, the peening effect is modeled in the same manner as in the DM weld program (see Section A.3.3); i.e., using a four-region piecewise equation that combines a compressive region near the surface with the pre-existing residual stresses while maintaining the same equivalent force through-wall (or through-weld) before and after peening. For that reason, the details of peening modeling will not be repeated here. Any differences in the way peening is applied in the DM weld program and the RPVHPN program are noted below:

- For RPVHPNs, the initial compressive surface stress and the penetration depth are sampled independently at each location. This is different from the DM weld program, which assumes that the peening is applied uniformly to all ID locations.
- For RPVHPNs, the compressive residual stress depths are sampled from separate distributions for the ID locations, as compared to the OD and weld locations. A peening compressive residual stress depth of 1.0 mm is assumed for the wetted nozzle OD and surface attachment area susceptible to PWSCC initiation, whereas a compressive residual stress depth of 0.25 mm is assumed for the nozzle inside surface. These assumptions are based on the peening performance criteria defined in Section 4.
- For weld locations, the through-element dimension is the weld path length instead of the penetration nozzle thickness (i.e., in Equations [A-18] through [A-21]).
- The effect of peening on growth is conservatively neglected for several scenarios described below:

- ID peening stresses above the weld are assumed to have no effect on the growth of circumferential through-wall cracks. The growth of circumferential through-wall cracks is based on stress intensity factors that were calculated with finite element software and these models did not include stresses representative of a peened nozzle.
- OD peening stresses below the weld are assumed to have no effect on the growth of partial through-wall axial OD cracks that have grown under the weld far enough that the upper crack surface tip is outside of the peened region (as demonstrated in Figure B-6).
- ID peening stresses do not affect nearly through-wall axial OD cracks (as demonstrated in Figure B-6), i.e., the thin compressive region near the ID is not given credit for abating the growth of mostly (90-100%) through-wall cracks.

B.3.4 Effect of Operating Temperature and Load Cycling

Residual stress relaxation due to temperature and load cycling can occur at penetration locations, as it can in DM weld components. As discussed for DM welds, the effects of thermal relaxation and load cycling (i.e., shakedown) must be considered when demonstrating that the minimum peening stress effect required by the applicable performance criteria will be obtained. Thus, the effects of thermal relaxation and load cycling subsequent to peening of RPVHPNs are implicitly addressed through modeling of the bounding stress effect meeting the performance criteria in the calculations of this appendix.

B.3.5 Summary of Load Model

The RPVHPN load model is used to attain through-wall (or through-weld) stress profiles on the different vectors that are attributed to the growth of the various cracking modes.

Total stresses and operational stresses (i.e., those stresses due to loads present during operation) are derived from FEA results and welding residual stresses are attained from the difference between the total and operational stresses. The total stress profile at each location is modeled with a second-order polynomial function of the through-wall fraction. The operational stress profile at each location is modeled with a constant stress.

Prior to peening, the total stress profiles used to predict crack growth are those derived from FEA results (plus the crack face pressure contribution).

The peening load model modifies the welding residual stress profiles to predict post-peening residual stresses. After peening is applied, the post-peening residual stress profile is superimposed with the operational stresses to attain the total stress profiles used to predict crack growth.

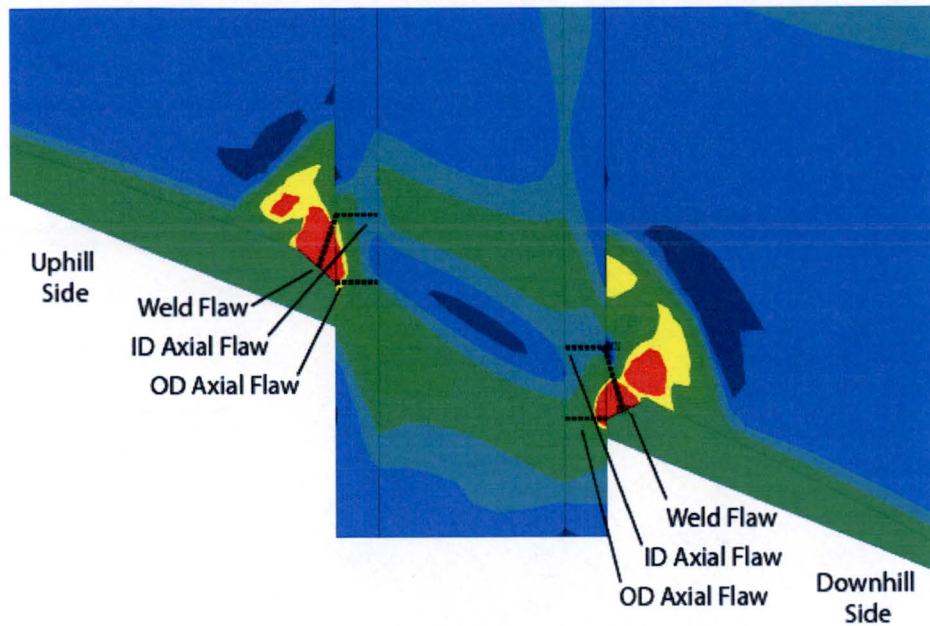


Figure B-5
Depiction of Stress Profile Vectors for Each Crack Mode Location (six bold dotted lines)
and Welding Residual Hoop Stress Contour Plot

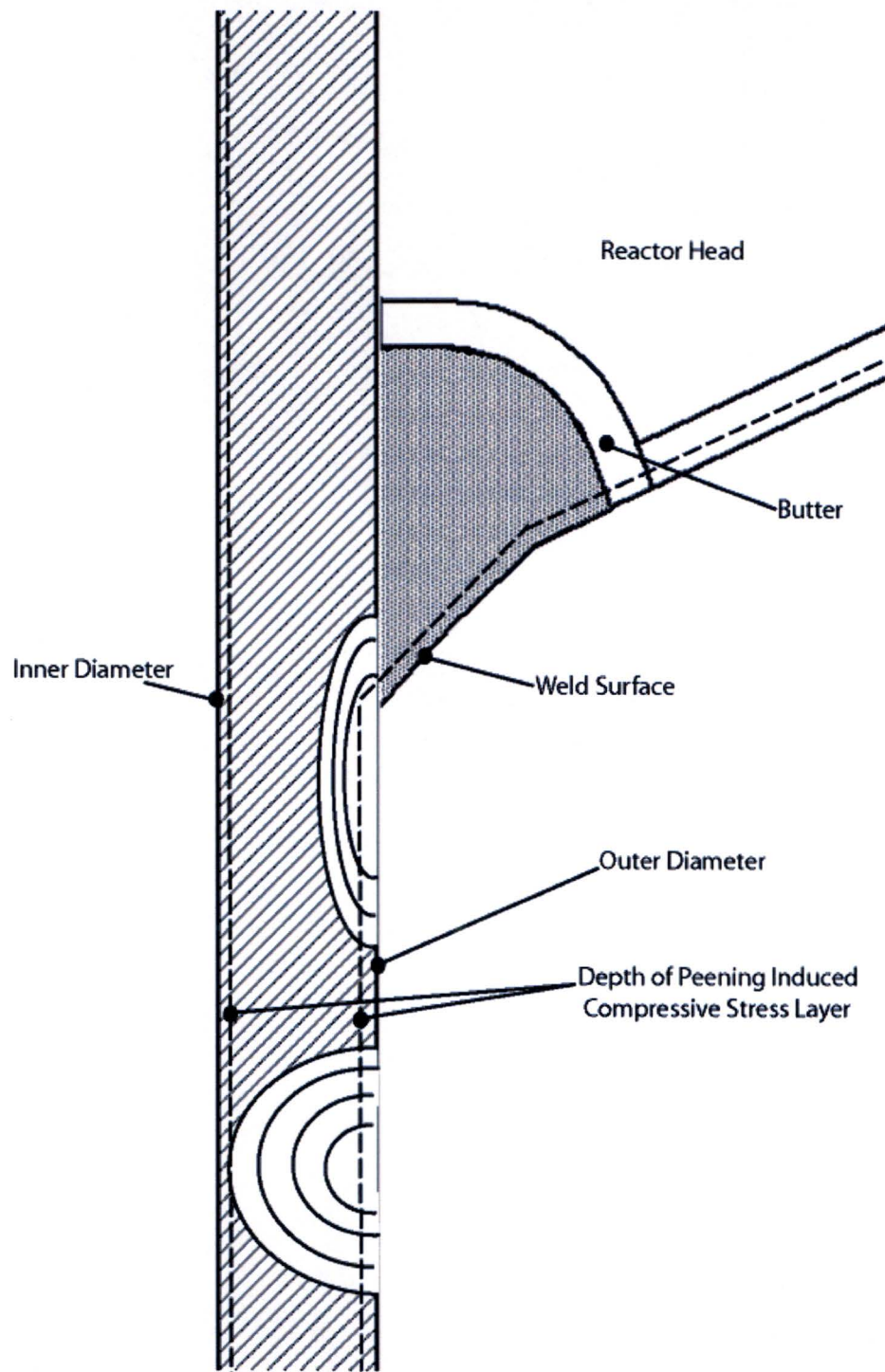


Figure B-6
Scenarios for Excluding Peening Effects in RPVHPNs: a) Crack Extends Below Weld, Past Reduced-Stress Layer (top flaw); b) OD Crack Depth Reaches ID Reduced-Stress Layer (bottom flaw)

B.4 Crack Initiation Model

This study employs a statistical Weibull approach for predicting crack initiation that is similar to the approach used by the DM weld program (discussed in Section A.4). As such, much of the information presented for DM welds will not be repeated in this section, which will instead focus on detailing the differences between the initiation models.

The key difference in the initiation models is that the RPVHPN initiation model does not include a surface stress adjustment. This adjustment was considered unfounded for RPVHPNs based on the following information:

- The surface stresses at all RPVHPN locations of interest are randomly sampled and are similar in tensile magnitude while surface stresses at DM weld locations vary systematically as a function of distance from the point of maximum tensile bending stress. Accounting for this systematic stress variation on the DM weld circumference is important for modeling coalescence.
- No clear stress-dependent location preference emerges from industry experience of PWSCC initiation on RPVHPNs.
- There is no known precedent for applying a stress-adjustment when modeling multiple initiation of PWSCC in different locations on individual RPVHPNs.

A second notable difference is that the RPVHPN initiation model predicts PWSCC initiation across all of the penetrations in a single head, as opposed to a single component.

B.4.1 Spatial Discretization of Crack Sites

The spatial discretization of the crack locations is described in Section B.2.2. To summarize, six cracking modes are considered for crack initiation in this study: axial cracks on the nozzle ID at the top of the weld (uphill/downhill), axial cracks on the nozzle OD at the bottom of the weld (uphill/downhill), and radially-directed cracks at center of the weld surface (uphill/downhill).

These six *locations* are considered for the number of penetrations in the head, N_{pen} , resulting in $6N_{pen}$ total initiation *sites*.

In this appendix, the subscript *loc* is used to denote the different locations and the subscript *i* is used to denote the different penetrations on the head.

B.4.2 Initiation Time of First Crack

As was done to predict time of first initiation on DM welds, a Weibull model has been selected for predicting the time of first initiation of PWSCC in RPVHPNs. The use of this statistical model reflects systematic and statistical variations in material properties and environmental conditions from head to head, across the industry. The advantages of the Weibull model, and a general description, can be found in Section A.4.2.

The Weibull slope, β , an arbitrary failure fraction, F_1 , (e.g., 0.1%, 1%, 10%, 63.2%, etc.), and the time at which this arbitrary failure fraction is reached, t_1 , are provided as inputs to the probabilistic model. The value of the Weibull characteristic time parameter, θ , is then determined during runtime using Equation [A-30]. The process by which β , F_1 , and t_1 are fit to existing data for first crack initiation in RPVHPNs is discussed in Section B.8.2.

Once β and θ are known for the current Monte Carlo realization, they can be used to sample a reference initiation time in EDY (t_{ref}). The sampled initiation time is adjusted for temperature (to convert to EFPY) using the Arrhenius relationship:

$$t_f = t_{ref} \times e^{\left(\frac{Q}{R}\right)\left(\frac{1}{T} - \frac{1}{T_{ref}}\right)} \quad [B-8]$$

The result of the above equation is considered to be the *average* time of the first PWSCC initiation for the head. Unlike the DM weld initiation model, this time is not applied to any specific initiation site. Similar to the DM weld initiation model, this time is used by the multiple crack initiation model, which is discussed next.

B.4.3 Initiation Times of Multiple Cracks

A Weibull model has been selected for use in predicting times of initiation of multiple PWSCC cracks on a head. The use of this statistical model reflects systematic and statistical variations in material properties and environmental conditions from location to location, and from penetration to penetration, on a single head.

The multiple crack initiation Weibull model uses a separate Weibull slope, $\beta_{mult,i}$, to reflect a new rate at which PWSCC degradation spreads to multiple sites on a head after the first crack initiation. This Weibull slope is sampled for each penetration to reflect the premise that each penetration has unique conditions relevant to multiple flaw initiation¹⁶. The distribution selected for $\beta_{mult,i}$ is discussed in Section B.8.2.

Since the time provided by Equation [B-8] is indicative of the average time of the first PWSCC initiation across all $6N_{pen}$ crack sites, it is therefore associated with the cumulative probability (F_{1st}) given in Equation [B-9] below:

$$F_{1st} = \frac{1 - 0.3}{6N_{pen} + 0.4} \quad [B-9]$$

For each penetration, the characteristic time parameter for the multiple flaw Weibull model, $\theta_{mult,i}$, is calculated from $\beta_{mult,i}$, t_{ref} , and F_{1st} above using Equation [A-30]. Then, an initiation time for each crack site, $t_{ref,i,loc}$, is sampled from the resulting Weibull distribution. Sampled initiation times are not truncated at t_{ref} as they were for DM welds.

The above approach allows for the initiation of multiple cracks and it can be shown that, on average, a single initiation across all initiation sites is expected prior to t_{ref} , the average time of first initiation based on industry experience.

¹⁶ It is noted that sampling the multiple flaw Weibull slope for each penetration results in the clustering of flaws on affected penetrations. This clustering effect may have a strong impact on leakage and ejection probabilities due to the detection, repair, and stability logic. In a sensitivity study, the Weibull slope will only be sampled for each reactor vessel head to demonstrate the relative effect of the sampling strategy.

B.4.4 Crack Initialization

Crack initialization refers here to assigning initial conditions to each crack at its initiation time. These initial conditions include size, location, and capacity for growth. The crack modes are fixed by the initiation site, as discussed in Section B.4.1.

Initial crack depth is sampled from a distribution of positive, non-zero, crack depths. This reflects both that the Weibull initiation models discussed above were fit to industry data recording first detection of crack indications and that crack detection is only possible for finite crack sizes. Initial crack lengths are attained by scaling the initial depth by a sampled aspect ratio.

Initiation location is not tracked for ID cracks. ID cracks are assumed to initiate at an arbitrary axial location near the weld top such that leakage occurs upon through-wall growth. Similarly, weld cracks are assumed to initiate at the weld center.

Initiation location is tracked for OD cracks. The variability in OD crack axial location affects the crack's susceptibility to leakage; i.e., the OD crack location together with the OD crack length provides a means to predict if the crack has grown long enough to reach the nozzle OD annulus. For OD cracks, the initial axial location is attained by taking a uniform sample between the weld toe and the axial location where the weld residual surface stress falls below 80% of yield stress. For a typical Alloy 600 penetration nozzle, this results in an initiation location threshold of approximately 30-40 ksi. This threshold is larger than the 20 ksi presumed to be required for PWSCC initiation [7], but conservatively results in initiation locations nearer to the OD nozzle annulus. Furthermore, crack initiation locations are likely to be biased toward the higher stress region. The location of 80% of yield was derived from results of J-groove welding residual stress FEA results [6].

In a similar fashion to the DM weld initialization, the capacity for growth of each crack is dependent on sampled crack growth variation terms: f_{weld} and $f_{ww,i}$ for Alloy 82/182 cracks or f_{heat} and $f_{wh,i}$ for Alloy 600 cracks. The accepted tendency of components that are more susceptible to PWSCC initiation to have higher flaw propagation rates can be included by correlating the sampled f_{weld} and f_{heat} terms with the average time of first initiation, t_{ref} .

B.5 Crack Growth Model

The RPVHPN crack growth model is similar to the DM weld model in many regards. Namely, both models allow the prediction of PWSCC growth rate as a function of crack geometry, component loading, and other conditions. However, the RPVHPN includes more conditionality due to the various different PWSCC locations and modes (e.g., Alloy 600 vs. Alloy 82/182, ID vs. OD, etc.) and the fact that cracking is modeled beyond through-wall crack growth such that ejection can be predicted.

This section details the model augmentation required to make growth predictions of the RPVHPN cracking modes. The new methods for the calculation of stress intensity factors, which are the result of new crack and component geometries, are presented in Sections B.5.1 through B.5.4. The rate equations for crack growth in Alloy 600 are presented in Section B.5.5. Section B.5.6 discusses other special considerations made for predicting growth given the geometry characteristics specific to a RPVHPN component. Section B.5.7 discusses the special

considerations made for predicting growth given a stress profile characteristic of a peened component (i.e., with a compressive stress region near the surface).

B.5.1 Stress Intensity Factor Calculation Using Influence Coefficient Method

The influence coefficient method for the calculation of stress intensity factor is presented in detail in Section A.5.1. This method assumes that the stress profile acting orthogonally to the crack face (i.e., hoop stresses for the cracking modes of interest in this study) is defined by a polynomial function in the direction of crack depth and is uniform along the crack length. The first of these two conditions is upheld prior to peening provided the second-order polynomial stress profiles described in Equation [B-7]. The second condition, stress profile uniformity along the crack length, is not upheld in reality due to the rapidly changing residual stress distributions near the J-groove weld. For modeling purposes, the stress results extracted from FEA on the approximate vectors shown in Figure B-5 are assumed uniform over the crack face; as can be observed from the hoop stress contour plot, these vectors tend to lie over more severe stress magnitudes, for the respective crack type.

The general form of the stress intensity factor calculation, for a second-order stress profile, by way of the influence coefficient method is:

$$K = \left[\sigma_0 G_0 + \sigma_1 G_1 \left(\frac{a}{D} \right) + \sigma_2 G_2 \left(\frac{a}{D} \right)^2 \right] \sqrt{a\pi} \quad [\text{B-10}]$$

where the G terms are the influence coefficients specific to the crack and component geometries and the location on the crack. Once again, D is a general dimension equal to the penetration nozzle thickness for ID and OD locations and equal to the weld path length for weld locations.

The influence coefficients for ID and OD crack locations are interpolated from tables built by way of finite element parametric analyses. In the DM weld study, lookup tables were used for ID, semi-elliptical, surface cracking (Tables 15 and 39 of Marie, et al. [8]). Tables 16 and 44 of Marie, et al. [8] provide lookup tables for OD, semi-elliptical, surface cracks. Interpolation and extrapolation of these tables use the criteria presented in Table A-1.

The calculation of stress intensity factors for weld cracks is not as clear as for the ID or OD crack locations. This is because there are no pre-determined influence coefficient lookup tables for cracks with the unique boundary conditions of the J-groove weld. As an approximation, cracks at the weld locations are treated as being on a flat plate with a thickness equal to the head thickness, t_{head} . Under this assumption, the influence coefficients may be interpolated from either the ID or OD lookup tables, using an R/t lookup value of 1000 and a through-wall fraction lookup value of a/t_{head} . For an R/t ratio value of 1000, both the ID and OD solutions have asymptotically converged to the solution for a flat plate.

B.5.2 Stress Intensity Factor Calculation Using Weight Function Method

After peening, the stress profile cannot be defined accurately by a polynomial function in the through-wall direction so the more versatile weight function method is used to calculate stress intensity factors.

The weight function method is fully detailed for calculating stress intensity factors of DM weld cracks in Section A.5.2. Since the methodology outlined in that section adequately covers stress intensity factor calculation at RPVHPN locations, no new information is given here.

B.5.3 Stress Intensity Factor Calculation for Through-Wall Axial Cracks

If an axial OD crack goes through-wall prior to reaching the nozzle OD annulus, growth continues in the length direction. In this case, the semi-elliptical crack shape assumed in Sections B.5.1 and B.5.2 breaks down and a through-wall model is required to accurately predict stress intensity factor at the crack tips.

Marie, et al. [8] provides an influence coefficient method for the prediction of stress intensity factor of a rectangular through-wall crack. The influence coefficient equation is:

$$K = \sigma_m F_m \sqrt{c\pi} \quad [\text{B-11}]$$

where c is the half-length of the through-wall crack, σ_m is the membrane elastic stress, and F_m is the lone influence coefficient.

In this study, the membrane elastic stress is approximated as the through-wall average of the total stress profile, attained by taking the analytical integral of the total stress polynomial. It is noted that this value does not change after peening because of the peening force balancing term; as a corollary, peening does not act to slow the growth of through-wall axial cracks in this study.

The influence coefficient is interpolated from a lookup table using the following dimensionless parameter:

$$\lambda = \frac{c}{\sqrt{R_m t}} \quad [\text{B-12}]$$

where R_m is the mid-radius of the penetration nozzle.

Table 35 of Marie, et al. [8] provides an FEA-based lookup table spanning values of λ from 0.2 to 5.0. Conservatively, for the rare case that a crack occurs with a value of λ less than 0.2, the stress intensity factor for $\lambda=0.2$ is used. Values of λ greater than 5.0 do not occur for typical RPVHPN geometries because at this size these hypothetical cracks will have reached the nozzle OD annulus resulting in a leak and a transition to the circumferential through-wall crack.

B.5.4 Stress Intensity Factor Calculation for Through-Wall Cracks on the Weld Contour (i.e. Circumferential Cracks)

In the RPVHPN probabilistic analysis, any crack predicted to leak is assumed to transition immediately to a through-wall crack along the J-groove weld contour. The growth of such cracks is required to be modeled until the nozzle ejection criterion is reached.

Because of the oblique growth direction of these cracks, and the complex stress profile along the length of the crack, there exists no parameterized method for predicting stress intensity factors at the crack tips as a function of the stress distribution characteristics (as has been done for all

previous K calculations). Instead, stress intensity factors are predicted as a function of crack length exclusively, using FEA results.

References [9] and [10] describe finite element analyses performed to predict stress intensity factors at the tips of through-wall cracks growing along the contour of RPVHPN J-groove welds, from both the uphill and downhill sides of the nozzle, at various elevations. These analyses include effects of welding residual stress and operational loads. Both analyses use the geometry of the outermost nozzle at the subject plant, resulting in a generally bounding welding residual stress profile along the crack face.

Across these studies, the most bounding average K versus crack length curves have been selected for use in this probabilistic analysis (those from Reference [10]). Figure B-7 shows these K curves, for the uphill and downhill sides of the nozzle. Linear interpolation is used between FEA evaluated points. (Extrapolation is never necessary because these cracks are modeled initiate at 30° , and ejection of the nozzle is modeled to occur at 300° , as will be discussed in forthcoming sections.)

Conservatively, the K curves presented in Figure B-7 are used for all through-wall cracks along the J-groove weld contour, regardless of the penetration angle of the nozzle being simulated.

Finally, although the analyses in References [9] and [10] are state-of-the-art, and are expected to give relatively accurate results in comparison to similar analyses performed in the nuclear industry, there still exists large uncertainty given welding process variation and plant-to-plant geometry variation. To include this uncertainty, a distributed variable, $K_{circ,mult}$, may be used to scale the circumferential through-wall crack K curves. The distribution selected for this variable is discussed in Section B.8.3.2.

B.5.5 MRP-115 Crack Growth Rate Model for Alloy 82/182 (weld) and MRP-55 Crack Growth Rate Model for Alloy 600 (tube)

The model selected in this study to estimate PWSCC crack growth in the Alloy 82/182 weld metal is the same model presented in MRP-115 [11]. This model is fully described in Section A.5.3 for DM welds and accordingly is not represented here.

The model selected in this study to estimate PWSCC crack growth in the Alloy 600 base metal is based on CGR data presented in MRP-55 [12]. This model uses the same equation form as the Alloy 82/182 crack growth rate model:

$$\frac{\delta}{\delta t}(d) = e^{\frac{Q_R}{R} \left(\frac{1}{T} - \frac{1}{T_{ref}} \right)} \alpha f_{heat} f_{wh} (K_I - K_{Ith})^b \quad [B-13]$$

where d is a general crack dimension (e.g., depth or length). The time-stepping procedure used to solve for RPVHPN crack growth is identical to the one presented for DM welds.

Some of the empirical parameters for Alloy 600 growth differ from those applied to Alloy 82/182 growth and those in MRP-55; specifically, these are the power-law coefficient α , the crack-tip stress intensity factor threshold K_{Ith} , and the stress intensity factor exponent b . Section B.8.3 presents the derivation of these parameters based on Alloy 600 data.

The additional factors, f_{heat} and f_{wh} , are used to describe the aleatory uncertainty in the Alloy 600 crack growth rate model. The within-heat variation, f_{wh} , is a value sampled for each flaw site from a distribution reflective of the growth rate variation observed in laboratory studies of cracks in a controlled Alloy 600 specimen. Similarly, the heat-to-heat growth rate variation, f_{heat} , is a value sampled for each reactor vessel head from a distribution reflective of the growth rate variation observed in laboratory studies of cracks in identically controlled Alloy 600 specimens, after accounting for the within-heat variation. Section B.8.3 describes derivation of these distributions.

The sampled heat-to-heat variation terms may be correlated with the average time of first initiation to simulate the premise that heads that are more susceptible to PWSCC initiation tend to have higher flaw propagation rates.

Finally, for circumferential through-wall cracks growing along the weld contour, a distributed variable, $C_{mult,circ}$, is used to scale the growth rate predicted using Equation [B-13]. This distributed variable is intended to capture the possibility of the growth rate being accelerated by the concentrated chemical environment that may develop in the annulus on the nozzle OD above the weld. The potential for chemical concentration in the annulus is discussed in MRP-55 [12]. The distribution selected for this variable is discussed in Section B.8.3.2.

B.5.6 Special Considerations for Crack Growth on RPVHPNs

This section discusses the special constraints and interactions applied to the various cracking modes modeled for RPVHPNs. Similar to DM welds, these constraints and interactions are imposed by a set of modeling “rules” used to approximate known physical behaviors. While these physical behaviors are complex in nature, the simple set of rules is applied in the probabilistic model in order to capture the most essential growth characteristics.

Axial ID cracks are not given any particularly special modeling considerations. As discussed, these cracks are assumed to initiate at the top of the weld, grow until through-wall, and subsequently transition to the weld contour through-wall growth model.

Axial OD cracks are assumed to initiate below the weld, somewhere between the weld toe and the point where surface stress falls below 80% of yield. If the upper crack tip of an axial OD crack reaches the weld root, i.e., the nozzle OD annulus, the crack transitions to the circumferential through-wall crack model. If the crack depth penetrates through-wall prior to reaching the nozzle OD annulus, the crack transitions to the through-wall axial crack model. The axial through-wall crack transitions to the circumferential through-wall crack model once the upper crack tip reaches the nozzle annulus.

Weld cracks are assumed to initiate at the center of the J-groove weld and grow under the influence of hoop stresses in the weld until reaching the weld root (i.e., nozzle annulus); at this point, the crack transitions to the circumferential through-wall crack model. Weld crack lengths are constrained from growing past the half-width of the weld—the width of the weld half-way along the weld path line as demonstrated in Figure B-8.

As mentioned several times previously, leakage of any crack is immediately followed by the formation of a through-wall crack growing along the J-groove weld contour. The crack is assumed to initiate with a length equivalent to 30° around the weld contour. This assumption has a precedent in MRP-105 [5] and, together with the immediate transition to through-wall growth

on the weld contour after leakage, is expected to result in conservative estimates for the time to ejection following leakage.

The program considers the rare case where through-wall crack growth along the weld contour initiates on both the uphill and downhill sides of the penetration nozzle. In this case, the lengths of the uphill and downhill cracks are combined to assess for nozzle ejection (as detailed in Section B.7).

B.5.7 Special Considerations for Crack Growth on a Peened Surface

The special considerations made for predicting growth in a component with a stress profile characteristic of a peened component (i.e., with a compressive stress region near the surface) are the same as those expressed for a DM weld component in Section A.5.5: accounting for crack closure and “balloon” growth. The strategies used to account for these effects on RPVHPN cracks are identical to those used on DM weld cracks.

Separate sensitivity studies are presented later to demonstrate the relative effect of the crack closure and “balloon” growth on ejection probability of RPVHPNs.

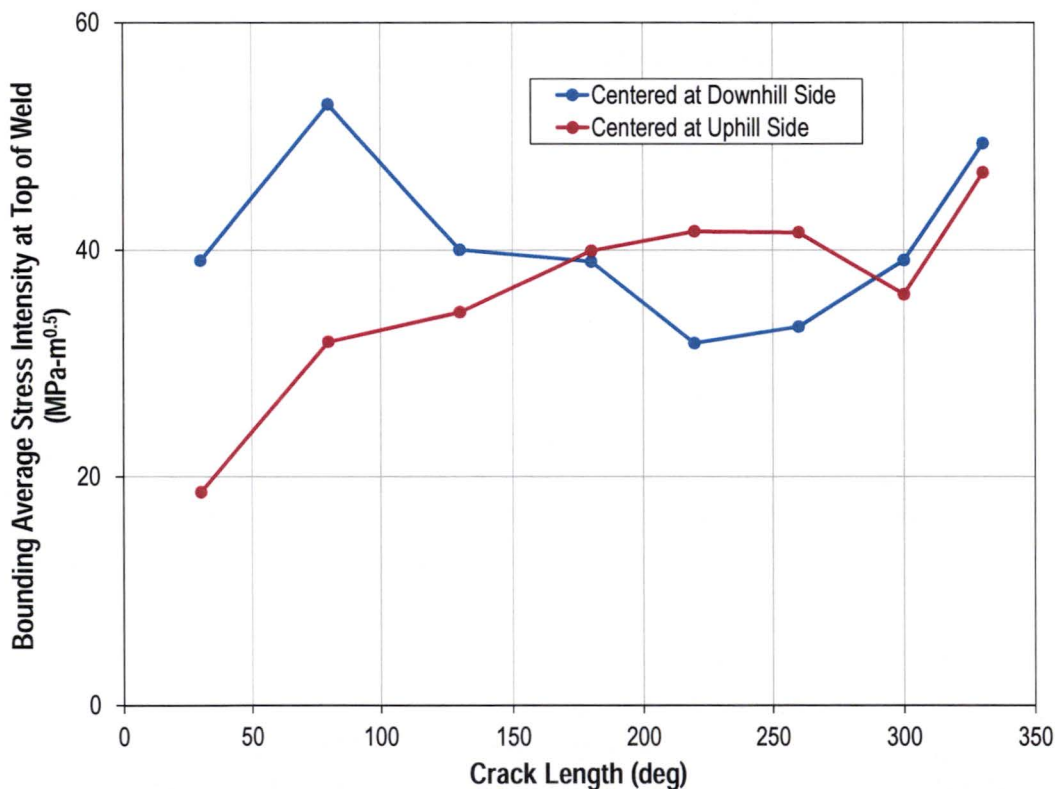


Figure B-7
Modeled Average Stress Intensity Factor vs. Crack Length for a Through-Wall Crack along the J-Groove Weld of a RPVHPN [10]

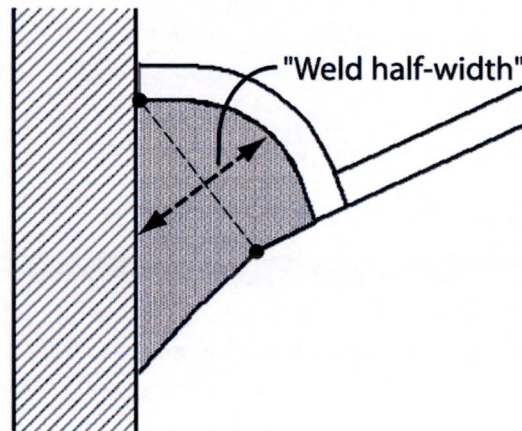


Figure B-8
Description of Weld Half-Width

B.6 Examination Model

This section describes the models applied to simulate ultrasonic and visual examinations of RPVHPNs.

Section B.6.1 discusses how examinations are scheduled, before and after peening, Section B.6.2 describes the inspection models, i.e., how POD is modeled, accounting for the geometry of the crack. Finally, Section B.6.3 describes the detection and repair modeling rules.

B.6.1 Examination Scheduling

UT inspection intervals for unmitigated RPVHPNs (e.g., prior to peening) are based on ASME Code Case N-729-1 [4], which gives the maximum number of operating cycles that are permitted between non-visual non-destructive examinations (NDEs) as a function of operating head temperature, cycle length, and capacity factor. The time of the first modeled UT inspection is set by the user.

Bare metal visual (BMV) inspection intervals for RPVHPNs are also based on N-729-1, which gives the VE (visual examination) interval as a function of the plant's effective degradation years (EDY). The first modeled BMV inspection is scheduled at the same outage of the first modeled UT inspection.

When peening is applied, different examination scheduling requirements and options are included in the model. First, during the peening application outage, immediately prior to peening, a UT inspection can be conducted to simulate a pre-peening inspection.

A follow-up UT examination is included before entering the relaxed in-service inspection (ISI) schedule. In this study, the follow-up inspection performed either one, two, three, or one and two cycles after the peening application for hot heads and either one, two, or three cycles after the peening application for cold heads.

After the follow-up examination, a new ISI schedule is used. The central goal of this probabilistic modeling effort is to demonstrate that the ISI inspection interval after peening can be relaxed, compared to N-729-1 requirements, without increasing the cumulative probability of

leakage and ejection over the entire plant service life. Accordingly, several different ISI intervals will be trialed after peening and compared to operation without peening.

For the base case, BMV inspection intervals are performed per the schedule prescribed in Section 4. Additionally, several sensitivity cases explore relaxed BMV inspection schedules after peening.

B.6.2 Inspection Modeling

This section describes the inspection models (i.e., the determination of POD) for UT and BMV inspections. The coverage requirements for each examination technique are discussed in Section 4.

For DM welds, the POD curve used for UT examinations was the result of a rigorous experimental study. Given the drastically different radius and thickness of a typical penetration nozzle, the UT curve from the DM weld study is not considered applicable here. Instead, a more general POD model described is used for UT inspection modeling of RPVHPNs. Instead of using absolute dimension as the POD argument, through-wall fraction is used to incorporate the dependence of UT performance on both the depth of the crack and the thickness of the component, resulting in the following POD equation:

$$POD\left(\frac{a}{t}\right) = \begin{cases} 0 & 0 \leq \frac{a}{t} < 0.1 \\ \frac{e^{\beta_{1,UT} + \beta_{2,UT} \ln\left(\frac{a}{t}\right)}}{1 + e^{\beta_{1,UT} + \beta_{2,UT} \ln\left(\frac{a}{t}\right)}} & 0.1 \leq \frac{a}{t} \leq 1 \end{cases} \quad [B-14]$$

Section B.8.4.2 gives the through-wall fraction/POD pairings used to define the probabilistic UT inspection curves for penetration nozzles (i.e., to calculate $\beta_{1,UT}$ and $\beta_{2,UT}$).

Similarly to the DM weld POD model, a POD of zero is conservatively applied for cracks with depths less than 10% through-wall. The model also includes the ability to linearly extrapolate the POD between the origin, i.e. 0% POD for an infinitesimal crack, and the POD given by Equation [B-14] for a 10% through-wall crack; this option is invoked in a sensitivity case.

It is noted that UT detection of both axial and circumferential through-wall cracks is modeled using an effective crack depth equal to the penetration nozzle thickness, i.e., a through-wall fraction of 1.

It is assumed for the purpose of the probabilistic model that any flaws located exclusively in the J-groove attachment weld are not detectable by UT inspection performed from the ID of the nozzle. In reality, it is possible that flaws in the weld metal that extend close to the fusion line with the base metal might be detectable by the UT examination.

BMV inspections are given a constant POD of p_{BMV} for leaking penetrations (i.e., RPVHPN with through-wall cracking to the nozzle annulus).

B.6.3 Detection and Repair Modeling

After probabilities of detection for the various examination methods have been calculated, detection is modeled in the same probabilistic manner as described for DM welds in Section A.6.3, including the capability to correlate back-to-back component inspections.

Leaking nozzles are inspected with the BMV probability a single time, regardless of the number of leaking cracks present on the nozzle.

If a crack is identified on a penetration, before or after the crack leads to leakage, the entire penetration is considered to be repaired or removed from service. The reactor vessel head is assumed to stay in operation after this repair/removal.

Credit can be taken for the condition that the unit(s) of interest have had no flaw detections prior to some user-defined past inspection time. If the detection occurs before this user-defined past inspection time, the Monte Carlo realization for the head is rejected and repeated with newly sampled inputs.

B.7 Nozzle Ejection Criterion

At the end of each Monte Carlo realization, the probabilistic model discussed in this report stores a limited number of metrics related to the extent of flaw growth and the repair status of individual penetrations and the head as a whole, including the timing and cracking mode type of related events. Most importantly, during each realization, the code tracks if any penetration nozzle is ejected and, if so, the number of the cycle of the ejection.

Credit can be taken for the condition that the unit(s) of interest have had no nozzle ejections prior to some user-defined past inspection time. If a nozzle is predicted to eject before this user-defined past inspection time, the Monte Carlo realization is rejected and repeated with newly sampled inputs, and the ejection is not counted toward the metric discussed above.

The critical size for a through-wall crack on the circumference of a penetration nozzle is a user-defined constant, in degrees. The choice of critical size for penetration nozzle ejection is discussed in Section B.8.6.

It is noted that credit is taken for penetration nozzle incidence angle when converting crack length to degrees. Specifically, crack angle, Θ , is calculated by the following equation:

$$\Theta = \frac{2c}{2\pi R_m} \cos(\phi) \quad [B-15]$$

where ϕ is the penetration nozzle incidence angle. It is noted that this results in a greater effective length for ejection for all nozzles with a non-zero penetration incidence angle.

B.8 Probabilistic Model Inputs

The RPVHPN probabilistic modeling framework takes both deterministic and distributed inputs. The values of the deterministic inputs are constant for every Monte Carlo realization. The values of the distributed inputs are determined by sampling probability distributions during each Monte Carlo realization.

The inputs selected for use in the probabilistic model are discussed in Section B.8.1 through B.8.5. Inputs for both hot and cold head base cases are included in Table B-2 through Table B-5 and Table B-8 through Table B-11. Input values are highlighted orange to indicate any differences between hot and cold heads.

B.8.1 Reactor Vessel Head Geometry, Operating Time, Temperature, and Loads

The choice of inputs for geometry, operating time, temperature, and loading are discussed in this section. These inputs are given for the two cases for which results will be presented: a hot and a cold head. There is currently a subpopulation of 24 reactor vessel top heads with Alloy 600 penetration nozzles operating in the U.S. Of these 24 heads, 19 operate at cold-leg temperature (i.e., cold heads) and five operate at a temperature significantly above cold-leg temperature (i.e., non-cold heads). The penetration nozzles of these heads are potential candidates for peening mitigation. The characteristics of these plants were incorporated to generate results in this report, inasmuch as possible. Namely, the hot head and cold head temperatures were selected to bound head temperatures from this subpopulation.

B.8.1.1 Component Geometry

The penetration nozzle wall thickness and outer diameter used for the hot and cold head are taken as deterministic inputs, assumed constant across penetration nozzles.

The nozzle thickness and OD that are applied for all hot head penetration nozzles are based on information provided in MRP-48 [1] for CRDM nozzles in Westinghouse-designed reactor vessel heads. ICI nozzles are modeled with the same geometries, despite the fact that, in reality, ICI nozzles have larger ODs and smaller thicknesses. This simplification is appropriate considering that indications of PWSCC have not been reported to date for any top head ICI nozzles ([3], [13]).

The nozzle thickness and OD that are applied for all cold head penetration nozzles are based on information provided in MRP-48 [1] for CRDM nozzles in Westinghouse and B&W heads.

The reactor vessel thickness for the hot and cold head is taken as 6.0 inches, a thickness that is representative of the heads in service.

The number of penetrations and the apportionment of penetration nozzle incidence angles are based on a specific hot head and on a specific cold head. For both the hot and cold heads, the number of penetrations includes all CRDM nozzles and is characteristic of heads with Alloy 600 nozzles in service in U.S. PWRs. A heat vent penetration is not included in this modeling effort.

As discussed in the modeling sections, crack initiation and growth are modeled through the J-groove weld region of the RPVHPNs. For various modeling aspects, some key J-groove weld geometries are required including: the distance from the weld toe to the weld root ("weld toe-to-root distance", the distance from the weld surface to the weld root ("weld path length"), and the weld width halfway along the weld path length ("weld half-width") as depicted in Figure B-8. The variation of these geometries across penetrations was incorporated by fitting normal distributions to inputs for various J-groove weld FEA studies [6] (which span different heads and

penetration locations), at the uphill and downhill locations separately.¹⁷ An example of such a fit (i.e., for the uphill weld path length) is given in Figure B-9. Lower and upper truncation limits were set based on the extreme values from the FEA studies. The ratio of the weld path length and the weld half-width was found to be approximately constant across penetration nozzles and accordingly was treated as a deterministic input.

General RPVHPN geometry inputs are included in Table B-2 and weld geometry inputs are included in Table B-3.

B.8.1.2 Operating Time

The hot and cold heads are simulated from plant startup until shutdown. Shutdown is considered to occur approximately 60 years after startup (i.e., a 40-yr original license and a 20-yr license renewal). Cumulative statistics are provided at the end of plant operational service period.

Both heads are assumed to have a capacity factor of 0.97. This value is representative of U.S. PWRs. Both heads are simulated with 24-month operating cycles. Five 24-month operating cycles results in the full 10-year interval between repeat ISI examinations that is required for peened heads in Section 4.3.

As discussed in the modeling sections, credit can be taken for the fact that the simulated unit has not experienced ejections or repairs before a user-defined outage. Monte Carlo realizations that predict repairs or ejections before some user-defined outage are rejected and rerun with new samples. This option is not invoked for the baseline results presented in this report. Accordingly the cumulative probabilities and ejection frequencies that are presented are not conditioned on any assumption of no ejection or repair before some date, and can be thought of as applying to the general population of heads with characteristics similar to those defined in Table B-2.

A user-defined outage, before which it is assumed that no ejections or repairs have occurred, will be set in a sensitivity case for each of the hot and the cold heads. The statistics presented in these two cases apply conditionally to heads that have experienced no ejections or repairs to date, but otherwise have characteristics similar to those defined in Table B-2.

B.8.1.3 Temperature

The mean hot and cold head temperatures were selected to bound the nominal operating temperatures for hot and cold heads with Alloy 600 RPVHPNs in service at U.S. PWRs [3].

Variation in head temperature and measurement error is incorporated into the model by using a normal distribution with a standard deviation of 5°F.

B.8.1.4 Operational Loads

As discussed in the modeling section, operational stresses (i.e., those stresses due to operational pressures and thermal gradients) are required to be separated from welding residual stresses. Results of finite element analyses of J-groove welding residual stresses [6] were used to estimate

¹⁷ Trends in the geometry characteristics as a function of penetration incidence angle were analyzed. The trends were not strong enough to justify their implementation in this study.

these operating stresses by subtracting the FEA-predicted stress state present during operation from the welding residual stress state.

The results of these analyses revealed that the penetration nozzle OD and weld surface stresses had a negligible contribution from operational loads.

At the penetration nozzle ID, the results of these analyses revealed a distribution on the hoop stress concentration factor, $F_{oper,ID}$, defined in Equation [B-2]. A normal distribution provides an adequate fit to describe the variation in this concentration factor across penetration locations, as demonstrated in Figure B-10.

B.8.1.5 Welding Residual Stresses

Welding residual stress profiles on six vectors of interest (shown in Figure B-5) on RPVHPNs were synthesized from the results of J-groove weld FEA analyses [6]. More accurately, curves were fit to the total stress profiles (operational plus residual) predicted by FEA analyses and the residual stresses are calculated during runtime by subtracting operational stresses from the total stress profiles.

Equation [B-3] describes the second-order polynomial form of the stochastic family of curves fit to the FEA results. The coefficients of each polynomial stress profile are solved for each Monte Carlo realization based on the constraint that the total stress curve must pass through sampled stresses at three locations: $x/D=0$, $x/D=1$, and $x/D=0.5$, where:

- $x/D=0$ is defined as the location where cracks are expected to initiate: the ID above the weld for ID axial cracks, the OD below the weld for OD axial cracks, or the weld surface center for weld cracks.
- $x/D=1$ is defined as the location toward which cracks are expected to grow in depth: the OD above the weld for ID axial cracks, the ID below the weld for OD axial cracks, or the weld root for weld cracks.
- $x/D=0.5$ is defined as being halfway between the previous two locations.

Equations [B-4] through [B-6] give parameterized equations for the stresses at $x/D=0$, $x/D=1$, and $x/D=0.5$. Uncertainty inherent in data, as well as the uncertainty due to unknown variation of missing data, is introduced by allowing distributed inputs for the parameters in these equations: the surface stress, $\sigma_{0,tot}$, the gradient quantifier, $R_{1,tot}$, and the curvature quantifier, $R_{0.5,tot}$.

For each location of interest, a semi-analytical, iterative procedure was used to derive parameter distributions that resulted in a family of stress profile curves that bound the data and provide an adequate excess of uncertainty. Fifty instances from each of these families of curves, overlaid on the FEA data, are shown for each location of interest in Figure B-11 through Figure B-16 (the median stress profile is shown with a dotted black line). The parameter distributions used to make these families of curves are summarized in Table B-4. Conservatively, a minimum of zero is used for all parameters to ensure tensile hoop stresses at the three interpolated depths.

Table B-2
Summary of General RPVHPN Inputs

Symbol	Description	Source	Units	Parameter Type	Hot Head Base Case	Cold Head Base Case
	Total number of trials	Convergence Study	# trials		1.00E+06	1.00E+06
	Number of operating cycles	Selected to yield desired cumulative operating time	# cycles		30	30
	Nominal cycle length	Upper end of cycle length of U.S. PWRs	years		2	2
CF	Operating capacity factor	Representative capacity factor for U.S. PWR	-		0.97	0.97
	Cycle of first UT inspection	Based on typical operating reactor service histories	Cycle number		10	10
	Pre-peening UT inspection interval	ASME Code Case N-729-1	# cycles		1	3
	Pre-peening BMV inspection interval	ASME Code Case N-729-1	# cycles		1	2
T	Operating temperature	Selected based on properties of units serving as characteristic hot/cold head	°F	type	Normal	Normal
				mean	605	561
				stdev	5	5
				min	575	520
				max	635	600
N_{pen}	Number of modeled penetrations	Selected based on properties of units serving as characteristic hot/cold head	-		78	78
N_{flaw}	Maximum number of part-depth flaws modeled per penetration	Selected to capture PWSCC locations and mechanisms observed in industry RPVHPNs	-		6	6
t	Nozzle thickness	Representative of CRDM nozzle thickness of units serving as characteristic hot/cold head	in.		0.62	0.62
D_o	Nozzle outer diameter	Representative of CRDM nozzle OD of units serving as characteristic hot/cold head	in.		4.00	4.00
t_{head}	Reactor head thickness	Representative of industry PWRs	in.		5.98	5.98

Table B-3
Summary of Weld Geometry Inputs

Symbol	Description	Source	Units	Parameter Type	Hot Head Base Case	Cold Head Base Case
	Representative length from weld surface to weld root, uphill	Inputs to finite element analyses of J-groove weld residual stresses; distribution considers various penetration geometries	in.	type	Normal	Normal
				mean	1.05	1.05
				stdev	0.18	0.18
				min	0.50	0.50
				max	1.70	1.70
	Representative length from weld surface to weld root, downhill	Inputs to finite element analyses of J-groove weld residual stresses; distribution considers various penetration geometries	in.	type	Normal	Normal
				mean	0.97	0.97
				stdev	0.23	0.23
				min	0.50	0.50
				max	1.70	1.70
	Representative length from weld toe to weld root, uphill	Inputs to finite element analyses of J-groove weld residual stresses; distribution considers various penetration geometries	in.	type	Normal	Normal
				mean	1.38	1.38
				stdev	0.30	0.30
				min	0.80	0.80
				max	2.90	2.90
	Representative length from weld toe to weld root, downhill	Inputs to finite element analyses of J-groove weld residual stresses; distribution considers various penetration geometries	in.	type	Normal	Normal
				mean	1.36	1.36
				stdev	0.37	0.37
				min	0.80	0.80
				max	2.90	2.90
	Ratio of weld path length to weld half-width, uphill	Inputs to finite element analyses of J-groove weld residual stresses; distribution considers various penetration geometries	-		1.62	1.62
	Ratio of weld path length to weld half-width, downhill	Inputs to finite element analyses of J-groove weld residual stresses; distribution considers various penetration geometries	-		1.24	1.24
	Incidence angles for penetrations	Selected based on properties of units serving as characteristic hot/cold head	degrees		Discrete List	Discrete List

Table B-4
Summary of Loading Inputs for RPVHPN Model

Symbol	Description	Source	Units	Parameter Type	Hot Head Base Case	Cold Head Base Case
P_{op}	Normal operating pressure	Representative of industry PWRs	ksi		2.248	2.248
$f_{oper,ID}$	Nozzle ID operating hoop stress concentration factor	Finite element analyses of operational stresses on CRDM nozzle; across various penetration angles	-	type	Normal	Normal
				mean	3.480	3.480
				stdev	0.729	0.729
				min	0.000	0.000
				max	7.850	7.850

Table B-4 (continued)
Summary of Loading Inputs for RPVHPN Model

Symbol	Description	Source	Units	Parameter Type	Hot Head Base Case	Cold Head Base Case
$\sigma_{0,tot,1}$	Total hoop stress at penetration ID above weld	Finite element analyses of operational stresses on CRDM nozzle; across various penetration angles	ksi	type	Normal	Normal
				mean	40.99	40.99
				stdev	7.34	7.34
				min	0.00	0.00
				max	85.02	85.02
$\sigma_{0,tot,2}$	Total hoop stress at penetration OD below weld, uphill	Finite element analyses of operational stresses on CRDM nozzle; across various penetration angles	ksi	type	Normal	Normal
				mean	53.78	53.78
				stdev	9.92	9.92
				min	0.00	0.00
				max	113.30	113.30
$\sigma_{0,tot,3}$	Total hoop stress at weld surface center, uphill	Finite element analyses of operational stresses on CRDM nozzle; across various penetration angles	ksi	type	Normal	Normal
				mean	59.97	59.97
				stdev	5.73	5.73
				min	25.60	25.60
				max	94.34	94.34
$\sigma_{0,tot,-1}$	Total hoop stress at penetration ID above weld, downhill	Finite element analyses of operational stresses on CRDM nozzle; across various penetration angles	ksi	type	Normal	Normal
				mean	43.18	43.18
				stdev	8.30	8.30
				min	0.00	0.00
				max	92.95	92.95
$\sigma_{0,tot,-2}$	Total hoop stress at penetration OD below weld, downhill	Finite element analyses of operational stresses on CRDM nozzle; across various penetration angles	ksi	type	Normal	Normal
				mean	67.08	67.08
				stdev	10.60	10.60
				min	3.47	3.47
				max	130.69	130.69
$\sigma_{0,tot,-3}$	Total hoop stress at weld surface center, downhill	Finite element analyses of operational stresses on CRDM nozzle; across various penetration angles	ksi	type	Normal	Normal
				mean	61.78	61.78
				stdev	5.77	5.77
				min	27.15	27.15
				max	96.42	96.42

Table B-4 (continued)
Summary of Loading Inputs for RPVHPN Model

Symbol	Description	Source	Units	Parameter Type	Hot Head Base Case	Cold Head Base Case
$R_{1,tot,1}$	Stress gradient quantifier at penetration ID above weld, uphill	Finite element analyses of J-groove weld residual stresses (14 independent analyses)	-	type	Normal	Normal
				mean	1.11	1.11
				stdev	0.24	0.24
				min	0.00	0.00
				max	2.55	2.55
$R_{1,tot,2}$	Stress gradient quantifier at penetration OD below weld, uphill	Finite element analyses of J-groove weld residual stresses (14 independent analyses)	-	type	Normal	Normal
				mean	0.84	0.84
				stdev	0.14	0.14
				min	0.00	0.00
				max	1.68	1.68
$R_{1,tot,3}$	Stress gradient quantifier at weld surface center, uphill	Finite element analyses of J-groove weld residual stresses (14 independent analyses)	-	type	Normal	Normal
				mean	0.89	0.89
				stdev	0.32	0.32
				min	0.00	0.00
				max	2.81	2.81
$R_{1,tot,-1}$	Stress gradient quantifier at penetration ID above weld, downhill	Finite element analyses of J-groove weld residual stresses (14 independent analyses)	-	type	Normal	Normal
				mean	0.60	0.60
				stdev	0.41	0.41
				min	0.00	0.00
				max	3.06	3.06
$R_{1,tot,-2}$	Stress gradient quantifier at penetration OD below weld, downhill	Finite element analyses of J-groove weld residual stresses (14 independent analyses)	-	type	Normal	Normal
				mean	0.51	0.51
				stdev	0.13	0.13
				min	0.00	0.00
				max	1.29	1.29
$R_{1,tot,-3}$	Stress profile curvature quantifier at weld surface center, downhill	Finite element analyses of J-groove weld residual stresses (14 independent analyses)	-	type	Normal	Normal
				mean	0.36	0.36
				stdev	0.17	0.17
				min	0.00	0.00
				max	1.38	1.38

Table B-4 (continued)
Summary of Loading Inputs for RPVHPN Model

Symbol	Description	Source	Units	Parameter Type	Hot Head Base Case	Cold Head Base Case
$R_{0.5, tot, 1}$	Stress profile curvature quantifier at penetration ID above weld, uphill	Finite element analyses of J-groove weld residual stresses (14 independent analyses)	-	type	Normal	Normal
				mean	1.08	1.08
				stdev	0.09	0.09
				min	0.54	0.54
				max	1.62	1.62
$R_{0.5, tot, 2}$	Stress profile curvature quantifier at penetration OD below weld, uphill	Finite element analyses of J-groove weld residual stresses (14 independent analyses)	-	type	Normal	Normal
				mean	0.87	0.87
				stdev	0.13	0.13
				min	0.09	0.09
				max	1.65	1.65
$R_{0.5, tot, 3}$	Stress profile curvature quantifier at weld surface center, uphill	Finite element analyses of J-groove weld residual stresses (14 independent analyses)	-	type	Normal	Normal
				mean	1.21	1.21
				stdev	0.12	0.12
				min	0.49	0.49
				max	1.93	1.93
$R_{0.5, tot, -1}$	Stress profile curvature quantifier at penetration ID above weld, downhill	Finite element analyses of J-groove weld residual stresses (14 independent analyses)	-	type	Normal	Normal
				mean	1.46	1.46
				stdev	0.13	0.13
				min	0.68	0.68
				max	2.24	2.24
$R_{0.5, tot, -2}$	Stress profile curvature quantifier at penetration OD below weld, downhill	Finite element analyses of J-groove weld residual stresses (14 independent analyses)	-	type	Normal	Normal
				mean	0.78	0.78
				stdev	0.09	0.09
				min	0.24	0.24
				max	1.32	1.32
$R_{0.5, tot, -3}$	Stress profile curvature quantifier at weld surface center, downhill	Finite element analyses of J-groove weld residual stresses (14 independent analyses)	-	type	Normal	Normal
				mean	1.47	1.47
				stdev	0.19	0.19
				min	0.33	0.33
				max	2.61	2.61

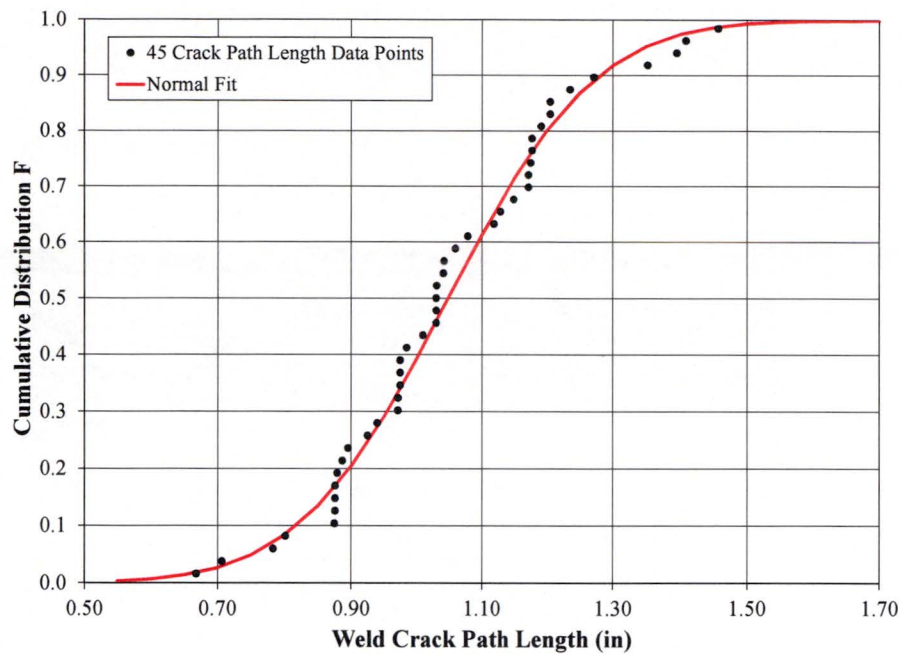


Figure B-9
Normal Distribution Fit to Geometry Data Varying Across Penetration Nozzle Incidence Angles: Uphill Weld Path Length

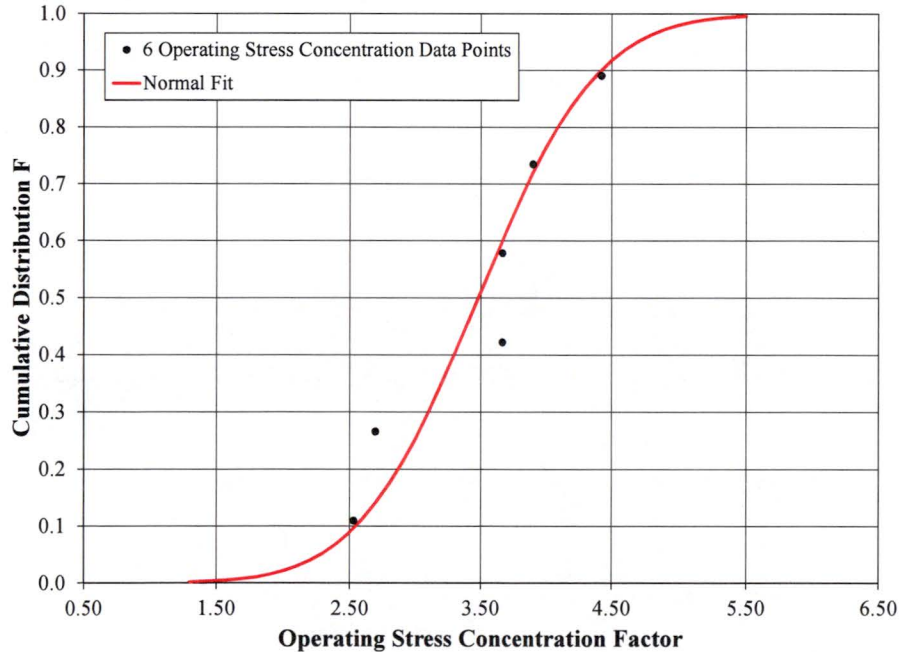


Figure B-10
Normal Distribution Fit to Penetration Nozzle ID Hoop Stress Concentration Factors Predicted by FEA Study

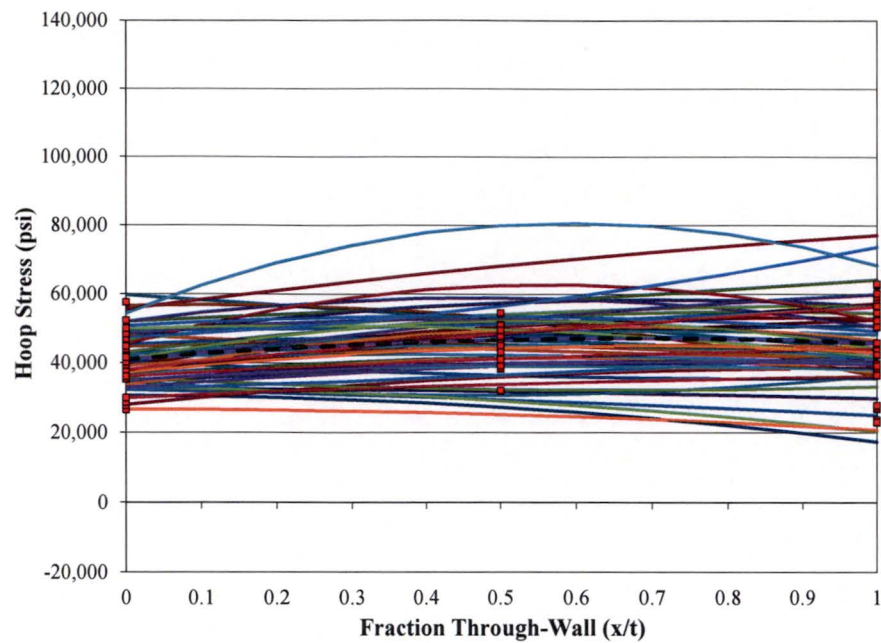


Figure B-11
Stochastic Family (50 instances) of Curves and FEA Results for the Total Stress Profile between the Penetration Nozzle ID Above the Weld and the Penetration Nozzle OD Above the Weld, Uphill Side

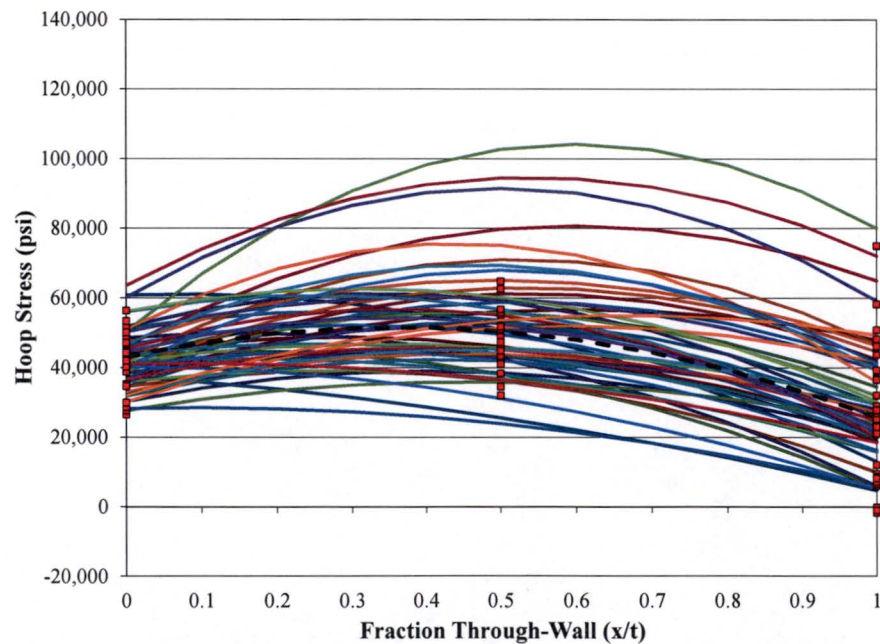


Figure B-12
Stochastic Family (50 instances) of Curves and FEA Results for the Total Stress Profile between the Penetration Nozzle ID Above the Weld and the Penetration Nozzle OD Above the Weld, Downhill Side

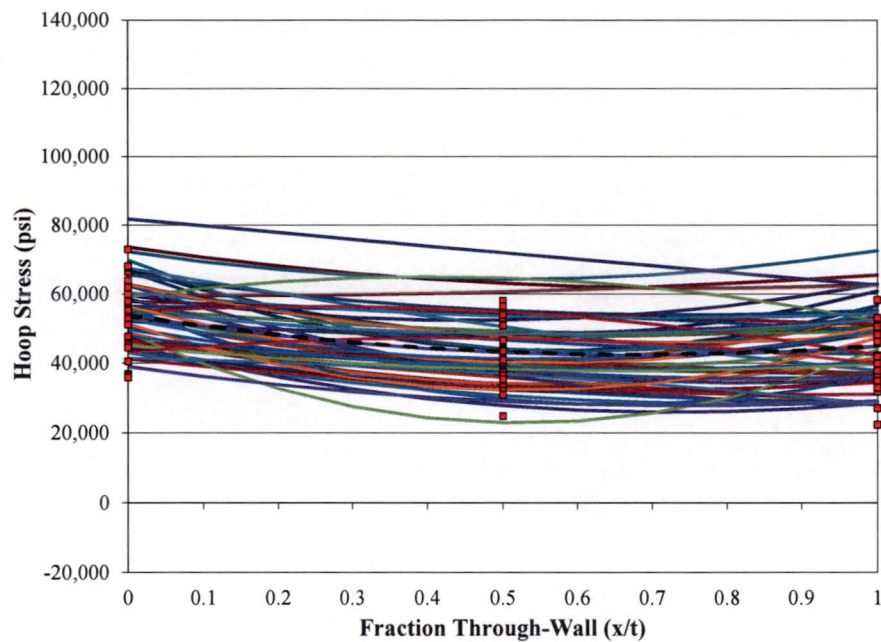


Figure B-13
Stochastic Family (50 instances) of Curves and FEA Results for the Total Stress Profile between the Penetration Nozzle OD Below the Weld and the Penetration Nozzle ID Below the Weld, Uphill Side

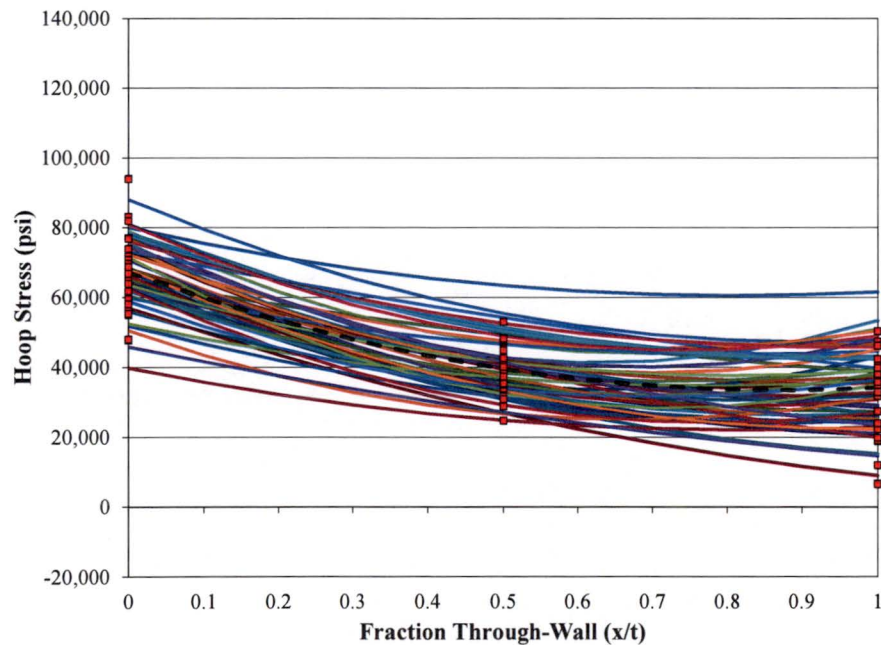


Figure B-14
Stochastic Family (50 instances) of Curves and FEA Results for the Total Stress Profile between the Penetration Nozzle OD Below the Weld and the Penetration Nozzle ID Below the Weld, Downhill Side

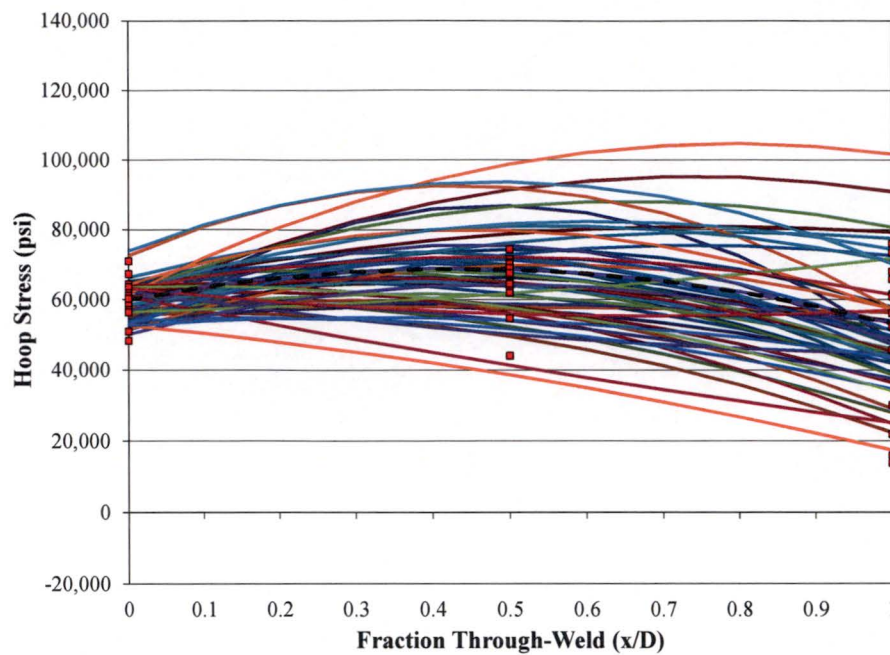


Figure B-15
Stochastic Family (50 instances) of Curves and FEA Results for the Total Stress Profile between the Weld Center and the Weld Root, Uphill Side

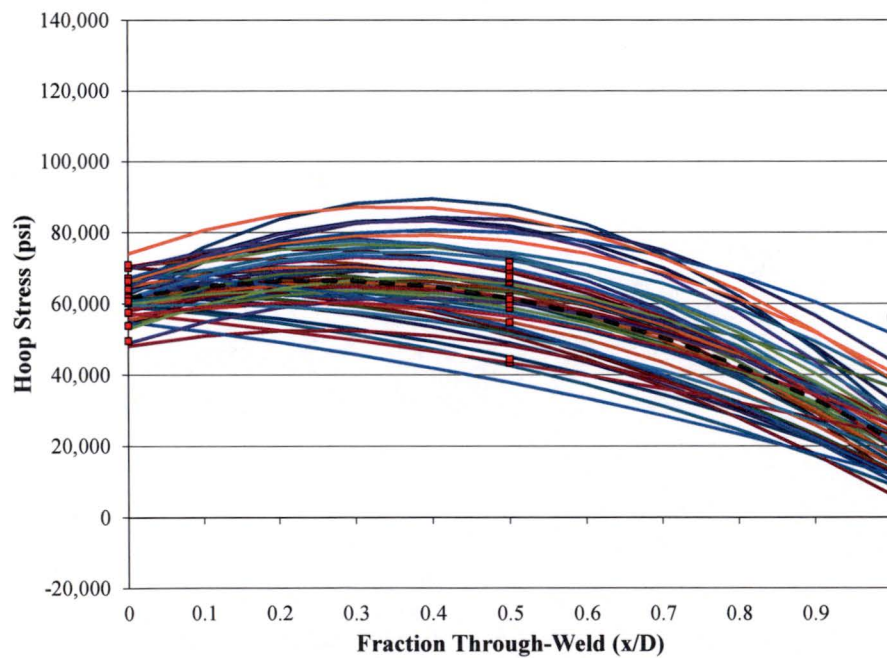


Figure B-16
Stochastic Family (50 instances) of Curves and FEA Results for the Total Stress Profile between the Weld Center and the Weld Root, Downhill Side

B.8.2 Crack Initiation Model

The set of inputs for the RPVHPN PWSCC initiation model is described in Table B-5 at the end of this section. Various inputs are detailed in the following subsections.

B.8.2.1 Industry Inspection Data used to Develop Initiation Model

Plant inspection data for RPVHPNs fabricated from Alloy 600 with J-groove welds fabricated from Alloys 82 and 182 were evaluated by DEI in MRP-395 [3]. Table B-6 lists the RPVHPNs in which cracking indications were detected that were used in this report.

B.8.2.2 Weibull Fitting Procedure for Average Time of First Initiation

The procedure used to fit a Weibull model to the time of first PWSCC initiation on a head differed from the like procedure for a DM weld, as presented in Section A.8.2. This is principally due to the fact that, generally, more than one cracking indication was discovered on heads during inspection, whereas inspection data for DM welds demonstrate only single cracking indications. In order to estimate the time of the first crack initiation on a particular head, a multiple flaw Weibull slope needed to be assumed; a value of 3.0 was chosen [3]. After the time of first PWSCC initiation on each head was estimated, the Weibull model was determined using a least squares fitting procedure.

B.8.2.3 Analysis Results for Average Time of First Initiation

Figure B-17 shows an example MLE Weibull distribution fit to the industry experience with RPVHPNs fabricated from Alloy 600 with welds from Alloys 82 and 182 given in Table B-6. The failure and suspension times were adjusted to a common reference temperature of 315°C (600°F) using a thermal activation energy of 184 kJ/mole (44 kcal/mole) (the mean value given in B.8.2.10). Table B-7 summarizes the MLE fit parameters of the Weibull analysis. Also included in Table B-7 are the standard errors in the Weibull fit parameter, β , and the vertical intercept of the linearized Weibull curve (which is used to determine the value of θ).

It is noted that the standard error in the vertical intercept of the linearized Weibull fit (referred to here as σ_c) is presented because it is used during runtime to account for the uncertainty in the value of the anchor point time, t_1 .

B.8.2.4 Uncertainty in First Initiation Time Weibull Slope

A constant value for the Weibull slope, β , is applied to the initiation model. Uncertainty in the time to cracking is incorporated in the Weibull intercept parameter,¹⁸ as discussed in Section B.8.2.5.

¹⁸ The Weibull intercept parameter (the product of the Weibull slope parameter and the natural log of the Weibull characteristic time parameter) is the y-intercept of the "linearized" equation that results after log-transforming the Weibull cumulative distribution function twice. This linearization is a common practice in Weibull modeling because it poses the relationship between failure fraction and time in a linear form, which is useful for visualization and regression.

B.8.2.5 Uncertainty in Anchor Point Time (t_1)

Uncertainty in the Weibull model is incorporated through the Weibull intercept parameter, and no anchor point is defined. The Weibull intercept parameter uncertainty is estimated by linearizing the Weibull model form and performing regression to the time to first crack data for RPVHPNs. To make a prediction with the model, the Weibull intercept parameter uncertainty is incorporated, effectively defining a Weibull characteristic time. Then, the initiation time is sampled from the Weibull distribution defined by the Weibull slope and characteristic time parameters.

B.8.2.6 Uncertainty in the Multiple Flaw Weibull Slope

As discussed in the modeling section, a second Weibull model is used to predict the initiation of multiple flaws on a single head. The key input to this model is the Weibull slope.

The slope of the multiple flaw Weibull model, β_{flaw} , quantifies the rate at which flaws occur after the initiation of the first flaw. An analytical data fitting procedure, as done for the first initiation time model, was not considered appropriate to fit β_{flaw} given the modeling complexities involved in sampling multiple flaw initiation times. Instead, a mean value of 2.0 was selected for the β_{flaw} . This value has a precedent in probabilistic modeling of SCC in steam generators [14]. A normal distribution with a mean of 2.0 and a standard deviation of 0.5 is employed to incorporate uncertainties due to material and manufacturing disparities. A lower truncation bound of 1.0 was selected to preclude a multiple flaw Weibull model in which the PWSCC initiation rate decreases over time.

A numerical experiment was run with a value of 2.0 for β_{flaw} in order to demonstrate the resulting number of cracks per head, given the parameter distributions discussed throughout this Section B.8. Figure B-18 depicts the resulting distribution of number of flaws in heads with at least a single flaw, at 21.5 EFPY, given an operating temperature of 605°F. The average number of flaws at 21.5 EFPY, given that at least a single flaw exists, is 20.9. This average number of flaws approximately matches industry data (depicted in Figure B-19) for which the average number of cracking indications per hot head with at least one cracking indication was 15.1.

To account for undetected flaws in industry, namely those located on the J-groove welds, a sensitivity study will be included in which the multiple flaw Weibull model is increased, resulting in a higher average number of flaws per head with at least one flaw.

B.8.2.7 Uncertainty in Initial Flaw Location

As discussed in the modeling section, an initial flaw location is required for OD axial flaws. This initial flaw location, together with the sampled weld toe to weld root distance, defines the OD axial crack half-length that would result in the opening of the OD nozzle annulus (i.e., leakage).

For each initiated OD axial flaw, the flaw center location is uniformly sampled between the weld toe and the location where the residual stresses in the penetration nozzle fall below 80% of yield stress. The distance from the weld toe to the 80% yield location (the “80% yield stress length”) is taken as a distributed input and is fit to results of finite analysis of J-groove welding residual

stresses [6]. The variation in the 80% yield stress length is due to process variation and geometrical variation across different penetration nozzle incidence angles¹⁹.

A unique normal distribution was used for the uphill and downhill sides of the penetration. The resulting fits are shown in Figure B-20 and Figure B-21. The distribution parameters are given in Table B-5.

B.8.2.8 Uncertainty in Initial Flaw Depth

The initial through-wall fraction for each flaw location is sampled at the time of flaw initiation. To remain consistent with the initial through-wall fractions used in the DM weld program (which are based on experimental data for UT inspection of cracking in DM welds), a log-normal distribution with a median of 5% through-wall and an upper 95% confidence bound of 9% through-wall is used. For the penetration nozzle thickness presented earlier (15.9 mm) this results in a median absolute initiation depth of 0.8 mm.

The lower truncation limit was defined to prevent the initiation of very small flaws for which the stress intensity factor (based on the input distributions of the surface welding residual stress) would be significantly less than the range of stress intensity factors (about 15-20 MPa-m^{1/2} or 14-18 ksi-in^{1/2}) evaluated in the laboratory studies used to define the flaw propagation models given in MRP-55.

A sensitivity case is used to explore an initial depth distribution that results in cracks that initiate approximately 5 times smaller. This is included to assess the potential effect on leakage probability of smaller cracks not being identified during inspections prior to peening.

A second sensitivity study is presented in which cracks initiate with the same *absolute* depths (as opposed to through-wall percentages) used for the DM weld program.

B.8.2.9 Uncertainty in Flaw Aspect Ratio

There was not enough data available for initial RPVHPN crack sizes to allow a distribution to be fit for aspect ratio, as was done for DM weld cracks. Instead, a log-normal distribution was applied to give a modal aspect ratio of 4.0 and a 99% confidence interval aspect ratio of 10.0.

B.8.2.10 Uncertainty in Temperature Effect

The uncertainty in temperature and its effect on initiation is handled in same manner as described for DM welds in Section A.8.2.10.

¹⁹ Trends in the 80% yield stress length as a function of penetration incidence angle were analyzed. The trends were not strong enough to justify their implementation in this study.

Table B-5
Summary of Inputs for RPVHPN Initiation Model

Symbol	Description	Source	Units	Parameter Type	Hot Head Base Case	Cold Head Base Case
t_1	Time at which failure fraction F_1 is reached on RPVHPNs	Flaw initiation data assessed in MRP-395	EDY		23.0	23.0
σ_c	Standard error in intercept of linearized Weibull fit	Linearized Weibull fit to flaw initiation data assessed in MRP-395	ln(EDY)		0.2705	0.2705
F_1	Arbitrary failure fraction selected to define Weibull PWSCC initiation function	Selected to reflect t_1 as the Weibull scale parameter (characteristic time)	-		0.6321	0.6321
β	Weibull slope for PWSCC flaw initiation on RPVHPNs	Flaw initiation data assessed in MRP-395	-		1.379	1.379
β_{flaw}	Weibull slope for PWSCC multiple flaw initiation on RPVHPNs	Based on representative value for formation of PWSCC at multiple locations in industry SGs	-	type	Normal	Normal
				mean	2.0	2.0
				stdev	0.5	0.5
				min	1.0	1.0
				max	5.0	5.0
ρ_{heat}	Correlation coefficient for PWSCC initiation and propagation of all cracks in Alloy 600	xLPR Input	-		0.0	0.0
ρ_{weld}	Correlation coefficient for PWSCC initiation and propagation of all cracks in Alloy 82/182 weld	xLPR Input	-		0.0	0.0

Table B-5 (continued)
Summary of Inputs for RPVHPN Initiation Model

Symbol	Description	Source	Units	Parameter Type	Hot Head Base Case	Cold Head Base Case
Q_i	Thermal activation energy for PWSCC flaw initiation	Distribution based on laboratory data and experience with Weibull analysis	kcal/mole	type	Normal	Normal
				mean	44.03	44.03
				stdev	3.06	3.06
				min	25.65	25.65
				max	62.41	62.41
$T_{ref,i}$	Reference temperature to normalize PWSCC flaw initiation data	Temperature used to adjust flaw initiation data assessed in this report	°R		1060	1060
a_0	Initial depth assigned to newly initiated flaw	Consistency with initial through-wall fractions of DM weld model	in.	type	Log-Normal	Log-Normal
				linear μ	3.32E-02	3.32E-02
				median	3.12E-02	3.12E-02
				log-norm μ	-3.47	-3.47
				log-norm σ	0.35	0.35
				min	0.02	0.02
AR	General initial aspect ratio assigned to newly initiated flaw	Based on aspect ratios of PWSCC cracks observed in inspections of DMW and RPVHPN components	-	max	0.62	0.62
				type	Log-Normal	Log-Normal
				linear μ	4.77	4.77
				median	4.50	4.50
				log-norm μ	1.50	1.50
				log-norm σ	0.34	0.34
	Distance from weld toe to location where welding residual stress is equal to 80% of yield stress, uphill side	Finite element analyses of J-groove weld residual stresses; across various units and penetration geometries	in.	min	0.57	0.57
				max	35.20	35.20
				type	Normal	Normal
				mean	0.25	0.25
	Distance from weld toe to location where welding residual stress is equal to 80% of yield stress, downhill side	Finite element analyses of J-groove weld residual stresses; across various units and penetration geometries	in.	stdev	0.13	0.13
				min	0.00	0.00
				max	1.03	1.03
				type	Normal	Normal
				mean	0.24	0.24
				stdev	0.06	0.06
				min	0.00	0.00
				max	0.61	0.61

Table B-6
Inspection Data Through Fall 2013 Extrapolated Back to Predicted Time to First Crack/Leak (Based on Weibull slope $\beta = 3$) [3]

Code	No. CRDM/ CEDM Nozzles	Replace Date	NDE Date, Scope, and Results											
			Outage	Year	EDY	All Nozzle Materials								
						NDE CRDM/ CEDM	Cum. Cracked	CDF (1st Crack)	CDF (# Cracked)	Time Factor (# Cracked)	EDYs at 1st Crack or Inspection (+8°F for all B&W Heads)	at Detection of Cracking	at 1st Crack Extrapolated Back using b=3	
												CDF of Units with Cracks (+8°F for all B&W Heads)	CDF of Units with Cracks (+8°F for all B&W Heads)	
Plant A	78		Fall	2006	2.56	78	0	0.0089			2.5559			
Plant B	78		Spring	2011	2.63	78	0	0.0089			2.6252			
Plant C	65	Spring	2007	Spring	2005	16.67	65	0	0.0107			16.6688		
Plant D	78		Fall	2012	3.87	78	0	0.0089			3.8692			
Plant E	69	Fall	2003	Spring	2002	23.16	23	5	0.0299	0.2009	0.5136	16.3672	0.86	0.45
Plant F	78		Fall	2012	4.30	78	0	0.0089			4.3015			
Plant G	78	Spring	2005	NONE		0	0	1.7500						
Plant H	45		Spring	2009	12.05	45	2	0.0154	0.0374	0.7412	8.9293	0.15	0.20	
Plant I	78	Fall	2014	Spring	2007	3.21	78	0	0.0089			3.2092		
Plant J	78		Spring	2013	19.09	78	0	0.0089			19.0900			
Plant K	65	Spring	2006	Fall	2004	15.01	65	4	0.0107	0.0566	0.5696	8.5493	0.23	0.16
Plant L	78		Spring	2013	4.00	78	0	0.0089			3.9989			
Plant M	65	Fall	2004	Spring	2003	18.17	65	0	0.0107			18.1659		
Plant N	78		Fall	2011	2.61	78	1	0.0089	0.0089	1.0000	2.0854	0.01	0.04	
Plant O	65	Spring	2003	Fall	2001	19.89	30	1	0.0230	0.0230	1.0000	19.8859	0.44	0.56
Plant P	65	Spring	2003	Fall	2001	19.12	16	6	0.0427	0.3476	0.4675	8.9394	0.34	0.22
Plant Q	65	Spring	2017	Fall	2009	14.84	65	2	0.0107	0.0260	0.7420	11.0115	0.20	0.33
Plant R	97	Fall	2009	Spring	2008	14.65	97	0	0.0072			14.6502		
Plant S	81		Fall	2013	19.10	81	0	0.0086			19.1000			
Plant T	97	Fall	2010	Spring	2009	15.19	97	0	0.0072			15.1860		
Plant U	91		Fall	2008	18.74	91	0	0.0077			18.7386			
Plant V	69	Fall	2011	Spring	2010	9.17	69	12	0.0101	0.1686	0.3801	3.4853	0.11	0.10
Plant W	78		Spring	2013	3.54	78	0	0.0089			3.5400			
Plant X	65		Fall	2013	4.00	65	6	0.0107	0.0872	0.4905	1.9615	0.07	0.03	
Plant Y	78		Spring	2008	1.76	78	0	0.0089			1.7611			
Plant Z	74	Fall	2009	Fall	2006	11.70	74	0	0.0094			11.7029		
Plant AA	65	Spring	2005	Fall	2003	18.50	65	0	0.0107			18.4957		
Plant AB	78	Fall	2007	Spring	2006	14.43	78	1	0.0089	0.0089	1.0000	10.1300	0.13	0.27
Plant AC	40	Fall	2004	NONE		0	0	1.7500						
Plant AD	69	Spring	2004	Fall	2002	23.61	69	19	0.0101	0.2695	0.3184	10.3475	0.93	0.29
Plant AE	79	Fall	2005	Spring	2004	12.90	79	0	0.0088			12.8951		
Plant AF	40	Spring	2005	NONE		0	0	1.7500						
Plant AG	78		Fall	2012	3.94	78	0	0.0089			3.9403			
Plant AH	79	Fall	2010	Spring	2009	13.24	79	0	0.0088			13.2412		
Plant AI	78		Spring	2012	3.11	78	1	0.0089	0.0089	1.0000	3.1055	0.05	0.08	

Table B-6 (continued)

Inspection Data Through Fall 2013 Extrapolated Back to Predicted Time to First Crack/Leak (Based on Weibull slope $\beta = 3$) [3]

Code	No. CRDM/ CEDM Nozzles	Replace Date		NDE Date, Scope, and Results												
				Outage	Year	EDY	All Nozzle Materials								at Detection of Cracking	at 1st Crack Extrapolated Back using b=
							NDE CRDM/ CEDM	Cum. Cracked	CDF (1st Crack)	CDF (# Cracked)	Time Factor (# Cracked)	EDYs at 1st Crack or Inspection (+8°F for all B&W Heads)				
													CDF of Units with Cracks (+8°F for all B&W Heads)	CDF of Units with Cracks (+8°F for all B&W Heads)		
Plant AJ	65	Fall	2003	NONE			0	0	1.7500							
Plant AK	78			Spring	2011	2.76	78	4	0.0089	0.0472	0.5703	1.5747	0.03	0.01		
Plant AL	69	Fall	2003	Fall	2001	16.20	9	1	0.0745	0.0745	1.0000	22.3057	0.51	0.71		
Plant AM	78			Fall	2007	1.94	78	0	0.0089			1.9383				
Plant AN	69	Fall	2004	Spring	2003	17.46	69	0	0.0101			17.4581				
Plant AO	49	Spring	2005	Fall	2003	16.60	49	0	0.0142			16.5959				
Plant AP	40	Spring	2006	NONE			0	0	1.7500							
Plant AQ	65	Spring	2003	Fall	2002	19.71	65	45	0.0107	0.6835	0.2107	4.1523	0.39	0.12		
Plant AR	69	Fall	2003	Fall	2001	18.08	12	8	0.0565	0.6210	0.3913	9.7426	0.58	0.24		
Plant AS	78			Spring	2011	3.11	77	0	0.0090			3.1111				
Plant AT	78	Spring	2007	NONE			0	0	1.7500							
Plant AU	78			Fall	2013	3.79	78	0	0.0089			3.7900				
Plant AV	69	Fall	2005	Spring	2004	21.69	69	0	0.0101			21.6900				
Plant AW	78			Spring	2013	4.08	78	0	0.0089			4.0800				
Plant AX	79	Fall	2006	Spring	2005	8.70	79	0	0.0088			8.7004				
Plant AY	69	Fall	2005	Spring	2004	16.70	69	0	0.0101			16.7000				
Plant AZ	78			Fall	2006	1.86	78	0	0.0089			1.8551				
Plant BA	91	Fall	2012	Fall	2009	19.78	91	0	0.0077			19.7833				
Plant BB	37	Fall	2003	NONE			0	0	1.7500							
Plant BC	97	Spring	2010	Fall	2008	15.29	97	0	0.0072			15.2946				
Plant BD	78			Spring	2013	4.02	78	0	0.0089			4.0200				
Plant BE	69	Fall	2005	Spring	2004	16.80	69	0	0.0101			16.8000				
Plant BF	97			Spring	2012	12.70	97	0	0.0072			12.7000				
Plant BG	78	Fall	2009	Spring	2008	14.37	78	0	0.0089			14.3701				
Plant BH	91	Fall	2007	Spring	2006	16.40	91	5	0.0077	0.0514	0.5261	8.6281	0.28	0.18		
Plant BI	65	Spring	2006	Spring	2004	16.42	65	0	0.0107			16.4150				
Plant BJ	69	Fall	2005	Spring	2004	22.62	69	8	0.0101	0.1110	0.4417	13.7499	0.79	0.36		
Plant BK	49	Fall	2005	Spring	2004	15.50	49	1	0.0142	0.0142	1.0000	15.5000	0.25	0.42		
Plant BL	69	Fall	2003	Spring	2002	26.50	69	5	0.0101	0.0677	0.5248	13.9070	0.65	0.39		
Plant BM	74	Spring	2010	Spring	2007	12.19	74	0	0.0094			12.1918				
Plant BN	91	Fall	2012	Fall	2012	24.68	91	0	0.0077			24.6800				
Plant BO	69	Spring	2005	Fall	2003	12.36	69	14	0.0101	0.1974	0.3586	4.4309	0.17	0.14		
Plant BP	41	Fall	2006	Spring	2005	13.09	41	0	0.0169			13.0947				
Plant BQ	69	Spring	2003	Fall	2001	22.39	69	16	0.0101	0.2262	0.3406	10.4982	0.72	0.31		
Plant BR	65			Fall	2012	4.08	65	4	0.0107	0.0566	0.5696	2.3210	0.09	0.06		

Table B-7

Summary of Weibull Probability Distribution Parameter Fitting for RPVHPN Analysis

Fitting Method	β	θ (EDY)	Standard Error in Vertical Intercept (ln(EDY))
Linearized Least Squares	1.379	23	0.2705

All inspection data adjusted to 600 °F ($Q = 50$ kcal/mole)

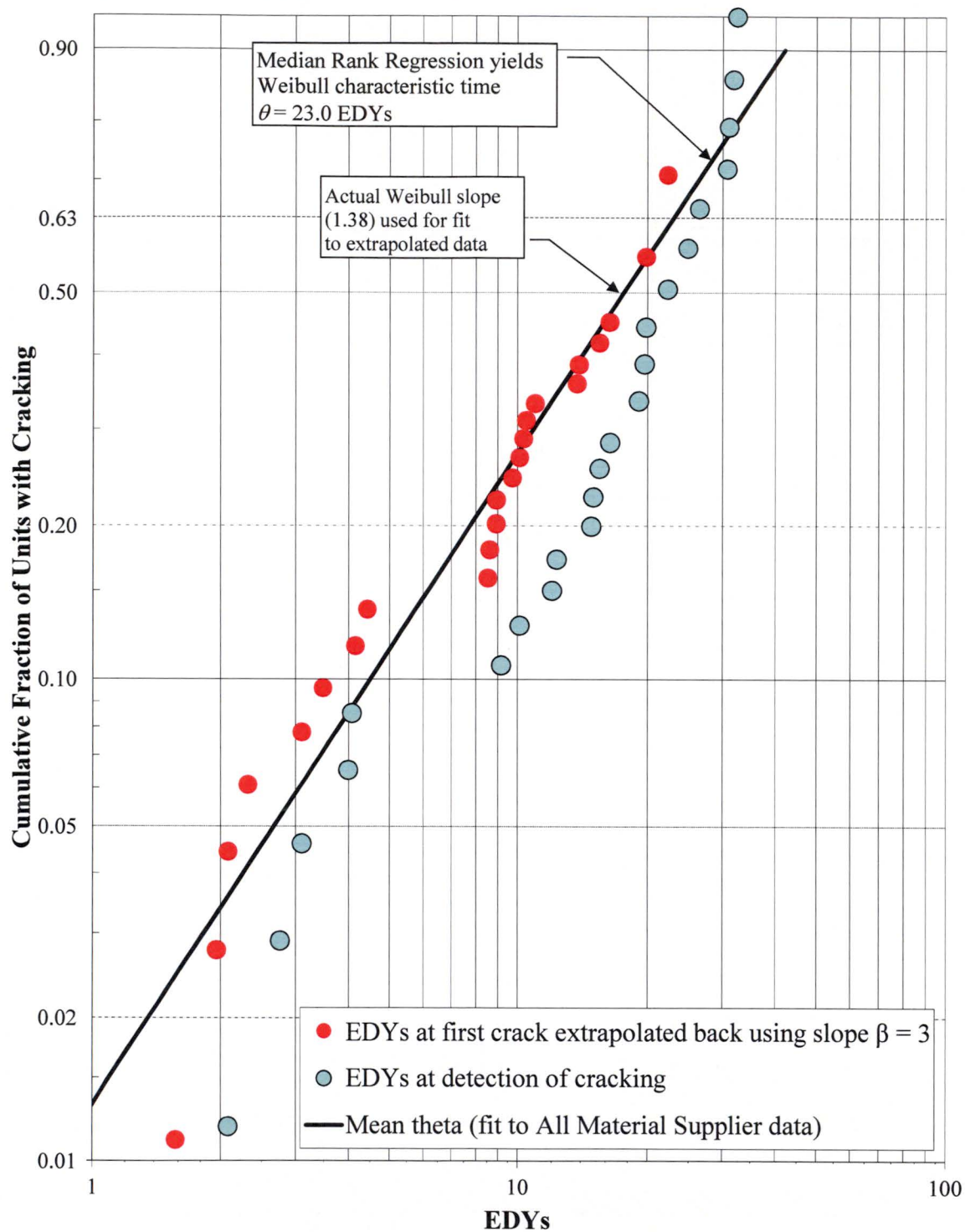


Figure B-17
Example MLE Weibull Probability Distribution for Alloy 600 RPVHPNs with Alloy 82/182 J-groove Welds

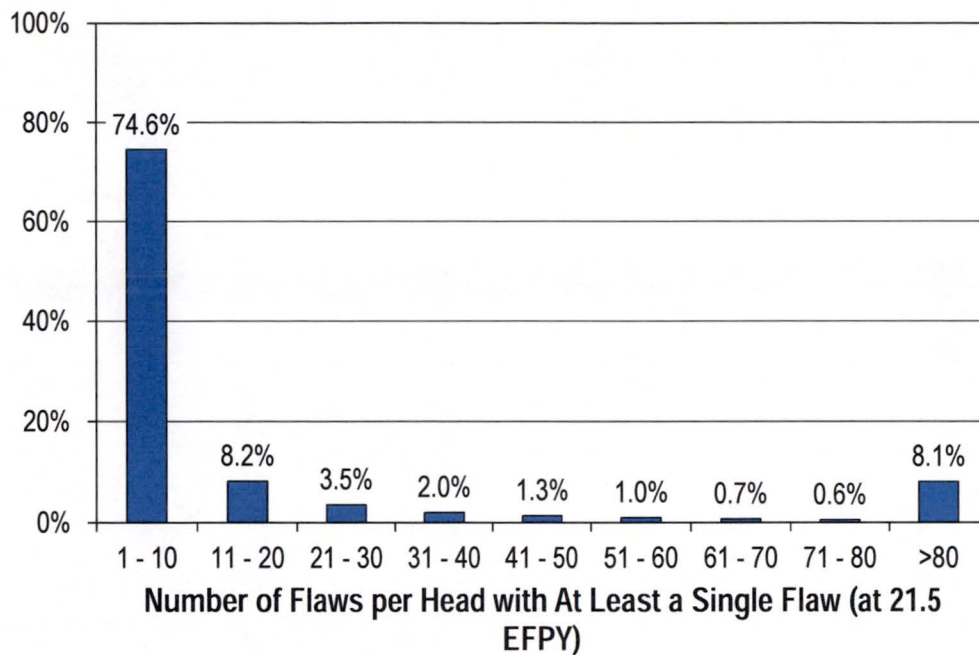


Figure B-18
Result of RPVHPN Numerical Initiation Study: Distribution of Number of Flaws per Hot Head with at Least a Single Flaw

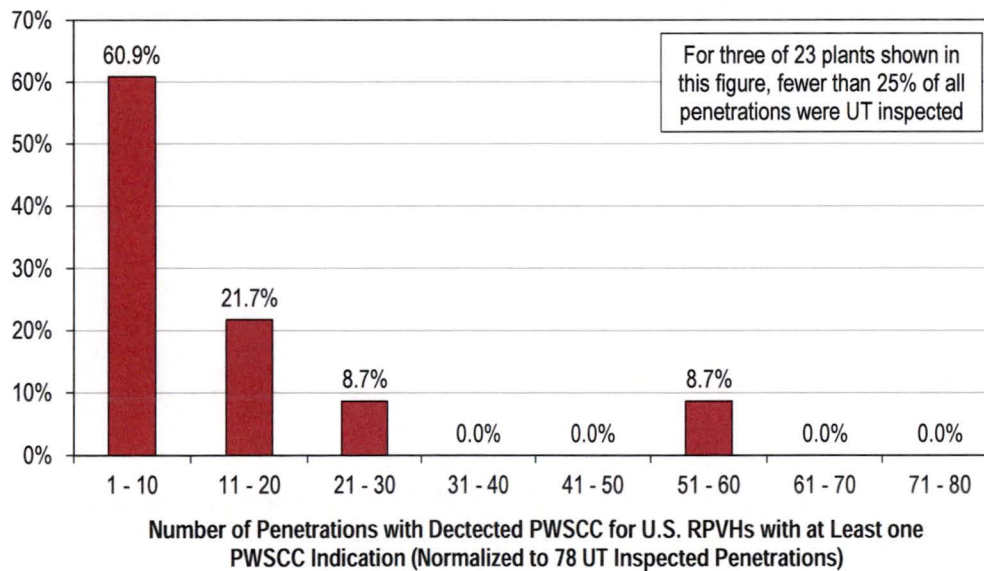


Figure B-19
Industry RPVHPN Flaw Initiation Data: Distribution of Normalized Number of Nozzles with PWSCC Indications per Head with at Least a Single Indication (23 Plants)

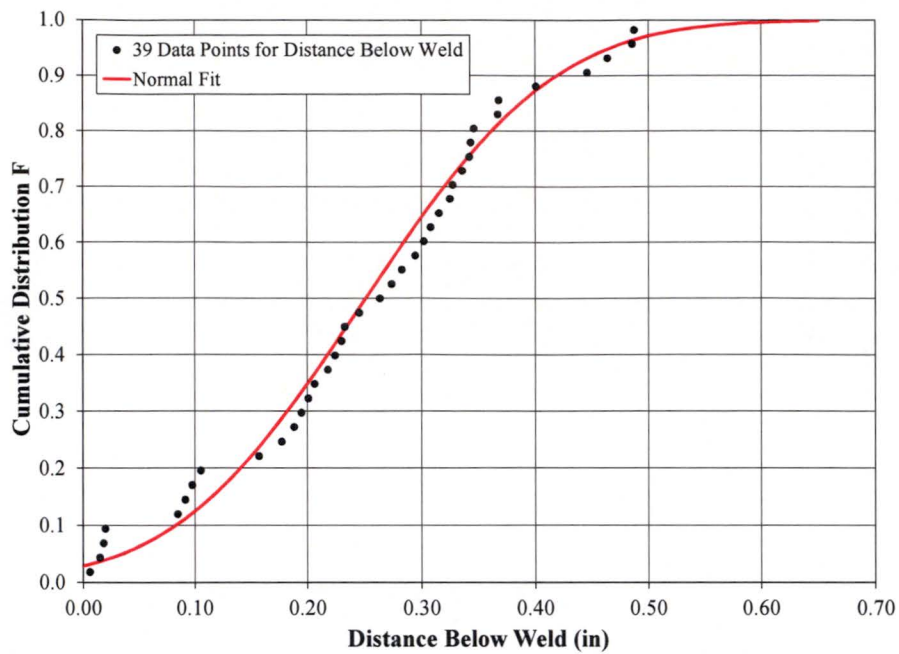


Figure B-20
Normal Distribution Fit to 80% Yield Stress Length on Uphill Side of Penetration Predicted by Different FEA Studies

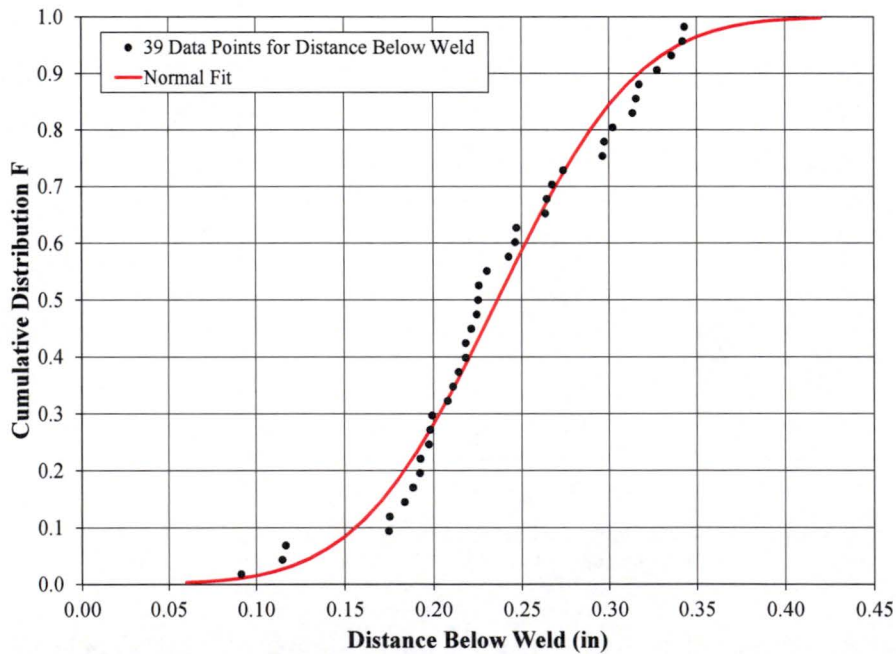


Figure B-21
Normal Distribution Fit to 80% Yield Stress Length on Downhill Side of Penetration Predicted by Different FEA Studies

B.8.3 Crack Growth Model

The set of inputs for the PWSCC propagation model is described in Table B-8 at the end of this section, including deterministic and distributed inputs. Various inputs are detailed in the following subsections.

B.8.3.1 Empirical Growth Parameters

The empirical growth parameters for Alloy 82/182 weld cracks are identical to those used for the DM weld program (see Section A.8.3.1).

The empirical growth parameters for Alloy 600 are based on the crack growth data compiled and presented in MRP-55 [12]. Instead of using a crack growth curve with a stress intensity factor threshold of $9 \text{ MPa}\cdot\text{m}^{1/2}$ and power law exponent of 1.16 (as suggested in MRP-55), a more bounding curve with a stress intensity factor threshold of 0.0 and power law exponent of 1.6 is fit to the data. Both curves are shown with the Alloy 600 CGR data in Figure B-22. The parameters for Alloy 600 curve that will be used in this study are given Table B-8.

B.8.3.2 Growth Variation Factors

The growth variation factor for Alloy 82/182 weld cracks are identical to those used for the DM weld program (see Section A.8.3.2).

Similar to the way growth uncertainty is accounted for in the weld material, the uncertainty of flaw propagation in Alloy 600 is characterized by f_{heat} and f_{wh} parameters.

The f_{heat} parameter is a common factor applied to all specimens fabricated from the same raw material to account for the effects of manufacturing variation. For this study, a log-normal distribution is fit to the heat factors for 26 laboratory heat specimens assessed in MRP-55 (see Figure B-23).

A “within-heat factor” (f_{wh}) describes the variability in flaw propagation rate for different Alloy 600 specimens from the same raw material (heat). A log-normal distribution was developed to describe the variability in f_{wh} for the data generated in MRP-55. The f_{wh} distribution describes the scatter in the flaw propagation rate model that remain after all effects addressed by the model are considered including the particular f_{heat} parameter calculated for the test heat. For this study, a log-normal distribution is fit to the heat factors for 140 laboratory crack specimens assessed in MRP-55 (see Figure B-24).

The lower and upper bounds for the growth variability distributions are set in the same manner as described for DM weld growth variation factors.

In addition to the heat-to-heat and within-heat variation terms, other forms of uncertainty are incorporated for the growth of circumferential through-wall cracks, as discussed in the modeling section.

- First, for the random multiplicative factor used to scale the FEA-derived K curves, a triangular distribution with a minimum and mode of 1.0 and a maximum of 2.0 is used. This results in a modestly increased K curve to account for any non-conservative bias in the FEA results.

- Second, for the environmental factor that scales the length growth rate predicted by the Alloy 600 CGR curve, a triangular distribution with a minimum and mode of 1.0 and a maximum of 2.0 is used. Based on the consensus of the international PWSCC expert panel convened by EPRI in 2001-2002, the crack growth rate for flaws connected to the OD annulus environment is most likely not significantly accelerated due to chemical concentration effects. However, as documented in MRP-55 [12], the expert panel conservatively recommended an environmental factor of 2 for deterministic calculations of growth of circumferential flaws in contact with the annulus environment. The triangular distribution described above was selected based on this work.

B.8.3.3 Uncertainty in Temperature Effect

The uncertainty in temperature and its effect on propagation is handled in same manner as described for DM welds in Section A.8.3.3.

B.8.3.4 Correlation in Relating Flaw Initiation and Propagation

As done for DM welds, the correlation in relating flaw initiation and propagation is not included for base case analysis.

Table B-8
Summary of Inputs for RPVHPN Flaw Propagation Model

Symbol	Description	Source	Units	Parameter Type	Hot Head Base Case	Cold Head Base Case
$1/\Delta t$	Number of time steps per year for crack size increment	The value chosen provides sufficient convergence	1/yr		12	12
f_{heat}	Heat-to-heat factor: common factor applied to all specimens fabricated from the same material to account for manufacturing variations	Fit to heat-to-heat variation data from MRP-55	-	type	Log-normal	Log-Normal
				linear μ	1.68	1.68
				median	1.00	1.00
				75%ile	1.98	1.98
				log-norm μ	0.00	0.00
				log-norm σ	1.016	1.016
				min	0.14	0.14
f_{wh}	Within-heat factor: factor accounting for the variability in crack growth rate for different specimens fabricated from the same raw material	Fit to within-heat variation from MRP-55 data after normalizing for heat-to-heat variation factor	-	max	5.32	5.32
				type	Log-Normal	Log-Normal
				linear μ	1.18	1.18
				median	1.00	1.00
				log-norm μ	0.00	0.00
				log-norm σ	0.5695	0.5695
				min	0.21	0.21
f_{weld}	Weld-to-weld factor: common factor applied to all specimens fabricated from the same weld to account for weld wire/stick heat processing and for weld fabrication	Fit to weld-to-weld variation data from MRP-115	-	max	3.68	3.68
				type	Log-Normal	Log-Normal
				linear μ	1.19	1.19
				median	1.00	1.00
				75%ile	1.49	1.49
				log-norm μ	0.00	0.00
				log-norm σ	0.5892	0.5892
f_{ww}	Within-weld factor: factor accounting for the variability in crack growth rate for different specimens fabricated from the same weld	Fit to within-weld variation from MRP-115 data after normalizing for weld-to-weld variation factor	-	min	0.313	0.313
				max	2.64	2.64
				type	Log-Normal	Log-Normal
				linear μ	1.12	1.12
				median	1.00	1.00
				log-norm μ	0.00	0.00
				log-norm σ	0.4807	0.4807
				min	0.309	0.309
				max	3.24	3.24

Table B-8 (continued)
Summary of Inputs for RPVHPN Flaw Propagation Model

Symbol	Description	Source	Units	Parameter Type	Hot Head Base Case	Cold Head Base Case
α_{heat}	Flaw propagation rate equation power law constant for Alloy 600	Fit to MRP-55 data with power law constant of 1.6 and stress intensity factor threshold of zero	(in/hr)/ (ksi-in. ^{0.5}) ^{1.6}		3.25E-08	3.25E-08
α_{weld}	Flaw propagation rate equation power law constant for Alloy 182 weld	MRP-115	(in/hr)/ (ksi-in. ^{0.5}) ^{1.6}		1.62E-07	1.62E-07
Q_g	Thermal activation energy for PWSCC flaw propagation	MRP-115	kcal/mole	type	Normal	Normal
				mean	31.07	31.07
				stdev	1.20	1.20
				min	23.90	23.90
				max	38.24	38.24
$T_{ref,g}$	Absolute reference temperature to normalize PWSCC flaw propagation data	MRP-55, MRP-115	°R		1077	1077
$K_{1,th,heat}$	Flaw propagation rate equation power law threshold for Alloy 600	Conservatively assumed threshold such that all cracks with positive K_I have a non-zero crack growth rate	ksi-in. ^{0.5}		0.0	0.0
$K_{1,th,weld}$	Flaw propagation rate equation power law threshold for Alloy 82/182 weld	MRP-115	ksi-in. ^{0.5}		0.0	0.0
$K_{1,min,heat}$	Minimum allowable K_I value for Alloy 600 components	No technical basis for non-zero value	ksi-in. ^{0.5}		0.0	0.0
$K_{1,min,weld}$	Minimum allowable K_I value for Alloy 182 components	No technical basis for non-zero value	ksi-in. ^{0.5}		0.0	0.0
n_{heat}	Flaw propagation rate equation power law exponent for Alloy 600	Fit to MRP-55 data with stress intensity factor threshold of zero	-		1.6	1.6
n_{weld}	Flaw propagation rate equation power law exponent for Alloy 182 weld	MRP-115	-		1.6	1.6
	Flag indicating if crack growth will be predicted considering the effect of crack closure	Crack closure effects are neglected for base case	Logical		FALSE	FALSE
	Flag indicating if cracks may grow in length without the effect of peening stresses	Approximates sub-surface balloon growth of crack	Logical		TRUE	TRUE

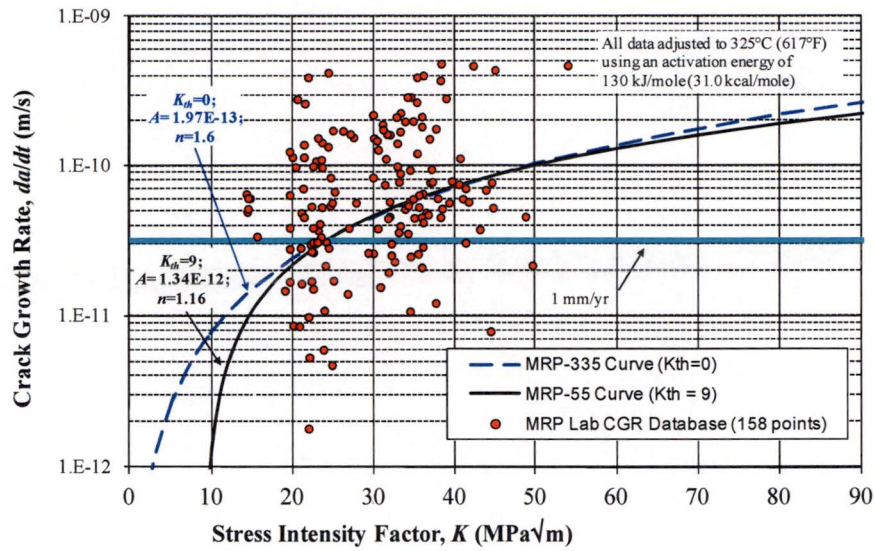


Figure B-22
Alloy 600 Crack Growth Rate Curves: MRP-55 ($K_{lth}=9$) Curve and MRP-335 ($K_{lth}=0$) Curve

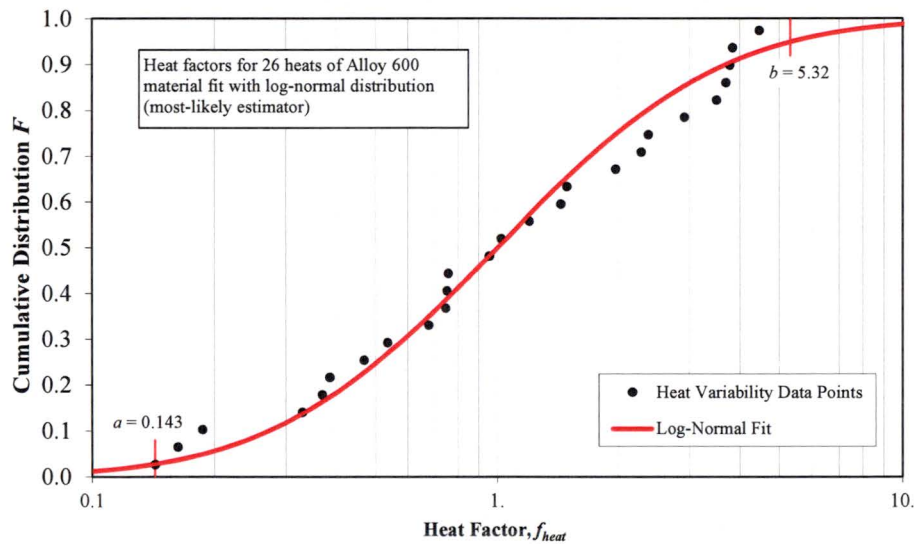


Figure B-23
Heat Factor f_{heat} Distribution with Log-Normal Fit for MRP-55 Alloy 600 Data

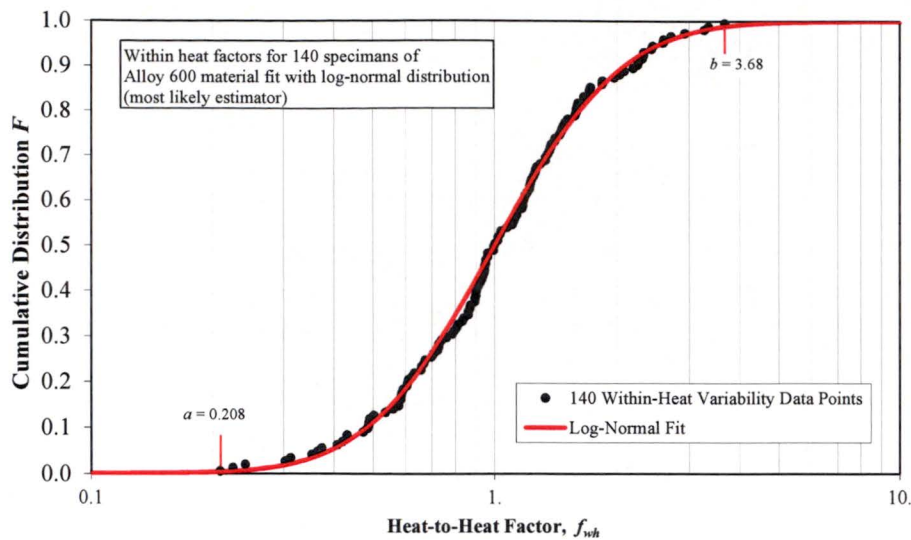


Figure B-24
Within-Heat Factor f_{wh} Distribution with Log-Normal Fit for MRP-55 Alloy 600 Data

B.8.4 Flaw Inspection and Detection Model

The set of inputs for the flaw examination models is described in Table B-9 at the end of this section, including deterministic and distributed inputs. Various inputs are detailed in the following subsections.

B.8.4.1 Examination Scheduling

As mentioned in the modeling section, UT inspection scheduling prior to peening for RPVHPNs is based on N-729-1 [4]. In accordance with this standard, a UT inspection is simulated once every cycle for the hot head (605°F operating temperature, 0.97 capacity factor, 24-month operating cycle) and once every three cycles for the cold head (561°F operating temperature, 0.97 capacity factor, 24-month operating cycle). The first UT inspection is modeled as occurring at the end of the 10th cycle for both the hot and cold reactor pressure vessel heads. These cycles correspond with the specific units that were used to develop the operating timeline, temperature, geometry inputs discussed in Section B.8.1.

In accordance with N-729-1, BMV inspections for leakage are conducted once every two cycles while a head has less than 8.0 EDY of operation and once every cycle afterward. This BMV schedule is not permitted to be relaxed after peening for hot heads but is relaxed to every third outage for cold heads (after follow-up examinations are performed).

In cases where peening is scheduled, the follow-up and in-service inspection intervals are varied to generate comparative results. The follow-up interval is varied between 1, 2, 3, or 1 and 2 cycles for hot heads and between 1, 2, and 3 cycles for cold heads. The in-service inspection interval is varied from 3 cycles to the plant operational service period for the hot and cold heads.

B.8.4.2 UT Probability of Detection

The probabilistic UT POD model is described by Equation [B-14]. The model is generated from upper and lower POD curves which each represent a two standard deviation offset from the median POD curve. The upper bound (favorable) curve was chosen such that there is an 80% POD for cracks 20% through-wall and a 95% POD for cracks 40% through-wall. The lower bound (unfavorable) curve was chosen such that there is a 65% POD for cracks 40% through-wall and a 90% POD for cracks 70% through-wall. Finally, a maximum POD of 95% is used to account for human/equipment error or other factors. The median POD curve is shown in Figure B-25.

This UT POD curve was calibrated to be consistent with a lower-end flaw detection rate for qualification testing of UT procedures and personnel used to inspect RPVHPNs. These UT qualification testing requirements are defined in 10 CFR 50.55a(g)(6)(ii)(D)(4) and in Table VIII-S10-1 of Supplement 10 to Appendix VIII of Section XI.

A correlation coefficient relating the results of successive inspections can be included to take into account the increasing likelihood of non-detection if a crack has already been missed in a previous inspection. Because this value has not been experimentally determined, a modest correlation coefficient of 0.5 is used for the base case input.

B.8.4.3 BMV Probability of Detection

The BMV inspection model employs a constant POD, irrespective of leak rate, duration of leak, etc. A value of 90% is used as a conservative assumption based on plant experience that through-wall cracking of CRDM and CEDM nozzles is accompanied by boric acid deposits that are reliably detected during direct visual examinations of the intersection of the nozzle with the upper surface of the reactor vessel head [13].

A strong correlation coefficient, 0.95, is used to correlate successive inspections of the same leaking penetration. It can be shown numerically that this results in approximately a 21%, 17%, and 14% POD for a leaking nozzle at the first, second, and third inspections following an original inspection in which a leaking nozzle was not detected.

Table B-9
Summary of Inputs for RPVHPN Examination Model

Symbol	Description	Source	Units	Parameter Type	Hot Head Base Case	Cold Head Base Case
	The through-wall fraction below which the small-flaw contingency (POD = 0) is used	Smallest flaw size used in UT mockup testing	-		0.10	0.10
$\rho_{insp,UT}$	Correlation coefficient for successive UT inspections	Conservative assumption	-		0.50	0.50
$(a/t_{U,1,UT}, p_{U,1,UT})$	First defined coordinate for favorable UT POD curve	Conservative assumption relative to UT qualification criteria	-		(0.2,0.80)	(0.2,0.80)
$(a/t_{U,2,UT}, p_{U,2,UT})$	Second defined coordinate for favorable UT POD curve	Conservative assumption relative to UT qualification criteria	-		(0.4,0.95)	(0.4,0.95)
$(a/t_{L,1,UT}, p_{L,1,UT})$	First defined coordinate for unfavorable UT POD curve	Conservative assumption relative to UT qualification criteria	-		(0.4,0.65)	(0.4,0.65)
$(a/t_{L,2,UT}, p_{L,2,UT})$	Second defined coordinate for unfavorable UT POD curve	Conservative assumption relative to UT qualification criteria	-		(0.7,0.90)	(0.7,0.90)
	Stdev between median UT POD curve and favorable/unfavorable curves	Conservative assumption relative to UT qualification criteria	-		2	2
$p_{max,UT}$	Maximum probability of detection for UT inspection	Conservative assumption relative to UT qualification criteria	-		0.95	0.95
p_{BMV}	Probability of detection for visual inspection of leaking nozzle	Conservative assumption	-		0.90	0.90
$\rho_{insp,BMV}$	Correlation coefficient for successive BMV inspections	Conservative assumption	-		0.95	0.95

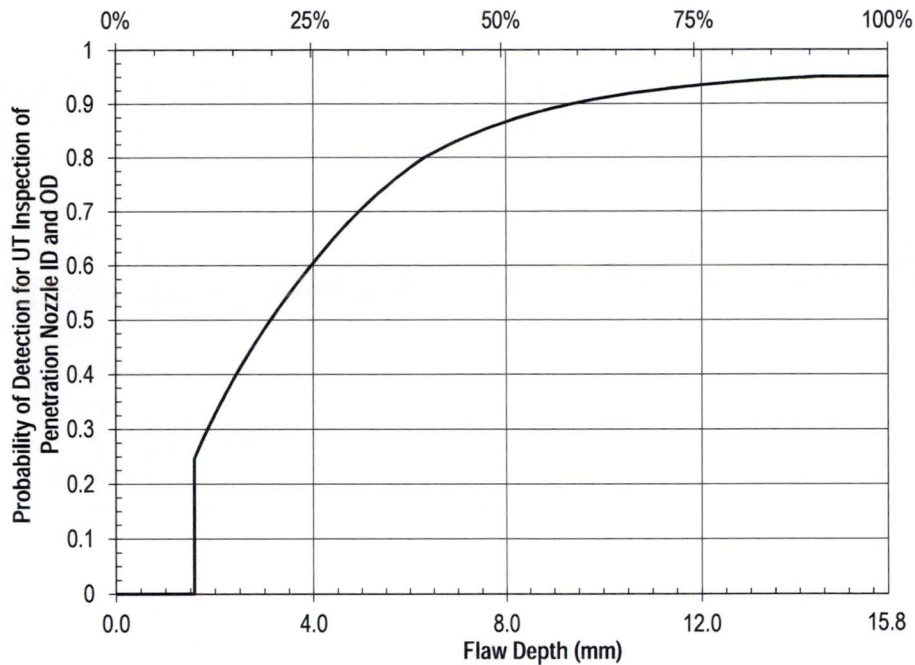


Figure B-25
Median Assumed UT Inspection POD Curve for Axial Cracking Initiating at the RPVHPN ID and OD

B.8.5 Effect of Peening on Residual Stress

The set of inputs related to peening considerations is described in Table B-10 at the end of this section, including deterministic and distributed inputs. Various inputs are detailed in the following subsections.

B.8.5.1 Peening Application Scheduling

The peening applications for the hot and cold head are scheduled based on the operating and inspection experience of the subpopulation of reactor vessel heads with Alloy 600 penetration nozzles that are still in service in U.S. PWRs. Peening application is considered to occur during a cycle that coincides with a scheduled UT inspection.

The hot head has peening scheduled at EOC 17 resulting in 7 UT inspections prior to peening (not including the pre-inspection).

The cold head has peening scheduled at EOC 12 resulting in 1 UT inspection prior to peening (not including the pre-inspection).

B.8.5.2 Post-Peening Residual Stresses

For RPVHPNs, the residual plus normal operating stress is modeled to result in a compressive stress prior to applying operating stresses. Once operating stresses are applied, the post-peening surface stress is deterministically modeled to be +10 ksi. This stress bounds the total steady-state surface stress permitted by the performance criteria in Section 4.

The peening compressive residual stress depth for the RPVHPN is modeled with a normal distribution. For the OD and weld surfaces, this distribution is given a mean of 1.0 mm (minimum allowable compressive residual stress depth defined in Section 4) and a standard deviation of 0.25 mm. For the ID surfaces, this distribution is given a mean of 0.25 mm (minimum allowable compressive residual stress depth defined in Section 4) and a standard deviation of 0.06 mm.

Finally, the same transition length ratios defined in Section A.8.5.2 are applied for peening stress profiles on RPVHPNs.

B.8.5.3 Effect of Thermal and Load Cycling

The peening performance requirements of Section 4 require the compressive stress effect produced by the mitigation process to be effective for at least the remaining service life of the component. As a bounding peening stress profile is applied to this analysis for the remainder of the plant operational period, relaxation effects are not modeled for the RPVHPN base case or for any model sensitivity studies.

B.8.5.4 Effect of Peening on Growth

For base case results, growth of cracks is simulated without consideration for crack closure. This effect is considered as a sensitivity case.

Also for the baseline results, full credit is given to growth of the length of a crack under the peening surface. As discussed in the modeling section, this is done by using the “balloon” growth approximation—neglecting peening stresses for the calculation of length growth. The “balloon” growth approximation is lifted for a sensitivity study.

B.8.6 Flaw Stability Model

The two key inputs to the flaw stability model presented in this report are the initial size of a circumferential through-wall crack and the critical crack length at which ejection is predicted to occur. Both are deterministic inputs and are presented in Table B-11.

Via the conservative precedent set in MRP-105 [5], circumferential through-wall cracks along the weld contour are assumed to initiate with a length equivalent to 30° around the weld contour. Together with the immediate transition to through-wall growth on the weld contour after leakage and accelerated growth parameters, this results in conservative estimates for the time to ejection following leakage.

The critical crack length for ejection, or net section collapse, is based on calculations presented in MRP-110 (Appendix D of Reference [13]). A length equivalent to 300° around the weld contour is used for all base case analyses in this report in order to bound the critical flaw angles calculated for CRDM and CEDM nozzles for all U.S. PWRs under standard design pressure. (For a sensitivity case presented later, the critical flaw length of 275° is used based on MRP-110 calculations in which a structural factor of 2.7 was applied to the standard design pressure.)

Table B-10
Summary of Peening-Specific Inputs

Symbol	Description	Source	Units	Parameter Type	Hot Head Base Case	Cold Head Base Case
	Outage of peening application	Scheduled at next outage coinciding with a UT inspection	Cycle number		17	12
	Number of cycles between peening application and final follow-up inspection	Section 4	# cycles		2	2
	Inspection interval after peening	Section 4	# cycles		5	5
	Interval for BMV post-peening (in number of cycles)	Section 4	# cycles		0	3
	Flag indicating if a UT pre-peening exam is performed	Section 4	-		TRUE	TRUE
	Flag indicating if a UT exam is included during all the cycle(s) between peening and the follow up exam	Section 4	-		TRUE	FALSE
	Flag indicating if BMV exams are performed after peening	Section 4	-		TRUE	TRUE
	Number of consecutive cycles in which BMV exams are performed after peening	Section 4	# cycles		Perform BMV post-peening per Section 4	2

Table B-10 (continued)
Summary of Peening-Specific Inputs

Symbol	Description	Source	Units	Parameter Type	Hot Head Base Case	Cold Head Base Case
$\sigma_{0,PPRS,ID}(t=0)$	Sum of post-peening residual plus normal operating stress on ID surface	Bounds minimum value from performance criteria (Section 4)	ksi		10.0	10.0
$x_{1,PPRS,ID}$	Depth of compressive residual stress layer from ID surface	Bounds minimum value from performance criteria (Section 4)	in.	type	Normal	Normal
				mean	0.010	0.010
				stdev	0.002	0.002
				min	0.000	0.000
				max	0.025	0.025
$\sigma_{0,PPRS,ext}(t=0)$	Sum of post-peening residual plus normal operating stress on OD and weld surface	Bounds minimum value from performance criteria (Section 4)	ksi	mean	10.0	10.0
$x_{1,PPRS,ext}$	Depth of compressive residual stress layer from OD and weld surface	Bounds minimum value from performance criteria (Section 4)	in.	type	Normal	Normal
				mean	0.039	0.039
				stdev	0.010	0.010
				min	0.000	0.000
				max	0.098	0.098
$f_{1,PPRS}$	Ratio of minimally-affected depth to penetration depth	Section A.3.3	-		2.0	2.0
$f_{2,PPRS}$	Fraction of depth between penetration depth and minimally-affected depth where peening results in no effect	Section A.3.3	-		0.7	0.7

Table B-11
Summary of Inputs for RPVHPN Stability Model

Symbol	Description	Source	Units	Parameter Type	Hot Head Base Case	Cold Head Base Case
$\theta_{circ,init}$	Initial angle for circumferential through-wall cracks immediately following a leak	MRP-105	degrees		30	30
$\theta_{circ,crit}$	Critical flaw angle for nozzle ejection	MRP-110	degrees		300	300
$K_{circ,mult}$	Circumferential through-wall crack K_I curve multiplier	Assumed to assure conservative application of FEA-predicted K_I curves	-	type	triangular	triangular
				mode	1	1
				lower limit	1	1
				upper limit	2	2
$C_{circ,mult}$	Circumferential through-wall crack environmental factor	Conservative factor applied based on anecdotal information about environment effects on circumferential TW cracks	-	type	triangular	triangular
				mode	1	1
				lower limit	1	1
				upper limit	2	2

B.9 Results of Probabilistic Cases

This section presents results generated using the integrated probabilistic model described in Sections B.2 through B.6, with particular focus on the prediction of the ejection criterion described in Section B.7. Using the inputs described in Section B.8, this section presents predictions for PWSCC on RPVHPNs on a hot and cold head, without peening mitigation (Section B.9.1) and with peening mitigation (Section B.9.2).

Section B.9.3 presents the results of sensitivity studies wherein one or more inputs or modeling methodologies are varied from those described in Sections B.2 through B.8. The aim of these sensitivity studies is to demonstrate the relative change in the predicted ejection risk for a head when an input or modeling assumption is varied.

Ejections and leakage are counted in two different ways within the simulation framework: in terms of the number of heads with at least one event (by counting only the first instance of leakage or ejection for a given MC realization) and in terms of the number of penetrations with at least one event (by counting the first instance of leakage or the occurrence of ejection for each unique penetration). The primary ejection and leakage statistics used to assess and compare the results of the probabilistic model are defined below:

- Incremental leakage frequency (ILF) is defined as the average number of new leaking nozzles per year on a reactor vessel top head. A simulated flaw causes leakage if it propagates through the entire material thickness to penetrate the annulus above the J-groove weld before it is detected and repaired. This statistic is derived for any given operational cycle by averaging the predicted number of new leaking nozzles for that operational cycle across all MC realizations. This is adjusted to a probability per year by dividing by the number of calendar years per cycle.

$$ILF = \frac{(\text{Number of new leaking nozzles predicted during cycle across all realizations})}{(\text{Number of realizations})(\text{Calendar years per cycle})} \quad [B-16]$$

- Average leakage frequency (ALF) is the average of the ILFs following the hypothetical time of peening until the end of the operational service period of the plant.

$$ALF = \frac{\sum_{i=i_{\text{peen}}}^{N_{\text{cycle}}} (\text{Number of new leaking nozzles predicted during cycle across all realizations})}{(\text{Number of realizations})(\text{Calendar years per cycle})(N_{\text{cycle}} - i_{\text{peen}})} \quad [B-17]$$

where:

- N_{cycle} = number of cycles in operational service period
- i_{peen} = cycle number associated with the hypothetical time of peening

- Cumulative probability of leakage (CPL) is defined as the fraction of heads with at least one predicted leak across all MC realizations across all cycles of interest. This document reports two versions of this statistic: (1) cumulated from the start of operation to a given cycle and (2) cumulated from the hypothetical time of peening to the end of plant operation.

$$CPL = \frac{(\text{Total number of heads with at least one predicted leak})}{(\text{Number of realizations})} \quad [B-18]$$

- Incremental ejection frequency (IEF) is defined as the average number of nozzle ejections per year on a reactor vessel top head. This statistic is derived for any given operational cycle by averaging the predicted number of ejections for that operational cycle across all MC realizations and dividing by the number of calendar years per cycle. If no ejections are predicted to occur during a given cycle across all MC realizations, 0.5 ejections are assumed for the sake of stability and conservatism in calculated statistic values.

$$IEF = \frac{\max\{(\text{Number of ejections leaks predicted during cycle across all realizations}), 0.5\}}{(\text{Number of realizations})(\text{Calendar years per cycle})} \quad [B-19]$$

- Average ejection frequency (AEF) is the average of the IEFs following the hypothetical time of peening until the end of the operational service period of the plant.

$$AEF = \frac{\sum_{i=i_{\text{peen}}}^{N_{\text{cycle}}} \max\{(\text{Number of ejections predicted during } i\text{th cycle across all realizations}), 0.5\}}{(\text{Number of realizations})(\text{Calendar years per cycle})(N_{\text{cycle}} - i_{\text{peen}})} \quad [B-20]$$

- Cumulative probability of ejection (CPE) is defined as the fraction of heads with at least one predicted ejection across all MC realizations across all cycles of interest. This document reports two versions of this statistic: (1) cumulated from the start of operation to a given cycle and (2) cumulated from the hypothetical time of peening to the end of plant operation.

$$CPE = \frac{(\text{Total number of heads with at least one predicted ejection})}{(\text{Number of realizations})} \quad [B-21]$$

The effect of nozzle ejection on nuclear safety can be assessed through multiplication of the frequency of nozzle ejection (i.e., the initiating event frequency) with appropriate conditional core damage probability (CCDP) value. The resulting core damage frequency is typically averaged over long-term operation and compared to the acceptance criteria of Regulatory Guide 1.174 [15]. Regulatory Guide 1.174 specifies an acceptable change in core damage frequency of 1×10^{-6} per reactor year for permanent changes in plant design parameters, technical specifications, etc.

In addition to comparison versus the absolute acceptance criterion of Regulatory Guide 1.174, the results of the probabilistic modeling can be used to make relative comparisons of the statistics predicted for different cases (e.g., between the AEF predicted for one peening schedule vs. the AEF predicted for the unmitigated case with standard inspection intervals). This comparative approach has the advantage of minimizing any potential for bias introduced by the various modeling assumptions.

B.9.1 Results for the Unmitigated Case

Using the inputs specified in Section A.8, predictions were made for unmitigated RPVHPNs. Ejection predictions for hot and cold heads are shown in Figure B-32 and Figure B-33, leakage

predictions are shown in Figure B-34 and Figure B-35. For these results, volumetric and visual examinations were scheduled based on N-729-1 for unmitigated reactor vessel heads.

For reference, the time of the first modeled inspection, as well as the hypothetical time of peening is shown on these plots. Between the hypothetical time of peening and 60 calendar years (58.2 EFPY), the model predicts an average ejection frequency (AEF) of 2.1×10^{-5} for the hot head and 1.9×10^{-6} for the cold head; the model predicts a cumulative probability of leakage of 18.6% for the hot head and 18.4% for the cold head.

These values will be important for assessing the performance of peening for leakage mitigation in the following section.

B.9.2 Results with Peening Mitigation

As discussed previously, a follow-up inspection is expected to be conducted either one, two, three, or the first and second cycles after peening for the hot head, and either one, two, or three cycles after peening for the cold head. After the follow-up inspection, a new in-service inspection interval is expected to be utilized through the end of plant service life. Various combinations of follow-up inspection time and in-service inspection frequency were used to make ejection and leakage predictions after peening. Ejection results are summarized in Figure B-36 for the hot head case and in Figure B-37 for the cold head case, and leakage results are summarized in Figure B-38 and Figure B-39 for the hot and cold head cases, respectively.

The RPVHPN results demonstrated a much larger trend with respect to the ISI frequency than the DM weld results. This is due in large part to the higher likelihood of cracks existing after the pre-peening inspection. It is conservatively predicted that, on average, two nozzles in each hot head and one nozzle in approximately two cold heads would have unrepaired cracks after the pre-peening inspection.

For both the hot and cold heads, the cumulative probability of leakage after peening is predicted to be reduced by a factor between 3.5 and 6 times, depending on the post-peening inspection schedule. For example, using a 10-year (one interval) UT inspection frequency, the cumulative probability of leakage after peening is predicted to be reduced by a factor of approximately five for both hot and cold heads. Furthermore, the probability of leakage vs. time decays rapidly for both hot and cold heads with relieve UT inspection intervals, as shown in Figure B-40.

For the hot head reactor, using a post-peening ISI interval of 10 years (one interval) combined with a follow-up examination either one or two cycles after peening resulted in somewhat higher ejection risks than the unmitigated case: 182% and 147% of the unmitigated head risk, respectively. However, the same interval with a follow-up inspection both one and two cycles after peening resulted in an ejection risk lower than (83% of) the unmitigated case.

For the cold head reactor, the AEF after peening was predicted to improve compared to the unmitigated case when a post-peening ISI frequency of every 10 years (one interval) is used with a follow-up within 6 calendar years after peening. A post-peening ISI of one interval resulted in somewhat lower ejection risks compared to the unmitigated case: 79%, 45%, and 66% of the unmitigated risk for follow-up inspections scheduled one, two, and three cycles after peening, respectively. This result suggests that it may be beneficial to delay the follow-up inspection to the second cycle after peening to allow more significant cracks to grow such that they are more easily detected at the follow-up inspection, i.e., before entering the ISI schedule.

It is important to consider the maximum incremental frequency of ejection (IEF) for any cycle, in addition to the AEF, in order to understand how concentrated the risk may be over particular spans of time and if there are particular cycles with considerably higher risk. For instance, for the peened cold head base case (with a follow-up inspection two cycles after peening and an ISI interval of 5 cycles), the ratio of maximum IEF to AEF is 4.0. The same ratio for the unmitigated cold head is 3.60. For a peened hot head (with a follow-up inspection one and two cycles after peening and an ISI interval of 5 cycles), the ratio of maximum IEF to AEF was 3.1. The same ratio for the unmitigated hot head is 1.4. The risk concentration was not substantially worse for the peened case than for the unmitigated case.

Comparing the leakage and ejection statistics recorded for the head as a whole and the statistics recorded for individual nozzles, it is possible to draw conclusions regarding the number of incidences per head *assuming that the head has one or more of such incidences (assuming one or more leaks or one or more ejections)*. For instance, hot heads that are predicted to have no ejections or repairs prior to the outage before peening are anticipated to have approximately 1.1 leaking penetrations between peening and the end of service; hot heads that are predicted to have no ejections or repairs prior to the outage before peening are anticipated to have only one ejection by the end of service (under the assumption that a unit would continue operating without head replacement after the first ejection). However, it is important to keep in mind that the average ejection frequency is four orders of magnitude lower than the average leakage frequency.

Finally, some location-specific information is output by the RPVHPN program. This information indicates that as modeled 75% to 90% or more of leaks that occur after peening occur due to weld-initiated cracks. The leakage probability as calculated is greatly influenced by the conservative assumptions that one third of the crack initiations occur on the wetted surface of the weld metal and that the weld flaws grow to cause leakage with no chance of becoming detectable via UT performed from the nozzle inside surface. On the contrary, plant experience shows that most CRDM nozzles leaks have been accompanied by cracking of the nozzle tube base metal detectable via UT from the nozzle inside surface. The assumptions made in the modeling conservatively increase the chance of developing circumferential cracks in the nozzle tube above the weld elevation since a 30° through-wall circumferential crack is assumed to be produced immediately upon leakage. The probability of leakage due to base metal cracking is also a more relevant measure to assess the benefit of periodic UT examinations because such examinations are not qualified to detect weld flaws.

B.9.3 Results for Sensitivity Cases

Various sensitivity studies were conducted with the RPVHPN probabilistic model in order to demonstrate the relative change in the predicted results given one or more changes to modeling or input assumptions. Each sensitivity case has been classified as either a Model Sensitivity Case (in which an approximated input or model characteristic is varied) or an Inspection Scheduling Sensitivity Case (in which a controllable inspection option is varied). Modified inputs for Model Sensitivity Cases are presented in Table B-12, modified inputs for Inspection Scheduling Sensitivity Cases are presented in Table B-13.

For hot heads, Figure B-41 compares the average ejection frequencies from the peening inspection scheduling sensitivity cases to those for the peening and non-peening base cases.

Figure B-42 and Figure B-43 compare the AEFs resulting from the model sensitivity cases with peening to those for the peening base case. Figure B-44 and Figure B-45 compare the AEFs resulting from the model sensitivity cases with no-peening to those for the no-peening base case.

For cold heads, Figure B-46 compares the average ejection frequencies from the peening inspection scheduling sensitivity cases to those for the peening and non-peening base cases. Figure B-47 compares the AEFs resulting from the model sensitivity cases with peening to those for the peening base case. Figure B-48 compare the AEFs resulting from the model sensitivity cases with no-peening to those for the no-peening base case.

The cases of greatest interest are discussed below:

Inspection Scheduling Sensitivity Case 1 – Entering Post-Peening ISI without a Follow-Up Inspection and Inspection Scheduling Sensitivity Case 2 – No Pre-Peening Inspection

Inspection Scheduling Sensitivity Case 1 explored that result of skipping the follow-up UT inspection after peening and immediately entering a post-peening ISI with a UT inspection frequency of once every 5 cycles (one interval). Inspection Scheduling Sensitivity Case 2 explored that result of skipping the pre-peening UT inspection but conducting a follow-up UT the first and second cycle after peening before entering a post-peening ISI defined in Section 4. In both cases, BMV inspection was performed according to N-729-1 schedule requirements.

Not performing follow-up inspections (Inspection Scheduling Sensitivity Case 1) resulted in an AEF of 1.0×10^{-4} for the peened hot-head, and an AEF of 2.1×10^{-6} for the peened cold-head. Not performing pre-peening inspections (Inspection Scheduling Sensitivity Case 2) resulted in an AEF of 8.0×10^{-5} for the peened hot-head, and an AEF of 1.9×10^{-6} for the peened cold-head. These sensitivity cases emphasize the importance of both the pre-peening and follow-up examinations.

Inspection Scheduling Sensitivity Case 3 through 5 and 7– Various Relief Options for Post-Peening Visual Examinations

As discussed previously, N-729-1 requires that VE be performed every cycle on unmitigated heads with more than 8.0 EDY. Inspection Scheduling Sensitivity Cases 3 through 5 and Case 7 explored the use of a different BMV schedule after peening:

- Case 3 used a two-cycle BMV interval after peening.
- Case 4 used a three-cycle BMV interval after peening.
- Case 5 stopped BMV examinations altogether after peening.
- Case 7 performed BMV examinations every refueling outage after peening.

Figure B-41 and Figure B-46 demonstrate the effect of each BMV scheduling change, relative to the base case.

The use of a two-cycle BMV interval after peening resulted in an AEF of 3.1×10^{-5} for the peened hot head, and an AEF of 1.1×10^{-6} for the peened cold head. Moving to a three-cycle BMV resulted in an AEF of 4.3×10^{-5} for the peened hot head. Not performing BMV altogether after peening resulted in an AEF of 2.4×10^{-4} for the peened hot head, and an AEF of 7.5×10^{-6} for the peened cold head, demonstrating the value in performing periodic BMV examinations. Performing BMV every cycle after peening results in a further slightly reduced AEF of 8.5×10^{-7}

for the peened cold head. It is noted that these probabilistic results do not credit the performance of required IWA-2212 VT-2 visual examinations of the head under the insulation through multiple access points every outage that a VE is not performed. Like the VE examinations, these VT-2 examinations are an opportunity to detect leakage. Moreover, the visual examinations only detect degradation after leakage has already occurred, so they do not act to prevent leakage in the nozzle being examined.

Model Sensitivity Case 2 –Reactor Vessel Heads with No Observed PWSCC to Date

Model Sensitivity Case 2 explored the result of resampling Monte Carlo realizations in which crack detection or nozzle ejection was predicted prior to the outage before that in which peening occurs.

This resampling logic results in probabilities that are conditioned on the premise that no detection of PWSCC or ejection has taken place by the specified time; of the 5 active hot heads and 19 active cold heads with Alloy 600 nozzles in U.S. PWRs, PWSCC has been reported for only six heads to date (one of which was a hot head) despite multiple volumetric examination having been performed of all the nozzles in each head [3].

Resampling early detections or ejections results in an AEF of 2.8×10^{-6} for the peened hot head, an AEF of 3.0×10^{-6} for the unmitigated hot head, an AEF of 5.3×10^{-7} for the peened cold head, and an AEF of 6.3×10^{-7} for the unmitigated cold head. Approximately three of every four Monte Carlo realizations are resampled for the hot head, and about one in 10 realizations are resampled for the cold head.

Figure B-49 shows a time-history of the incremental ejection frequency and cumulative probabilities of ejection for this sensitivity case. By comparing these results to the base case results shown in Figure B-32, it is clear that resampling MC realizations that are conditioned on no early detection or ejections results in a lower IEF and CPE. Comparing this sensitivity case to the equivalent peening or unmitigated base case, the average ejection frequency is about a factor of 6.2 lower for the peened hot head, a factor of 6.9 lower for the unmitigated hot head, a factor of 2.4 lower for the peened cold head, and a factor of 3.1 lower than the base case for the unmitigated cold head.

Model Sensitivity Cases 7 and 9 – Removal of Inspection Correlation

As discussed in the modeling and inputs section, the base case assumed correlation between successive inspections, i.e., a crack that goes undetected by a UT examination would be more likely to be missed in subsequent UT inspections (assuming it does not grow significantly); a leak that goes undetected by visual examination is more likely to be missed in subsequent visual examinations.

Removing correlation between subsequent UT inspections (M7) results in an AEF of 1.1×10^{-5} for the peened hot head, and an AEF of 1.6×10^{-5} for the unmitigated hot head. Removing correlation between subsequent BMV inspections (M9) results in an AEF of 3.3×10^{-6} for the peened hot head, an AEF of 1.6×10^{-5} for the unmitigated hot head, an AEF of 5.6×10^{-7} for the peened cold head, and an AEF of 9.9×10^{-7} for the unmitigated cold head.

The inclusion of these correlations results in higher probabilities of leakage and ejection because it reduces the benefit of performing multiple examinations over time to detect a crack or leak, allowing longer spans of time for growth.

Model Sensitivity Case 13 – Earlier Initiation of First PWSCC

Similar to DMW Model Sensitivity Case 13, this case explored the shifting of the initiation time model to earlier times. For this sensitivity case, t_1 , the time at which 1% of all RPVHPNs are expected to initiate PWSCC, was reduced by a factor of 5.

This shift in the initiation model resulted in an AEF of 3.3×10^{-5} for the peened hot head, an AEF of 2.9×10^{-5} for the unmitigated hot head, an AEF of 8.3×10^{-6} for the peened cold head, and an AEF of 1.0×10^{-5} for the unmitigated cold head. The predicted AEF and ALF for this sensitivity case result in the greatest increase with respect to the base case. However, it is noted that this initiation model results in a prediction of at least one leaking nozzle before 20 EFPY in over 95% of hot-heads and in over 35% of cold-heads. This is not in line with U.S. PWR operating experience.

Model Sensitivity Case 16 – Correlation Between Initiation and Growth

Similar to DMW Model Sensitivity Case 15, this case explored the generally accepted tendency for cracks that initiate earlier to grow faster.

Including this correlation results in an AEF of 1.7×10^{-5} for the peened hot-head, an AEF of 3.7×10^{-5} for the unmitigated hot-head, an AEF of 4.1×10^{-6} for the peened cold-head, and an AEF of 1.0×10^{-5} for the unmitigated cold-head.

This significant increase for cold-heads is due to the fact that any instance of PWSCC that initiates prior to the end of the unit operating lifetime are relatively early given the initiation frequency at temperatures characteristic of a cold head. The growth rates of these cracks could be biased upward of laboratory crack growth rate predictions (assuming that the conditions that led to early initiation also foster more rapid growth).

Model Sensitivity Case 26 – Compressive Total Stress at Peened Surface

As is the case for the peening performance requirements for DMWs defined in Section 4, this case explores the effect of applying a total (normal operating plus residual) stress of 0 ksi to the peened surface. This is a change from the base case inputs, in which the total (normal operating plus residual) stress at the peened surface of an RPVHPN is +10 ksi (tensile) (+70 MPa).

The more compressive surface stress resulted in an AEF of 1.7×10^{-5} for the peened hot head, and an AEF of 1.1×10^{-6} for the peened cold head. This minimal reduction in AEF from the base case is due to the fact that peening is credited with no future PWSCC initiation for both the base case and for this sensitivity case. Additionally, this change in the post-peening stress profile has a minor effect on the crack growth rates for the small subset of flaws that are not detected by the pre-peening examinations.

Model Sensitivity Case 27 – Total Stress Compressive to Nominal Compressive Stress Depth

Similar to DMW Model Sensitivity Case 25, this sensitivity case explores the effect of a compressive total stress to the nominal compressive stress depth of 0.04 in. (1.0 mm) on the RPVHPN outer surfaces and 0.01 in. (0.25 mm) on the RPVHPN inner surfaces. To do so, this sensitivity case is modeled by assigning a greater value for the compressive residual stress depth and a more compressive peening surface residual stress compared to the base cases. The stress

profiles used in this sensitivity case are compared to the base case peened stress profile in Figure B-26 through Figure B-31.

Setting the total (residual plus operating) stress to be compressive from the surface to the nominal compressive residual stress depth results in an AEF of 1.5×10^{-5} for the peened hot head, and an AEF of 9.3×10^{-7} for the peened cold head. Comparing these results to the base case and RPVHPN Model Sensitivity Case 26 results indicates that there is only a limited risk benefit for a total (normal operating plus residual) stress that remains compressive to the nominal compressive stress depth. The results of Model Sensitivity Cases 26 and 27 show that there would be very limited benefit to requiring a more compressive stress effect than that specified by the performance criteria in Section 4.3.8.1 for RPVHPNs.

Probabilistic Assessment Cases for Reactor Pressure Vessel Head Penetration Nozzles (RPVHPNs)

Table B-12
Summary of Modified Inputs for RPVHPN Model Sensitivity Cases

Sensitivity Case	Description	Symbol	Units	Parameter Type	Hot Base Case Value	Hot Sensitivity Case Value	Cold Base Case Value	Cold Sensitivity Case Value
M1	Reduce operating capacity factor	CF	-		0.97	0.92		11
M2	Reject trials with detections/ejections before given cycle (i.e. present day)		Cycle number		0	16		
M3	Increase number of modeled penetrations	N_{pen}	-		78	97		
M4	Decrease nozzle thickness and OD	t	in.		0.62	0.39		
		D_o	in.		4.00	3.50		
M5	Halve growth integration time step	$1/\Delta t$	1/yr		12	24		
M6	Linearly extrapolate POD to zero below 10% TW		-		Assume POD = 0 below 10% TW	Linearly extrapolate		
M7	Remove correlation between UT inspections	$\rho_{map,UT}$	-		0.50	0.00		
M8	Decrease maximum UT probability of detection to 90%	$P_{max,UT}$	-		0.95	0.90	0.95	0.90
M9	Remove correlation between BMV inspections	$\rho_{map,BMV}$	-		0.95	0.00	0.95	0.00
M10	Decrease critical flaw angle for nozzle ejection	$\theta_{crit,crit}$	degrees		300	275	300	275

Table B-12 (continued)
Summary of Modified Inputs for RPVHPN Model Sensitivity Cases

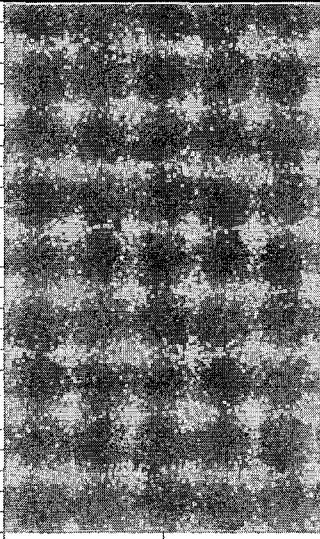
Sensitivity Case	Description	Symbol	Units	Parameter Type	Hot Base Case Value	Hot Sensitivity Case Value	Cold Base Case Value	Cold Sensitivity Case Value
M11	Double standard deviation of peening penetration depth	$x_{1,PPRS,ID}$	in.	type	Normal	Normal		
				mean	0.010	0.010		
				stdev	0.002	0.005		
				min	0.000	0.000		
				max	0.025	0.049		
		$x_{1,PPRS,ext}$	in.	type	Normal	Normal		
				mean	0.039	0.039		
				stdev	0.010	0.020		
				min	0.000	0.000		
				max	0.098	0.236		
M12	Increase peening compressive surface stress and penetration depth	$\sigma_{0,PPRS,ID}(t=0)$	ksi		Normal operating plus residual stress is +10 ksi tensile	Residual stress is 100 ksi compressive		
		$x_{1,PPRS,ID}$	in.	type	Normal	Normal		
				mean	0.010	0.020		
				stdev	0.002	0.005		
				min	0.000	0.000		
				max	0.025	0.049		
		$\sigma_{0,PPRS,ext}(t=0)$	ksi		Normal operating plus residual stress is +10 ksi tensile	Residual stress is 100 ksi compressive		
		$x_{1,PPRS,ext}$	in.	type	Normal	Normal		
				mean	0.039	0.118		
				stdev	0.010	0.059		
				min	0.000	0.000		
				max	0.098	0.295		
M13	Decrease initiation characteristic time by factor of 5	t_1	EDY		23.0	4.6	23.0	4.6
M14	Increase multiple flaw initiation slope	β_{flow}	-	type	Normal	Normal	Normal	Normal
				mean	2.0	3.0	2.0	3.0
				stdev	0.5	0.5	0.5	0.5
				min	1.0	2.0	1.0	2.0
				max	5.0	6.0	5.0	6.0

Table B-12 (continued)
Summary of Modified Inputs for RPVHPN Model Sensitivity Cases

Sensitivity Case	Description	Symbol	Units	Parameter Type	Hot Base Case Value	Hot Sensitivity Case Value	Cold Base Case Value	Cold Sensitivity Case Value
M15	Sample multiple flaw initiation slope a single time per head		-		Sample multiple flaw initiation slope once per penetration	Sample multiple flaw initiation slope once per head		
M16	Include initiation-growth correlation	P_{heat}	-		0.0	-0.8	0.0	-0.8
		P_{weld}	-		0.0	-0.8	0.0	-0.8
M17	Decrease initiation activation energy	Q_i	kcal/mole	type			Normal	Normal
				mean			44.03	40.03
				stdev			3.06	3.06
				min			25.65	21.64
				max			62.41	58.41
M18	Decrease median initial crack depth by factor of 5 and remove minimum, impose minimum K_I value	a_0	in.	type	Log-Normal	Log-Normal	Log-Normal	Log-Normal
				linear μ	0.033	0.006	0.033	0.006
				median	0.031	0.006	0.031	0.006
				log-norm μ	-3.467	-5.127	-3.467	-5.127
				log-norm σ	0.354	0.354	0.354	0.354
				min	0.020	0.000	0.020	0.000
				max	0.622	0.622	0.622	0.622
		$K_{I,min,heat}$	ksi-in. ^{0.5}		0.00	10.92	0.00	10.92
		$K_{I,min,weld}$	ksi-in. ^{0.5}		0.00	10.92	0.00	10.92
M19	Utilize crack closure methodology and decrease initial flaw depth		-		Do not utilize crack closure	Utilize crack closure	Do not utilize crack closure	Utilize crack closure
		a_0	in.	type	Log-Normal	Log-Normal	Log-Normal	Log-Normal
				linear μ	0.033	0.006	0.033	0.006
				median	0.031	0.006	0.031	0.006
				log-norm μ	-3.467	-5.127	-3.467	-5.127
				log-norm σ	0.354	0.354	0.354	0.354
				min	0.020	0.000	0.020	0.000
				max	0.622	0.622	0.622	0.622
M20	Increase median initial crack depth	a_0	in.	type	Log-Normal	Log-Normal	Log-Normal	Log-Normal
				linear μ	0.033	0.146	0.033	0.146
				median	0.031	0.137	0.031	0.137
				log-norm μ	-3.467	-1.987	-3.467	-1.987
				log-norm σ	0.354	0.354	0.354	0.354
				min	0.020	0.020	0.020	0.020
				max	0.622	0.622	0.622	0.622

Table B-12 (continued)
Summary of Modified Inputs for RPVHPN Model Sensitivity Cases

Sensitivity Case	Description	Symbol	Units	Parameter Type	Hot Base Case Value	Hot Sensitivity Case Value	Cold Base Case Value	Cold Sensitivity Case Value
M21	MRP-55 Crack Growth Rate Model Parameters	a_{heat}	(in/hr)/(ksi-in. ^{0.5, 1.5})		3.25E-08	2.21E-07		
		$K_{10,heat}$	ksi-in. ^{0.5}		0.00	8.19		
		n_{heat}	-		1.60	1.16		
M22	Decrease growth activation energy	Q_g	kcal/mole	type			Normal	Normal
				mean			31.07	28.68
				stdev			1.20	1.20
				min			23.90	21.51
				max			38.24	35.85
M23	Prevent balloon growth		-		Allow balloon growth	Prevent balloon growth		
M24	Remove crack environmental factor	$C_{circ, mult}$	-	type	triangular	constant	triangular	constant
				mode	1	1	1	1
				lower limit	1	-	1	-
				upper limit	2	-	2	-
M25	Increase peening compressive surface stress and penetration depth, prevent balloon growth, utilize crack closure	$\sigma_{0,PPRS,ID}(t=0)$	ksi		Normal operating plus residual stress is +10 ksi tensile	Residual stress is 100 ksi compressive		
		$x_{1,PPRS,ID}$	in.	type	Normal	Normal		
				mean	0.010	0.020		
				stdev	0.002	0.005		
				min	0.000	0.000		
				max	0.025	0.049		
		$\sigma_{0,PPRS,ext}(t=0)$	ksi		Normal operating plus residual stress is +10 ksi tensile	Residual stress is 100 ksi compressive		
		$x_{1,PPRS,ext}$	in.	type	Normal	Normal		
				mean	0.039	0.118		
				stdev	0.010	0.059		
				min	0.000	0.000		
				max	0.098	0.295		
			-		Do not utilize crack closure	Utilize crack closure		
			-		Allow balloon growth	Prevent balloon growth		

Table B-12 (continued)
Summary of Modified Inputs for RPVHPN Model Sensitivity Cases

Sensitivity Case	Description	Symbol	Units	Parameter Type	Hot Base Case Value	Hot Sensitivity Case Value	Cold Base Case Value	Cold Sensitivity Case Value
M26	Compressive total stress at peened surface	$\sigma_{0,PPRS,ID}(t=0)$	ksi		Normal operating plus residual stress is +10 ksi tensile	Normal operating plus residual stress is zero ksi	Normal operating plus residual stress is +10 ksi tensile	Normal operating plus residual stress is zero ksi
		$\sigma_{0,PPRS,ext}(t=0)$	ksi		Normal operating plus residual stress is +10 ksi tensile	Normal operating plus residual stress is zero ksi	Normal operating plus residual stress is +10 ksi tensile	Normal operating plus residual stress is zero ksi
M27	Total stress compressive to nominal compressive stress depth	$\sigma_{0,PPRS,ID}(t=0)$	ksi		Normal operating plus residual stress is +10 ksi tensile	Residual stress is 34.88 ksi compressive	Normal operating plus residual stress is +10 ksi tensile	Residual stress is 34.88 ksi compressive
		$x_{1,PPRS,ID}$	in.	type	Normal	Constant	Normal	Constant
				mean	0.010	0.016	0.010	0.016
				stdev	0.002	-	0.002	-
				min	0.000	-	0.000	-
				max	0.025	-	0.025	-
		$\sigma_{0,PPRS,ext}(t=0)$	ksi		Normal operating plus residual stress is +10 ksi tensile	Residual stress is 13.49 ksi compressive	Normal operating plus residual stress is +10 ksi tensile	Residual stress is 13.49 ksi compressive
		$x_{1,PPRS,ext}$	in.	type	Normal	Normal	Normal	Normal
				mean	0.039	0.047	0.039	0.047
				stdev	0.010	-	0.010	-
				min	0.000	-	0.000	-
				max	0.098	-	0.098	-
		$f_{1,PPRS}$	-		2.0	1.8	2.0	1.8

Table B-13
Summary of Modified Inputs for RPVHPN Inspection Scheduling Sensitivity Cases

Sensitivity Case	Description	Symbol	Units	Parameter Type	Hot Base Case Value	Hot Sensitivity Case Value	Cold Base Case Value	Cold Sensitivity Case Value
S1	Skip follow-up UT inspection and enter post peening ISI schedule		-		Perform follow-up UT 1st and 2nd cycle after peening	Skip follow-up UT inspection; first ISI after 5 cycles	Perform follow-up UT 2nd cycle after peening	Skip follow-up UT inspection; first ISI after 5 cycles
S2	Skip UT during pre-peening inspection		-		Perform UT during pre-peening inspection	Skip UT during pre-peening inspection	Perform UT during pre-peening inspection	Skip UT during pre-peening inspection
S3	BMV every other cycle post-peening		-		Perform BMV post-peening per Section 4	Perform BMV every 2nd outage post-peening	Perform BMV post-peening per Section 4	Perform BMV every 2nd outage post-peening
S4	BMV every third cycle post-peening		-		Perform BMV post-peening per Section 4	Perform BMV every 3rd outage post-peening		
S5	Do not perform BMV after peening		-		Perform BMV post-peening per Section 4	Do not perform BMV after peening	Perform BMV post-peening per Section 4	Do not perform BMV after peening
S6	Do not perform UT during all cycles between peening and follow-up exam		-		Perform follow-up UT 1st and 2nd cycle after peening	Perform follow-up UT 2nd cycle after peening		
S7	BMV every cycle post-peening		-				Perform BMV post-peening per Section 4	Perform BMV every outage post-peening

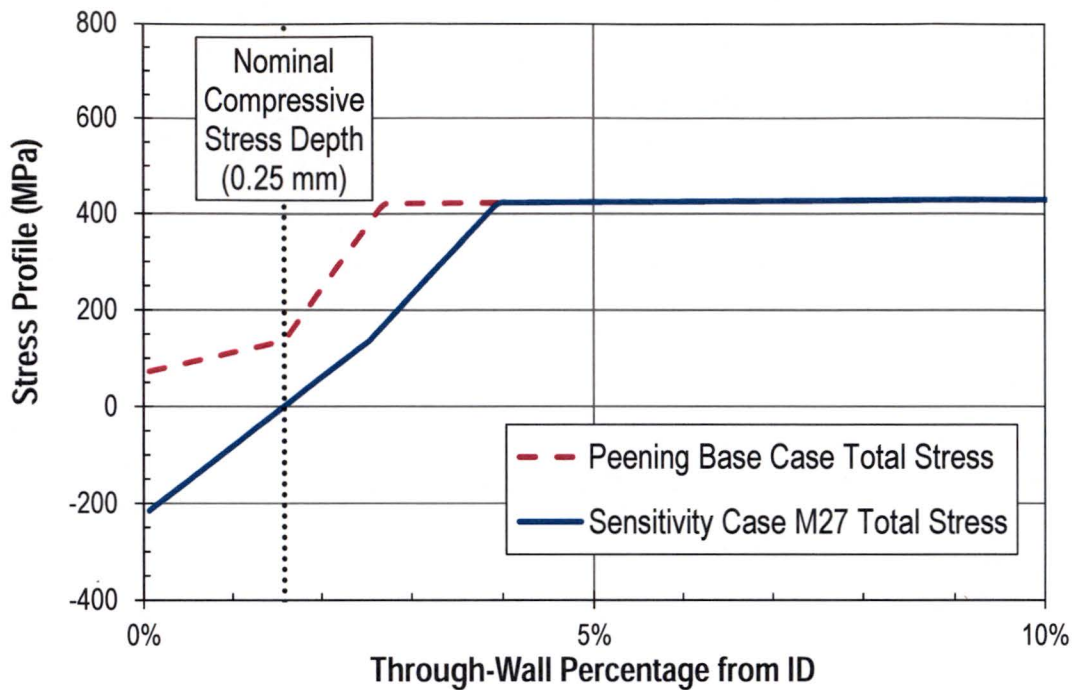


Figure B-26
Post-Peening Total (Normal Operating Plus Residual) Stress Profile for a Crack Initiating on the ID of an RPVHPN, Uphill Side

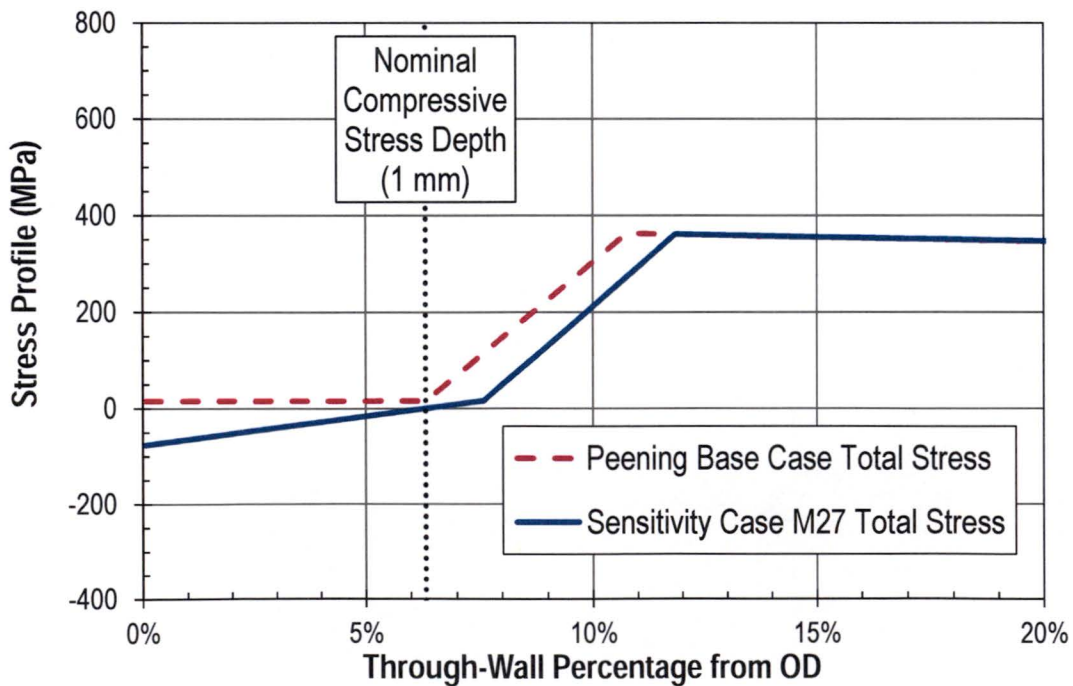


Figure B-27
Post-Peening Total (Normal Operating Plus Residual) Stress Profile for a Crack Initiating on the OD of an RPVHPN, Uphill Side

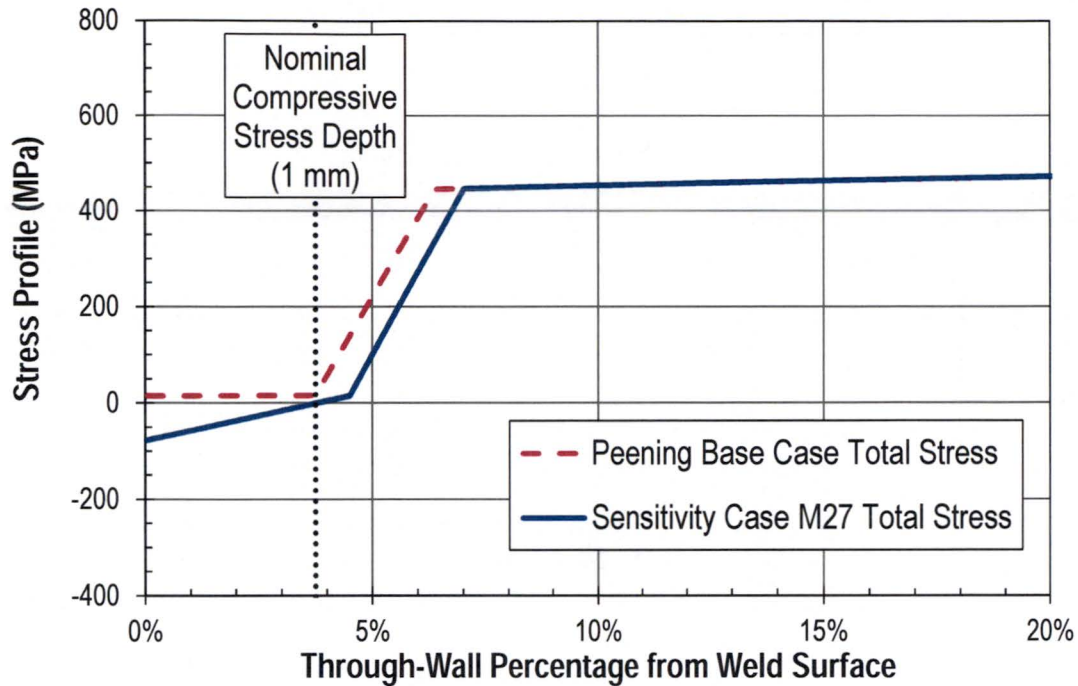


Figure B-28
Post-Peening Total (Normal Operating Plus Residual) Stress Profile for a Crack Initiating on the Weld of an RPVHPN, Uphill Side

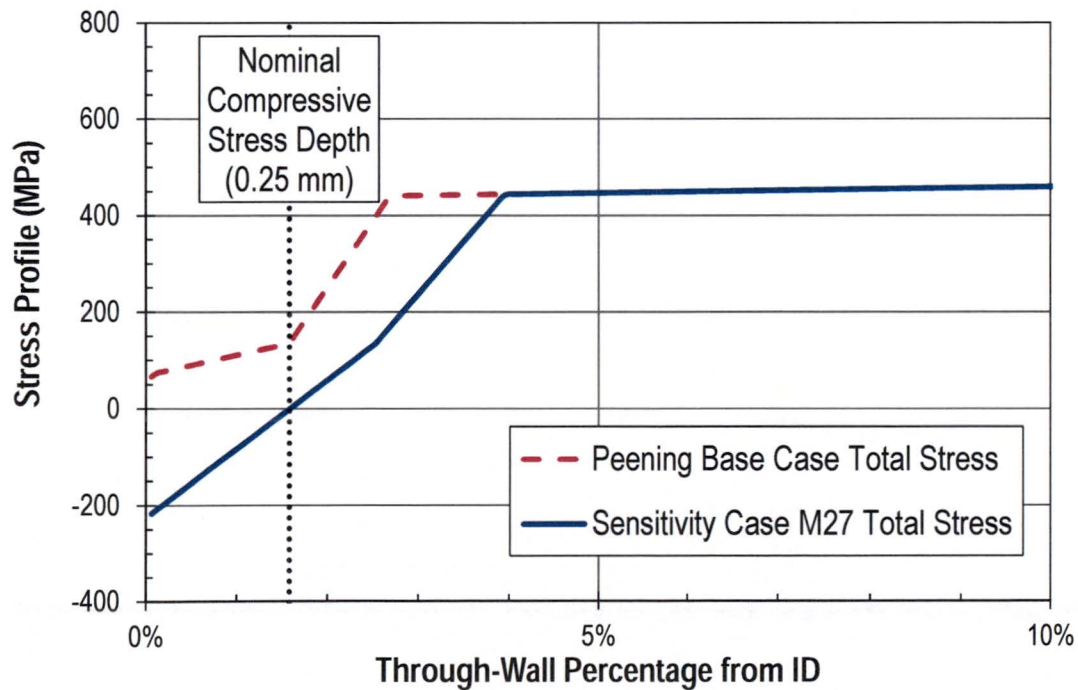


Figure B-29
Post-Peening Total (Normal Operating Plus Residual) Stress Profile for a Crack Initiating on the ID of an RPVHPN, Downhill Side

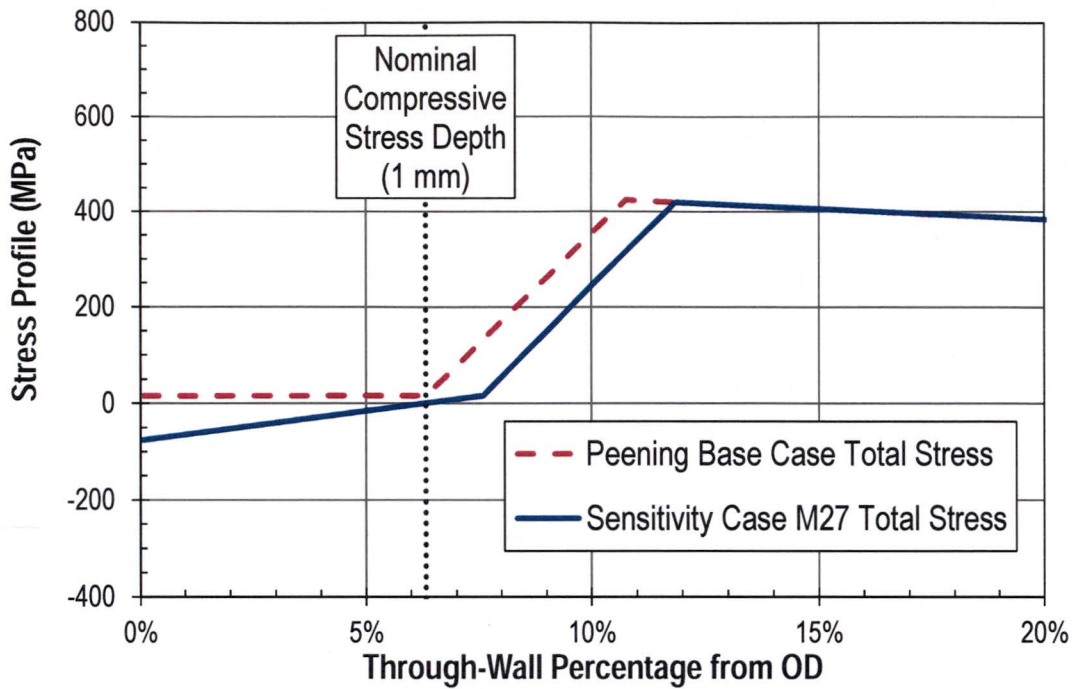


Figure B-30
Post-Peening Total (Normal Operating Plus Residual) Stress Profile for a Crack Initiating on the OD of an RPVHPN, Downhill Side

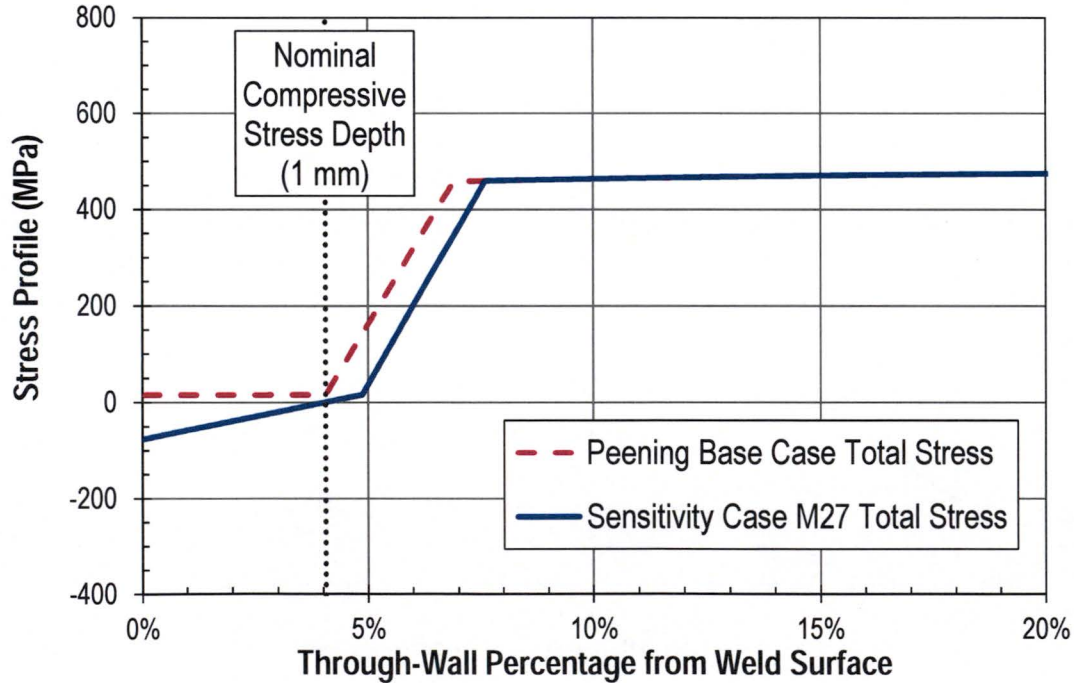


Figure B-31
Post-Peening Total (Normal Operating Plus Residual) Stress Profile for a Crack Initiating on the Weld of an RPVHPN, Downhill Side

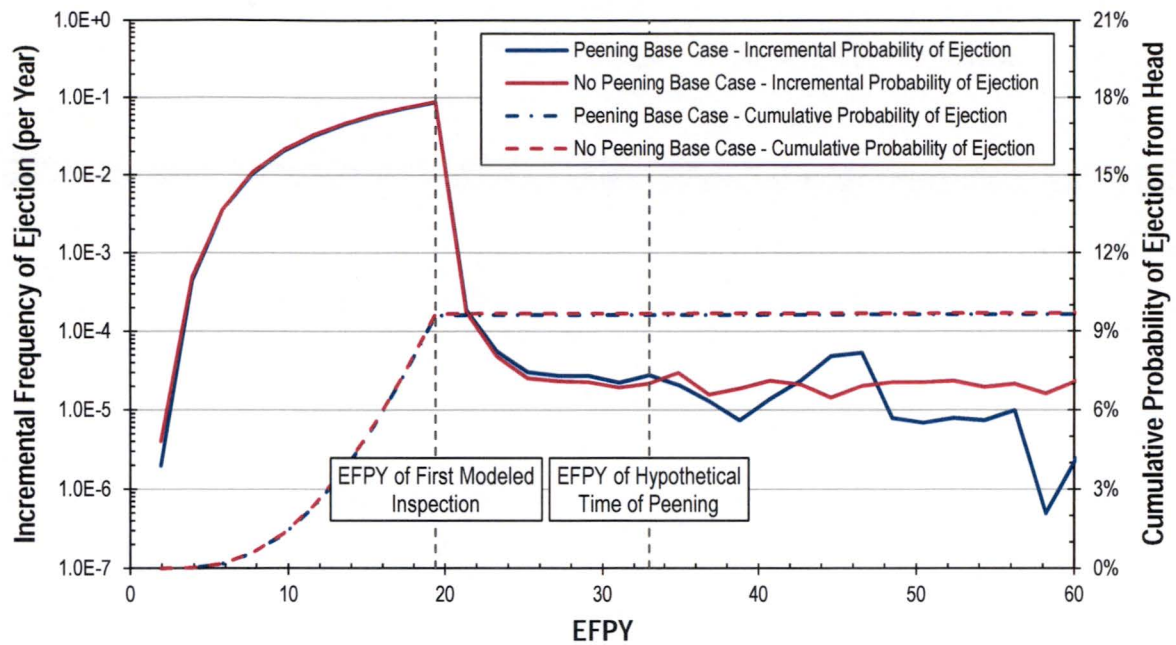


Figure B-32
Prediction of Ejection vs. Time for Hot RPVHPNs

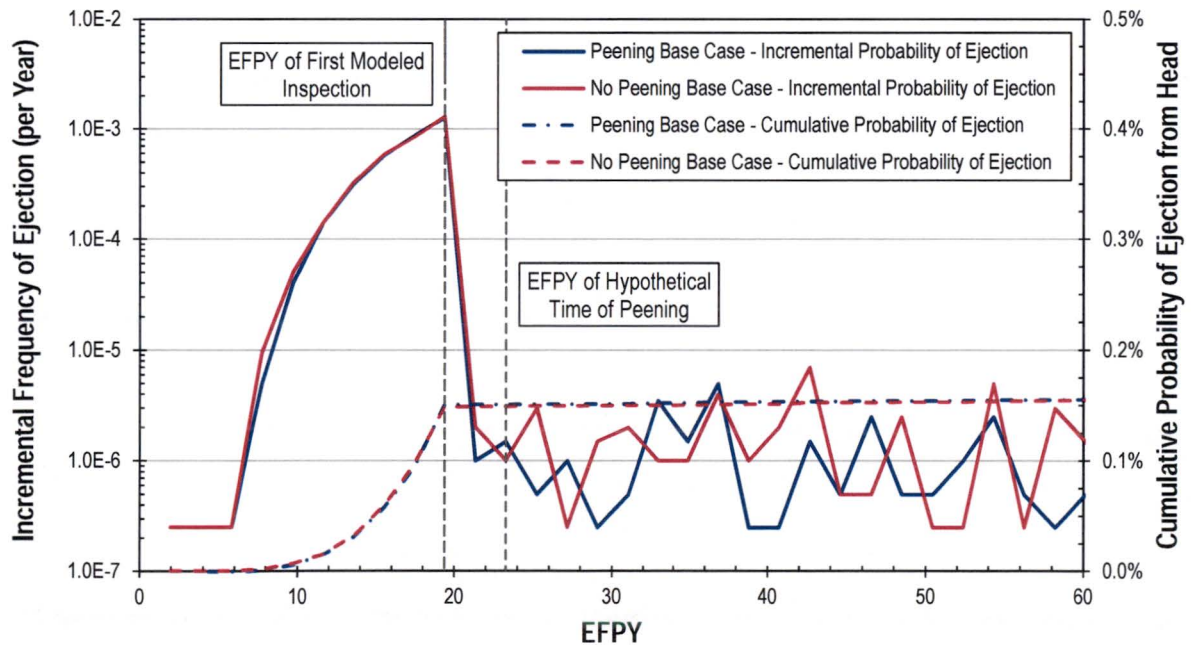


Figure B-33
Prediction of Ejection vs. Time for Cold RPVHPNs

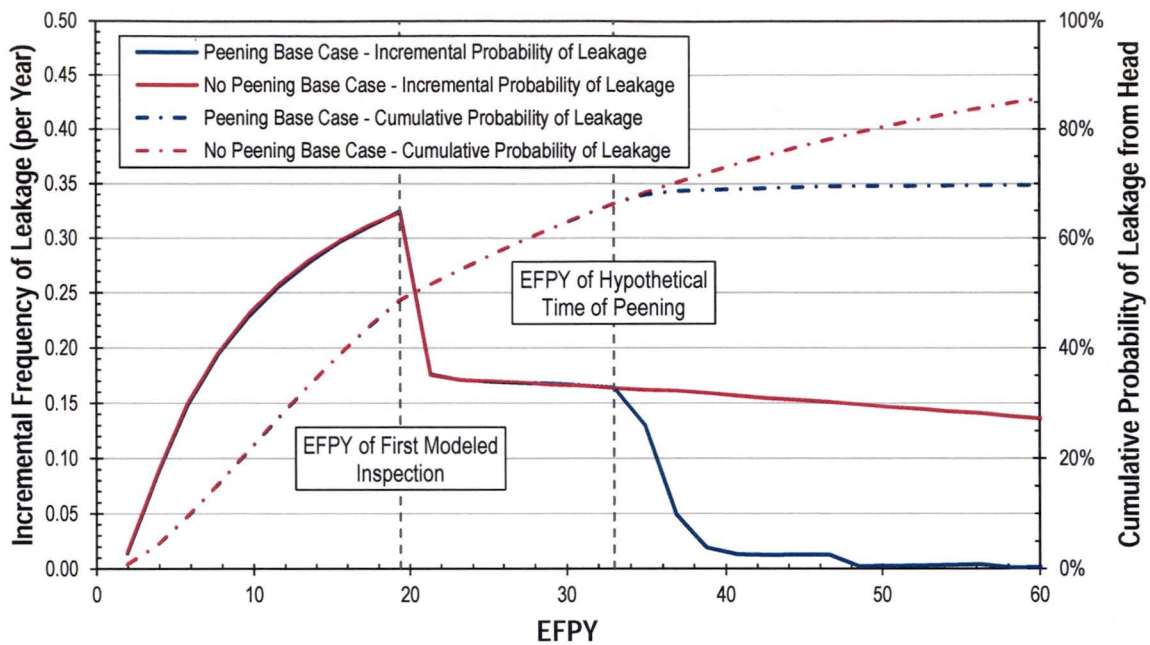


Figure B-34
Prediction of Leakage vs. Time for Hot RPVHPNs

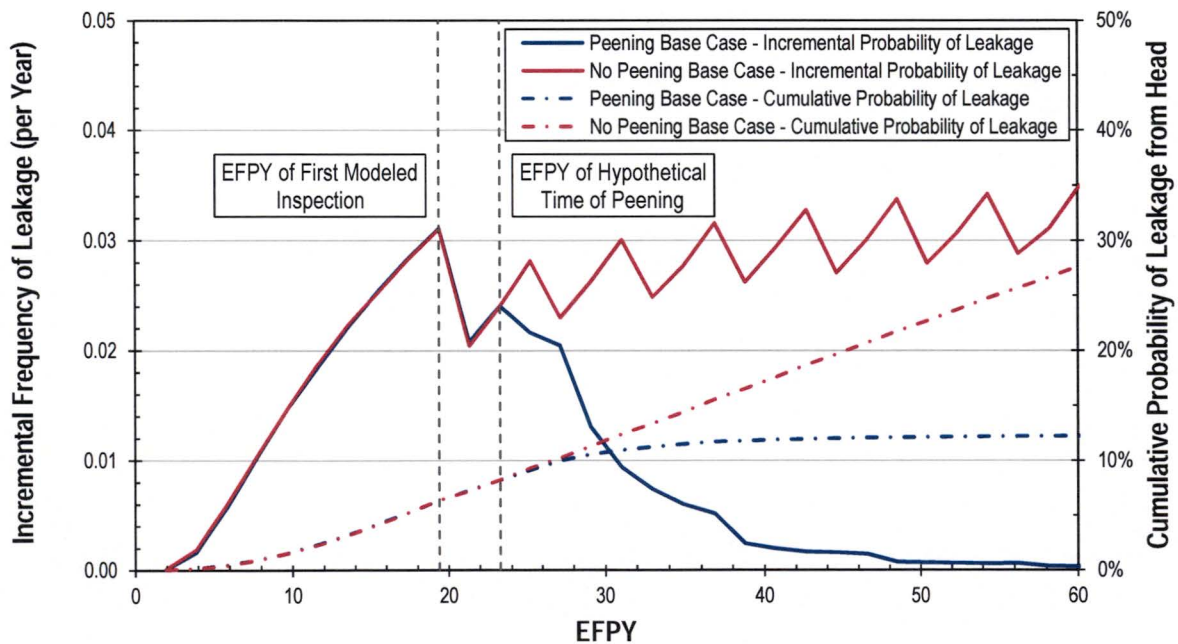


Figure B-35
Prediction of Leakage vs. Time for Cold RPVHPNs

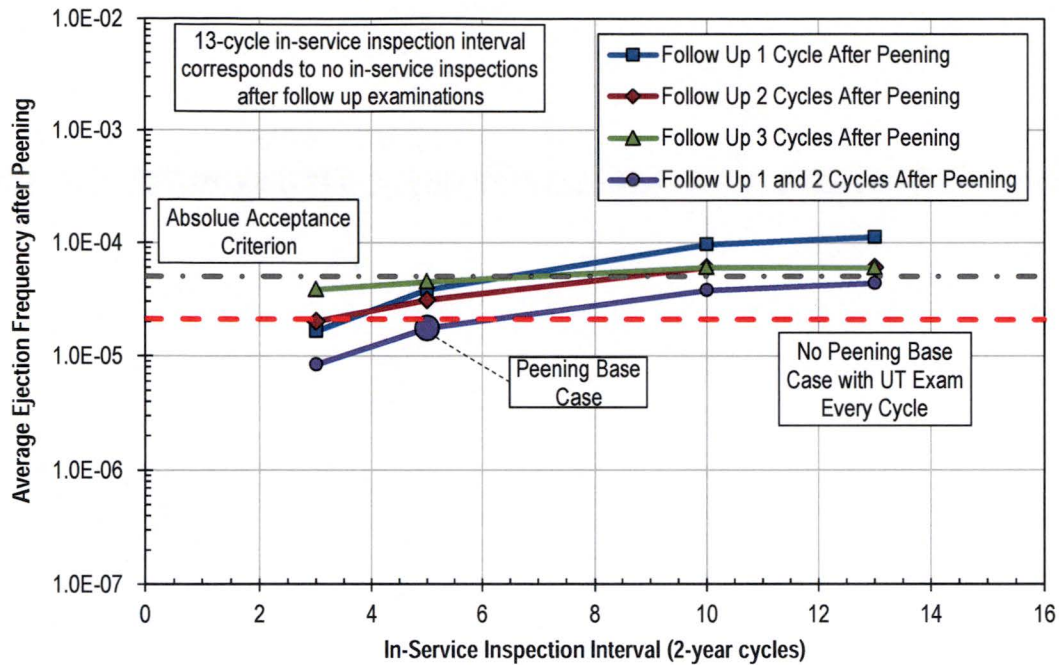


Figure B-36
Average Ejection Frequency from Hypothetical Time of Peening to End of Operational Service Period vs. ISI Frequency for Hot Reactor Vessel Head

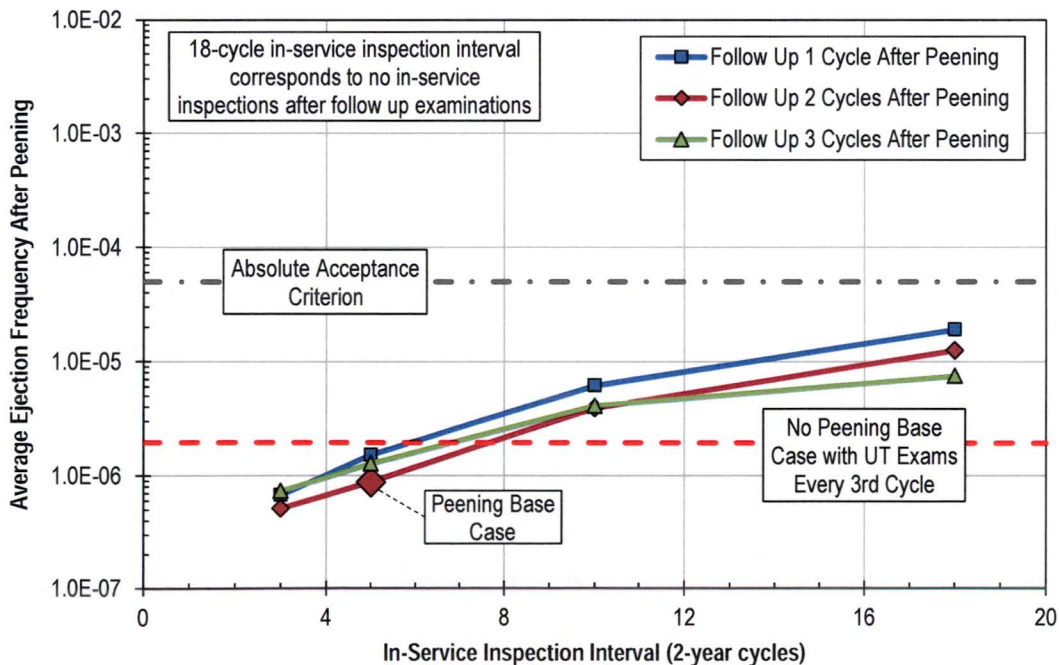


Figure B-37
Average Ejection Frequency from Hypothetical Time of Peening to End of Operational Service vs. ISI Frequency for Cold Reactor Vessel Head

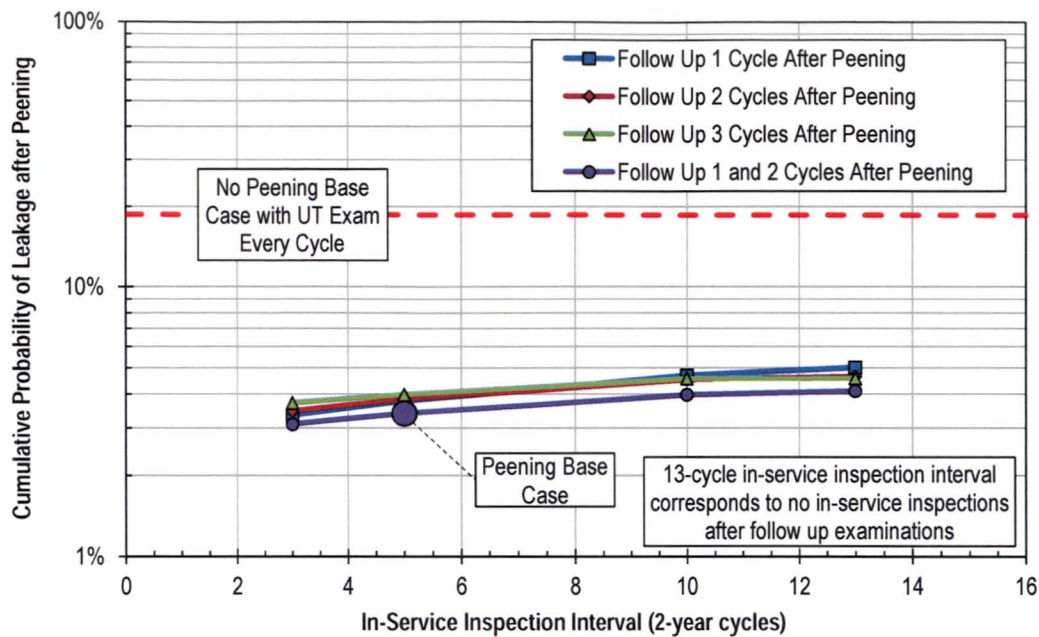


Figure B-38
Cumulative Probability of Leakage from Hypothetical Time of Peening to End of Operational Service Period vs. ISI Frequency for Hot Reactor Vessel Head

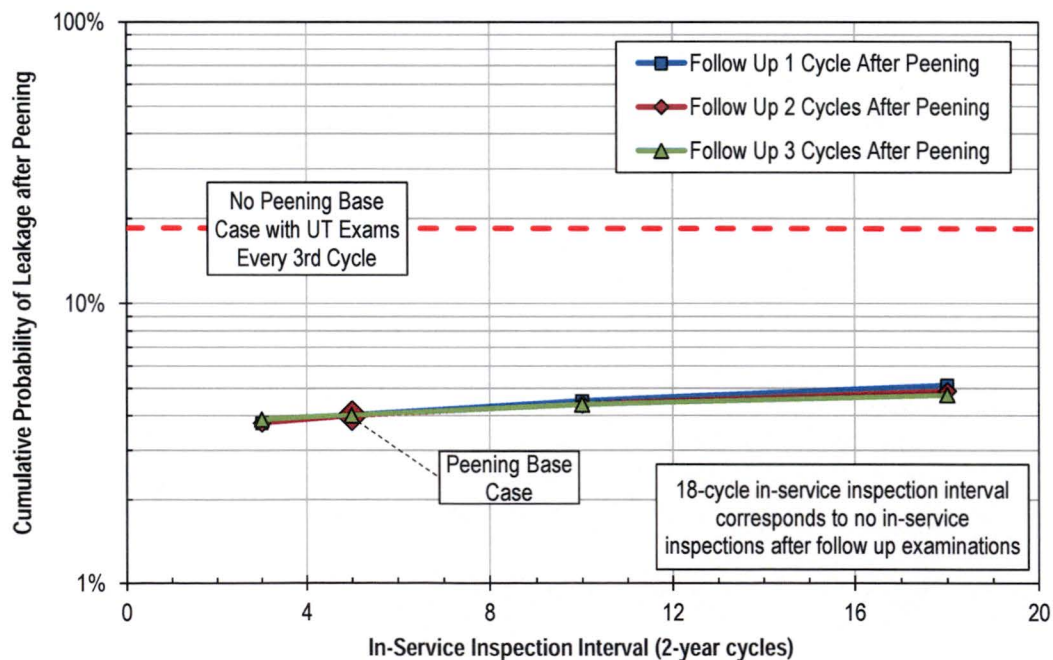


Figure B-39
Cumulative Probability of Leakage from Hypothetical Time of Peening to End of Operational Service Period vs. ISI Frequency for Cold Reactor Vessel Head

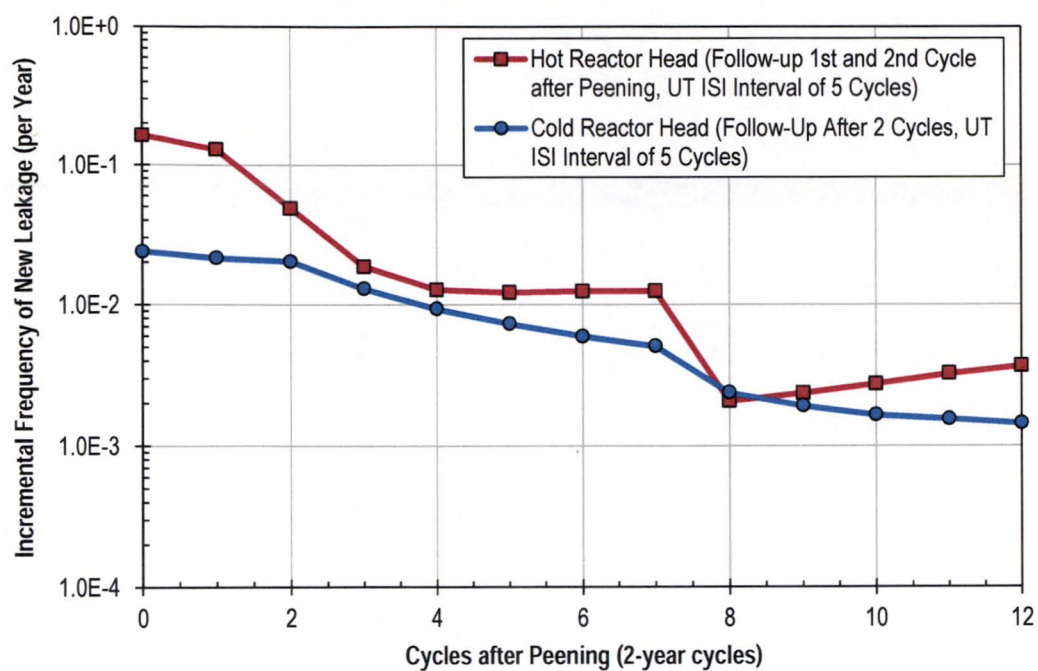


Figure B-40
Incremental Frequency of Leakage after Peening with Relaxed ISI Intervals

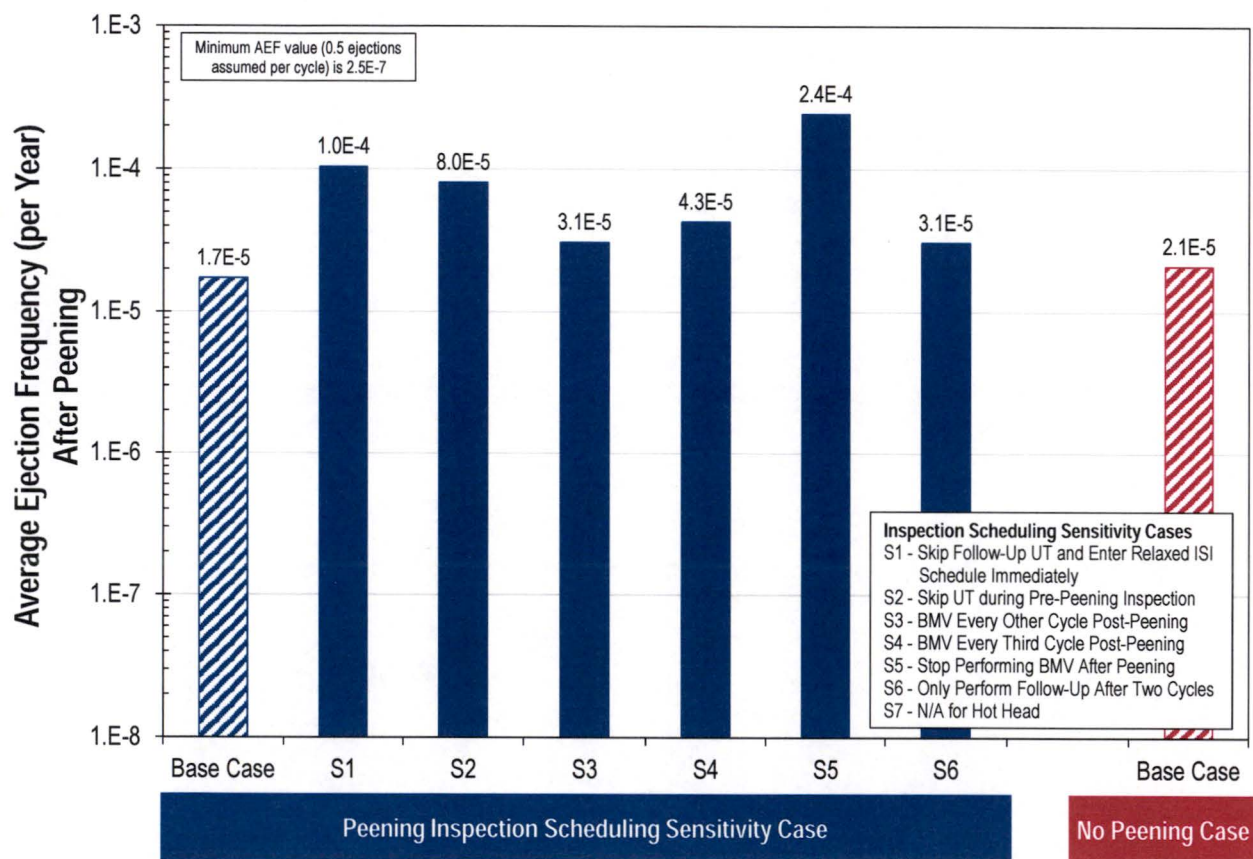


Figure B-41
Summary for Inspection Scheduling Sensitivity Results for Hot RPVHPN Probabilistic Model with Peening

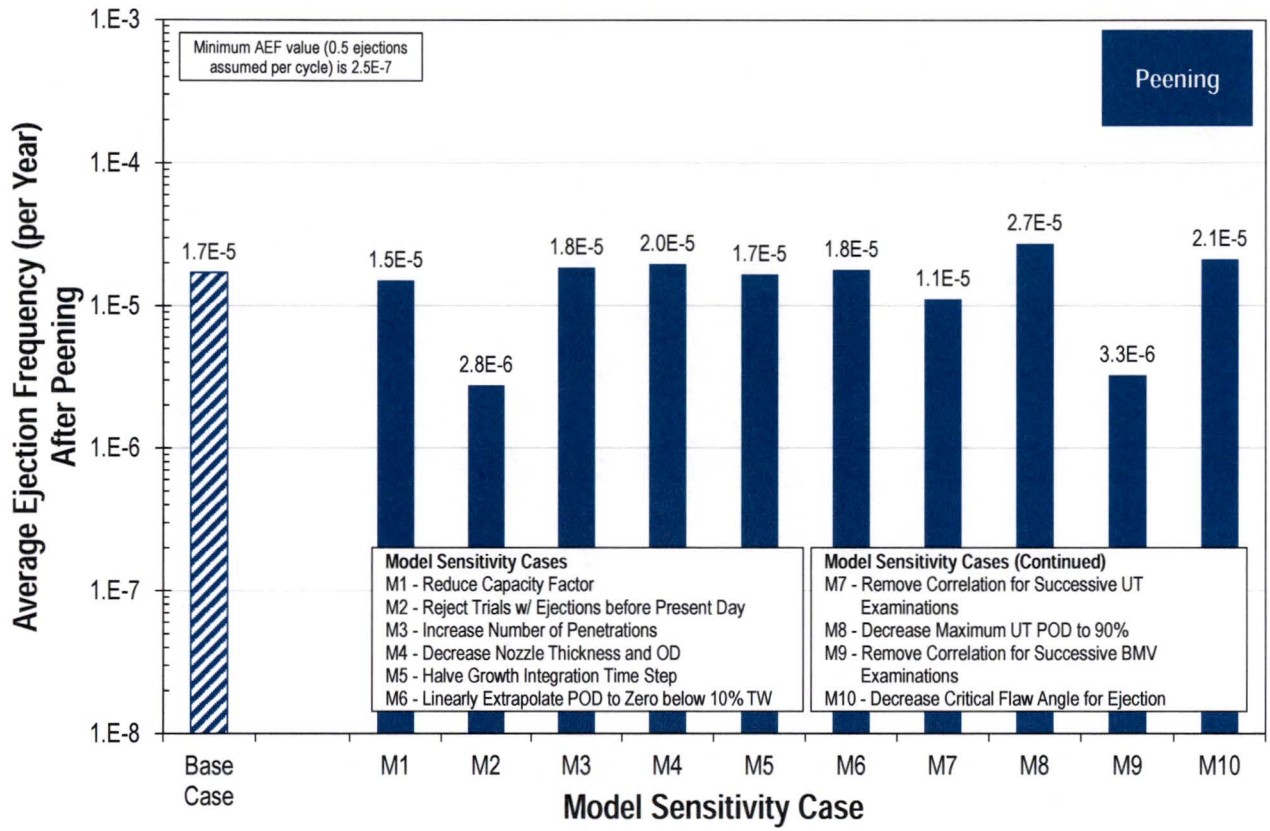


Figure B-42
Summary of Model Sensitivity Results for Hot RPVHPN Probabilistic Model with Peening

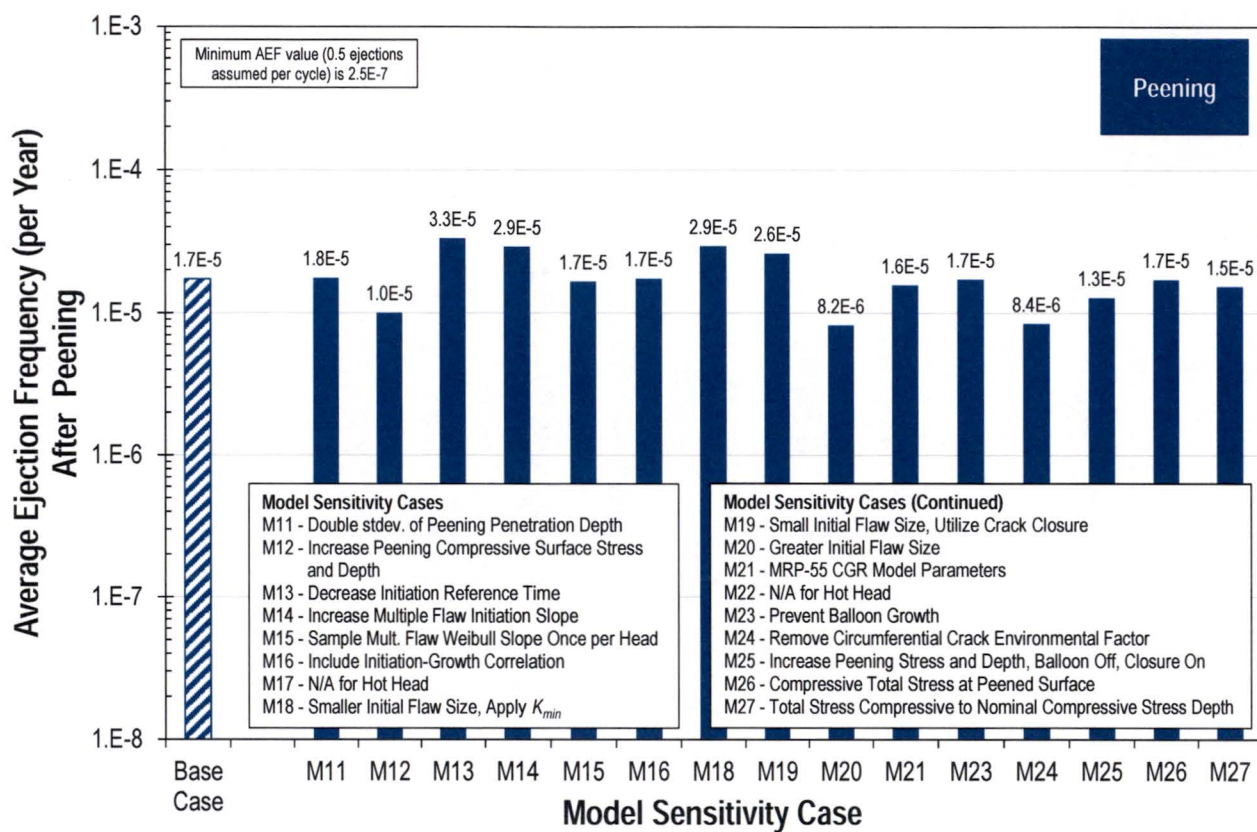


Figure B-43
Summary of Model Sensitivity Results for Hot RPVHPN Probabilistic Model with Peening (continued)

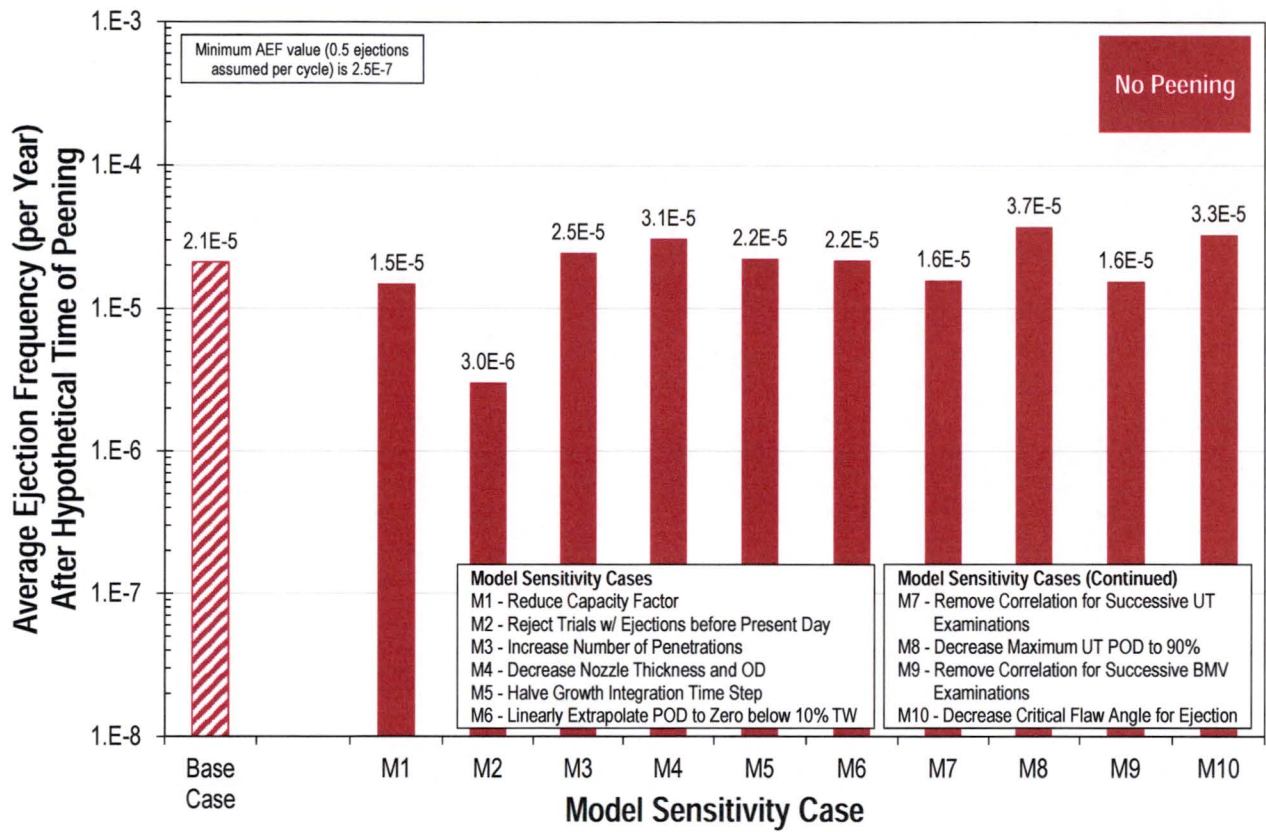


Figure B-44
Summary of Model Sensitivity Results for Hot RPVHPN Probabilistic Model without Peening

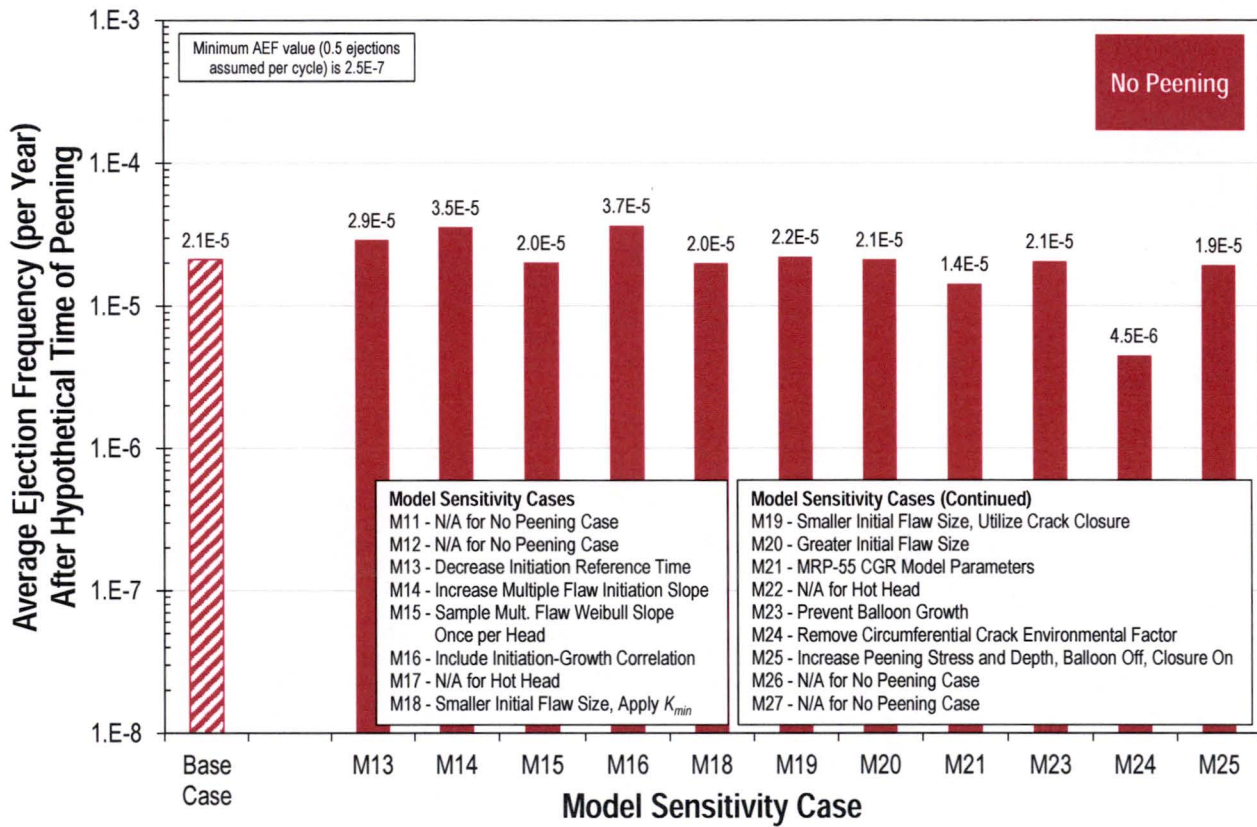


Figure B-45
Summary of Model Sensitivity Results for Hot RPVHPN Probabilistic Model without Peening (continued)

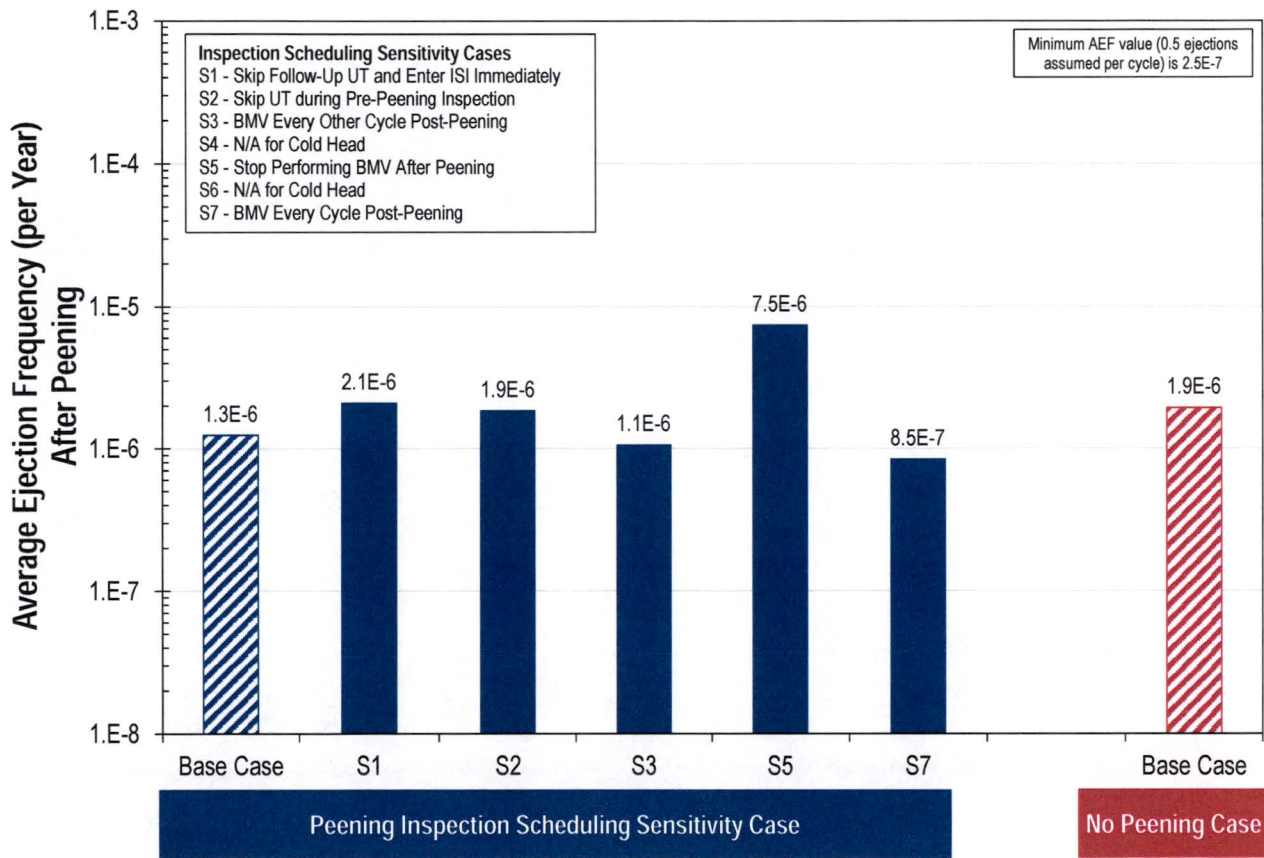


Figure B-46
Summary for Inspection Scheduling Sensitivity Results for Cold RPVHPN Probabilistic Model with Peening

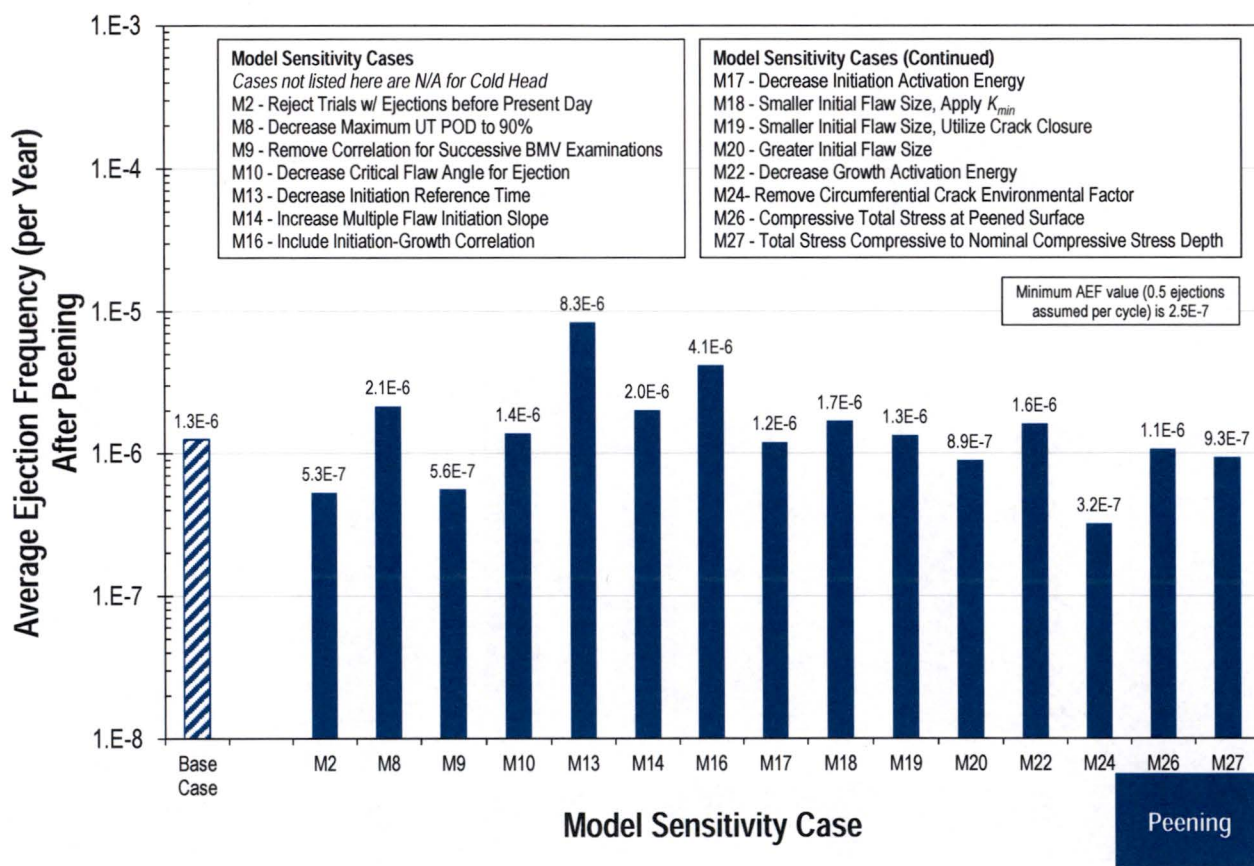


Figure B-47
 Summary of Model Sensitivity Results for Cold RPVHPN Probabilistic Model with Peening

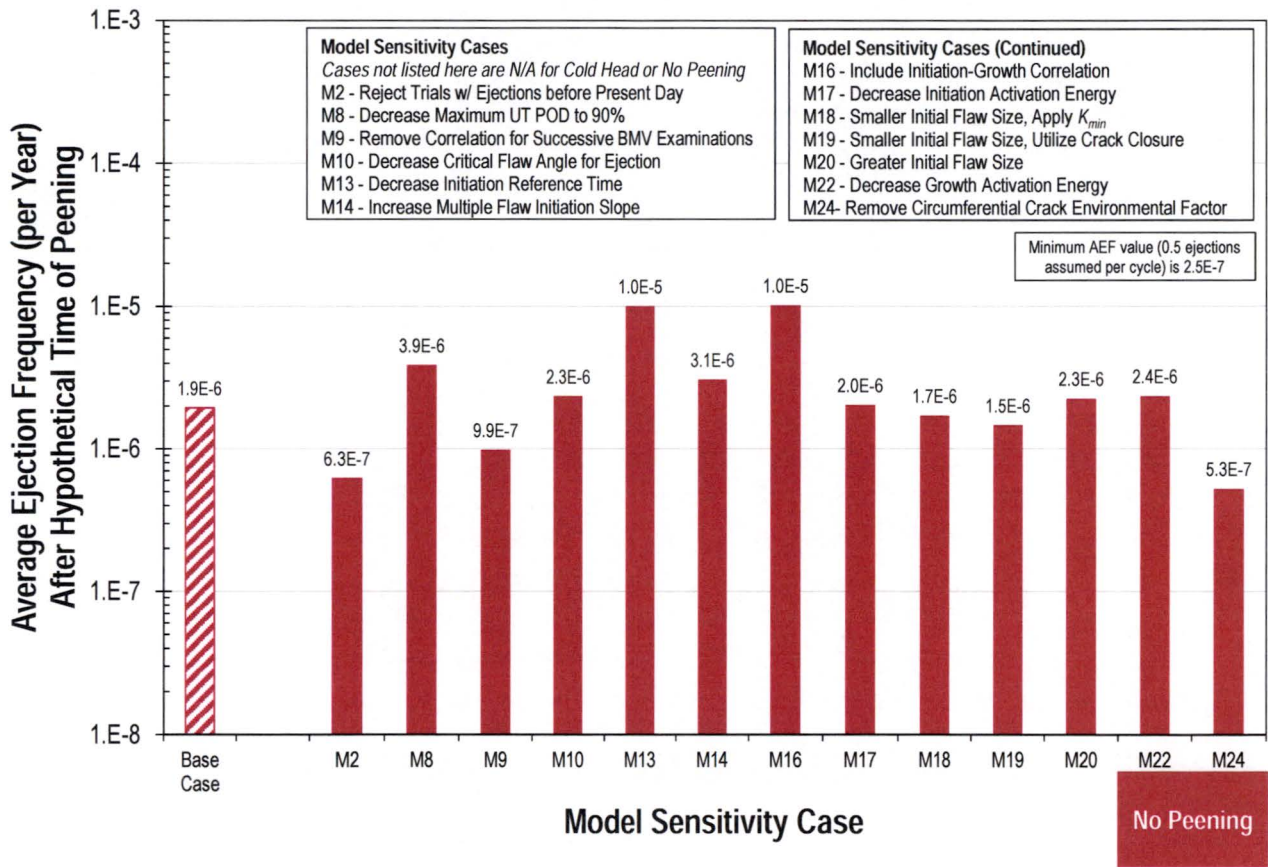


Figure B-48
 Summary of Model Sensitivity Results for Cold RPVHPN Probabilistic Model without Peening

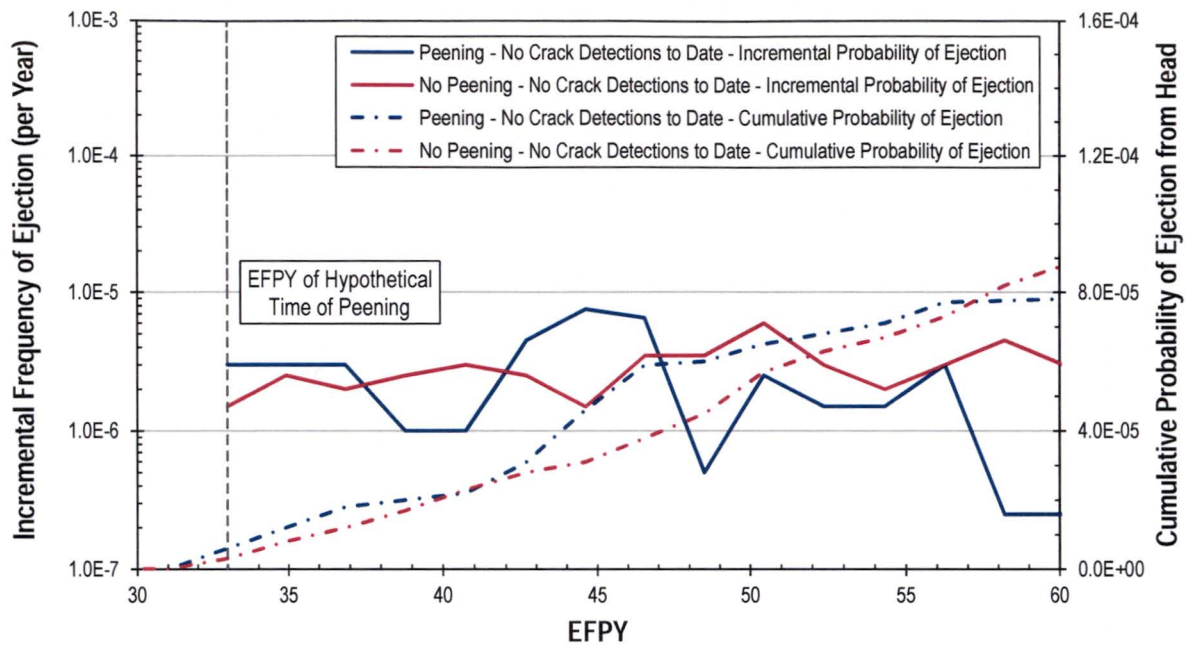


Figure B-49
Prediction of Nozzle Ejection vs. Time for Hot RPVHPNs with No Crack Detections to Date
(Model Sensitivity Study 2)

B.10 Conclusions Regarding Appropriate In-Service Examination Requirements for RPVHPNs Mitigated by Peening

The results of the probabilistic analysis of PWSCC on a general hot head support the relaxed UT inspection schedules prescribed in Section 4 of this report. Specifically, cases where the follow-up UT inspection is scheduled for the first and second cycle after peening and subsequent UT inspections are scheduled every 10 years (every interval) result in the following:

- The cumulative leakage probability after the hypothetical time of peening is predicted to be reduced by a factor of approximately 5.5 relative to the unmitigated case per N-729-1.
- The average ejection frequency after the hypothetical time of peening is predicted to be reduced to 81% of the average ejection frequency of the unmitigated case.

The results of the probabilistic analysis of PWSCC on a general cold head support the relaxed UT inspection schedules prescribed in Section 4 of this report. Specifically, cases where the follow-up UT inspection is scheduled two cycles after peening and subsequent UT inspections are scheduled every 10 years (every interval) result in the following:

- The cumulative leakage probability after the hypothetical time of peening is predicted to be reduced by a factor of approximately 4.6 relative to the unmitigated case per N-729-1.
- The average ejection frequency after the hypothetical time of peening is predicted to be reduced to 64% of the average ejection frequency of the unmitigated case.

For both hot and cold leg components, the probabilistic model predicts the rapid decay of incremental leakage probabilities after peening. The calculations also demonstrate the value of visual examinations performed to detect leakage as part of the program of follow-up examinations.

Many key input or modeling assumptions have been varied for Model Sensitivity Cases. The following subset of these cases resulted in an increase in average ejection frequency for the peened component relative to the unmitigated component:

- Hot Model Sensitivity Case 13 – Arbitrarily reducing the initiation reference time by a factor of five results in an AEF of 3.3×10^{-5} for the peened component and an AEF of 2.9×10^{-5} for the unmitigated component. The predicted AEF and ALF for this sensitivity case result in the greatest increase with respect to the base case. However, it is noted that this initiation model results in a prediction of leakage before 20 EFPY in over 95% of hot heads. This is not in line with U.S. PWR operating experience.
- Hot Model Sensitivity Case 18 – Applying a smaller initial flaw size and enforcing a minimum allowable stress intensity factor (regardless of crack size and loading) results in an AEF of 2.9×10^{-5} for the peened component and an AEF of 2.0×10^{-5} for the unmitigated component. The results of this hypothetical case are bounding of the actual stress intensity factors.
- Hot Model Sensitivity Case 19 – Applying a smaller initial flaw size and utilizing crack closure results in an AEF of 2.6×10^{-5} for the peened component and an AEF of 2.2×10^{-5} for the unmitigated component. The reduced initial flaw size provides most of this effect.
- Hot Model Sensitivity Case 21 – Applying the unmodified MRP-55 CGR Model results in an AEF of 1.6×10^{-5} for the peened component and an AEF of 1.4×10^{-5} for the unmitigated component. The predicted AEF for this sensitivity case is less than that of the corresponding base case values.
- Hot Model Sensitivity Case 24 – Removing the circumferential crack environmental factor results in an AEF of 8.4×10^{-6} for the peened component and an AEF of 4.5×10^{-6} for the unmitigated component. The predicted AEF for this sensitivity case is about half of the AEF for the corresponding base case values.
- No Cold Model Sensitivity Cases resulted in a greater AEF for the peened component than for the unmitigated component.
- The average leakage frequencies remain below 0.05 new leaking penetrations per year per head for all peening cases evaluated.

B.11 References

1. *PWR Materials Reliability Program Response to NRC Bulletin 2001-01 (MRP-48)*, EPRI, Palo Alto, CA: 2001. 1006284. [Freely Available at www.epri.com]
2. *PWR Materials Reliability Program, Interim Alloy 600 Safety Assessments for US PWR Plants (MRP-44): Part 2: Reactor Vessel Top Head Penetrations*, EPRI, Palo Alto, CA: 2001. TP-1001491, Part 2.
3. *Materials Reliability Program: Reevaluation of Technical Basis for Inspection of Alloy 600 PWR Reactor Vessel Top Head Nozzles (MRP-395)*. EPRI, Palo Alto, CA: 2014. 3002003099. [Freely Available at www.epri.com]
4. ASME Code Case N-729-1, "Alternative Examination Requirements for PWR Reactor Vessel Upper Heads With Nozzles Having Pressure-Retaining Partial-Penetration Welds," Section XI, Division 1, American Society of Mechanical Engineers, New York, Approved March 28, 2006.
5. *Materials Reliability Program: Probabilistic Fracture Mechanics Analysis of PWR Reactor Vessel Top Head Nozzle Cracking (MRP-105NP)*, EPRI, Palo Alto, CA: 2004. 1007834. [NRC ADAMS Accession No.: ML041680489]
6. D. Rudland, J. Broussard, et al., "Comparison of Welding Residual Stress Solutions for Control Rod Drive Mechanism Nozzles," *Proceedings of the ASME 2007 Pressure Vessels & Piping Division Conference: PVP2007*, San Antonio, Texas, July 2007.
7. *Materials Reliability Program Generic Evaluation of Examination Coverage Requirements for Reactor Pressure Vessel Head Penetration Nozzles, Revision 1 (MRP-95R1)*, EPRI, Palo Alto, CA: 2004. 1011225. [Freely Available at www.epri.com]
8. S. Marie, et al., "French RSE-M and RCC-MR code appendices for flaw analysis: Presentation of the fracture parameters calculation – Part III: Cracked Pipes," *International Journal of Pressure Vessels and Piping*, 84, pp. 614-658, 2007.
9. *Technical Basis for RPV Head CRDM Nozzle Inspection Interval H. B. Robinson Steam Electric Plant, Unit No. 2*. Dominion Engineering Inc.: Reston, VA: 2003. R-3515-00-1.
10. *Farley CRDM Through-Wall Circumferential Crack Fracture Mechanics*. Dominion Engineering Inc.: Reston, VA: 2003. C-7781-00-1.
11. *Materials Reliability Program: Crack Growth Rates for Evaluating Primary Water Stress Corrosion Cracking (PWSCC) of Alloy 82, 182, and 132 Welds (MRP-115)*, EPRI, Palo Alto, CA: 2004. 1006696. [Freely Available at www.epri.com]
12. *Materials Reliability Program (MRP) Crack Growth Rates for Evaluating Primary Water Stress Corrosion Cracking (PWSCC) of Thick-Wall Alloy 600 Materials (MRP-55) Revision 1*, EPRI, Palo Alto, CA: 2002. 1006695. [Freely Available at www.epri.com]
13. *Materials Reliability Program: Reactor Vessel Closure Head Penetration Safety Assessment for U.S. PWR Plants (MRP-110NP): Evaluations Supporting the MRP Inspection Plant*, EPRI, Palo Alto, CA: 2004. 1009807. [NRC ADAMS Accession No.: ML041680506]
14. *PWSCC Prediction Guidelines*, EPRI, Palo Alto, CA: 1994. TR-104030.

15. U.S. NRC, Regulatory Guide 1.174, "An Approach for Using Probabilistic Risk Assessment in Risk-Informed Decisions on Plant-Specific Changes to the Licensing Basis," Revision 2, May 2011.

C

TENSILE BALANCING STRESSES IN RESIDUAL STRESS PROFILE IN RESPONSE TO PEENING

C.1 Introduction

C.1.1 Deformation and Tensile Stress Response of Components to Peening

In addition to producing a surface compressive residual stress layer, peening causes deformation of the treated component. Some of the compressive stress at the peened layer is immediately relieved by deformation of the part. As the stiffness of the treated component is assumed to be greater, the resulting deformation decreases, and more of the initial compressive stress at the treated surface is retained.

The retained compressive stress at the peened surface is balanced by residual stresses generated through the component thickness. In order to satisfy static equilibrium, the internal forces and internal bending moments integrated over any cross section through the component must balance to zero or be balanced by a reaction force on the component. If the through-wall stress profile is suitably uniform over a cross section (and the plate length-to-width aspect ratio is suitably large such that beam theory holds), the residual stress profile for an unrestrained flat plate must self-balance by force and through-wall bending moment before and after peening. Thus, the peak balancing tensile stress in the post-peening through-wall profile for an unrestrained flat plate depends on both the force and moment imparted by the surface compressive residual stress layer.

The balancing stress for peened thick-wall pipes behaves in a similar manner, but the more constrained pipe geometry does not deflect as much as the plate case for equivalent peening compressive stress effect and equivalent wall thickness. As shown in the analyses presented below, the result is that the balancing stress profile for a thick-wall pipe is more nearly uniform than for the case of an unrestrained flat plate of equivalent wall thickness.

C.1.2 Purpose and Approach

The purpose of this appendix is to investigate the magnitude and distribution of tensile stresses developed in response to the peening compressive stresses produced at the treated surface. Any pre-existing flaws located beyond the compressive stress zone would grow during subsequent operation under the influence of these balancing stresses (as well as weld residual stresses and operating stresses).

Specifically, a straightforward linear-elastic finite-element analysis (FEA) approach is taken for flat plate and thick-wall cylinder geometries. Peening is assumed to be applied to a substantial fraction of the plate area or inside diameter surface of a thick-walled cylinder, and the through-wall stress profile developed in the peened region is investigated for different wall thicknesses. The stress source approach ([1], [2], [3]) originally developed to assess the stress effects of shot

peening of a flat plate is applied to calculate the bending stress and axial membrane stress generated in response to peening:

$$\sigma(x) = \sigma_p(x) + \sigma_b(x) + \sigma_a \quad [C-1]$$

where:

- $\sigma(x)$ = through-wall equilibrium stress profile, as function of through-wall position x
- $\sigma_p(x)$ = peening stress source function
- $\sigma_b(x)$ = bending stress generated in response to peening (linear function of x)
- σ_a = axial membrane stress generated in response to peening

The stress source function, $\sigma_p(x)$, is the stress that would result from peening of an infinitely thick plate. For sufficiently thick plates, the stress source depends only on the peening process applied (i.e., intensity and duration). The form of the stress source function is chosen to fit data for the particular peening process of interest. As described below, published data are used to determine the most appropriate form of the stress source function. Published stress measurements and modeling results also illustrate the expected trends.

The stress source function is imposed in the FEA model as an initial condition for the stress state in the region of the “peened” surface, and the FEA solver is used to calculate the equilibrium stress response. The two-dimensional FEA model for the unrestrained flat plate case is used to demonstrate how more of the compressive stress near the surface is retained as the wall thickness is increased for a constant peening intensity (i.e., stress source function). Additional cases for the flat plate geometry show how the equilibrium stress profile, including the peak tensile stress, varies with wall thickness while holding constant the amount of compressive stress retained at the “peened” surface (surface magnitude and compressive depth) by varying the stress source function. These results are then extended to the thick-wall cylinder geometry.

The form of the stress source function is validated based on a published set of experimental stress measurements performed on a peened flat plate. The FEA approach is further validated through application of a simple bilinear stress profile that is analytically constrained to satisfy through-wall force and moment balances.

The FEA model is described in Section C.2, the simulated cases are listed in Section C.3, the results are presented in Section C.4, and the model validation is presented in Section C.5. Conclusions are made in Section C.6.

C.1.3 Relevant Literature

Researchers have studied tensile balancing effects in post-peening residual stress profiles in a range of geometries for shot peening, laser peening, and water-jet peening. The following findings are relevant to the tensile balancing stress in the post-peening residual stress profile:

- Buchanan and John [4] show that for a constant residual surface stress, the peak tensile stress decreases as component thickness increases. With increased component thickness, the

balancing force is spread over a greater distance and the difference in balancing tensile stress required to develop a balancing through-wall moment is decreased.

- Hill, et al. [5] show that the peak tensile stress indirectly induced by a peening process decreases as the compressive residual stress at the surface decreases. As the peening intensity is increased and a larger compressive surface residual stress is produced, the peak tensile stress beyond the compressive residual stress layer tends to increase.
- Menig, et al. [6] investigated the nature of the tensile stress field beyond the peening compressive residual stress layer. The results presented in this paper indicate that the compressive residual stresses generated by peening are balanced by rather low tensile residual stresses extending over the whole cross-section of the component.
- DeWald and Hill [7] measured stresses and performed strain and stress modeling for four different specimen geometries treated by laser peening, including thick-wall cylinders peened on the outer diameter. The through-wall residual stress measurements were made using the contour method. The stress profile measured for the thick-wall cylinder case is comparable to that observed in other studies for peening of flat plates, although the profile near the inside surface (not peened) showed greater curvature than for flat plate cases. This case is not directly applicable to peening of reactor vessel primary nozzles because the peening was performed on the OD and because of the especially small inner-radius-to-thickness ratio, $R_i / t = 15 \text{ mm} / 15 \text{ mm} = 1.0$.

C.2 ANSYS Model Description

A two-dimensional linear-elastic ANSYS [8] FEA model is used to simulate the balancing stress effects of either:

- (1) a cross section of a flat plate peened on one side, or
- (2) a thick-wall pipe that is subjected to axisymmetric peening on the pipe inside surface.

The peening process itself is not simulated. Instead the balancing stress profile generated in response to the peening compressive residual stress layer at the treated surface is calculated considering the effect of the component geometry and stiffness. The standard peening stress source approach, also known as the “eigenstress” approach, is taken in which the initial stress profile due to peening (prior to deformation of the component and development of the balancing stress) is directly input to the model as an initial condition. This initial stress source function is independent of the component geometry given a sufficiently large wall thickness. The final stress state at equilibrium, which reflects both the reduction in peening compressive stress due to component deformation as well as generation of the balancing residual stress, is calculated using the ANSYS FEA solver. Although the peening process itself results in substantial local yielding and plastic strains, the redistribution of stress beyond the surface compressive residual stress zone in response to peening is an elastic unloading problem [1], and thus amenable to the linear-elastic stress source approach.

The material properties, geometry, boundary conditions, and loading are described in the following subsections.

C.2.1 Material Properties

The ANSYS model is a linear-elastic model. Thus the needed properties are limited to Young's Modulus and Poisson's Ratio. As shown in Table C-1, room-temperature values were input using the physical properties tabulated in Section II Part D of the ASME Boiler and Pressure Vessel Code [9] for Alloy 600 and another nickel-based alloy, Alloy 22. The material properties for Alloy 22 were applied in the case used to validate the chosen form of the stress source function.

Table C-1
Material Properties [9]

Material	Parameter	Units	Value
Alloy 600	Young's Modulus	Pa	2.13E+11
	Poisson's Ratio	-	0.31
Alloy 22	Young's Modulus	Pa	2.06E+11
	Poisson's Ratio	-	0.31

C.2.2 Geometry

The same two-dimensional mesh is used to model a flat plate or an axisymmetric pipe. The ANSYS PLANE183 element type is applied under the generalized plane strain assumption for the flat plate geometry and in axisymmetric mode for the pipe geometry.

It was shown that the choice of either generalized plane strain or plane stress for the plate geometry does not significantly affect the in-plane stress results presented in this appendix. The reason is that the calculated profile for the in-plane (Y-direction) stress must satisfy the same force and moment balances regardless of whether the plane strain or plane stress assumption is made for two-dimensional treatment of Hooke's Law.

The geometry of the plate and pipe models is defined by the example mesh shown in Figure C-1. When modeling a plate, the model can be considered to be infinitely wide in the out-of-plane direction. When modeling a pipe, the out-of-plane direction is the azimuthal dimension and the axis of rotation is to the left of the mesh of Figure C-1. The pipe geometry boundary conditions make the pipe behave as though it is infinite in length. As shown in red in this figure, the model includes a distinct area on the left (inner diameter) surface where the stress source function is applied to simulate the effects of peening. This area is assigned an initial stress profile, as described by Section C.2.4, to model the effects of peening while the initial stress state in the remainder of the mesh is zero.

The mesh spacing is controlled in the model to ensure the results are accurate in the areas of interest. The mesh is refined in the region where the stress source function is applied because this is the area with the largest stress gradient. The effect of overall mesh refinement was checked to confirm model convergence. The length of the peened area is chosen to result in a region of reasonably uniform stresses that are reasonably fully developed without edge effects, and the solution is confirmed to be converged with respect to the modeled length of the mesh. The modeled geometry satisfied a study of the spatial uniformity of the peak stress and of the compressive residual stress layer depth.

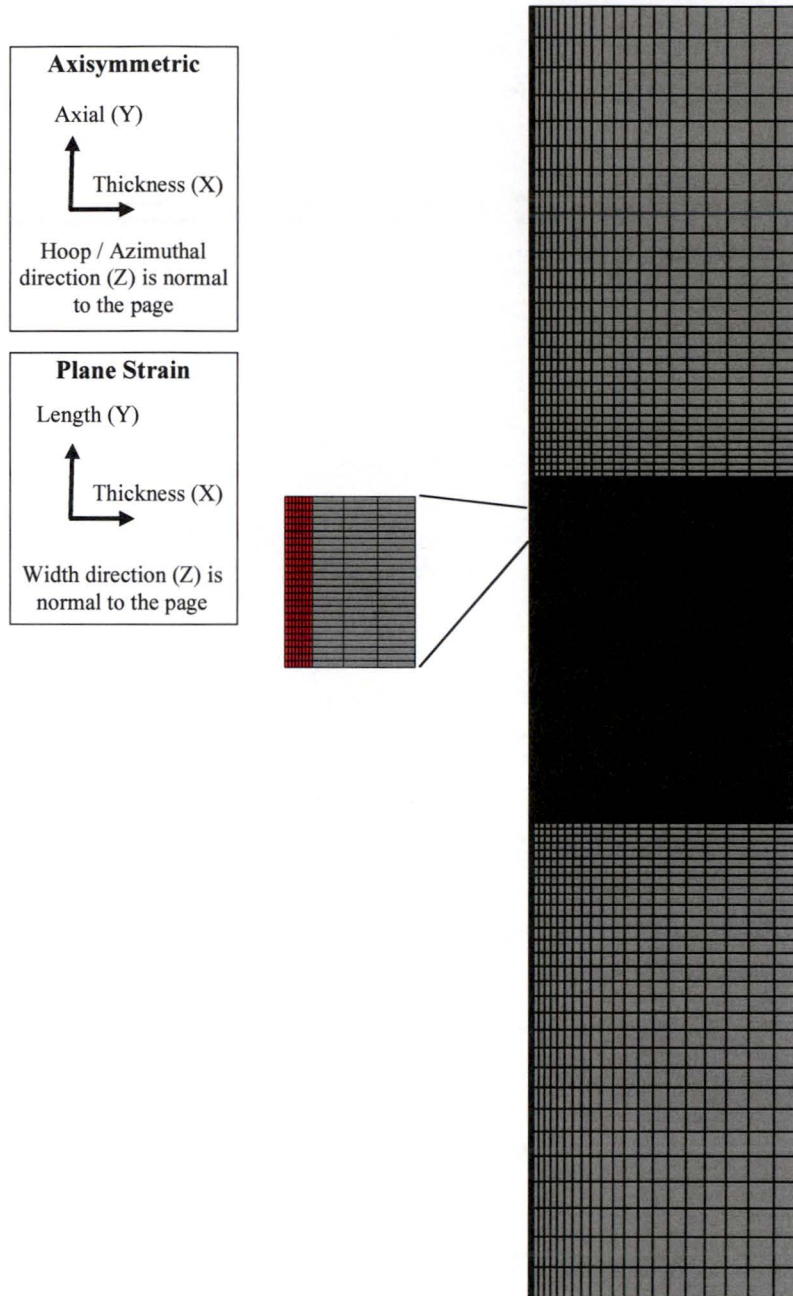


Figure C-1
Example Mesh with Region of Application of Stress Source Function in Red (wall thickness = 63.5 mm)

C.2.3 Boundary Conditions

To prevent rigid-body motion of the model, the following boundary conditions are applied:

Flat Plate Geometry

- Midpoint of Left Side of Cross Section: Zero displacement in the X- and Y-directions
- Midpoint of Right Side of Cross Section: Zero displacement in the Y-direction

Thick-Wall Pipe Geometry

- Bottom Row of Nodes: Zero displacement in Y-direction
- Top Row of Nodes: Displacement in Y-direction is uniformly the same (coupled)

C.2.4 Loading

The only load source in the model is the biaxial initial stress state specified in the region where the stress source function is applied. The initial stress state is specified using the ANSYS INISTATE command and applied to the nodes of the elements in the stress source region according to the nodal position. The profile is applied to both the SY and SZ stress components. No initial stress is input for the through-thickness component (SX).

Per the validation exercise described below in Section C.4.1, the stress source function is assumed to have an exponential form. An improved fit to the validation data resulted from a small refinement to a pure exponential decay function. The stress source function is based on an exponential function scaled to reach zero at a depth of δ_p :

$$\sigma_p(x) = \sigma_{p,0} \left[\frac{e^{-x/\tau} - R}{1 - R} \right] \quad \text{for } x < \delta_p \quad [C-2]$$
$$\tau = -\frac{\delta_p}{\ln(R)}$$

where:

- δ_p = depth of region subjected to initial stress source function
- x = through-wall depth from “peened” surface
- $\sigma_p(x)$ = peening stress source function
- $\sigma_{p,0}$ = initial peening compressive stress at peened surface prior to deformation
- R = fraction of exponential remaining at $x = \delta_p$, taken to be 0.04 based on the comparison in Section C.4.1

Examples of a stress source function having the form of Equation [C-2] and the final equilibrium stress state in the component are shown in Figure C-2 and Figure C-3.

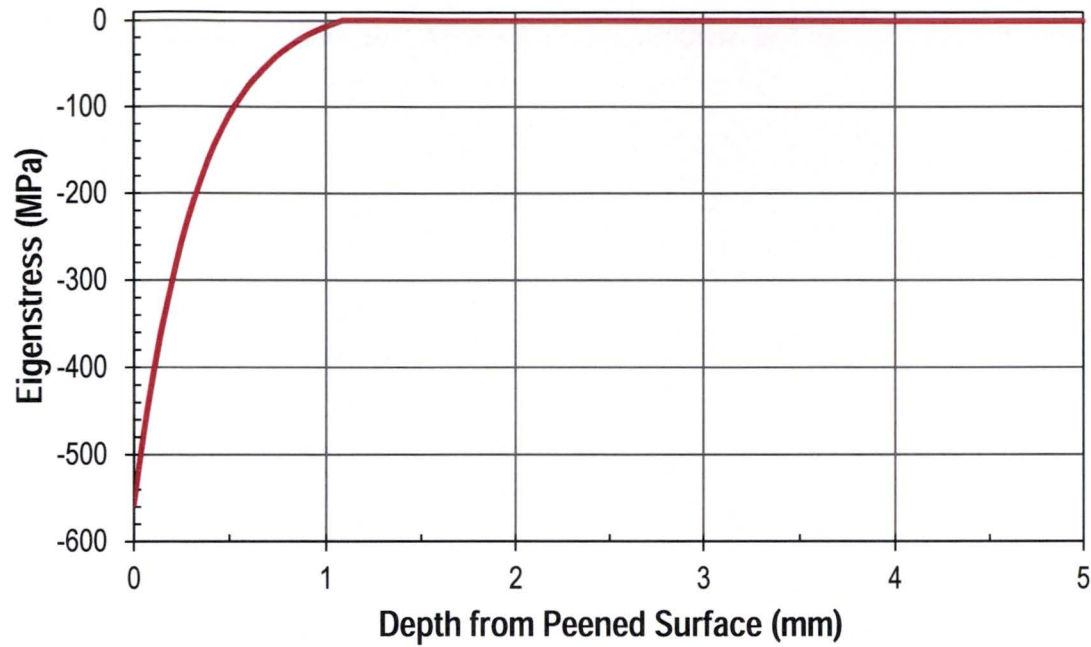


Figure C-2
Example Stress Source Function for $\sigma_{p,0} = -558$ MPa (-80.9 ksi) and $\delta_p = 1.09$ mm (0.043 in.)

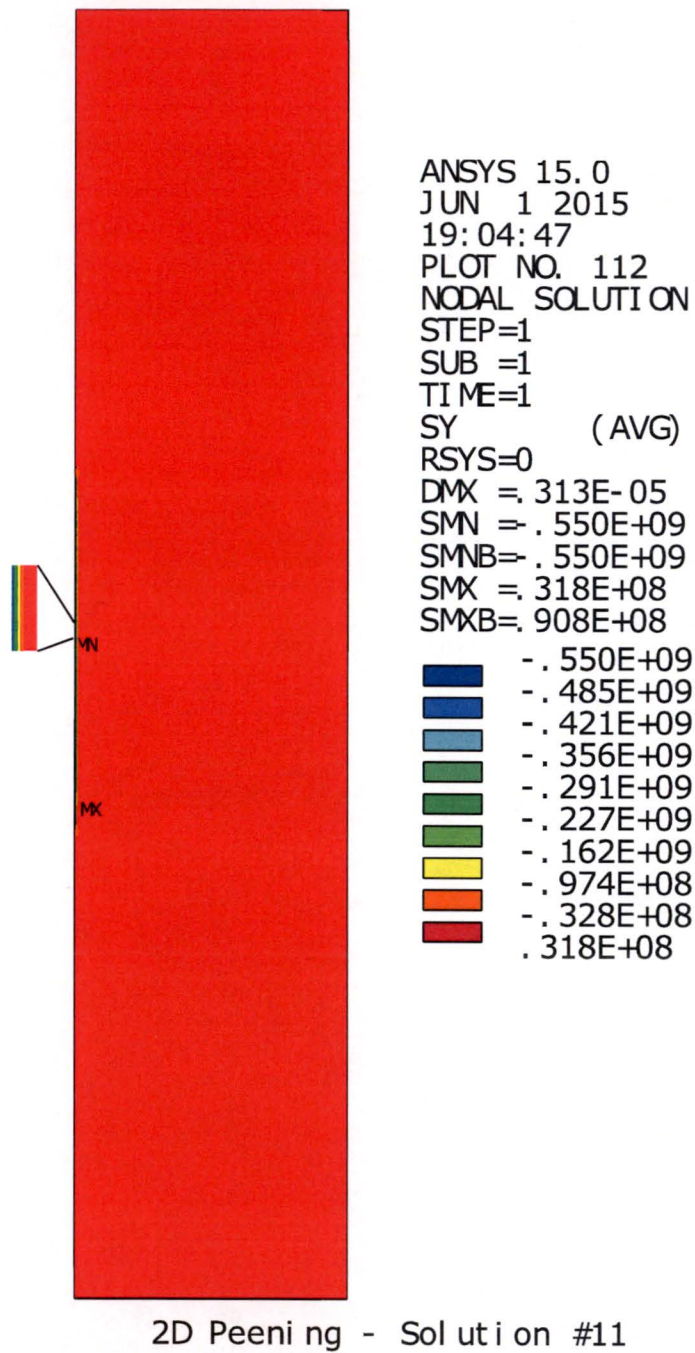


Figure C-3
Example Equilibrium Stress Solution Contour Plot for the Length (Y) Direction Stress (SY)
for Flat Plate Model (wall thickness = 63.5 mm)

C.3 ANSYS Model Cases

The FEA model was used to investigate the following cases:

- **Validation of Exponential Form of Stress Source Function**
 - Simulates the stress profile for a flat plate treated by laser peening (measured by Hill et al. [5]) (Figure C-4)
 - Material: Alloy 22
 - Plate with thickness of 20 mm and length of 38 mm
 - Peened area length of 30 mm
 - Modeled using an equilibrium surface compressive stress of ~ 470 MPa (68.2 ksi) and depth of 2.74 mm
- **Plate with Thickness of Reactor Vessel Outlet Nozzle (Two-Dimensional)**
 - Simulates an unrestrained flat plate with thickness comparable to the reactor vessel outlet nozzle pipe case to show the effect of modeling a plate vs. a pipe. The simpler plate geometry is a common geometry for published testing and modeling efforts.
 - Material: Alloy 600
 - Plate length of 300 mm and peened area length of 80 mm
 - Plate wall thickness:
 - Base case thickness of 2.5 inches (63.5 mm), which is close to the lower bound thickness of 2.4 inches (61 mm) cited in MRP-109 [10]
 - Sensitivity cases illustrating effect of wall thickness ranging from a factor of 8 thinner to a factor of 6 thicker
 - Peening stress source function assumptions:
 - Constant stress source function ($\sigma_{p,0} = -558$ MPa (-80.9 ksi) and $\delta_p = 1.09$ mm) to illustrate greater retention of initial compressive stress as thickness is increased
 - Vary stress source function to obtain equilibrium surface compressive stress of ~ 550 MPa (80 ksi) and compressive stress depth of 1.0 mm
- **Reactor Vessel Outlet Nozzle (Axisymmetric)**
 - Simulates effects of peening on the ID of a thick-wall pipe with the dimensions of a typical reactor vessel outlet nozzle (RVON) dissimilar metal weld.
 - Material: Alloy 600
 - Pipe length of 300 mm, peened area length of 80 mm, and ratio of inner radius to thickness of 5.8 (yields an outer diameter of 34 inches (864 mm) for a thickness of 2.5 inches (63.5 mm))
 - Pipe wall thickness:
 - Base case thickness of 2.5 inches (63.5 mm), which is close to the lower bound thickness of 2.4 inches (61 mm) cited in MRP-109 [10]
 - Sensitivity cases illustrating effect of wall thickness ranging from a factor of 8 thinner to a factor of 6 thicker (evaluated both for a constant outer diameter of 34 inches and for a constant ratio of inner radius to wall thickness of 5.8)

- Peening stress source function assumptions:
 - Vary stress source function to obtain equilibrium surface compressive stress of ~550 MPa (80 ksi) and compressive stress depth of 1.0 mm
 - Sensitivity cases illustrating effect of compressive stress depth using 0.5 mm and 1.5 mm equilibrium surface compressive stress depths for RVON base case dimensions

C.4 ANSYS Model Results

C.4.1 Validation of Exponential Form of Stress Source Function

The parameters for the exponential stress source function ($\sigma_{p,0}$ and δ_p in Equation [C-2]) were varied until the match between the measured stress profile and the calculated equilibrium profile in Figure C-4 was obtained. The magnitude of the peak stress obtained in this case reflects the magnitude of the compressive stress depth (2.7 mm) in comparison to the wall thickness (20 mm).

The very good agreement between the measured and predicted stress profiles shows that the exponential form of Equation [C-2] is a good choice to model the peening effect for the type of laser peening performed by Hill et al. [5]. Furthermore, the measured peening compressive stress profiles presented in MRP-267R1 [11] for a variety of laser peening and water jet peening processes have shapes that are generally reasonably approximated by the shape of the peening compressive stress profile measured by Hill et al. [5] and shown in Figure C-4. Hence, the stress source functional form defined in Equation [C-2] is applied in all the FEA cases.

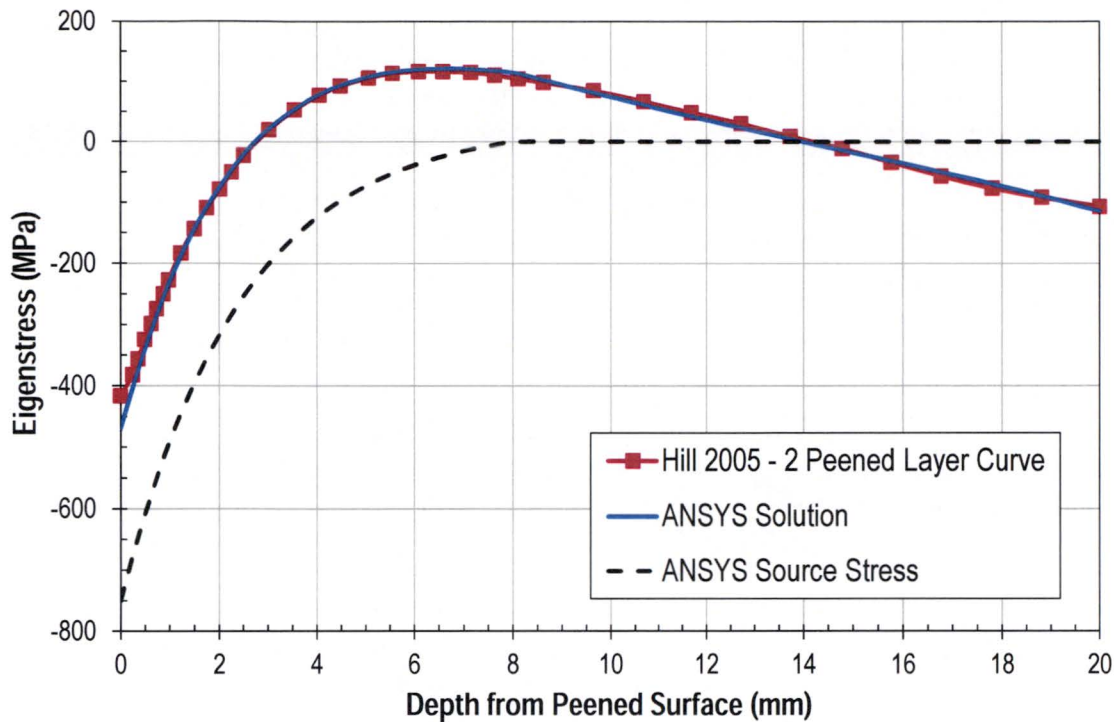


Figure C-4
Validation of Exponential Form of Stress Source Function Using Through-Wall Stress Profile Measured by Hill et al. [5]

C.4.2 Calculated Stress Profiles for Flat Plate and Thick-Wall Pipe Geometries

The FEA analyses results are shown in Figure C-5 through Figure C-13, where in each figure the stress profile is taken at the midpoint of the peened region (i.e., the symmetry plane of the model):

Effect of Wall Thickness on Retained Peening Compressive Stress (Flat Plate)

- Figure C-5 illustrates how the compressive stress effect developed by peening increases (in terms of surface compressive stress magnitude and compressive stress depth) for the same peening intensity as the wall thickness is increased. More of the initial peening compressive stress would be retained for the thick-wall pipe geometry for equivalent wall thickness because of its greater level of constraint. Because the peening performance criteria are based on the stress profile achieved following peening (including the relaxation in compressive stress at the surface due to elastic deformation of the component upon peening), the results presented below for a consistent equilibrium compressive stress effect are more important to the conclusions of this investigation.

Effect of Wall Thickness on Balancing Stress Profile (Flat Plate and Thick-Wall Pipe)

- Figure C-6 clearly illustrates how the peak tensile stress is reduced as the wall thickness is increased for the flat plate geometry with the stress source function parameters varied to obtain constant equilibrium values of the surface compressive stress magnitude and compressive depth. The profiles show how a linear stress profile (through-wall bending) and an axial membrane stress component are produced in response to the peening effect. As discussed by Bernasconi and Roth [1], this is the expected behavior of a peened plate and reflects simple beam behavior. Note that it was numerically confirmed that these calculated stress profiles satisfy both force and moment balance. This is a requirement of the model since the through-thickness profile for stress in the Y-direction is necessarily uniform in the Z-direction (into the page) given the two-dimensional assumption.
- Figure C-7 shows similar behavior for the axial stress profile for the thick-wall pipe geometry. For equivalent wall thickness, the peak tensile stress is smaller for the pipe axial stress case. The pipe geometry is more constrained than a flat plate and does not deflect as much as the plate case for equivalent peening compressive stress effect and equivalent wall thickness. The reduced curvature for the pipe case means that a smaller through-wall bending stress component is produced in the axial direction than would be the case for the corresponding flat plate. In addition, the gradient in cross sectional area between the inner and outer portions of the pipe cross section tends to increase the contribution of a given through-wall stress gradient to the through-wall force and bending moment in comparison to the situation for a flat plate. Note that it was numerically confirmed that these calculated stress profiles satisfy force balances. Force balance over a given through-wall profile is a requirement of the model since the axial stress profile is necessarily uniform in the azimuthal direction given the axisymmetric assumption. The pipe geometry does not satisfy the moment balance in the same manner as for the unrestrained flat plate as shear stresses contribute to the balance for the pipe.
- While the results in Figure C-7 represent a constant outer diameter while the thickness is varied, Figure C-8 plots the equivalent axial stress results for a constant inner-radius-to-thickness ratio. The peak tensile stress for the pipe geometry cases remains smaller than the peak tensile stress in the plate geometry case for equivalent wall thickness. Note that the curves with a positive slope in Figure C-8 have a lower peak tensile stress than the equivalent constant outer diameter curves (having a negative slope). These cases with positive slope correspond to relatively small wall thicknesses and are the result of a more complex deformed shape of the pipe compared to cases with greater wall thickness or greater diameter. It was numerically confirmed that these calculated stress profiles also satisfy force balance.
- Figure C-9 and Figure C-10 show the calculated profiles for the case of the hoop stress for the thick-wall pipe geometry. Note that the compressive stress depth at equilibrium for the hoop stress profile varies slightly for the different thickness cases because the stress source function was varied to maintain the compressive stress depth for the axial stress profile. Regardless of this point, the magnitude of the tensile stress response is substantially smaller for the hoop stress profile in comparison to that for the axial stress for equivalent wall thickness. This lower peak magnitude occurs because the force balance in the hoop direction is enforced over the entire modeled area, permitting a

distribution of the tensile balancing stress over a greater area. The hoop profiles have smaller slopes than the axial profiles because the axial change in curvature upon peening is greater than the change in curvature of the pipe in the circumferential direction. The pipe geometry is most constrained in the circumferential direction.

Effect of Wall Thickness on Peak Balancing Tensile Stress (Flat Plate and Thick-Wall Pipe)

- Figure C-11 and Figure C-12 plot the peak tensile stress of the profiles in Figure C-6 through Figure C-10 directly as a function of wall thickness. The peak tensile stress is plotted as a percentage of the surface compressive stress value as the shape of the stress profile does not depend on the magnitude of the surface compressive stress.

Effect of Peening Compressive Stress Depth on Balancing Stress Profile (RVON Pipe Geometry)

- The results in Figure C-6 through Figure C-12 assumed a post-peening compressive stress depth of 1 millimeter. Figure C-13 illustrates how the axial stress profile for the RVON geometry is affected by this assumption. Profiles are shown for compressive depths of 0.5 mm and 1.5 mm in addition to 1.0 mm. The magnitude of the peak tensile stress has an approximate linear dependence on the compressive stress depth. This is expected given that the force and moment created by the compressive profile close to the peened surface are each approximately proportional to the compressive depth.

As shown in the figures, the calculated maximum tensile stress for a given peening compressive stress effect (surface magnitude and compressive depth) decreases with increasing wall thickness. This applies in both the axial and hoop directions for the pipe.

For the reactor vessel outlet nozzle (RVON) thick-wall pipe geometry, the peak tensile balancing stresses are less than about 2% of the magnitude of the compressive surface stress for the case of a compressive residual stress layer at the pipe ID that is 1 millimeter deep. This relatively small magnitude for the peak tensile balancing stress is the result of the balancing force and moment being spread over the large wall thickness of this component, plus the fact that the pipe geometry is more constrained than a flat plate and does not deflect as much as the plate case for equivalent peening compressive stress effect and equivalent wall thickness.

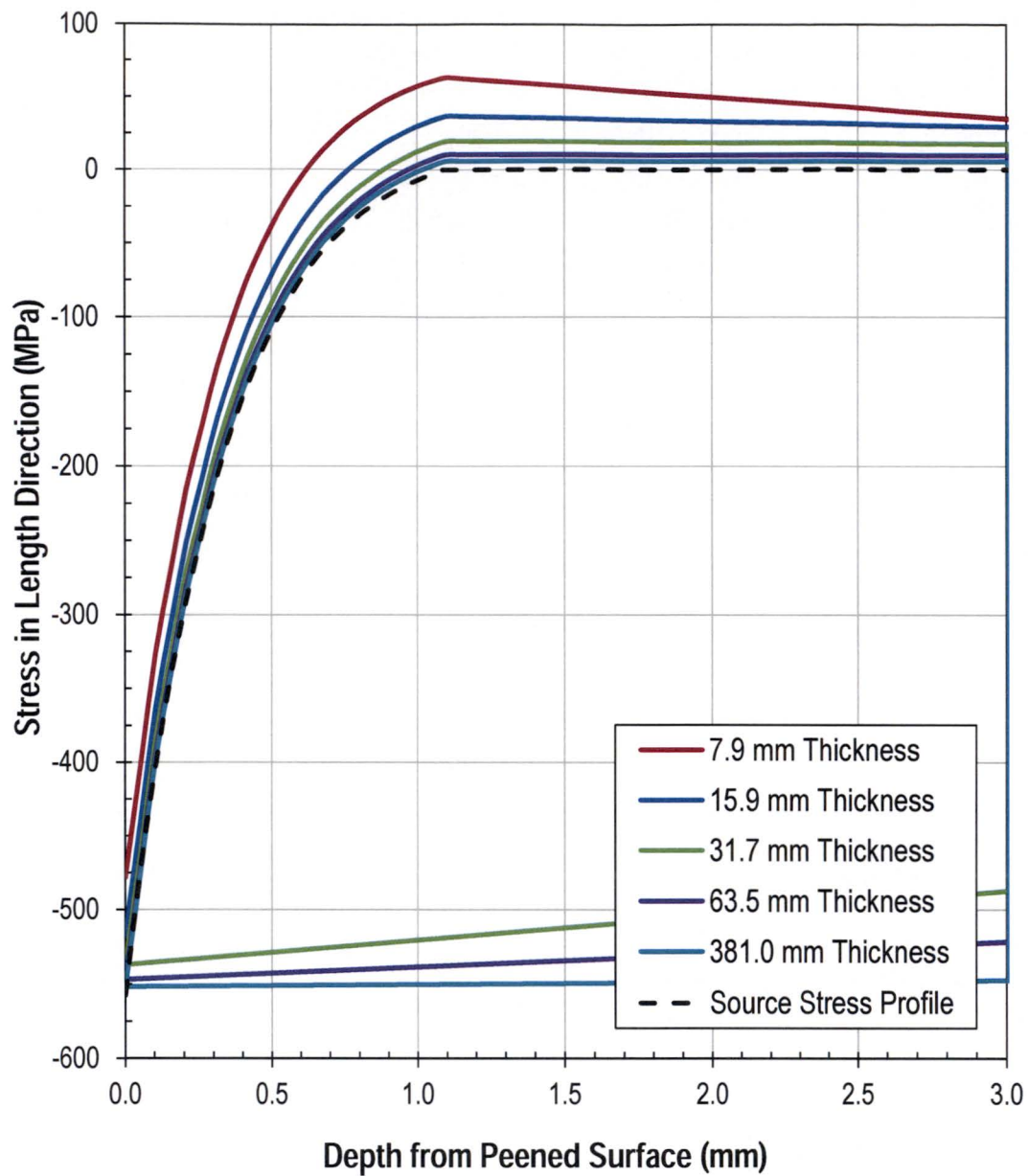


Figure C-5
Equilibrium Through-Wall Stress Profiles for Flat Plate for Common Stress Source
Function

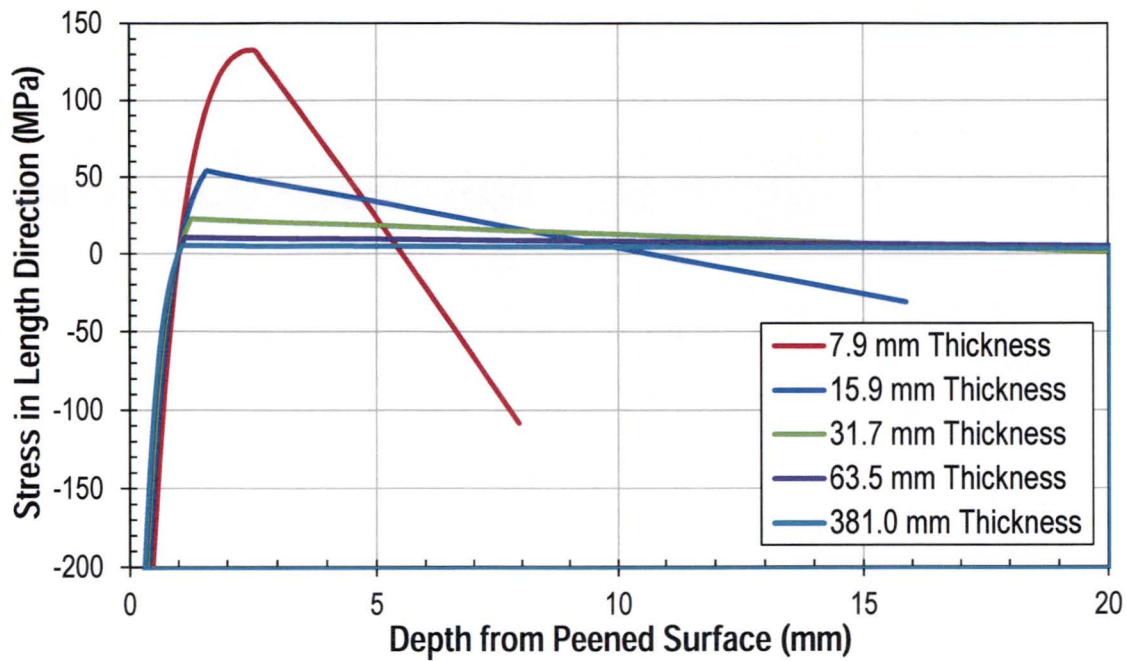


Figure C-6
Effect of Wall Thickness on Through-Wall Stress Profile for Plate Geometry for Same Equilibrium Surface Compressive Stress and Compressive Depth

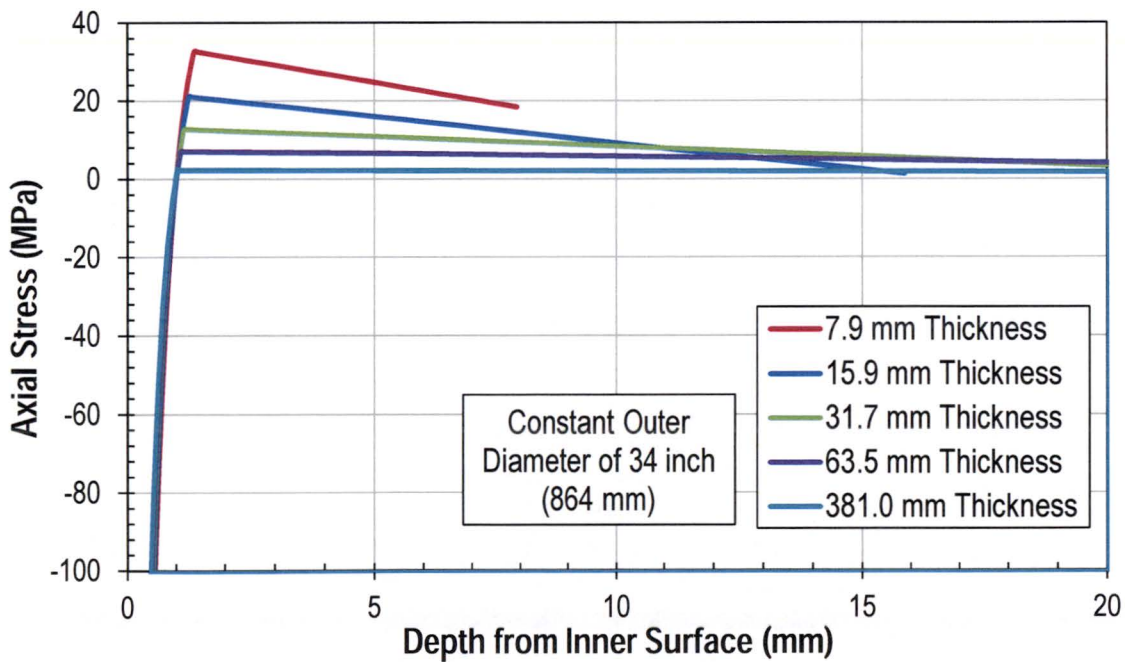


Figure C-7
Effect of Wall Thickness on Through-Wall Axial Stress Profile for Constant Outer Diameter Pipe Geometry for Same Equilibrium Surface Compressive Stress and Compressive Depth

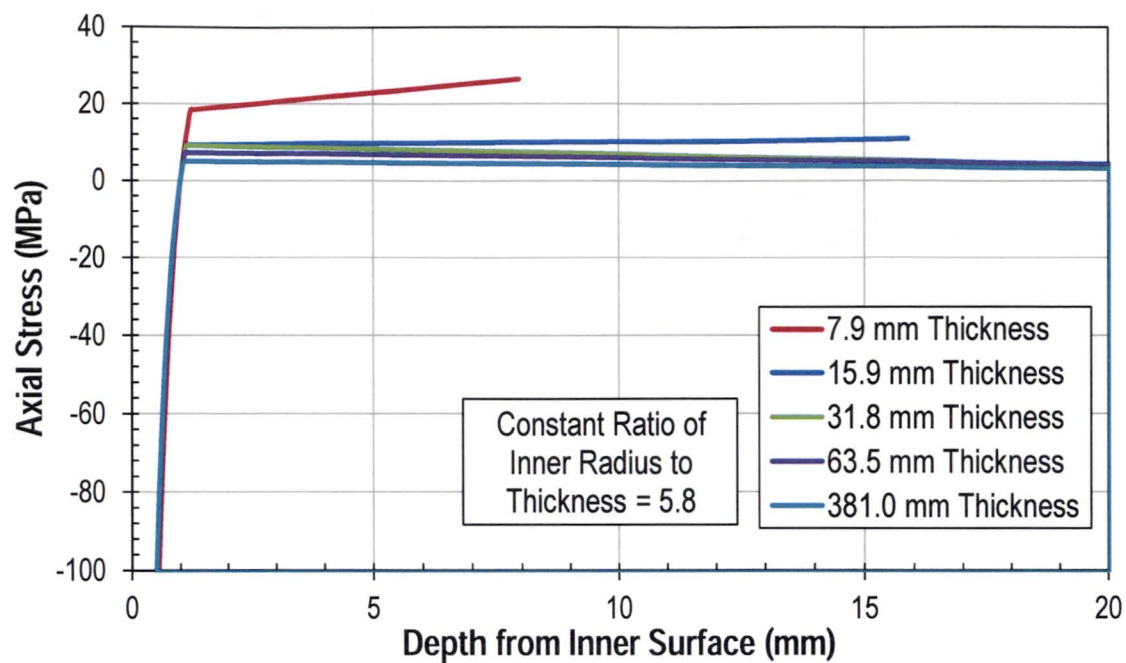


Figure C-8
Effect of Wall Thickness on Through-Wall Axial Stress Profile for Constant R_i / t Pipe Geometry for Same Equilibrium Surface Compressive Stress and Compressive Depth

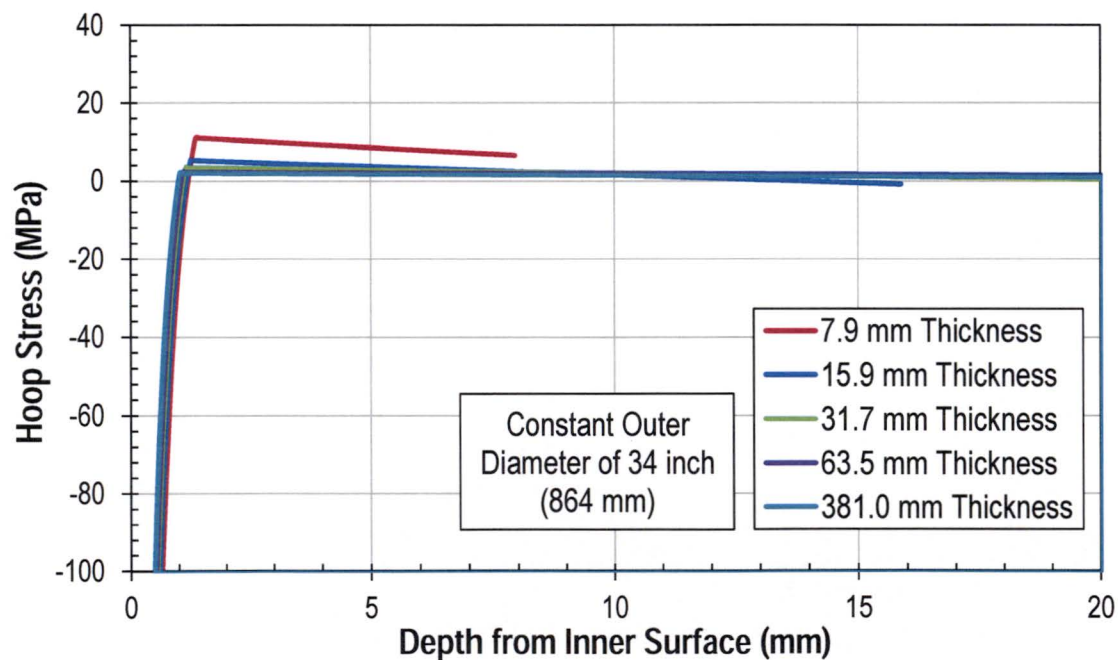


Figure C-9
Effect of Wall Thickness on Through-Wall Hoop Stress Profile for Constant Outer Diameter Pipe Geometry for Same Equilibrium Surface Compressive Stress and Compressive Depth

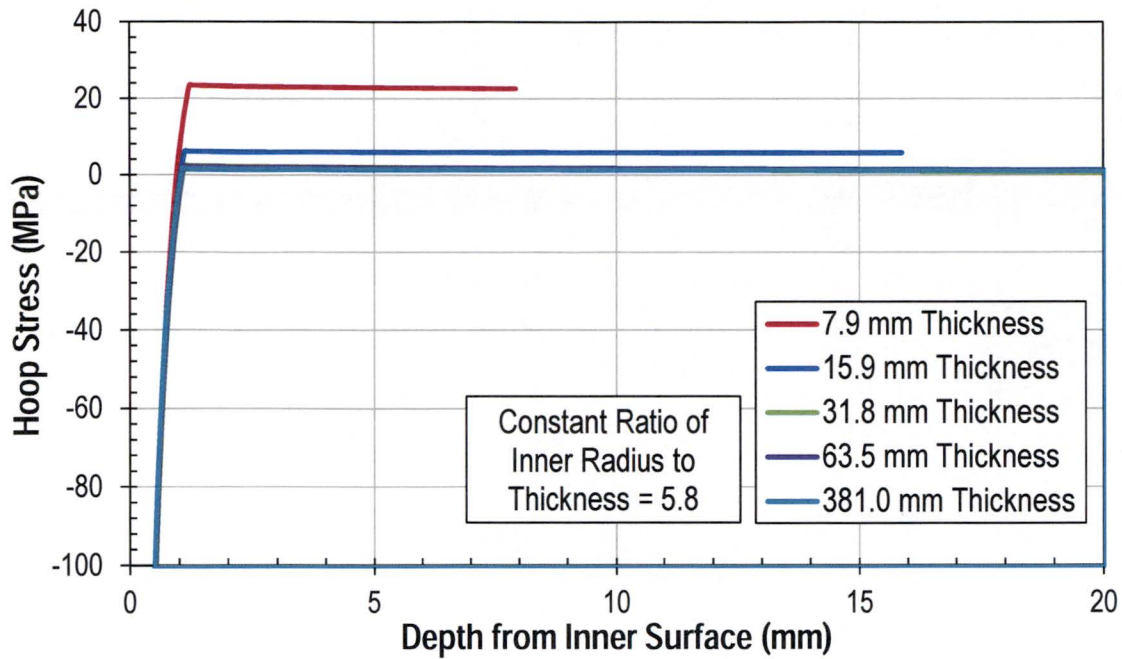


Figure C-10
Effect of Wall Thickness on Through-Wall Hoop Stress Profile for Constant R_i / t Pipe Geometry for Same Equilibrium Surface Compressive Stress and Compressive Depth

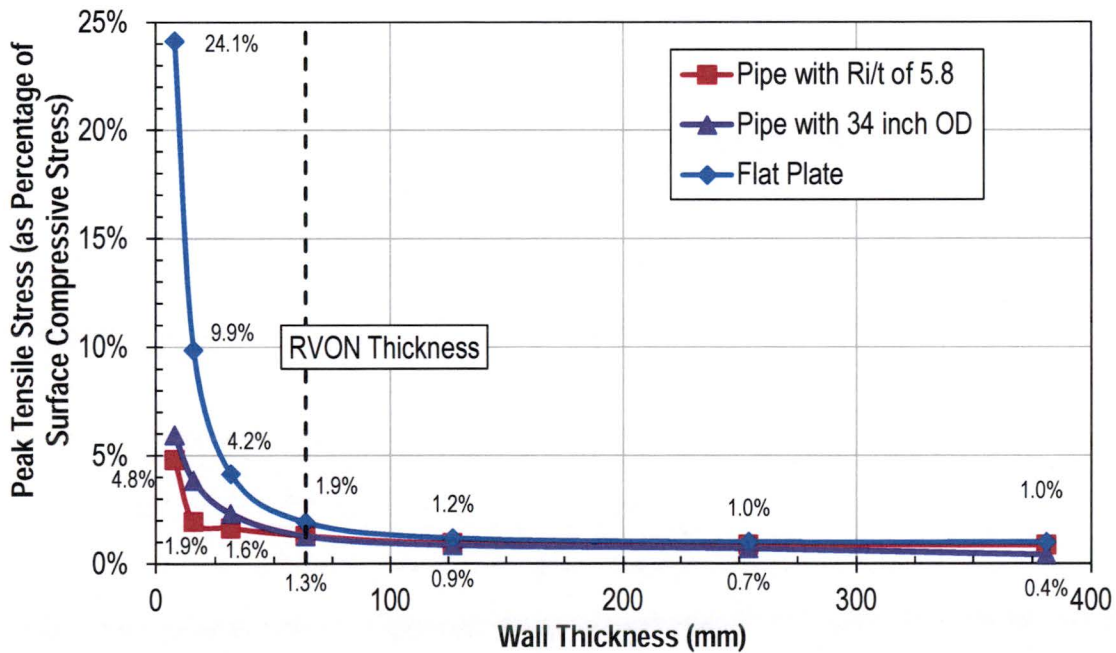


Figure C-11
Effect of Wall Thickness on Peak Tensile Axial Stress for Same Equilibrium Surface Compressive Stress and Compressive Depth

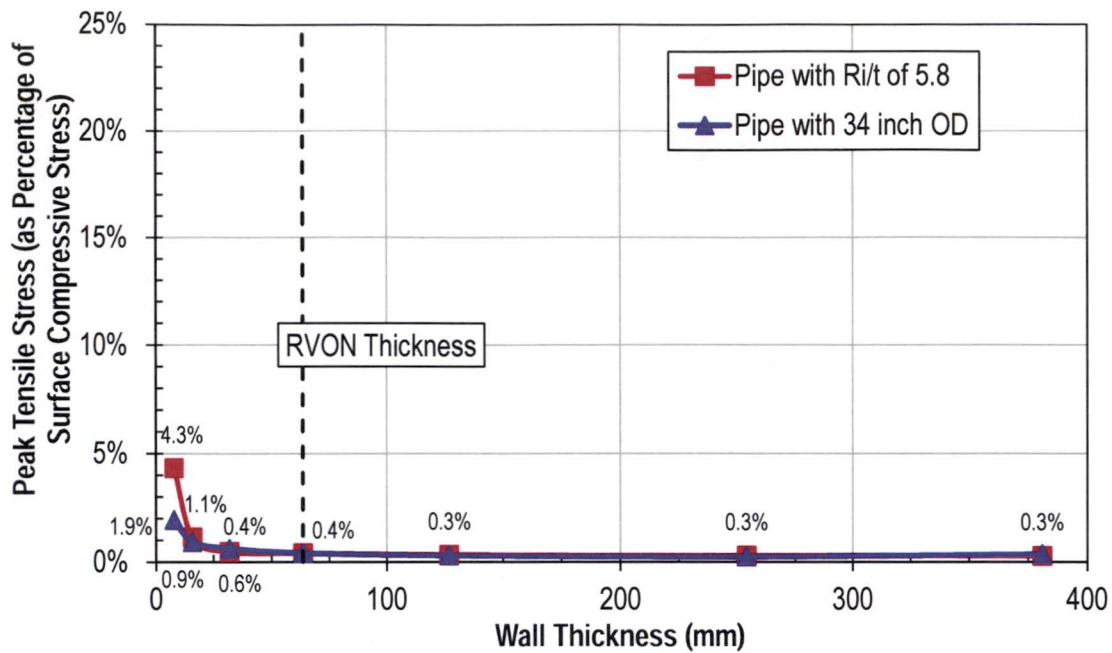


Figure C-12
Effect of Wall Thickness on Peak Tensile Hoop Stress for Same Equilibrium Surface Compressive Stress and Compressive Depth

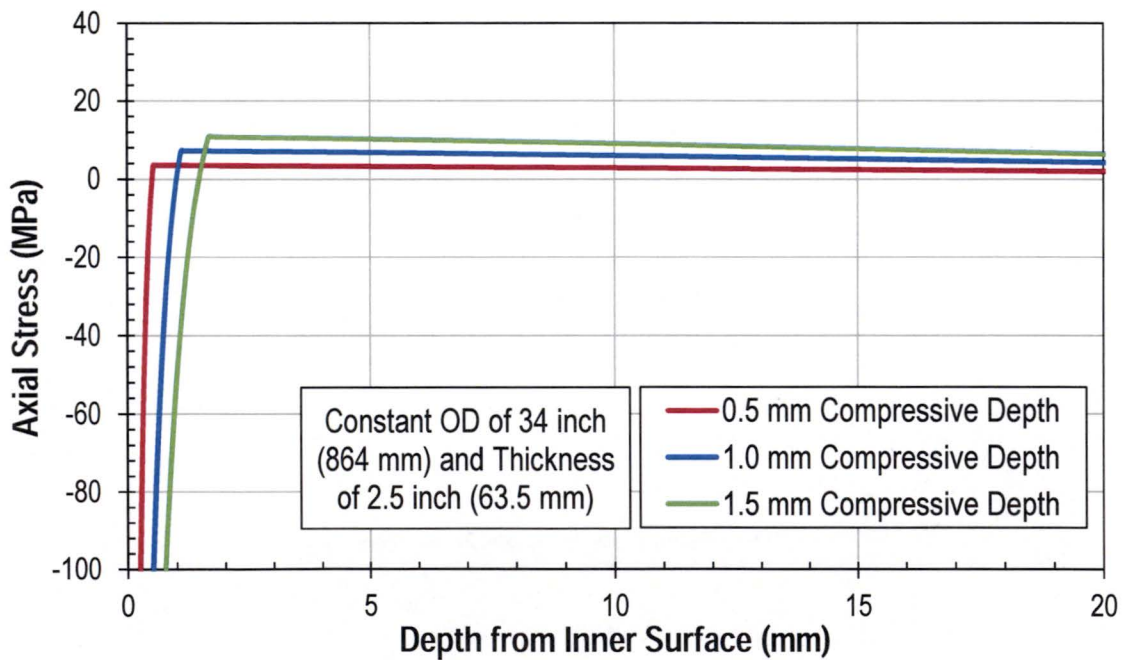


Figure C-13
Effect of Compressive Stress Depth on Through-Wall Axial Stress Profile for RVON Pipe Geometry (Surface Stress Held Constant)

C.5 Model Validation Using Bilinear Stress Profile

The ANSYS model is validated by comparing the resulting stresses to a simple piecewise linear stress profile. The piecewise linear stress profile, which ensures that the applicable force and moment balances are satisfied for the simplest possible profile, is subject to the following assumptions:

1. The profile models the effect of peening only.
2. The compressive surface stress is set to an assumed value, $\sigma(x=0) = \sigma_0$.
3. The stress profile transitions to tensile stresses at a pre-defined point, x_0 . This is where $\sigma(x=x_0) = 0$.
4. The internal forces must balance to zero through the thickness of the peened component assuming that the profile is uniform over the cross section of an unrestrained flat plate:

$$F_{net} = \int_0^t \sigma(x) dx = 0 \quad [C-3]$$

5. The internal moments must balance to zero through the thickness of the peened component assuming that the profile is uniform over the cross section of an unrestrained flat plate:

$$M_{net} = \int_0^t x\sigma(x) dx = 0 \quad [C-4]$$

The piecewise linear stress profile is defined by two line segments; the first is defined by assumptions (2) and (3), whereas the second is defined by assumptions (4) and (5). For the case of the axial stress profile of a thick-wall pipe, Equations [C-3] and [C-4] are assumed to hold except that the force and moment integration are each weighted by the radial coordinate to account for the increase in cross sectional area toward the OD. In each validation case, the values of σ_0 and x_0 were selected to match the FEA profile.

Figure C-14 and Figure C-15 compare the bilinear profile with the FEA results for two cases.

- Figure C-14 shows reasonable agreement versus the FEA solution and measured stress profile for the flat plate case investigated by Hill et al. [5], including similar peak tensile stress values.
- Figure C-15 shows a similar peak tensile stress for the FEA case investigated for a thick-wall pipe with dimensions applicable to reactor vessel outlet and inlet nozzles. The somewhat smaller peak stress for the FEA case is the result of the curvature in the FEA stress profile close to the peened surface. This curvature results in a reduced force and a reduced moment to be balanced by the remainder of the stress profile. This particular FEA stress profile is from a region with a rather uniform curvature that is close to a through-wall moment balance without considering the effect of shear stress on the moment balance.

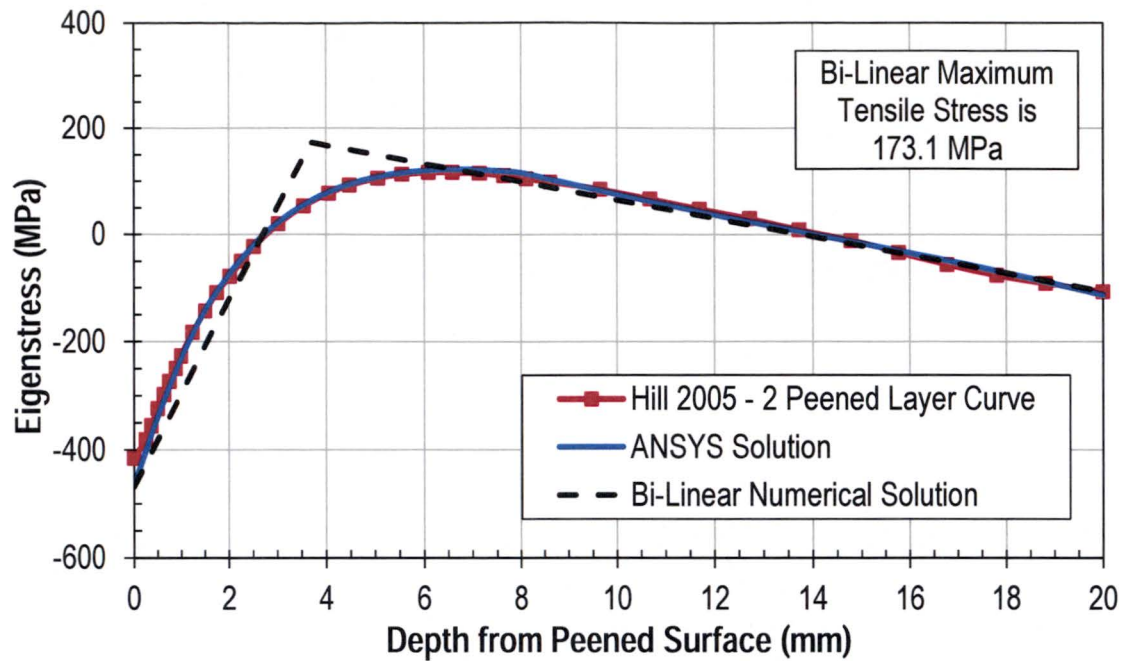


Figure C-14
ANSYS Model Validation for Profile Measured by Hill et al. [5] Using Bilinear Stress Profile

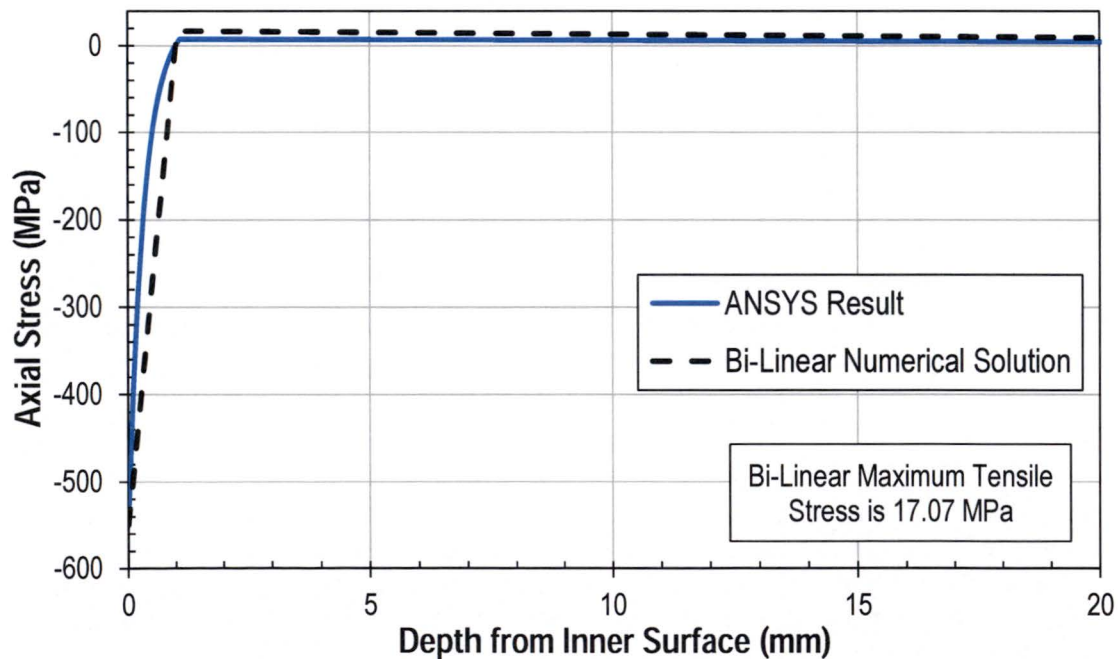


Figure C-15
ANSYS Model Validation for Reactor Vessel Outlet Nozzle (RVON) Case Using Bilinear Stress Profile

C.6 Conclusions

The literature review and analyses presented in this appendix demonstrate the following:

- A balancing stress profile develops beyond the compressive residual stress induced by peening at the treated surface. This balancing stress consists of a through-wall bending component and an axial membrane stress. These residual stress components act to balance the force and change in curvature associated with the peening compressive residual stress developed in the region of the treated surface. The peak tensile stress generally forms in the region just beyond the peening compressive residual stress layer. The peak tensile stress location represents the location beyond the compressive stress zone where the through-wall bending stress is maximum.
- For a given compressive residual stress effect (surface magnitude and depth of compression) retained upon peening, the peak tensile balancing stress decreases as the component thickness increases. As the component thickness increases, the balancing force and moment are each spread over a greater distance. The difference in balancing stress required to develop the balancing through-wall moment is decreased. The increase in moment arm distance means that a smaller stress difference will create the same moment. Similar trends are produced for thick-wall pipes peened on the inside diameter as for flat plates.
- The peak balancing tensile stress for the case of a peened thick-wall pipe is reduced compared to an unrestrained flat plate of equivalent wall thickness. This is because the more constrained pipe geometry does not deflect as much as the plate case for equivalent peening compressive stress effect and equivalent wall thickness, corresponding to a reduced through-wall drop in the balancing stress profile. The pipe geometry does not satisfy the moment balance in the same manner as for the unrestrained flat plate as shear stresses contribute to the balance for the pipe. The result is that the balancing stress profile for a thick-wall pipe is more nearly uniform than for the case of an unrestrained flat plate of equivalent wall thickness.
- For the reactor vessel outlet nozzle (RVON) geometry evaluated with the FEA model, the peak tensile balancing stresses are less than about 2% of the magnitude of the compressive surface stress for the case of a compressive residual stress layer at the pipe ID that is 1 millimeter deep. This relatively small magnitude for the peak tensile balancing stress is the result of the balancing force and moment being spread over the large wall thickness of this component, plus the fact that the pipe geometry is more constrained than a flat plate and does not deflect as much as the plate case for equivalent peening compressive stress effect and equivalent wall thickness.

In summary, because of the thick-wall for reactor vessel outlet and inlet nozzles, peening of these components has a small effect on the peak tensile stress below the surface compressive stress zone. With regard to reactor pressure vessel head penetration nozzles (RPVHPNs), the effective thickness of the nozzle at the weld elevation is increased by the presence of the J-groove weld and head. This effect tends to limit the peak tensile balancing stress near the peened ID at the weld elevation. Below the J-groove weld, both the OD and ID surfaces are peened, tending to make the balancing stress uniform over the wall thickness.

C.7 References

1. J. Bernasconi and M. Roth, "The Niku-Lari Method and the Stress Source Method: Application to Residual Stress Distribution of Shot Peened Plates," *Advances in Surface Treatments, Residual Stresses*, Vol. 4, pp. 221-250, Pergamon Press, 1987.
2. S. T. S. Al-Hassani, "Mechanical Aspects of Residual Stress Development in Shot Peening," *Proceedings of ICSP-1*, edited by A. Niku-Lari, pp. 583-602, Pergamon Press, 1981.
3. A. Niku-Lari, "Methode De La Fleche Methode De La Source Des Contraintes Residuelles," *Proceedings of ICSP-1*, edited by A. Niku-Lari, pp. 237-247, Pergamon Press, 1981.
4. D. J. Buchanan and R. John, "Residual Stress Redistribution in Shot Peened Samples Subject to Mechanical Loading," *Materials Science & Engineering A*, Vol. 615, pp. 70-78, 2014.
5. M. R. Hill, et al., "Measurement of Laser Peening Residual Stresses," *Journal of Materials Science & Technology*, Vol. 21, No. 1, pp. 3-9, 2005.
6. R. Menig, et al., "Depth Profiles of Macro Residual Stresses in Thin Shot Peened Steel Plates Determined by X-Ray and Neutron Diffraction," *Scripta Materialia*, Vol. 45, No. 8, pp. 977-983, 2001.
7. A. T. DeWald and M. R. Hill, "Eigenstrain-Based Model for Prediction of Laser Peening Residual Stresses in Arbitrary Three-Dimensional Bodies. Part 2: Model Verification," *Journal of Strain Analysis for Engineering Design*, Vol. 44, No. 1, pp. 13-27, 2009.
8. ANSYS Version 15.0, Mallett Technology, Inc., Canonsburg, PA: 2015.
9. ASME Boiler and Pressure Vessel Code, Section II, Materials, Part D, Properties (Customary), ASME, 2013 Edition, July 1, 2013.
10. *Materials Reliability Program: Alloy 82/182 Pipe Butt Weld Safety Assessment for the US PWR Plant Designs: Westinghouse and CE Design Plants (MRP-109NP)*, EPRI, Palo Alto, CA: 2004. 1009804. [NRC ADAMS Accession No. ML042430093]
11. *Materials Reliability Program: Technical Basis for Primary Water Stress Corrosion Cracking Mitigation by Surface Stress Improvement (MRP-267, Revision 1)*, EPRI, Palo Alto, CA: 2012. 1025839. [Freely Available at www.epri.com]

The Electric Power Research Institute, Inc. (EPRI, www.epri.com) conducts research and development relating to the generation, delivery and use of electricity for the benefit of the public. An independent, nonprofit organization, EPRI brings together its scientists and engineers as well as experts from academia and industry to help address challenges in electricity, including reliability, efficiency, affordability, health, safety and the environment. EPRI members represent 90% of the electric utility revenue in the United States with international participation in 35 countries. EPRI's principal offices and laboratories are located in Palo Alto, Calif.; Charlotte, N.C.; Knoxville, Tenn.; and Lenox, Mass.

Together...Shaping the Future of Electricity

Program:

Pressurized Water Reactor Materials Reliability Program (MRP)

© 2016 Electric Power Research Institute (EPRI), Inc. All rights reserved. Electric Power Research Institute, EPRI, and TOGETHER...SHAPING THE FUTURE OF ELECTRICITY are registered service marks of the Electric Power Research Institute, Inc.

3002009241

Electric Power Research Institute

3420 Hillview Avenue, Palo Alto, California 94304-1338 • PO Box 10412, Palo Alto, California 94303-0813 USA
800.313.3774 • 650.855.2121 • askepri@epri.com • www.epri.com